Molecular biological and biochemical investigations on the biosynthetic enzymes of prenylated indole alkaloids from fungi

Molekularbiologische und biochemische Untersuchungen zu Enzymen in der Biosynthese von prenylierten Indolalkaloiden aus Pilzen

DISSERTATION

zur

Erlangung des Doktorgrades

der Naturwissenschaften

(Dr. rer. nat.)

dem Fachbereich Pharmazie

der Philipps-Universität Marburg

vorgelegt von

Xia Yu

aus Hunan, China

Marburg/Lahn, 2013

Vom Fachbereich Pharmazie der Philipps-Universität Marburg als Dissertation am 10. Juli 2013 angenommen.

Erstgutachter: Prof. Dr. Shu-Ming Li
Zweitgutachter: Prof. Dr. Michael Keusgen

Tag der mündlichen Prüfung am 11. Juli 2013

Dedicated to
my parents

Contents

Publications and presentations

Publications (*: equal contribution)

1. Yin, S.*, **Yu, X.***, Wang, Q., Liu, X. Q. & Li, S.-M. (2013). Identification of a brevianamide F reverse prenyltransferase BrePT from *Aspergillus versicolor* with a broad substrate specificity towards tryptophan-containing cyclic dipeptides. *Appl. Microbiol. Biotechnol.* 97, 1649-1660.
2. **Yu, X.**, Liu, Y., Xie, X., Zheng, X.-D. & Li, S.-M. (2012). Biochemical characterization of indole prenyltransferases: Filling the last gap of prenylation positions by a 5-dimethylallyltryptophan synthase from *Aspergillus clavatus*. *J. Biol. Chem.* 287, 1371-1380.
3. **Yu, X.**, Yang, A., Lin, W. & Li, S.-M. (2012). Friedel-Crafts alkylation on indolocarbazoles catalyzed by two dimethylallyltryptophan synthases from *Aspergillus*. *Tetrahedron Lett.* 53, 6861-6864.
4. **Yu, X.**, Li, S.-M. (2012). Prenyltransferases of the dimethylallyltryptophan synthase superfamily. *Methods Enzymol.* 516, 259-278.
5. Wollinsky, B., Ludwig, L., Hamacher, A., **Yu, X.**, Kassack, M. U. & Li, S.-M. (2012). Prenylation at the indole ring leads to a significant increase of cytotoxicity of tryptophan-containing cyclic dipeptides. *Bioorg. Med. Chem. Lett.* 22, 3866-3869.
6. **Yu, X.**, Li, S.-M. (2011). Prenylation of flavonoids by using a dimethylallyltryptophan synthase 7-DMATS from *Aspergillus fumigatus*. *Chembiochem* 12, 2280-2283.
7. **Yu, X.**, Xie, X. & Li, S.-M. (2011). Substrate promiscuity of secondary metabolite enzymes: prenylation of hydroxynaphthalenes by fungal indole prenyltransferases. *Appl. Microbiol. Biotechnol.* 92, 737-748.
8. Yin, W.-B.*, **Yu, X.***, Xie, X.-L. & Li, S.-M. (2010). Preparation of pyrrolo[2,3-b]indoles carrying a ß-configured reverse C3-dimethylallyl moiety by using a recombinant prenyltransferase CdpC3PT. *Org. Biomol. Chem.* 8, 2430-2438.
9. **Yu, X.**, Xie, X. & Li, S.-M., Complementary stereospecific synthesis of *cis*-configured prenylated pyrroloindoline diketopiperazines by indole prenyltransferases of the DMATS superfamily. (manuscript)

Presentations at scientific meetings

1. **Yu, X.**, Xie, X. & Li, S.-M., “Prenylation of hydroxynaphthalenes and flavonoids by indole prenyltransferases from fungi”. Poster presentation, *Annual Conference of the*

Association for General and Applied Microbiology (VAAM), 2012, March, Tuebingen, Germany.

2. **Yu, X.**, Xie, X. & Li, S.-M., "Chemoenzymatic synthesis of bacterial and plant metabolites by enzymes from mould fungi". Oral presentation. *DAAD-GCLB Conference*, 2011, September, Bonn, Germany.
3. Wunsch, C., Mundt, K., **Yu, X.** & Li, S.-M., "Nicht-ribosomale Peptidsynthetasen und Prenyltransferasen als Instrument zur Herstellung neuer Wirkstoffe". Poster presentation, *Synthetische Mikrobiologie Perspektiven für Biotechnologie und Pharmazie*, 2011, May, Marburg, Germany.

Erklärung zum Eigenanteil

Titel der Publikation	**Autoren**	**geschätzter Eigenanteil in %**
Preparation of pyrrolo[2,3-b]indoles carrying a ß-configured reverse C3-dimethylallyl moiety by using a recombinant prenyltransferase CdpC3PT (published)	Yin, W.-B., Yu, X., Xie, X.-L. & Li, S.-M.	35
Biochemical characterization of indole prenyltransferases: Filling the last gap of prenylation positions by a 5-dimethylallyl tryptophan synthase from *Aspergillus clavatus* (published)	Yu, X., Liu, Y., Xie, X., Zheng, X.-D. & Li, S.-M.	70
Identification of a brevianamide F reverse prenyltransferase BrePT from *Aspergillus versicolor* with a broad substrate specificity towards tryptophan-containing cyclic dipeptides (published)	Yin, S., Yu, X., Wang, Q., Liu, X. Q. & Li, S.-M.	35
Complementary stereospecific synthesis of *cis*-configurated prenylated pyrroloindoline diketopiperazines by indole prenyltransferases of the DMATS superfamily (manuscript)	Yu, X., Xie, X. & Li, S.-M.	72
Friedel–Crafts alkylation on indolocarbazoles catalyzed by two dimethylallyltryptophan synthases from *Aspergillus* (published)	Yu, X., Yang, A., Lin, W. & Li, S.-M.	70
Substrate promiscuity of secondary metabolite enzymes: prenylation of hydroxynaphthalenes by fungal indole prenyltransferases (published)	Yu, X., Xie, X. & Li, S.-M.	72
Prenylation of flavonoids by using a dimethylallyltryptophan synthase 7-DMATS from *Aspergillus fumigatus* (published)	Yu, X., Li, S.-M.	75
Prenyltransferases of the dimethylallyltryptophan synthase superfamily (published review)	Yu, X., Li, S.-M.	75

…… **……**

Kandidatin **Unterschrift Betreuer**

Abbreviations

2D	two-dimensional
4-DMATS	4-dimethylallyltryptophan synthase
A. clavatus	*Aspergillus clavatus*
A. flavus	*Aspergillus flavus*
A. fumigatus	*Aspergillus fumigatus*
A. nidulans	*Aspergillus nidulans*
Ar	aromatic ring
A. terreus	*Aspergillus terreus*
A. versicolor	*Aspergillus versicolor*
BAC	bacterial artificial chromosome
BLAST	basic local alignment search tool
bp	base pair
cDNA	complementary DNA
Da	dalton
dd	double doublet
DMA	dimethylallyl
DMAPP	dimethylallyl diphosphate
DMATS	dimethylallyltryptophan synthase
DMSO	dimethyl sulfoxide
DNA	deoxyribonucleic acid
E. coli	*Escherichia coli*
EDTA	ethylenediamine tetraacetic acid
EI	electron ionization
ESI	electrospray ionization
FPLC	fast protein liquid chromatography
FPP	farnesyl diphosphate
gDNA	genomic DNA
GPP	geranyl diphosphate
HAS	hexadehydroastechrome
His_6	hexahistidine
HPLC	high performance liquid chromatography
HMBC	heteronuclear multiple-bond correlation

HR	high-resolution
HSQC	heteronuclear single-quantum correlation
Hz	hertz
IPTG	isopropyl β-thiogalactopyranoside
k_{cat}	turnover number
kb	kilo base pairs
K_M	Michaelis-Menten constant
LB	Luria-Bertani
L. maculans	*Leptosphaeria maculans*
m	multiplet
ml	milliliter
m/z	mass-to-charge ratio
mRNA	messenger RNA
MS	mass spectrometry
N. fischeri	*Neosartorya fischeri*
Ni-NTA	nickel-nitrilotriacetic acid
NMR	nuclear magnetic resonance
NOESY	nuclear overhauser effect spectroscopy
NRPS	nonribosomal peptide synthetase
OD_{600}	optical density at 600 nm
PCR	polymerase chain reaction
PPi	pyrophosphate
ppm	parts per million
RNA	ribonucleic acid
RP	reverse phase
rpm	revolutions per minute
s	singlet
SAM	*S*-adenosyl methionine
S. cerevisiae	*Saccharomyces cerevisiae*
SCU	synthetic medium devoid of uracil
SDS	sodium dodecyl sulfate
SDS-PAGE	sodium dodecyl sulfate polyacrylamide gel electrophoresis
t	triplet
TB	Terrific-Broth
TFA	trifluoroacetic acid
UV	ultraviolet
v/v	volume per volume

w/v	weight per volume
× g	gravitational acceleration

Summary

Prenylated indole alkaloids are widely distributed in plants, fungi and bacteria, especially in the family of Clavicipitaceae and Trichocomaceae of Ascomycota, and commonly exhibit interesting biological and pharmaceutical activities. In the biosynthetic pathway of prenylated indole alkaloids, prenylation catalyzed by prenyltransferases contributes significantly to the large structure diversity of these compounds in nature. Investigation on indole prenyltransferases would help to understand the construction of prenylated indole alkaloids in nature and also be useful for structural modification of indole derivatives and other substances to produce analogues of prenylated derivatives.

Three indole prenyltransferases belonging to the dimethylallyltryptophan synthase (DMATS) superfamily were biochemically identified and characterized in *vitro*, including CdpC3PT from *Neosartorya fischeri* (*N. fischeri*), BrePT from *Aspergillus versicolor* (*A. versicolor*) and 5-DMATS from *Aspergillus clavatus* (*A. clavatus*). The responsible genes *cdpC3PT* and *brePT* were cloned into expression vector and heterologously expressed in *Escherichia coli* (*E. coli*). These works were carried out by Dr. Wen-Bing Yin, Suqin Yin and Qing Wang, respectively. In this thesis, CdpC3PT was confirmed to catalyze the formation of C3-prenylated products with a characteristic 6/5/5/6-fused tetracyclic ring system from tryptophan-containing cyclic dipeptides in one-step reaction. The NotF homologue BrePT showed much higher flexibility towards its aromatic substrates than NotF, and was proven to catalyze the highly regiospecific reverse prenylation at C-2 of the indole nucleus. The cloning of *5-dmats* was carried out by Yan Liu. Functional proof of this gene was provided within this thesis by heterologous expression in *E. coli* and subsequent structure elucidation of enzyme products by mass spectrometry (MS) and nuclear magnetic resonance (NMR) analyses. 5-DMATS established high regiospecific activity to catalyze C5-prenylation on indole derivatives.

Given the importance of prenylation in structure diversity and bioactivity enhancement, CdpC3PT, BrePT, 5-DMATS and other known prenyltransferases of the DMATS superfamily were applied for the chemoenzymatic synthesis of prenylated compounds. By using AnaPT, CdpC3PT and CdpNPT, eight and six stereoisomers of *cis*-configured prenylated pyrroloindoline diketopiperazines from cyclo-Trp-Ala and cyclo-Trp-Pro isomers were produced, respectively. The stereospecificity of AnaPT and CdpC3PT depended mainly on the configuration of tryptophanyl moiety in cyclo-Trp-Ala and cyclo-Trp-Pro isomers, while CdpNPT showed lower stereoselectivity, but higher conversion ability towards most tested substrates.

5-DMATS and FgaPT2 from *Aspergillus* were used for chemoenzymatic synthesis of prenylated indolocarbazoles. Reconstitution of enzyme activity of 5-DMATS and FgaPT2 in

vitro revealed that they catalyzed regiospecific prenylation of indolocarbazoles at the *para*-position of the indole N-atom. This is the first report for prenylated indolocarbazoles. Subsequently, some indole prenyltransferases of the DMATS superfamily were found to accept also hydroxynaphthalenes and flavonoids, which were substrates for enzymes from the CloQ/NphB group and the UbiA superfamily, respectively. Nine prenylated flavonoids and twenty prenylated hydroxynaphthalenes have been isolated, and their structures were elucidated by MS and NMR analyses. It has been shown that, for an accepted hydroxynaphthalene, different enzymes produced usually the same major prenylated product, *i.e.* with a regular C-prenyl moiety at *para*- or *ortho*-position to a hydroxyl group. For flavonoids accepted by 7-DMATS, C-6 between two hydroxyl groups was the favorable prenylation position. The Michaelis-Menten constants (K_M) and turnover numbers (k_{cat}) of some prenyltransferases towards selected hydroxynaphthalenes are comparable to those obtained by using indole derivatives.

In addition to indole prenyltransferases, other genes in the biosynthetic cluster of prenylated indole alkaloids were also investigated. A putative O-methyltransferase gene *hasC* and a putative cytochrome P450 gene *hasH* involved in the biosynthesis of hexadehydroastechrome (HAS) in *Aspergillus fumigatus* (*A. fumigatus*) were cloned into pQE60 and pESC-URA, respectively. Soluble His_6-HasC was successfully overproduced in *E. coli* SG13009 and purified to near homogeneity by Ni-NTA. Constructs for co-expression with the reductase gene *NFIA_083630* from *N. fischeri* in pESC-URA and for expression as His_6-tagged protein in pESC-URA were also prepared for the putative cytochrome P450 gene *hasH*.

Zusammenfassung

Prenylierte Indolalkaloide sind ubiquitär in Pflanzen, Bakterien und Pilzen verbreitet, vor allem in den Familien Clavicipitaceae und Trichocomaceae der Ascomyceten. Gemeinsam weisen sie interessante biologische und pharmazeutische Aktivitäten auf. Bei der Biosynthese von Indolalkaloiden ist die Prenylierung durch Prenyltransferasen maßgeblich für die hohe Strukturvielfalt dieser Substanzen in der Natur verantwortlich. Biochemische Untersuchungen zu Indolprenyltransferasen können helfen, die Entstehung von prenylierten Indolalkaloiden in der Natur zu verstehen. Außerdem können Indolderivate und anderen Substanzen durch Prenyltransferasen modifiziert werden.

Drei Indolprenyltransferasen der Dimethylallyltryptophan Synthase (DMATS) Superfamilie wurden biochemisch identifiziert und *in vitro* charakterisiert, diese beinhalteten CdpC3PT aus *Neosartorya fischeri* (*N. fischeri*), BrePT aus *Aspergillus versicolor* (*A. versicolor*) und 5-DMATS aus *Aspergillus clavatus* (*A. clavatus*). Die verantwortlichen Gene *cdpC3PT* und *brePT* wurden jeweils in einen Expressionsvektor kloniert und heterolog in *Escherichia coli* (*E. coli*) exprimiert. Diese Arbeiten wurden von Dr. Wen-Bing Yin, Suqin Yin und Qing Wang durchgeführt. In der vorliegenden Arbeit wurde herausgefunden, dass CdpC3PT die Entstehung von C3-prenylierten Produkten mit einem charakteristischen 6/5/5/6-tetrazyklischen Ringsystem aus tryptophan-haltigen zyklischen Dipeptiden in einem Reaktionsschritt katalysiert. Das NotF-Homolog BrePT zeigte eine sehr viel höhere Flexibilität gegenüber seinen aromatischen Substraten im Vergleich zu NotF. Dabei konnte eine hohe Regiospezifität einer reversen Prenylierung an Position C-2 des Indolrings nachgewiesen werden. Bei der Charakterisierung von 5-DMATS wurde die Klonierung von Yan Liu durchgeführt. Im weiteren Verlauf dieser Arbeit erfolgte meinerseits die Aufklärung der Genfunktion durch heterologe Expression in *E. coli* und die anschließende Strukturaufklärung der Enzymprodukte mit Hilfe von Massenspektrometrie (MS) und Kernresonanzspektroskopie (NMR). 5-DMATS katalysiert eine regiospezifische Prenylierung von Indolderivaten an Position C-5.

Aufgrund der enormen Bedeutung der Prenylierung an der Strukturvielfalt und damit der biologischen Aktivität, wurden CdpC3PT, BrePT, 5-DMATS und andere bekannte Prenyltransferasen der DMATS-Superfamile zur chemoenzymatischen Synthese von prenylierten Substanzen verwendet. Durch Einsatz von AnaPT, CdpC3PT und CdpNPT, konnten jeweils acht und sechs Stereoisomere von *cis*-konfigurierten prenylierten Pyrroloindolin-Diketopiperazinen von cyclo-Trp-Ala und cyclo-Trp-Pro Isomeren produziert werden. Die Stereospezifität von AnaPT und CdpC3PT hängt dabei hauptsächlich von der Konfiguration der Tryptophaneinheit in cyclo-Trp-Ala und cyclo-Trp-Pro Isomeren ab. Im

Vergleich dazu, zeigte CdpNPT eine geringere Stereoselektivität, aber eine höhere Umsetzungsrate gegenüber den getesteten Substraten.

Weiterführend wurden 5-DMATS und FgaPT2 für die chemoenzymatische Synthese von prenylierten Indolcarbazolen eingesetzt. Die Rekonstruktion der Enzymaktivität von 5-DMATS und FgaPT2 *in vitro* zeigte, dass sie in der Lage sind, die regiospezifische Prenylierung von Indolcarbazolen an der *para*-Position des N-Atoms zu katalysieren. Dies ist der erste Bericht über derartige prenylierte Indolcarbazole. Desweiteren konnte auch die Akzeptanz einiger Hydroxynaphthalene und Flavonoide durch Indolprenyltransferasen der DMATS Superfamilie nachgewiesen werden, wobei diese eigentlich Substrate der Enzyme der CloQ/NphB-Gruppe, oder der UbiA-Superfamilie darstellen. Neun prenylierte Flavonoide und zwanzig prenylierte Hydroxynaphthalene wurden isoliert und deren Strukturen anschließend durch MS- und NMR-Analysen aufgeklärt. Dabei konnte festgestellt werden, dass für ein akzeptiertes Hydroxynaphthalen, unterschiedliche Enzyme das gleiche prenylierte Hauptprodukt produzieren, natürlich mit einer regulären C-Prenylierung an *para*- oder *ortho*-Position zu einer Hydroxygruppe. Bei Flavonoiden, welche von 7-DMATS akzeptiert wurden, war Position C-6 zwischen zwei Hydroxygruppen die bevorzugte Prenylierungsstelle. Die erhaltenen Michaelis-Menten Konstanten (K_M) und die Wechselzahlen (k_{cat}) einiger Prenyltransferasen für ausgewählte Hydroxynaphthalene waren vergleichbar mit denen von Indolderivaten.

Ergänzend zu Prenyltransferasen wurden noch weitere Gene aus einem putativen Biosynthesecluster für ein prenyliertes Indolalkaloid, das Hexadehydroastechrom (HAS) untersucht. Ein putatives O-Methyltransferasegen *hasC* und ein putatives Cytochrome P450-Gen *hasH*, welche in dessen Biosynthese in *Aspergillus fumigatus* (*A. fumigatus*) involviert sind. Sie wurden jeweils in die Expressionsvektoren pQE60 und pESC-URA kloniert. Das lösliche His_6-HasC wurde erfolgreich in *E.coli* SG13009 überexprimiert und über Ni-NTA aufgereinigt. Konstrukte für die Co-Expression mit dem Reduktasegen NFIA_083630 aus *N. fischeri* in pESC-URA und für die Expression als His_6-getaggtes Protein in pESC-URA wurden auch für das putative Cytochrome P450-Gen *hasH* angefertigt.

1 Introduction

1.1 Prenylated aromatic compounds

Prenylated aromatic compounds are hybrid natural products containing an aromatic scaffold and one or more prenyl moieties derived from prenyl diphosphates. These compounds are widely distributed in nature and often possess impressive better biological activities than their non-prenylated precursors (Li, 2010; Botta *et al.*, 2005b; Schardl *et al.*, 2006; El-Seedi *et al.*, 2010; Sunassee and Davies-Coleman, 2012). Considering the various types of precursors, the prenylated aromatic compounds represent a broad range of structural diversity, such as prenylated indole alkaloids, flavonoids, xanthones, naphthalenes and quinones. According to the connection patterns of the prenyl moiety to the aromatic ring, these compounds can be classified into two types, *i.e.* “regularly” and “reversely” prenylated derivatives. The prenyl moiety is substituted to the aromatic ring *via* C-1' in a regularly prenylated derivative, while reverse prenylation represents the bridge between C-3' of the prenyl moiety and the aromatic ring (Figure 1-1).

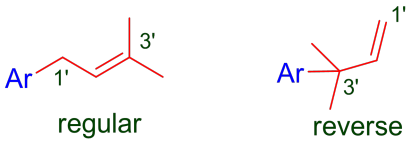

Figure 1-1: Regular and reverse prenyl moieties. Ar: aromatic ring.

1.1.1 Prenylated indole alkaloids

Prenylated indole alkaloids represent a group of compounds with diverse chemical structures and are widely distributed in nature, especially in the family of Clavicipitaceae and Trichocomaceae of Ascomycota (Li, 2010; Ruiz-Sanchis *et al.*, 2011). Due to their impressive pharmacological and biological activities as drugs or toxins (Li, 2010; Wallwey and Li, 2011), prenylated indole alkaloids attract attention of scientists from different scientific disciplines including chemistry, ecology, biology, pharmacology and biochemistry (Lindel *et al.*, 2012; Williams *et al.*, 2000; Li, 2010; Schardl *et al.*, 2006; Uhlig *et al.*, 2009). This thesis deals with enzymes for C2-, C3- and C5-prenylation of indole alkaloids. Therefore more details on C2-, C3- and C5-prenylated indole alkaloids are described below.

1.1.1.1 C2-prenylated indole alkaloids

Prenylated indole alkaloids in this group carry one prenyl moiety at position C-2 on the indole ring (Figure 1-2). A series of C2-prenylated cyclic dipeptides were isolated. For example, echinulin (**1**) with antitubercular activity was isolated from several *Aspergillus* strains and

other sources (Stipanovic and Schroeder, 1976; Wang *et al.*, 2007a; Kanokmedhakul *et al.*, 2002). The anticancer agent tryprostatin A (**2**) from *A. fumigatus* is the methoxylated derivative of regularly C2-prenylated cyclo-L-Trp-L-Pro (Cui *et al.*, 1996; Wang *et al.*, 2008; Cui *et al.*, 1995; Jain *et al.*, 2008; Zhao *et al.*, 2002). Cyclo-L-Trp-L-Trp is the precursor of fellutanine B (**3**) from *Penicillium fellutanum* (Kozlovsky *et al.*, 2000; Kozlovsky *et al.*, 2001). Another example is variecolortide B (**4**) from *Aspergillus variecolor*, which contains an additional anthraquinone molecule (Wang *et al.*, 2007b).

In addition to C2-prenylated cyclic dipeptides, derivatives of other indole alkaloids were also reported. Ergot alkaloid (8S,9S)-fumigaclavine C (**5**) with a reverse prenyl moiety at C-2 of the indole ring was identified in *A. fumigatus* (Ge *et al.*, 2009). The prenylated bisindolyl benzoquinone asterriquinone CT5 (**6**) from *A. terreus* bears a regular prenyl moiety at position C-2 on both indole rings (Mocek *et al.*, 1996; Kaji *et al.*, 1994).

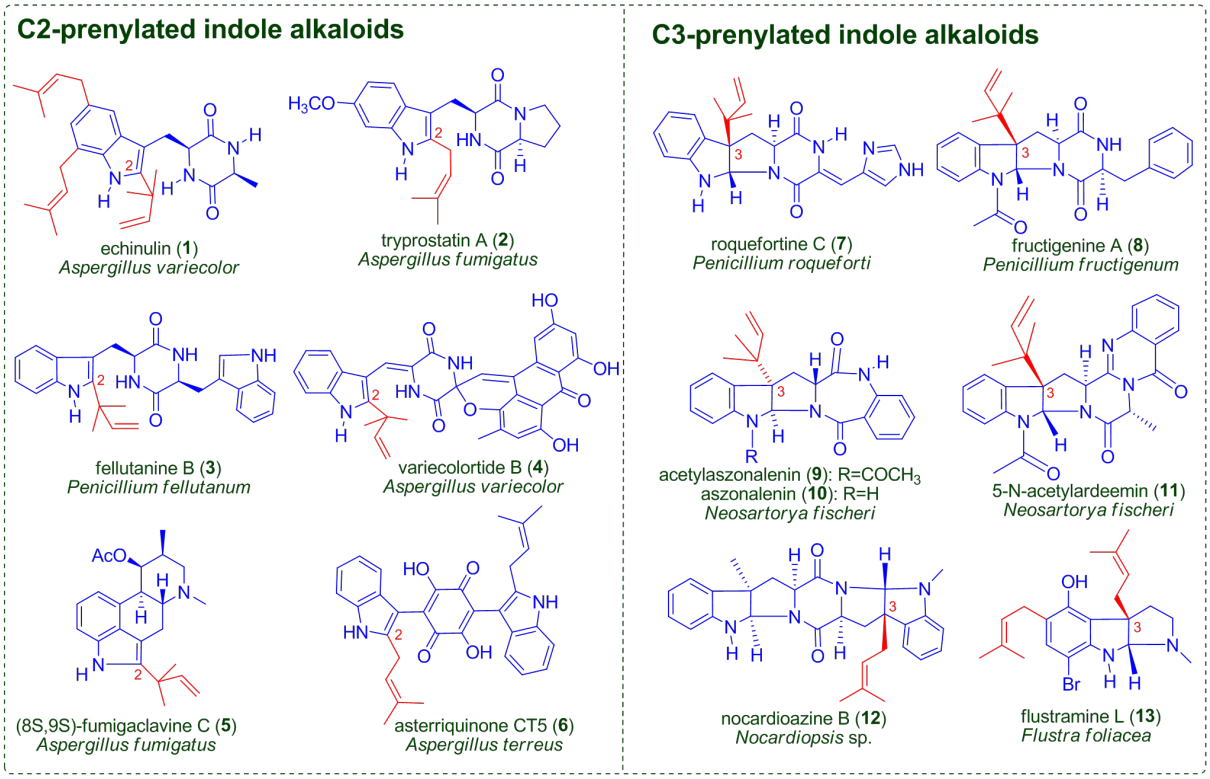

Figure 1-2: Examples of C2- and C3-prenylated indole alkaloids.

1.1.1.2 C3-prenylated indole alkaloids

C3-prenylated indole alkaloids represent a characteristic fused multicyclic ring system with the prenyl moiety at the position C-3 on the indoline ring (Figure 1-2). Most of these compounds are reversely C3-prenylated derivatives of cyclic dipeptides. For example, roquefortine C (**7**) identified in *Penicillium* strains is a cyclic dipeptide derivative of tryptophan and histidine (Ohmomo *et al.*, 1977; O'Brien *et al.*, 2006). Another example is fructigenine A (**8**) from *Penicillium fructigenum* (Arai *et al.,* 1989). This compound is a derivative of cyclo-L-

Trp-L-Phe and was reported to be a plant growing inhibitor (Arai *et al.,* 1989). The mycotoxin acetylaszonalenin (**9**) and its non-acetylated form aszonalenin (**10**) were identified in various fungal strains, *e.g. N. fischeri* (Wakana *et al.*, 2006; Yin *et al.*, 2009; Ellestad *et al.*, 1973). Their stereoisomers *epi*-aszonalenins A and C were isolated from *Aspergillus novofumigatus* (Rank *et al.,* 2006). These four compounds are derived from the amino acids tryptophan and anthranilic acid. The cytotoxic compound 5-N-acetylardeemin (**11**) identified in *N. fischeri* represents a cyclo-Trp-Ala derivative connected with an anthranilic acid moiety (Hochlowski *et al.*, 1993; Ge *et al.*, 2010).

A detailed database search showed that only one regularly C3-prenylated cyclic dipeptide nocardioazine B (**12**) was found in nature. Nocardioazine B (**12**) from *Nocardiopsis* sp. is derived from cyclo-L-Trp-L-Trp (Raju *et al.*, 2011). Besides prenylated derivatives of cyclic dipeptides, a series of C3-prenylated simple indole derivatives with the C3-regular or reverse prenyl moieties were isolated from the bryozoan *Flustra foliacea* (Peters *et al.*, 2002; Peters *et al.*, 2003; Rochfort *et al.*, 2009). One example is flustramine L (**13**) with regular prenyl moieties at positions C-3 and C-5 (Rochfort *et al*., 2009). Antimicrobial activity was reported for this compound (Rochfort *et al*., 2009).

1.1.1.3 C5-prenylated indole alkaloids

A number of biologically active indole alkaloids carrying a regular prenyl moiety at position C-5 were discovered (Figure 1-3). The regularly C5-prenylated bisindolyl benzoquinones were derived from two tryptophan molecules like semicochliodinol A (**14**) from the fungus *Chrysosporium merdarium* (Fredenhagen *et al.*, 1997) and petromurin B (**15**) from the fungus *Petromyces muricatus* (Ooike *et al.*, 1997). Semicochliodinol A (**14**) was reported to inhibit HIV-1 protease (Fredenhagen *et al*., 1997). Regularly C5-prenylated derivatives were also found for tryptophan-containing cyclic dipeptides like cyclo-L-Trp-L-Ala, *e.g.* echinulin (**1**) from *Aspergillus* strains or tardioxopiperazine A (**16**) from the fungus *Microascus tardifaciens* (Fujimoto *et al.*, 1999). Immunosuppressive activity has been observed with tardioxopiperazine A (**16**) (Fujimoto *et al.*, 1999). Another type of C5-prenylated indole alkaloids are derived from indole diterpenes. These compounds carry one prenyl moiety at C-5, *e.g.* 21-isopentenylpaxilline (**17**) from *Eupenicillium shearii* (Belofsky *et al.*, 1995), or more prenyl moieties, *e.g.* shearinine K (**18**) from *Penicillium* sp. (Xu *et al*., 2007). 21-isopentenylpaxilline showed antiinsectant activity in a previous report (Belofsky *et al.*, 1995). Only a few reversely C5-prenylated indole alkaloids have been found in nature, such as lansai B (**19**) from *Streptomyces* sp. (Tuntiwachwuttikul *et al.*, 2008).

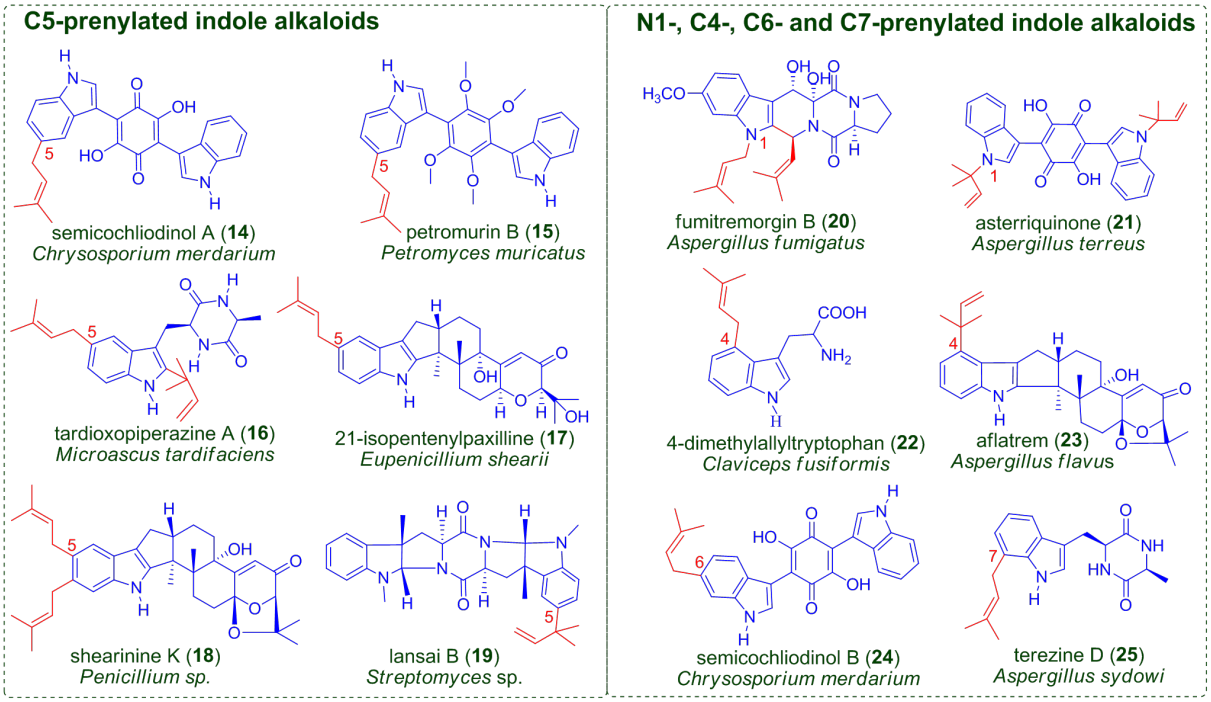

Figure 1-3: Examples of C5-, N1-, C4-, C6- and C7-prenylated indole alkaloids.

1.1.1.4 Other prenylated indole alkaloids

Besides positions C-2, C-3 and C-5, the prenyl moiety can be connected to positions N-1, C-4, C-6 and C-7 on the indole ring in nature (Figure 1-3). N1-prenylated indole alkaloids were found in various fungi. The mycotoxin fumitremorgin B (**20**) identified in a number of *Aspergillus* and *Penicillium* strains bears two prenyl moieties at positions N-1 and C-2 of the indole ring (Yamazaki *et al.*, 1974; Yamazaki and Suzuki, 1986; Gallagher and Latch, 1977; Sabater-Vilar *et al.*, 2003). Asterriquinone (**21**) isolated from *A. terreus* contains one reverse prenyl moiety at the position N-1 on each tryptophanyl moiety (Yamamoto *et al.,* 1976b). This compound showed inhibitory activity against tumour cells (Yamamoto *et al.,* 1976a). Another example of N1-prenylated benzoquinone is isoasterriquinone from *A. terreus,* which contains reversely N1-prenylated and regularly C2-prenylated tryptophanyl moieties (Kaji *et al.,* 1994). 4-dimethylallyltryptophan (**22**) firstly isolated from *Claviceps fusiformis* (Barrow and Quigley, 1975) is the precursor of ergot alkaloids in many strains (Wallwey and Li, 2011). A further example of C4-prenylated indole alkaloids is the tremorgenic mycotoxin aflatrem (**23**) from *Aspergillus flavus* (*A. flavus*) (Cole *et al.*, 1981; Gallagher and Wilson, 1978), which is a monoprenylated derivative of the indole diterpene. The potent antiflea agent nodulisporic acid E containing two prenyl moieties at both positions C-5 and C-6 of the indole diterpene scaffold was isolated from *Nodulisporium* sp. mutant MF6227 (ATCC74473) (Singh *et al.*, 2004). Semicochliodinol B (**24**) from *Chrysosporium merdarium* (Fredenhagen *et al.,* 1997) and isocochliodinol from *Chaetomium* sp. (Sekita, 1983) are prenylated bisindolyl benzoquinone with prenyl moieties substituted at position C-6 on one and both indole rings,

respectively. Semicochliodinol B (**24**) exhibits inhibitory activity against HIV-1 protease (Fredenhagen *et al*., 1997). Terezine D (**25**) from fungi *Sporormiella teretispora* and *Aspergillus sydowi* is a C7-prenylated derivative of cyclo-L-Trp-L-Ala (Wang *et al.*, 1995; Zhang *et al.*, 2008), which is very likely the precursor of the tryptophan-derived iron(III)-complex HAS (see section 1.2.1.3) (Yin *et al.*, 2013b).

1.1.2 Prenylated flavonoids

Prenylated flavonoids are a group of compounds consisting of one or more prenyl moieties on the flavonoid nucleus (C6-C3-C6). They are mainly distributed in the plant kingdom, especially in the family Leguminosae and Moraceae (Botta *et al*., 2005b; Botta *et al.*, 2009; Tahara, 2007; Barron and Ibrahim, 1996). These compounds are well known for their numerous pharmacological effects (Botta *et al*., 2005b; Botta *et al*., 2009). According to their chemical structures, they can be classified into prenylated flavones, flavonols, flavanones, flavanonols, isoflavones, isoflavanones, isoflavans, chalcones and so on. An example of prenylated flavones is kuwanon C (**26**) isolated from various species of the genera *Morus* and *Artocarpus* (Cho *et al.*, 2011; Yang *et al.*, 2011; Arung *et al.*, 2006; Ko *et al.*, 1997). Inhibitory activities against β-secretase, melanin biosynthesis and nitric oxide production were reported for kuwanon C (**26**) (Cho *et al*., 2011; Yang *et al*., 2011; Arung *et al*., 2006). The diprenylated isoflavanone papyriflavonol A (**27**) was isolated from *Broussonetia papyrifera* and *Broussonetia kazinoki* and showed inhibitory activities against 5-LOX, 12-LOX and α-glucosidase (Zhang *et al.*, 2001; Ryu *et al.*, 2010; Chi *et al.*, 2001). The prenylated flavanone 8-prenylnaringenin (**28**) was purified from diverse plants, *e.g. Azadirachta indica* and *Macaranga conifera* (Nakahara *et al.*, 2003; Jang *et al.*, 2002; Lukaseder *et al.*, 2009; Akazawa *et al.*, 2012; Sasaki *et al.*, 2012; Versiani *et al.*, 2011). This compound exhibits ABCG2 inhibitory, estrogenic, antibacterial and antitumor activities (Akazawa *et al*., 2012; Sasaki *et al*., 2012; Versiani *et al*., 2011; Overk *et al.*, 2005).

Wighteone (**29**) is the prenylated derivative of the isoflavone genistein and has been isolated from many plants, especially from the species of the genus *Erythrina* (Morikawa *et al.*, 2006; Wang *et al.*, 2005; Erasto *et al.*, 2004; Bankeu *et al.*, 2011; Tanaka *et al.*, 2001; El-Masry *et al.*, 2002; Djiogue *et al.*, 2009). Broad biological activities, including antifungal, antibacterial, nitric oxide production inhibitory and β-glucuronidase inhibitory activities, were observed for wighteone (**29**) (Morikawa *et al*., 2006; Wang *et al*., 2005; Erasto *et al*., 2004; Bankeu *et al*., 2011). The prenylated isoflavan (3S)-(+)-7-methoxymanuifolin K (**30**) was found in the plant *Dalea aurea* and exhibits antiprotozoal activity (Belofsky *et al.*, 2006). Xanthohumol (**31**) is the main prenylated flavonoid of hops and represents a wide range of biological activities, especially well known for the potential cancer chemopreventive activity (Gerhauser *et al.*, 2002; Stevens and Page, 2004; Albini *et al.*, 2006). The distribution, chemistry and biological

activities of xanthohumol (**31**) were reviewed (Stevens and Page, 2004; Magalhaes *et al.*, 2009; Gerhauser, 2005).

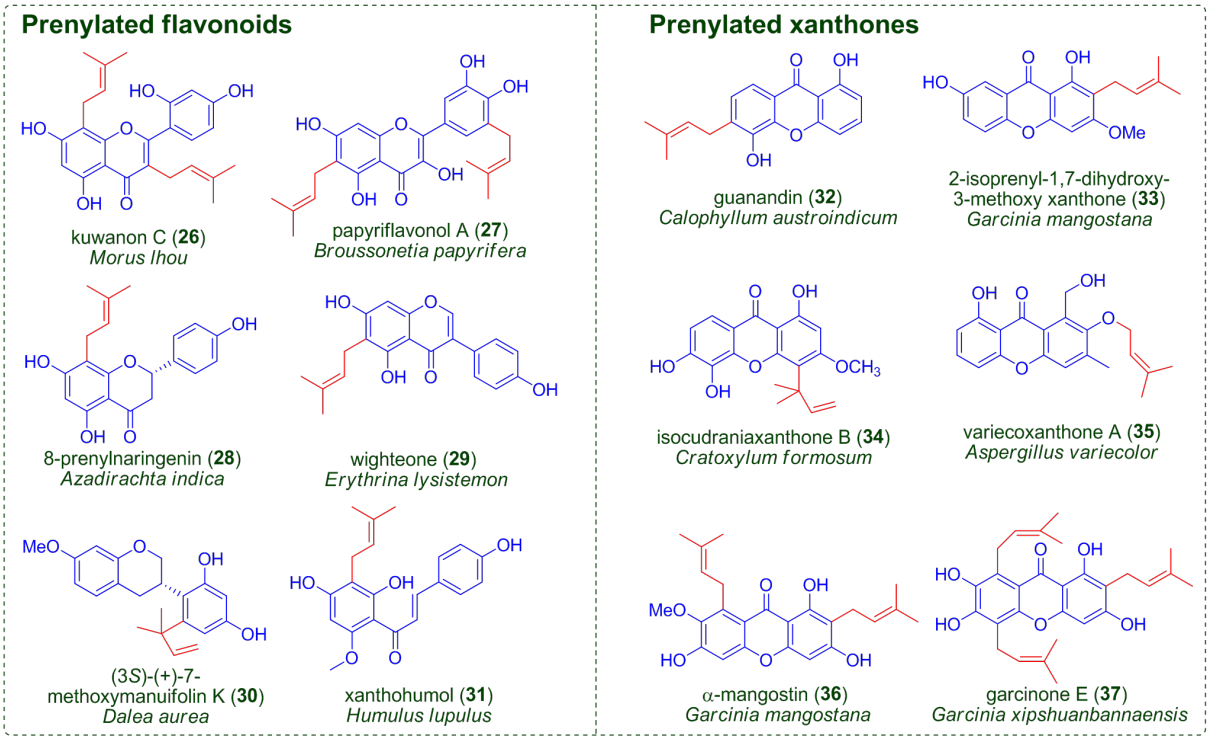

Figure 1-4: Examples of prenylated flavonoids and xanthones.

1.1.3 Prenylated xanthones

Xanthones are a group of secondary metabolites found in higher plants, fungi and lichens (El-Seedi *et al.*, 2009; Vieira and Kijjoa, 2005). The key structure feature of these compounds is the 9*H*-xanthen-9-one nucleus (Figure 1-4). Prenylated xanthones are emerged as an important subgroup of naturally occurring xanthones and exhibit interesting biological and pharmaceutical activities (El-Seedi *et al.*, 2010; Pinto *et al.*, 2005). Xanthone derivatives with prenyl moieties at diverse positions were reported. In most cases, regular prenyl moieties were found in prenylated xanthones, for example, the antihypotensive agent guanandin (**32**). The compound found in various species of the plant genus *Calophyllum* is a dioxygenated xanthone carrying a regular prenyl moiety at the *para*-position to the carbonyl moiety in the structure (Iinuma *et al.*, 1996; Gunasekera *et al.*, 1977; Oku *et al.*, 2005). Another example of C-prenylated xanthone is 2-isoprenyl-1,7-dihydroxy-3-methoxy xanthone (**33**). This compound was isolated from various species of the plant genus *Garcinia* (Huang *et al.*, 2001; Deachathai *et al.*, 2005; Rukachaisirikul *et al.*, 2003) and showed inhibitory effect towards human leukemia HL60 cells (Matsumoto *et al.*, 2003). Isocudraniaxanthone B (**34**) isolated from the plants *Cratoxylum formosum* and *Cudrania tricuspidata* is a reversely prenylated tetraoxygenated xanthone derivative (Park *et al.*, 2006; Boonnak *et al.*, 2006; Lee *et al.*,

2005). Park *et al*. reported significant antioxidant activity of isocudraniaxanthone B (**34**) (Park *et al*., 2006).

Besides C-prenylated xanthones, O-prenylated derivatives were also reported, *e.g.* variecoxanthone A (**35**) from fungi *A. nidulans* and *A. variecolor* (Scherlach and Hertweck, 2006; Chexal *et al.*, 1975). In addition, several prenylated xanthones with more than one prenyl moieties were found in nature, such as the diprenylated xanthone α-mangostin (**36**) and triprenylated xanthone garcinone E (**37**). The compound α-mangostin (**36**) isolated from the plant genera *Garcinia*, *Cratoxylum* and *Pentadesma* (Ren *et al.*, 2011; Lenta *et al.*, 2011a; Ryu *et al.*, 2011; Kikuchi *et al.*, 2010) carries one regular prenyl moiety on each aromatic ring and was reported to have broad biological activities, such as inhibiting and dissociating the Aβ aggregation, which indicated that α-mangostin is a potential candidate for treatment of Alzheimer's disease, as well as significant anti-inflammatory activity (Wang *et al.*, 2012; Chen *et al.*, 2008). Garcinone E (**37**) isolated from various species of the plant genus *Garcinia* as well as the species *Pentadesma butyracea* (Na and Xu, 2010; Jung *et al.*, 2006; Lenta *et al.*, 2011b) also exhibits a wide range of biological activities, *e.g.* antiproliferative and antiplasmodial activities (Han *et al.*, 2008; Lenta *et al*., 2011b; Ho *et al.*, 2002).

1.1.4 Prenylated naphthalenes and quinones

In comparison to the large number of prenylated indole alkaloids, flavonoids and xanthones, database search showed that the number of natural occurring prenylated naphthalenes is limited. Known prenylated naphthalenes with intact prenyl moieties were mostly isolated from plants (Hussein *et al.*, 2004; Monache *et al.*, 1985; Hussein *et al.*, 2003). Vismione E (**38**) and adenaflorin C (**39**) are two examples of prenylated naphthalenes. Vismione E (**38**) containing one prenyl moiety at the aromatic ring was isolated from *Cratoxylum cochinchinense*, *Cratoxylum formosum* and *Psorospermum febrifugum* (Boonnak *et al.*, 2007; Botta *et al.*, 1983; Laphookhieo *et al.*, 2009). Vismione E (**38**) has antimalarial and antibacterial activities (Boonnak *et al*., 2007; Laphookhieo *et al*., 2009). Adenaflorin C (**39**) from *Adenaria floribunda* exhibits moderate cytotoxic activity (Hussein *et al*., 2004).

Prenylated quinones are widely distributed in plants, microorganisms as well as animals and have broad biological activities (Sunassee and Davies-Coleman, 2012). For example, the bis-prenylated quinone (**40**) isolated from the brown algae *Perithalia capillaris* and *Sporochnus comosus* represents anti-inflammatory and antiproliferative properties (Sansom *et al.*, 2007; Ovenden *et al.*, 2011). The naphthoquinone lapachol (**41**) containing one prenyl moiety on the quinone ring has been found from dozens of plants. A wide range of pharmacological activities were reported for lapachol (**41**), *e.g*. anticancer, anti-inflammatory and antiviral activities. The occurrence, biological activities, synthesis and biosynthesis of lapachol (**41**) has been reviewed (Hussain *et al.*, 2007; Epifano *et al.*, 2013). Another

example is the prenylated anthraquinone 1-methyl-2-(3'-methyl-but-2'-enyloxy)-anthraquinone (**42**). This compound was isolated from the plant *Aegle marmelos* and showed antifungal activity (Mishra *et al.*, 2010a; Mishra *et al.*, 2010b). The antioxidative agent naphterpin (**43**) derived from a hybrid structure containing a naphthoquinone unit and a geranyl side chain has been isolated from the bacteria *Streptomyces aeriouvifer* and *Streptomyces* sp. (Shin-Ya *et al.*, 1990b; Seto *et al.*, 1996). 1,3,6,8-tertrahydroxynaphthalene is the precursor for the biosynthesis of naphterpin (**43**) in *Streptomyces* (Shin-Ya *et al.*, 1990a).

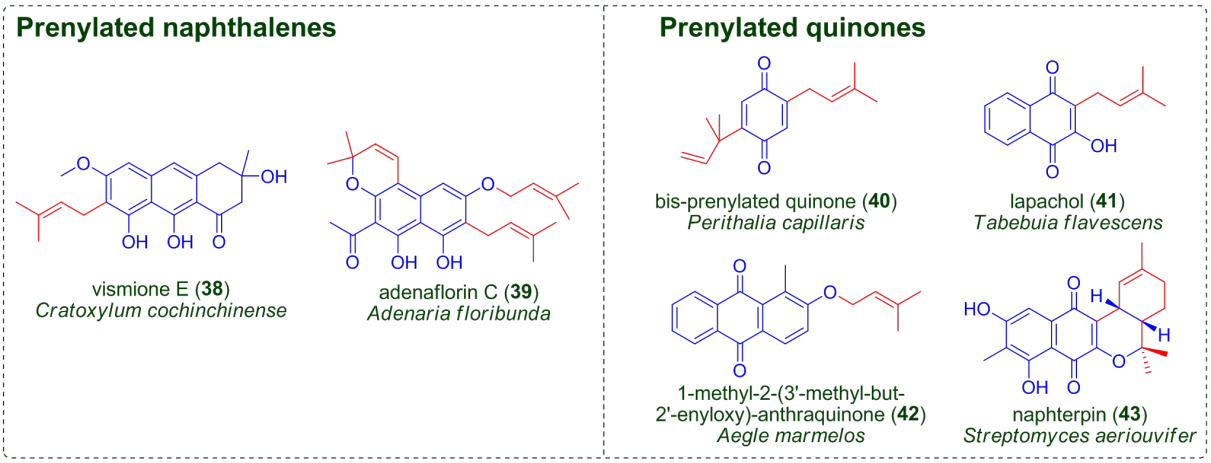

Figure 1-5: Examples of prenylated naphthalenes and quinones.

1.2 Biosynthetic pathways of prenylated indole alkaloids in *Aspergillus*

Recently, significant progress has been achieved in the discovery of gene clusters responsible for the biosynthesis of prenylated indole alkaloids in *Aspergillus*. Several biosynthetic genes were identified by feeding experiments, gene deletion experiments and biochemical characterization *in vitro*. Gene clusters related to enzymes used in this thesis are described below.

1.2.1 Biosynthetic pathways of prenylated indole alkaloids derived from cyclic dipeptides

1.2.1.1 The biosynthesis of fumitremorgins/verruculogen

In *A. fumigatus*, a gene cluster for the biosynthesis of fumitremorgins/verruculogen was identified. The end product of this cluster is verruculogen (Steffan *et al.*, 2009b), while three tryprostatins together with three fumitremorgins are synthesized as intermediates (Figure 1-

6). The biosynthesis of these compounds starts with the formation of brevianamide F from L-tryptophan and L-proline by the nonribosomal peptide synthetase (NRPS) FtmPS, followed by a prenylation reaction catalyzed by FtmPT1 to produce tryprostatin B (Maiya *et al.*, 2006; Grundmann and Li, 2005). The genes *ftmPT1* and *ftmPS* were overexpressed in *E. coli* and *Aspergillus*, respectively. The cytochrome P450 enzyme FtmP450-1 and the putative methyltransferase FtmMT catalyze the addition of small functional groups, *i.e.* hydroxyl and methyl groups, resulting in the formation of tryprostatin A (Kato *et al.*, 2009). The second cytochrome P450 enzyme FtmP450-2 is responsible for cyclization of tryprostatin A, and next the hydroxylation is catalyzed by the third cytochrome P450 enzyme FtmP450-3 consequently for the production of 12,13-dihydroxyfumitremorgin C (Kato *et al.*, 2009). The identification of three cytochrome P450 genes was carried out by gene disruption (Kato *et al.*, 2009). The second prenyltransferase FtmPT2 was proven to catalyze the conversion of 12,13-dihydroxyfumitremorgin C to fumitremorgin B (Grundmann *et al.,* 2008). The non-heme Fe(II) α-ketoglutarate-dependent dioxygenase FtmOx1 catalyzes the formation of verruculogen from fumitremorgin B (Steffan *et al.,* 2009b).

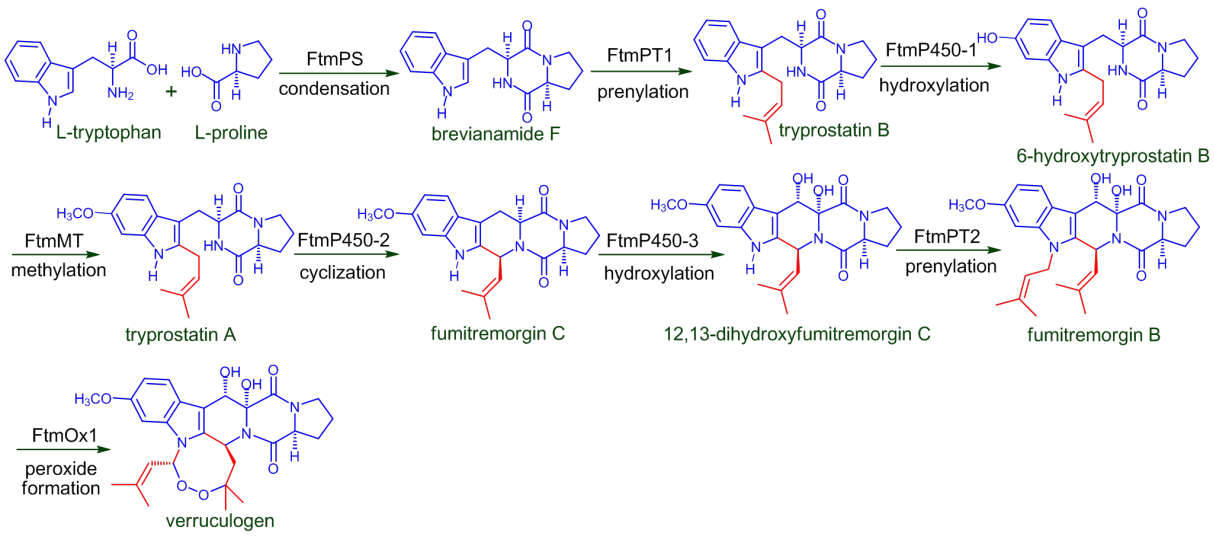

Figure 1-6: The biosynthesis of fumitremorgins/verruculogen in *A. fumigatus.*

1.2.1.2 The biosynthesis of notoamides

A gene cluster for the biosynthesis of notoamides was found in a marine-derived strain *Aspergillus* sp. MF297-2 (Ding *et al.*, 2010). Similar to verruculogen, the biosynthesis of notoamides also begins with the formation of brevianamide F from L-tryptophan and L-proline (Figure 1-7). The prenyltransferase NotF catalyzes the prenylation of brevianamide F to yield deoxybrevianamide E (Ding *et al*., 2010). Another prenyltransferase NotC generates a regularly C7-prenylated derivative of 6-hydroxy-deoxybrevianamide E (Ding *et al*., 2010). NotB was reported to catalyze the indole 2,3-oxidation of notoamide E through an apparent

pinacol-like rearrangement to produce notoamides C and D (Li *et al.*, 2012). The biochemical characterization of NotF, NotC and NotB has been carried out in *vitro* (Ding *et al.*, 2010; Li *et al.*, 2012). Feeding experiment with doubly ^{13}C-labeled racemic stephacidin A carried out in *Aspergillus* sp. MF297-2 showed that (+)-stephacidin A was converted into (-)-notoamide B in the biosynthetic pathway of notoamides (Finefield *et al.*, 2011b). The biosynthesis of notoamides in *A. versicolor* was also reported, which was demonstrated by feeding experiments with isotope-labelled precursors (Finefield *et al.*, 2011b; Finefield *et al.*, 2011c; Finefield *et al.*, 2011a).

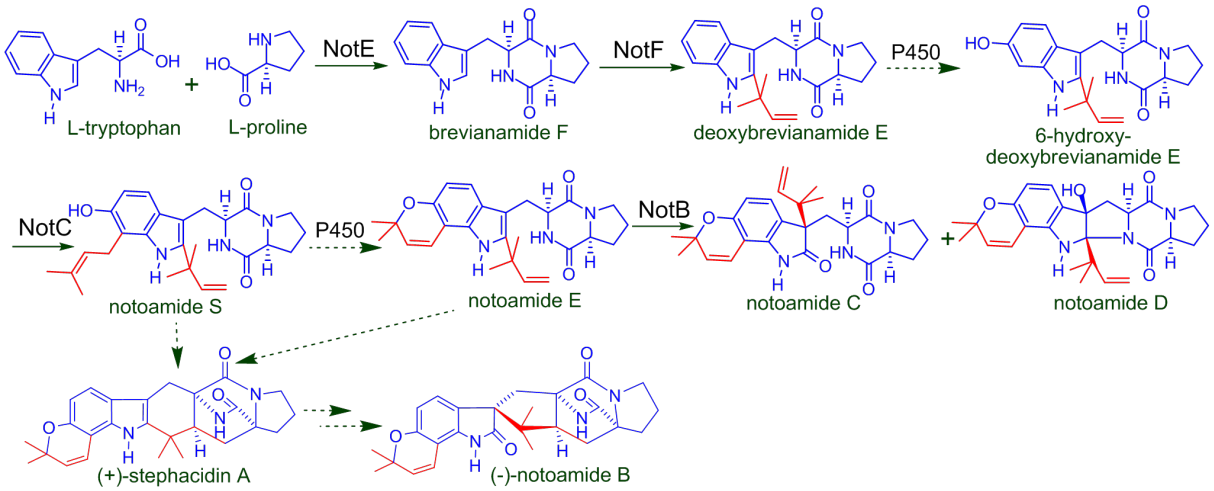

Figure 1-7: The biosynthesis of notoamides in *Aspergillus* sp. MF297-2.

1.2.1.3 The biosynthesis of hexadehydroastechrome

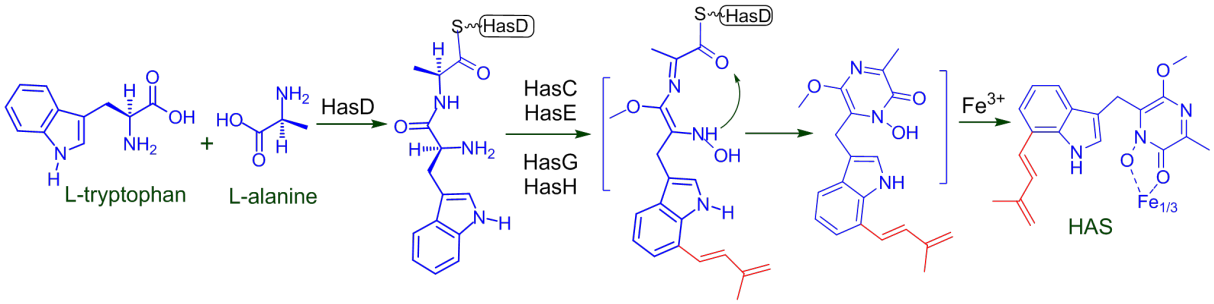

Figure 1-8: The proposed biosynthetic pathway of HAS in *A. fumigatus* (Yin *et al.*, 2013b).

Gene disruption experiments of the HAS cluster in *A. fumigatus* revealed that the end product of this cluster is a tryptophan-derived iron(III)-complex, HAS (Figure 1-8) (Yin *et al.*, 2013b). Five putative biosynthetic genes are proposed to be involved in this pathway, including one NRPS gene *hasD*, one 7-dimethylallyltryptophan synthase gene *hasE* (also named *7-dmats*) (Kremer *et al.*, 2007), one putative FAD binding protein gene *hasG*, one putative O-methyltransferase gene *hasC* and one putative cytochrome P450 gene *hasH*. In

addition, two putative C6 transcription factor genes *hasA* and *hasF* and one putative transporter gene *hasB* are also located in this cluster. It was suggested that the intermediates produced by this cluster are all in a NRPS-bound mode (Figure 1-8) (Yin *et al.*, 2013b). However, C7-prenylated L-tryptophan and C7-prenylated cyclo-L-Trp-L-Ala (terezine D) were isolated as precursors for HAS. Orthologues of these genes (Table 1-1) were also found in *N. fischeri* and *A. terreus* (Kremer *et al.*, 2007).

Table 1-1: Orthologous proteins of HasA-HasH.

A. fumigatus Af293	*N. fischeri* NRRL181		*A. terreus* NIH2624	
Protein	Protein	Identity*	Protein	Identity*
HasA (EAL92294)	EAW21279	93	EAU31597	73
HasB (EAL92293)	EAW21278	96	EAU31598	87
HasC (EAL92292)	EAW21277	96	EAU31599	88
HasD (EAL92291)	EAW21276	93	EAU31600	76
HasE (EAL92290, *i.e.* 7-DMATS)	EAW21275	95	EAU31601	82
HasF (EAL92289)	EAW21274	96	EAU31602	84
HasG (EAL92288)	EAW21273	95	-	-
HasH (EAL92287)	EAW21272	92	EAU31603	85

*: the identity to the orthologous protein from *A. fumigatus* Af293.

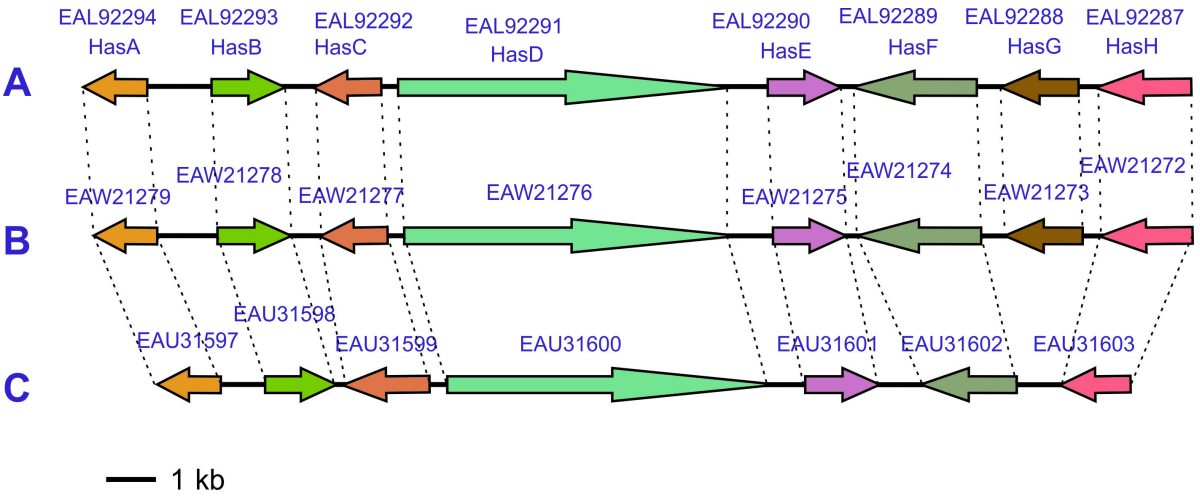

Figure 1-9: Biosynthetic clusters of HAS in different strains (A-C). A: *A. fumigatus*; B: *N. fischeri*; C: *A. terreus*.

In a previous work in our group, 7-DMATS was overproduced in *E. coli* and characterized biochemically (Kremer *et al.*, 2007). However, the biochemical functions of HasC and HasH are still unknown. In this thesis, *hasC* and *hasH* were cloned from *A. fumigatus* and overexpressed in *E. coli* and *Saccharomyces cerevisiae* (*S. cerevisiae*), respectively.

1.2.2 Biosynthetic pathway of ergot alkaloids in *Aspergillus fumigatus*

Another subgroup of prenylated indole alkaloids in *A. fumigatus* are ergot alkaloids. The biosynthesis of ergot alkaloids (Figure 1-10) starts with the conversion of L-tryptophan to 4-dimethylallyltryptophan by the 4-dimethylallyltryptophan synthase (4-DMATS), *i.e.* FgaPT2 (Unsöld and Li, 2005). Formation of the 4-dimethylallyl-L-abrine is catalyzed by the methyltransferase FgaMT (Rigbers and Li, 2008), followed by the production of chanoclavine-1 (Coyle *et al.*, 2010). FgaDH has been proven to catalyze the formation of chanoclavine-I aldehyde from chanoclavine-I (Wallwey *et al.*, 2010a). The conversion of chanoclavine-1 aldehyde to festuclavine needs two enzymes, *i.e.* FgaOx3 and FgaFS (Wallwey *et al.*, 2010b). Subsequently, a further hydroxylation reaction leads to the formation of (8S,9S)-fumigaclavine B, and this reaction was speculated to be catalyzed by the cytochrome P450 enzyme FgaP450-2 (Wallwey and Li, 2011). FgaAT was proven to catalyze the next step, which produces (8S,9S)-fumigaclavine A by an acetylation reaction (Liu *et al.*, 2009). Finally, the second prenyltransferase FgaPT1 catalyzes the formation of (8S,9S)-fumigaclavine C from (8S,9S)-fumigaclavine A (Unsöld and Li, 2006). The biochemical characterization of FgaPT2, FgaMT, FgaDH, FgaOx3, FgaFS, FgaAT and FgaPT1 has been carried out in *vitro* after overexpression of the encoding genes in *E. coli* or *S. cerevisiae* (Unsöld and Li, 2005; Rigbers and Li, 2008; Wallwey *et al.*, 2010a; Wallwey *et al.*, 2010b; Liu *et al.*, 2009; Unsöld and Li, 2006).

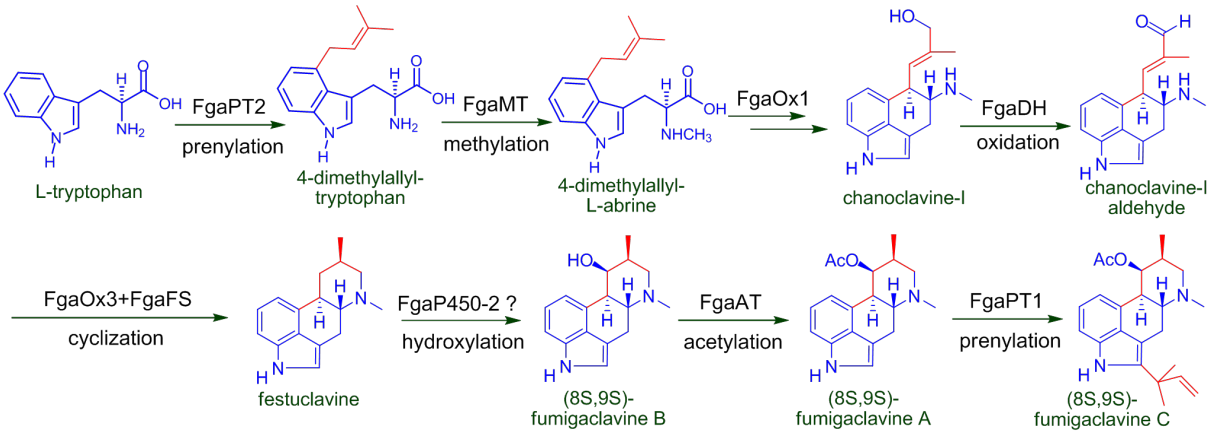

Figure 1-10: The biosynthesis of fumigaclavine C in *A. fumigatus*.

1.3 Aromatic prenyltransferases

Aromatic prenyltransferases are responsible for the attachment of prenyl moieties to an aromatic ring and contribute significantly to the structural and biological diversity of prenylated compounds in nature. In the last decade, significant progress has been achieved

in the molecular biological, biochemical and structural biological investigation of the aromatic prenyltransferases, since a vast volume of sequences from genome projects were released.

1.3.1 Prenyltransferases of the DMATS superfamily

As mentioned above, 4-DMATS was identified as the first pathway-specific enzyme in the biosynthesis of ergot alkaloids (Tsai *et al.*, 1995; Unsöld and Li, 2005). It catalyzes the prenylation of L-tryptophan at C-4 of the indole ring and therefore functions as an indole prenyltransferase (Unsöld and Li, 2005; Steffan *et al.*, 2009a). Genes with sequence homology to 4-DMATS are classified as prenyltransferase genes of the **dim**ethyl**a**llyl**t**ryptophan **s**ynthase (DMATS) superfamily. Prenyltransferases of the DMATS superfamily are involved in the biosynthesis of fungal secondary metabolites and mainly catalyze prenylation of diverse indole derivatives, including tryptophan and tryptophan-containing cyclic dipeptides.

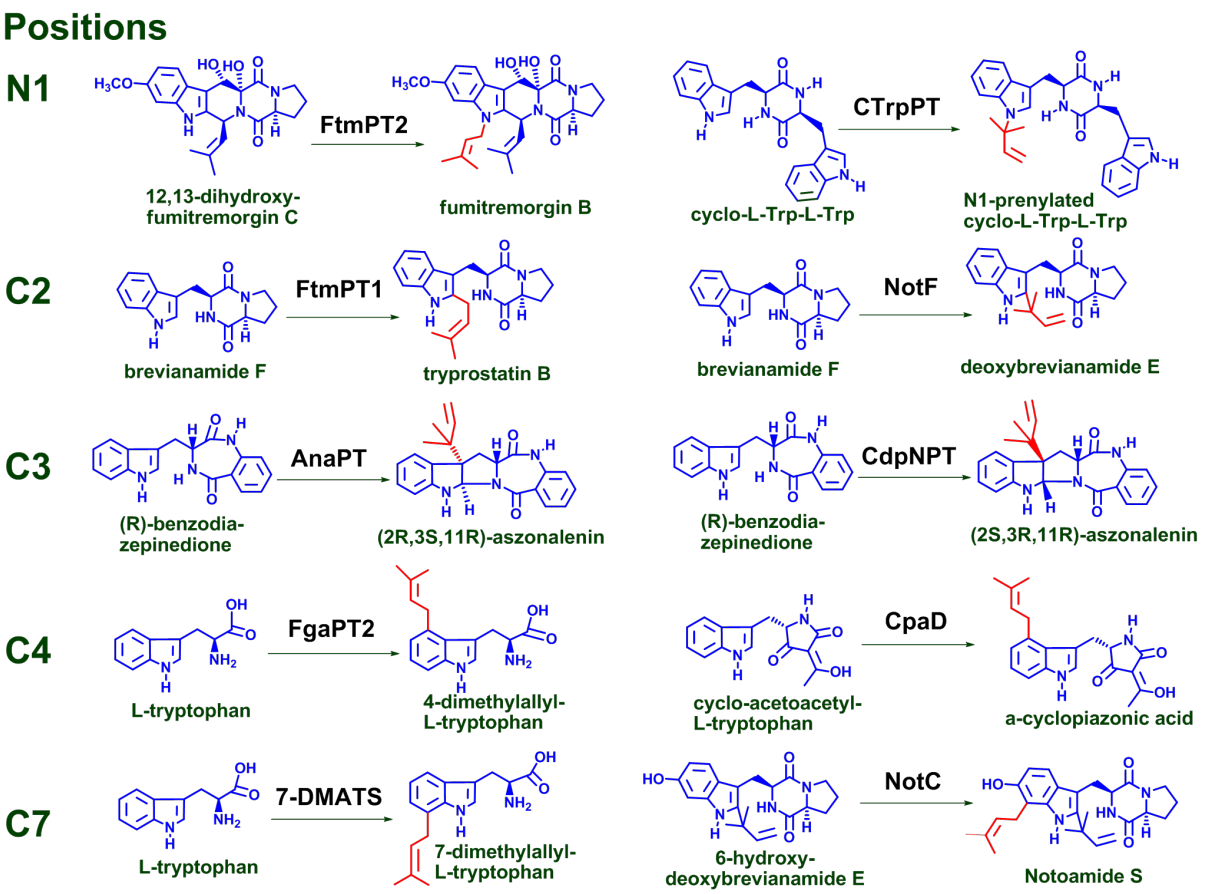

Figure 1-11: Known examples of fungal indole prenyltransferases of the DMATS superfamily prior to this thesis.

Biochemical characterization of the encoded enzymes began in summer 2004 after availability of the genome sequence for *A. fumigatus* (Unsöld and Li, 2005). A number of indole prenyltransferases have been biochemically identified and characterized from that

time (Figure 1-11). For example, FtmPT2 from *A. fumigatus* catalyzes the regular N1-prenylation of 12,13-dihydroxyfumitremorgin C (Grundmann *et al.*, 2008). An additional example of N1-prenyltransferase is CTrpPT from *Aspergillus oryzae*, which uses cyclo-L-Trp-L-Trp as the best substrate (Zou *et al.*, 2010). The regular and reverse C2-prenylations were observed for FtmPT1 (Grundmann and Li, 2005) and NotF (Ding *et al.*, 2010) from *Aspergillus* strains, respectively. C3-prenylations of cyclic dipeptides by AnaPT from the fungus *N. fischeri* (Yin *et al.*, 2009) and CdpNPT from *A. fumigatus* (Schuller *et al.*, 2012), lead to the formation of indoline derivatives with a reverse prenyl moiety at opposite sides. As described above, FgaPT2 and its orthologues from different fungi catalyze the regular prenylation of L-tryptophan at position C-4 (Unsöld and Li, 2005; Wallwey and Li, 2011). CpaD from *Aspergillus* sp. catalyzes regular C4-prenylation as well, but uses cyclo-acetoacetyl-L-tryptophan as natural substrate (Liu and Walsh, 2009). 7-DMATS from *A. fumigatus* was reported to prenylate L-tryptophan at position C-7 (Kremer *et al.*, 2007). Another C7-prenyltransferase NotC from a marine-derived *Aspergillus* sp. catalyzes the prenylation of 6-hydroxy-deoxybrevianamide E (Ding *et al.*, 2010).

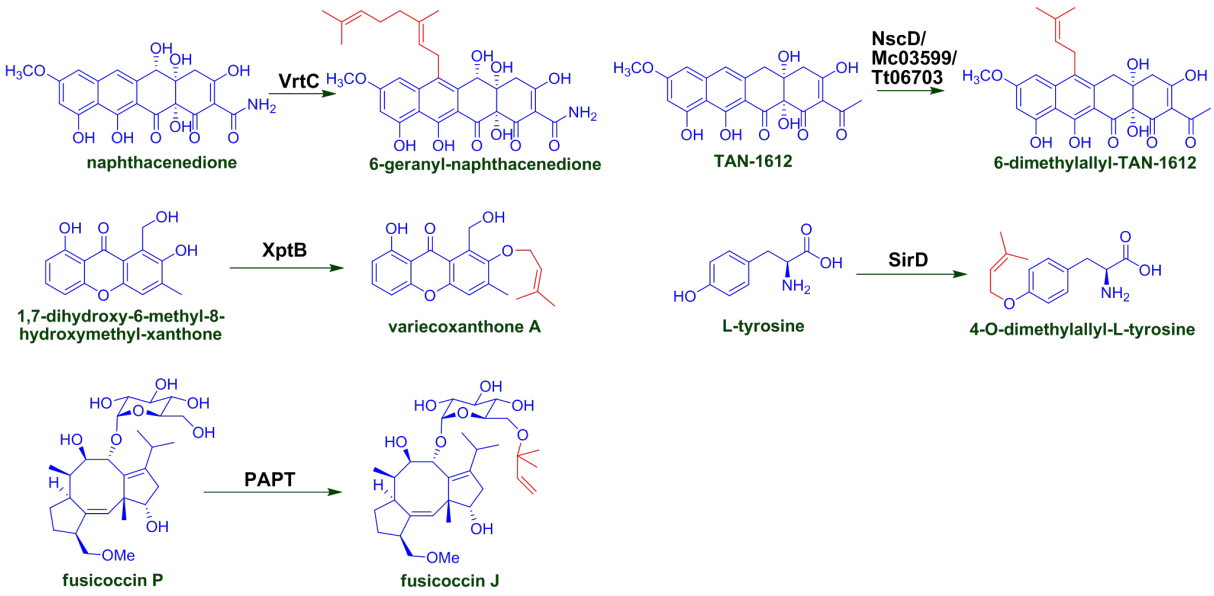

Figure 1-12: Prenyltransferases of the DMATS superfamily which use compounds other than indole alkaloids as substrates.

In addition to the indole prenyltransferases, some members of the DMATS superfamily catalyze prenylations of other substances (Figure 1-12). VrtC from *Penicillium aethiopicum*, and its homologues NscD from *N. fischeri*, Mc03599 from *Microsporum canis* as well as Tt06703 from *Trichophyton tonsurans* transfer a geranyl and a dimethylallyl moiety to tetracyclic naphthacenedione compounds, respectively (Figure 1-12) (Chooi *et al.*, 2012; Chooi *et al.*, 2013). XptB from *A. nidulans*, SirD from *Leptosphaeria maculans* (*L. maculans*) and PAPT from *Phomopsis amygdali* are O-prenyltransferases. XptB uses 1,7-dihydroxy-6-

methyl-8-hydroxymethyl-xanthone (Pockrandt *et al.*, 2012), while SirD and PAPT accept L-tyrosine and fusicoccin P as natural substrates, respectively (Kremer and Li, 2010; Noike *et al.*, 2012).

1.3.2 Prenyltransferases of the LtxC group

Prenyltransferases from the LtxC group are soluble proteins from bacteria. Although the enzymes from this group show very low sequence similarity to the members of the DMATS superfamily, they also utilize indole derivatives as common substrates (Figure 1-13). CymD from *Salinispora arenicola*, SCO7467 from *Streptomyces coelicolor* and IptA from *Streptomyces* sp. SN-593 prenylate L-tryptophan at positions N-1, C-5 and C-6, respectively (Schultz *et al.*, 2010; Subramanian *et al.*, 2012; Ozaki *et al.*, 2013; Takahashi *et al.*, 2010). The results on SCO7467 were published after those of 5-DMATS in this thesis. MpnD from *Marinactinospora thermotolerans* catalyzes the reverse C7-prenylation of (-)-indolactam-Ile (Ma *et al.*, 2012). LtxC is the first known member of this group and responsible for transfer of a geranyl group to (-)-indolactam V to give lyngbyatoxin A in *Lyngbya majuscule* (Edwards and Gerwick, 2004).

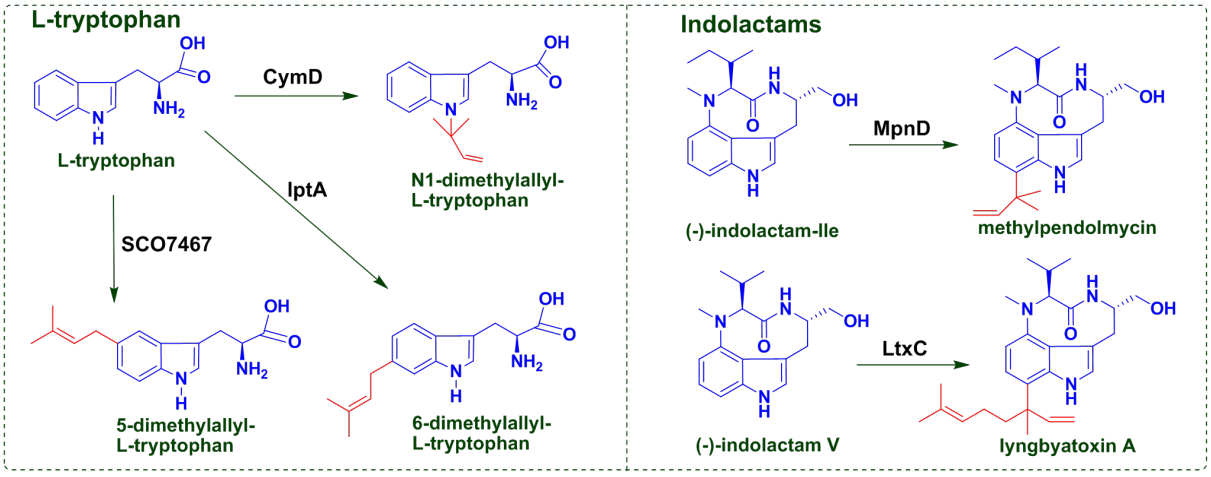

Figure 1-13: Prenyltransferases of the LtxC group.

1.3.3 Prenyltransferases of the CloQ/NphB group

Prenyltransferases of the CloQ/NphB group catalyze the prenylation of naphthalenes, quinones, simple phenols and phenzines (Figure 1-14) (Heide, 2009). These enzymes are mainly found in bacterial, but also in some fungi. NphB from *Streptomyces* sp. and the homologue SCO7190 from *Streptomyces coelicolor* accept 1,6-dihydroxynaphthalene as substrate, and catalyze the transfer of a geranyl and a dimethylallyl group to the substrate, respectively (Kuzuyama *et al.*, 2005; Kumano *et al.*, 2008). Fur7 from *Streptomyces* sp. and Fnq26 from *Streptomyces cinnamonensis* transfer the geranyl groups to 2-methoxy-3-

methylflaviolin and flaviolin, respectively (Kumano *et al.*, 2010; Haagen *et al.*, 2007). CloQ from *Streptomyces roseochromogenes*, which is the first known member of this group, and its homologue NovQ from *Streptomyces niveus* were reported to prenylate 4-hydroxyphenylpyruvic acid (Metzger *et al.*, 2010; Ozaki *et al.*, 2009). Both EpzP from *Streptomyces cinnamonensis* and PpzP from *Streptomyces anulatus* catalyze the C-prenylation of 5,10-dihydrophenazine-1-carboxylic acid (Seeger *et al.*, 2011; Saleh *et al.*, 2009).

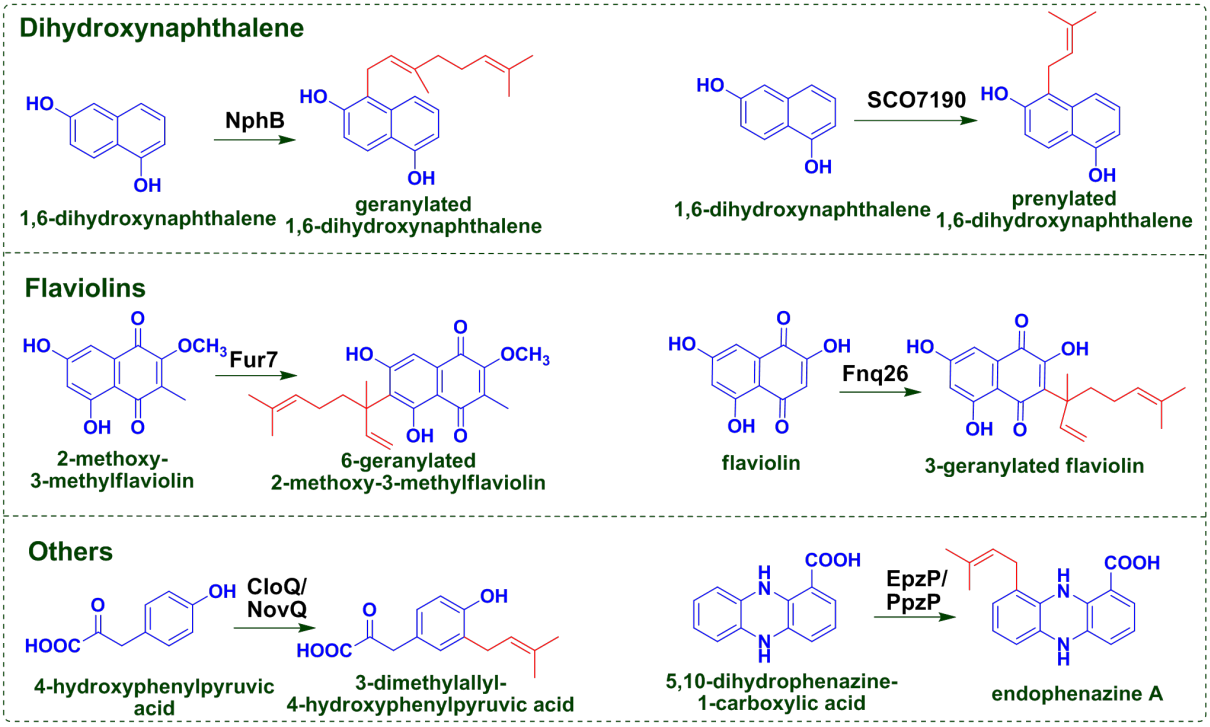

Figure 1-14: Prenyltransferases of the CloQ/NphB group.

1.3.4 Prenyltransferases of the UbiA superfamily

Prenyltransferases of the UbiA superfamily are membrane-bound proteins and widely distributed in bacteria, fungi and plants. These enzymes accept diverse aromatic compounds as substrates (Figure 1-15). Four plant flavonoid prenyltransferases of the UbiA superfamily have been identified and characterized. LaPT1 from *Lupinus albus* and SfG6DT from *Sophora flavescens* are responsible for the prenylation of genistein to produce isowighteone and wighteone, respectively (Shen *et al.*, 2012; Sasaki *et al.*, 2011). SfN8DT-1 identified from *Sophora flavescens* transfers the dimethylallyl group to position C-8 of naringenin (Sasaki *et al.*, 2008), while G4DT from *Glycine max* shows activity to prenylate (-)-glycinol (Akashi *et al.*, 2009). Three enzymes LePGT1, Coq2p and UbiA, which were identified from the medicinal plant *Lithospermum erythrorhizon*, *S. cerevisiae* and *E. coli*, respectively, catalyze the transfer of a short or long-chain prenyl moiety to 4-hydroxybenzoic acid (Ohara *et al.*, 2009;

Pierrel *et al.*, 2010; Melzer and Heide, 1994). AuaA from the bacterium *Stigmatella aurantiaca* is responsible for transfer of a farnesyl group to 2-methyl-4-hydroxyquinoline to yield aurachin D in the biosynthetic pathway of aurachin A (Stec *et al.*, 2011). The plant prenyltransferase HlPT-1 from *Humulus lupulus* has the ability to prenylate phlorisovalerophenone (Tsurumaru *et al.*, 2012).

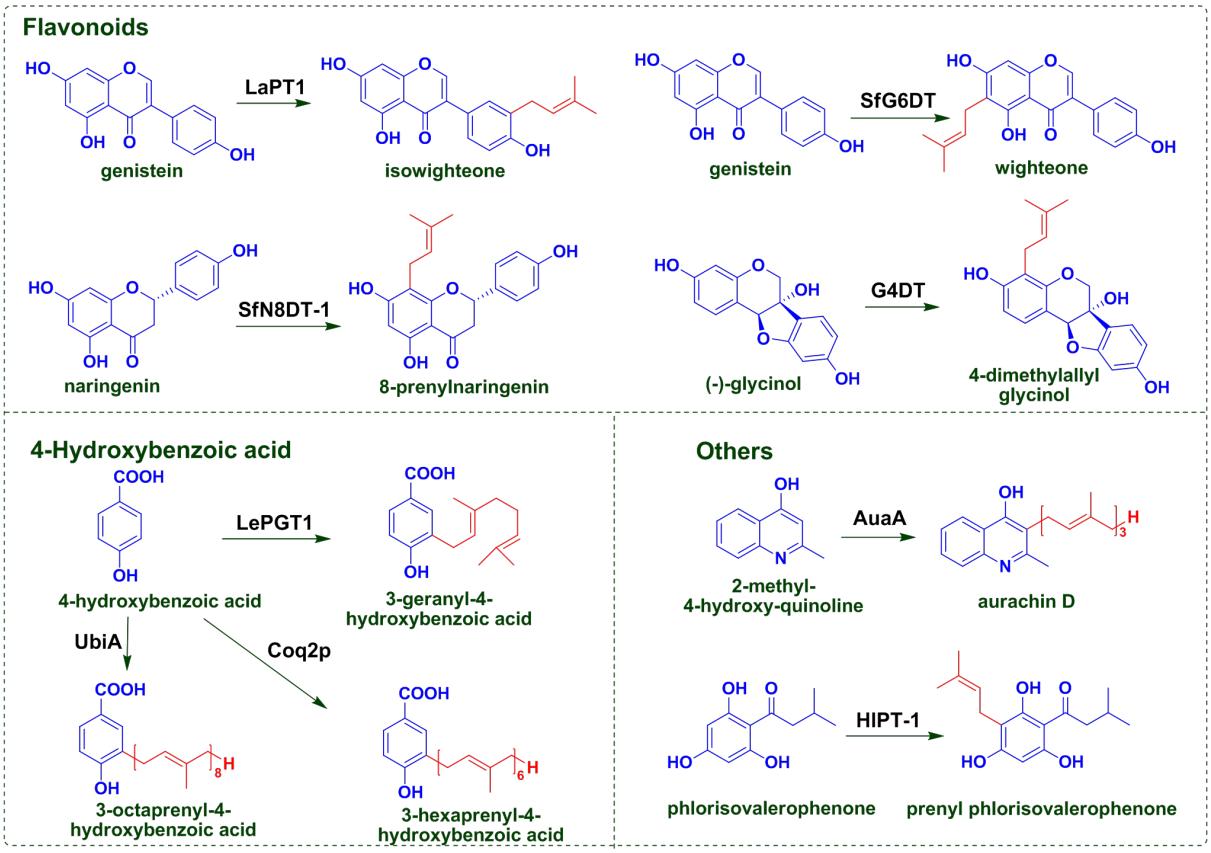

Figure 1-15: Prenyltransferases of the UbiA superfamily

1.3.5 Chemoenzymatic synthesis of prenylated derivatives by using aromatic prenyltransferases

Prenylation improves often the affinity of a compound to biomembranes and the interaction of the substance with proteins (Botta *et al.*, 2005b), leading to dramatically increased biological activities. Therefore, it is attractive for scientists to use prenyltransferases as strategies for regioselective chemoenzymatic synthesis of prenylated derivatives. Aromatic prenyltransferases, especially the soluble indole prenyltransferases of the DMATS superfamily, show promising flexibility towards their aromatic substrates and catalyze highly regio- and stereoselective prenyltransfer reactions. These features provided evidence for the potential of aromatic prenyltransferases as biocatalysts for chemoenzymatic synthesis. Many series of prenylated derivatives have been successfully synthesized by these enzymes. Details are described below.

1.3.5.1 Chemoenzymatic synthesis of prenylated indole alkaloids

Dimethylallyltryptophan synthases 7-DMATS, FgaPT2, MaPT and IptA showed noble substrate flexibility towards simple indole derivatives (Kremer and Li, 2008; Steffan *et al.*, 2007; Ding *et al.*, 2008; Takahashi *et al.*, 2010) (Figure 1-16). Eleven C7-prenylated, ten C4-prenylated, four C4-prenylated and five C6-prenylated simple indole derivatives were successfully produced by 7-DMATS, FgaPT2, MaPT and IptA, respectively (Kremer and Li, 2008; Steffan *et al.*, 2007; Takahashi *et al.*, 2010; Ding *et al.*, 2008; Unsöld and Li, 2005). At higher enzyme concentration, FgaPT2 accepted as well tryptophan-containing cyclic dipeptides and five C4-prenylated derivatives were obtained (Figure 1-17) (Steffan and Li, 2009). CpaD showed substrate promiscuity towards tryptophan-containing diketopiperazines and catalyzed the formation of five enzyme products (Liu and Walsh, 2009). In addition, CpaD accepted three tryptophan-containing thiohydantoins and produced C4-prenylated products (Liu and Walsh, 2009). Cyclic dipeptide prenyltransferase FtmPT1 catalyzed high efficient prenylation of fourteen tryptophan-containing cyclic dipeptides to produce regularly C2-prenylated derivatives (Figure 1-17) (Wollinsky *et al.*, 2012a). The cytotoxic study showed that prenylation at C-2 led to a significant increase of the cytotoxicity of all the fourteen tested cyclic dipeptides (Wollinsky *et al.*, 2012a). Detailed analysis of the incubation mixtures of FtmPT1 with cyclic dipeptides revealed the presence of additional product peaks for regularly C3-prenylated hexahydropyrrolo[2,3-b]indoles in the high performance liquid chromatography (HPLC) chromatograms (Wollinsky *et al.*, 2012b). Seven regularly C3-prenylated hexahydropyrrolo[2,3-b]indoles were obtained (Wollinsky *et al.*, 2012b).

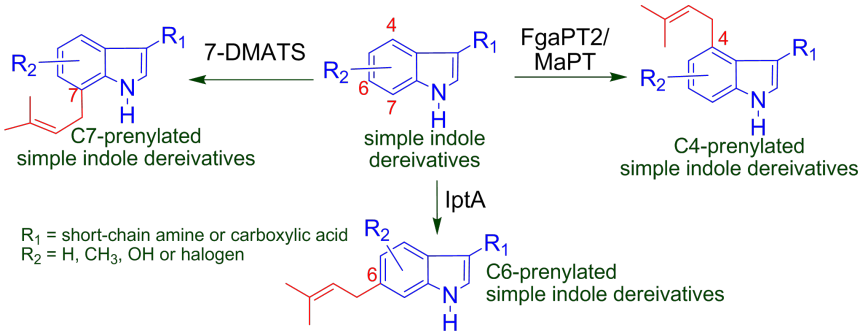

Figure 1-16: Chemoenzymatic synthesis of prenylated simple indole derivatives by 7-DMATS, FgaPT2, MaPT and IptA.

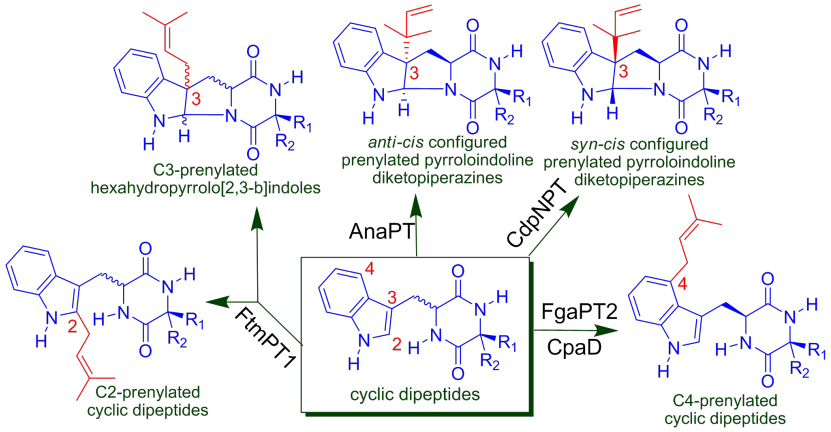

Figure 1-17: Chemoenzymatic synthesis of prenylated derivatives of tryptophan-containing cyclic dipeptides.

As shown in Figure 1-17, the enzyme reactions catalyzed by AnaPT and CdpNPT were found to be not only regiospecific, but also stereospecific towards tryptophan-containing cyclic dipeptides (Yin *et al.*, 2010a; Schuller *et al.*, 2012).

1.3.5.2 Chemoenzymatic synthesis of other prenylated derivatives

The tyrosine prenyltransferase SirD (Figure 1-18) of the DMATS superfamily showed substrate promiscuity towards phenylalanine/tyrosine derivatives and has successfully applied for synthesis of eight regularly O-prenylated products (Kremer and Li, 2010; Zou *et al.*, 2011). The xanthone prenyltransferase XptB could be applied for chemoenzymatic synthesis of O-prenylated xanthones (Pockrandt *et al.*, 2012). Four prenylated xanthones were obtained. Six hydroxyquinolines were well accepted by AuaA as substrates and converted to the respective C3-farnesylated products (Stec *et al.*, 2011). NphB, Fur7 and NovQ from the CloQ/NphB group showed also broad substrate promiscuity towards several substrates. However, low specificity was observed for these enzymes, since more than one enzyme products were detected for most substrates (Kumano *et al.*, 2008; Shindo *et al.*, 2011; Kumano *et al.*, 2010; Ozaki *et al.*, 2009; Macone *et al.*, 2009).

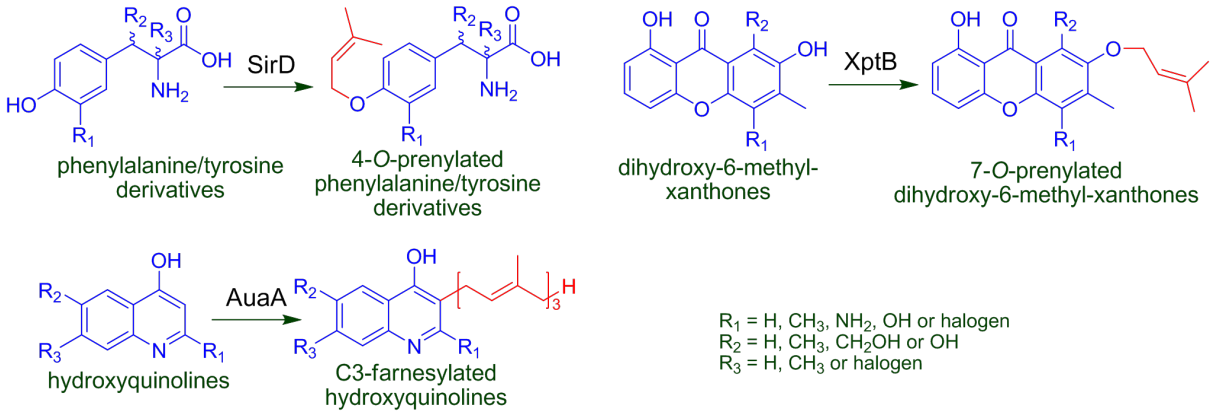

Figure 1-18: Chemoenzymatic synthesis of prenylated derivatives from other substrates.

1.3.6 Relationship of aromatic prenyltransferases

The enzymes of the DMATS superfamily share very low sequence similarity with the members of the LtxC group and almost no sequence similarity with other known prenyltransferases, *e.g.* the soluble prenyltransferases of the CloQ/NphB group from bacteria and fungi as well as the membrane-bound prenyltransferases of the UbiA superfamily from bacteria, fungi and plants. Similar to enzymes of the DMATS superfamily, the members of the CloQ/NphB group don't contain a DDxxD motif. In contrast to those enzymes, the members of the UbiA superfamily contain a NQxxDxxxD motif for prenyl diphosphate binding and are strictly dependent on Mg^{2+} or other divalent cations.

Surprisingly, structure analysis revealed that FgaPT2, FtmPT1 and CdpNPT of the DMATS superfamily contain a PT-barrel (Figure 1-19) (Metzger *et al.*, 2009; Jost *et al.*, 2010; Schuller *et al.*, 2012), which has been only found in the bacterial aromatic prenyltransferases of the CloQ/NphB group (Metzger *et al.*, 2010; Kuzuyama *et al.*, 2005). Therefore, it is proposed that all the proteins from both the DMATS superfamily and the CloQ/NphB group share a common ancestry (Bonitz *et al.*, 2011). It would be interesting to test the acceptance of substrates for the members of the CloQ/NphB group by the prenyltransferases of the DMATS superfamily. An acceptance of hydroxynaphthalenes by a member of the DMATS superfamily was not reported previously. Correspondingly, substrates tyrosine or indole derivatives for the DMATS superfamily were not prenylated by enzymes of the CloQ/NphB group. In *vitro* assays were carried out in this thesis to test the enzyme activity of prenyltransferases of the DMATS superfamily towards hydroxynaphthalenes. Furthermore, the acceptance of flavonoids by members of the DMATS superfamily was also tested in this thesis.

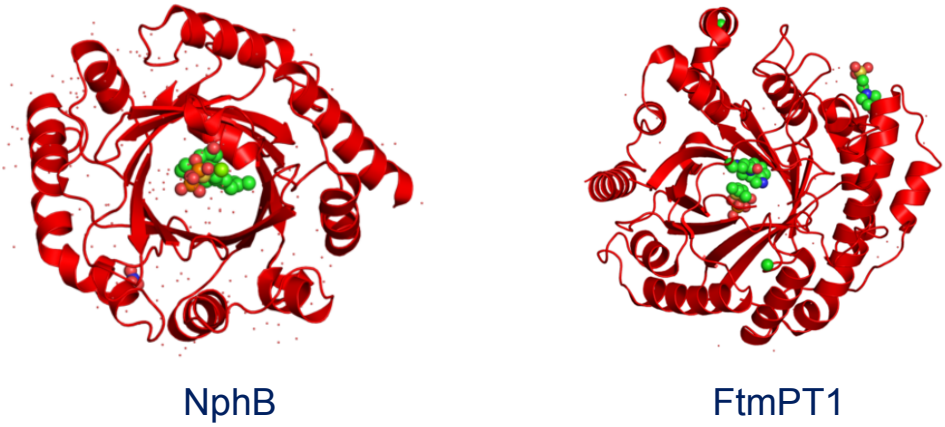

Figure 1-19: The structures of NphB (also named Orf2, PDB 1ZB6) and FtmPT1 (PDB 3O2K) in cartoon representation (Kuzuyama *et al.*, 2005; Jost *et al.*, 2010).

2 Aims of this thesis

The following issues have been addressed in this thesis:

Functional proof of putative indole prenyltransferase genes in *Neosartorya* and *Aspergillus*

Blast search in GenBank indicated two proteins which showed significant sequence similarity to members of the DMATS superfamily: 5-DMATS from *A. clavatus* and CdpC3PT from *N. fischeri*. 5-DMATS and CdpC3PT showing 52% identity with FgaPT2 and 53% identity with CdpNPT, respectively, indicated similar roles. BrePT from *A. versicolor* is an orthologue of NotF from *Aspergillus* sp. MF297-2 and was expected to compensate for low substrate promiscuity of NotF. In order to characterize 5-DMATS, BrePT and CdpC3PT biochemically, the following experiments were carried out:

- Overproduction of *cdpC3PT*, *5-dmats* and *brePT* in *E. coli*.
- Enzyme assays with CdpC3PT, 5-DMATS and BrePT. Analysis and isolation of enzyme products by HPLC.
- Structure elucidation of enzyme products by NMR and MS.
- Kinetic study of CdpC3PT, 5-DMATS and BrePT reactions.

Chemoenzymatic synthesis of prenylated indole derivatives by indole prenyltransferases of the DMATS superfamily

AnaPT, CdpC3PT and CdpNPT were reported to catalyze reverse prenylation at opposite sides in tryptophan-containing cyclic dipeptides to produce *cis*-configured prenylated pyrroloindoline diketopiperazines in previous studies (Yin *et al*., 2010a; Yin *et al.*, 2010b; Schuller *et al*., 2012). In this thesis, the stereoselectivity of these three enzymes was demonstrated by analysis of product formation from four cyclo-Trp-Ala and four cyclo-Trp-Pro isomers. In addition, indolocarbazoles, a class of natural products with well known remarkable biological inhibitory effects against protein kinases, were tested for the acceptance by indole prenyltransferases. The following experiments were carried out:

- Synthesis of stereoisomers of several cyclic dipeptides and indolocarbazoles.
- Enzyme assays of cyclic dipeptides and indolocarbazoles with indole prenyltransferases. Analysis and isolation of enzyme products by HPLC.
- Structure elucidation of enzyme products by NMR and MS.
- Kinetic study of the enzyme reactions.

Chemoenzymatic synthesis of prenylated hydroxynaphthalenes and flavonoids by indole prenyltransferases of the DMATS superfamily

As mentioned previously, indole prenyltransferases of the DMATS superfamily showed no sequence similarity and catalytic activity to known aromatic prenyltransferases of the CloQ/NphB group and the UbiA superfamily. However, recent studies indicated that prenyltransferases of the DMATS superfamily share structure similarity with those of the CloQ/NphB group. Therefore, it is interesting to prove if the members of the DMATS superfamily could also accept the substrates for enzymes of the CloQ/NphB group, *e.g.* hydroxynaphthalenes. In addition, it is also interesting to know if the members of the DMATS superfamily could catalyze the prenylation of substrates for other known aromatic prenyltransferases, *e.g.* flavonoids accepted by the members of the UbiA superfamily. In order to investigate the acceptance of hydroxynaphthalenes and flavonoids by the members of the DMATS superfamily, the following experiments were carried out:

- Enzyme assays of hydroxynaphthalenes and flavonoids with indole prenyltransferases. Analysis and isolation of enzyme products by HPLC.
- Structure elucidation of enzyme products by NMR and MS.
- Kinetic study of the enzyme reactions.

Biosynthetic genes other than prenyltransferases involved in the biosynthesis of a prenylated indole alkaloid in *A. fumigatus*

A gene cluster for the biosynthesis of HAS was identified in *A. fumigatus*. One NRPS, one putative transporter, two putative C6 transcription factors, one 7-dimethylallyltryptophan synthase (7-DMATS), one putative FAD binding protein, one putative O-methyltransferase (HasC) and one putative cytochrome P450 (HasH) were proposed to be involved in the biosynthesis (Yin *et al*., 2013b). HasC and HasH were expected to catalyze the O-methylation and N-hydroxylation, respectively. In order to elucidate the biochemical function of HasC and HasH in the biosynthesis of HAS, the following experiments were carried out:

- Cloning of *hasC* and *hasH* into cloning vector pGEM-T easy.
- Preparing the expression vector of *hasC* in pQE60.
- Preparing expression constructs containing *hasH*: expression vectors of *hasH* in pESC-URA with or without His_6-tag, and the co-expression vector of *hasH* with a reductase gene *NFIA_083630* in pESC-URA.
- Overproduction of *hasC* in *E. coli* and *hasH* in *S. cerevisiae*.
- Enzyme assays with HasC and HasH.

3 Materials and methods

3.1 Chemicals

Dimethylallyl diphosphate (DMAPP), geranyl diphosphate (GPP) and farnesyl diphosphate (FPP)

DMAPP, GPP and FPP were prepared according to the method described for GPP (Woodside *et al*., 1988). DMAPP was prepared by Lena Ludwig and Dr. Marco Matuschek (Institut für Pharmazeutische Biologie und Biotechnologie, Philipps-Universität Marburg), while GPP and FPP were synthesized by Dr. Edyta Stec.

Cyclic dipeptides

Cyclo-L-Trp-L-Pro and cyclo-L-Trp-D-Pro were synthesized in this thesis, while cyclo-D-Trp-L-Pro and cyclo-D-Trp-D-Pro were synthesized by Beate Wollinsky. The four isomers of cyclo-Trp-Ala were synthesized by Lena Ludwig. These compounds were synthesized from tryptophan methyl ester and N-Boc protected proline according to the method published previously (Cacciatore *et al.*, 2005; Caballero *et al.*, 1998). Cyclo-L-Trp-L-Pro and cyclo-L-Trp-D-Pro were synthesized from H-L-Trp-OMe·HCl and N-Boc-D-Pro-OH, cyclo-D-Trp-L-Pro and cyclo-D-Trp-D-Pro from H-D-Trp-OMe·HCl and N-Boc-D-Pro-OH. Similarly, the two pairs H-L-Trp-OMe·HCl and N-Boc-D-Ala-OH as well as H-D-Trp-OMe·HCl and N-Boc-D-Ala-OH were used for the preparation of the four stereoisomers of cyclo-Trp-Ala.

Cyclo-L-Trp-L-His was synthesized in this thesis from N-Boc-L-Trp-OH and H-L-His-OMe·HCl according to the literature (Bivin *et al*., 1993; Cacciatore *et al*., 2005). Other cyclic dipeptides were purchased from Bachem (Bubendorf, Switzerland).

Synthesis of indolocarbazoles in this thesis

Treatment of indole-3-acetamide with methyl indolyl-3-glyoxylate in the presence of KOBu^t afforded the intermediate arcyriarubin A (Faul *et al*., 1998), which was converted to N-methylarcyriarubin A by treatment with methyl iodide (Nakazono *et al*., 2007). Arcyriaflavin A and its N6-methylated derivative were obtained after oxidative cyclization of the two bisindolylmaleimides arcyriarubin A and N-methylarcyriarubin A, respectively (Burtin *et al*., 2000; Wilson *et al*., 2007). Reduction of arcyriaflavin A with tin metal in AcOH/HCl and $LiAlH_4$ in THF resulted in the formation of K252c (Wilson *et al*., 2007) and 7-hydroxy-K252c (Harris *et al*., 1993), respectively.

Simple indole derivatives, hydroxynaphthalenes and flavonoids

These substrates were purchased from Fluka, TCI, Acros Organics, Aldrich, Roth, Sigma, Bachem and Alfa Aesar.

3.2 Bacterial and yeast strains, plasmids and oligonucleotides

Table 3-1: Overview of the used *E. coli* and *S. cerevisiae* strains.

Strain	Genotype	Supplier/ Manufacturer
E. coli XL1 Blue MRF'	Δ*(mcrA)183* Δ*(mcrCB-hsdSMR-mrr)173 endA1 supE44 thi-1 recA1 gyrA96 relA1 lac [F' proAB lacI^{q}ZΔM15* Tn10 (Tet^r)]	Agilent (Waldbronn)
E. coli BL21 (DE3) pLysS	F$^-$ *ompT hsdS$_B$*(r$_B^-$ m$_B^-$) *gal dcm* (DE3) pLysS (Cam^R)	Novagen (Darmstadt)
E. coli M15 [pREP4]	Nal^S, Str^S, Rif^S, Thi$^-$, Lac$^-$, Ara$^+$, Gal$^+$, Mtl$^-$, F$^-$, RecA$^+$, Uvr$^+$, Lon$^+$.	Qiagen (Hilden)
E. coli SG13009 [pREP4]	Nal^S, Str^S, Rif^S, Thi$^-$, Lac$^-$, Ara$^+$, Gal$^+$, Mtl$^-$, F$^-$, RecA$^+$, Uvr$^+$, Lon$^+$	Qiagen (Hilden)
S. cerevisiae INVSc1	MATa/α *his3Δ1/his3Δ1 leu2/leu2 trp1-289/trp1-289 ura3-52/ura3-52*	Invitrogen (Karlsruhe)

Table 3-2: Commercial cloning and expression vectors.

Vector	Description	Supplier/ Manufacturer
pESC-URA	Expression vector for *S. cerevisiae*, *GAL1* and *GAL10* promoters, *URA3*, with epitope tags	Agilent (Waldbronn)
pGEM®-T easy	Cloning vector with T-overhangs for PCR cloning	Promega (Mannheim)
pQE60	Expression vector for *E. coli*, T5-promoter, Amp^R, with C-terminal His$_6$-tag	Qiagen (Hilden)

Table 3-3: List of plasmids used in this work.

Plasmid	Description	Reference
pAG012	Construct of *ftmPT1* from *A. fumigatus* B5233 in pQE70 for expression in *E. coli.*	(Grundmann and Li, 2005)
pAK2	Construct of *sirD* from *L. maculans* M1 in pQE70 for expression in *E. coli.*	(Kremer and Li, 2010)
pHL5	Construct of *cdpNPT* from *A. fumigatus* B5233 in pQE60 for expression in *E. coli.*	(Yin *et al*., 2007)
pIU18	Construct of *fgaPT2* from *A. fumigatus* B5233 in pHis8 for expression in *E. coli.*	(Steffan *et al*., 2007)
pLW40	Construct of *7-dmats* from *A. fumigatus* B5233 in pQE60 for expression in *E. coli.*	(Kremer *et al*., 2007)
pSY1	Construct of *brePT* from *A. versicolor* NRRL573 in pET28a for expression in *E. coli.*	(Yin *et al.*, 2013a)
pVW41	Construct of *NFIA_083630* from *N. fischeri* NRRL181 in pESC-URA for expression in *S. cerevisiae.*	Viola Wohlgemuth, unpublished
pWY22	Construct of *anaPT* from *N. fischeri* NRRL181 in pQE70 for expression in *E. coli.*	(Yin *et al*., 2009)
pWY25	Construct of *cdpC3PT* from *N. fischeri* NRRL181 in pQE60 for expression in *E. coli.*	(Yin *et al.*, 2010b)
pXY01	*AFUA_3G12910* in pGEM-T easy, containing the PCR product (10-1296 under the accession number XM_749237.1 at GenBank) amplified from gDNA from the bacterial artificial chromosome (BAC) AfB28B10 (616042-693705 under the accession number AAHF01000002.1 at GenBank) of *A. fumigatus* Af293 by using fusion PCR. In the first round, primers AFUA_3G12910_1 and AFUA_3G12910_4 were used for amplification of the first exon of *hasC*, and AFUA_3G12910_2 and AFUA_3G12910_3 for the second exon of *hasC*. In the second round, primers AFUA_3G12910_1 and AFUA_3G12910_2 were used.	this thesis
pXY02	904 bp BamHI-BglII fragment from pXY01 in the same sites of pQE60, containing the sequence of 394-1296 under the accession number XM_749237.1 at GenBank.	this thesis
pXY03	*AFUA_3G12910* from *A. fumigatus* Af293 between the sites BamHI and BglII of pQE60 for expression in *E. coli*, containing the entire coding sequence of *AFUA_3G12910* (10-1296 under the accession number XM_749237.1 at GenBank). 389 bp BamHI-BamHI fragment from pXY01 was cloned into the site BamHI in pXY02 to give pXY03.	this thesis
pXY11	*AFUA_3G12960* from *A. fumigatus* B5233 in pGEM-T easy, containing the PCR product (58-1228, 1262-1653 under the accession number XM_749232.1 at GenBank) by using cDNA from a cDNA library of *A. fumigatus* B5233 as template and AFUA_3G12960_1 as well as	this thesis

	AFUA_3G12960_2 as primers.	
pXY12	Construct of *AFUA_3G12960* from *A. fumigatus* B5233 in pESC-URA for expression in *S. cerevisiae*, containing the entire coding sequence of *AFUA_3G12960* (58-1228, 1262-1653 under the accession number XM_749232.1 at GenBank). 1569 bp XhoI-NheI fragment from pXY11 was cloned into the same sites in pESC-URA to give pXY12.	this thesis
pXY13	Co-expression construct of *AFUA_3G12960* from *A. fumigatus* B5233 with *NFIA_083630* from *N. fischeri* in pESC-URA for *S. cerevisiae*, containing the entire coding sequence of *AFUA_3G12960* (58-1228, 1262-1653 under the accession number XM_749232.1 at GenBank). 1569 bp XhoI-NheI fragment from pXY11 was cloned into the same sites in pVW41 to give pXY13.	this thesis
pXY14	Construct of *AFUA_3G12960* (58-1228, 1262-1653 under the accession number XM_749232.1 at GenBank) with six His residues, obtained by inserting a double-stranded oligonucleotide (prepared from PXY12-1 and PXY12-2) into the sites BamHI and XhoI of the plasmid pXY12 to give pXY14.	this thesis
pYL09	Construct of *5-dmats* from *A. clavatus* NRRL1 between the sites SphI and BglII of pQE70 for expression in *E. coli.*	(Yu *et al.*, 2012)

Table 3-4: List of oligonucleotides used in this thesis.

Primer	Sequence (5'→3')	Plasmid
AFUA_3G12910_1	TGGGATCCGAACTTGAGCATTTGA (BamHI)	pXY01
AFUA_3G12910_2	CCAGATCTCAACTCAGACTCCCATT (BglII)	pXY01
AFUA_3G12910_3	GGTAGATGGAGTTTTTGCTTTTACGAACAGCAAGG	pXY01
AFUA_3G12910_4	CCTTGCTGTTCGTAAAAGCAAAAACTCCATCTACC	pXY01
AFUA_3G12960_1	AACTCGAGGATTCCGCTCAACCTA (XhoI)	pXY11
AFUA_3G12960_2	TAGCTAGCTCAAGACTCTCTTGGC (NheI)	pXY11
PXY12-1	GATCCATGCATCATCATCATCATCATTCCGGAC (BamHI + ATG + CAT×6 + BspEI + XhoI)	pXY14
PXY12-2	TCGAGTCCGGAATGATGATGATGATGATGCATG (XhoI + BspEI + ATG×6 + CAT + BamHI)	pXY14

3.3 Gene cloning

3.3.1 PCR amplification

Table 3-5: Standard components for PCR amplification from gDNA or cDNA. Expand High Fidelity Kit (Roche, Mannheim) was used.

Substance	Final concentration
gDNA or cDNA	ca. 3 nmol/µl
primers (10 pmol/µl)	each 0.2 pmol/µl
dNTPs (each 10 mM)	each 0.2 mM
Expand High Fidelity Buffer (10×)	1 ×
Expand High Fidelity Enzyme mix (3.3 U/µl)	0.05 U/µl
final volume	50 µl

Table 3-6: Components for the second round PCR to amplify *hasC.* Expand High Fidelity Kit (Roche, Mannheim) was used.

Substance	Final concentration
PCR products of the two exons	a molar ratio of 1:1
primer AFUA_3G12910_1	0.2 pmol/µl
primer AFUA_3G12910_2	0.2 pmol/µl
dNTPs (each 10 mM)	each 0.2 mM
Expand High Fidelity Buffer (10×)	1 ×
Expand High Fidelity Enzyme mix (3.3 U/µl)	0.05 U/µl
final volume	50 µl

Table 3-7: Conditions used for PCR amplification.

Step	Temperature	Duration	Cycles
initialization	94 °C	5 min	1 x
denaturation	94 °C	45 sec	30 x
annealing	60 °C for *hasC* 52 °C for *hasH*	1 min	
elongation	72 °C	1 min 30 sec for *hasC* 2 min for *hasH*	
final elongation	72 °C	10 min	1 x
final hold	4 °C	forever	final temperature

The coding regions of *hasC* and *hasH* were amplified by using gDNA from the BAC AfB28B10 of *A. fumigatus* Af293 and cDNA from a cDNA library of *A. fumigatus* B5233 as templates, respectively. Fusion PCR consisting of two rounds was used for amplification of *hasC* from gDNA. In the first round, primers AFUA_3G12910_1 and AFUA_3G12910_4 were used for amplification of the first exon of *hasC* (239 bp), and AFUA_3G12910_2 and AFUA_3G12910_3 for the second exon of *hasC* (1099 bp). Then the PCR products of the two exons from the first round PCR were used as templates (in a molar ratio of 1:1) for the second round PCR in the presence of primers AFUA_3G12910_1 and AFUA_3G12910_2 to

obtain the entire coding region of *hasC* (1303 bp). Amplification of *hasH* (1579 bp) was performed with primers AFUA_3G12960_1 and AFUA_3G12960_2. The components and conditions for PCR reactions are listed in Tables 3-5, 3-6 and 3-7.

3.3.2 DNA sequencing and sequence analysis

DNA sequencing of the plasmids were performed by Eurofins MWG Operon (Ebersberg) and Sequence Laboratories Göttingen GmbH (Göttingen) by using Chain-termination methods. Sequence identities were obtained by alignments of amino acid sequences using the program “BLAST 2 SEQUENCES” (www.ncbi.nlm.nih.gov). Multiple sequence alignments at the amino acid level were carried out with ClustalW2 (http://www.ebi.ac.uk/Tools/msa/clustalw2). The hydrophobic transmembrane domains of the putative cytochrome P450 protein HasH were analyzed by the SOSUI server (http://bp.nuap.nagoya-u.ac.jp/sosui/) and the TMHMM server v.2.0 (http://www.cbs.dtu.dk/services/TMHMM/).

3.4 Protein overproduction

3.4.1 Growth media

All growth media were sterilized at 121 °C for 20 min.

Luria-Bertani (LB) medium

LB medium contains 1.0% (w/v) tryptone, 1.0% (w/v) NaCl and 0.5% (w/v) yeast extract.
Add the corresponding antibiotics before use.
Solid medium for agar plates contains 2% (w/v) agar.

Terrific-Broth (TB) medium

TB medium contains 12 g tryptone, 24 g yeast extract and 4 ml glycerol for per 900 ml medium.
Add 100 ml sterile potassium phosphate buffer (0.17 M KH_2PO_4 and 0.72 M K_2HPO_4) and the corresponding antibiotics to per 900 ml medium before use.
Solid medium for agar plates contains 2% (w/v) agar.

SCU (synthetic medium devoid of uracil) minimal medium

SCU minimal medium contains 0.67% (w/v) yeast nitrogen base (without amino acids but with ammonium sulfate), 0.01% each of adenine, arginine, cysteine, leucine, lysine,

threonine and tryptophan, 0.005% each of aspartic acid, histidine, isoleucine, methionine, phenylalanine, proline, serine, tyrosine and valine.
Add filter-sterilized carbon source after cooling down, *i.e.* glucose and galactose with a final concentration of 2% and 3% in medium, respectively.
Solid medium for agar plates contains 2% (w/v) agar.

3.4.2 Gene expression in *Escherichia coli* and purification of proteins

E. coli cells harboring an expression plasmid were cultivated in 2000 ml Erlenmeyer flasks containing 1000 ml liquid TB or LB medium supplemented with the respective antibiotics, and then grown at 37 °C to an adsorption of approximate 0.6 at 600 nm. For induction, isopropyl β-thiogalactopyranoside (IPTG) was added to a final concentration of 0.1-1.0 mM and the cells were cultivated for further 6-16 h at 22-37 °C before harvest. The cells were collected by centrifugation and stored at -20 °C.
Protein purification was performed at 4 °C. The cell pellets were resuspended in lysis buffer (10 mM imidazole, 50 mM NaH_2PO_4 and 300 mM NaCl, pH 8.0) at 2-5 ml per gram wet weight. After addition of lysozyme to a final concentration of 1 $mg \cdot ml^{-1}$ and incubation for 30 min, the cells were sonicated six times for 10 s each at 200 W, with 10 s for cooling after each burst. To separate soluble proteins from cellular debris, the lysate was centrifuged at 13,000 rpm for 30 min. The supernatant was mixed with nickel-nitrilotriacetic acid (Ni-NTA) agarose resin (Qiagen, Hilden) according to the manufacturer's instruction and then stirred for 1 h. The mixture was then loaded to an 8 ml empty column with bottom sieve. The obtained residue was washed with 4 ml wash buffer (20 mM imidazole, 50 mM NaH_2PO_4 and 300 mM NaCl, pH 8.0) for twice, followed by elution of protein with 2.5 ml elution buffer (250 mM imidazole, 50 mM NaH_2PO_4 and 300 mM NaCl, pH 8.0). Finally, the protein was obtained after buffer changing by using a PD-10 column with Sephadex G-25 (GE Healthcare, Freiburg), which has been equilibrated with PD-10 buffer (50 mM Tris-HCl containing 15% (v/v) glycerol, pH 7.5). The aliquots of purified protein were stored at -80 °C for enzyme assays and the purity was proven by sodium dodecyl sulfate polyacrylamide gel electrophoresis (SDS-PAGE).

3.4.3 Gene expression in *Saccharomyces cerevisiae* and purification of proteins

S. cerevisiae cells harboring an expression plasmid were grown in 2000 ml Erlenmeyer flasks with 400 ml SCU minimal medium containing 2% (w/v) glucose at 30°C and 300 rpm for 24 h. Then the cells were washed with SCU minimal medium without glucose for twice and subsequently cultivated in 2000 ml Erlenmeyer flasks with 400 ml SCU liquid medium containing 3% (w/v) galactose for further 23 h before harvest by centrifugation (5 min, 3,000 × g, 4°C).

Protein purification was performed at 4 °C. The cell pellets were resuspended in 250 µl 50 mM Tris-HCl (pH 7.5) for per 100 ml culture. After transfer of the suspension into a mortar with liquid nitrogen by using an injection syringe, the frozen suspension was grinded into fine powder. Then per volume of the powder was resuspend in 2 volumes buffer containing 50 mM Tris-HCl pH 7.5, 15 % (v/v) glycerol, 1 mM DTT, 1 mM EDTA, 1 µM FAD, 1 µM FMN and 1 mM PMSF (add freshly before use), and the mixture was stirred on ice for 1h. After centrifugation at a low speed (20,000 × g, 20 min, 4°C), the obtained supernatant was centrifuged at a high speed (200,000 × g, 1 h 30 min, 4°C) to separate “microsomes” (pellet) from the “soluble proteins” (supernatant). The “microsomes” was resuspended in 50 mM Tris-HCl (with 15 % glycerol, pH 7.5). For the recombinant His_6-tagged fusion protein, affinity chromatography with Ni-NTA agarose resin (Qiagen, Hilden) was used for purification after centrifugation at the low speed. “Soluble proteins”, “microsomes” and “purified His_6-tagged protein” were detected on SDS-PAGE gel by using Western Blot for the myc epitope tagged proteins and Coomassie Brilliant Blue dye staining for the His_6-tagged protein. All these proteins were stored at -80 °C and used for further experiments.

3.5 Enzyme assays

3.5.1 Assays with prenyltransferases

The enzyme reaction mixtures (100 µl) for determination of the relative activities with different aromatic substrates contained 50 mM Tris-HCl (pH 7.5), 5 or 10 mM $CaCl_2$, 0.5-1 mM aromatic substrate, 1-2 mM DMAPP, GPP or FPP, 0.15-5% (v/v) glycerol, 0-5% (v/v) DMSO and 1-20 µg of purified recombinant protein. The reaction mixtures were incubated at 30 or 37 °C for 0.5-24 h. The enzyme reactions were terminated by addition of 100 µl methanol per 100 µl reaction mixture or extraction with ethyl acetate for three times. For determination of kinetic parameters, protein amount and incubation time in the linear region of reactions were used.

To isolate the enzyme products, reactions were carried out in large scales (5-50 ml) with the same condition described above. After incubation for overnight, reaction mixtures were treated in different ways due to solubility difference of the enzyme products. For assays with simple indoles, the reactions were terminated by addition of 1 volume of methanol each. After removal of the precipitated protein by centrifugation at 13,000 rpm for 20 min, the reaction mixtures were concentrated on a rotating vacuum evaporator at 30 °C to a final volume of 1 ml before injection onto HPLC. For assays with tryptophan-containing cyclic dipeptides, indolocarbazoles, hydroxynaphthalenes or flavonoid aglycones, the reaction mixtures were extracted three times with ethyl acetate. After evaporation of the solvent, the

residues of the ethyl acetate phase containing both substrate and enzyme products were dissolved in methanol before injection onto HPLC.

3.5.2 Assays with the putative methyltransferase HasC

The enzyme reaction mixtures (100 µl) contained 50 mM Tris-HCl (pH 7.5), 5 mM $MgCl_2$ or KCl, 1 mM aromatic substrate, 0.5 mM *S*-adenosyl methionine (SAM), 0.15-5% (v/v) glycerol, 0-5% (v/v) DMSO and 10 µg of purified recombinant protein. The enzyme reactions were terminated by addition of 100 µl methanol. The proteins were removed by centrifugation at 13,000 rpm for 20 min.

3.5.3 Assays with the putative cytochrome P450 enzyme HasH

The enzyme reaction mixtures (100 µl) contained 50 mM Tris-HCl (pH 7.5), 0.1-1 mM aromatic substrate, 1 mM freshly prepared NADPH and NADH, 0-5 mM $MgCl_2$, 0-5 mM freshly prepared $Fe(NH_4)_2(SO_4)_2$, 5-15% glycerol and different fractions of proteins (see section 3.4.3). The enzyme reactions were terminated by addition of 100 µl methanol or extraction with ethyl acetate for three times.

3.6 Analytic methods

3.6.1 HPLC methods

HPLC on an Agilent series 1200 with a Multospher 120 RP-18 column (250 x 4 mm, 5 µm, C+S Chromatographie Service, Langenfeld) at a flow rate of 1 ml•min^{-1} was used for analysis of incubation mixtures. A non-gradient HPLC method with acetonitrile and water as solvents was used for analysis of incubation mixtures of four cyclo-Trp-Ala and four cyclo-Trp-Pro isomers with AnaPT, CdpC3PT and CdpNPT, while different gradient HPLC methods by increasing methanol (with or without 0.5% TFA) in water (with or without 0.5% TFA) were used for analysis of those with other aromatic substrates. For isolation of enzyme products, the same HPLC equipment with a Multospher 120 RP-18 column (250×10 mm, 5 µm, C+S Chromatographie) was used at a flow rate of 2.5 ml•min^{-1}. Enzyme products were purified by using gradient methods by increasing methanol in water or acetonitrile in water.

3.6.2 NMR spectroscopic analysis and high-resolution mass spectrometry

NMR spectra were recorded on a JEOL ECX-400, JEOL ECX-500, Bruker Avance 500 MHz or Bruker Avance 600 MHz spectrometer. Chemical shifts were referenced to the signal of acetone-d_6 at 2.05 ppm, $CDCl_3$ at 7.26 ppm, CD_3OD at 3.31 ppm or DMSO-d_6 at 2.50 ppm.

All spectra were processed with MestReNova 5.2.2. The isolated products were also analyzed by mass spectroscopy on a Q-Trap Quantum (Applied Biosystems) using a high resolution electron spray ionization (HR-ESI) mode or on an Auto SPEC with an electron impact (HR-EI) mode.

4 Results and discussion

4.1 Biochemical characterization of a cyclic dipeptide prenyltransferase CdpC3PT from *Neosartorya fischeri*

Based on the bioinformatic analysis of prenyltransferase genes from the genome sequence of *N. fischeri* NRRL181, one putative gene *NFIA_074280* was found. Its deduced product, EAW17508, showed significant sequence similarity to known indole prenyltransferases of the DMATS superfamily. To identify its function, the coding sequence of *NFIA_074280*, termed *cdpC3PT*, was amplified from gDNA by fusion PCR through three rounds reactions. The PCR fragment consisting exclusively of the two exons was cloned *via* pGEM-T easy vector into pQE60, resulting in the expression construct pWY25. The plasmid pWY25 was transformed into *E. coli* for protein overproduction. The soluble His_6-tagged protein CdpC3PT was purified with Ni-NTA agarose to near homogeneity as judged by SDS-PAGE. HPLC analysis of incubation mixtures of CdpC3PT with tryptophan-containing cyclic dipeptides in the presence of DMAPP showed clearly the formation of enzyme products. The parts of works described above were carried out by Dr. Wen-Bing Yin. In this thesis, enzyme products of CdpC3PT were isolated on HPLC and their structures were elucidated by HR-ESI-MS and NMR analyses, including ^{1}H- and ^{13}C-NMR analyses as well as by long-range ^{1}H-^{13}C connectivities in heteronuclear multiple-bond correlation (HMBC) spectra. ^{1}H-^{1}H spatial correlations in nuclear overhauser effect spectroscopy (NOESY) were used to determine absolute configuration.

The results showed that CdpC3PT catalyzed regio- and stereospecific reverse prenylations of cyclo-L-Trp-L-Leu, cyclo-L-Trp-L-Trp, cyclo-L-Trp-L-Phe, cyclo-L-Trp-L-Tyr as well as cyclo-L-Trp-Gly and meanwhile the formation of a five-membered ring between the original indole and diketopiperazine rings with a *cis*-configuration between H-2 and C3-dimethylallyl moiety in one-step reaction. To understand the biochemical behavior of CdpC3PT, kinetic parameters were determined for DMAPP and all the five aromatic substrates. The range of K_M as well as the k_{cat} values indicated different preference of CdpC3PT towards these substrates. Comparing the enzyme activity of CdpC3PT with AnaPT, both enzymes catalyzed the formation of reversely C3-prenylated cyclic dipeptides, however, they introduced the prenyl moiety from opposite sides, so that two compounds with different stereochemistry at position C-2 and C-3 can be obtained from one substrate. They therefore complement to each other regarding the prenylation and the results expand their potential usage for chemoenzymatic synthesis.

For details of this work see please the publication (section 5.1):

Yin, W.-B.*, **Yu, X.***, Xie, X.-L. & Li, S.-M. (2010). Preparation of pyrrolo[2,3-b]indoles carrying a ß-configured reverse C3-dimethylallyl moiety by using a recombinant prenyltransferase CdpC3PT. *Org. Biomol. Chem.* 8, 2430-2438. (*: equal contribution)

4.2 Biochemical characterization of a 5-dimethylallyltryptophan synthase from *Aspergillus clavatus*

Before we started this work, a literature search of indole prenyltransferases showed that 20 enzymes from bacteria and fungi have been characterized biochemically (Li, 2010; Yin *et al*., 2010b; Zou *et al*., 2010; Schultz *et al*., 2010; Takahashi *et al*., 2010; Ding *et al*., 2010; Li, 2009). These enzymes catalyzed the transfer of prenyl moieties onto positions N-1, C-2, C-3, C-4, C-6 or C-7 at the indole ring resulting in the formation of “regularly” or “reversely” prenylated derivatives (Figures 1-11 and 1-13). However, a prenyltransferase being responsible for transferring a prenyl moiety onto position C-5 of the indole ring has not been reported. Database searching revealed, on the other hand, the presence of a number of biologically active indole alkaloids carrying a prenyl moiety at position C-5 in nature (see section 1.1.1.3). The discrepancy between the natural occurrence of a large number of C5-prenylated indole derivatives on one hand and undiscovered C5-prenyltransferases on the other hand prompted us to search for such enzymes. One putative prenyltransferase EAW08391, encode by the *ACLA_031240* from the genome sequence of *A. clavatus* NRRL1 raised our attention. EAW08391 shares on the amino acid level sequence identity 52% with 4-dimthylallyltryptophan synthase FgaPT2, therefore it can be expected that EAW08391 catalyzes a similar reaction as FgaPT2. To prove the function of EAW08391, the coding region of *ACLA_031240*, termed *5-dmats*, was amplified by PCR from cDNA synthesized from mRNA. The PCR product was cloned *via* pGEM-T easy vector into pQE70, resulting in the expression construct pYL09. The works described above were carried out by Yan Liu. In this thesis, the plasmid pYL09 was transformed into *E. coli* for overproduction of His_6-5-DMATS. The soluble His_6-tagged protein 5-DMATS was purified to near homogeneity and used for biochemical investigation with diverse aromatic substrates in the presence of different prenyl diphosphates.

Due to the high sequence similarity with tryptophan C4-prenyltransferase FgaPT2 mentioned above, L-tryptophan and 17 simple indole derivatives were firstly incubated with 5-DMATS in the presence of DMAPP. With the exception for C5-substituted derivatives, the most tested simple indole derivatives with modifications at the indole ring or side chain have been well accepted by 5-DMATS with L-tryptophan as the best substrate. A previous study showed that FgaPT2 accepted also tryptophan-containing cyclic dipeptides as substrates (Steffan and Li, 2009). 5-DMATS was therefore assayed with five such cyclic dipeptides in the presence of DMAPP. It has been shown that these compounds were also substrates for 5-DMATS, but

accepted with significantly lower yields than most of the simple indole derivatives in the presence of DMAPP. In addition, 5-DMATS was also incubated with L-tyrosine in the presence of DMAPP or with L-tryptophan in the presence of GPP or FPP. However, no formation of any enzyme product was detected in these assays.

To confirm the prenylation position, enzyme products of 12 well accepted substrates were isolated on HPLC and subjected to HR-ESI-MS and NMR analyses. The results revealed unequivocally the highly regioselective regular prenylation at C-5 of the indole nucleus of the 12 enzyme products. 5-DMATS was therefore a 5-dimethylallyltryptophan synthase and filled therewith the last gap in the toolbox of indole prenyltransferases regarding their prenylation positions. To study the behavior of 5-DMATS towards indole derivatives and DMAPP, kinetic parameters including K_M and k_{cat} values, were determined. K_M values of 5-DMATS were found for L-tryptophan and DMAPP at 34 µM and 76 µM, respectively. Average k_{cat} value at 1.1 s^{-1} was calculated from kinetic data of L-tryptophan and DMAPP. Catalytic efficiencies of 5-DMATS were detected for L-tryptophan at 25,588 $s^{-1} \cdot M^{-1}$ and for other 11 simple indole derivatives up to 1,538 $s^{-1} \cdot M^{-1}$. It can be therefore expected that 5-DMATS could serve as an effective biocatalyst for chemoenzymatic synthesis of prenylated derivatives in the program of drug discovery and development.

For details of this part see please the publication (section 5.2):

Yu, X., Liu, Y., Xie, X., Zheng, X.-D. & Li, S.-M. (2012). Biochemical characterization of indole prenyltransferases: Filling the last gap of prenylation positions by a 5-dimethylallyltryptophan synthase from *Aspergillus clavatus*. *J. Biol. Chem.* 287, 1371-1380.

4.3 Biochemical characterization of a brevianamide F reverse prenyltransferase BrePT from *Aspergillus versicolor*

A prenyltransferase NotF involved in the biosynthesis of notoamides in *Aspergillus* sp. MF297-2 was reported by the work group of Prof. Sherman from University of Michigan (Ding *et al.*, 2010). NotF is responsible for the reverse prenylation of brevianamide F at position C-2 of the indole ring resulting in the formation of deoxybrevianamide E and uses a limited number of compounds as clearly favorable prenylation substrates. The low flexibility of NotF towards aromatic substrates prohibits its usage as biocatalyst for production of desired compounds. It was necessary to find a NotF homologue with broad substrate specificity and to be used as biocatalyst for synthesis of reversely C2-prenylated indole derivatives.

Literature search revealed that several *A. versicolor* strains produced brevianamides or notoamides, which are very likely derived from deoxybrevianamide E and therefore a *notF* homologue must be involved in their biosynthesis. To amplify the *notF* homologue *brePT* from *A. versicolor* NRRL573, the PCR reaction using primers deduced from *notF* sequence was performed. The PCR fragment was cloned into pET28a *via* pGEM-T easy vector to

create the expression construct pQW2 with a C-terminal His_6-tag. After failed expression with pQW2, *brePT* was recloned in pET28a by introducing five histidine residues directly connected to the C-terminus of the overproduced protein. The new expression vector pSY1 was transformed and overexpressed in *E. coli*. The His_5-BrePT was obtained after one-step purification on Ni-NTA agarose. HPLC analysis of incubation mixtures of BrePT with 14 tryptophan-containing cyclic dipeptides in the presence of DMAPP showed clearly the formation of enzyme products. The works described above were carried out by Qing Wang and Suqin Yin. In this thesis, the enzyme products were isolated and their structures were identified by ^{1}H-NMR and MS analyses. The data proved unequivocally the attachment of the reverse prenyl (tert-prenyl) moiety at C-2 of the indole ring and the regiospecific C2-prenylation catalyzed by BrePT. BrePT showed much higher substrate flexibility than NotF. To study the behavior of BrePT towards DMAPP and twelve different cyclic dipeptides, kinetic parameters including K_M and k_{cat} values, were measured. Average turnover number (k_{cat}) at 0.4 s^{-1} was calculated from kinetic data of brevianamide F and DMAPP. K_M values in the range of 0.082-2.9 mM and k_{cat} values from 0.003 to 0.15 s^{-1} were determined for other eleven cyclic dipeptides. To test the acceptance of other prenyl donors, GPP or FPP instead of DMAPP was used in the reaction mixtures of the 14 tryptophan-containing cyclic dipeptides and His_5-BrePT. Similar to known fungal indole prenyltransferases, BrePT did not accept GPP or FPP as a prenyl donor for its prenylation.

For details of this work see please the publication (section 5.3):

Yin, S.*, **Yu, X.***, Wang, Q., Liu, X. Q. & Li, S.-M. (2013). Identification of a brevianamide F reverse prenyltransferase BrePT from *Aspergillus versicolor* with a broad substrate specificity towards tryptophan-containing cyclic dipeptides. *Appl. Microbiol. Biotechnol.* 97, 1649-1660. (*: equal contribution)

4.4 Production of enantiomers of *cis*-configured prenylated pyrroloindoline diketopiperazines by fungal indole prenyltransferases

Previously, three C3-prenyltransferases belonging to the DMATS superfamily were identified and characterized biochemically in our group (Yin *et al*., 2009; Yin *et al*., 2010b; Schuller *et al*., 2012), *i.e.*, AnaPT and CdpC3PT from *N. fischeri* and CdpNPT from *A. fumigatus*. They could introduce a dimethylallyl moiety to position C-3 of the tryptophanyl moiety and catalyze the formation of a five-membered ring between the original indole and diketopiperazine rings with a *cis*-configuration between H-2 and C3-dimethylallyl moiety to produce prenylated pyrroloindoline diketopiperazines. However, the used cyclic dipeptides usually contained only L-configured amino acid moieties, and little was known about their behavior on substrates with D-configured amino acid moieties. This feature prohibits their usage as biocatalysts for

producing stereoisomers of prenylated pyrroloindoline diketopiperazines. In order to understand the different stereoselectivity of AnaPT, CdpC3PT and CdpNPT, four cyclo-Trp-Ala and four cyclo-Trp-Pro isomers were synthesized and incubated with these enzymes in the presence of DMAPP.

HPLC analysis showed that all the substrates were accepted by AnaPT, CdpC3PT and CdpNPT in the incubation mixtures. The enzyme products were isolated on HPLC from incubation mixtures and their structures were elucidated by NMR and MS analyses as prenylated pyrroloindoline diketopiperazines. The results showed that AnaPT always transfer the prenyl moiety to C-3 at the opposite side to the carbonyl moiety at C-11 to produce *anti-cis* configured prenylated pyrroloindoline diketopiperazines, while CdpC3PT transfer it to C-3 at the same side as the carbonyl moiety at C-11 to produce *syn-cis* configured prenylated pyrroloindoline diketopiperazines. Therefore, it could be concluded that the stereospecificity of AnaPT and CdpC3PT depends largely on the configuration of tryptophanyl moiety in cyclic dipeptides. CdpNPT was reported to catalyze the same reaction as CdpC3PT in the previous study (Schuller *et al.*, 2012). However, we found in this thesis that CdpNPT could also produce enzyme products catalyzed by AnaPT. CdpNPT could catalyze the formation of both *anti-cis* and *syn-cis* configured prenylated pyrroloindoline diketopiperazines but showed different stereoselectivity towards isomers of cyclo-Trp-Ala and cyclo-Trp-Pro. It is likely that not the configuration of amino acids moiety in cyclic dipeptides, but the structure of the second amino acid moiety plays an important role for the stereoselectivity of CdpNPT.

The enzyme reactions with tested substrates catalyzed by AnaPT and CdpC3PT always complemented to each other, and the stereoselectivity of both enzymes were approximately 100%. Although CdpNPT showed lower stereoselectivity compared to AnaPT and CdpC3PT, higher conversion ability towards most tested substrates was observed. Thereby CdpNPT could be useful for prenylation of poor substrates of AnaPT and CdpC3PT. These results expand the usage of the three C3-prenyltransferases as biocatalysts for production of stereoisomers of prenylated pyrroloindoline diketopiperazines.

For details of this work see please the manuscript (section 5.4):

Yu, X., Xie, X. & Li, S.-M., Complementary stereospecific synthesis of *cis*-configured prenylated pyrroloindoline diketopiperazines by indole prenyltransferases of the DMATS superfamily. (manuscript)

4.5 Production of prenylated indolocarbazoles by using 5-DMATS and FgaPT2 from *Aspergillus*

Indolocarbazoles are a class of natural products with well known remarkable biological activities, especially their inhibitory effects against protein kinases in various organisms (Sánchez *et al.*, 2006; Nakano and Ômura, 2009). However, prenylated indolocarbazoles

have been reported, neither from natural sources, nor from chemical synthetic approaches, although diverse prenylated carbazoles have been isolated from different sources (Schmidt *et al.*, 2012). In this thesis, we used prenyltransferases of the DMATS superfamily to catalyze regiospecific prenylation of indolocarbazoles.

For this purpose, four indolocarbazoles arcyriaflavin A, N6-methylarcyriaflavin A, K252c and 7-hydroxy-K252c and two non-bridged intermediates arcyriarubin A and N-methylarcyriarubin A were synthesized. The six synthesized compounds together with two indolocarbazole glycosides staurosporine and K252d, which had been isolated from *Streptomyces nitrosporeus* CQT14-24, were incubated with nine prenyltransferases of the DMATS superfamily in the presence of DMAPP. The tested enzymes included five cyclic dipeptide prenyltransferases AnaPT, BrePT, CdpC3PT, CdpNPT and FtmPT1, three dimethylallyltryptophan synthases FgaPT2, 5-DMATS and 7-DMATS and one tyrosine *O*-prenyltransferase SirD (Yin *et al*., 2010a; Yin *et al*., 2013a; Yin *et al*., 2010b; Schuller *et al*., 2012; Grundmann and Li, 2005; Steffan *et al*., 2007; Yu *et al*., 2012; Kremer and Li, 2008; Kremer and Li, 2010). HPLC analysis showed that 5-DMATS from *A. clavatus* and FgaPT2 from *A. fumigatus* displayed more substrate flexibilities towards the tested substances than other enzymes and were studied in details.

Arcyriaflavin A was poor substrates for both 5-DMATS and FgaPT2, while other three indolocarbazoles were clearly accepted. The two non-bridged intermediates of indolocarbazoles were not accepted by 5-DMATS and FgaPT2, indicating the importance of the presence of the indolocarbazole skeleton. Glycosides of indolocarbazoles were also not substrates for the enzymes of the DMATS superfamily.

The enzyme products were isolated and their structures were elucidated by NMR and MS analyses. C3-prenylated products were isolated from the incubation mixtures of K252c and 7-hydroxy-K252c with both 5-DMATS and FgaPT2 as well as the incubation mixture of N6-methylatedarcyriaflavin A with 5-DMATS. In addition to those products, C9-prenylation and diprenylation at both C-3 and C-9 were also catalyzed by 5-DMATS in the incubation mixture with K252c. This proved that both 5-DMATS and FgaPT2 catalyzed regiospecific C-prenylation on the indolocarbazole system, *i.e.* the *para*-position to the indole N-atom (C3, C9 or both) and function therefore as biocatalysts for Friedel-Crafts alkylations. To elucidate the behavior of 5-DMATS and FgaPT2 towards indolocarbazoles, kinetic parameters were determined for the best accepted substrate 7-hydroxy-K252c with both enzymes. K_M values were calculated to be at 87 and 136 μM for 5-DMATS and FgaPT2, respectively, while k_{cat} values were found at 6.8 and 7.3 min^{-1}. This work expands the potential usage of enzymes of the DMATS superfamily in the structural modifications. To best of our knowledge, this is the first reported on the (chemoenzymatic) synthesis of prenylated indolocarbazoles.

For details of this work see please the publication (section 5.5):

Yu, X., Yang, A., Lin, W. & Li, S.-M. (2012). Friedel-Crafts alkylation on indolocarbazoles catalyzed by two dimethylallyltryptophan synthases from *Aspergillus*. *Tetrahedron Lett.* 53, 6861-6864.

4.6 Production of prenylated hydroxynaphthalenes by using fungal indole prenyltransferases

As described in section 1.3.6, fungal prenyltransferases of the DMATS superfamily share no sequence, but structure similarity with prenyltransferases of the CloQ/NphB group. However, an acceptance of substrates for CloQ/NphB group by a member of the DMATS superfamily was not reported previously. This prompted us to investigate the acceptance of hydroxynaphthalenes by enzymes of the DMATS superfamily.

For initial investigation, eight prenyltransferases of the DMATS superfamily including five cyclic dipeptide prenyltransferases AnaPT, CdpC3PT, CdpNPT, CTrpPT and FtmPT1, two dimethylallyltryptophan synthases FgaPT2 and 7-DMATS and one tyrosine O-prenyltransferase SirD (Yin *et al*., 2010a; Yin *et al*., 2010b; Schuller *et al*., 2012; Grundmann and Li, 2005; Zou *et al*., 2010; Steffan *et al*., 2007; Kremer and Li, 2008; Kremer and Li, 2010) were incubated with the simple naphthalene derivative 1-naphthol in the presence of DMAPP. HPLC analysis showed clear formation of one additional peak each in all the incubation mixtures with an exception of SirD. The intriguing results obtained with 1-naphthol encouraged us to test the acceptance of more hydroxynaphthalenes by the members of the DMATS family. Five enzymes including AnaPT, CdpC3PT, CdpNPT, 7-DMATS and SirD were selected for incubation with naphthalene and 11 hydroxynaphthalenes in the presence of DMAPP. HPLC analysis showed that non-hydroxylated naphthalene was not accepted by the tested enzymes, indicating the importance of an activation of the naphthalene ring, *e.g.* by hydroxylation. Most of the 11 hydroxynaphthalenes were accepted by AnaPT, 7-DMATS, CdpNPT and CdpC3PT, while they were very poor substrates for SirD. The enzyme activities and preference of the tested prenyltransferases towards hydroxynaphthalenes differed clearly from each other.

For structure elucidation, enzyme products were isolated on HPLC and sent for NMR and MS analyses. Inspection of the structures of the enzyme products revealed clearly that different enzymes catalyzed usually the formation of the same major prenylated product. The prenylation has preferentially taken place at *para*-position of the hydroxyl group at C-1. If this was impossible, the *ortho*-position to the hydroxyl group at C-2 was prenylated. Regularly O-prenylated and diprenylated derivatives were also identified as enzyme products of substrates with low conversion rates and regioselectivity. To get information on the catalytic efficiencies of indole prenyltransferases towards hydroxynaphthalenes, kinetic parameters of AnaPT, CdpNPT, CdpC3PT and 7-DMATS with six selected substrates were determined.

The K_M and k_{cat} values were determined to be in the range of 0.064-2.8 mM and 0.038-1.30 s^{-1}, respectively. These data are in the similar concentration range as those for indole derivatives. In this study, we have shown that the substrate specificity of the members of the DMATS superfamily towards hydroxynaphthalene derivatives doesn't correlate with those obtained for tyrosine or indole derivatives, and provided experimental evidence for their potential application as biocatalysts for chemoenzymatic synthesis of prenylated hydroxynaphthalenes.

For details of this work see please the publication (section 5.6):

Yu, X., Xie, X. & Li, S.-M. (2011). Substrate promiscuity of secondary metabolite enzymes: prenylation of hydroxynaphthalenes by fungal indole prenyltransferases. *Appl. Microbiol. Biotechnol.* 92, 737-748.

4.7 Production of prenylated flavonoids by using 7-DMATS from *Aspergillus fumigatus*

Prenylated flavonoids are a group of compounds predominantly found in plants (Botta *et al.*, 2009; Botta *et al.*, 2005b). Due to their broad pharmacological activities (Botta *et al*., 2009; Botta *et al*., 2005b; Wätjen *et al.*, 2007), various strategies have been developed for both regioselective chemical and chemoenzymatic synthesis of prenylated flavonoids, especially for C-prenylated derivatives (Tischer and Metz, 2007; Hossain *et al.*, 2006; Yazaki *et al.*, 2009). In previous studies, many prenylated flavonoids have been produced by using recombinant enzymes (Sasaki *et al.*, 2011; Sasaki *et al.*, 2008; Ozaki *et al.*, 2009; Kumano *et al*., 2008). However, only a few of such derivatives carry a dimethylallyl moiety at position C-6. Our studies in section 4.6 have shown that several members of the DMATS superfamily accepted also hydroxynaphthalene derivatives. These results encouraged us to test the acceptance of flavonoids including chalcones, flavanones and isoflavonoids by the members of the DMATS superfamily.

For initial investigation, seven fungal prenyltransferases including 7-DMATS, AnaPT, CdpC3PT, CdpNPT, SirD, FtmPT1 and FgaPT2 (Yin *et al*., 2010a; Yin *et al*., 2010b; Schuller *et al*., 2012; Grundmann and Li, 2005; Steffan *et al*., 2007; Kremer and Li, 2008; Kremer and Li, 2010) were incubated with up to thirty flavonoids in the presence of DMAPP. HPLC analysis showed that 7-DMATS has a more flexible substrate specificity towards these compounds than other enzymes. Detailed study was therefore carried out with 7-DMATS from *A. fumigatus*. 7-DMATS was then incubated with 16 flavonoids and analogues in the presence of DMAPP. Product formation was detected for 14 substrates after incubation with 14 µg protein per 100 µl assay at 37°C for 16 h. Six of them, *i.e.* genistein, biochanin A, naringenin, eriodictyol, hesperetin and phloretin, represented a yield of more than 12% and were selected for further research.

For structure elucidation, enzyme products of the six substrates were isolated on HPLC and sent for NMR and MS analyses. The results showed that C6-prenylated products were found in all the six incubation mixtures. In cases of eriodictyol and hesperetin, products with prenylation at ring B were also isolated from the incubation mixtures. From the structures of the enzyme products, it is obviously that the favorable prenylation position for 7-DMATS was C-6 between the two hydroxyl groups. To get information on the catalytic efficiencies of 7-DMATS towards flavonoids, kinetic parameters were determined for the six substrates. The K_M and k_{cat} values for flavonoids were determined to be in the range of 0.07-1.26 mM and 0.02-0.4 s^{-1}, respectively. These data provided evidence that the tryptophan prenyltransferase 7-DMATS can also be used for production of prenylated flavonoids, especially for C6- or ring B-prenylated flavanones and isoflavonoids by chemoenzymatic approach and therefore complements the production gap of other reported prenyltransferases for prenylated flavonoids (Kumano *et al*., 2008; Ozaki *et al*., 2009; Sasaki *et al*., 2011; Botta *et al.*, 2005a).

For details of this work see please the publication (section 5.7):

Yu, X., Li, S.-M. (2011). Prenylation of flavonoids by using a dimethylallyltryptophan synthase 7-DMATS from *Aspergillus fumigatus*. *Chembiochem* 12, 2280-2283.

4.8 Prenyltransferases of the dimethylallyltryptophan synthase superfamily

Besides the experimental works on prenyltransferases of the DMATS superfamily, general methods for biochemical characterization of these enzymes were summarized in a review article. The first part in this review was devoted to a general introduction of prenyltransferases of the DMATS superfamily. Subsequently the procedures for spore preparation as well as cultivation of fungi were described. RNA and DNA isolation and cDNA synthesis were followed by gene cloning, in which both normal PCR amplification from cDNA and fusion PCR amplification from gDNA were described. Protein overproduction in *E. coli* as well as *S. cerevisiae* and protein purification were detailed after gene cloning.

The next part described details on carrying enzyme assays. General procedures for biochemical characterization of prenyltransferases were then described, including test of enzyme activities and determination of kinetic parameters. For chemoenzymatic synthesis of prenylated compounds, protocols of enzyme reactions and sample preparation before product isolation on HPLC were presented. HPLC components and conditions used for assays with diverse types of substrates were then shown in this review.

For details of this review see please the publication (section 5.8):

Yu, X., Li, S.-M. (2012). Prenyltransferases of the dimethylallyltryptophan synthase superfamily. *Methods Enzymol.* 516, 259-278.

4.9 Cloning and overexpression of a putative methyltransferase gene *hasC* from *Aspergillus fumigatus*

4.9.1 Cloning of *hasC* from *Aspergillus fumigatus*

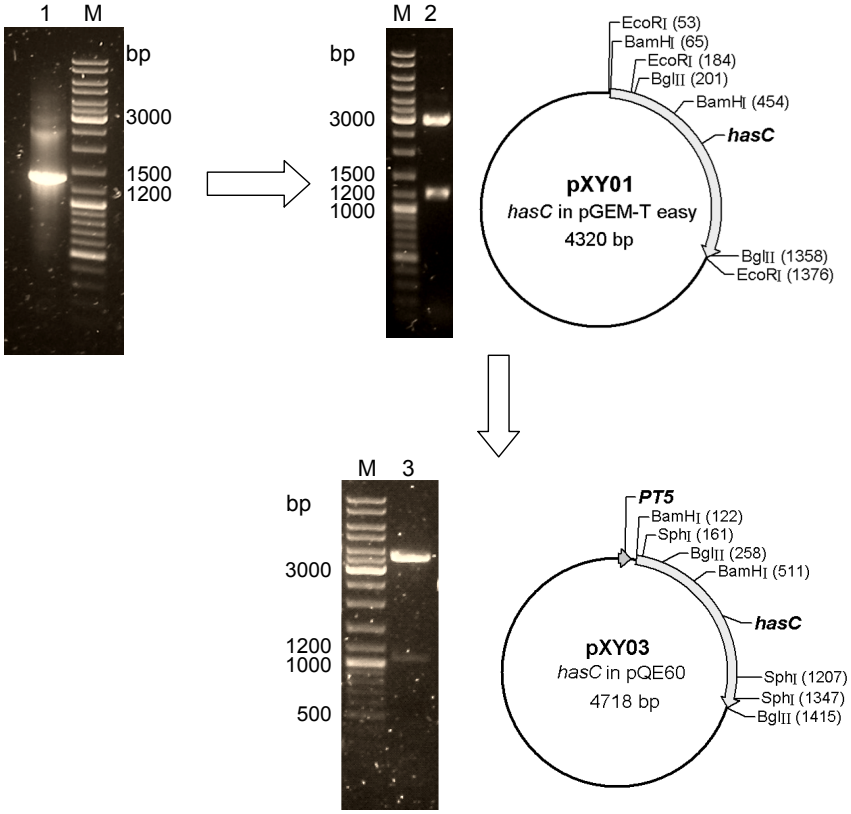

Lane	PCR product or plasmid	Restriction enzyme	Expected sizes (bp)	Observed sizes (kb)
1	PCR product produced after the second round PCR	-	1303	1.3
2	pXY01	EcoRI	131/ 1192/ 2997	1.2/3.0
3	pXY03	SphI	140/1046/3532	1.0/3.5

Figure 4-1: Cloning of *hasC* into pQE60. Lane M: DNA ladder.

The putative methyltransferase gene *hasC* is proposed to be involved in the biosynthesis of a prenylated indole alkaloid HAS in *A. fumigatus* (see section 1.2.1.3). In order to identify the function of *hasC*, the coding sequence of *hasC* was cloned from *A. fumigatus*.

This gene consists of two exons of 223 and 1079 bp interrupted by one intron of 60 bp. The whole coding sequence of *hasC* was amplified from gDNA from the BAC AfB28B10 of *A. fumigatus* Af293 by using two rounds fusion PCR (see section 3.3.1). Primers AFUA_3G12910_1 and AFUA_3G12910_4 as well as AFUA_3G12910_2 and AFUA_3G12910_3 were used for amplification of the first and second exons in the first round PCR, respectively. In the second round of PCR, a PCR fragment of 1303 bp containing the entire coding sequence of *hasC* was obtained by using two PCR products from the first

round as templates in the presence of primers AFUA_3G12910_1 and AFUA_3G12910_2 (Figure 4-1).

The PCR product (1303 bp) was cloned into pGEM-T easy vector resulting in plasmid pXY01 (Figure 4-1), which was subsequently confirmed to be correct by sequencing. The plasmid pXY01 was digested with BamHI alone or together with BglII to obtain BamHI-BamHI fragment of 389 bp and BamHI-BglII fragment of 904 bp, respectively. In order to get the expression construct pXY03 (Figure 4-1), the two fragments were cloned into pQE60 subsequently.

4.9.2 Overexpression of *hasC* in *Escherichia coli*

Table 4-1: Induction conditions tested for expression of *hasC* (pXY03) in *E. coli* XL1 Blue, M15 and SG13009.

Strain	Medium	Temperature (°C)	IPTG (mM)	Induction time (h)	Speed (rpm)
XL1 Blue	LB, TB	37, 30, 22	0.05, 0.1, 0.2, 0.4, 0.6, 0.8	0, 1, 3, 4, 5, 6, 9, 16	220
			0	0, 1, 3, 4, 5, 6, 9, 16, 24, 48, 72	
M15	LB, TB	37, 30, 22	0.1, 0.8	1, 2, 3, 16	
SG13009	TB	30	0	6, 9, 16	
		37, 30, 22	0.05, 0.1, 0.3, 0.5	3, 6, 16	
		4	0.1	5, 16	200
		22	0.1	5, 16	150

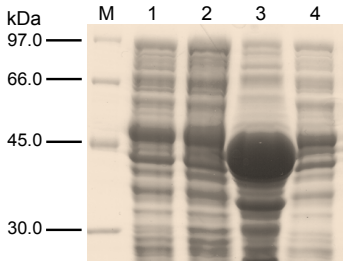

Lane M: protein marker.

Lane 3: total protein obtained after induction without IPTG at 30°C for 16h by using *E. coli* XL1 Blue cells.

Other lanes: total proteins obtained after induction under other conditions.

Figure 4-2: SDS-PAGE analysis of *hasC* overexpression in the absence of IPTG.

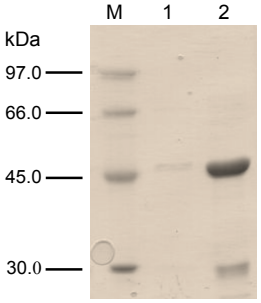

Lane M: protein marker.

Lanes 1 and 2: purified His_6-HasC. Different induction conditions were used. The induction condition for lane 2 was the best condition described above.
Expected size: 49.6 kDa.
Observed size: with migration near the 45.0 kDa size marker.

Figure 4-3: Analysis of purified His_6-HasC on SDS-PAGE.

For overexpression of *hasC*, pXY03 was firstly transformed into *E. coli* XL1 Blue. The cells were induced with IPTG at different conditions (Table 4-1). A high yield of insoluble protein was detected instead of soluble protein. Comparison of the total protein obtained before induction and after induction on SDS-PAGE showed that IPTG was not necessary for gene expression (Figure 4-2, lane 3). Therefore, different induction conditions in the absence of IPTG were tested (Table 4-1). Unfortunately, no soluble protein was obtained. Then another two *E. coli* host strains, *i.e.* M15 and SG13009, were used for overexpression of *hasC.* After condition optimization (Table 4-1), the best condition was found to be 16 h induction in TB medium with 0.1 mM IPTG at 22 °C and 150 rpm by using *E. coli* SG13009 cells (Figure 4-3, lane 2). A yield of 500 µg of purified protein was achieved from 100 ml of bacterial culture. A significant band with migration near the 45.0 kDa size marker was observed on SDS-PAGE of the purified protein, corresponding to the calculated mass of 49.6 kDa for His_6-HasC (Figure 4-3, lane 2).

Table 4-2: Conditions of enzyme assays with HasC.

Substrate	Ion	Other components
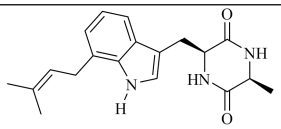 terezine D	5 mM $MgCl_2$	50 mM Tris-HCl (pH 7.5), 0.5 mM SAM, 1 mM tryptophan derivatives, 10 µg protein, in 100 µl assay, 37 °C incubation, 19 h
	5 mM KCl	
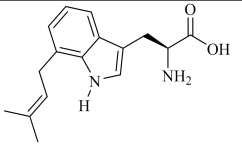 7-dimethylallyl-L-tryptophan	5 mM $MgCl_2$	
	5 mM KCl	
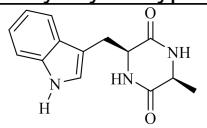 cyclo-L-Trp-L-Ala	5 mM KCl	
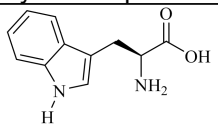 L-tryptophan	5 mM $MgCl_2$	
	5 mM KCl	

Motif search of amino acid sequences revealed the presence of motif I of SAM-dependent methyltransferases in HasC: VVDVGAGVG (238-246 amino acids under the accession number EAL92292 at GenBank). SAM is therefore probably the methyl donor for the reaction catalyzed by HasC (Kagan and Clarke, 1994). HasC doesn't possess the typical CxxxCxxC motif for [4Fe-4S] cluster nucleating (Sofia *et al.*, 2001), indicating that HasC is likely a normal SAM-dependent protein rather than a radical SAM-dependent protein. Enzyme reactions of HasC were carried out with several possible precursors of HAS in the presence of SAM (Table 4-2). Unfortunately, no product formation was observed.

4.10 Cloning of a putative cytochrome P450 gene *hasH* from *Aspergillus fumigatus*

4.10.1 Cloning of *hasH* from *Aspergillus fumigatus*

As described in section 1.2.1.3, the putative cytochrome P450 gene *hasH* is proposed to be involved in the biosynthesis of a prenylated indole alkaloid HAS (Figure 1-8) in *A. fumigatus*. For functional proof of *hasH*, this gene was cloned from *A. fumigatus*.

Sequence analysis showed that *hasH* comprises six exons of 192, 185, 631, 220, 206 and 219 bp, interrupted by five introns of 51, 76, 59, 31 and 56 bp. Multiple alignments of HasH with the two orthologues EAW21272 and EAU31603 (Table 1-1), showed that HasH from *A. fumigatus* contains one additional fragment of 18 amino acids at the N-terminus of the sequence (Figure 4-4), which could be due to a prediction error. So we decided to start the amplification of the coding sequence at the 58th base pair in the sequence.

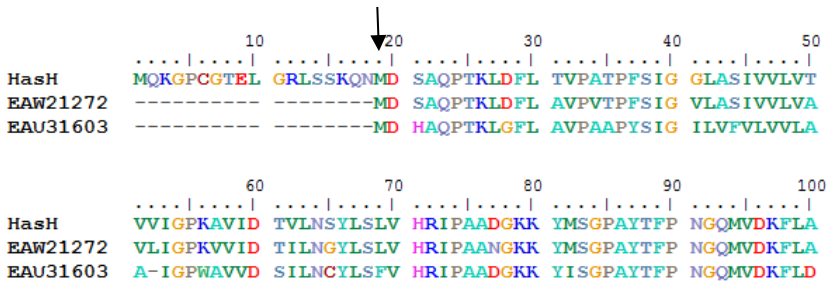

Figure 4-4: Multiple alignment of HasH with the two orthologues EAW21272 and EAU31603.

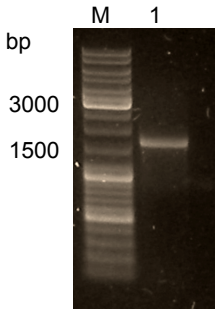

Expected size	Observed size
1612 bp	1.6 kb

Figure 4-5: The entire coding sequence of *hasH* obtained after PCR reaction. Lane M: DNA ladder; lane 1: the PCR product.

The whole coding sequence of *hasH* was amplified by using cDNA from a cDNA library of *A. fumigatus* B5233 as template and primers AFUA_3G12960_1 and AFUA_3G12960_2. A PCR fragment with a size of about 1.6 kb was observed on the agarose gel, corresponding to the calculated size of 1612 bp. The PCR fragment was cloned into pGEM-T easy vector resulting in plasmid pXY11 (Figure 4-6), which was subsequently sequenced to confirm the sequence.

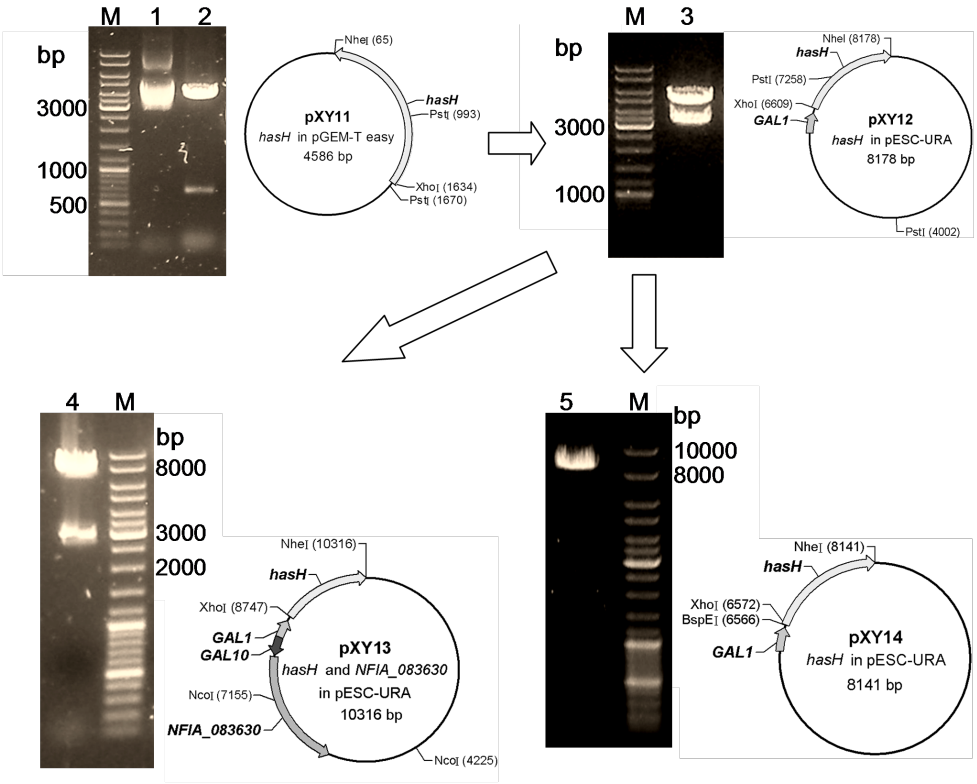

Lane	plasmid	Restriction enzyme	Expected sizes (bp)	Observed sizes (kb)
1	pXY11	Before digestion	-	-
2	pXY11	PstI	677/3909	0.7/4.0
3	pXY12	PstI	3256/4922	3.3/4.9
4	pXY13	NcoI	2930/7386	2.9/7.4
5	pXY14	BspEI	8141	8.1

Figure 4-6: Cloning and expression construction of *hasH*. Lane M: DNA ladder.

Comparing the sequencing results with the sequence of *hasH* obtained from NCBI under the accession number XM_749232.1, one additional gap of 33 bp was found in the PCR product (Figure 4-7, pXY11). This gap was directly connected to one intron in the genome sequence, therefore it could be speculated that the gap was also a part of the intron. Interestingly, the gap was also observed in the homologue gene *NFIA_064360* from *N. fischeri* under the accession number XM_001263168.1 (Figure 4-7), which provided an evidence for our speculation. The true size of the PCR product was calculated to be 1579 bp.

Figure 4-7: Multiple alignment of sequence of pXY11 with the sequence of *hasH* from *A. fumigatus* Af293 and *NFIA_064360* from *N. fischeri* NRRL 181.

Plasmid pXY11 was digested with XhoI and NheI to obtain a fragment of 1569 bp. The XhoI-NheI fragment was cloned into pESC-URA vector to give the single expression vector pXY12 (Figure 4-6). For construct of co-expression vector with a reductase gene, the XhoI-NheI fragment was inserted into pVW41 containing the coding sequence of *NFIA_083630* from *N. fischeri* to give pXY13 (Figure 4-6).

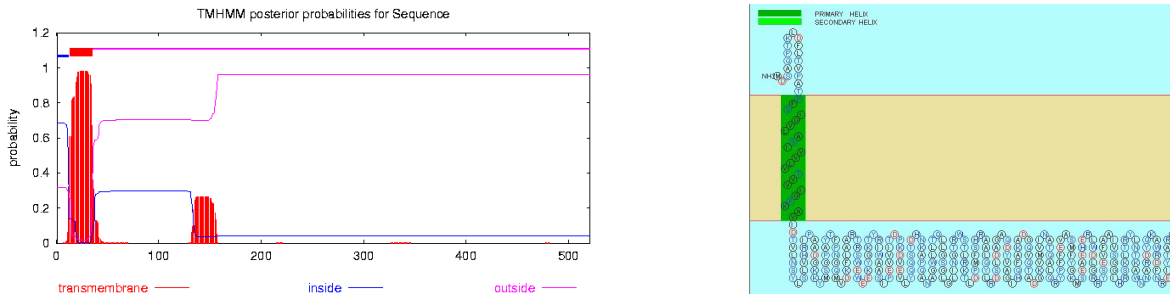

Figure 4-8: Amino acids sequence analysis of HasH by using TMHMM and SOSUI servers.

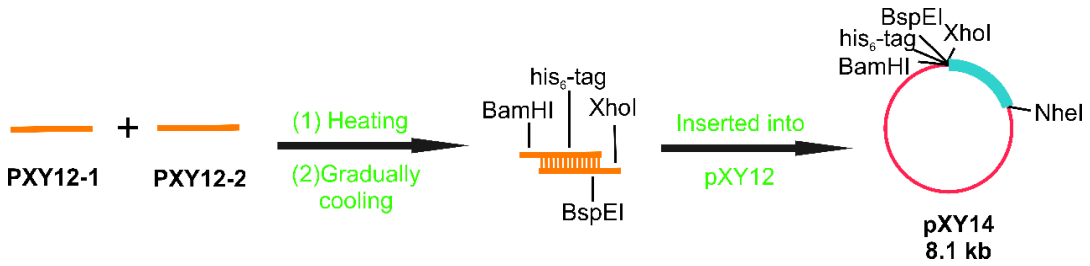

Figure 4-9: Construct of expression vector pXY14.

Amino acid sequence analysis by using SOSUI and TMHMM servers predicted that HasH is a membrane-bound protein (Figure 4-8). However, due to little information on fungal cytochrome P450 enzymes on these servers, the solubility of HasH remains unclear. We would like to prepare one additional expression vector with His_6-tag for purification of HasH from crude extracts, in case that HasH is a soluble protein. Therefore, the expression plasmid pXY14 was obtained after insertion of a double-stranded oligonucleotide containing amino acid codons for six His residues and BspEI restriction site for validation between BamHI and XhoI sites in the plasmid pXY12, which was digested with BamHI and XhoI previously (Figures 4-6 and 4-9). The double-stranded oligonucleotide was prepared by heating primers PXY12-1 and PXY12-2 and gradually cooling.

4.10.2 Overexpression of *hasH* in *Saccharomyces cerevisiae*

For protein overproduction, the plasmids pXY12, pXY13 and pXY14 were transformed into *S. cerevisiae* INVSc-1 separately. The resulting transformants were proven by yeast colony

PCR reactions with primers AFUA_3G12960_1 and AFUA_3G12960_2. The PCR reaction with *S. cerevisiae* INVSc-1 cells was used as negative control.

Both “soluble proteins” and “microsomes” (see section 3.4.3) from the transformants of *S. cerevisiae* cells harbouring pXY12 or pXY13 and “purified His_6-tagged protein” (see section 3.4.3) from cells harbouring pXY14 after induction with 3% galactose at 30 °C for 23 h were obtained and analyzed by SDS-PAGE. A Western Blot and Coomassie Brilliant Blue dye staining were used for detection of myc epitope tagged and His_6-tagged proteins, respectively. However, no obvious band of target protein was observed on SDS-PAGE. Allowing for the possibility of low protein yield, enzyme assays were carried out with high volume of proteins. Terezine D, 7-dimethylallyl-L-tryptophan, L-tryptophan, cyclo-L-Trp-L-Ala and tryptophan methyl ester were incubated with different fractions of HasH in the presence of NADPH and NADH at 30 or 37 °C. Unfortunately, no product formation was observed on HPLC.

5 Publications and manuscript

5.1 Preparation of pyrrolo[2,3-b]indoles carrying a ß-configured reverse C3-dimethylallyl moiety by using a recombinant prenyltransferase CdpC3PT

PAPER www.rsc.org/obc | Organic & Biomolecular Chemistry

Preparation of pyrrolo[2,3-b]indoles carrying a β-configured reverse C3-dimethylallyl moiety by using a recombinant prenyltransferase CdpC3PT†

Wen-Bing Yin,‡§[a] Xia Yu,‡[a] Xiu-Lan Xie[b] and Shu-Ming Li*[a]

Received 14th January 2010, Accepted 19th February 2010
First published as an Advance Article on the web 22nd March 2010
DOI: 10.1039/c000587h

Six β-configured reversely C3-prenylated pyrrolo[2,3-b]indoles were successfully prepared by using a recombinant prenyltransferase from *Neosartorya fischeri*. For this purpose, the putative prenyltransferase gene *NFIA_074280* (termed herewith *cdpC3PT*) was cloned into pQE60 and overexpressed in *Escherichia coli*. The overproduced His_6-CdpC3PT was purified to near homogeneity and incubated with five cyclic tryptophan-containing dipeptides in the presence of dimethylallyl diphosphate (DMAPP). All of the substrates were accepted by CdpC3PT and converted to reversely C3-prenylated pyrrolo[2,3-b]indoles. Using cyclo-L-Trp-L-Trp as substrate, both mono- and diprenylated derivatives were obtained. The structures of the enzymatic products were confirmed by HR-ESI-MS, ^{1}H- and ^{13}C-NMR analyses as well as by long-range ^{1}H-^{13}C connectivities in heteronuclear multiple-bond correlation (HMBC) spectra after preparative isolation. ^{1}H-^{1}H spatial correlations in nuclear overhauser effect spectroscopy (NOESY) were used for determination of absolute configuration. The K_M values were determined at about 1.5 mM for DMAPP and in the range from 0.22 to 5.5 mM for cyclic dipeptides. The turnover number k_{cat} were found in the range of 0.023 to 0.098 s^{-1} and specificity constants k_{cat}/K_M from 14.2 to 122.7 M^{-1} s^{-1}. In contrast to the products of AnaPT bearing α-configured C3-dimethylallyl residues, the C3-prenyl moieties in the products of CdpC3PT have a β-configuration. Discovery and characterisation of CdpC3PT expand the usage of the chemoenzymatic approach for stereospecific synthesis of C3-prenylated derivatives.

Introduction

A number of naturally occurring indoline alkaloids carry a reverse prenyl moiety at position C3 of the indoline ring and a five-membered ring system between the indoline and the diketopiperazine ring (Fig. 1). These compounds are mainly found in the genera *Penicillium* and *Aspergillus* of ascomycota.[1] All of the known natural products from this group have a *cis*-configuration between H-2 and C3-prenyl moiety. Both α- and β-configured C3-dimethylallyl residues have been identified (Fig. 1). 5-*N*-acetylardeemin,[2] aszonalenin and epiaszonalenin as well as their acetylated form[1,3,4] belong to the first subgroup. Examples of β-configured derivatives are roquefortines C and D,[5–7] fructigenines A and B (verrucofortine),[8,9] rugulosuvines A and B,[10] brevicompanines A, B and C,[11,12] as well as amauromine.[13] Both α- and β-configured C3-dimethylallyl residues are found in the structure of epiamauromine derived from two tryptophan molecules.[14] Until now, more β-configured derivatives have been isolated from fungal strains than the α-configured ones. C3-prenylated indolines have been reported to show diverse biological activities.[15]

By using two indole prenyltransferases AnaPT and CdpNPT, four aszonalenin stereoisomers were synthesised successfully from (R)- and (S)-benzodiazepinedione.[16] Seven C3-prenylated pyrrolo[2,3-b]indoles (**2a–2f** and **4**) have been obtained by enzymatic conversion of six tryptophan-containing cyclic dipeptides (**1a–1f**) with AnaPT (Scheme 1).[15] By using HPLC, only one stereoisomer each was detected from the incubation mixtures with the mentioned prenyltransferases. MS, CD and NMR analyses, including nuclear overhauser effect spectroscopy (NOESY), showed clearly that all of the isolated products of AnaPT reactions carried an α-configured C3-dimethylallyl moiety. To expand the usage of prenyltransferases for chemoenzymatic synthesis, we identified an additional **c**yclic **d**ipe**p**tide **C3-p**renyl**t**ransferase (CdpC3PT) gene from the genome sequence of *Neosartorya fischeri*. In contrast to those of AnaPT, the products of CdpC3PT bear β-configured C3-dimethylallyl residues. Here, we report the gene cloning, protein overproduction and biochemical investigation of CdpC3PT.

Results and discussion

In the course of our investigation on indole prenyltransferases, one putative gene *NFIA_074280* from the genome sequence of *Neosartorya fischeri* NRRL181 raised our attention. *NFIA_074280* spans bp 569563-570866 of DS027696.1 in GenBank. Its deduced product, EAW17508, comprises 423 amino acids and showed significant sequence similarity to known indole prenyltransferases.[17,18] *NFIA_074280* and a putative

[a]*Philipps-Universität Marburg, Institut für Pharmazeutische Biologie, Deutschhausstrasse 17A, D-35037 Marburg, Germany. E-mail: shuming.li@Staff.uni-Marburg.de; Fax: +49-6421-2825365; Tel: +49-6421-2822461*
[b]*Philipps-Universität Marburg, Fachbereich Chemie, Hans-Meerwein-Strasse, 35032 Marburg, Germany*
† Electronic supplementary information (ESI) available: Spectra of compounds. See DOI: 10.1039/c000587h
‡ These authors contributed equally to this work
§ Present address: University of Wisconsin-Madison, Medical Microbiology and Immunology, 3455 Microbial Sciences Building, 1550 Linden Drive, Madison WI 53706, USA.

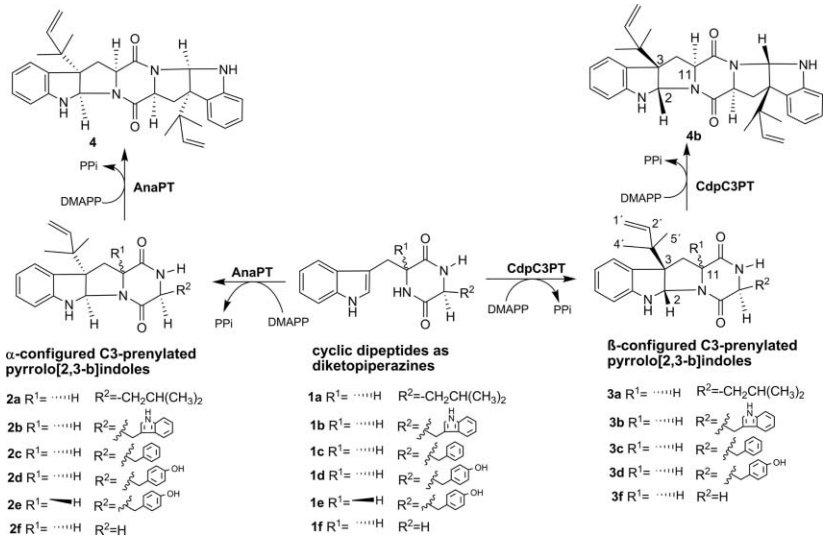

Scheme 1 Preparation of C3-prenylated pyrrolo[2,3-b]indoles by using recombinant prenyltransferases.

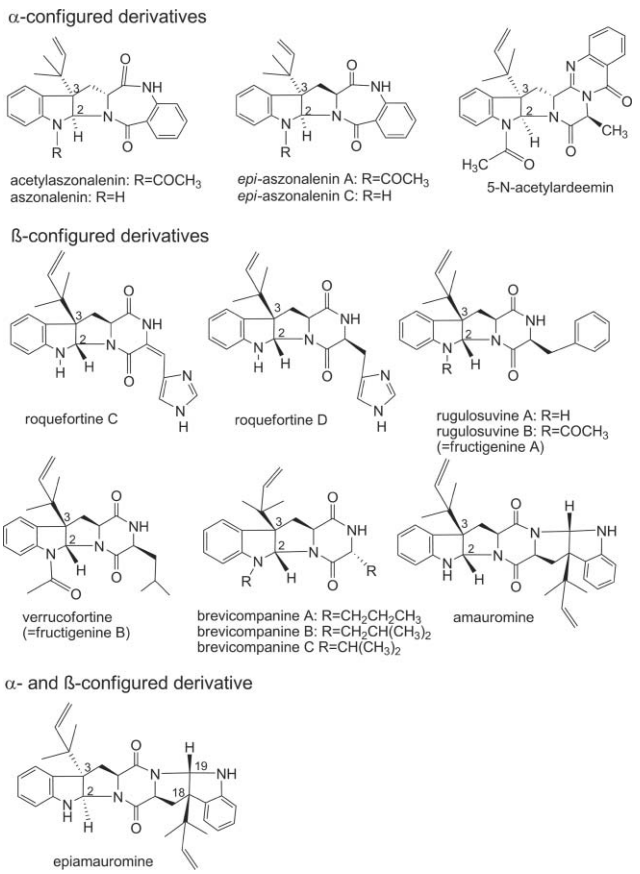

Fig. 1 Examples of C3-prenylated pyrrolo[2,3-b]indoles.

non-ribosomal peptide synthetase (NRPS) gene *NFIA_074300* are separated from each other by only 3.9 kb (Fig. 2) and could therefore belong to a same gene cluster for a secondary metabolite. The deduced product of *NFIA_074300*, EAW17510, showed a similar domain structure as the cyclic dipeptide synthetase FtmPT1 (brevianamide F synthetase) involved in the biosynthesis of fumitremorgins,[19] *i.e.* ATCATC (A: adenylation; T: thiolation and C: condensation), and could therefore be responsible for the formation of a cyclic dipeptide. Thus, we speculated that EAW17508 would function as a cyclic dipeptide prenyltransferase. By sequence comparison and analysis, it was neither possible to propose the natural substrate for the putative prenyltransferase, nor its prenylation pattern, *i.e.* regular or reverse, or prenylation position at the indole ring. The end product encoded by this cluster is also unknown. One putative cytochrome P450 oxidoreductase gene *NFIA_074290* is located between the putative prenyltransferase gene *NFIA_074280* and the putative NRPS gene *NFIA_074300*. Orthologous genes, *i.e. pc21g15430*, *pc21g15470* and *pc21g15480*, with sequence identities of 67, 60 and 59% on the amino acid level to *NFIA_074280*, *NFIA_074290* and *NFIA_074300*, respectively, have been identified in the genome sequence of *Penicillium chrysogenum* (Fig. 2).[20] Three additional genes *pc21g15440*, *pc21g15450* and *pc21g15460* are located between *pc21g15430* and *pc21g15470*, indicating that the product encoded by the cluster from *P. chrysogenum* is very likely different from that in *N. fischeri*.

To prove the function of EAW17508, *i.e.* CdpC3PT, the coding region of *NFIA_074280* was amplified by homologous recombinant DNA technique through three rounds PCR.[1,21] The PCR fragment consisting exclusively of the two exons was cloned *via* pGEM-T easy vector into pQE60 to create the expression construct pWY25 (see Experimental section). Soluble proteins were obtained from transformants of *E. coli* cells harbouring pWY25 after 6 h induction by 0.5 mM of IPTG at 37 °C. His_6-CdpC3PT was purified with Ni-NTA agarose to near homogeneity as judged by SDS-PAGE (Fig. 3) and a protein yield of 7 mg of purified His_6-tagged CdpC3PT per litre of cultures was obtained. A major protein band with migration near the 45 kDa size marker was observed, which corresponded well to the calculated value of 47.6 kDa for His_6-CdpC3PT.

In analogy to AnaPT,[15] the purified CdpC3PT (1.3 μM) was incubated with five tryptophan-containing cyclic dipeptides (**1a–1d** and **1f**) (1 mM) in the presence of DMAPP (2 mM) for different time. HPLC analysis of the incubation mixtures (Fig. 4) showed that all of the five substrates were accepted by

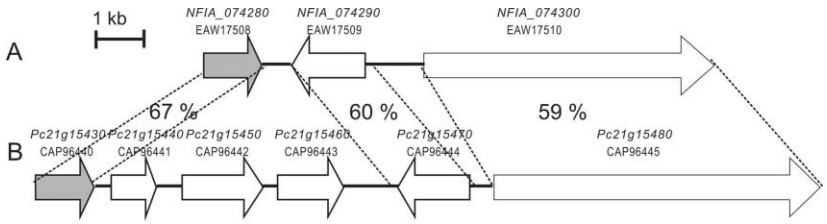

Fig. 2 Putative clusters containing *cdpC3PT* and its orthologue from *Neosartorya fischeri* (A) and *Penicillium chrysogenum* (B).

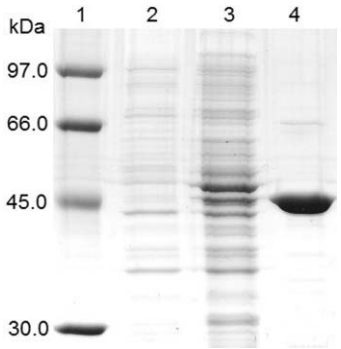

Fig. 3 Purification of CdpC3PT as a His_6-tagged protein. The 12% (w/v) SDS polyacrylamide gel was stained with Coomassie brilliant blue G-250. Lanes 1: molecular mass standard; 2: total protein before induction; 3: total protein after induction; 4: purified His_6- CdpC3PT.

CdpC3PT. In all the cases, product formation has been clearly observed already after incubation for 1 h (Fig. 4) and was dependent on the presence of active protein and DMAPP (data not shown). Increasing of product formation with extension of incubation time has also been observed. After incubation for 24 h, conversion rates of 31, 12, 6, 30 and 37% were determined for cyclo-L-Trp-L-Leu (**1a**), cyclo-L-Trp-L-Trp (**1b**), cyclo-L-Trp-L-Phe (**1c**), cyclo-L-Trp-L-Tyr (**1d**) and cyclo-L-Trp-Gly (**1f**), respectively, which were calculated from the ^{1}H-NMR signal intensity of the enzymatic products and remained respective substrate in the reaction mixtures (see Experimental section). One product peak each was detected for **1a**, **1c**, **1d** and **1f** (Fig. 4). In the HPLC chromatogram of the incubation mixture of **1b** (Fig. 4), two product peaks have been observed.

For structure elucidation, the enzymatic products were isolated on a preparative scale and substances in the range of 0.2–1 mg were subjected to high resolution ESI-MS and NMR analyses. HR-ESI-MS (Table 1) confirmed the presence of one dimethylallyl moiety in the structures of **3a–3d** and **3f** by detection of $[M+1]^+$ or $[M+Na]^+$ ions, which are 68 daltons larger than those of the respective substrates. The assignments of the NMR data listed in Table 2 were

Table 1 HR-ESI-MS data of the enzymatic products

Comp.	Chemical Formula	HR-ESI-MS data		Deviation
		Calculated	Measured	ppm
3a	$C_{22}H_{29}N_3O_2$	368.2338 $[M+1]^+$	368.2362	6.5
3b	$C_{27}H_{28}N_4O_2$	441.2291 $[M+1]^+$	441.2308	3.9
3c	$C_{25}H_{27}N_3O_2$	402.2182 $[M+1]^+$	402.2216	8.4
3d	$C_{25}H_{27}N_3O_3$	418.2131 $[M+1]^+$	418.2112	4.5
3f	$C_{18}H_{21}N_3O_2$	334.1531 $[M+Na]^+$	334.1540	2.7
4b	$C_{32}H_{36}N_4O_2$	509.2917 $[M+1]^+$	509.2920	0.6

verified by analysing the ^{1}H-^{13}C heteronuclear single-quantum correlation (HSQC) and heteronuclear multiple bond correlation (HMBC) spectra (Figures S1–S6, ESI†). Comparison of the ^{1}H-NMR data of the isolated products **3a–3d** and **3f** (Table 2) with those of the respective substrates (data not shown) revealed clearly the presence of signals for a reverse dimethylallyl moiety in the spectra of the isolated compounds at 5.08–5.14 (d or dd) for H-1′, 5.95–5.98 (dd) for H-2′, 1.00–1.01 ppm (s) for H-4′ and 1.11–1.13 (s) for H-5′, respectively. The signals of H-2 were strongly upfield shifted from approximately 7.0–7.2 in the spectra of the substrates to 5.50–5.56 ppm in the spectra of the enzymatic products (Figures S1–S6, ESI†). This indicated that the prenylation has very likely taken place at position C3 of the cyclic dipeptides and pyrrolo[2,3-b]indole derivatives were formed during the enzymatic reactions. Cross peaks in the HSQC spectra of **3a–3d** and **3f** revealed that the singlets of H-2 at 5.5 ppm correlated with the signals of C-2 at 77.5–77.6 ppm, proving the disappearance of the double bonds between C-2 and C-3 of the indole rings in the structures of **3a–3d** and **3f**. HMBC spectra showed clear connectivity from H-2 to C-11, which is conducted by the formation of a chemical bond between C-2 and N-12 of the diketopiperazine ring. Furthermore, HMBC spectra showed strong connectivities from H2 to C3′, H4′ to C3, and H5′ to C3. These results proved that the structures of **3a–3d** and **3f** are indeed C3-prenylated indolines with a fused five-membered ring between the indoline and diketopiperazine ring. This means that CdpC3PT catalysed, in analogy to AnaPT,[15] the reverse C3-prenylation of tryptophan-containing cyclic dipeptides and meanwhile the formation of a pyrrolo[2,3-b]indole structure.

The ^{1}H-NMR spectra and the assigned chemical shifts of **3a–3d** and **3f** (Table 2) are similar to those of **2a–2d** and **2f** (Scheme 1) reported previously.[15] Without considering the NOESY spectra, however, clear differences of chemical shifts were found for H-2 and H-10_{syn}. The chemical shifts of H-2 in **3a–3d** and **3f** were detected at approximately 5.5 ppm, while those of **2a–2d** and **2f** with α-configured C3-prenyl moieties at approximately 5.4 ppm.[15] The chemical shifts of H-10_{syn} in **3a–3d** and **3f** are found from 2.52 to 2.56 ppm, about 0.3 ppm upfield shifted in comparison to those of **2a–2d** and **2f** at 2.79 to 2.84 ppm.[15] These data indicated that the structures of **3a–3d** and **3f** differ from those of **2a–2d** and **2f** very likely by different configurations at C-2 and C-3 of the indoline rings.

Unambiguous proof of the stereochemistry was provided by NOESY experiments for **3a–3d** and **3f** (Table 3). Strong NOE correlations between H-2 and the protons of the prenyl moiety, *i.e.* H-2′, H-4′and H-5′, proved the *cis*-configuration between H-2 and C3-prenyl moieties of the indoline rings.

For compounds **3a–3d** and **3f**, only very weak NOE correlation was observed between H-2 and H-11. In the cases of **2a–2d** and **2f**, the NOE correlation for these protons was determined as

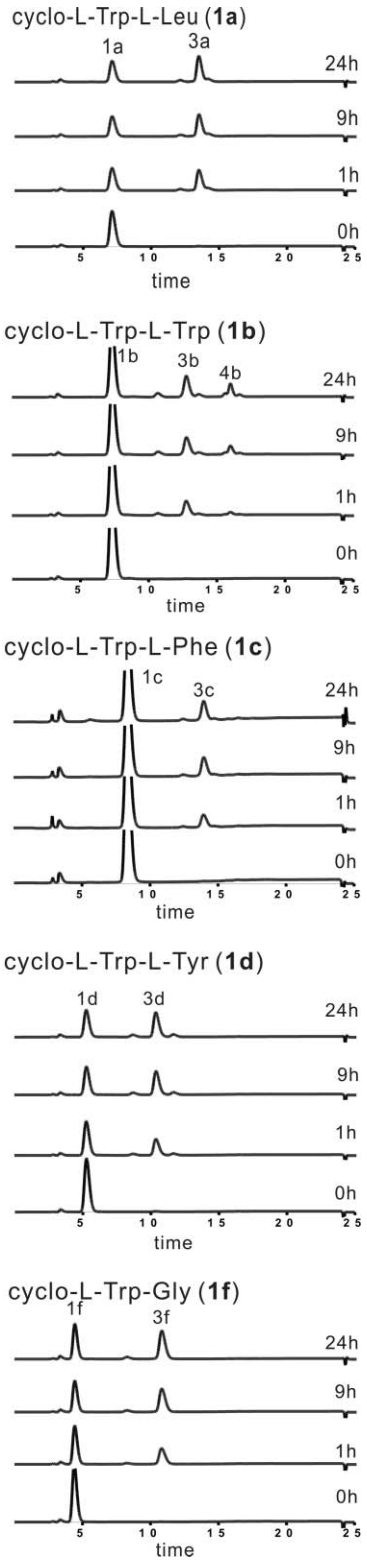

Fig. 4 HPLC chromatograms of incubation mixtures of five tryptophan–containing cyclic dipeptides with recombinant CdpC3PT. Detection was carried with a diode array detector and illustrated for absorption at 254 nm.

medium. Moreover, H-10_{anti} in **3a–3d** and **3f** instead of H-10_{syn} in **2a–2d** and **2f**,[15] showed medium or strong NOE correlations with protons of the prenyl moiety (Table 3). H-10_{syn} in **3a–3d** and **3f** as well as **2a–2d** and **2f** showed strong correlation with H-11. The correlations observed for **2a–2d** and **2f** between H-11 and those of the prenyl group were not detected in **3a–3d** and **3f**. From the results of NOE correlations, we concluded that H-2 and C3-prenyl moiety must be substituted on the opposite side to H-11. This demonstrated that, in contrast to **2a–2d** and **2f**, **3a–3d** and **3f** carry β-configured C3-dimethylallyl moieties as illustrated in Table 2 and Scheme 1. The steric hindrance of the β-configured prenyl residue makes the indoline ring bend in opposite direction and causes a spatial proximity between H4 and $H10_{syn}$. This is confirmed by the observation of strong NOE correlation between these two protons (Table 3).

The NMR data of **3a** and **3c** corresponded also well to those reported for brevicompanine B[22] and rugulosuvine A,[23] respectively.

The second product peak **4b** of cyclo-L-Trp-L-Trp (**1b**) (Fig. 4) was also isolated by repeated chromatography and subjected to MS analysis. The positive HR-ESI-MS of **4b** showed an ion at *m/z* 509.2920 (Table 1), which could be interpreted as $[M+1]^+$ of a diprenylated derivative with a molecular mass 136 daltons larger than that of the substrate.

The ^{1}H-NMR spectrum of **4b** showed signals of two identical tryptophanyl moieties, which are reversely prenylated at position C3 of the indoline rings. C3-diprenylated derivatives of cyclo-L-Trp-L-Trp containing two pyrrolo[2,3-b]indole systems have been reported, *e.g.* amauromine (Fig. 1) from *Amauroascus sp*[13] and epiamauromine (Fig. 1) from *Aspergillus ochraceus*.[14] ^{1}H-NMR data of **4b** (Table 2) corresponded perfectly to those of amauromine,[13] indicating that **4b** has an identical structure as amauromine or both compounds are enantiomers. The absolute configuration of **4b** was not determined in this study. However, it can be expected that the symmetrical **4b** was formed by a second prenylation and cyclisation of **3b** under the catalysis of CdpC3PT (Scheme 1). Therefore, both tryptophanyl moieties must have the same configuration as in **3b**. Therefore, **4b** and amauromine have same configuration as illustrated in Fig. 1 and Scheme 1.

The results provided in this study proved that both AnaPT and CdpC3PT catalyse the formation of indoline derivatives carrying fused five-membered rings with a *cis*-configuration. However, they introduced the ring system from opposite sides. Similar as observed with AnaPT,[15,16] the reaction catalysed by CdpC3PT includes at least three steps, *i.e.* attachment of a reverse prenyl moiety to C3 of the indole ring, breaking of the double bond between C2 and C3 and the formation of a C–N bond between C2 and N12. The detailed mechanism of this reaction is unknown. As proposed for AnaPT,[15] it can be speculated that attacking of dimethylallyl cation *via* its C3′ to C3 of the indole ring of the cyclic dipeptides would result in formation of an intermediate with a positive charge at C2. Formation of a C–N bond between C2 and N12 would lead to an intermediate with positive charge at N12, which is to be converted to the enzymatic products by releasing of a proton.

After structure elucidation of the enzymatic products, CdpC3PT was characterised biochemically. For determination of the dependence of the CdpC3PT activity on metal ions, incubations of **1a** with DMAPP were carried out in the presence of different metal ions at a final concentration of 5 mM. Incubations with EDTA at a final concentration of 5 mM and without additives were used as controls. Our results showed that product

Table 2 ^{1}H-NMR and ^{13}C-NMR data of enzymatic products ($CDCl_3$)

Compound	**3a** 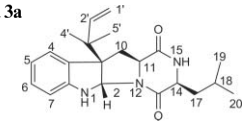		**3b** 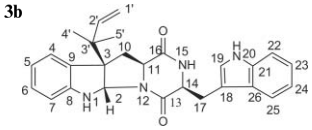		**3c** 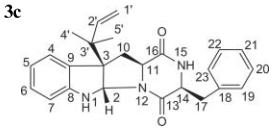		**3d** 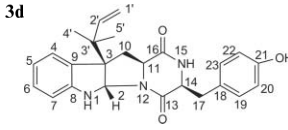		**3f** 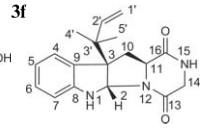		**4b** 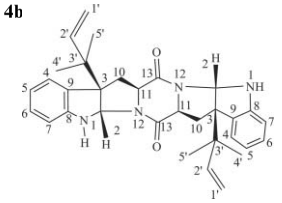
Position	δ_C	δ_H, multi., J in Hz	δ_C	δ_H, multi., J in Hz	δ_C	δ_H, multi., J in Hz	δ_C	δ_H, multi., J in Hz	δ_C	δ_H, multi., J in Hz	δ_H, multi., J in Hz
2	77.6	5.50, s	77.5	5.55, s	77.6	5.54, s	77.5	5.54, s	77.5	5.56, s	5.44, s
3	61.3	—	61.3	—	61.4	—	61.4	—	61.2	—	—
4	124.9	7.16, d, 7.4	124.9	7.14[a]	124.9	7.14, d, 7.4	125.0	7.14, d, 7.4	124.9	7.16, d, 7.2	7.09, dd, 7.6, 1.1
5	118.7	6.76, t, 7.5	118.8	6.75, td, 7.5, 0.8	118.8	6.76, td, 7.5, 0.9	118.8	6.76, t, 7.7	118.8	6.77, t, 7.5	6.70, td, 7.4, 1.0
6	128.7	7.10, t, 7.6	128.8	7.11[a]	128.8	7.10, td, 7.6, 1.0	128.8	7.11, t, 7.5	128.8	7.11, t, 8.1	7.02, td, 7.6, 1.2
7	109.1	6.58, d, 7.8	109.0	6.61, d, 7.8	109.0	6.60, d, 7.6	109.0	6.60, d, 7.9	109.0	6.60, d, 7.9	6.48, d, 7.9
8	149.8	—	149.7	—	149.7	—	149.6	—	149.7	—	—
9	128.9	—	128.7	—	128.7	—	128.6	—	128.6	—	—
10_{syn}[b]	35.7	2.55, dd, 12.7, 6.4	35.7	2.52, dd, 12.6, 6.3	35.9	2.52, dd, 12.6, 6.2	35.9	2.52, dd, 12.6, 6.1	36.2	2.56, dd, 12.6, 6.2	2.50, dd, 12.8, 6.6
10_{anti}[b]		2.47, t, 11.9		2.42, t, 11.9		2.40, t, 11.9		2.38, t, 11.9		2.45, t, 12.0	2.45, t, 11.9
11	58.6	3.95, m	58.8	3.92, ddd, 11.1,6.2, 1.6	58.7	3.93, ddd, 11.2, 6.2, 1.6	58.7	3.93,ddd,10.7,6.1, 2.0	58.0	3.97, ddd, 11.0, 5.9, 2.1	3.88, dd, 10.5, 6.4
13	166.3	—	165.8	—	165.3	—	165.1	—	163.4	—	—
14	53.3	3.95,m	54.4	4.31, ddd, 10.9, 3.6, 1.8	55.9	4.21, ddd, 10.4, 3.3, 1.5	56.0	4.15, dd, 8.9, 2.2	46.3	4.05, dd, 17.0, 1.9	—
	—	—	—	—	—	—	—	—	—	3.90, dd, 17.1, 4.0	—
15	—	5.67, s	—	5.69, s	—	5.54, s	—	5.64, s	—	6.24, br.s	—
16	169.3	—	168.8	—	168.8	—	168.8	—	169.5	—	—
17	38.6	2.02, ddd, 14.2, 10.2, 3.8	26.8	3.74, ddd, 14.7, 3.3, 0.8	36.7	3.59, dd, 14.4, 3.5	35.9	3.47, dd, 16.9, 2.5	—	—	—
		1.57, ddd, 14.5, 9.6, 5.0		2.98, dd, 15.0, 11.0		2.79, dd, 14.5, 10.6		2.76, dd, 14.3, 10.3		—	—
18	24.4	1.68, m	109.5	—	135.3	—	127.1	—	—	—	—
19	23.0	0.99, d, 6.6	123.1	7.11, s	128.8	7.19, d, 7.1	130.2	7.06, d, 8.4	—	—	—
20	20.8	0.92, d, 6.6	—	8.13, s	129.1	7.34, t, 7.3	116.0	6.79, d, 8.4	—	—	—
21	—	—	136.3	—	127.5	7.29, t, 7.4	154.8	—	—	—	—
22	—	—	111.3	7.38, d, 8.2	129.1	7.34, t, 7.3	116.0	6.79, d, 8.4	—	—	—
23	—	—	122.7	7.22, td, 7.7, 0.9	128.8	7.19, d, 7.1	130.2	7.06, d, 8.4	—	—	—
24	—	—	119.9	7.13[a]	—	—	—	—	—	—	—
25	—	—	118.2	7.55, d, 8.1	—	—	—	—	—	—	—
26	—	—	126.3	—	—	—	—	—	—	—	—
1′	114.4	5.12, d, 10.8	114.3	5.12, dd, 10.8, 1.0	114.3	5.13, dd, 10.8, 1.0	114.3	5.13, d, 10.8	114.4	5.14, dd, 10.8, 0.7	5.13, dd, 10.9, 1.1
		5.08, d, 17.3		5.08, dd, 17.4, 1.0		5.08, dd, 17.4, 0.9		5.08, d, 17.6		5.09, dd, 17.4, 0.6	5.08, dd, 17.4, 1.1
2′	143.3	5.97, dd, 17.3, 10.8	143.3	5.97, dd, 17.4, 10.8	143.3	5.96, dd, 17.3, 10.8	143.3	5.95, dd, 17.5, 10.8	143.2	5.98, dd, 17.4, 10.8	5.99, dd, 17.4, 10.8
3′	40.5	—	40.6	—	40.6	—	40.6	—	40.7	—	—
4′	22.7	1.01, s	22.6	1.01, s	22.6	1.01, s	22.7	1.00, s	22.7	1.01, s	1.01, s
5′	22.2	1.12, s	22.2	1.11, s	22.2	1.11, s	22.2	1.11, s	22.3	1.13, s	1.11, s

[a] Overlapping signals; [b] H-10_{syn} has a *cis*-configuration to H-11, H-10_{anti} a *trans*-configuration.

Table 3 NOE results of C3-prenylated pyrrolo[2,3-b]indoles (with an exception for **4b**)

Protons	Strength
H-2 to H-1′	Weak
H-2 to H-2′	Strong
H-2 to H-4′	Strong
H-2 to H-5′	Strong
H-2 to H-11	Weak
H-10$_{anti}$ to H-1′	Weak
H-10$_{anti}$ to H-2′	Medium
H-10$_{anti}$ to H-4′	Strong
H-10$_{anti}$ to H-5′	Strong
H-10$_{anti}$ to H-11	Medium
H-10$_{syn}$ to H-11	Strong
H-10$_{syn}$ to H-4	Strong
H-11 to H-2′	Not observed
H-11 to H-4′	Not observed
H-11 to H-5′	Not observed

Table 4 Preliminary parameters of the tested substrates[a]

Substrate	K_M/mM	k_{cat}/s^{-1}	k_{cat}/K_M/M^{-1} s^{-1}
1a	2.1	0.085	40.5
1b	0.35	0.023	65.7
1c	0.22	0.027	122.7
1d	1.5	0.06	40.0
1f	5.5	0.078	14.2
DMAPP[b]	1.4	0.098	70.0
DMAPP[c]	1.6	0.035	21.9

[a] Due to low solubility, the aromatic substrates were only tested up to 1 mM (**1b–1d**) or 5 mM (**1a** and **1f**). [b] **1a** as aromatic substrate. [c] **1b** as aromatic substrate.

formation was independent of the presence of metal ions. Even in the presence of the chelating agent EDTA, no decreasing of the enzyme activity was detected, in comparison to that of incubation without additives. This finding corresponded well to the behaviour of other known prenyltransferases.[17,18] The enhancing effect of Ca^{2+} on the activity of CdpC3PT seems stronger than other prenyltransferases. Addition of Ca^{2+}, Mg^{2+} and Mn^{2+} to the reaction mixtures increased the enzyme activity to 400, 240 and 220% of that without additives, respectively.

For comparison of the behaviour of CdpC3PT towards the cyclic dipeptides, kinetic parameters were determined for DMAPP and all of the five aromatic substrates by incubation with CdpC3PT at 37 °C for 30 min. For this purpose, the dependence of the product formation on incubation time had been proven and found to be linear up to 30 min for **1a**, nearly linear up to 30 min for **1b** and 45 min for **1c**, **1d** and **1f** (see please Figure S7, ESI†). Michaelis–Menten constants (K_M) as well as the turnover numbers (k_{cat}) were determined by Hanes-Woolf analysis and are given in Table 4. The obtained values were also confirmed by Lineweaver–Burk and Eadie-Hofstee analyses.

Using **1a** and **1b** as aromatic substrates, comparable K_M values for DMAPP were determined at 1.4 and 1.6 mM, respectively, which are much higher than the K_M values of other cyclic dipeptide prenyltransferases for DMAPP, *e.g.* FtmPT1 at 56 μM[24] and AnaPT at 156 μM.[1] However, the natural substrates were used for determination of kinetic parameters of FtmPT1 and AnaPT. In the case of CdpC3PT, the natural substrate is still unknown. **1b** and **1c** were found to have similar K_M values of 0.35 and 0.22 mM and turnover numbers of 0.023 and 0.027 s^{-1}, respectively (Table 4). **1a**, **1d** and **1f** with K_M values of 2.1, 1.5 and 5.5 mM, respectively, showed much lower affinity towards CdpC3PT than **1b** and **1c**. Interestingly, the turnover numbers of these three substrates were two- to three-fold of those of **1b** and **1c**. Consequently, CdpC3PT showed similar catalytic efficiency towards **1a**, **1b** and **1d** with specificity constants k_{cat}/K_M of 40.5, 65.7 and 40 M^{-1} s^{-1}, respectively. Using **1c** as substrate, CdpC3PT was found to have the best catalytic efficiency with a specificity constant of 122.7 M^{-1} s^{-1}. This value is however only 1.9% of that of AnaPT at 6522 M^{-1} s^{-1} determined by using its natural substrates DMAPP and (R)-benzodiazepinedinone.[1]

Conclusions

In this study, we described the cloning and biochemical investigation of a new indole prenyltransferase CdpC3PT, which catalysed the reverse prenylation of cyclic dipeptides at position C3 of the indole ring. Similar to AnaPT from the biosynthetic gene cluster of acetylaszonalenin[1] from the same fungus, *i.e.* *N. fischeri* NRRL181, CdpC3PT showed also broad substrate specificity and accepted all of the five tryptophan-containing cyclic dipeptides tested. Both AnaPT and CdpC3PT catalysed the formation of a five-membered ring between the original indole and diketopiperazine rings with a *cis*-configuration between H-2 and C3-dimethylallyl moiety. However, they introduce the prenyl moiety from different sides, *i.e.* AnaPT from behind and CdpC3PT from the front, so that two compounds with different stereochemistry at position C2 and C3 could be obtained from one substrate. They are therefore complement to each other regarding the prenylation and expand their potential to be used for chemoenzymatic synthesis.

Experimental section

Chemicals

Dimethylallyl diphosphate was prepared according to the method described for geranyl diphosphate by Woodside.[25] Cyclo-L-Trp-L-Leu (**1a**), cyclo-L-Trp-L-Trp (**1b**), cyclo-L-Trp-L-Phe (**1c**), cyclo-L-Trp-L-Tyr (**1d**) and cyclo-L-Trp-Gly (**1f**) were purchased from Bachem (Bubendorf, Switzerland).

Bacterial strains, plasmids and cultural conditions

pGEMT easy vector and pQE60 were obtained from Promega (Mannheim, Germany) and Qiagen (Hilden, Germany), respectively.

Escherichia coli XL1 Blue MRF′ (Stratagene) was used for cloning and over expression experiments and grown in liquid or on solid Luria-Bertani medium with 1.5% (w/v) agar at 37° C.[26] Carbenicillin (50 μg mL^{-1}) was used for selection of recombinant *E. coli* strains.

Neosartorya fischeri NRRL181 was kindly provided by ARS Culture Collection (Peoria, Illinois USA).

Cultivation of *N. fischeri* and DNA isolation

For DNA isolation, mycelia of *N. fischeri* from plates were inoculated into 300 mL Erlenmeyer flask containing 100 mL YES

media consisting of yeast extract (0.6% (w/v)), sucrose 0.2% (w/v) (pH 5.8) and cultivated at 30 °C and 170 rpm for 48 h. DNA isolation from *N. fischeri* was carried out according to the protocol described by Ausubel *et al.*[27]

DNA isolation, PCR amplification and gene cloning

Standard procedures for DNA isolation and manipulation were performed as described.[26]

PCR amplification was carried out on an iCycler from BioRad (Munich, Germany). The entire coding sequence of *cdpC3PT* was obtained after three rounds PCR amplification by using genomic DNA as template and Expand High Fidelity Kit (Roche Diagnostics GmbH, Mannheim, Germany). The first round PCR is used for amplification of the two exons. The primers for the first exon were CdpC3PT_a1 (5′-TCGTCTGATAAACCTCATCCT-3′) at the 5′-end and CdpC3PT_a2 (5′- **TCTGTGGCAATAGC-CAAGTCCTCGCCAGGG**TAATATGATTG CAGATTCTCC-3′) at the 3′-end. The primers for the second exon were CdpC3PT_b1 (5′- **GGGTCTACCCGGAGAATCTGCAAT-CATATTA**CCCTGGCGAG GACTTGGCT-3′) at the 5′-end and CdpC3PT_b2 (5′- AACAGGAAGGCACTAATAAGC-3′) at the 3′-end. Bold letters represent overlapping region of the two exons. The PCR products of the first and second exon were mixed in a molar ratio of 1 : 1 and used as template for a second round of PCR to get a fragment consisting of the two exons with help of the overlapping region. A third round PCR was then carried out by using a nested primer pair and the PCR product from the second round as template. The nested primers are CdpC3PT_for (5′-**ATTCC**ATG**G**CAGTGTCGTCGACCG-3′) at the 5′-end and CdpC3PT_rev (5′-**GAAGATCT**GTGGTAGTACATGGTCA-3′) at the 3′-end of the gene. Bold letters represent mutations inserted in comparison to the original genome sequence to give the underlined restriction sites NcoI located in the start codon in CdpC3PT_for and BglII located in the predicted stop codon in CdpC3PT_rev, respectively. A PCR fragment of 1286 bp containing the entire coding sequence of *cdpC3PT* could be amplified after the third round PCR. The PCR fragment was cloned into pGEMT easy vector resulting in plasmid pWY24, which was subsequently sequenced (Eurofins MWG Operon, Ebersberg, Germany) to confirm the sequence. To create the expression vector pWY25, pWY24 was digested with NcoI and BglII and the resulted NcoI-BglII fragment of 1278 bp was ligated into pQE60, which had been digested with the same enzymes, previously.

Overproduction and purification of His_6-CdpC3PT

For *cdpC3PT* expression, *E. coli* XL1 Blue MRF′ cells harbouring the plasmid pWY25 were cultivated in 300 mL Erlenmeyer flasks containing 100 mL liquid Luria-Bertani medium supplemented with carbenicillin (50 μg mL^{-1}) and grown at 37 °C to an absorption at 600 nm of 0.6. For induction, isopropyl thiogalactoside (IPTG) was added to a final concentration of 0.5 mM and the cells were cultivated for further 6 h at 37 °C before harvest. The bacterial cultures were centrifuged and the pellets were resuspended in lysis buffer (10 mM imidazole, 50 mM NaH_2PO_4, 300 mM NaCl, pH 8.0) at 2–5 mL per gram wet weight. After addition of 1 mg mL^{-1} lysozyme and incubation on ice for 30 min, the cells were sonicated 6 times for 10 s each at 200 W. To separate the cellular debris from the soluble proteins, the lysate was centrifuged at 13,000 x *g* for 30 min at 4 °C. One-step purification of the recombinant His_6-tagged fusion protein by affinity chromatography with Ni-NTA agarose resin (Qiagen, Hilden, Germany) was carried out according to the manufacturer's instructions. The protein was eluted with 250 mM imidazole in 50 mM NaH_2PO_4, 300 mM NaCl, pH 8.0. In order to change the buffer, the protein fraction was passed through a NAP-5 column (GE Healthcare, Freiburg, Germany), which had been equilibrated with 50 mM Tris-HCl, 15% (v/v) of glycerol, pH 7.5, previously. CdpC3PT was eluted with the same buffer and stored frozen at –80 °C for enzyme assays.

Protein analysis and determination of molecular mass of active His_6-CdpC3PT

Proteins were analysed by SDS-PAGE according to the method of Laemmli[28] and stained with Coomassie brilliant blue G-250.

The molecular mass of the recombinant His_6-CdpC3PT was determined by size exclusion chromatography on a HiLoad 16/60 Superdex 200 column (GE Health Care, Freiburg, Germany), which had been equilibrated with 20 mM Tris-HCl buffer (pH 7.5) containing 150 mM NaCl. The column was calibrated with dextran blue 2000 (2000 kDa), ferritin (440 kDa), aldolase (158 kDa), conalbumin (75 kDa), carbonic anhydrase (29 kDa) and ribonuclease A (13.7 kDa) (GE Health Care, Freiburg, Germany). The proteins were eluted with 20 mM Tris-HCl buffer (pH 7.5) containing 150 mM NaCl. The molecular mass of the recombinant His_6-CdpC3PT was determined as 130 kDa. This indicated that CdpC3PT acts likely as a homotrimer.

Assay for CdpC3PT activity

For quantitative determination of the enzyme activity, the reaction mixture (100 μL) contained 50 mM Tris-HCl (pH 7.5), 5 mM $CaCl_2$, 1 mM aromatic substrates, 1 mM DMAPP, 1.5% (v/v) glycerol, and 0.07 μM of purified recombinant CdpC3PT. The reaction mixtures were incubated at 37 °C and the reactions were terminated by addition of 100 μl methanol per 100 μl reaction mixtures. The protein was removed by centrifugation at 13,000 x g for 20 min. The enzymatic products were analysed by HPLC under conditions described below. For quantitative measurement of the enzyme activity, duplicate values were determined routinely. For determination of kinetic parameters of DMAPP, cyclic dipeptides at 1 mM, DMAPP at final concentrations of 0.0, 0.16, 0.40, 0.81, 1.62 and 4.05 mM were used as substrates. For determination of the kinetic parameters of cyclic dipeptides, DMAPP at a final concentration of 5 mM was used. Due to low solubility, concentrations of **1a** and **1f** up to 5.0 mM and **1b–1d** up to 1 mM were used.

Quantification of the enzymatic products

For quantification of the enzymatic products, CdpC3PT was incubated in a large scale (10 mL) containing each of the five cyclic dipeptides (1 mM), DMAPP (2 mM), $CaCl_2$ (5 mM), Tris-HCl (50 mM, pH 7.5), glycerol 1.5% (v/v) and CdpC3PT (2 mg). The reaction mixtures were extracted after incubation at 37 °C for 24 h with ethyl acetate. After evaporation of the solvent, the residues of

the ethyl acetate phase containing both enzymatic products and substrates were subjected to ^{1}H-NMR analysis. The conversion rate of a given substrate was determined by comparison of the integrals of the enzymatic product and the remained substrate in ^{1}H-NMR spectra. The absorption coefficients of the enzymatic products were then calculated by HPLC analysis of the samples after NMR analysis.

Preparative synthesis of enzymatic products for structure elucidation

The NMR samples for quantification of the enzymatic products were then purified on HPLC under the conditions described below for structure elucidation. The isolated products were subjected to ^{1}H-NMR, ^{13}C-NMR, ^{1}H-^{1}H COSY, ^{1}H-^{13}C HSQC and HMBC as well as high resolution electrospray ionization mass spectrometry (HR-ESI-MS).

HPLC conditions for analysis and isolation of enzymatic products of CdpC3PT

The enzymatic products of the incubation mixtures of CdpC3PT were analysed by HPLC on an Agilent series 1200 by using a LiChrospher RP 18-5 column (125 × 4 mm, 5 µm, Agilent) at a flow rate of 1 mL min^{-1}. Water (solvent A) and methanol (solvent B) were used as solvents. For analysis of enzymatic products, linear gradients of 50–80% (v/v) solvent B in 10 min and then of 80–100% (v/v) solvent B in 5 min were used. The column was then washed with 100% solvent B for 5 min and equilibrated with 50% (v/v) solvent B for 5 min. Detection was carried out by a Photo Diode Array detector and illustrated at 254 nm in the figures in this paper.

For isolation, the same HPLC equipment with a Multospher 120 RP-18 column (250 × 10 mm, 5 µm, C+S Chromatographie Service, Langenfeld, Germany) was used. Linear gradients of 50–80% (v/v) solvent B in 10 min and then of 80–100% (v/v) solvent B in 5 min at a flow rate of 2.5 mL min^{-1} were used. The column was then washed with 100% solvent B for 5 min and equilibrated with 50% (v/v) solvent B for 5 min.

NMR experiments

Small amount (less than 1 mg) of each sample was dissolved in 0.2 mL of $CDCl_3$. Samples were filled into Wilmad 3 mm tubes from Rototec Spintec. Spectra were recorded at room temperature on a Bruker Avance 600 MHz spectrometer equipped with an inverse probe with z-gradient. The HSQC and HMBC spectra were recorded with standard methods.[29] Gradient-selected NOESY experiment[30] was performed in phase-sensitive mode. For all two-dimensional spectra, 32 to 64 transients were used. For NOESY spectra, a mixing time of 1.5 s and a relaxation delay of 3.0 s. ^{1}H spectra were acquired with 65 536 data points, while 2D spectra were collected using 4096 points in the F_2 dimension and 512 increments in the F_1 dimension. Typical experiment time for the HMBC and NOESY measurements was about 12 h. Chemical shifts were referenced to $CDCl_3$. All spectra were processed with Bruker TOPSPIN 2.1.

Mass spectrometry

The isolated products were analysed by HR-ESI-MS with a Q-Trap Quantum (Applied Biosystems).Positive HR-ESI-MS data of the enzymatic products are given in Table 1.

Nucleotide sequence accession number

The nucleotide sequence of the genomic DNA from *Neosartorya fischeri* NRRL181 reported in this study is available at GenBank under accession number DS027696. The coding sequence of *cdpC3PT* is available at GenBank under the name *NFIA_074280*.

Acknowledgements

This work was supported by a grant from the LOEWE program des Landes Hessen (SynMikro to S.-M. Li). Xie acknowledges the Deutsche Forschungsgemeinschaft for funding the Bruker AVANCE 600 spectrometer. Xia Yu is a recipient of a fellowship from China Scholarship Council.

References

1 W.-B. Yin, A. Grundmann, J. Cheng and S.-M. Li, *J. Biol. Chem.*, 2008, **284**, 100–109.
2 J. P. Karwowski, M. Jackson, R. R. Rasmussen, P. E. Humphrey, J. B. Poddig, W. L. Kohl, M. H. Scherr, S. Kadam and J. B. McAlpine, *J. Antibiot. (Tokyo)*, 1993, **46**, 374–379.
3 Y. Kimura, T. Hamasaki, H. Nakajima and A. Isogai, *Tetrahedron Lett.*, 1982, **23**, 225–228.
4 C. Rank, R. K. Phipps, P. Harris, J. C. Frisvad, C. H. Gotfredsen and T. O. Larsen, *Tetrahedron Lett.*, 2006, **47**, 6099–6102.
5 P. M. Scott and B. P. C. Kennedy, *J. Agric. Food Chem.*, 1976, **24**, 865–868.
6 T. Rundberget, I. Skaar and A. Flaoyen, *Int. J. Food Microbiol.*, 2004, **90**, 181–188.
7 C. Finoli, A. Vecchio, A. Galli and I. Dragoni, *J. Food Prot.*, 2001, **64**, 246–251.
8 R. P. Hodge, C. M. Harris and T. M. Harris, *J. Nat. Prod.*, 1988, **51**, 66–73.
9 K. Arai, K. Kimura, T. Mushiroda and Y. Yamamoto, *Chem. Pharm. Bull.*, 1989, **37**, 2937–2939.
10 A. G. Kozlovsky, V. M. Adanin, H. M. Dahse and U. Gräfe, *Appl. Biochem. Microbiol.*, 2001, **37**, 253–256.
11 M. Kusano, G. Sotoma, H. Koshino, J. Uzawa, M. Chijimatsu, S. Fujioka, T. Kawano and Y. Kimura, *J. Chem. Soc., Perkin Trans. 1*, 1998, 2823–2826.
12 K. Sprogoe, S. Manniche, T. O. Larsen and C. Christophersen, *Tetrahedron*, 2005, **61**, 8718–8721.
13 S. Takase, Y. Kawai, I. Uchida, H. Tanaka and H. Aoki, *Tetrahedron Lett.*, 1984, **25**, 4673–4676.
14 F. S. De Guzman and J. B. Glober, *J. Nat. Prod.*, 1992, **55**, 931–939.
15 W.-B. Yin, X.-L. Xie, M. Matuschek and S.-M. Li, *Org. Biomol. Chem.*, 2010, **8**, 1133–1141.
16 W.-B. Yin, J. Cheng and S.-M. Li, *Org. Biomol. Chem.*, 2009, **7**, 2202–2207.
17 N. Steffan, A. Grundmann, W.-B. Yin, A. Kremer and S.-M. Li, *Curr. Med. Chem.*, 2009, **16**, 218–231.
18 S.-M. Li, *Phytochemistry*, 2009, **70**, 1746–1757.
19 S. Maiya, A. Grundmann, S.-M. Li and G. Turner, *ChemBioChem*, 2006, **7**, 1062–1069.
20 M. A. van den Berg, R. Albang, K. Albermann, J. H. Badger, J. M. Daran, A. J. Driessen, C. Garcia-Estrada, N. D. Fedorova, D. M. Harris, W. H. Heijne, V. Joardar, J. A. Kiel, A. Kovalchuk, J. F. Martin, W. C. Nierman, J. G. Nijland, J. T. Pronk, J. A. Roubos, d. K. van, I. N. N. van Peij, M. Veenhuis, H. von Dohren, C. Wagner, J. Wortman and R. A. Bovenberg, *Nat. Biotechnol.*, 2008, **26**, 1161–1168.
21 J. H. Yu, Z. Hamari, K. H. Han, J. A. Seo, Y. Reyes-Dominguez and C. Scazzocchio, *Fungal Genet. Biol.*, 2004, **41**, 973–981.

22 L. Du, X. Yang, T. Zhu, F. Wang, X. Xiao, H. Park and Q. Gu, *Chem. Pharm. Bull.*, 2009, **57**, 873–876.
23 J. H. Chang and H. Moon, *Biotechnol. Bioprocess Eng.*, 2004, **9**, 59–61.
24 A. Grundmann and S.-M. Li, *Microbiology*, 2005, **151**, 2199–2207.
25 A. B. Woodside, Z. Huang and C. D. Poulter, *Org. Synth.*, 1988, **66**, 211–215.
26 J. Sambrook, and D. W. Russell, *Molecular Cloning: a Laboratory Manual*, Cold Spring Harbor Laboratory Press, New York, 2001.
27 F. M. Ausubel, R. Brent, R. E. Kingston, D. D. Moore, J. G. Seidman, J. A. Smith, and K. Struhl, *Current Protocols in Molecular Biology*, John Wiley and Sons Inc, New York, 1996.
28 U. K. Laemmli, *Nature*, 1970, **227**, 680–685.
29 S. Berger, and S. Braun, *200 and More NMR Experiments. A Practical Course*, Weiley-VCH, Weinheim, Germany, 2004.
30 T.-L. Hwang and A. J. Shaka, *J. Am. Chem. Soc.*, 1992, **114**, 3157–3159.

Electronic supporting information to:

Preparation of pyrrolo[2,3-b]indoles carrying a ß-configured reverse C3-dimethylallyl moiety by using a recombinant prenyltransferase CdpC3PT

Wen-Bing Yin,[a,b,c] Xia Yu,[a,b] Xiu-Lan Xie,[d] and Shu-Ming Li [a,*]

[a] *Philipps-Universität Marburg, Institut für Pharmazeutische Biologie, Deutschhausstrasse 17A, D-35037 Marburg, Germany. Email: shuming.li@Staff.uni-Marburg.de, Tel: 0049-6421-2822461 Fax: 0049-6421-2825365*

[b] *These authors contributed equally to this work*

[c] *Present address: University of Wisconsin-Madison, Medical Microbiology and Immunology, 3455 Microbial Sciences Building, 1550 Linden Drive, Madison WI 53706, USA.*

[d] *Philipps-Universität Marburg, Fachbereich Chemie, Hans-Meerwein-Strasse, 35032 Marburg, Germany.*

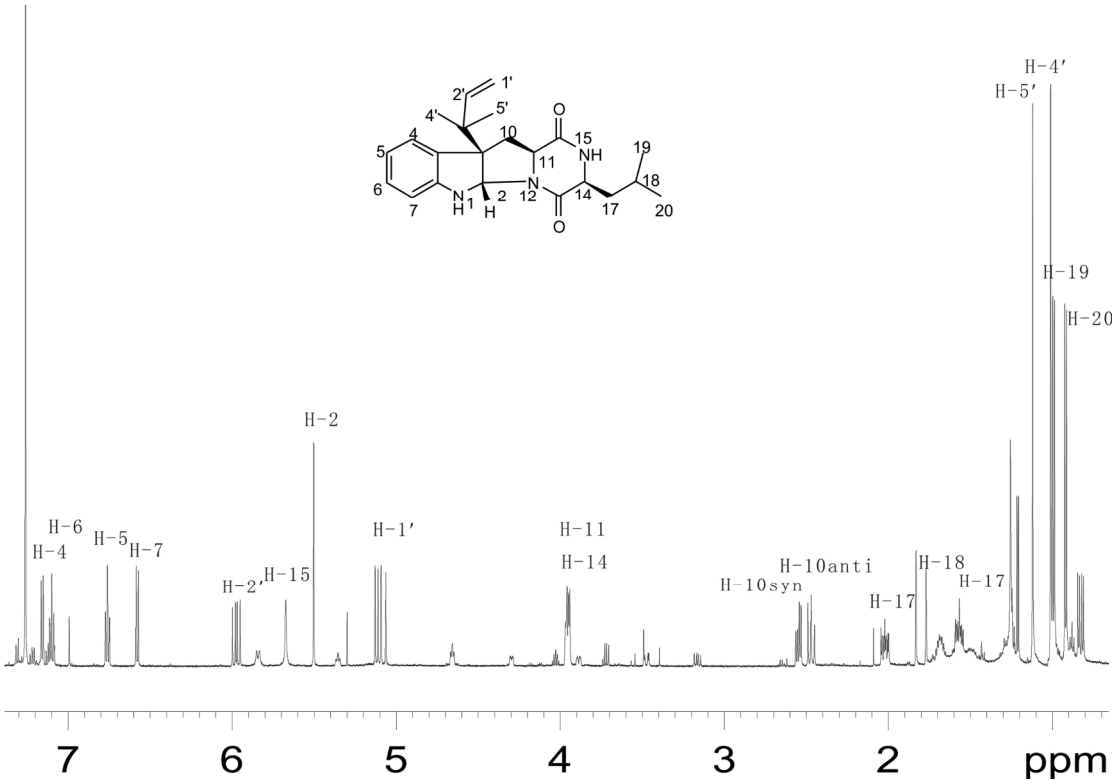

Figure S1.1: ^{1}H-NMR spectrum of **3a** in $CDCl_3$.

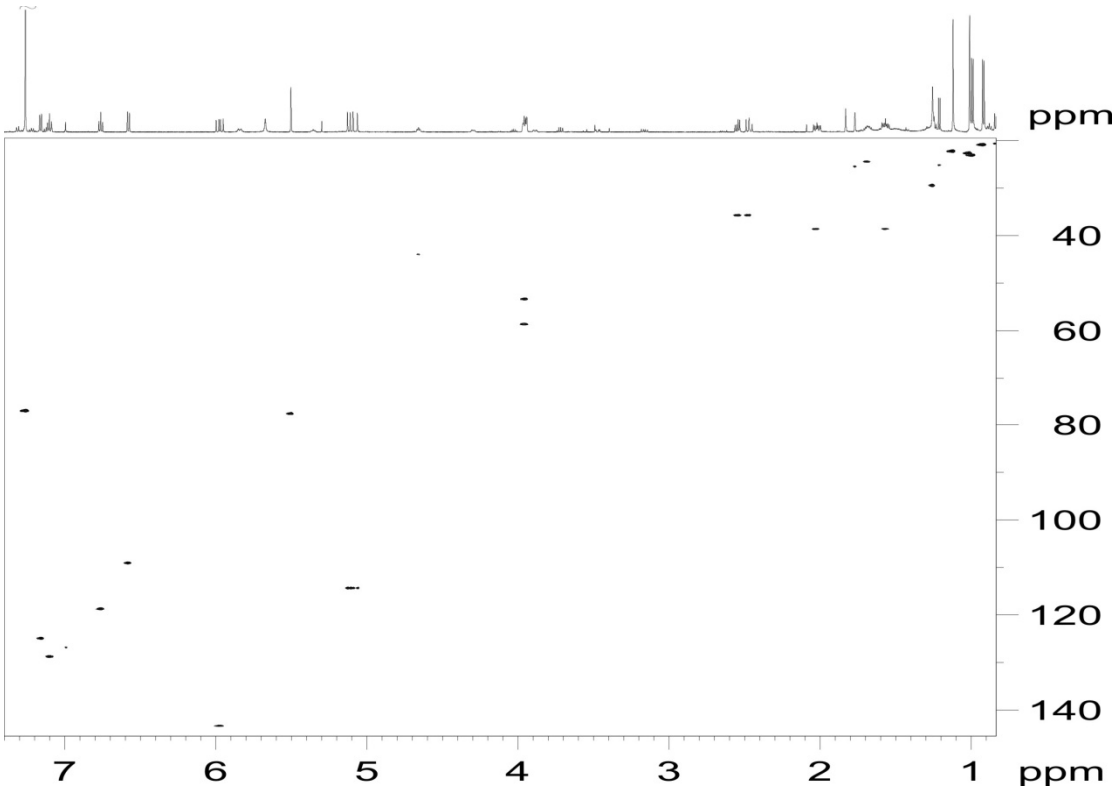

Figure S1.2: HSQC spectrum of **3a** in $CDCl_3$. The solvent signal is partially cut in the 1D projection for clarity.

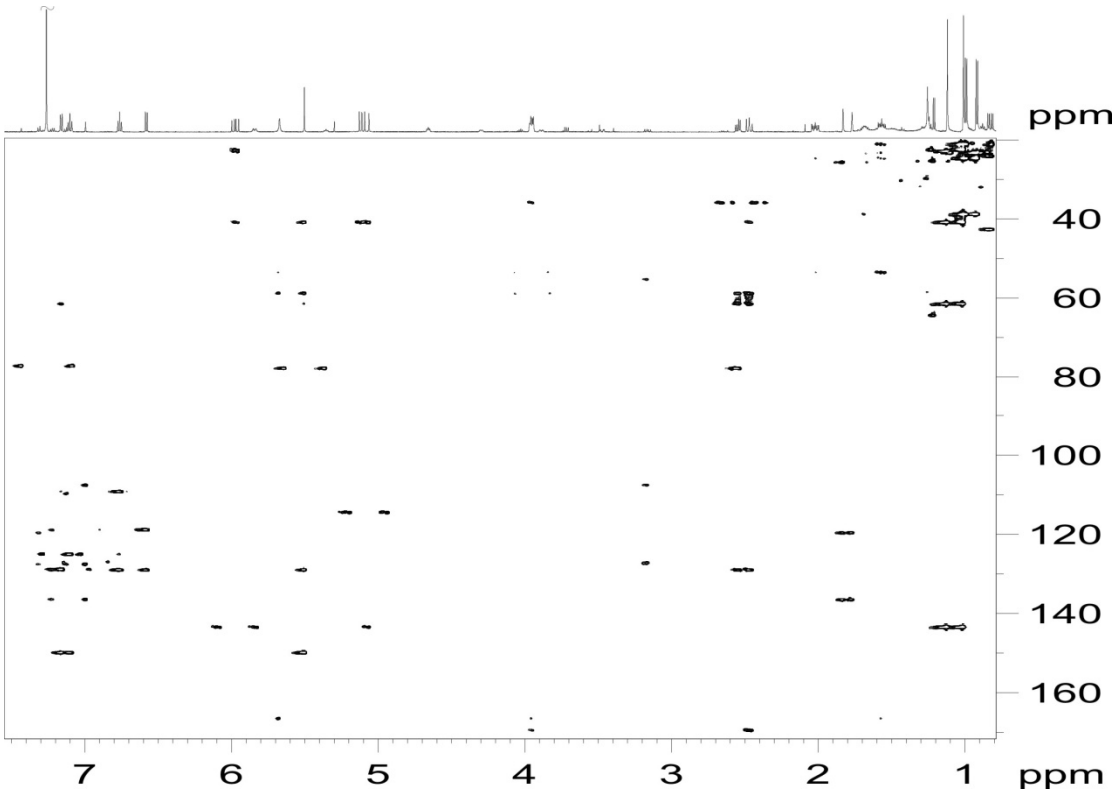

Figure S1.3: HMBC spectrum of **3a** in $CDCl_3$. The solvent signal is partially cut in the 1D projection for clarity.

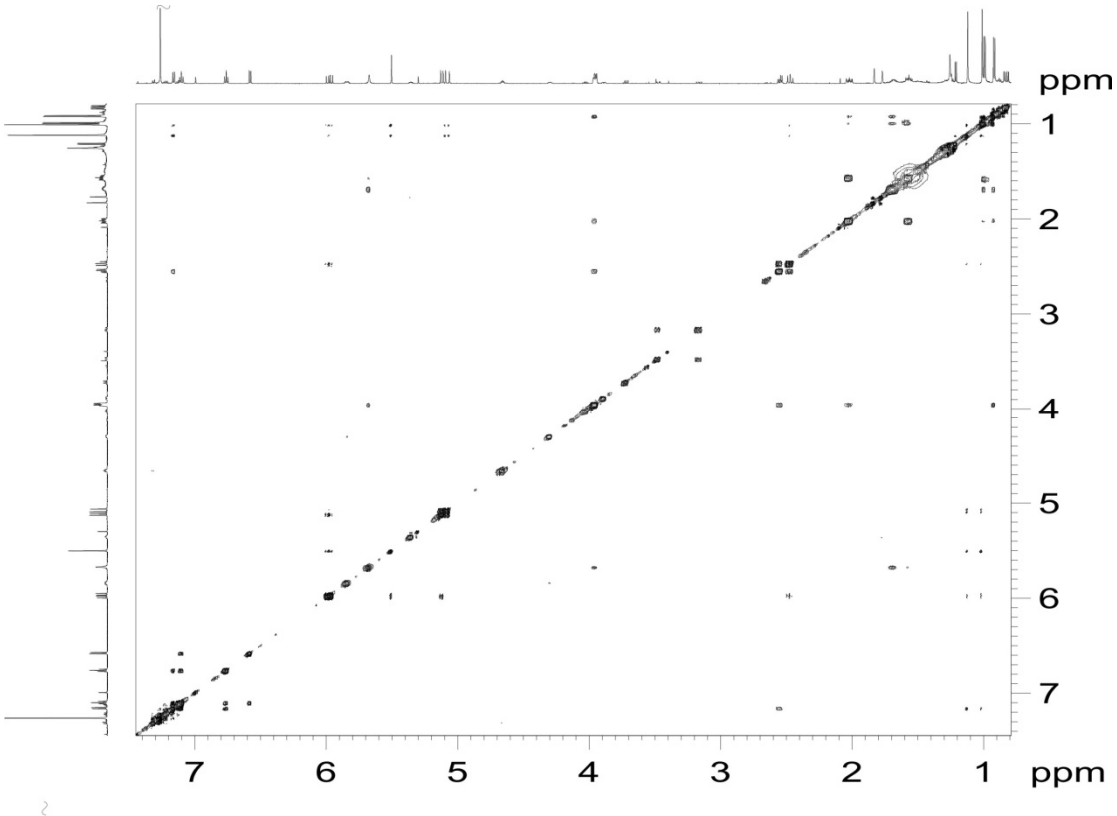

Figure S1.4: NOESY spectrum of **3a** in $CDCl_3$. The solvent signal is partially cut in the 1D projection for clarity.

4

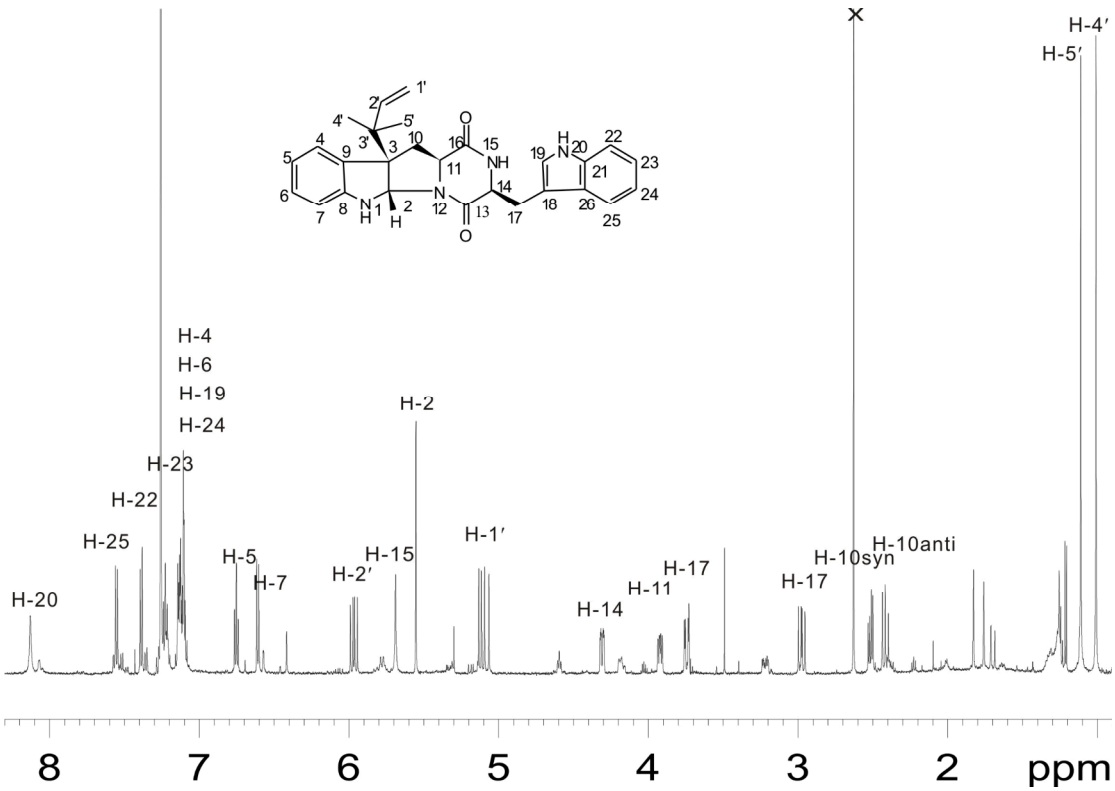

Figure S2.1: ^{1}H-NMR spectrum of **3b** in $CDCl_3$. The label X indicates signal of impurity.

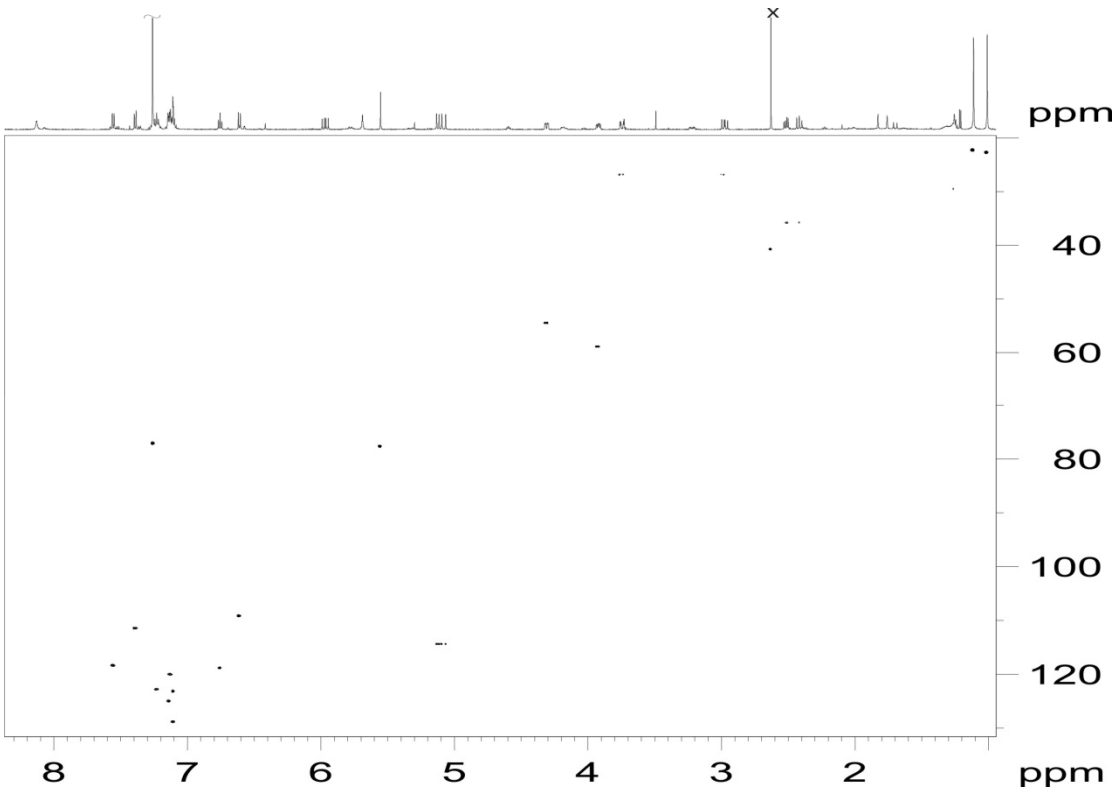

Figure S2.2: HSQC spectrum of **3b** in $CDCl_3$. The label X indicates signal of impurity and the solvent signal is partially cut in the 1D projection for clarity.

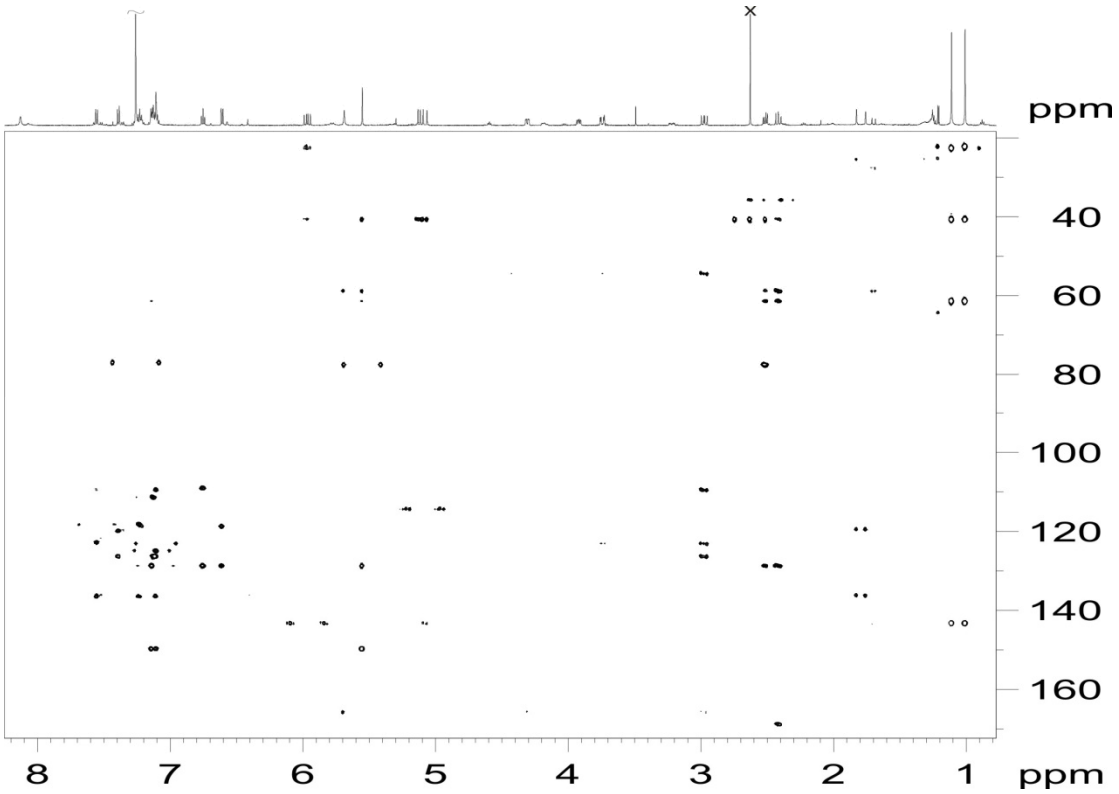

Figure S2.3: HMBC spectrum of **3b** in $CDCl_3$. The label X indicates signal of impurity and the solvent signal is partially cut in the 1D projection for clarity.

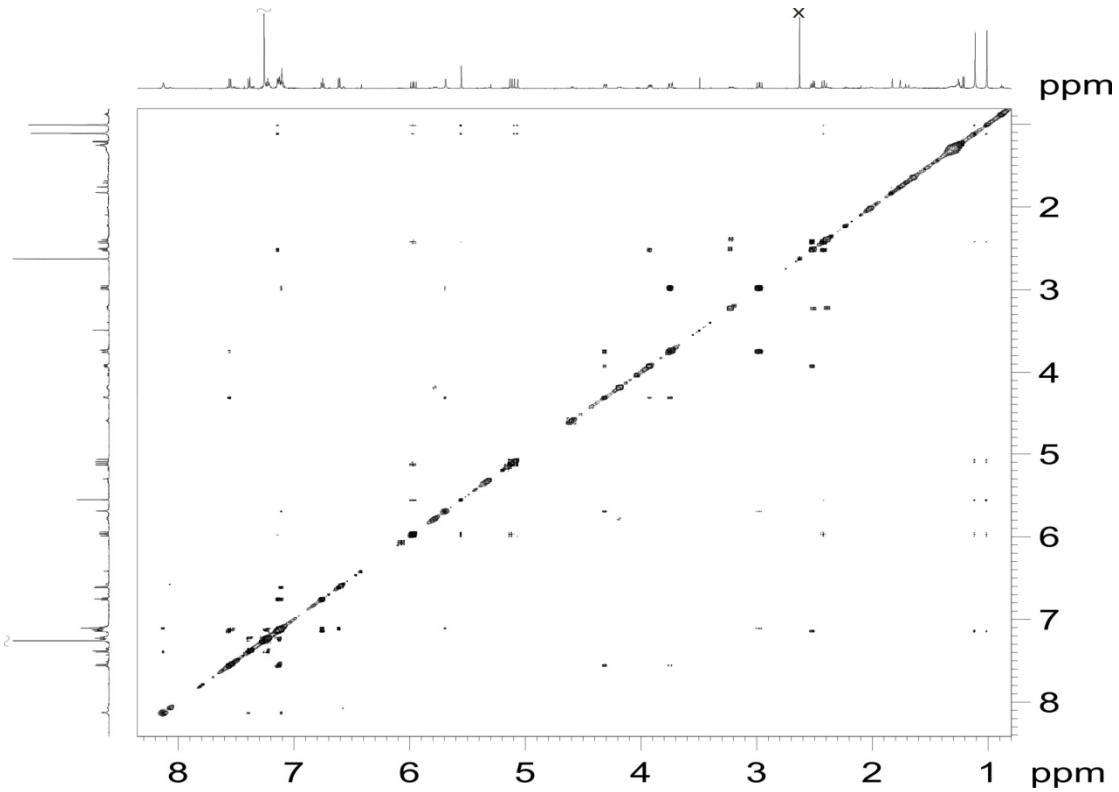

Figure S2.4: NOESY spectrum of **3b** in $CDCl_3$. The label X indicates signal of impurity and the solvent signal is partially cut in the 1D projection for clarity.

6

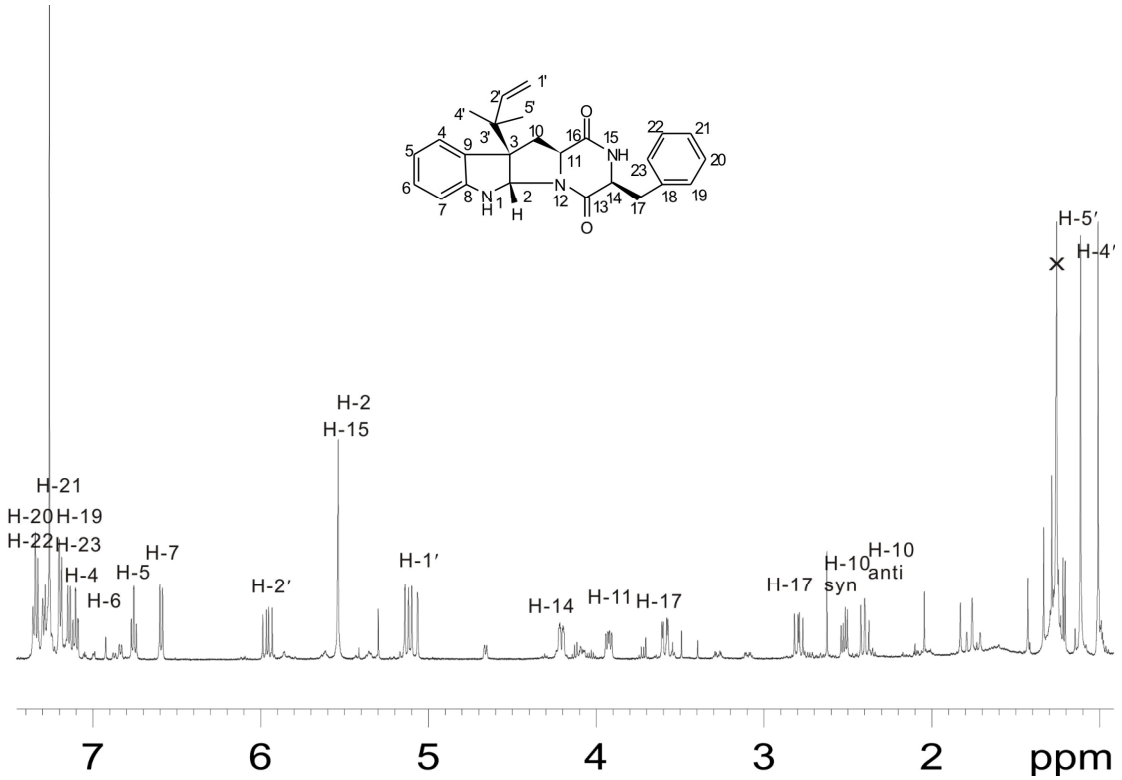

Figure S3.1: ^{1}H-NMR spectrum of **3c** in $CDCl_3$. The label X indicates signal of impurity.

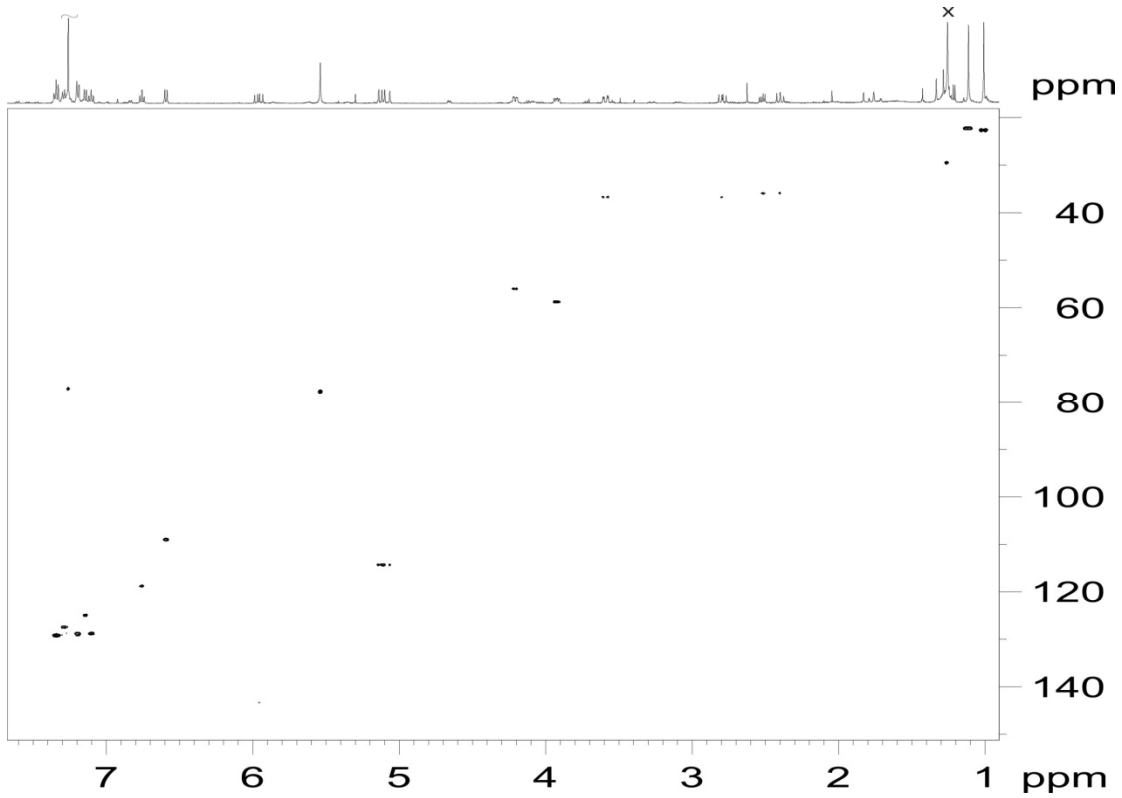

Figure S3.2: HSQC spectrum of **3c** in $CDCl_3$. The label X indicates signal of impurity and the solvent signal is partially cut in the 1D projection for clarity.

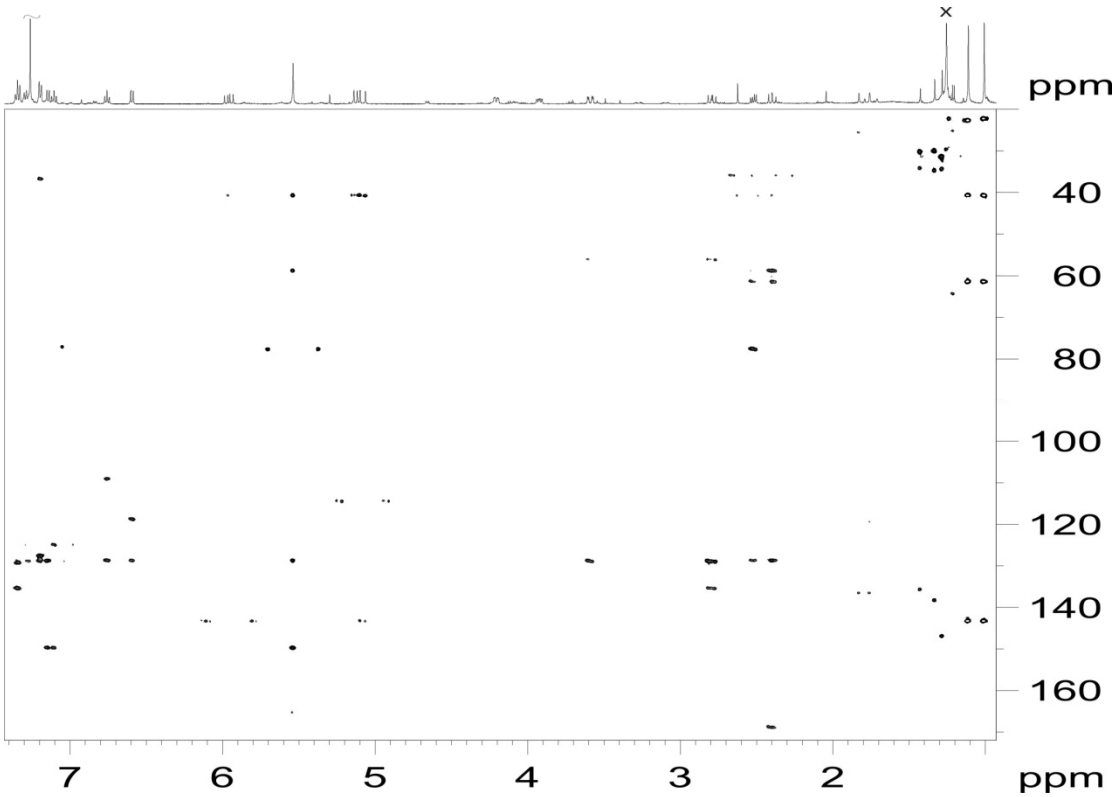

Figure S3.3: HMBC spectrum of **3c** in $CDCl_3$. The label X indicates signal of impurity and the solvent signal is partially cut in the 1D projection for clarity.

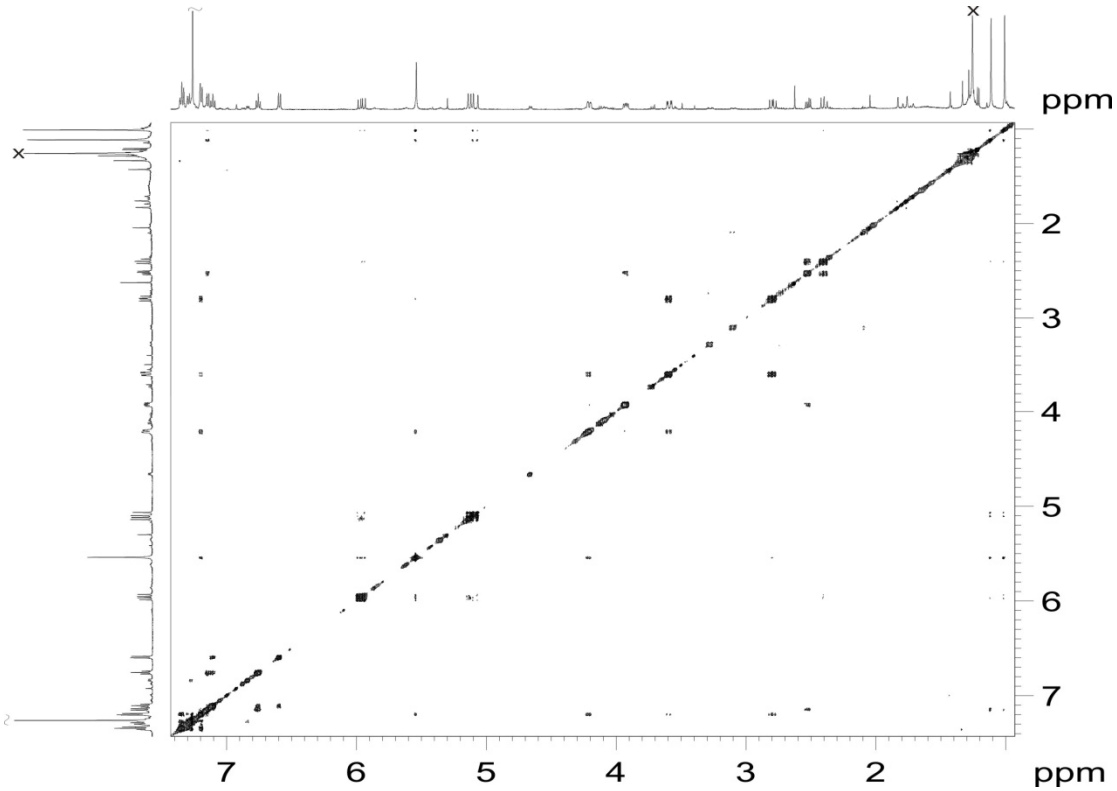

Figure S3.4: NOESY spectrum of **3c** in $CDCl_3$. The label X indicates signal of impurity and the solvent signal is partially cut in the 1D projection for clarity.

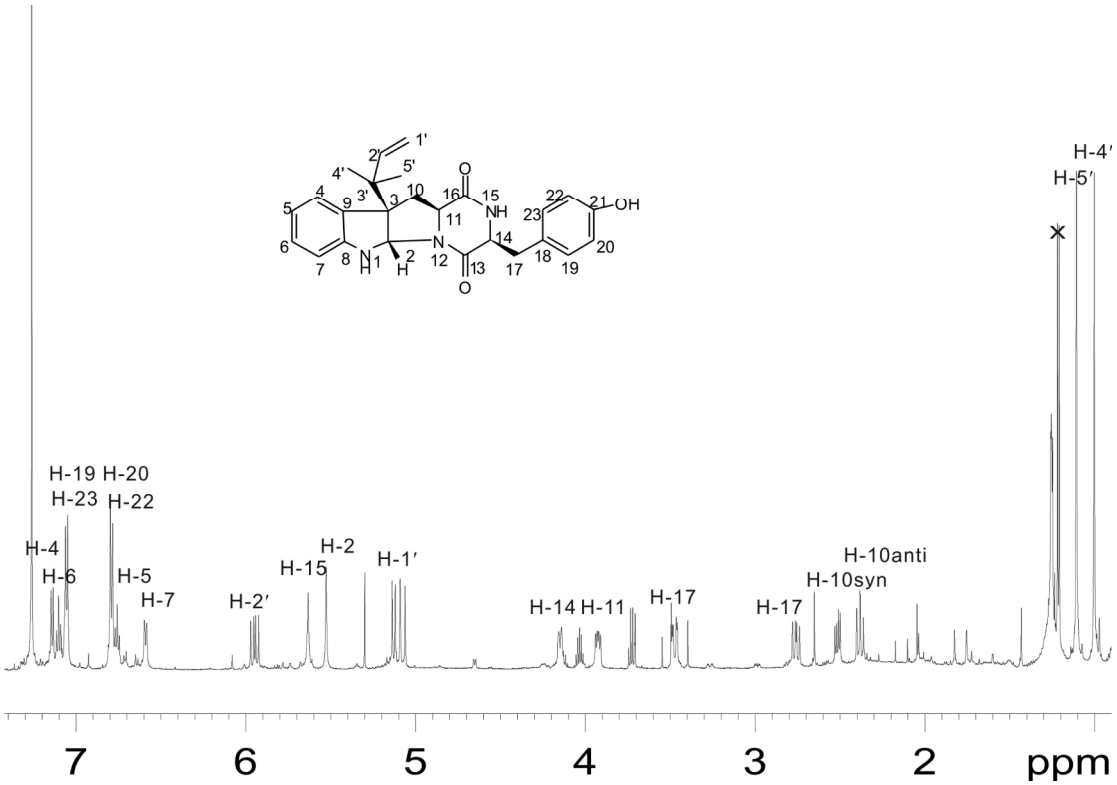

Figure S4.1: ^{1}H-NMR spectrum of **3d** in $CDCl_3$. The label X indicates signal of impurity.

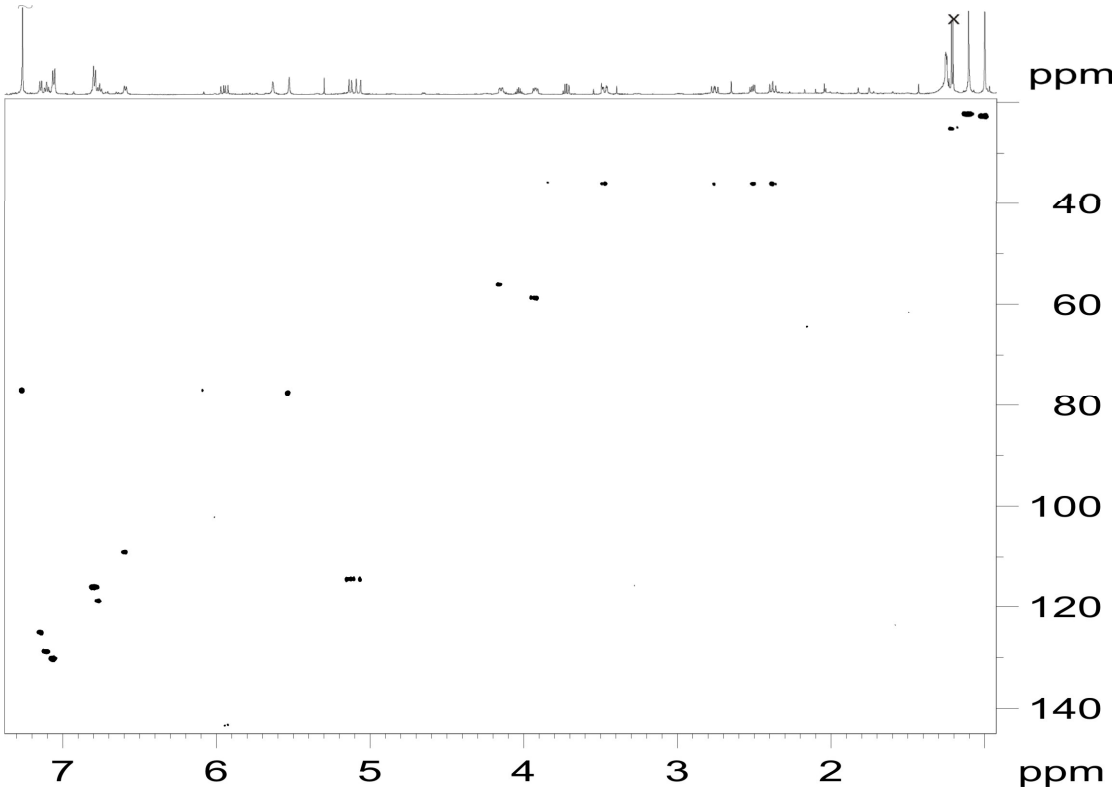

Figure S4.2: HSQC spectrum of **3d** in $CDCl_3$. The label X indicates signal of impurity and the solvent signal is partially cut in the 1D projection for clarity.

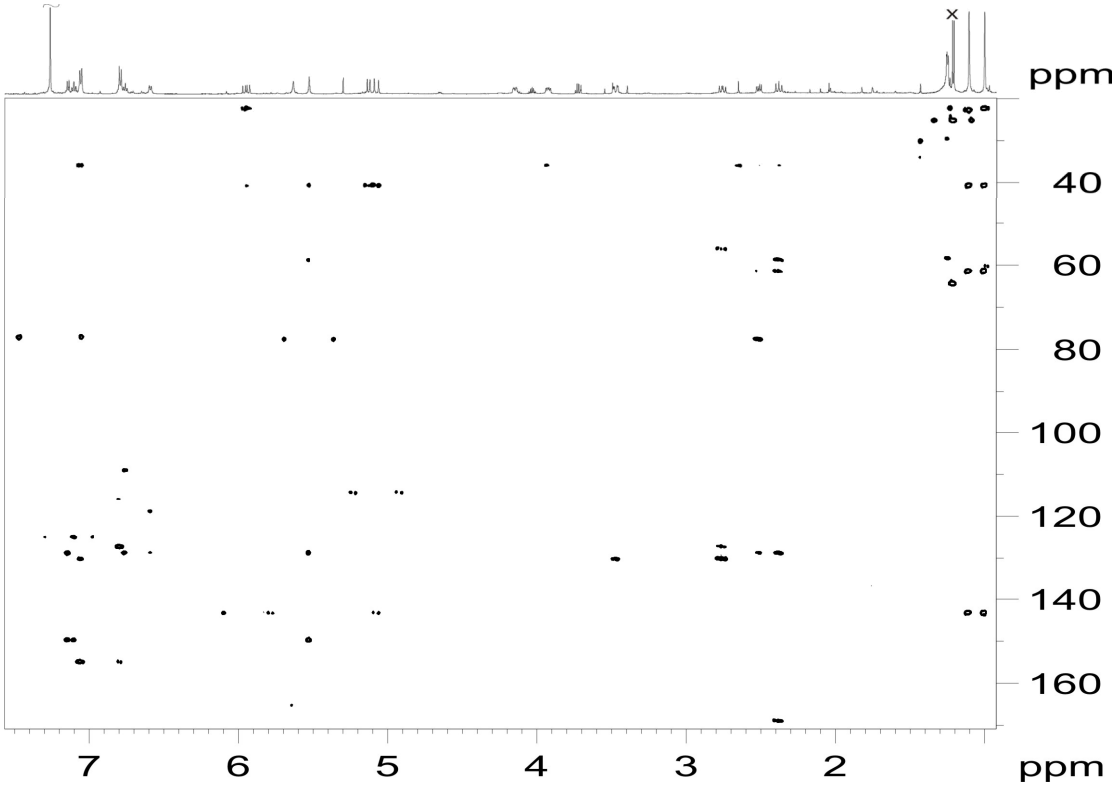

Figure S4.3: HMBC spectrum of **3d** in $CDCl_3$. The label X indicates signal of impurity and the solvent signal is partially cut in the 1D projection for clarity.

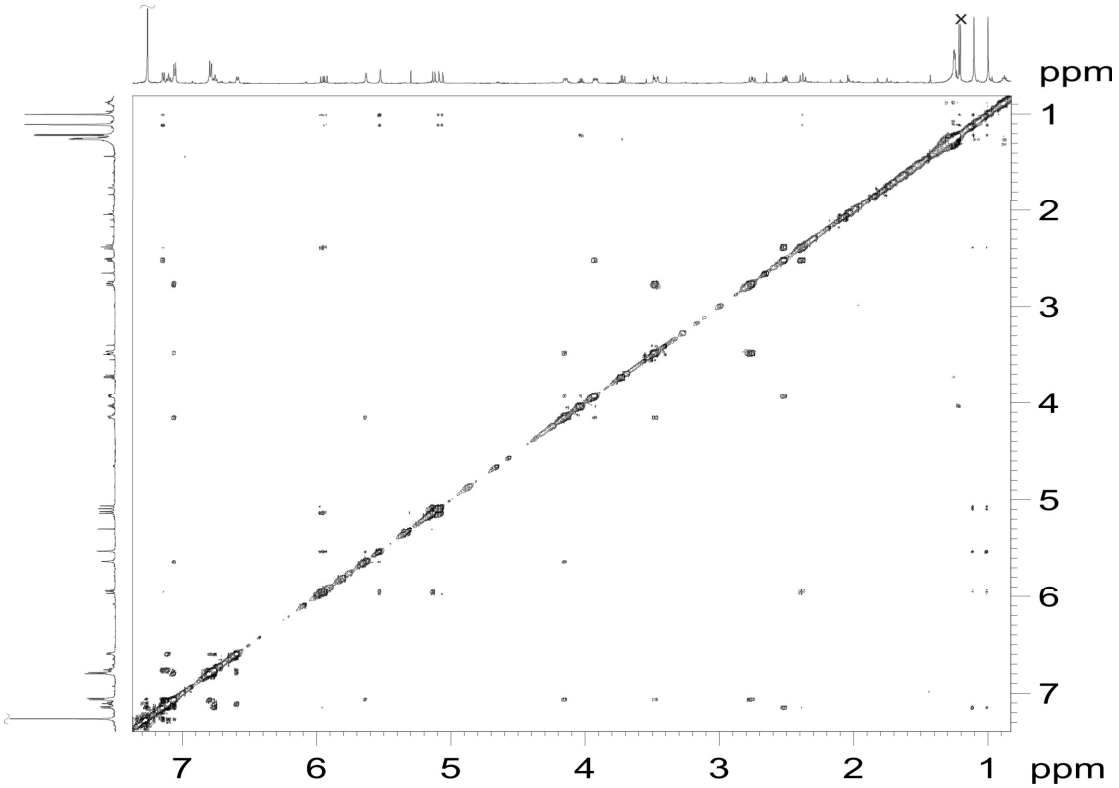

Figure S4.4: NOESY spectrum of **3d** in $CDCl_3$. The label X indicates signal of impurity and the solvent signal is partially cut in the 1D projection for clarity.

10

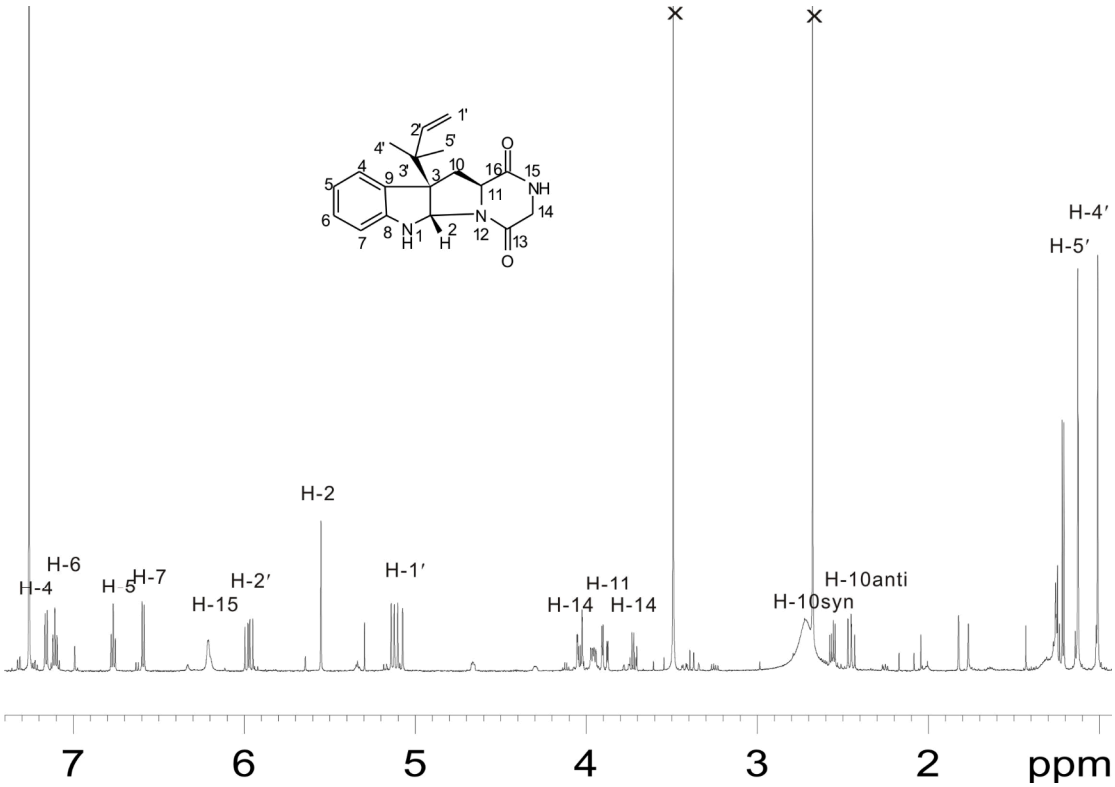

Figure S5.1: ^{1}H-NMR spectrum of **3f** in $CDCl_3$. The label X indicates signals of impurity.

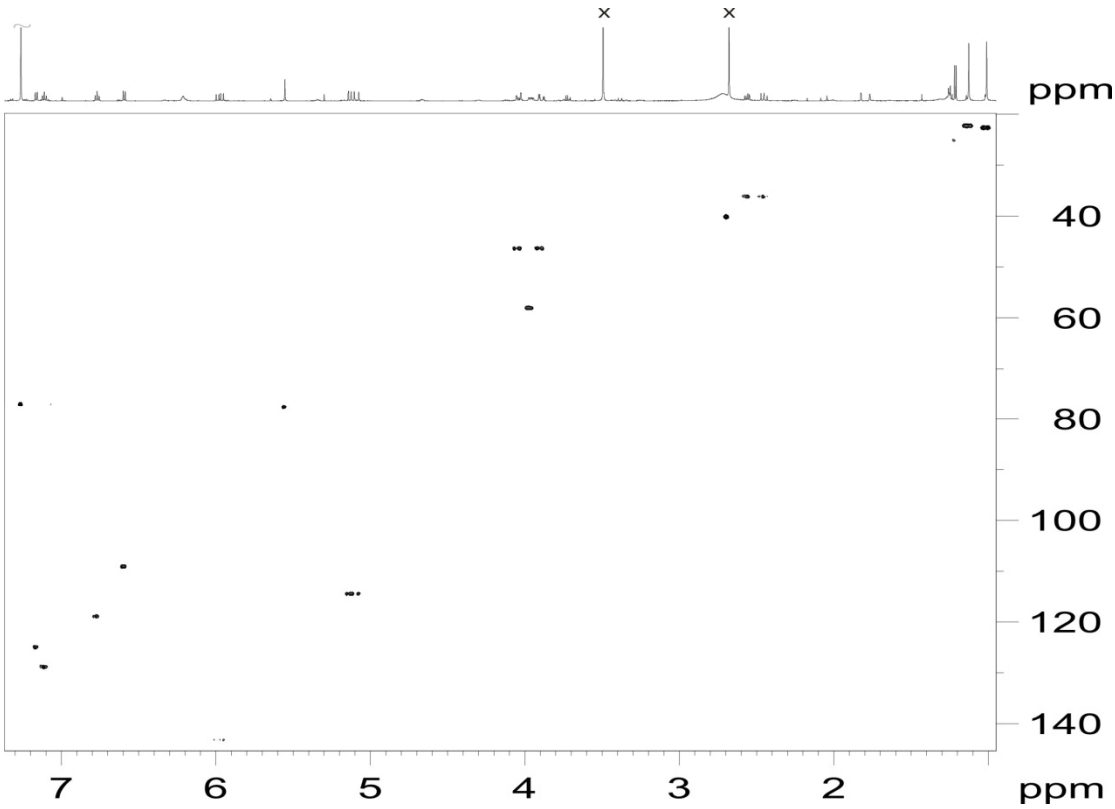

Figure S5.2: HSQC spectrum of **3f** in $CDCl_3$. The label X indicates signals of impurity and the solvent signal is partially cut in the 1D projection for clarity.

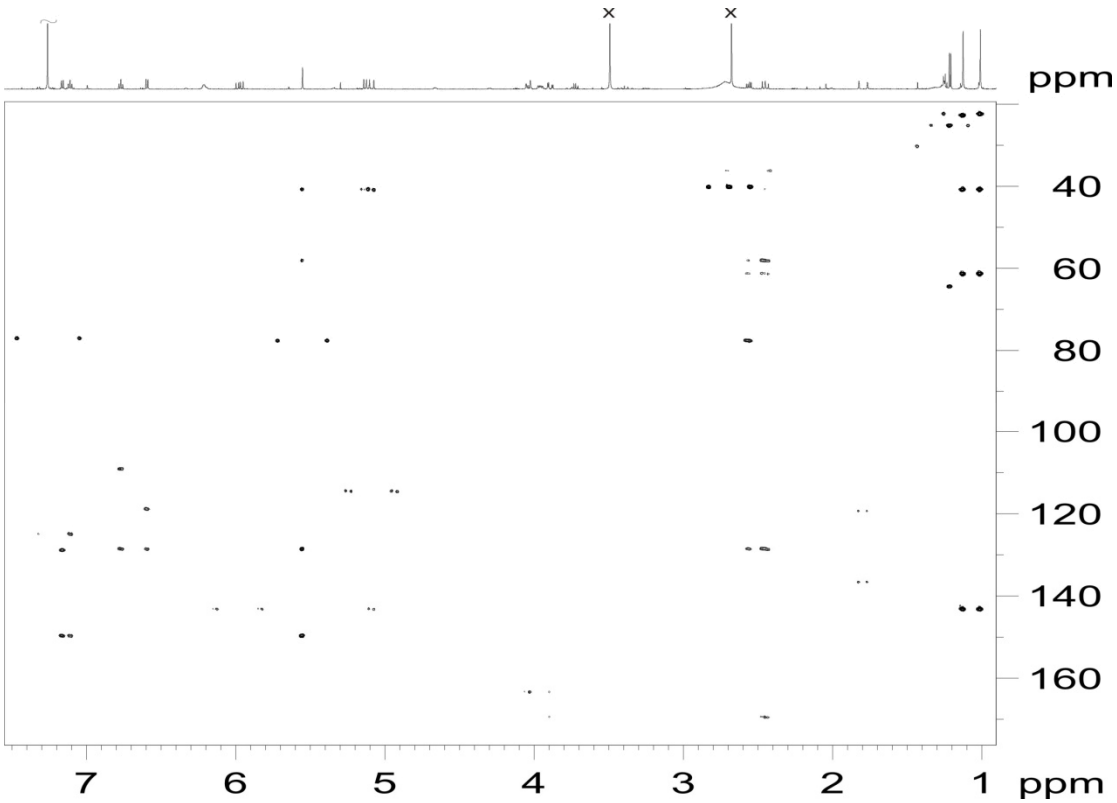

Figure S5.3: HMBC spectrum of **3f** in $CDCl_3$. The label X indicates signals of impurity and the solvent signal is partially cut in the 1D projection for clarity.

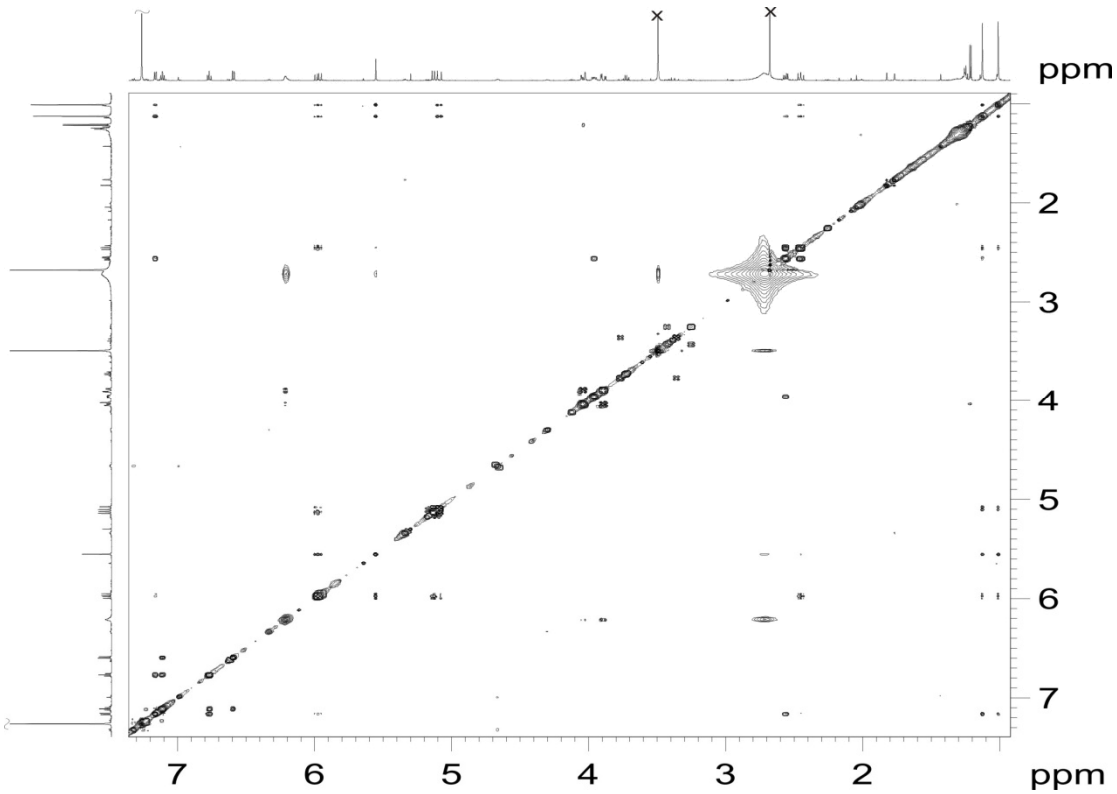

Figure S5.4: NOESY spectrum of **3f** in $CDCl_3$. The label X indicates signals of impurity and the solvent signal is partially cut in the 1D projection for clarity.

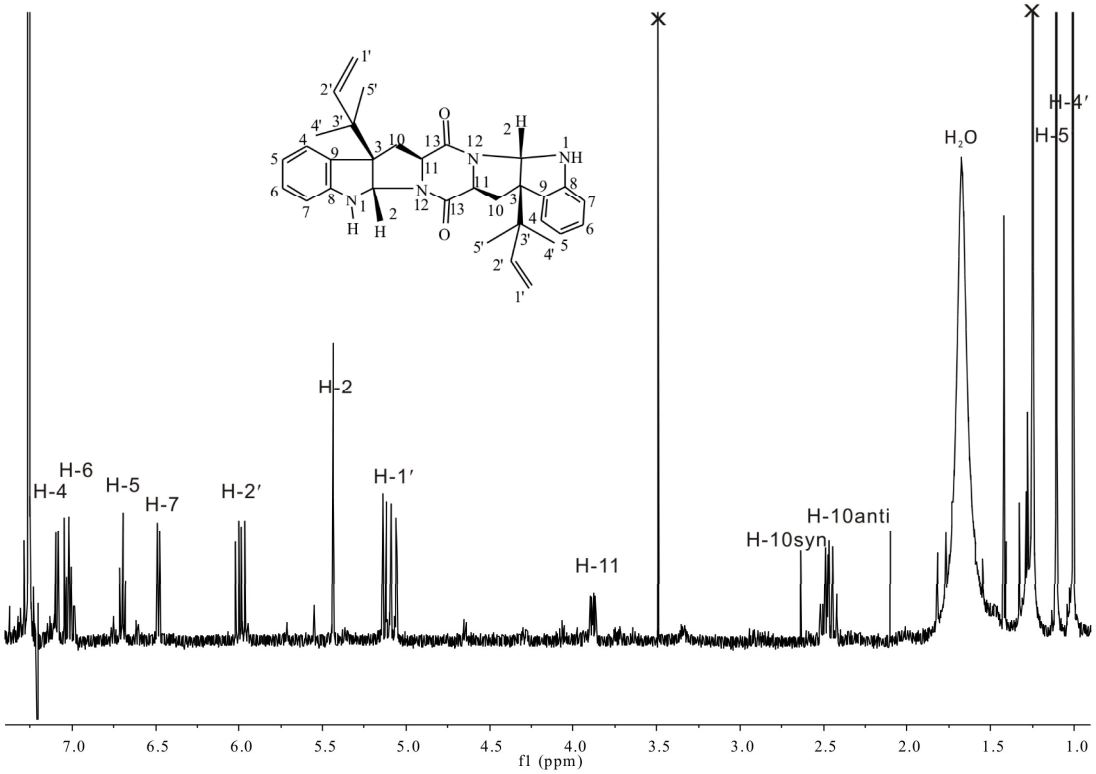

Figure S6.1: ^{1}H-NMR spectrum of **4b** in $CDCl_3$. The label X indicates signals of impurity.

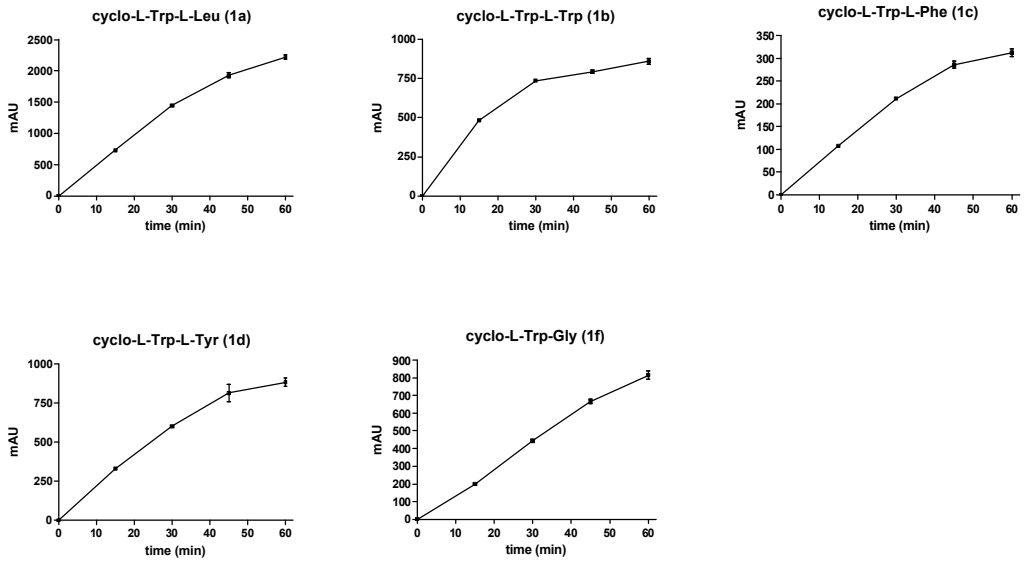

Figure S7: Time dependence of the product formation. The assay condition including components, substrate and enzyme concentrations as well as incubation temperature was identical to that for determination of the kinetic parameters

5.2 Biochemical characterization of indole prenyltransferases: Filling the last gap of prenylation positions by a 5-dimethylallyltryptophan synthase from *Aspergillus clavatus*

THE JOURNAL OF BIOLOGICAL CHEMISTRY VOL. 287, NO. 2, pp. 1371–1380, January 6, 2012

Biochemical Characterization of Indole Prenyltransferases

FILLING THE LAST GAP OF PRENYLATION POSITIONS BY A 5-DIMETHYLALLYLTRYPTOPHAN SYNTHASE FROM ASPERGILLUS CLAVATUS[*] [S]

Received for publication, October 27, 2011, and in revised form, November 26, 2011 Published, JBC Papers in Press, November 28, 2011, DOI 10.1074/jbc.M111.317982

Xia Yu (于霞)[‡1], Yan Liu (刘燕)[‡§2], Xiulan Xie (谢秀兰)[¶], Xiao-Dong Zheng (郑晓冬)[§], and Shu-Ming Li (李书明)[‡3]

From the [‡]Institut für Pharmazeutische Biologie und Biotechnologie, Philipps-Universität Marburg, Deutschhausstrasse 17A, 35037 Marburg, Germany, the [§]Department of Food Science and Nutrition, Zhejiang University, 310058 Hangzhou, Zhejiang, China, and the [¶]Fachbereich Chemie, Philipps-Universität Marburg, Hans-Meerwein-Strasse, 35032 Marburg, Germany

Background: Known indole prenyltransferases catalyzed regioselective prenylations at N-1, C-2, C-3, C-4, C-6, and C-7 of the indole ring.
Results: Recombinant 5-DMATS was assayed with tryptophan and derivatives in the presence of DMAPP.
Conclusion: 5-DMATS prenylated indole derivatives at C-5.
Significance: 5-DMATS fills the last prenylation gap of indole derivatives and could be used as a potential catalyst for chemoenzymatic synthesis.

The putative prenyltransferase gene *ACLA_031240* belonging to the dimethylallyltryptophan synthase superfamily was identified in the genome sequence of *Aspergillus clavatus* and overexpressed in *Escherichia coli*. The soluble His-tagged protein EAW08391 was purified to near homogeneity and used for biochemical investigation with diverse aromatic substrates in the presence of different prenyl diphosphates. It has shown that in the presence of dimethylallyl diphosphate (DMAPP), the recombinant enzyme accepted very well simple indole derivatives with L-tryptophan as the best substrate. Product formation was also observed for tryptophan-containing cyclic dipeptides but with much lower conversion yields. In contrast, no product formation was detected in the reaction mixtures of L-tryptophan with geranyl or farnesyl diphosphate. Structure elucidation of the enzyme products by NMR and MS analyses proved unequivocally the highly regiospecific regular prenylation at C-5 of the indole nucleus of the simple indole derivatives. EAW08391 was therefore termed 5-dimethylallyltryptophan synthase, and it filled the last gap in the toolbox of indole prenyltransferases regarding their prenylation positions. K_m values of 5-dimethylallyltryptophan synthase were determined for L-tryptophan and DMAPP at 34 and 76 μM, respectively. Average turnover number (k_{cat}) at 1.1 s^{-1} was calculated from kinetic data of L-tryptophan and DMAPP. Catalytic efficiencies of 5-dimethylallyltryptophan synthase for L-tryptophan at 25,588 $s^{-1} \cdot M^{-1}$ and for other 11 simple indole derivatives up to 1538 $s^{-1} \cdot M^{-1}$ provided evidence for its potential usage as a catalyst for chemoenzymatic synthesis.

Prenylated indole alkaloids represent a group of natural products with diverse chemical structures and are widely distributed in bacteria, fungi, plants, and marine organisms (1, 2). Because of their impressive pharmacological and biological activities as drugs or as toxins (1, 3), prenylated indole alkaloids attract the attention of scientists from different scientific disciplines, including chemistry, ecology, biology, pharmacology, and biochemistry (1, 4–7). These compounds are hybrid molecules containing prenyl moieties derived from prenyl diphosphates and indole or indoline ring from tryptophan or its precursors (1, 5). Indole prenyltransferases catalyze the connection of these two characteristic structural features and contribute significantly to the structural diversity of the prenylated indole alkaloids. Significant progress has been achieved for molecular biological, biochemical, and structural biological investigations on different prenyltransferase groups, including indole prenyltransferases (1, 8, 9). By the end of October 2011, 20 indole prenyltransferases from bacteria and fungi have been characterized biochemically (1, 10–15). These enzymes catalyzed the transfer of prenyl moieties onto nitrogen or carbon atoms at the indole ring resulting in formation of "regularly" or "reversely" prenylated derivatives (15). More interestingly, indole prenyltransferases showed the usually broad substrate specificity but catalyzed regiospecific prenylation at different positions of indole or indoline rings (Fig. 1) (15). CymD from the marine actinobacterium *Salinispora arenicola* catalyzed the reverse prenylation at the indole nitrogen of L-tryptophan (12), whereas FtmPT2 from the fungus *Aspergillus fumigatus* catalyzed the regular prenylation of 12,13-dihydroxyfumitremorgin C at this position (16). Regular and reverse C2-prenylations were observed for FtmPT1 (17) and FgaPT1 (18), both from *A. fumigatus*, respectively. Prenylations at C-3 of cyclic dipeptides by AnaPT (19) and CdpC3PT (10), both from the fungus *Neosartorya fischeri,* lead to the formation of indoline derivatives with an α- and β-configured reverse

* This work was supported in part by Deutsche Forschungsgemeinschaft Grant Li844/4-1 (to S.-M. L.) and by the Deutscher Akademischer Austauschdienst within the Programme des Projektbezogenen Personenaustauschs.
The nucleotide sequence(s) reported in this paper has been submitted to the GenBank™/EBI Data Bank with accession number(s) XM_001269816.
[S] This article contains supplemental Tables S1–S4 and Figs. S1–S14.
[1] Recipient of a Ph.D. scholarship from the China Scholarship Council for fellowships.
[2] Recipient of a project-related person exchange program from the China Scholarship Council for fellowships.
[3] To whom correspondence should be addressed. Tel.: 49-6421-2822461; Fax: 49-6421-2825365; E-mail: shuming.li@staff.uni-marburg.de.

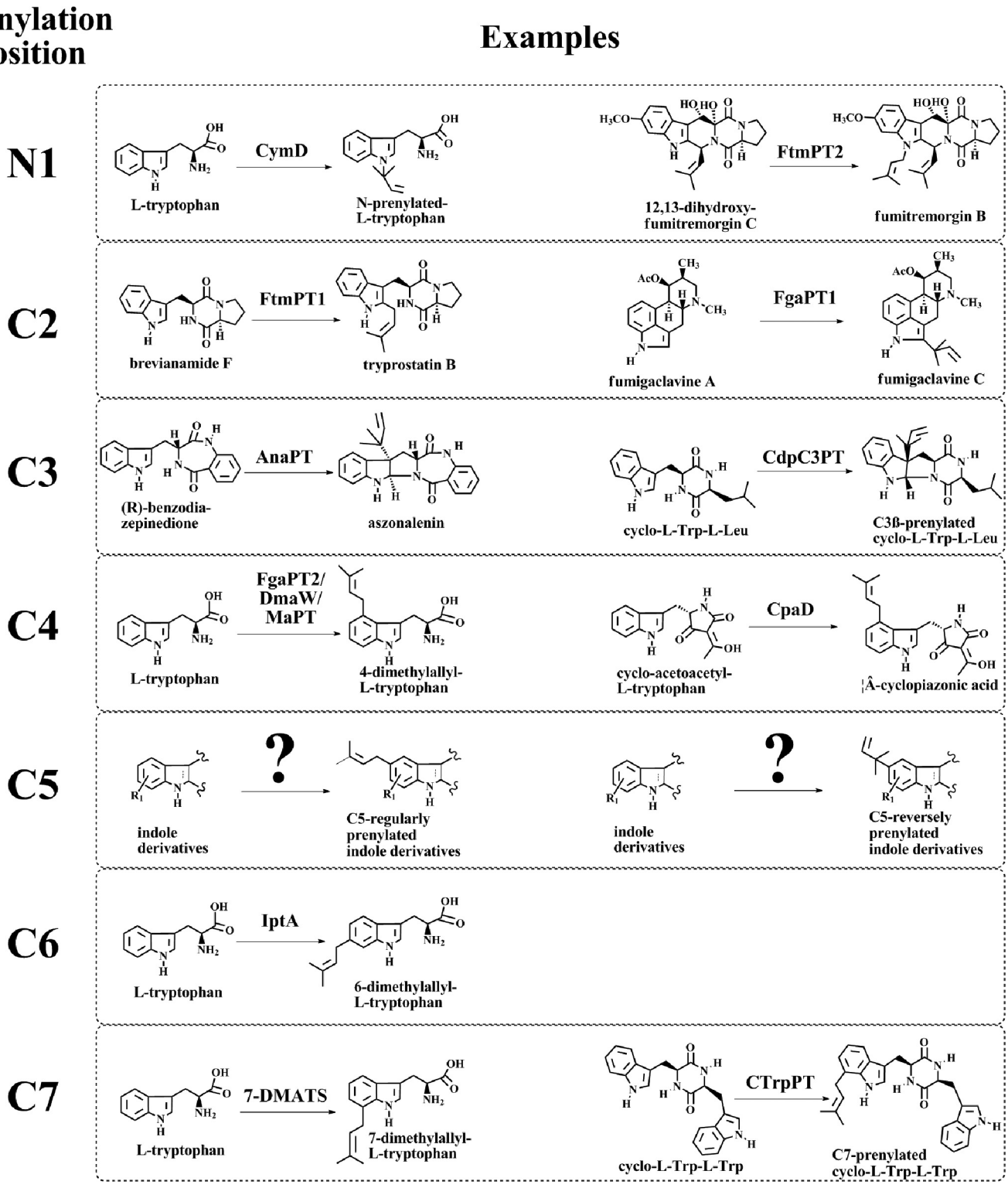

FIGURE 1. **Examples of indole prenyltransferases with different prenylation positions.**

prenyl moiety, respectively. FgaPT2 and its orthologues from different fungi represent the first pathway-specific enzyme in the biosynthesis of ergot alkaloids and catalyzed the regular prenylation of L-tryptophan at C-4 (3, 20). CpaD from *Aspergillus oryzae* catalyzed regular C4-prenylation as well but used cyclo-acetoacetyl-L-tryptophan as substrate (21). IptA from a soil bacterium *Streptomyces* sp. was reported to prenylate L-tryptophan at C-6 (13) and 7-DMATS[4] from *A. fumigatus* at C-7 (22). An additional

[4] The abbreviations used are: 7-DMATS, 7-dimethylallyltryptophan synthase; DMAPP, dimethylallyl diphosphate; 5-DMATS, 5-dimethylallyltryptophan synthase; HMBC, heteronuclear multiple-bond correlation spectroscopy; FPP, farnesyl diphosphate; GPP, geranyl diphosphate.

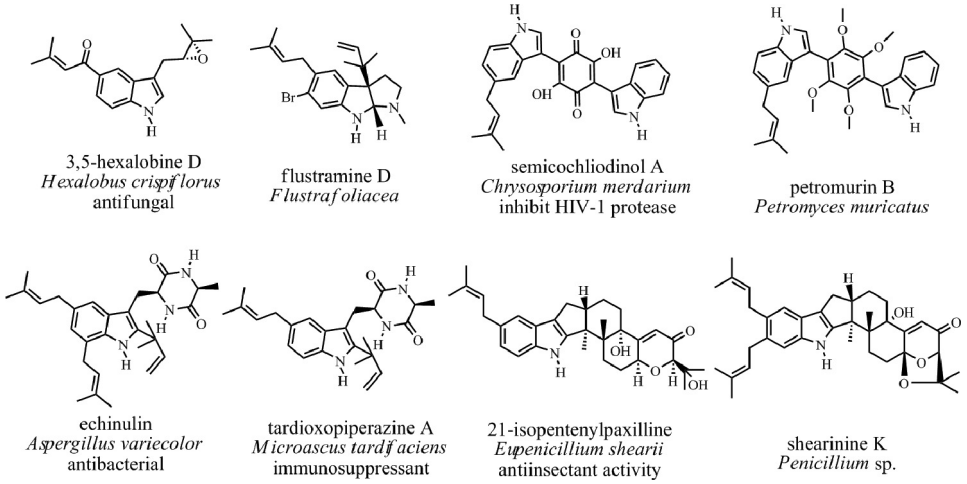

FIGURE 2. **Examples of naturally occurring C5-prenylated indole alkaloids.**

example of C7-prenyltransferase is CTrpPT from *A. oryzae*, which used cyclo-L-Trp-L-Trp as the best substrate (11).

In summary, indole prenyltransferases with regioselectivity for N-1, C-2, C-3, C-4, C-6, and C-7 have already been identified and characterized in detail (Fig. 1). However, a prenyltransferase responsible for transferring a prenyl moiety to C-5 of the indole ring has not been reported prior to this study. However, database searching revealed the presence of a number of biologically active indole alkaloids carrying a prenyl moiety at C-5 in nature (Fig. 2). These compounds include simple prenylated indole derivatives like the antifungal compound 3,5-hexalobine D from the plant *Hexalobus crispiflorus* (23) or the brominated tryptamine derivative flustramine D from the bryozoan *Flustra foliacea* (24). Semicochliodinol A from the fungus *Chrysosporium merdarium* (25) and petromurin B from the fungus *Petromyces muricatus* (26) are C5-prenylated indolyl benzoquinones derived from two tryptophan molecules (27). Semicochliodinol A was reported to inhibit HIV-1 protease (25). C5-prenylated derivatives were also found for tryptophan-containing cyclic dipeptides like cyclo-L-Trp-L-Ala, *e.g.* echinulin from *Aspergillus* strains (28) or tardioxopiperazine A from the fungus *Microascus tardifaciens* (29). A relatively large indole alkaloid group are the indole diterpenes from *Penicillium* (30) and other Ascomycetes (31). The members of this group carry prenyl moieties at C-5 (21-isopentenylpaxilline) (32), C-6, or at both positions (shearinine K) (30), or modified structures thereof.

The discrepancy between the natural occurrence of a large number of C5-prenylated indole derivatives on the one hand and undiscovered C5-prenyltransferases on the other hand prompted us to search for such enzymes. In this study, we reported the identification and characterization of the first C5-prenyltransferase of indoles, *i.e.* 5-dimethylallyltryptophan synthase (5-DMATS) from *Aspergillus clavatus* and its potential usage as a catalyst for chemoenzymatic synthesis.

EXPERIMENTAL PROCEDURES

Computer-assisted Sequence Analysis—Sequence identities were obtained by alignments of amino acid sequences using the program "BLAST 2 SEQUENCES" (www.ncbi.nlm.nih.gov). FGENESH from Softberry and the DNASIS software package (version 2.1, Hitachi Software Engineering, San Bruno, CA) were used for exon prediction and sequence analysis, respectively.

Chemicals—Dimethylallyl diphosphate (DMAPP), geranyl diphosphate (GPP), and farnesyl diphosphate (FPP) were prepared according to the method described for geranyl diphosphate by Woodside *et al.* (33). Indole derivatives of the highest available purity were purchased from TCI, Acros Organics, Aldrich, Sigma, Bachem, and Alfa Aesar.

Bacterial Strains, Plasmids, and Culture Conditions—pGEM-T Easy and pQE70 were obtained from Promega and Qiagen (Hilden, Germany), respectively. *Escherichia coli* XL1 Blue MRF′ (Stratagene, Amsterdam, the Netherlands) and M15 [*pREP4*] (Qiagen) were used for cloning and expression experiments, respectively. They were grown in liquid Terrific-Broth (TB) or Luria-Bertani (LB) medium and on solid LB medium with 1.5% (w/v) agar at 37 or 22 °C. 50 $\mu g \cdot ml^{-1}$ of carbenicillin were used for selection of recombinant *E. coli* XL1 Blue MRF′ strains. Addition of carbenicillin at 50 $\mu g \cdot ml^{-1}$ and kanamycin at 25 $\mu g \cdot ml^{-1}$ was used for selection of recombinant *E. coli* M15 [*pREP4*] strains.

Cultivation of A. clavatus, RNA Isolation, and cDNA Synthesis—*A. clavatus* NRRL1 was kindly provided by Agricultural Research Service Culture Collection, United States Department of Agriculture, and was cultivated on solid YME media consisting of 0.4% (w/v) yeast extract, 1% (w/v) malt extract, 0.4% (w/v) glucose, pH 7.3, and 2% (w/v) agar at 26 °C. For RNA isolation, mycelia of *A. clavatus* NRRL1 from plates were inoculated into a 300-ml Erlenmeyer flask containing 100 ml of liquid YME media and cultivated at 26 °C and 160 rpm for 7 days. After separation of mycelia from the medium, RNA was isolated by using the High Pure RNA isolation kit (Roche Diagnostics) according to the manufacturer's protocol. cDNA was synthesized with the Transcriptor High Fidelity cDNA synthesis kit (Roche Diagnostics).

PCR Amplification and Gene Cloning—PCR amplification was carried out on a MiniCycler from Bio-Rad. A PCR fragment of 1300 bp containing the entire coding sequence of *5-dmats* was amplified from cDNA by using Expand high fidelity kit (Roche Diagnostics). The primers were 5-DMATS_for (5′-

GCCCAGC/ATGCCTCACCAAAACAGC-3′) at the 5′-end, and 5-DMATS_rev (5′- **GGTCGAAGATCT**CAATTTCCAAGACTT-3′) at the 3′-end of the gene. Bold letters represent mutations inserted in comparison with the original genome sequence to give the underlined restriction site SphI at the start codon in 5-DMATS_for and BglII located at the predicted stop codon in 5-DMATS_rev. A program of 30 cycles with annealing at 58 °C for 50 s and elongation at 72 °C for 90 s was used for PCR amplification. The PCR fragment was cloned into pGEM-T easy vector resulting in plasmid pYL08, which was subsequently sequenced (Eurofins MWG Operon, Ebersberg, Germany) to confirm the sequence. Plasmid pYL08 was digested with BglII alone or together with SphI to obtain BglII-BglII fragment of 748 bp and SphI-BglII fragment of 531 bp, respectively. To get the expression construct pYL09, these two fragments were cloned into pQE70 subsequently.

Overproduction and Purification of His_6-5-DMATS—For overproduction of 5-DMATS, *E. coli* M15 [*pREP4*] cells harboring the plasmid pYL09 were cultivated in 2000-ml Erlenmeyer flasks containing 1000 ml of liquid TB medium, supplemented with carbenicillin (50 $\mu g \cdot ml^{-1}$) and kanamycin (25 $\mu g \cdot ml^{-1}$), and then grown at 37 °C to an absorption at 600 nm of 0.6. For induction, isopropyl thiogalactoside was added to a final concentration of 0.4 mM, and the cells were cultivated for a further 16 h at 22 °C before harvest. The bacterial cultures were centrifuged, and the pellets were resuspended in lysis buffer (10 mM imidazole, 50 mM NaH_2PO_4, 300 mM NaCl, pH 8.0) at 2–5 ml/g wet weight. After addition of 1 $mg \cdot ml^{-1}$ lysozyme and incubation on ice for 30 min, the cells were sonicated six times for 10 s each at 200 watts. To separate the cellular debris from the soluble proteins, the lysate was centrifuged at 13,000 × *g* for 30 min at 4 °C. One-step purification of the recombinant His_6-tagged fusion protein by affinity chromatography with nickel-nitrilotriacetic acid-agarose resin (Qiagen) was carried out according to the manufacturer's instructions. The protein was eluted with 250 mM imidazole in 50 mM NaH_2PO_4, 300 mM NaCl, pH 8.0. To change the buffer, the protein fraction was passed through a PD-10 column (GE Healthcare), which had been equilibrated with 50 mM Tris-HCl, 15% (v/v) of glycerol, pH 7.5, previously. 5-DMATS was eluted with the same buffer and frozen at −80 °C for enzyme assays.

Protein Analysis and Determination of Relative Molecular Mass of Active His_6-5-DMATS—Proteins were analyzed by 12% (w/v) SDS-polyacrylamide gels according to the method of Laemmli (34) and stained with Coomassie Brilliant Blue G-250. The M_r value of the recombinant active His_6-5-DMATS was determined by size exclusion chromatography on a HiLoad 16/60 Superdex 200 column (GE Healthcare), which had been equilibrated with 50 mM Tris-HCl buffer, pH 7.5, containing 150 mM NaCl. The column was calibrated with dextran blue 2000 (2000 kDa), ferritin (440 kDa), aldolase (158 kDa), conalbumin (75 kDa), carbonic anhydrase (29 kDa), and ribonuclease A (13.7 kDa) (GE Healthcare). The proteins were eluted with the same buffer as for equilibration.

Enzyme Assays with 5-DMATS—The enzyme reaction mixtures for determination of the relative activities with different indole derivatives or L-tyrosine (100 μl) contained 50 mM Tris-HCl, pH 7.5, 5 mM $CaCl_2$, 1 mM aromatic substrate, 2 mM DMAPP, GPP, or FPP, 0.15–5% (v/v) glycerol, 0–5% (v/v) DMSO, and 1 μM purified recombinant protein. The reaction mixtures were incubated at 37 °C for 7 h (with DMAPP) or 24 h (with GPP or FPP). The enzyme reactions were terminated by addition of 100 μl of methanol per 100 μl reaction mixture.

For determination of kinetic parameters of DMAPP, L-tryptophan at 1 mM and DMAPP at final concentrations of up to 3 mM were used as substrates. For determination of kinetic parameters of L-tryptophan and derivatives, the assays contained 2 mM DMAPP. Because of the difference of solubility in the aqueous system, various concentrations were used for aromatic substrates as follows: for **8a** and **12a** up to 5 mM, for **1a–3a**, **7a,** and **9a–11a** up to 2 mM, and for **4a–6a** up to 1 mM. The protein concentration was 20 nM (**1a**), 40 nM (DMAPP), or 200 nM (other substrates), and the incubation time was 30 min (**1a**), 40 min (DMAPP) or 60 min (other substrates).

Preparative Synthesis of Enzyme Products for Structure Elucidation—For isolation of the enzyme products, reactions were carried out in large scale (10 ml) containing each of the 12 substrates **1a–12a** (1 mM), DMAPP (2 mM), $CaCl_2$ (5 mM), Tris-HCl (50 mM, pH 7.5), glycerol 0.15–5% (v/v), and 5-DMATS (1.4 μM). After incubation for 16 h, the reactions were terminated by addition of 10 ml of methanol each. After removal of the precipitated protein by centrifugation at 6000 rpm for 30 min, the reaction mixtures were concentrated on a rotating vacuum evaporator at 30 °C to a final volume of 1 ml before injection onto HPLC.

HPLC Conditions for Analysis and Isolation of Enzyme Products—The enzyme products of the incubation mixtures were analyzed by HPLC on an Agilent series 1200 by using a Multiphor 120 RP-18 column (250 × 4 mm, 5 μm, C+S Chromatographie Service, Langerwehe, Germany) at a flow rate of 1 $ml \cdot min^{-1}$. Water (solvent A) and methanol (solvent B) each with 0.5% (v/v) trifluoroacetic acid were used as solvents. For analysis of enzyme products of tryptophan, simple indole derivatives and L-tyrosine, a linear gradient of 20–100% (v/v) solvent B, for 15 min were used. The column was then washed with 100% (v/v) solvent B for 5 min and equilibrated with 20% (v/v) solvent B for 5 min. For analysis of enzyme products of tryptophan-containing cyclic dipeptides, the gradient began with 40% (v/v) solvent B and increased from 40 to 100% (v/v) solvent B in 15 min. After washing with 100% (v/v) solvent B for 5 min, the column was equilibrated with 40% (v/v) solvent B after each run. For assays with GPP or FPP, a linear gradient of 20–84% (v/v) solvent B for 12 min and then 84–100% (v/v) solvent B for 18 min was used. The column was then washed with 100% (v/v) solvent B for 10 min and equilibrated with 20% (v/v) solvent B for 5 min. Detection was carried out with a Photo Diode Array Detector.

For isolation of the enzyme products, the same HPLC equipment with a Multospher 120 RP-18 column (250 × 10 mm, 5 μm, C+S Chromatographie Service) was used. The flow rate was 2.5 $ml \cdot min^{-1}$. Water (solvent C) and methanol (solvent D) without acid were used as solvents. Gradients of 20–100% (v/v) solvent D for different times were used for isolation. The column was then washed with 100% (v/v) solvent D for 8 min and equilibrated with 20% (v/v) solvent D for 8 min.

NMR Spectroscopic Analysis and High Resolution ESI-MS—^{1}H NMR spectra were recorded on a Bruker Avance 500 MHz spectrometer or a JEOL ECX-400 spectrometer. The HSQC and HMBC spectra were recorded with standard methods (35) on the Bruker Avance 500 MHz spectrometer. Chemical shifts were referenced to the signal of CD_3OD at 3.31 ppm or DMSO-d_6 at 2.50 ppm. All spectra were processed with MestReNova 5.2.2.

The isolated products were also analyzed by high resolution ESI-MS with a Q-Trap Quantum (Applied Biosystems). Positive ESI-MS data are given in supplemental Table S3.

Nucleotide Sequence Accession Number—The coding sequence of *5-dmats* (*ACLA_031240*) is available at GenBank™ under the accession number XM_001269816.

RESULTS

Sequence Analysis and Cloning of 5-Dimethylallyltryptophan Synthase Gene 5-dmats—In the course of our search for prenyltransferases responsible for prenylation of tryptophan or indole derivatives at C-5, one putative gene *ACLA_031240* from the genome sequence of *A. clavatus* NRRL1 raised our interest. The deduced gene product EAW08391 consists of 427 amino acids and shares high sequence similarities with C4-prenyltransferases of tryptophan, *e.g.* 52% identity with FgaPT2 from *A. fumigatus* (20) at the amino acid level. Based on this homology, it can be expected that EAW08391 catalyzes a similar reaction as FgaPT2.

Inspection of down- and upstream genes of *ACLA_031240* in the genome sequence of *A. clavatus* (www.ncbi.nlm.nih.gov) revealed that the enzymes encoded by these genes are very likely involved in the fungal development and biosynthesis of primary rather than secondary metabolites, *e.g.* prenylated indole alkaloids. This means that *ACLA_031240* is very likely not clustered with genes for the biosynthesis of secondary metabolites. For example, in the downstream sequence of *ACLA_031240*, the putative gene *ACLA_031250* is separated from *ACLA_031240* by a segment of 13 kb and encodes a putative MYB family conidiophore development protein. *ACLA_031260*, downstream of *ACLA_031250*, was predicted to be a glycosyl hydrolase gene. In the upstream sequence of *ACLA_031240*, *ACLA_031230* was predicted to encode a UDP-*N*-acetylglucosaminyltransferase involved in the cell wall biosynthesis. *ACLA*_031220 is likely a 60 S ribosomal protein gene.

Blast search with EAW08391 from *A. clavatus* in GenBank™ indicated the presence of three homologues as follows: XP_001818057 encoded by *AOR_1_1880174* from *A. oryzae* RIB40; EED57628 encoded by *AFLA_083250* from *Aspergillus flavus* NRRL3357, and EEQ32624 encoded by *MCYG_05443* from *Arthroderma otae* CBS113480. EAW08391 shares on the amino acid level sequence identities of 76, 75, and 74% with XP_001818057, EED57628, and EEQ32624, respectively. It can be expected that these three enzymes catalyze the same reaction as EAW08391.

Inspection of down- and upstream genes of *AOR_1_1880174* in the genome sequence of *A. oryzae*, *AFLA_083250* of *A. flavus*, and *MCYG_05443* of *A. otae* (www.ncbi.nlm.nih.gov) indicated also their nonclustering with other secondary metabolite biosynthesis genes. The direct neighboring genes of *AOR_1_1880174* were predicted to encode L-arabitol/xylitol dehydrogenase (*AOR_1_1878174*) and a putative transporter gene for choline, γ-aminobutyric acid, or other amino acids (*AOR_1_1882174*). Orthologues of these two genes (*AFLA_083240* and *AFLA_083270*) were also found directly at *AFLA_083250*. A gene *AFLA_083260* coding for a small hypothetical protein with 84 amino acids was located between *AFLA_083250* and *AFLA_083270*. In the genome of *A. otae*, *MCYG_05443* was found between an L-allothreonine aldolase gene (*MCYG_05442*) and a hypercellular protein HypA gene (*MCYG_05444*).

To prove the function of EAW08391, the coding region of *ACLA_031240*, termed *5-dmats* in this study, was amplified by PCR from cDNA synthesized from mRNA. The PCR product was cloned via pGEM-T easy vector into pQE70, resulting in the expression construct pYL09. For overproduction of His_6-5-DMATS, *E. coli* M15 cells harboring pYL09 were cultivated in TB medium and induced with 0.4 mM isopropyl thiogalactoside at 22 °C for 16 h. A significant band with migration near the 45-kDa size marker was observed on SDS-PAGE of the purified protein (see supplemental Fig. S1), corresponding to the calculated M_r value of 50,411 for His_6-5-DMATS. The yield was calculated to be 1.8 mg of purified protein/liter of culture. The M_r value of the native recombinant His_6-5-DMATS was determined by size exclusion chromatography at about 79,000. This indicated that 5-DMATS acted likely as a homodimer.

5-DMATS Accepted Well L-Tryptophan and Simple Indole Derivatives as Substrates—Because of the high sequence similarity with tryptophan C4-prenyltransferases mentioned above, L-tryptophan and 17 simple indole derivatives (Table 1 and supplemental Table S1) were incubated with the purified 5-DMATS in the presence of DMAPP (2 mM). These substances included eight tryptophan derivatives with modification at the indole ring and nine at the side chain. The reaction mixtures were incubated with 5-DMATS at a final concentration of 1 μM for 7 h. HPLC analysis was used for monitoring the enzyme product formation. Assays with heat-inactivated protein by boiling for 20 min were used as negative control.

HPLC analysis of the incubation mixtures showed clear product formation for 17 of the 18 tested indole derivatives with L-tryptophan as the best substrate (Table 1 and supplemental Table S1). HPLCs of incubation mixtures of 12 substrates (**1a–12a**, Table 1) showed clearly the presence of one product peak for each substrate. Similar behavior was also observed for other five accepted substrates (data not shown). Under this condition, L-tryptophan was almost completely consumed, and the 11 other substrates (**2a–12a**) were accepted with total yields between 38 and 91%. Even in the incubation mixtures with 0.40 μM protein for 1 h, the conversion yield for L-tryptophan was calculated to be 95.4% (see supplemental Table S2).

Inspection of the activities of the tested substances (Table 1 and supplemental Table S1) revealed that, with the exceptions for C5-substituted derivatives, all of the substances with modifications by fluoro or methyl group at the indole ring were well accepted by 5-DMATS. These results could indicate the prenylation position at C-5 of the indole rings of the accepted substrates. 5-Bromo-DL-tryptophan was not accepted by

TABLE 1

Enzyme activity of 5-DMATS towards tryptophan and other simple indole derivatives (1a–12a)

The reaction mixtures containing indole derivatives and DMAPP were incubated with 1 μM protein for 7 h. Under this condition, L-tryptophan was completely consumed.

Substrate	Structure	Product yield (%)
L-tryptophan (**1a**)	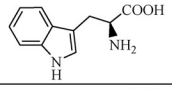	100
1-methyl-DL-tryptophan (**2a**)	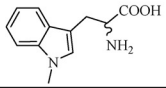	46.9
4-methyl-DL-tryptophan (**3a**)	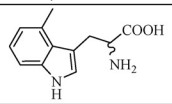	56.6
6-methyl-DL-tryptophan (**4a**)	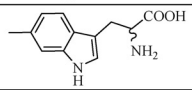	53.2
6-fluoro-DL-tryptophan (**5a**)	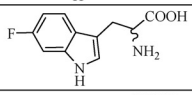	69.5
7-methyl-DL-tryptophan (**6a**)	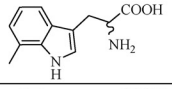	57.8
L-abrine (**7a**)	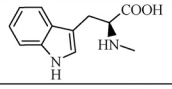	90.9
N-acetyl-DL-tryptophan (**8a**)	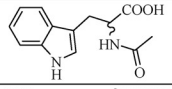	54.4
L-β-homotryptophan (**9a**)	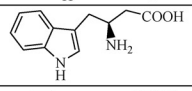	48.8
DL-indole-3-lactic acid (**10a**)	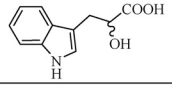	67.3
indole-3-propionic acid (**11a**)	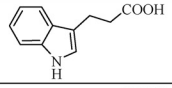	70.7
trans-indole-3-acrylic acid (**12a**)	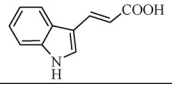	38.0

5-DMATS. The conversion yields of 5-fluoro-L-tryptophan and 5-methyl-DL-tryptophan at 7.4 and 1.7%, respectively, were significantly lower than those with substitution at other positions of the indole ring. The prenylation of these substances had very likely taken place at other positions rather than C-5 (see under "Discussion"). Modification at the side chain of tryptophan reduced enzyme activity, especially by shortening the chain length, as in the case of indole-3-acetic acid and tryptamine. In comparison, changes at the amino group such as *N*-methylation (L-abrine, **7a**), replacement by a hydroxyl group (DL-indole-3-lactic acid, **10a**), or deamination (indole-3-propionic acid, **11a**) showed less influence on the enzyme activity.

A previous study (36) showed that the tryptophan C4-prenyltransferase FgaPT2 also accepted tryptophan-containing cyclic dipeptides as substrates. 5-DMATS was therefore also assayed with five such cyclic dipeptides and analyzed on HPLC. It has been shown that these compounds were also substrates for

TABLE 2

Signals for aromatic protons in the ^{1}H NMR spectra of the selected products (CD_3OD)

For structures, see Fig. 3. The signals are arranged in an order from low to high magnetic field so that the relative signal positions caused by C5-prenylation can be better compared.

Compd	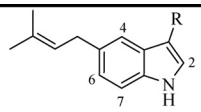			
	H-4	H-7	H-2	H-6
1b	7.49, d, 1.6	7.27, d, 8.4	7.15, s	6.95, dd, 8.4, 1.6
2b	7.49, br s	7.25, d, 8.4	7.05, s	7.02, dd, 8.4, 1.5
7b	7.47, br s	7.26, d, 8.4	7.18, s	6.95, dd, 8.4, 1.5
8b	7.35, br s	7.19, d, 8.3	7.05, s	6.88, dd, 8.3, 1.5
9b	7.36, d, 1.6	7.27, d, 8.4	7.13, s	6.95, dd, 8.4, 1.6
10b	7.45, br s	7.19, d, 8.3	7.09, s	6.88, dd, 8.3, 1.5
11b	7.33, br s	7.20, d, 8.3	7.00, s	6.89, dd, 8.3, 1.5
12b	7.61, br s	7.33, d, 8.3	7.60, s#	7.05, dd, 8.3, 1.5

#,Due to the presence of a double bond between C-10 and C-11, the signal of H-2 was downshifted in the ^{1}H NMR spectrum.

5-DMATS but were accepted with significantly lower yields (<10%) than most of the simple indole derivatives (see supplemental Table S1). Incubations of 5-DMATS with L-tyrosine in the presence of DMAPP or with L-tryptophan in the presence of GPP or FPP did not result in the formation of any enzyme product, even after incubation with 1 μM protein for 24 h (see supplemental Table S2).

5-DMATS Catalyzed the Regular C5 Prenylation at the Indole Ring—To confirm the prenylation position, enzyme products of 12 substrates (**1a–12a**, Table 1) were isolated on HPLC and subjected to high resolution MS and NMR analyses. High resolution ESI-MS (see supplemental Table S3) confirmed the presence of one dimethylallyl moiety each in the products of **1a–12a** by detection of masses, which are 68 daltons larger than those of the respective substrates.

In the ^{1}H NMR spectra of all the enzyme products (taken in CD_3OD or DMSO-d_6), signals at δ_H 3.34–3.47 (d, 2H-1′), 5.17–5.40 (t or m, H-2′), 1.71–1.78 (s, 3H-4′), and 1.67–1.77 (s, 3H-5′) were observed (see supplemental Table S4 and supplemental Figs. S3–S14), proving unequivocally the attachment of a regular dimethylallyl moiety to a carbon atom (37, 38).

Substrates **2a** and **7a–11a** are derivatives of L-tryptophan (**1a**) with modifications at N-1 at the indole ring or at the side chain. Characteristic signals of the four coupling protons at the indole ring (H-4, -5, -6, and -7) appeared as two doublets and two triplets, all with coupling constants of 7–9 Hz in the ^{1}H NMR spectra of **1a**, **2a,** and **7a–11a** (data not shown). In comparison, the two triplets had disappeared in the ^{1}H NMR spectra of their enzyme products **1b**, **2b**, and **7b–11b**. One additional singlet or doublet with a coupling constant smaller than 2 Hz was observed instead. These changes indicated that prenylations had taken place at C-5 or C-6. As given in Table 2, the signals of the remaining three protons at H-4, H-5 or H-6 and H-7 in the ^{1}H NMR spectra (all taken in CD_3OD) were found to be in the same order, *i.e.* (from low to high magnetic field) doublet (1.6 Hz) or broad singlet, doublet (8.3–8.4 Hz), and double doublet (8.3–8.4 and 1.5–1.6 Hz). The singlets for H-2 were found between the doublet (8.3–8.4 Hz) and double doublet. It is plausible that the structures of these compounds have the same prenylation position.

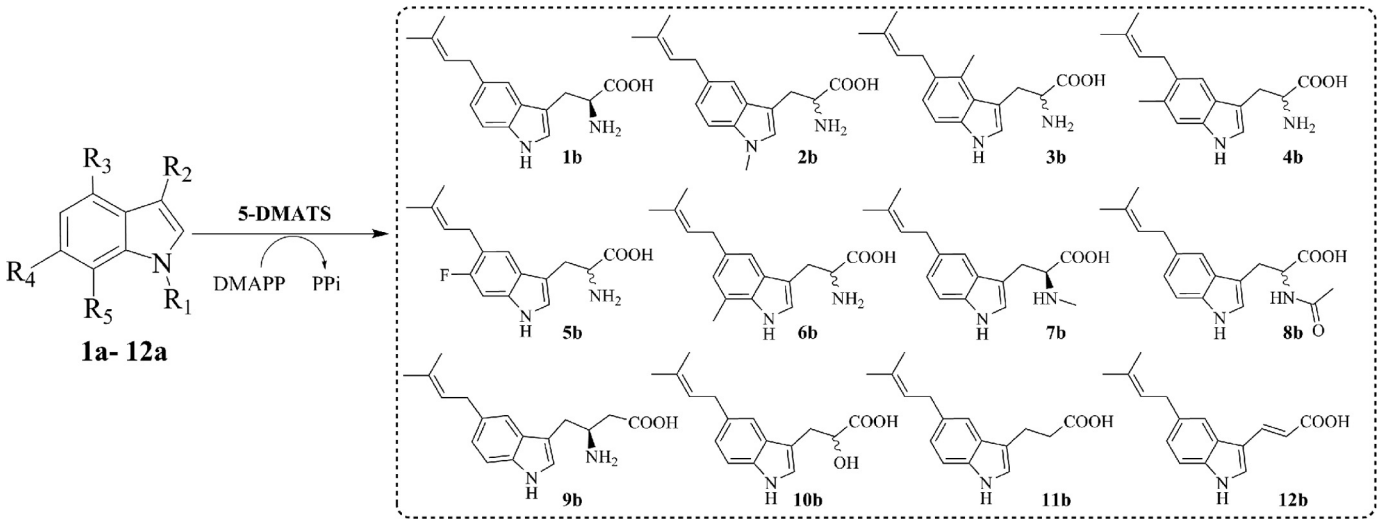

FIGURE 3. **Prenyl transfer reactions catalyzed by 5-DMATS, exemplified with simple indole derivatives 1a–12a.**

Enzyme products of **1a** and **7a** with prenylation at C-6 were reported by Takahashi *et al.* (13). The NMR data of 6-dimethylallyl-L-tryptophan and 6-dimethylallyl-L-abrine (also taken in CD_3OD) differed clearly from those of **1b** and **7b**, especially in the region for aromatic protons. The aromatic protons in the ^1H NMR spectra of 6-dimethylallyl-L-tryptophan and 6-dimethylallyl-L-abrine appeared (from low to high magnetic field) in a different order than in the spectra of **1b** and **7b**, *i.e.* doublet (7.8 – 8.2 Hz), two singlets, and double doublet. Therefore, the prenylation position in **1b** and **7b** must be C-5. This conclusion was also confirmed by interpretation of the two-dimensional NMR spectra of **1b** (in DMSO-d_6) and **7b** (in CD_3OD). In the HMBC spectrum of **1b** (see supplemental Figs. S2 and S3), connectivity from δ_H 7.32 (1H, br. s, H-4) to C-1′ of the prenyl moiety at δ_C 34.1 proved unequivocally the attachment of the dimethylallyl moiety to C-5. The signal at δ_H 7.32 (1H, s) for proton H-4 was unambiguously confirmed by the detected connectivities between this signal and C-8 at 134.9 ppm as well as C-3 at 109.3 ppm. For **7b**, similar phenomena were also observed in the HMBC spectrum (see supplemental Figs. S2 and S9). It can be concluded that the prenyl moieties in **1b**, **2b,** and **7b–11b** are attached to C-5 of the indole rings.

Substrate **12a** is also a derivative of L-tryptophan with alteration at the side chain. Because of the presence of a double bond between C-10 and C-11, the signal of H-2 was downshifted in ^1H NMR spectrum to δ_H 7.60 (1H, s), in comparison with those of **1b**, **2b,** and **7b–11b** between 7.00 and 7.18 ppm. However, the signals for H-4, H-6, and H-7 of **12b** appeared in the same order as in the spectra of **1b**, **2b**, and **7b–11b** (Table 2), proving the C5-prenylation in the structure of **12b**.

In the ^1H NMR spectrum of **3b** (see supplemental Fig. S5), the two doublets at δ_H 6.85 (1H, d, 8.2 Hz, H-6) and δ_H 7.08 (1H, d, 8.2 Hz, H-7) represent signals for two protons at the *ortho*-position and indicated the prenylation at C-5 or C-7. The connectivity from H-6 to δ_C 31.4 of C-1′ and from δ_H 2.55 (3H, s, H-13) of the methyl group at C-4 to δ_C 128.9 of C-5 in the HMBC spectrum confirmed the prenylation at C-5 in **3b** (see supplemental Fig. S2).

The structures of **4b**, **5b**, and **6b** were elucidated by interpretation of their ^1H NMR spectra (see supplemental Figs. S6 – S8). Three singlets observed at δ_H 7.14 (1H, s, H-2), δ_H 7.44 (1H, s, H-4), and δ_H 7.08 (1H, s, H-7) in the ^1H NMR spectrum of **4b** proved the prenylation at C-5. In the ^1H NMR spectrum of **5b**, the two doublets at δ_H 7.02 (1H, d, 10.8 Hz, H-7) and δ_H 7.49 (1H, d, 7.3 Hz, H-4) with clearly different coupling constants are caused by the different distances of the protons to fluoro atom at C-6. In the ^1H NMR spectrum of the enzyme product of **6a**, signals for two products **6b** and **6c** with a ratio of 1.5:1 were detected. Unfortunately, these two compounds could not be separated from each other. Based on their different contents in the mixture, we were able to identify the major product **6b** as C5-prenylated derivative, which is characteristic of the presence of three singlets at δ_H 7.14 (1H, br. s), 7.14 (1H, br. s), and 6.69 (1H, br. s) for H-2, H-4, and H-6, respectively.

In conclusion, 5-DMATS catalyzed the C5-prenylation of L-tryptophan and simple indole derivatives (Fig. 3). To the best of our knowledge, the structures **1b–12b** were not described previously. The structure of **6c** could not be unequivocally elucidated in this study. The presence of two doublets with a coupling constant of 8.1 Hz in the ^1H NMR spectrum indicated a prenylation at C-4 or C-6.

Biochemical Characterization and Kinetic Parameters of 5-DMATS—For determination of the metal ion dependence of 5-DMATS, incubations of L-tryptophan (**1a**) with DMAPP were carried out in the presence of different metal ions at a final concentration of 5 mM. Incubations with the chelating agent EDTA or without additives were used as controls. In the incubation mixture with EDTA, no decrease of the enzyme activity was observed, in comparison with that of incubation without additives. As observed for other members of the DMATS superfamily (15, 39), several divalent metal ions enhanced slightly the enzyme activity of 5-DMATS. For example, the enzyme activities with Ca^{2+} and Mg^{2+} were found to be 250 and 204% of that without additives, respectively.

To study the behavior of 5-DMATS toward 12 indole derivatives (**1a–12a**) and DMAPP in detail, kinetic parameters,

TABLE 3
Kinetic parameters of 5-DMATS for selected substrates

Substrate	K_m	k_{cat}	k_{cat}/K_m
	mM	s^{-1}	$s^{-1}\cdot M^{-1}$
L-Tryptophan (**1a**)	0.034	0.87	25,588
1-Methyl-DL-tryptophan (**2a**)	0.10	0.059	590
4-Methyl-DL-tryptophan (**3a**)	0.25	0.29	1160
6-Methyl-DL-tryptophan (**4a**)	1.0	0.76	760
6-Fluoro-DL-tryptophan (**5a**)	0.27	0.29	1074
7-Methyl-DL-tryptophan (**6a**)	0.47	0.40	851
L-Abrine (**7a**)	0.26	0.40	1538
N-Acetyl-DL-tryptophan (**8a**)	0.35	0.10	286
L-β-Homotryptophan (**9a**)	0.97	0.15	155
DL-Indole-3-lactic acid (**10a**)	0.67	0.43	642
Indole-3-propionic acid (**11a**)	0.39	0.39	1000
trans-Indole-3-acrylic acid (**12a**)	0.40	0.14	350
DMAPP	0.076	1.3	17,105

including Michaelis-Menten constants (K_m) and turnover numbers (k_{cat}), were determined by Hanes-Woolf and Eadie-Hofstee plots and are given in Table 3. The reactions catalyzed by 5-DMATS apparently followed Michaelis-Menten kinetics. The K_m values for DMAPP and L-tryptophan (**1a)** were found to be 76 and 34 μM, respectively, whereas K_m values of 0.10–1.0 mM were determined for **2a–12a**, much higher than that observed for **1a**. The turnover numbers were calculated for DMAPP and **1a** at 1.3 and 0.87 s^{-1}, respectively. Lower turnover numbers of 0.059–0.76 s^{-1} were determined for **2a–12a**. The catalytic efficiencies (k_{cat}/K_m) of 5-DMATS toward DMAPP and **1a** were calculated to be 17,105 and 25,588 $s^{-1}\cdot M^{-1}$, respectively. In comparison, lower catalytic efficiencies at 155–1538 $s^{-1}\cdot mM^{-1}$ were found for **2a–12a**, only 0.6–6.0% that of **1a**.

DISCUSSION

Prenyltransferases catalyze transfer reactions of prenyl moieties from prenyl diphosphates to diverse aliphatic or aromatic receptors, including proteins, terpenes, benzoic acids, naphthalenes, flavonoids, and indole alkaloids (1, 8, 9, 40, 41). These enzymes are involved in both primary and secondary metabolism, play an important role in living organisms (42), and contribute significantly to the structural diversity of natural products (43). Prenylated indole alkaloids represent a large group of natural products, predominantly identified as mycotoxins in Ascomycetes (1, 44). Indole prenyltransferases catalyze transfer reactions of prenyl moieties onto the indole nucleus and are involved in the biosynthesis of diverse natural products, especially mycotoxins (1, 15). A large number of indole prenyltransferases, mainly belonging to the DMATS superfamily from fungi of Ascomycetes, have been identified in the last years and characterized biochemically (1, 10, 11). The members of the DMATS superfamily are soluble proteins, showed usually broad substrate specificity and accepted tryptophan, simple indole derivatives, tryptophan-containing cyclic dipeptides, or other indole-containing structures as aromatic substrates and DMAPP as prenyl donor (1, 10, 11). A few examples of soluble indole prenyltransferases have also been identified in bacteria (13, 45). One of the important features of indole prenyltransferases is the regioselectivity of their prenylation reactions. With the exception for C-5, diverse indole prenyltransferases for the other six positions (N-1, C-2, C-3, C-4, C-6, and C-7) have been identified and characterized (Fig. 1). No enzyme for prenylation at C-5 of the indole ring was reported prior to this study, although a number of C5-prenylated derivatives have been isolated from different organisms (Fig. 2). Therefore, there is a need to find enzymes for C5-prenylation at the indole nucleus, so that these enzymes could be better used as tools for chemoenzymatic synthesis of prenylated indole derivatives or even for synthesis of prenylated hydroxynaphthalenes and flavonoids, which have been very recently described for several members of the DMATS superfamily (46, 47).

In this study, we identified and characterized the first tryptophan C5-prenyltransferase 5-DMATS from *A. clavatus*, which catalyzes the regiospecific C5-prenylation of indole derivatives and fills herewith the last gap in the search for indole prenyltransferases regarding their prenylation positions. Blast searching in the database with 5-DMATS from *A. clavatus* NRRL1 revealed the presence of three orthologues in the genome sequences of *A. oryzae* RIB40 (48), *A. flavus* NRRL3357 (49), and *A. otae* CBS 113480 (GenBank™). Analysis of genes in the genomic region of these prenyltransferase genes in all four strains did not provide any indication for their clustering with genes for secondary metabolite biosynthesis. No C5-prenylated derivative was reported for these fungi. Therefore, their roles in these strains could not be predicted in this study. It seems that these genes are the results of redundant copies in the evolution. Nevertheless, considering the low K_m values of 34 and 76 μM for L-tryptophan and DMAPP, respectively, as well as the high turnover number of 1.1 s^{-1} (Table 3), it can be speculated that L-tryptophan and DMAPP are very likely the natural substrates of 5-DMATS in the four fungal strains. Inactivation of these genes in the fungal strains could provide detailed information about their roles in nature, if the genes are expressed and the gene products involved in the biosynthesis of certain substance. Therefore, we tried to detect the production of C5-prenylated indole derivatives by *A. clavatus* NRRL1. For this purpose, the fungus was cultivated in different liquid media like YME. Culture filtrates and mycelia were extracted with ethyl acetate and methanol, respectively. In the ^{1}H NMR spectra of both extracts, no signal for aromatic protons was observed, which could be assigned to C5-substituted indole rings. Signals for prenyl moieties were also absent in their ^{1}H NMR spectra (data not shown). This means that C5-substituted indole derivatives were not or only in a very low yield produced by this fungus under the tested conditions. These results could indicate that 5-DMATS is not involved in the biosynthesis of secondary metabolites in *A. clavatus*. It cannot be excluded, however, that 5-DMATS catalyzed a C5-prenylation in the biosynthesis of a fungal product. It is plausible that the expression level of *5-dmats* and other related genes would be too low to produce a substantial amount of prenylated derivative. In both cases, cultivation of *A. clavatus* NRRL1 and *5-dmats*-defective mutants would very likely not result in significant changes of secondary metabolite accumulation, which prohibited the potential usage of knock-out experiments to prove gene function. Therefore, optimization of culture conditions should be carried out to improve the level of gene expression in *A. clavatus*. Cultivation of *A. oryzae*, *A. flavus,* or *A. otae* under different conditions and proof of the accumulated C5-prenylated secondary metabolites, *e.g.* by NMR analysis, after purification or

as extracts, would also be a prerequisite for gene knock-out experiments in these strains. This work is now in progress.

In addition to 5-DMATS described in this study, several DMATSs using L-tryptophan as natural or best aromatic substrate with different regioselectivity have been studied biochemically in detail, *e.g.* the 4-DMATS FgaPT2 from *A. fumigatus* (20) and its orthologues MaPT from *Malbranchea aurantiaca* (50) and DmaW from a clavicipitalean fungus (51, 52), the 6-DMATS IptA from *Streptomyces* sp. SN-593 (13), and the 7-DMATS from *A. fumigatus* (22). All of these enzymes catalyzed regular C-prenylation (13, 20, 22, 50, 51). As mentioned above, 5-DMATS shares high sequence similarities on the amino acid level with 4-DMATSs, *e.g.* 52% with FgaPT2 from *A. fumigatus*, 50% with MaPT from *M. aurantiaca,* and 47% with DwaW from the clavicipitalean fungus. As observed for the low sequence similarity between FgaPT2 and 7-DMATS (22), 5-DMATS also showed low sequence similarity (27%) to 7-DMATS. No meaningful similarity was found for 5-DMATS and IptA. These data proved again that substrates of indole prenyltransferases and their prenylation positions could not be predicted by sequence analysis and comparison (15).

As observed for other members of the DMATS superfamily (15, 39), the enzyme activity of 5-DMATS was enhanced by some metal ions such as Ca^{2+} or Mg^{2+}. 5-DMATS accepted only DMAPP but not GPP or FPP as prenyl donor. It showed, however, similar to many members of the DMATS superfamily, broad promiscuity toward its aromatic substrates. With the exception for C5-substituted derivatives, the most tested simple indole derivatives with modifications at the indole ring or side chain have been well accepted by 5-DMATS (Table 1 and supplemental Table S1). It is not surprising that C5-substituted derivatives were poor substrates for a 5-DMATS with a high regioselectivity at C-5. No product formation was observed for 5-bromo-DL-tryptophan, although low conversion yields of 7.4 and 1.7% were detected for 5-fluoro-L-tryptophan and 5-methyl-DL-tryptophan, respectively. These results indicated a limited feasibility of 5-DMATS to prenylate C5-substituted tryptophan derivatives. Similar phenomena were also observed for the tryptophan C6-prenyltransferase IptA, which also accepted 6-methyl-DL-tryptophan as substrate and catalyzed a C7-prenylation (13). Because of the low amounts, the enzyme products of 5-fluoro-L-tryptophan and 5-methyl-DL-tryptophan were not identified in this study. It could be speculated, however, that prenylation had taken place at another position rather than C-5. We have shown in this study that 5-DMATS prenylated predominantly tryptophan and derivatives at C-5 but occasionally also catalyzed prenylations at other positions, as observed in the incubation mixture of 7-methyl-DL-tryptophan. Both C5- and C4- or C6-prenylated derivatives were identified in this case (supplemental Table S4). The acceptance of C5-substituted tryptophan derivatives by 5-DMATS could also be explained by the substrate promiscuity of indole prenyltransferases of the DMATS superfamily, which accepted even hydroxynaphthalenes and flavonoids as substrates and catalyzed C-, O-, or both prenylations (46, 47).

As given in Table 1, high conversion yields of more than 38% were detected for 12 simple indole derivatives after incubation with 1 μM 5-DMATS for 7 h. NMR and MS analyses proved unequivocally that the reaction catalyzed by 5-DMATS was highly regioselective regular prenylation at C-5 of the indole nucleus in most cases. It can therefore be expected that 5-DMATS could serve as an effective catalyst for chemoenzymatic synthesis of prenylated derivatives in the program of drug discovery and development. Acceptance of tryptophan-containing cyclic dipeptides by 5-DMATS could also be used to increase the structural diversity of prenylated derivatives, although the conversion yields detected in this study were still very low, which perhaps could be improved in the future by mutagenesis experiments.

Acknowledgments—We thank Dr. Laufenberg for taking mass spectra and Marco Matuschek and Edyta Stec for synthesis of DMAPP, GPP, and FPP.

REFERENCES

1. Li, S. M. (2010) Prenylated indole derivatives from fungi. Structure diversity, biological activities, biosynthesis, and chemoenzymatic synthesis. *Nat. Prod. Rep.* **27,** 57–78
2. Ruiz-Sanchis, P., Savina, S. A., Albericio, F., and Álvarez, M. (2011) Structure, bioactivity, and synthesis of natural products with hexahydropyrrolo[2,3-*b*]indole. *Chemistry* **17,** 1388–1408
3. Wallwey, C., and Li, S. M. (2011) Ergot alkaloids. Structure diversity, biosynthetic gene clusters, and functional proof of biosynthetic genes. *Nat. Prod. Rep.* **28,** 496–510
4. Lindel, T., Marsch, N., and Adla, S. K. (2011) Indole prenylation in alkaloid synthesis. *Top. Curr. Chem.* DOI: 10.1007/128_2011_204
5. Williams, R. M., Stocking, E. M., and Sanz-Cervera, J. F. (2000) Biosynthesis of prenylated alkaloids derived from tryptophan. *Top. Curr. Chem.* **209,** 97–173
6. Schardl, C. L., Panaccione, D. G., and Tudzynski, P. (2006) Ergot alkaloids, biology and molecular biology. *Alkaloids Chem. Biol.* **63,** 45–86
7. Uhlig, S., Botha, C. J., Vrålstad, T., Rolén, E., and Miles, C. O. (2009) Indole-diterpenes and ergot alkaloids in *Cynodon dactylon* (Bermuda grass) infected with *Claviceps cynodontis* from an outbreak of tremors in cattle. *J. Agric. Food Chem.* **57,** 11112–11119
8. Heide, L. (2009) Prenyl transfer to aromatic substrates. Genetics and enzymology. *Curr. Opin. Chem. Biol.* **13,** 171–179
9. Yazaki, K., Sasaki, K., and Tsurumaru, Y. (2009) Prenylation of aromatic compounds, a key diversification of plant secondary metabolites. *Phytochemistry* **70,** 1739–1745
10. Yin, W. B., Yu, X., Xie, X. L., and Li, S. M. (2010) Preparation of pyrrolo[2,3-*b*]indoles carrying a β-configured reverse C3-dimethylallyl moiety by using a recombinant prenyltransferase CdpC3PT. *Org. Biomol. Chem.* **8,** 2430–2438
11. Zou, H. X., Xie, X. L., Linne, U., Zheng, X. D., and Li, S. M. (2010) Simultaneous C7- and N1-prenylation of cyclo-L-Trp-L-Trp catalyzed by a prenyltransferase from *Aspergillus oryzae*. *Org. Biomol. Chem.* **8,** 3037–3044
12. Schultz, A. W., Lewis, C. A., Luzung, M. R., Baran, P. S., and Moore, B. S. (2010) Functional characterization of the cyclomarin/cyclomarazine prenyltransferase CymD directs the biosynthesis of unnatural cyclic peptides. *J. Nat. Prod.* **73,** 373–377
13. Takahashi, S., Takagi, H., Toyoda, A., Uramoto, M., Nogawa, T., Ueki, M., Sakaki, Y., and Osada, H. (2010) Biochemical characterization of a novel indole prenyltransferase from *Streptomyces* sp. SN-593. *J. Bacteriol.* **192,** 2839–2851
14. Ding, Y., de Wet, J. R., Cavalcoli, J., Li, S., Greshock, T. J., Miller, K. A., Finefield, J. M., Sunderhaus, J. D., McAfoos, T. J., Tsukamoto, S., Williams, R. M., and Sherman, D. H. (2010) Genome-based characterization of two prenylation steps in the assembly of the stephacidin and notoamide anticancer agents in a marine-derived *Aspergillus* sp. *J. Am. Chem. Soc.* **132,** 12733–12740
15. Li, S. M. (2009) Evolution of aromatic prenyltransferases in the biosynthe-

sis of indole derivatives. *Phytochemistry* **70,** 1746–1757
16. Grundmann, A., Kuznetsova, T., Afiyatullov, S. Sh., and Li, S. M. (2008) FtmPT2, an *N*-prenyltransferase from *Aspergillus fumigatus*, catalyzes the last step in the biosynthesis of fumitremorgin B. *ChemBioChem* **9,** 2059–2063
17. Grundmann, A., and Li, S. M. (2005) Overproduction, purification, and characterization of FtmPT1, a brevianamide F prenyltransferase from *Aspergillus fumigatus*. *Microbiology* **151,** 2199–2207
18. Unsöld, I. A., and Li, S. M. (2006) Reverse prenyltransferase in the biosynthesis of fumigaclavine C in *Aspergillus fumigatus*. Gene expression, purification, and characterization of fumigaclavine C synthase FGAPT1. *ChemBioChem* **7,** 158–164
19. Yin, W. B., Grundmann, A., Cheng, J., and Li, S. M. (2009) Acetylaszonalenin biosynthesis in *Neosartorya fischeri*. Identification of the biosynthetic gene cluster by genomic mining and functional proof of the genes by biochemical investigation. *J. Biol. Chem.* **284,** 100–109
20. Unsöld, I. A., and Li, S. M. (2005) Overproduction, purification, and characterization of FgaPT2, a dimethylallyltryptophan synthase from *Aspergillus fumigatus*. *Microbiology* **151,** 1499–1505
21. Liu, X., and Walsh, C. T. (2009) Characterization of cyclo-acetoacetyl-L-tryptophan dimethylallyltransferase in cyclopiazonic acid biosynthesis. Substrate promiscuity and site -directed mutagenesis studies. *Biochemistry* **48,** 11032–11044
22. Kremer, A., Westrich, L., and Li, S. M. (2007) A 7-dimethylallyltryptophan synthase from *Aspergillus fumigatus*. Overproduction, purification, and biochemical characterization. *Microbiology* **153,** 3409–3416
23. Achenbach, H., Renner, C., and Waibel, R. (1995) Constituents of tropical medicinal plants, LXIX. The hexalobines, diprenylated indoles from *Hexalobus crispiflorus* and *Hexalobus monopetalus. Liebigs Ann. Recl.* **1995,** 1327–1337
24. Peters, L., König, G. M., Terlau, H., and Wright, A. D. (2002) Four new bromotryptamine derivatives from the marine bryozoan *Flustra foliacea*. *J. Nat. Prod.* **65,** 1633–1637
25. Fredenhagen, A., Petersen, F., Tintelnot-Blomley, M., Rösel, J., Mett, H., and Hug, P. (1997) Semicochliodinol A and B. Inhibitors of HIV-1 protease and EGF-R protein-tyrosine kinase related to asterriquinones produced by the fungus *Chrysosporium merdarium*. *J. Antibiot.* **50,** 395–401
26. Ooike, M., Nozawa, K., Udagawa, S I., and Kawai, K. I. (1997) Bisindolylbenzenoids from ascostromata of *Petromyces muricatus*. *Can. J. Chem.* **75,** 625–628
27. Balibar, C. J., Howard-Jones, A. R., and Walsh, C. T. (2007) Terrequinone A biosynthesis through L-tryptophan oxidation, dimerization and bisprenylation. *Nat. Chem. Biol.* **3,** 584–592
28. Wang, W. L., Lu, Z. Y., Tao, H. W., Zhu, T. J., Fang, Y. C., Gu, Q. Q., and Zhu, W. M. (2007) Isoechinulin-type alkaloids, variecolorins A–L, from halotolerant *Aspergillus variecolor*. *J. Nat. Prod.* **70,** 1558–1564
29. Fujimoto, H., Fujimaki, T., Okuyama, E., and Yamazaki, M. (1999) Immunomodulatory constituents from an ascomycete, *Microascus tardifaciens*. *Chem. Pharm. Bull.* **47,** 1426–1432
30. Xu, M., Gessner, G., Groth, I., Lange, C., Christner, A., Bruhn, T., Deng, Z., Li, X., Heinemann, S. H., Grabley, S., Bringmann, G., Sattler, I., and Lin, W. (2007) Shearinines D-K, new indole triterpenoids from an endophytic *Penicillium* sp. (strain HKI0459) with blocking activity on large-conductance calcium-activated potassium channels. *Tetrahedron* **63,** 435–444
31. Sings, H., and Singh, S. (2003) Tremorgenic and nontremorgenic 2,3-fused indole diterpenoids. *Alkaloids Chem. Biol.* **60,** 51–163
32. Belofsky, G. N., Gloer, J. B., Wicklow, D. T., and Dowd, P. F. (1995) Antiinsectan alkaloids: Shearinines A-C and a new paxilline derivative from the ascostromata of *Eupenicillium shearii. Tetrahedron* **51,** 3959–3968
33. Woodside, A. B., Huang, Z., and Poulter, C. D. (1988) Trisammonium geranyl diphosphate. *Org. Synth.* **66,** 211–215
34. Laemmli, U. K. (1970) Cleavage of structural proteins during the assembly of the head of bacteriophage T4. *Nature* **227,** 680–685
35. Berger, S., and Braun, S. (2004) *200 and More NMR Experiments. A Practical Course*, pp. 1–854, Wiley-VCH, Weinheim, Germany
36. Steffan, N., and Li, S. M. (2009) Increasing structure diversity of prenylated diketopiperazine derivatives by using a 4-dimethylallyltryptophan synthase. *Arch. Microbiol.* **191,** 461–466
37. Steffan, N., Unsöld, I. A., and Li, S. M. (2007) Chemoenzymatic synthesis of prenylated indole derivatives by using a 4-dimethylallyltryptophan synthase from *Aspergillus fumigatus*. *ChemBioChem* **8,** 1298–1307
38. Kremer, A., and Li, S. M. (2008) Potential of a 7-dimethylallyltryptophan synthase as a tool for production of prenylated indole derivatives. *Appl. Microbiol. Biotechnol.* **79,** 951–961
39. Steffan, N., Grundmann, A., Yin, W. B., Kremer, A., and Li, S. M. (2009) Indole prenyltransferases from fungi. A new enzyme group with high potential for the production of prenylated indole derivatives. *Curr. Med. Chem.* **16,** 218–231
40. Li, S. M. (2009) Applications of dimethylallyltryptophan synthases and other indole prenyltransferases for structural modification of natural products. *Appl. Microbiol. Biotechnol.* **84,** 631–639
41. Liang, P. H. (2009) Reaction kinetics, catalytic mechanisms, conformational changes, and inhibitor design for prenyltransferases. *Biochemistry* **48,** 6562–6570
42. Turunen, M., Olsson, J., and Dallner, G. (2004) Metabolism and function of coenzyme Q. *Biochim. Biophys. Acta* **1660,** 171–199
43. Sacchettini, J. C., and Poulter, C. D. (1997) Creating isoprenoid diversity. *Science* **277,** 1788–1789
44. Nielsen, K. F., and Smedsgaard, J. (2003) Fungal metabolite screening. Database of 474 mycotoxins and fungal metabolites for dereplication by standardized liquid chromatography-UV-mass spectrometry methodology. *J. Chromatogr. A* **1002,** 111–136
45. Edwards, D. J., and Gerwick, W. H. (2004) Lyngbyatoxin biosynthesis. Sequence of biosynthetic gene cluster and identification of a novel aromatic prenyltransferase. *J. Am. Chem. Soc.* **126,** 11432–11433
46. Yu, X., Xie, X., and Li, S. M. (2011) Substrate promiscuity of secondary metabolite enzymes: prenylation of hydroxynaphthalenes by fungal indole prenyltransferases. *Appl. Microbiol. Biotechnol.* **92,** 737–748
47. Yu, X., and Li, S. M. (2011) Prenylation of flavonoids by using a dimethylallyltryptophan synthase 7-DMATS from *Aspergillus fumigatus*. *ChemBioChem* **12,** 2280–2283
48. Machida, M., Asai, K., Sano, M., Tanaka, T., Kumagai, T., Terai, G., Kusumoto, K., Arima, T., Akita, O., Kashiwagi, Y., Abe, K., Gomi, K., Horiuchi, H., Kitamoto, K., Kobayashi, T., Takeuchi, M., Denning, D. W., Galagan, J. E., Nierman, W. C., Yu, J., Archer, D. B., Bennett, J. W., Bhatnagar, D., Cleveland, T. E., Fedorova, N. D., Gotoh, O., Horikawa, H., Hosoyama, A., Ichinomiya, M., Igarashi, R., Iwashita, K., Juvvadi, P. R., Kato, M., Kato, Y., Kin, T., Kokubun, A., Maeda, H., Maeyama, N., Maruyama, J., Nagasaki, H., Nakajima, T., Oda, K., Okada, K., Paulsen, I., Sakamoto, K., Sawano, T., Takahashi, M., Takase, K., Terabayashi, Y., Wortman, J. R., Yamada, O., Yamagata, Y., Anazawa, H., Hata, Y., Koide, Y., Komori, T., Koyama, Y., Minetoki, T., Suharnan, S., Tanaka, A., Isono, K., Kuhara, S., Ogasawara, N., and Kikuchi, H. (2005) Genome sequencing and analysis of *Aspergillus oryzae*. *Nature* **438,** 1157–1161
49. Cleveland, T. E., Yu, J., Fedorova, N., Bhatnagar, D., Payne, G. A., Nierman, W. C., and Bennett, J. W. (2009) Potential of *Aspergillus flavus* genomics for applications in biotechnology. *Trends Biotechnol.* **27,** 151–157
50. Ding, Y., Williams, R. M., and Sherman, D. H. (2008) Molecular analysis of a 4-dimethylallyltryptophan synthase from *Malbranchea aurantiaca*. *J. Biol. Chem.* **283,** 16068–16076
51. Markert, A., Steffan, N., Ploss, K., Hellwig, S., Steiner, U., Drewke, C., Li, S. M., Boland, W., and Leistner, E. (2008) Biosynthesis and accumulation of ergoline alkaloids in a mutualistic association between *Ipomoea asarifolia* (Convolvulaceae) and a clavicipitalean fungus. *Plant Physiol.* **147,** 296–305
52. Steiner, U., Leibner, S., Schardl, C. L., Leuchtmann, A., and Leistner, E. (2011) *Periglandula*, a new fungal genus within the Clavicipitaceae and its association with Convolvulaceae. *Mycologia* **103,** 1133–1145

SUPPLEMENTAL DATA FOR

Biochemical characterization of indole prenyltransferases: Filling the last gap of prenylation positions by a 5-dimethylallyltryptophan synthase from *Aspergillus clavatus*

Xia Yu (于霞)[1], Yan Liu (刘燕) [1,2], Xiulan Xie (谢秀兰)[3], Xiao-Dong Zheng (郑晓冬)[2], Shu-Ming Li (李书明)[1]

[1]Institut für Pharmazeutische Biologie und Biotechnologie, Philipps-Universität Marburg, Deutschhausstrasse 17A, 35037 Marburg, Germany

[2] Department of Food Science and Nutrition, Zhejiang University, 310058 Hangzhou, Zhejiang, People's Republic of China

[3]Fachbereich Chemie, Philipps-Universität Marburg, Hans-Meerwein-Strasse, 35032 Marburg, Germany

Correspondence to: Shu-Ming Li, Institut für Pharmazeutische Biologie und Biotechnologie, Philipps-Universität Marburg, Deutschhausstrasse 17A, 35037 Marburg, Germany, Tel: 0049-6421-2822461, Fax: 0049-6421-2825365, email: shuming.li@staff.uni-marburg.de

Table S1. Enzyme activity of 5-DMATS towards aromatic compounds, which are not included in Table 1.

Name	Structure	Product yield (%)
5-methyl-DL-tryptophan	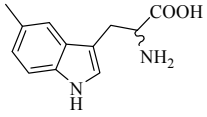	1.7
5-bromo-DL-tryptophan	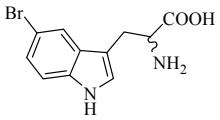	< 0.5
5-fluoro-L-tryptophan	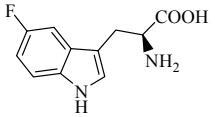	7.4
indole-3-butyric acid	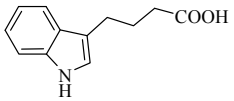	20.2
indole-3-acetic acid	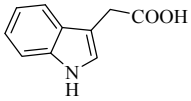	1.8
tryptamine	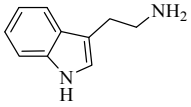	6.1
cyclo-L-Trp-L-Ala	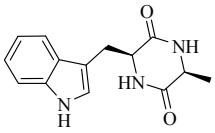	1.9
cyclo-L-Trp-L-Leu	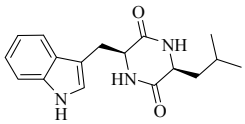	6.4
cyclo-L-Trp-L-Phe	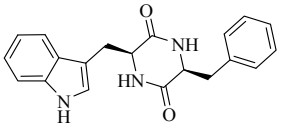	2.2
cyclo-L-Trp-L-Pro	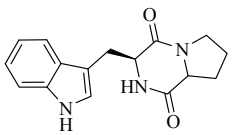	0.9
cyclo-L-Trp-L-Trp	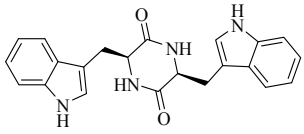	9.0

The reaction mixtures containing aromatic compounds and DMAPP were incubated with 1 μM protein for 7 h.

Table S2. Enzyme activity of 5-DMATS towards prenyl diphosphates

Name	Structure	Product yield (%)		
		1h incubation 0.40 µM 5-DMATS	7h incubation 1 µM 5-DMATS	24h incubation 1 µM 5-DMATS
DMAPP	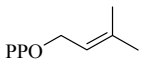	95.4	100	100
GPP	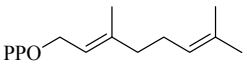	< 0.5	< 0.5	< 0.5
FPP	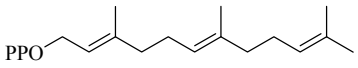	< 0.5	< 0.5	< 0.5

L-tryptophan was used as aromatic substrate.

Table S3. HR-ESI-MS data of enzyme products of 5-DMATS

		HR-ESI-MS data		
Comp.	Chemical formula	Calculated	Measured	Deviation (ppm)
1b	$C_{16}H_{20}N_2O_2$	273.1603 $[M+H]^+$	273.1604	-0.3
2b	$C_{17}H_{22}N_2O_2$	287.1760 $[M+H]^+$	287.1746	4.5
3b	$C_{17}H_{22}N_2O_2$	287.1760 $[M+H]^+$	287.1753	2.4
4b	$C_{17}H_{22}N_2O_2$	287.1760 $[M+H]^+$	287.1791	-11.0
5b	$C_{16}H_{19}FN_2O_2$	291.1509 $[M+H]^+$	291.1473	12.4
6b and **6c**	$C_{17}H_{22}N_2O_2$	287.1760 $[M+H]^+$	287.1725	11.9
7b	$C_{17}H_{22}N_2O_2$	287.1760 $[M+H]^+$	287.1750	3.3
8b	$C_{18}H_{22}N_2O_3$	337.1528 $[M+Na]^+$	337.1499	8.7
9b	$C_{17}H_{22}N_2O_2$	287.1760 $[M+H]^+$	287.1744	5.4
10b	$C_{16}H_{19}NO_3$	296.1263 $[M+Na]^+$	296.1245	5.9
11b	$C_{16}H_{19}NO_2$	280.1313 $[M+Na]^+$	280.1346	-11.6
12b	$C_{16}H_{17}NO_2$	278.1157 $[M+Na]^+$	278.1153	1.4

Table S4. ^{1}H- and ^{13}C- NMR data of enzyme products obtained in CD_3OD or DMSO- d_6.

Compd	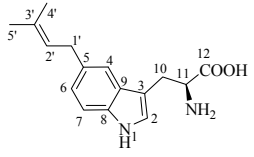 **1b** (in DMSO- d_6)		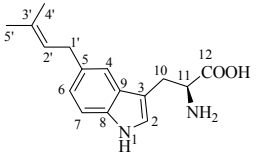 **1b** (in CD_3OD)	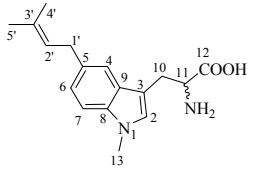 **2b** (in CD_3OD)	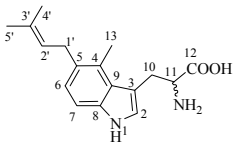 **3b** (in DMSO- d_6)		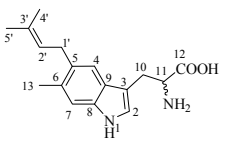 **4b** (in CD_3OD)	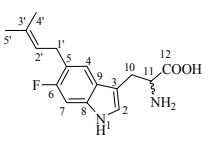 **5b** (in CD_3OD)	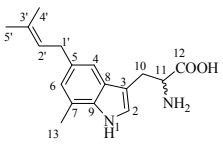 **6b** (in DMSO- d_6)
Pos.	δ_C	δ_H, multi., *J*	δ_H, multi., *J*	δ_H, multi.,*J*	δ_C	δ_H, multi.,*J*	δ_H, multi., *J*	δ_H, multi., *J*	δ_H, multi., *J*
2	124.1	7.18, s	7.15, s	7.05, s	124.5	7.11, s	7.14, s	7.14, s	7.14, br. s
3	109.3	-	-	-	§	-	-	-	-
4	117.2	7.32, br. s	7.49, d, 1.6	7.49, br. s	126.5	-	7.44, s	7.49, d, 7.3	7.14, br. s
5	131.0	-	-	-	128.9	-	-	-	-
6	121.8	6.88, br. d, 8.3	6.95, dd, 8.4, 1.6	7.02, dd, 8.4, 1.5	123.0	6.85, d, 8.2	-	-	6.69, br. s
7	111.2	7.25, d, 8.3	7.27, d, 8.4	7.25, d, 8.4	108.8	7.08, d, 8.2	7.08, s	7.02, d, 10.8	-
8	134.9	-	-	-	135.6	-	-	-	-
9	127.4	-	-	-	125.5	-	-	-	-
10	27.2	3.30, dd, 15.1, 3.6	3.51, dd, 15.3, 4.0	3.48, dd, 15.3, 4.0	29.2	3.63, d, 15.2	3.50, dd, 15.2, 3.7	3.48, dd, 15.2, 3.8	#
10		2.90, dd, 15.1, 9.3	3.10, dd, 15.2, 9.8	3.09, dd, 15.3, 9.5		2.89, dd, 15.4, 10.6	3.08, dd, 15.2, 9.8	3.09, dd, 15.3, 9.6	2.87, dd, 14.9, 9.5
11	54.8	3.44, dd, 9.3, 3.6	3.86, dd, 9.8, 4.0	3.83, dd, 9.5, 4.0	§	#	3.85, dd, 9.8, 3.7	3.83, dd, 9.6, 3.8	#
12	170.2	-	-	-	§	-	-	-	-
13	-	-	-	3.75, s	14.9	2.55, s	2.34, s	-	2.40, s
14	-	-	-	-	-	-	-	-	-
1'	34.1	3.36, d, 7.4	3.43, d, 7.4	3.44, d, 7.3	31.4	3.34	3.41, d, 6.8	3.41, d, 7.1	#
2'	124.9	5.33, t, 7.4	5.37, m	5.37, m	124.3	5.17, t, 7.1	5.24, m	5.33, t, 7.1	5.32, m
3'	130.4	-	-	-	129.5	-	-	-	
4'	17.7	1.72, s	1.76, s	1.76, s	17.3	1.73, s	1.77, s	1.76, s	1.71, s
5'	25.5	1.70, s	1.74, s	1.74, s	25.1	1.67, s	1.72, s	1.72, s	1.69, s

Chemical shifts (δ) were given in ppm and coupling constants (*J*) in Hz. #: overlapping signals with those of solvents; §: due to low amount, the signals were not observed.

Table S4 (continued)

Compd	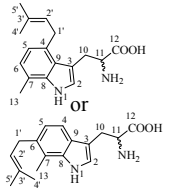 **6c** (in DMSO- d_6)		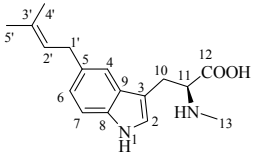 **7b** (in CD_3OD)		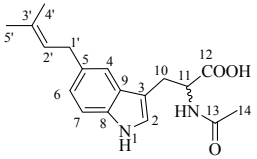 **8b** (in CD_3OD)	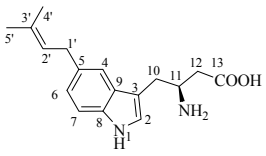 **9b** (in CD_3OD)	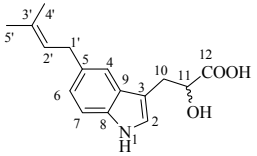 **10b** (in CD_3OD)	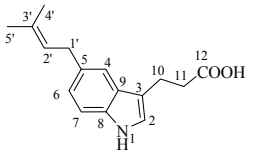 **11b** (in CD_3OD)	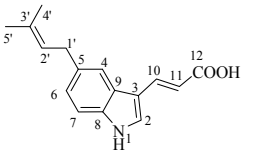 **12b** (in CD_3OD)
Pos.	$\delta_{H,}$ multi., *J*	δ_C	$\delta_{H,}$ multi., *J*	$\delta_{H,}$ multi., *J*	$\delta_{H,}$ multi., *J*	$\delta_{H,}$ multi., *J*	$\delta_{H,}$ multi., *J*	$\delta_{H,}$ multi., *J*	
2	7.12, d, 2.2	125.3	7.18, s	7.05, s	7.13, s	7.09, s	7.00, s	7.60, s	
3	-	108.6	-	-	-	-	-	-	
4	7.29, d, 8.1	118.3	7.47, br. s	7.35, br. s	7.36, d, 1.6	7.45, br. s	7.33, br. s	7.61, br. s	
5	6.80, d, 8.1	133.8	-	-	-	-	-	-	
6		123.8	6.95, dd, 8.4, 1.5	6.88, dd, 8.3, 1.5	6.95, dd, 8.4, 1.6	6.88, dd, 8.3, 1.5	6.89, dd, 8.3, 1.5	7.05, dd, 8.3, 1.5	
7	-	112.3	7.26, d, 8.4	7.19, d, 8.3	7.27, d, 8.4	7.19, d, 8.3	7.20, d, 8.3	7.33, d, 8.3	
8	-	136.9	-	-	-	-	-	-	
9	-	128.7	-	-	-	-	-	-	
10	#	27.6	3.46, dd, 15.5, 4.6	3.34, dd, 14.6, 4.8	2.54, dd, 16.8, 3.9	3.26, dd, 14.8, 3.4	2.57, m	6.34, d, 15.9	
10	2.90, dd, 14.3, 9.3		3.23, dd, 15.5, 8.2	3.13, dd, 14.6, 6.7	2.35, dd, 16.8, 9.2	2.92, dd, 14.8, 8.2	-	-	
11	#	65.4	3.77, dd, 8.2, 4.6	4.58, dd, 6.7, 4.8	3.66, m	4.21, dd, 8.2, 3.4	3.01, m	7.90, d, 15.9	
12	-	173.4	-	-	3.05, d, 7.2	-	-	-	
13	2.36, s	33.1	2.56, s	-	-	-	-	-	
14	-	-	-	1.86, s	-	-	-	-	
1'	#	35.6	3.43, d, 7.3	3.40, d, 7.3	3.42, d, 6.9	3.40, d, 7.3	3.40, d, 7.2	3.47, d, 7.3	
2'	5.18, m	126.0	5.37, m	5.37, m	5.37, m	5.38, m	5.37, m	5.40, m	
3'	-	132.0	-	-	-	-	-	-	
4'	1.72, s	17.9	1.76, s	1.76, s	1.76, s	1.76, s	1.76, s	1.78, s	
5'	1.67, s	25.9	1.74, s	1.74, s	1.74, s	1.74, s	1.75, s	1.77, s	

#: overlapping signals with those of solvents; §: due to low amount, the signals were not observed.

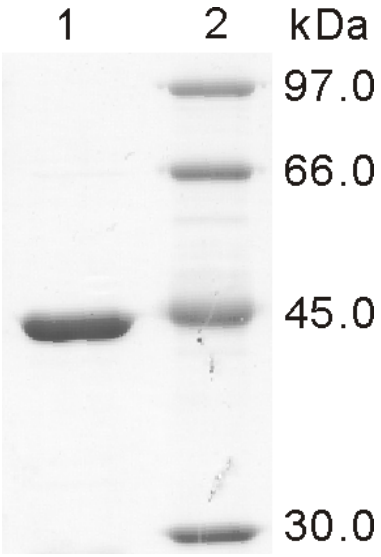

Figure S1. Analysis of purified His_6-5-DMATS on SDS-PAGE. Lane 1: purified His_6-5-DMATS; 2: molecular mass standard.

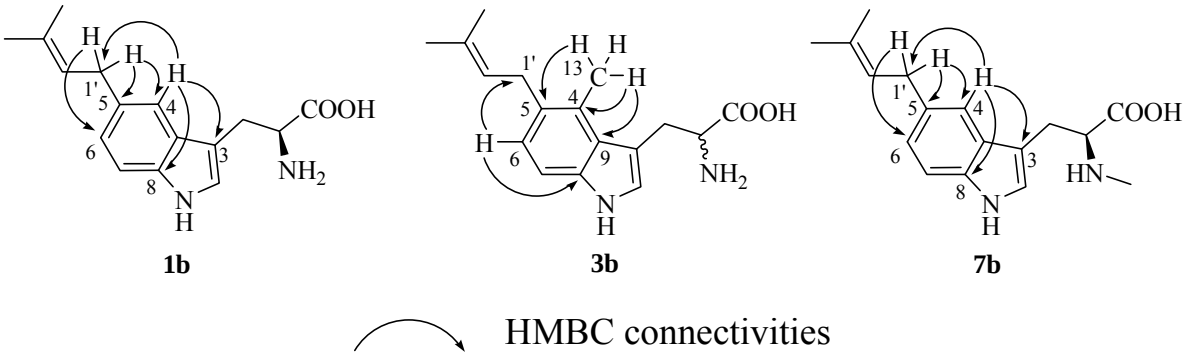

Figure S2. Summary of the HMBC connectivities of enzyme products **1b**, **3b** and **7b**.

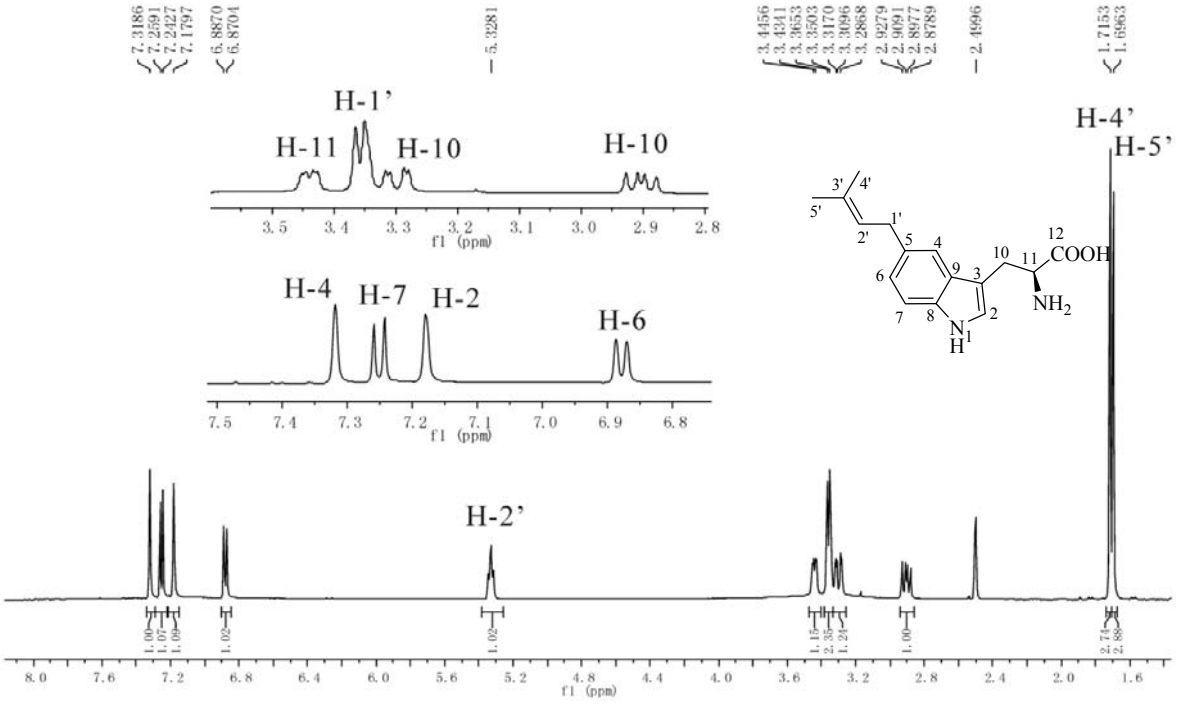

Figure S3.1. [1]H-NMR spectrum of **1b** in DMSO-d_6 (500 MHz)

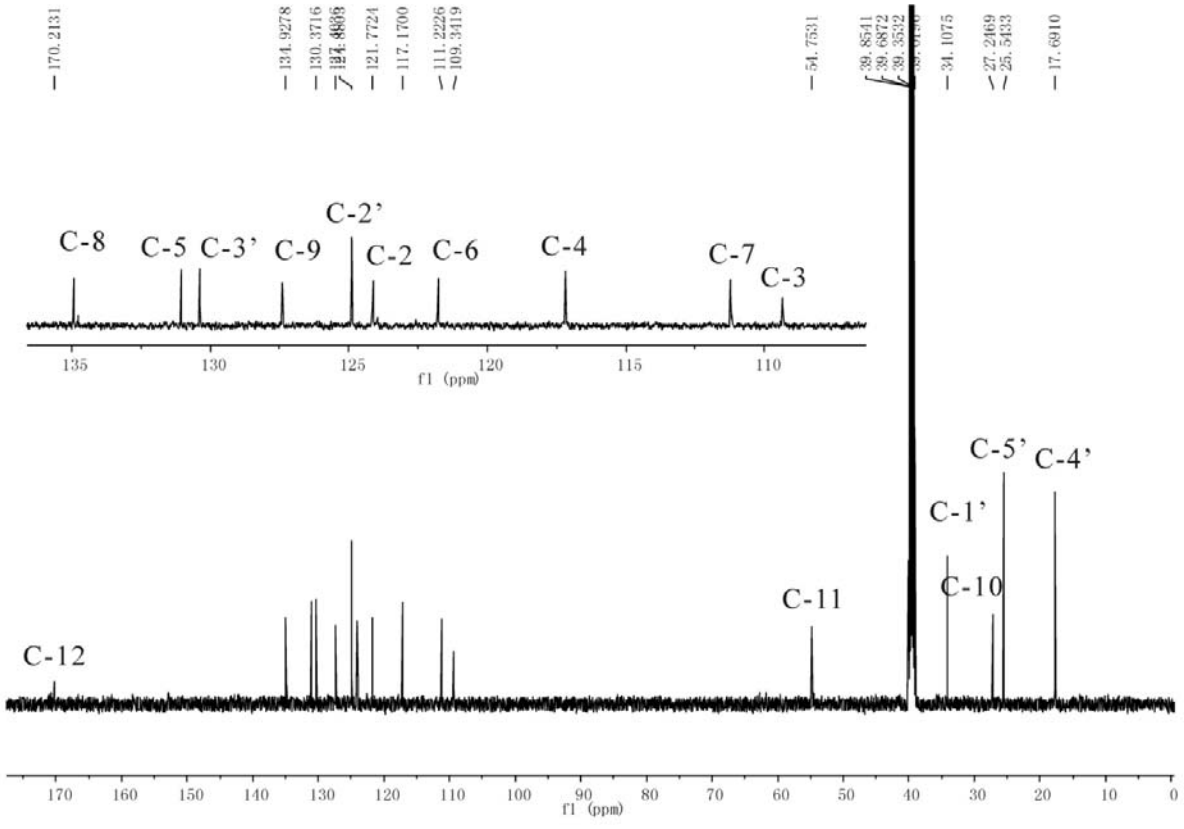

Figure S3.2. [13]C-NMR spectrum of **1b** in DMSO-d_6 (500 MHz)

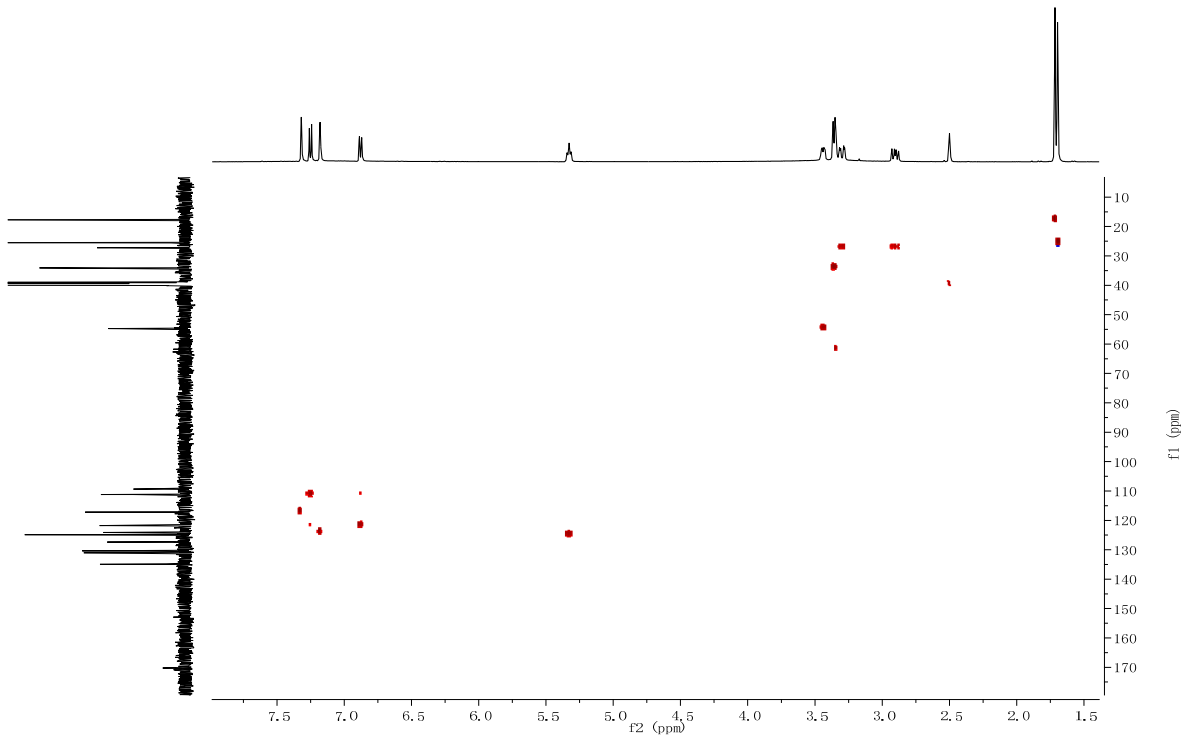

Figure S3.3. HSQC spectrum of **1b** in DMSO-d_6 (500 MHz)

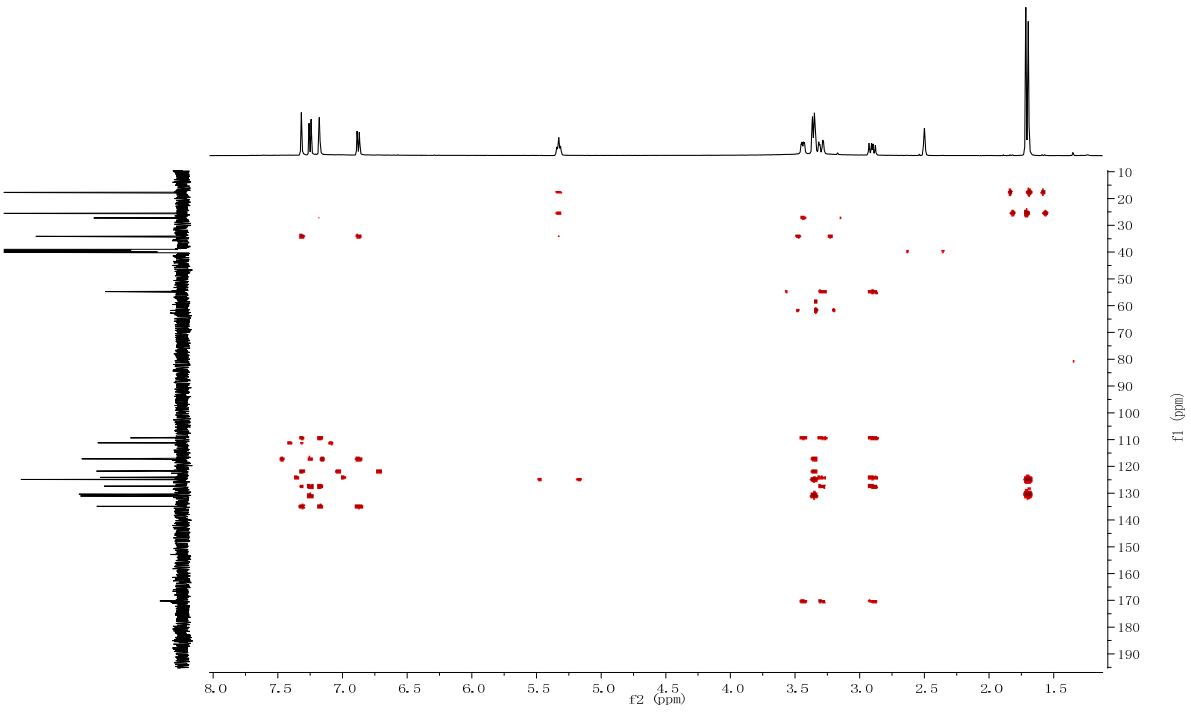

Figure S3.4. HMBC spectrum of **1b** in DMSO-d_6 (500 MHz)

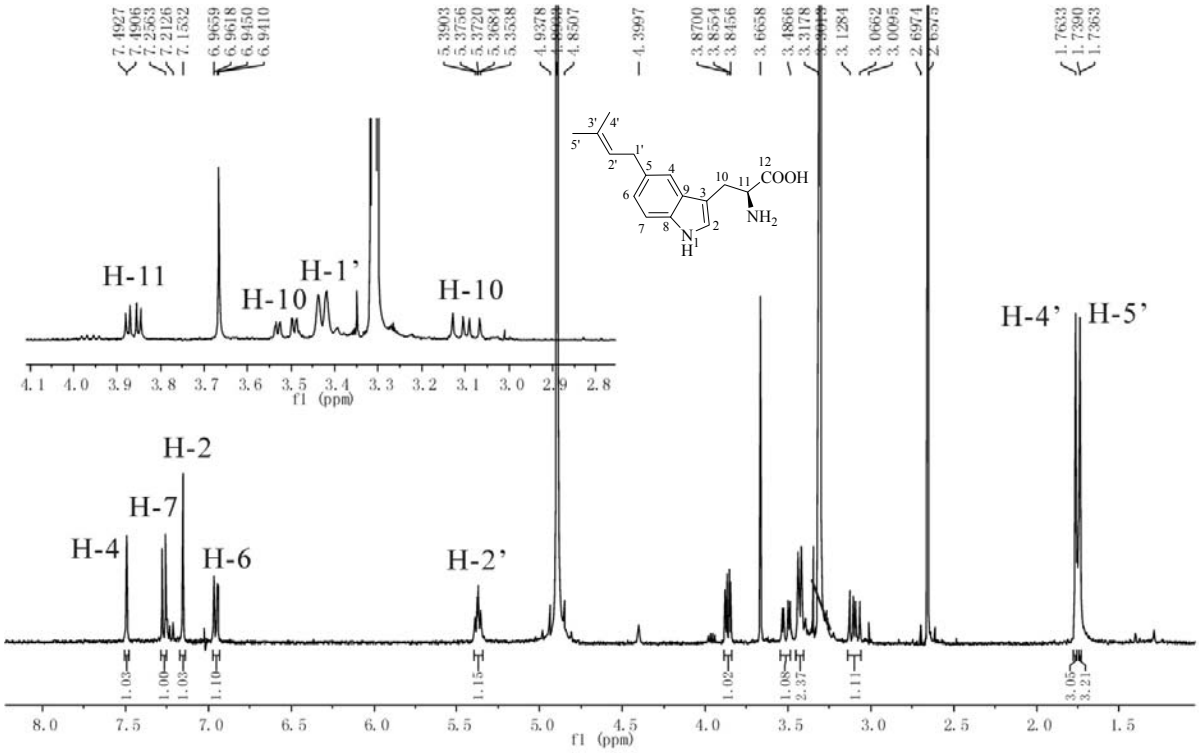

Figure S3.5. ^{1}H-NMR spectrum of **1b** in CD_3OD (400 MHz)

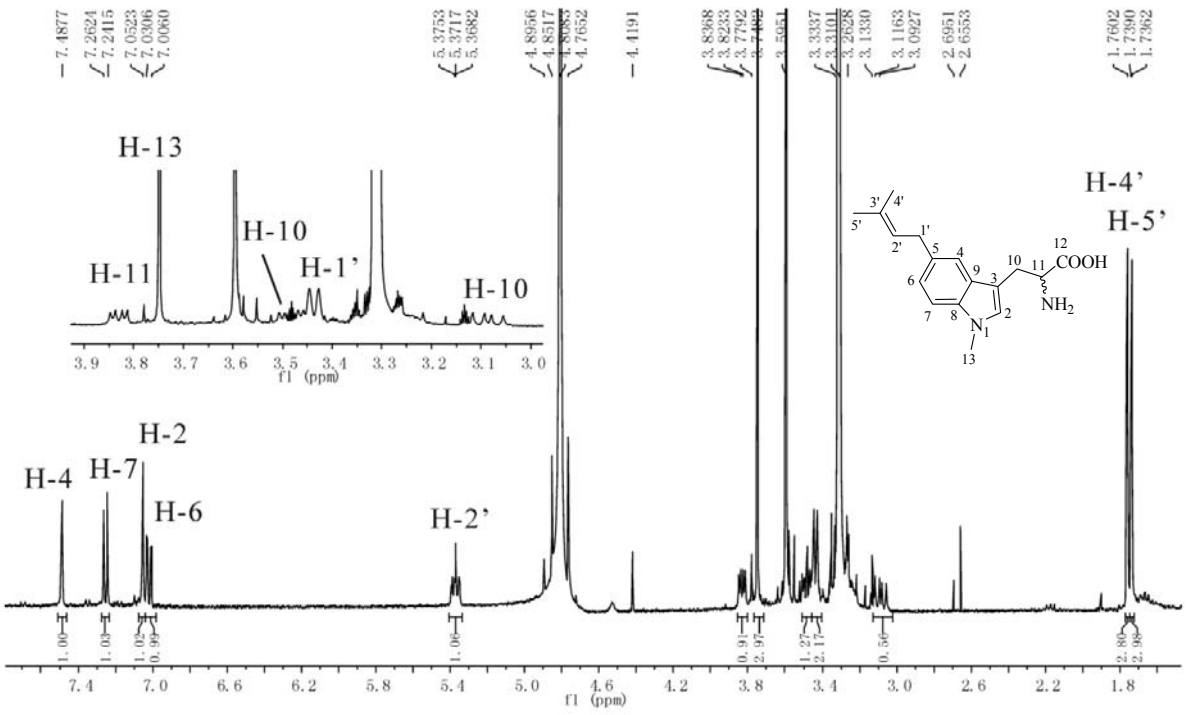

Figure S4. ^{1}H-NMR spectrum of **2b** in CD_3OD (400 MHz)

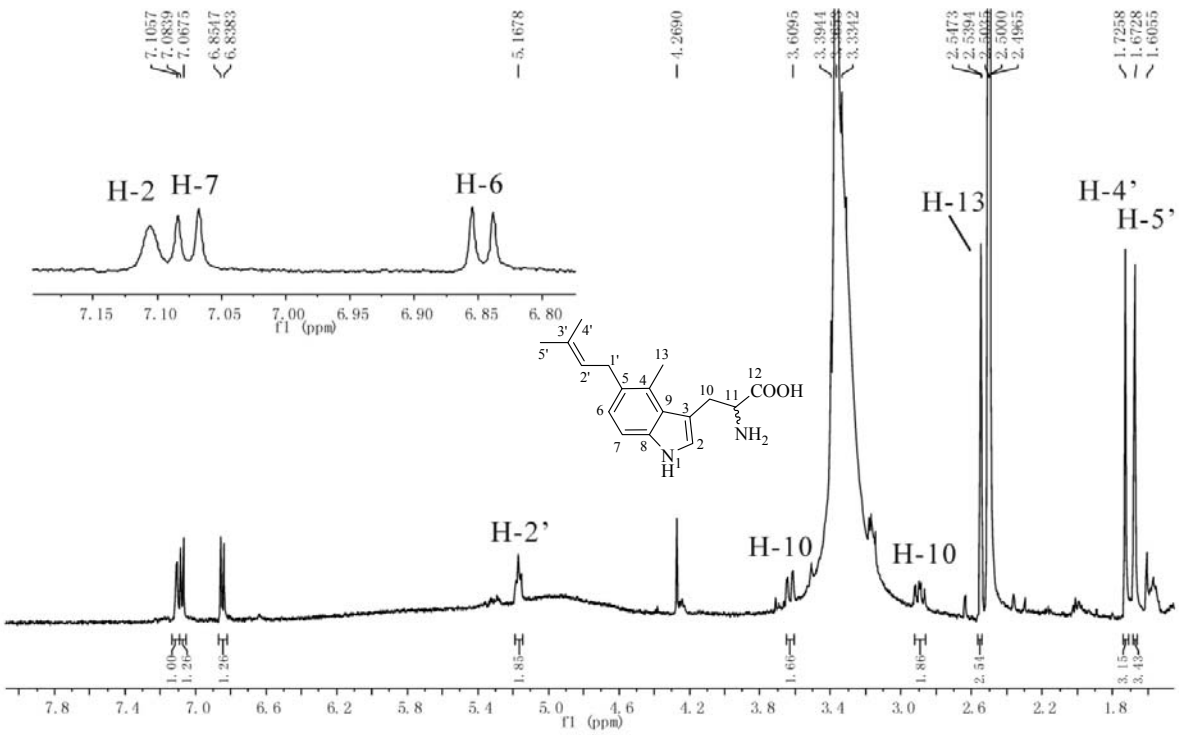

Figure S5.1. ^{1}H-NMR spectrum of **3b** in DMSO-d_6 (500 MHz)

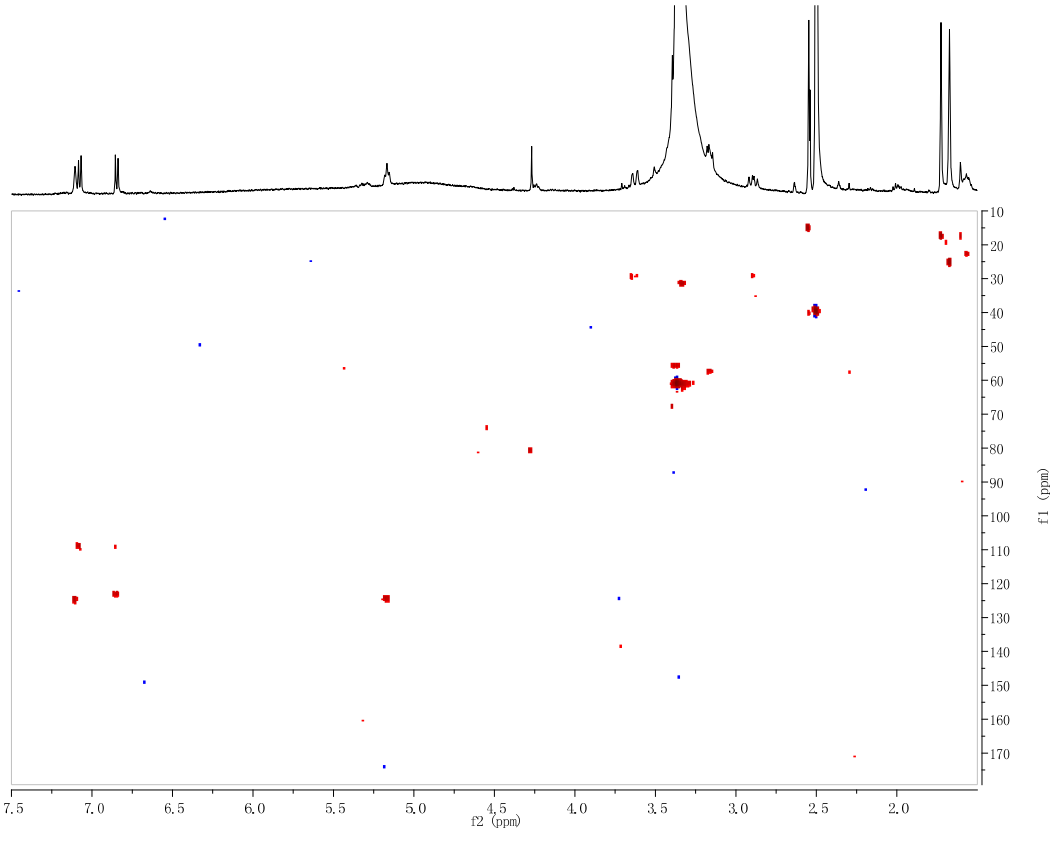

Figure S5.2. HSQC spectrum of **3b** in DMSO-d_6 (500 MHz)

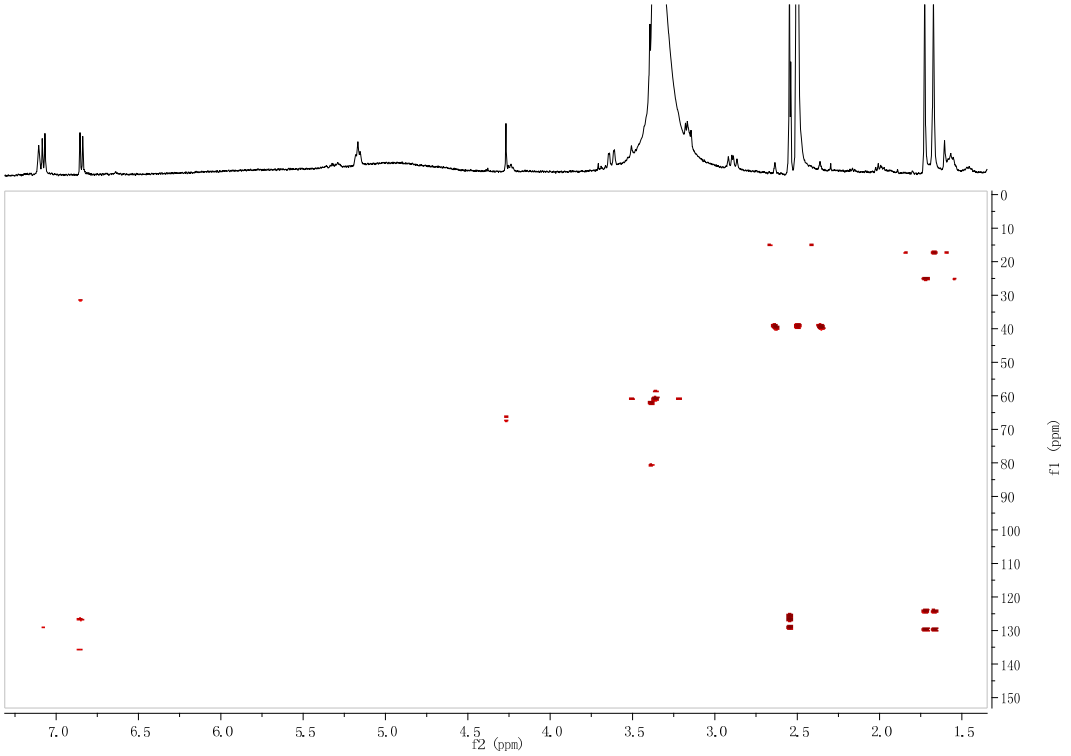

Figure S5.3. HMBC spectrum of **3b** in DMSO-d_6 (500 MHz)

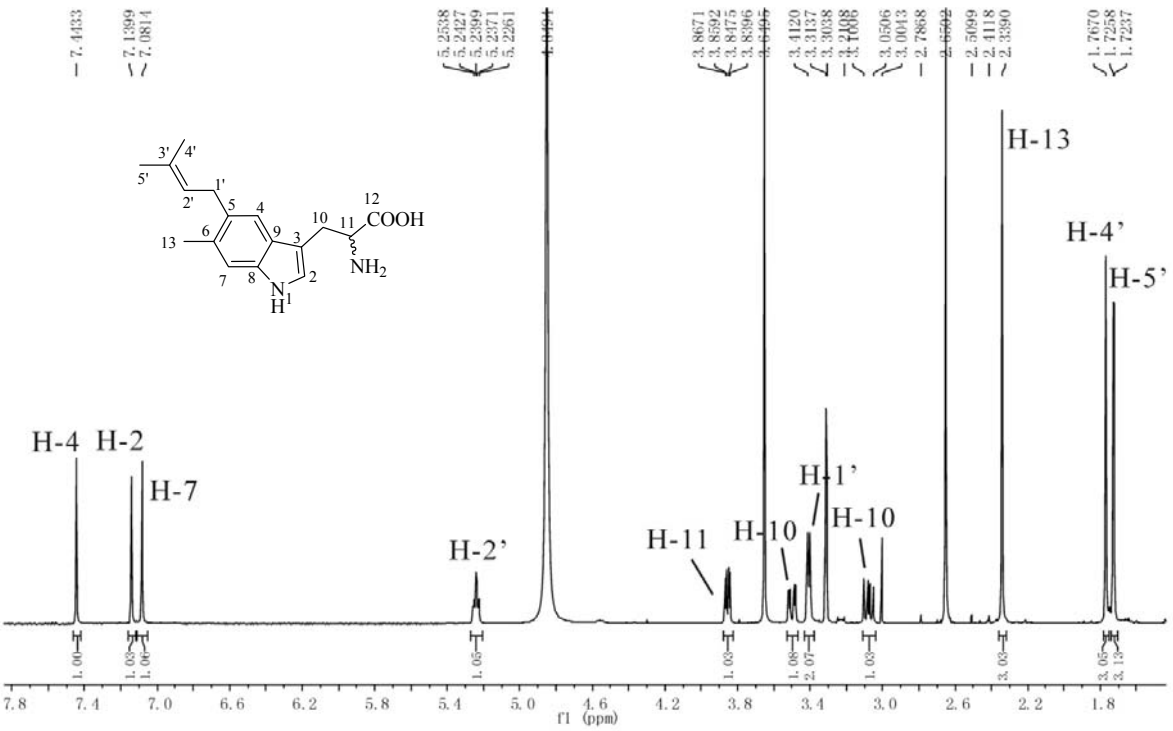

Figure S6. ^{1}H-NMR spectrum of **4b** in CD_3OD (500 MHz)

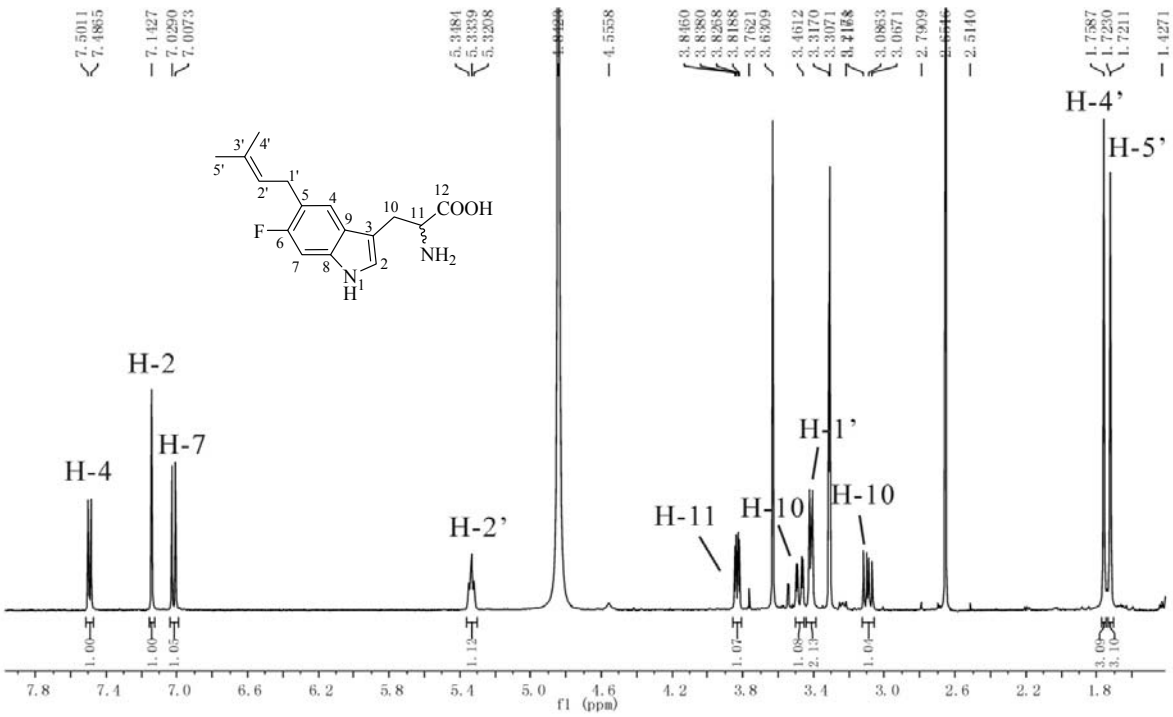

Figure S7. ^{1}H-NMR spectrum of **5b** in CD_3OD (500 MHz)

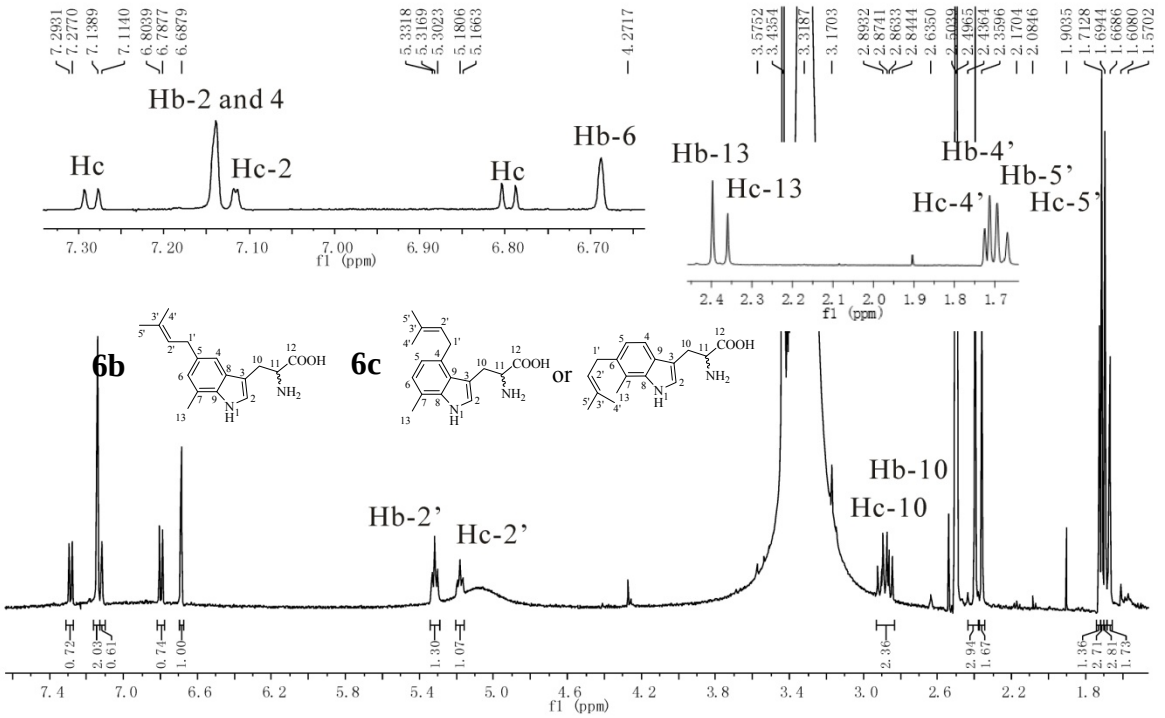

Figure S8. ^{1}H-NMR spectrum of **6b** and **6c** in DMSO-d_6 (500 MHz). The protons of **6b** and **6c** were labeled with Hb and Hc, respectively.

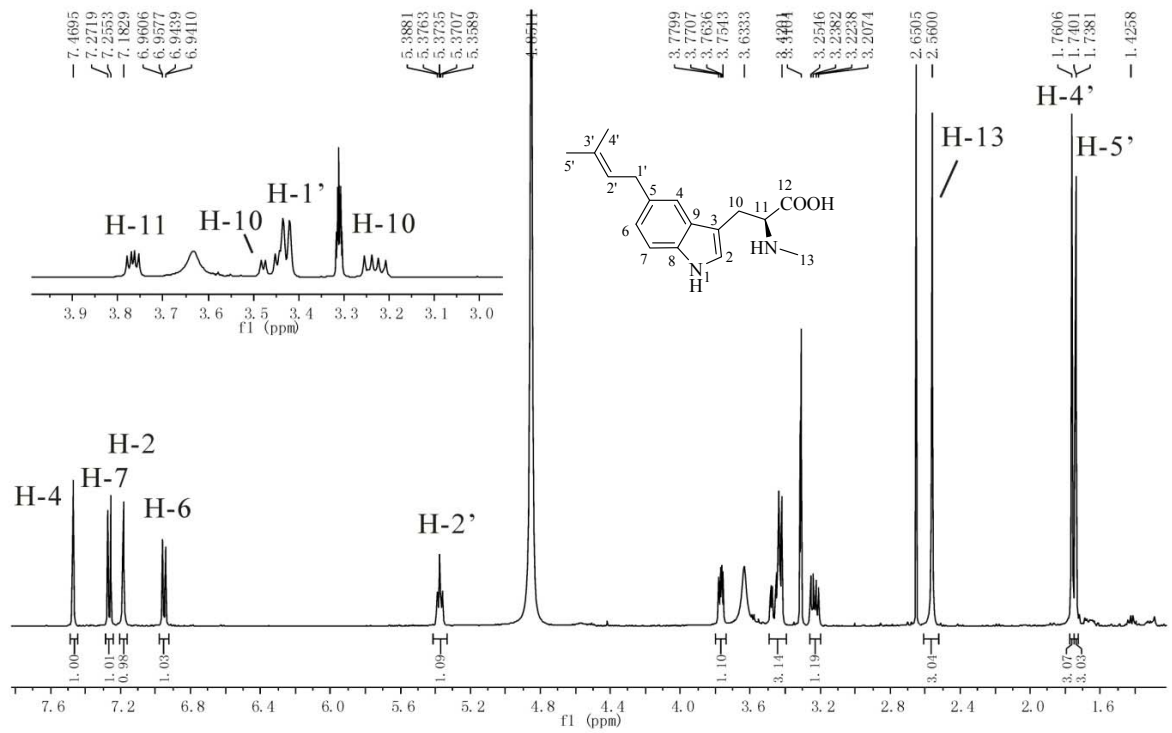

Figure S9.1. ^{1}H-NMR spectrum of **7b** in CD_3OD (500 MHz)

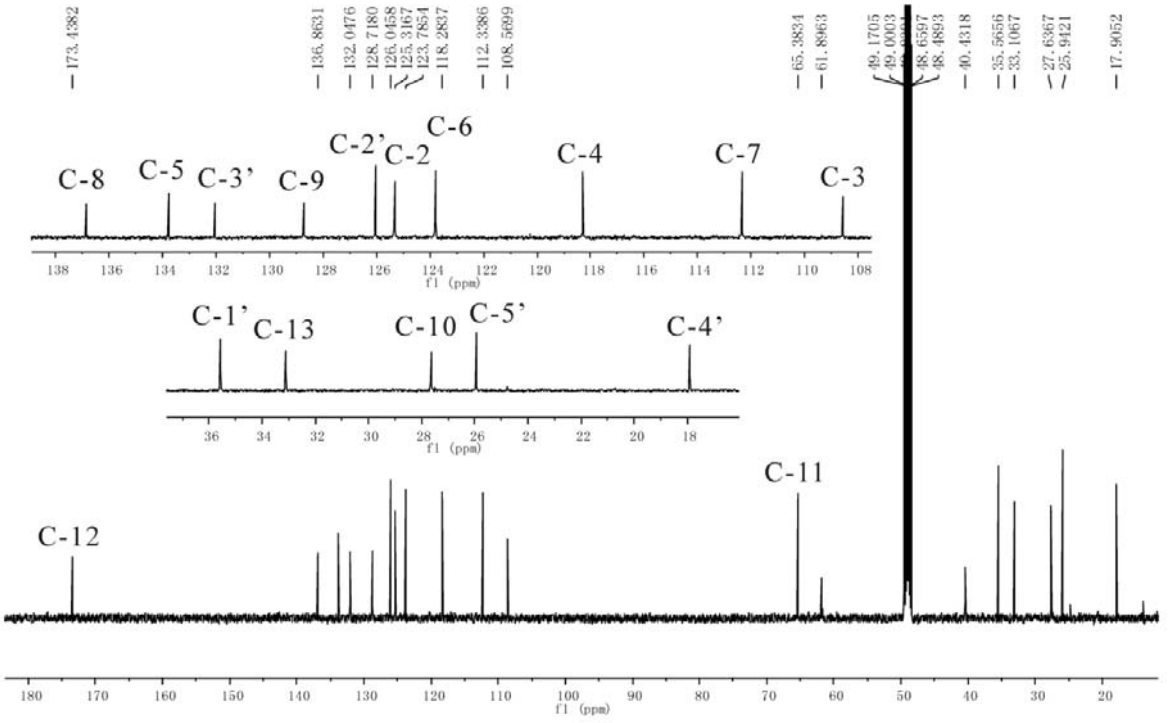

Figure S9.2. ^{13}C-NMR spectrum of **7b** in CD_3OD (500 MHz)

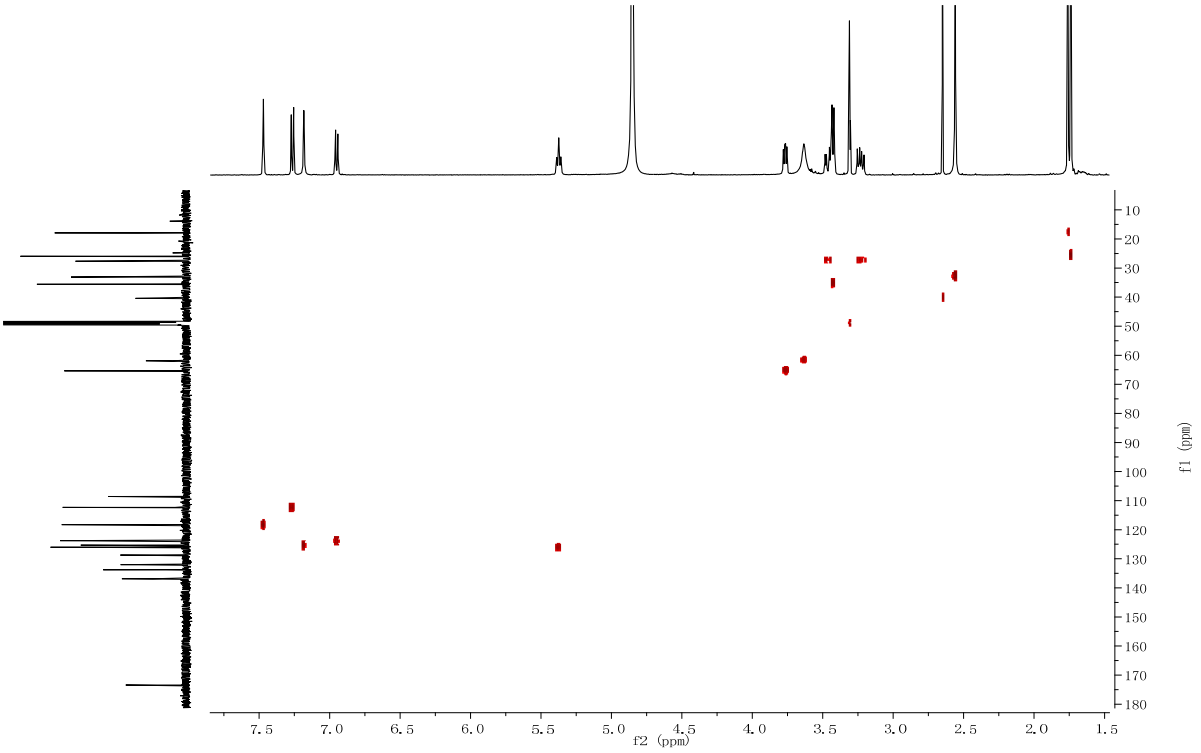

Figure S9.3. HSQC spectrum of **7b** in CD_3OD (500 MHz)

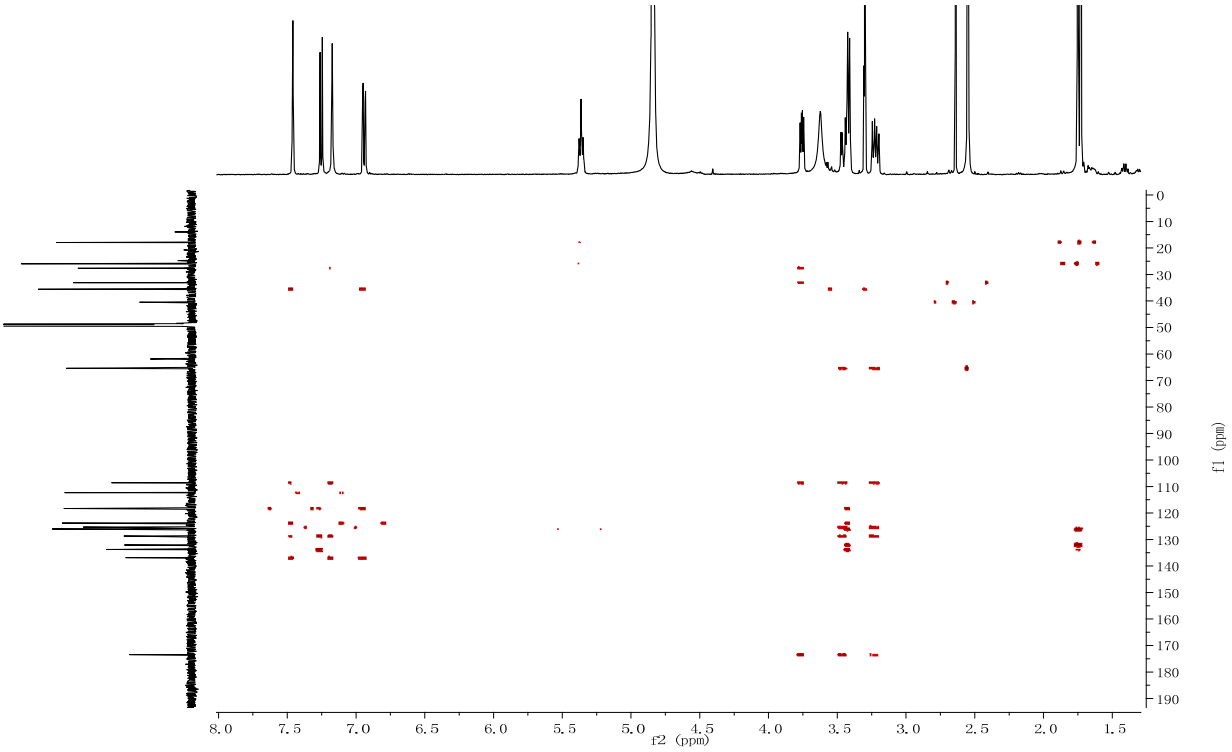

Figure S9.4. HMBC spectrum of **7b** in CD_3OD (500 MHz)

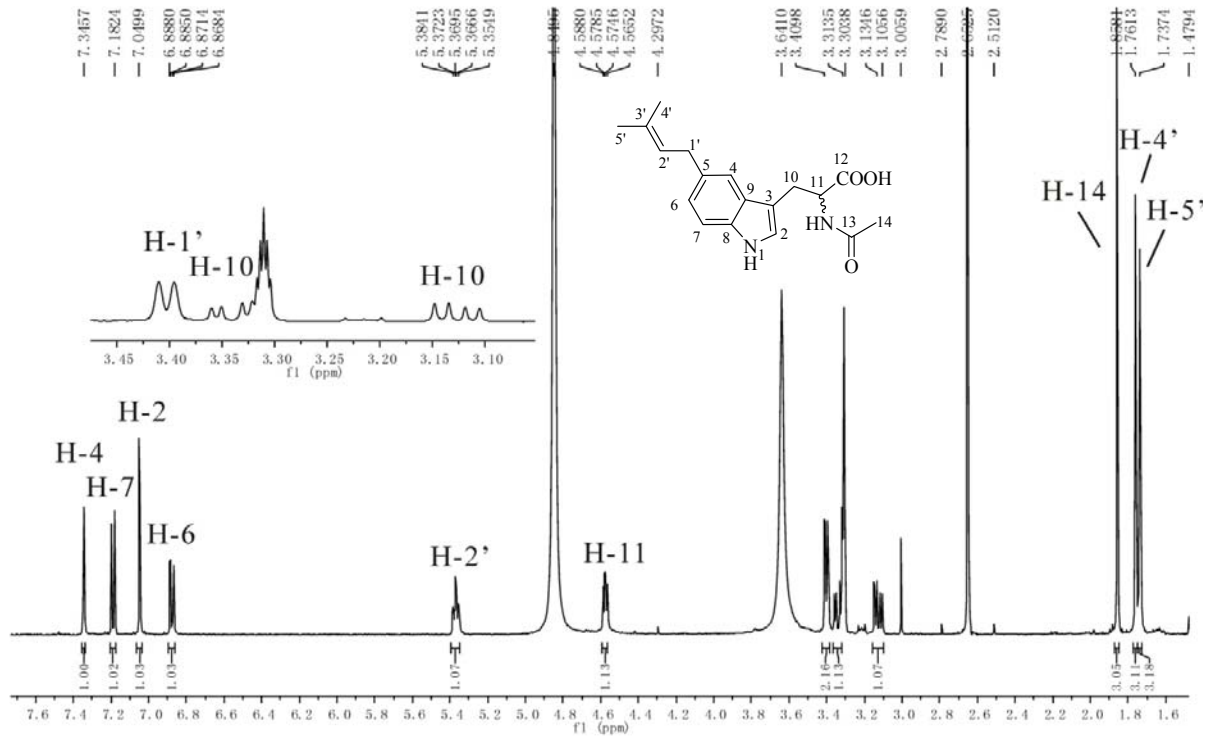

Figure S10. ^{1}H-NMR spectrum of **8b** in CD_3OD (500 MHz)

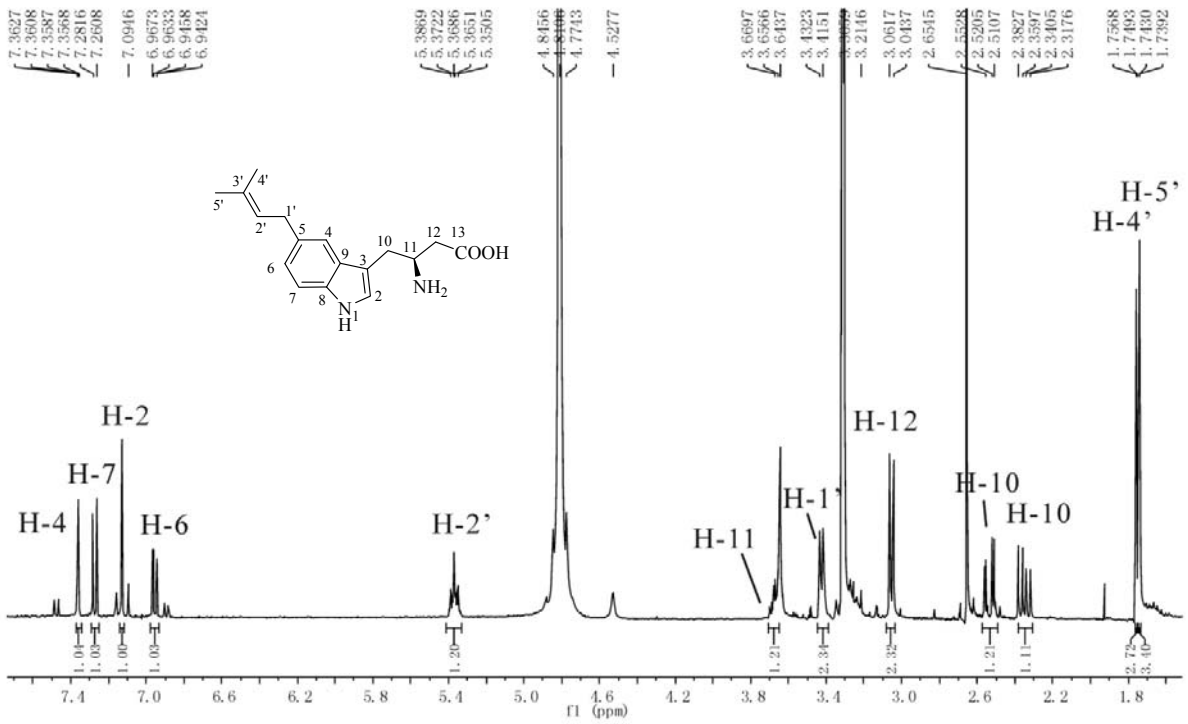

Figure S11. ^{1}H-NMR spectrum of **9b** in CD_3OD (400 MHz)

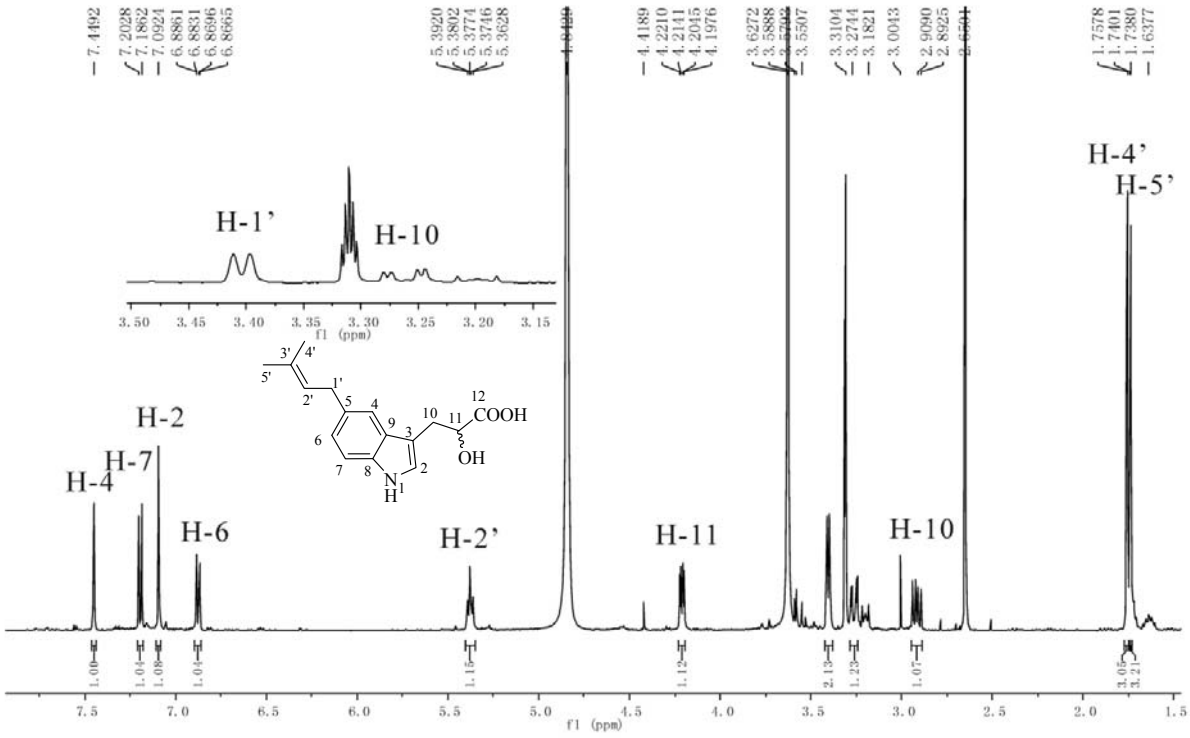

Figure S12. ^{1}H-NMR spectrum of **10b** in CD_3OD (500 MHz)

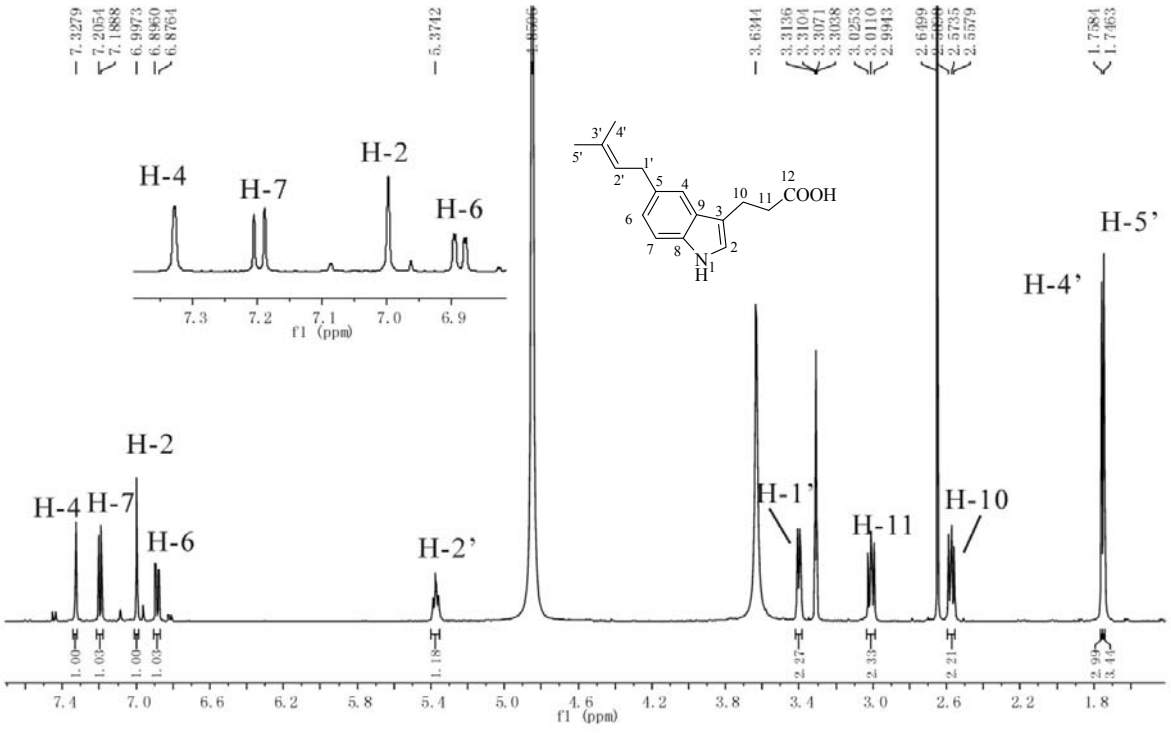

Figure S13. ^{1}H-NMR spectrum of **11b** in CD_3OD (500 MHz)

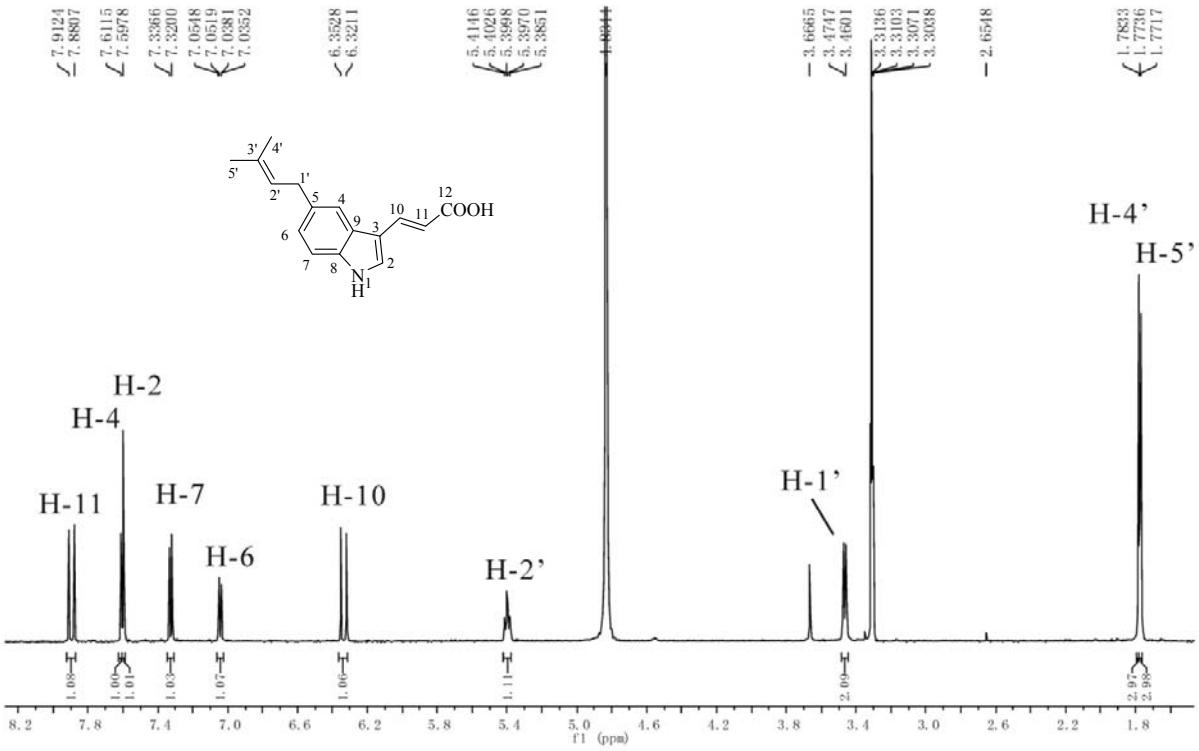

Figure S14. ^{1}H-NMR spectrum of **12b** in CD_3OD (500 MHz)

5.3 Identification of a brevianamide F reverse prenyltransferase BrePT from *Aspergillus versicolor* with a broad substrate specificity towards tryptophan-containing cyclic dipeptides

Appl Microbiol Biotechnol (2013) 97:1649–1660
DOI 10.1007/s00253-012-4130-0

BIOTECHNOLOGICALLY RELEVANT ENZYMES AND PROTEINS

Identification of a brevianamide F reverse prenyltransferase BrePT from *Aspergillus versicolor* with a broad substrate specificity towards tryptophan-containing cyclic dipeptides

Suqin Yin · Xia Yu · Qing Wang · Xiao-Qing Liu · Shu-Ming Li

Received: 18 April 2012 / Accepted: 20 April 2012 / Published online: 3 June 2012

Abstract A putative brevianamide F reverse prenyltransferase gene *brePT* was amplified from *Aspergillus versicolor* NRRL573 by using primers deduced from its orthologue *notF* in *Aspergillus* sp. MF297-2 and overexpressed in *Escherichia coli*. The soluble His-tagged protein BrePT was purified to near homogeneity and assayed with tryptophan-containing cyclic dipeptides in the presence of dimethylallyl diphosphate. BrePT showed much higher flexibility towards its aromatic substrates than NotF and accepted all of the 14 tested tryptophan-containing cyclic dipeptides. Structure elucidation of the enzyme products by NMR and MS analyses proved unequivocally the highly regiospecific reverse prenylation at C2 of the indole nucleus. K_M values of BrePT were determined for its putative substrates brevianamide F and DMAPP at 32 and 98 μM, respectively. Average turnover number (k_{cat}) at 0.4 s^{-1} was calculated from kinetic data of brevianamide F and DMAPP. K_M values in the range of 0.082–2.9 mM and k_{cat} values from 0.003 to 0.15 s^{-1} were determined for other 11 cyclic dipeptides. Similar to known fungal indole prenyltransferases, BrePT did not accept geranyl or farnesyl diphosphate as prenyl donor for its prenylation.

Keywords Brevianamide · Cyclic dipeptide · DMATS superfamily · Prenylated derivative · Prenyltransferase

Suqin Yin and Xia Yu contributed equally to this work.

Electronic supplementary material The online version of this article (doi:10.1007/s00253-012-4130-0) contains supplementary material, which is available to authorized users.

S. Yin · Q. Wang · X.-Q. Liu (✉)
College of Life Sciences, Capital Normal University,
No.105 Xisanhuan Beilu,
Beijing 100048, China
e-mail: liuxq@mail.cnu.edu.cn

S. Yin · X. Yu · Q. Wang · S.-M. Li (✉)
Institut für Pharmazeutische Biologie und Biotechnologie,
Philipps-Universität Marburg,
Deutschhausstrasse 17A,
35037 Marburg, Germany
e-mail: shuming.li@Staff.uni-Marburg.de

Introduction

Prenyltransferases are found in all domains of the life and are involved in the biosynthesis of primary and secondary metabolites in nature (Heide 2009; Li 2009a; Liang 2009; Yazaki et al. 2009). They catalyze the transfer reactions of a prenyl moiety from a prenyl donor, usually as diphosphate, to a terpenoid, serine residue of a protein or an aromatic nucleus (Li 2009a). The later mentioned enzymes are known as aromatic prenyltransferases, which are mainly found in plants, bacteria and fungi (Heide 2009; Li 2009a; Yazaki et al. 2009). A subgroup of the aromatic prenyltransferases from ascomycetes show clear sequence homology to dimethylallyltryptophan synthase (DMATS) in the biosynthesis of ergot alkaloids from *Claviceps purpurea* (Tudzynski et al. 1999) and are therefore classified as prenyltransferases of the DMATS superfamily. The members of this group catalyze mainly the prenylation of diverse indole derivatives including tryptophan and tryptophan-containing cyclic dipeptides at different positions of the indole ring and are involved in the biosynthesis of a number of prenylated indole alkaloids (Li 2009b; Li 2010; Steffan et al. 2009). Prenylated indole alkaloids are widely distributed in terrestrial and marine organisms, especially in the genera *Claviceps*, *Penicillium*, and *Aspergillus*. They are important mycotoxins like fumitremorgin- or roquefortine-type alkaloids (Li 2010; Williams et al. 2000) and drugs, e.g., ergot alkaloids (Wallwey and Li 2011).

The characteristic features of the enzymes of the DMATS superfamily are their flexibility towards aromatic substrates and high regioselectivity regarding prenylation position at the indole ring. Usually, tryptophan prenyltransferases, e.g., FgaPT2 and 7-DMATS from *Aspergillus fumigatus* (*A. fumigatus*), MaPT from *Malbranchea aurantiaca*, or 5-DMATS from *Aspergillus clavatus*, accepted also very well a number of tryptophan derivatives with modifications both at the side chain and the indole ring as substrates (Ding et al. 2008; Kremer et al. 2007; Steffan et al. 2007; Yu et al. 2012). FgaPT2 used even a number of tryptophan-containing cyclic dipeptides as substrates (Steffan and Li 2009). The same prenylation position at the indole ring was however found for products of a given enzyme, i.e., at C-4 with FgaPT2 and MaPT (Ding et al. 2008; Steffan et al. 2007), C-5 with 5-DMATS (Yu et al. 2012) and C-7 in the case of 7-DMATS (Kremer and Li 2008). Similar phenomena were also observed for cyclic dipeptide prenyltransferases from this family. For example, the regular prenyltransferase FtmPT1 from *A. fumigatus* catalyzes the prenylation of brevianamide F (cyclo-L-Trp-L-Pro) at C2 of the indole ring (Grundmann and Li 2005). The reverse prenyltransferases AnaPT and CdpC3PT from *Neosartorya fischeri* used almost all of the tested tryptophan-containing cyclic dipeptides as substrates and catalyzed regiospecific prenylation at C-3 of the indole ring (Yin et al. 2009, 2010).

Until now, two cyclic dipeptide prenyltransferases were reported to use a limited number of compounds as clearly favorable prenylation substrates. CTrpPT from *Aspergillus oryzae* accepted cyclo-L-Trp-L-Trp much better than other cyclic dipeptides as substrate (Zou et al. 2010). NotF from *Aspergillus* sp. MF297-2 is involved in the biosynthesis of notoamides and only used brevianamide F as aromatic substrate (Ding et al. 2010). This feature prohibits their usage as catalysts for production of desired compounds. It was necessary to find a NotF homologue with broad substrate specificity and to be used as catalyst for synthesis of reversely C2-prenylated indole derivatives.

Literature search revealed that several *Aspergillus versicolor* strains produced brevianamides or notoamides (Finefield et al. 2011; Li et al. 2009), which are very likely derived from deoxybrevianamide E and therefore a brevianamide F reverse prenyltransferase must be involved in their biosynthesis. We decided therefore to amplify *notF* homologue from *A. versicolor* NRRL573 by using PCR primers deduced from *notF* sequence in *Aspergillus* sp. MF297-2. In this paper, we report the cloning and expression of a *notF* homologue *brePT* from *A. versicolor*. Biochemical characterization with BrePT revealed its high flexibility towards tryptophan-containing cyclic dipeptides.

Materials and methods

Chemicals

Dimethylallyl diphosphate (DMAPP), geranyl diphosphate (GPP), and farnesyl diphosphate (FPP) were prepared according to the method described for GPP (Woodside et al. 1988). The four cyclo-Trp-Pro isomers were synthesized from tryptophan methyl ester and N-Boc protected proline according to the method published previously (Caballero et al. 2003). Cyclo-L-Trp-L-Pro and Cyclo-L-Trp-D-Pro were synthesized from H-L-Trp-OMe·HCl and N-Boc-D-Pro-OH, cyclo-D-Trp-L-Pro and cyclo-D-Trp-D-Pro from H-D-Trp-OMe·HCl and N-Boc-D-Pro-OH. Similarly, the two pairs H-L-Trp-OMe·HCl and N-Boc-D-Ala-OH as well as H-D-Trp-OMe·HCl and N-Boc-D-Ala-OH were used for the preparation of the four stereoisomers of cyclo-Trp-Ala. Cyclo-L-Trp-L-His was synthesized from N-Boc-L-Trp-OH and H-L-His-OMe·HCl according to the literature (Bivin et al. 1993; Cacciatore et al. 2005). The other cyclic dipeptides were purchased from Bachem (Bubendorf, Switzerland).

Computer-assisted sequence analysis

FGENESH (Softberry, Inc.) and the DNASIS software package (version 2.1: Hitachi Software Engineering, San Bruno, CA) were used for intron prediction and sequence analysis, respectively. Amino acid sequence similarity searches were carried out by using BLAST program from GenBank.

Bacterial strains, plasmids, and culture conditions

pGEM-T easy and pET28a were obtained from Promega (Mannheim, Germany) and Novagen (Beijing, China), respectively. *Escherichia coli* XL1 Blue MRF' (Stratagene, Amsterdam, the Netherlands) and BL21 (DE3) pLysS (Newprobo, Beijing, China) were used for cloning and expression experiments, respectively. They were grown in liquid Luria-Bertani (LB) medium or on solid LB medium with 1.5 % (*w*/*v*) agar at 37 or 20 °C. 50 $\mu g \cdot ml^{-1}$ of kanamycin were used for selection of recombinant *E. coli* cells.

Cultivation of *A. versicolor* NRRL573 for DNA isolation

A. versicolor NRRL573 was kindly provided by Agricultural Research Service Culture Collection of the United States Department of Agriculture. For DNA isolation, the fungus was cultivated in liquid potatoe dextrose medium at 25 °C and 160 rpm for 5 days. Fungal mycelia were collected and washed with phosphate-buffered saline consisting of 137 mM NaCl, 2.7 mM KCl, 1 mM Na_2HPO_4, and 0.18 mM KH_2PO_4 (pH 7.3). Genomic DNA was isolated by using freeze–thaw method.

DNA propagation in *E. coli*, PCR amplification, and gene cloning

Standard procedures for DNA isolation and manipulation were performed as described (Sambrook and Russell 2001). PCR amplification was carried out on an iCycler from BioRad (Munich, Germany). A PCR fragment of 1,384 bp was amplified from genomic DNA of *A. versicolor* by using the DNA sequences of *Aspergillus* sp. MF297-2, 5′-ATAT**ATG**ACGGCCCCAGAGCTCCGT-3′ and 5′-GGCC**TCA**ATCTTCTTCCCACAGATAGG-3′ as primers. The underlined bold triplets ATG and TCA represent the start and stop codon of *notF*, respectively.

To delete the intron sequence, a two round fusion PCR was carried out as described previously (Yin et al. 2009). Two primers brePT1-for (5′-CATG**CCATGG**CA ATGACGGCCCCAGAGCTCCGTG-3′) and brePT1-rev (5′-ACGTCCAGGTCCGGGTACAGCTGTTGCAA CATATC-3′) were used for amplification of the first exon, and brePT2-for (5′-TATGTTGCAACAGCT GTACCCGGACCTGGACGTTT-3′) and brePT2-rev (5′-ATAAGAAT**GCGGCCGC**ATCTTCTTCCCACAG ATAGGTACTTTGT-3′) for the second exon. The underlined sequences with bold letter in brePT1-for and brePT2-rev represent the restriction sites *Nco*I and NotI for cloning in pET28a vector, respectively. The underlined letters in bePT1-rev and brePT2-for indicated the overlapping region of the two exons with a length of 1,178 and 130 bp, respectively. The entire coding sequence of *brePT* was obtained as a PCR fragment of 1,333 bp and subsequently cloned into pGEM-T easy vector, resulting in plasmid pQW1. pQW1 was sequenced (Eurofins MWG Operon, Ebersberg, Germany) to confirm the sequence. To create the expression vector pQW2, pQW1 was digested with *Nco*I and NotI and the resulted *Nco*I–NotI fragment of 1,314 bp was ligated into pET28a, which had been digested with the same enzymes, previously. After unsuccessful expression with pQW2 in *E. coli* under different conditions, the *brePT* sequence was amplified from pQW2 by using the primers 5′-TACCATGGATATGACGGCCCCA-3′ and 5′-ATGCGGCCGCTCA ATGATGATGATGATGA TGATCTTCTTCC-3′. The underlined sequence codes five histidine residues for purification on Ni-NTA agarose. The PCR product of 1,343 bp was then cloned into the restriction sites *Nco*I and NotI in pET28a, resulting in the new expression plasmid pSY1.

Overproduction and purification of His_5-BrePT

For gene expression, *E. coli* BL21 (DE3) pLysS cells harboring the plasmid pSY1 were cultivated in liquid LB medium supplemented with kanamycin (50 μg ml^{-1}) and grown at 37 °C to an A_{600} of 0.7 and induced with 0.1 mM IPTG for 5 h at 20 °C. Protein extraction and purification were carried out as described previously (Yu et al. 2012).

Protein analysis and determination of molecular mass of active His_5-BrePT

Proteins were analyzed on SDS-PAGE according to the method described by Laemmli (Laemmli 1970) and stained with Coomassie Brilliant Blue G-250. The molecular mass of the recombinant His_5-BrePT was determined by size exclusion chromatography on a HiLoad 16/60 Superdex 200 column (GE Healthcare) that had been equilibrated with 50 mM Tris–HCl buffer (pH 7.5) containing 150 mM NaCl. The column was calibrated with dextran blue 2000 (2,000 kDa), ferritin (440 kDa), aldolase (158 kDa), conalbumin (75 kDa), carbonic anhydrase (29 kDa), and ribonuclease A (13.7 kDa; GE Healthcare). The proteins were eluted with 50 mM Tris–HCl buffer (pH 7.5) containing 150 mM NaCl.

Assays for BrePT activity

For determination of the BrePT activity, the reaction mixtures (100 μl) contained 50 mM Tris–HCl (pH 7.5), 10 mM $CaCl_2$, 1 mM cyclic dipeptide, 2 mM DMAPP, GPP, or FPP, and 18 μg of purified recombinant BrePT and were incubated at 37 °C for 4 h. The reactions were then terminated by addition of 100 μl of methanol. After removal of protein by centrifugation at 13,000×*g* for 20 min, the enzyme products were analyzed on HPLC under the conditions described below. For quantitative measurement of the enzyme activity, duplicate values were determined routinely. The assays for determination of the kinetic parameters (100 μl) of cyclic dipeptides contained 2 mM DMAPP, 0.5–10 μg of BrePT. Due to the difference in solubility in assay system, various concentrations were used for cyclic dipeptides: **1d–1g**, **1i**, and **1j** up to 5 mM, **1b** and **1c** up to 2 mM, **1a** up to 0.8 mM, and **1h**, **1k**, and **1l** up to 0.5 mM. For determination of the kinetic parameters of DMAPP, the assays (100 μl) contained 1 μg of BrePT, 1 mM cyclo-L-Trp-L-Pro and DMAPP at final concentrations of up to 2 mM. The incubation time was 30 min.

Preparative synthesis of the enzyme products for structural elucidation

BrePT assays for isolation of the enzyme products (10 ml) contained 1 mM DMAPP, 1 mM cyclic dipeptide, 10 mM $CaCl_2$, 50 mM Tris–HCl (pH 7.5), and 2 mg of BrePT. The reaction mixtures were incubated at 37 °C for 16 h and extracted subsequently with ethyl acetate. After evaporation of the solvent, the residues were dissolved in methanol and purified on HPLC under the conditions described below.

Table 1 HR-ESI-MS and HR-EI-MS data of the enzyme products of BrePT

Compounds	Chemical formula	HR-MS data			Deviation (ppm)
		MS	Calculated	Measured	
2a	$C_{21}H_{25}N_3O_2$	HR-ESI-MS	374.1844 $[M+Na]^+$	374.1811	8.9
2b	$C_{21}H_{25}N_3O_2$	HR-ESI-MS	374.1844 $[M+Na]^+$	374.1808	9.8
2c	$C_{21}H_{25}N_3O_2$	HR-ESI-MS	374.1844 $[M+Na]^+$	374.1814	8.1
2d	$C_{21}H_{25}N_3O_2$	HR-EI-MS	351.1947 $[M]^+$	351.1928	5.3
2e	$C_{19}H_{23}N_3O_2$	HR-EI-MS	325.1790 $[M]^+$	325.1777	4.0
2f	$C_{19}H_{23}N_3O_2$	HR-ESI-MS	348.1688 $[M+Na]^+$	348.1672	4.6
2g	$C_{19}H_{23}N_3O_2$	HR-EI-MS	325.1790 $[M]^+$	325.1773	5.3
2h	$C_{19}H_{23}N_3O_2$	HR-EI-MS	325.1790 $[M]^+$	325.1771	5.8
2i	$C_{18}H_{21}N_3O_2$	HR-ESI-MS	312.1712 $[M+H]^+$	312.1710	0.8
2j	$C_{22}H_{29}N_3O_2$	HR-ESI-MS	368.2338 $[M+H]^+$	368.2328	2.8
2k	$C_{25}H_{27}N_3O_2$	HR-ESI-MS	424.2001 $[M+Na]^+$	424.2039	−9.0
2l	$C_{25}H_{27}N_3O_3$	HR-ESI-MS	440.1950 $[M+Na]^+$	440.1952	−0.4

HPLC conditions for analysis and isolation of the enzyme products of BrePT

The enzyme products of the incubation mixtures of BrePT were analyzed on HPLC with an Agilent series 1200 by using a Multospher 120 RP-18 column (250×4 mm, 5 μm, C+S Chromatographie Service, Langerwehe, Germany) at a flow rate of 1 ml min^{-1}. Water (solvent A) and methanol (solvent B) each with 0.5 % (*v*/*v*) trifluoroacetic acid were used as solvents. For analysis of enzyme products, a linear gradient of 40–100 % (*v*/*v*) solvent B in 15 min was used. The column was then washed with 100 % solvent B for 5 min and equilibrated with 40 % (*v*/*v*) solvent B for 5 min. Detection was carried out by a photodiode array detector at 296 nm.

For isolation, the same HPLC equipment with a Multospher 120 RP-18 column (250×10 mm, 5 μm, C+S Chromatographie) was used. Water (solvent C) and methanol (solvent D) without acid were used as solvents. A linear gradient of 40–100 % (*v*/*v*) solvent D in 30 min at a flow rate of 2.5 ml min^{-1} was used. The column was then washed with 100 % solvent D for 8 min and equilibrated with 40 % (*v*/*v*) solvent D for 8 min.

NMR spectroscopic analysis and high resolution mass spectra

^{1}H-NMR spectra were recorded on a JEOL ECX-400 or ECX-500 spectrometer. Chemical shifts were referenced to the signal of CD_3OD at 3.31 ppm or DMSO-d_6 at 2.50 ppm. All spectra were processed with MestReNova 5.2.2. The isolated products were also analyzed by mass spectroscopy on a Q-Trap Quantum (Applied Biosystems) using a high resolution electron spray ionization (HR-ESI) mode or on an AutoSPEC with an electron impact (HR-EI) mode. Positive MS data are given in Table 1.

Nucleotide sequence accession number

The genomic and coding sequences of *brePT* from *A. versicolor* NRRL573 is available at GenBank under the accession number JQ013953.

Results

Cloning and sequence analysis of a *notF* homologue *brePT* from *A. versicolor* as well as protein overproduction and purification

Whole genome sequencing of the marine-derived *Aspergillus* sp. MF297-2 led to the identification of a biosynthetic gene cluster for notoamides (Ding et al. 2010). NotF from this cluster was found to be responsible for the reverse prenylation of brevianamide F at position C2 of the indole ring resulting in

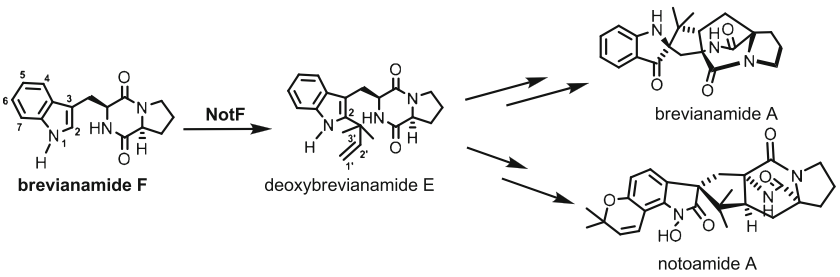

Fig. 1 Prenyl transfer reaction catalyzed by NotF as well as its role in the biosynthesis of fungal natural products

```
BrePT   1   MTAPELR-----APAGHPQEP-------PARSSPAQALSSYHHFPTSDQERWYQETGSLC  48
NotF    1   MTAPELRVDTFRAPEDAPKEPSAQQPRLPSSPSPAQALASYHHFPTNDQERWWEETGSLF  60

BrePT   49  SRFLEAGQYGLHQQYQFMFFFMHHLIPALGPYPQKWRSTISRSGLPIEFSLNFQKGSHRL  108
NotF    61  SRFLEAGQYGLPQQYQFMFFFMHHLIPALGPYPQKWRSTISRSGLPIEFSLNFQKGSHRL  120

BrePT   109 LRIGFEPVNFLSGSSQDPFNRIPIADLLAQLARLQLRGFDTQCFQQLLTRFQLSLDEVRQ  168
NotF    121 LRIGFEPVSFLSGSSQDPFNRIPITDLLNRLSKLQLSNFDTPFFQHLLSKFQLSLSEVRQ  180

BrePT   169 LP-----PDDQPLKSQGAFGFDFNPDGAILVKGYVFPYLKAKAAGVPVATLIAESVRAID  223
NotF    181 LQKQGSGPDAHPLKSQAAFGFDFNPDGAILVKGYVFPYLKAKAADVPVGTLIAEAVRTID  240

BrePT   224 ADRNQFMHAFSLINDYMQESTGYNEYTFLSCDLVEMSRQRVKIYGAHTEVTWAKIAEMWT  283
NotF    241 VERNQFTHAFGLINDYMQESTGYNEYTFLSCDFVETSEQRLKIYGAHTEVTWAKIAEMWT  300

BrePT   284 LGGRLIEEPEIMEGLARLKQIWSLLQIGEGSRAFKGGFDYGKASATDQIPSPIIWNYEIS  343
NotF    301 LGGRLIEEPEIIAGLARLKQIWSLLQIGEGSRAFKGGFDYDKSSATDQIASPIIWNYEIH  360

BrePT   344 PGSSFPVPKFYLPVHGENDLRVARSLAQFWDSLGWSEHACAYPDMLQQLYPDLDVSRTSR  403
NotF    361 PGSRFPVPKFYLPVHGENDLHVARALAQFWDSLGWPEHACAYPDTLQQLYPDQDISQTTR  420

BrePT   404 LQSWISYSYTAKKGVYMSVYFHSQSTYLWEED  435
NotF    421 LQSWISYSYTAKRGVYMSVYYHSQSTYLWEED  452
```

Fig. 2 Alignments of BrePT from *Aspergillus versicolor* NRRL573 (JQ013953) with NotF from *Aspergillus* sp. MF297-2 (ADM34132.1). Identical amino acids in both proteins are highlighted with *grey* background

the formation of deoxybrevianamide E (Fig. 1) (Ding et al. 2010). It was also reported that NotF was highly specific towards its aromatic substrate and no prenylated product was detected for L-tryptophan, cyclo-L-Trp-L-Trp or cyclo-L-Trp-L-Tyr by LC-MS analysis (Ding et al. 2010).

In course of our search for NotF homologues with broad substrate specificity, a 1,384 bp PCR fragment was amplified from genomic DNA of *A. visicolor* NRRL573 by using two oligonucleotides containing sequences at the beginning and the end of *notF*. The obtained fragment was cloned into pGEM-T easy vector and sequenced subsequently. Sequencing results showed that the putative *notF* homologue from *A. versicolor*, termed *brePT* (**bre**vianamide F **p**renyl**t**ransferase) in this study, has a size of 1,376 bp consisting of two predicted exons of 1,178 and 130 bp, respectively, disrupted by one intron of 68 bp. *brePT* shares an identity of 87 % on the nucleotide level with *notF* from *Aspergillus* sp. MF297-2. The deduced polypeptide BrePT has a length of 435 amino acids and is therefore of 17 amino acids shorter than NotF. These amino acids correspond to two gaps of five and seven amino acids at the N terminus and one gap of five amino acids between amino acids 183 and 187 in NotF (Fig. 2). BrePT and NotF share an identity of 83 % with each other on the amino acid level.

To clone the entire coding region of *brePT*, the two exons were amplified parallel from the genomic DNA and combined with the help of a short overlapped region by further PCR amplification (see Materials and methods). The successfully amplified PCR product was cloned via pGEM-T easy vector into the expression vector pET28a to create the expression construct pQW2. After failed expression with pQW2, we recloned *brePT* in pET28a by introducing five histidine residues in the C-terminus of the overproduced protein. *E. coli* BL21 cells harboring the newly constructed expression vector pSY1 were cultivated in LB medium and induced with 0.1 mM IPTG at 20 °C for 5 h. One-step purification on Ni-NTA agarose resulted in a significant band with similar migration behavior as the 45 kDa size marker on SDS-PAGE (Fig. 3), corresponding to the calculated mass

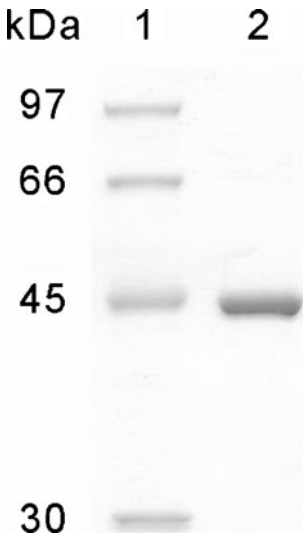

Fig. 3 Analysis of the purified His_5-BrePT on SDS-PAGE. The proteins were separated on a 12 % SDS-polyacrylamide gel and stained with Coomassie Brilliant *Blue* G-250. *Lane 1* molecular mass standard and *lane 2* purified His_5-BrePT

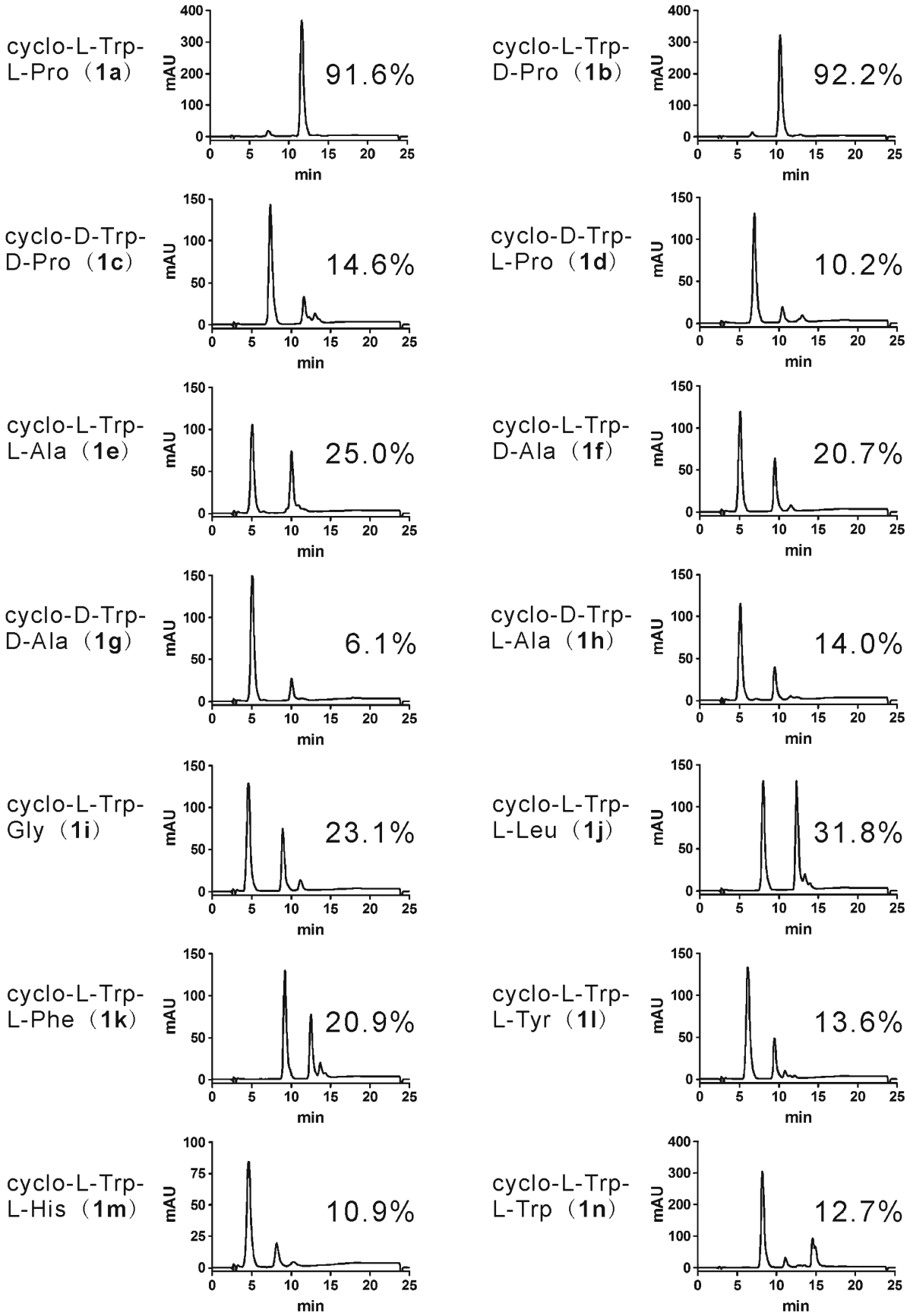

Fig. 4 HPLC analysis of reaction mixtures of BrePT with cyclic dipeptides

Table 2 ^{1}H-NMR data of C2-prenylated cyclic dipeptides produced by using BrePT

Compd	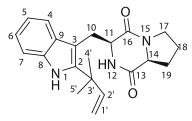 Cyclo-2-tert-prenyl-L-Trp-L-Pro (**2a**) in CD_3OD	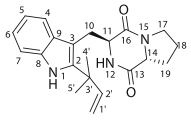 Cyclo-2-tert-prenyl-L-Trp-D-Pro (**2b**) in CD_3OD	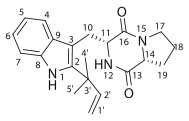 Cyclo-2-tert-prenyl-D-Trp-D-Pro (**2c**) in CD_3OD	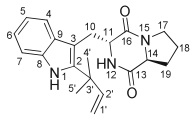 Cyclo-2-tert-prenyl-D-Trp-L-Pro (**2d**) in CD_3OD
Pos.	δ_H, multi., *J*	δ_H, multi., *J*	δ_H, multi., *J*	δ_H, multi., *J*
4	7.47, d, 8.1	7.46, d, 8.0	7.47, d, 8.1	7.46, d, 8.0
5	7.02, dd, 8.1, 7.1	6.97, dd, 8.0, 7.0	7.02, dd, 8.1, 7.1	6.97, dd, 8.0, 7.0
6	7.09, dd, 8.1, 7.1	7.04, dd, 8.0, 7.0	7.09, dd, 8.1, 7.1	7.04, dd, 8.0, 7.0
7	7.37, d, 8.1	7.30, d, 8.0	7.37, d, 8.1	7.30, d, 8.0
10	3.65, dd, 15.1, 4.3 3.14, dd, 15.1, 11.2	3.45, dd, 14.8, 5.1 3.38, dd, 14.8, 6.5	3.65, dd, 15.1, 4.3 3.15, dd, 15.1, 11.2	3.45, dd, 14.7, 5.1 3.38, dd, 14.7, 6.6
11	4.52, ddd, 11.2, 4.3, 2.0	4.18, dd, 6.5, 5.1	4.52, dd, 11.2, 4.3	4.18, dd, 6.5, 5.1
14	4.23, dd, 8.5, 6.4	3.47, ddd, 11.4, 9.8, 7.4	4.23, m	3.47, m
17	3.61, m 3.55, m	3.3[a] 3.3[a]	3.61, m 3.55, m	3.3[a] 3.3[a]
18	2.02, m 1.94, m	1.89, m 1.52, m	2.03, m 1.94, m	1.89, m 1.52, m
19	2.28, m 1.94, m	2.09, m 1.74, tdd, 12.1, 11.4, 7.4	2.28, m 1.94, m	2.09, m 1.74, m
1'	5.13, d, 17.5 5.10, d, 10.6	5.16, d, 17.5 5.12, d, 10.6	5.13, d, 17.5 5.10, d, 10.6	5.16, d, 17.5 5.12, d, 10.6
2'	6.22, dd, 17.5, 10.6	6.21, dd, 17.5, 10.6	6.22, dd, 17.5, 10.6	6.21, dd, 17.5, 10.6
4'	1.57, s	1.54, s	1.58, s	1.54, s
5'	1.56, s	1.54, s	1.56, s	1.54, s

of 50 kDa for His_5-BrePT. The yield was calculated to be 1.5 mg of purified protein per liter of culture. The molecular mass of the native recombinant His_5-BrePT was determined by size exclusion chromatography as 56 kDa, which indicated that BrePT likely acts as a monomer.

BrePT accepted all of the tested tryptophan-containing cyclic dipeptides as substrates in the presence of DMAPP

BrePT was firstly assayed with brevianamide F (**1a**), the natural substrate of its homologue NotF from *Aspergillus* sp. MF297-2 (Ding et al. 2010), in the presence of DMAPP. A product peak was clearly detected in the HPLC chromatogram of the incubation mixture (Fig. 4). A conversion yield of about 91 % was achieved after incubation with 18 μg of His_5-BrePT for 4 h. Detection of this peak was strictly dependent on the presence of DMAPP and the active enzyme (data not shown). Incubation of His_5-BrePT with 13 additional tryptophan-containing cyclic dipeptides (**1b**–**1n**) showed also clearly product formation with conversion yields from 6 to 92 % (Fig. 4). L-tryptophan and L-tyrosine were not accepted by His_5-BrePT in the presence of DMAPP under this condition. No production formation was observed, when GPP or FPP instead of DMAPP was used as a prenyl donor in reaction mixtures of the 14 tryptophan-containing cyclic dipeptides and His_5-BrePT.

The accepted substrates included all of the four diketopiperazine stereoisomers of tryptophan and proline as well as of tryptophan and alanine. As shown in Fig. 4, cyclo-L-Trp-D-Pro (**1b**) was also well accepted by BrePT with an almost same conversion yield as **1a**. In contrast, the other two isomers cyclo-D-Trp-D-Pro (**1c**) and cyclo-D-Trp-L-Pro (**1d**) showed conversion yields of less than 15 %. It seems that the stereochemistry of tryptophanyl moiety in these dipeptides plays an important role for their binding to BrePT and L-form is the preferable configuration. Similar phenomena were

Table 2 (continued)

Compd	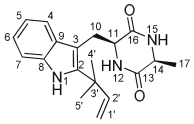 Cyclo-2-tert-prenyl-L-Trp-L-Ala (**2e**) in CD_3OD	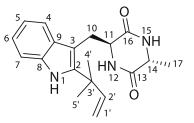 Cyclo-2-tert-prenyl-L-Trp-D-Ala (**2f**) in CD_3OD	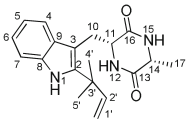 Cyclo-2-tert-prenyl-D-Trp-D-Ala (**2g**) in CD_3OD	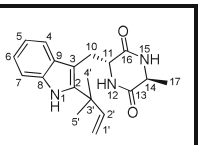 Cyclo-2-tert-prenyl-D-Trp-L-Ala (**2h**) in CD_3OD
Pos.	δ_H, multi.,*J*	δ_H, multi., *J*	δ_H, multi., *J*	δ_H, multi., *J*
4	7.51, d, 7.8	7.52, d, 8.0	7.51, d, 8.0	7.52, d, 8.0
5	6.99, dd, 7.8, 7.0	6.99, dd, 8.0, 7.1	6.99, dd, 8.0, 7.1	6.99, dd, 8.0, 7.1
6	7.06, dd, 7.8, 7.0	7.05, dd, 8.0, 7.1	7.06, dd, 8.0, 7.1	7.05, dd, 8.0, 7.1
7	7.33, d, 7.8	7.32, d, 8.0	7.33, d, 8.0	7.32, d, 8.0
10	3.54, dd, 14.6, 3.8 3.3[a]	3.45, dd, 14.6, 4.4 3.3[a]	3.54, dd, 14.6, 3.8 3.3[a]	3.45, dd, 14.6, 4.4 3.3[a]
11	4.28, dd, 9.6, 3.8	4.21, dd, 8.5, 4.4	4.28, dd, 9.6, 3.8	4.21, dd, 9.2, 4.4
14	3.94, q, 7.1	3.81, q, 6.8	3.94, q, 7.0	3.81, q, 7.0
17	1.30, d, 7.1	1.33, d, 6.8	1.30, d, 7.0	1.33, d, 7.0
1'	5.15, d, 17.5 5.11, d, 10.6	5.15, d, 17.5 5.10, d, 10.6	5.15, d, 17.5 5.11, d, 10.6	5.15, d, 17.5 5.10, d, 10.6
2'	6.21, dd, 17.5, 10.6	6.22, dd, 17.5, 10.6	6.21, dd, 17.5, 10.6	6.22, dd, 17.5, 10.6
4'	1.56, s	1.55, s	1.56, s	1.55, s
5'	1.56, s	1.54, s	1.56, s	1.54, s

also observed with the four isomers of cyclic dipeptides from tryptophan and alanine (Fig. 4). Cyclo-L-Trp-L-Ala (**1e**) and cyclo-L-Trp-D-Ala (**1f**) showed comparable activities with conversion yields of 25 and 21 %, respectively. The two isomers with D-tryptophanyl moiety, i.e., cyclo-D-Trp-D-Ala (**1g**) and cyclo-D-Trp-L-Ala (**1h**) showed significantly lower conversion yields of 6 and 14 %, respectively. In comparison to that of cyclo-L-Trp-L-Ala (**1e**), comparable activities were detected for cyclo-L-Trp-Gly (**1i**) and cyclo-L-Trp-L-Leu (**1j**) with conversion yields of 23 and 32 %, respectively. BrePT showed slightly lower activities towards tryptophan-containing dipeptides with an additional aromatic amino acid such as cyclo-L-Trp-L-Phe (**1k**), cyclo-L-Trp-L-Tyr (**1l**), cyclo-L-Trp-L-His (**1m**), and cyclo-L-Trp-L-Trp (**1n**) than those consisting of L-tryptophan and an aliphatic amino acid (Fig. 4).

BrePT catalyzed reverse C2-prenylation of tryptophan-containing cyclic dipeptides

For structure elucidation, enzyme products of 12 selected substrates (**1a–1l**, Fig. 4) were isolated on HPLC in preparative scales and subjected to MS and NMR analyses. High-resolution electron spray ionization mass spectroscopy (HR-ESI-MS) and high resolution electron impact mass spectroscopy (HR-EI-MS) confirmed that the molecular masses of the isolated products are 68 Daltons larger than those of the respective substrates (Table 1), indicating the monoprenylation of these substrates. Comparing the ^{1}H-NMR data of the enzyme products (**2a–2l**, Table 2; for spectra see Figs. S1–S12 in the Electronic supplementary material) with those of the respective substrates (data not shown) revealed clearly the presence of the characteristic signals for reverse prenyl residues, i.e., δ_H 6.08–6.22 (dd, 1H-2′), 4.98–5.16 (d, 1H-1′), 4.97–5.12 (d, 1H-1′), 1.43–1.58 (s, 3H-4′), and 1.43–1.56 ppm (s, 3H-5′). Inspection of the ^{1}H-NMR spectra of the enzyme products revealed also the disappearance of the singlets for H-2 of the substrates. Other signals for aromatic protons did not changed significantly. This proved unequivocally the attachment of the reverse prenyl (tert-prenyl) moieties at C2 of the indole ring and the regiospecific C2-prenylation catalyzed by BrePT (Fig. 5). The ^{1}H-NMR data of **2a**, **2d**, **2e**, **2h**, and **2i** corresponded to those reported previously (Guo et al. 2011; Kuramochi et al. 2008; Ritchie and Saxton 1981).

Table 2 (continued)

Compd	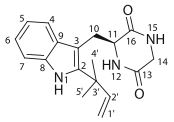 Cyclo-2-tert-prenyl-L-Trp-Gly (**2i**) in CD_3OD	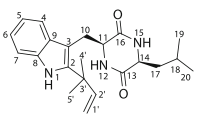 Cyclo-2-tert-prenyl-L-Trp-L-Leu (**2j**) in CD_3OD	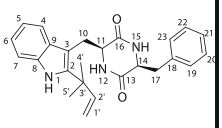 Cyclo-2-tert-prenyl-L-Trp-L-Phe (**2k**) in DMSO-d_6[b]	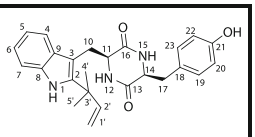 Cyclo-2-tert-prenyl-L-Trp-L-Tyr (**2l**) in DMSO-d_6[b]
Pos.	δ_H, multi., *J*	δ_H, multi., *J*	δ_H, multi., *J*	δ_H, multi., *J*
4	7.50, d, 8.0	7.52, d, 7.7	7.27, d, 7.1	7.27, d, 7.9
5	6.97, dd, 8.0, 7.0	6.97, t, 7.7	6.92, dd, 8.1, 7.1	6.92, dd, 7.9, 7.1
6	7.03, dd, 8.0, 7.0	7.05, t, 7.7	7.00, dd, 8.1, 7.1	7.00, dd, 7.9, 7.1
7	7.30, d, 8.0	7.32, d, 7.7	7.20, d, 7.1	7.23, d, 7.9
10	3.44, dd, 14.6, 4.4 3.34, dd, 14.6, 9.0	3.51, dd, 14.8, 4.0 3.3[a]	2.86, dd, 13.6, 5.2 2.79, dd, 13.6, 5.2	2.78, dd, 13.7, 4.8 2.73, dd, 13.7, 4.8
11	4.19, dd, 9.0, 4.4	4.26, dd, 8.3, 4.0	4.07, t, 5.2	4.00, t, 4.8
14	3.3[a]	3.80, dd, 9.5, 4.5	3.84, dd, 9.1, 3.8	3.83, dd, 9.1, 3.6
17	-	1.43, ddd, 13.6, 9.5, 4.5 1.16, ddd, 13.6, 9.5, 4.5	3.08, dd, 14.7, 3.8 2.33, dd,14.7, 9.1	3.10, dd, 14.5, 3.6 2.25, dd, 14.5, 9.1
18	-	1.30, m	-	-
19	-	0.88, d, 6.6	7.10, d, 7.0	6.91, d, 8.5
20	-	0.86, d, 6.6	7.30, t, 7.0	6.68, d, 8.5
21	-	-	7.21, t, 7.0	-
22	-	-	7.30, t, 7.0	6.68, d, 8.5
23	-	-	7.10, d, 7.0	6.91, d, 8.5
1'	5.14, d, 17.5 5.09, d, 10.6	5.16, d, 17.5 5.11, d, 10.6	4.98, d, 10.6 4.97, d, 17.4	4.99, d, 10.5 4.98, d, 17.4
2'	6.20, dd, 17.5, 10.6	6.21, dd, 17.5, 10.6	6.08, dd, 17.4, 10.6	6.08, dd, 17.4, 10.5
4'	1.53, s	1.56, s	1.43, s	1.43, s
5'	1.52, s	1.56, s	1.43, s	1.43, s

[a] Overlapping signals with those of solvents

[b] After addition of D_2O

Biochemical characterization and kinetic parameters of BrePT

For determination of the ion dependence of BrePT, incubations of cyclo-L-Trp-L-Pro (**1a**) with DMAPP were carried out in the presence of different metal ions at a final concentration of 5 mM. Incubations with the chelating agent EDTA or without additives were used as controls. In the incubation mixture with EDTA, slight increase of the enzyme activity to 116 % was observed, in comparison to that of incubation without additives. As observed for other members of the DMATS superfamily (Li 2009b; Steffan et al. 2009), Ca^{2+} clearly enhanced the enzyme activity of BrePT. The enzyme activity with Ca^{2+} was found to be 266 % of that without additives.

To study the behavior of BrePT towards DMAPP and twelve different cyclic dipeptides (**1a–1l**) in detail, kinetic parameters including Michaelis–Menten constants (K_M) and turnover numbers (k_{cat}), were determined by Hanes–Woolf and Eadia–Hofstee plots and are given in Table 3. The reactions catalyzed by BrePT apparently followed Michaelis–Menten kinetics. BrePT showed the best affinity to cyclo-L-Trp-L-Pro (**1a**) with the largest reaction velocity. K_M values for DMAPP and cyclo-L-Trp-L-Pro (**1a**) were found to be 98 and 32 μM, respectively. The turnover number and catalytic efficiency were calculated for **1a** at

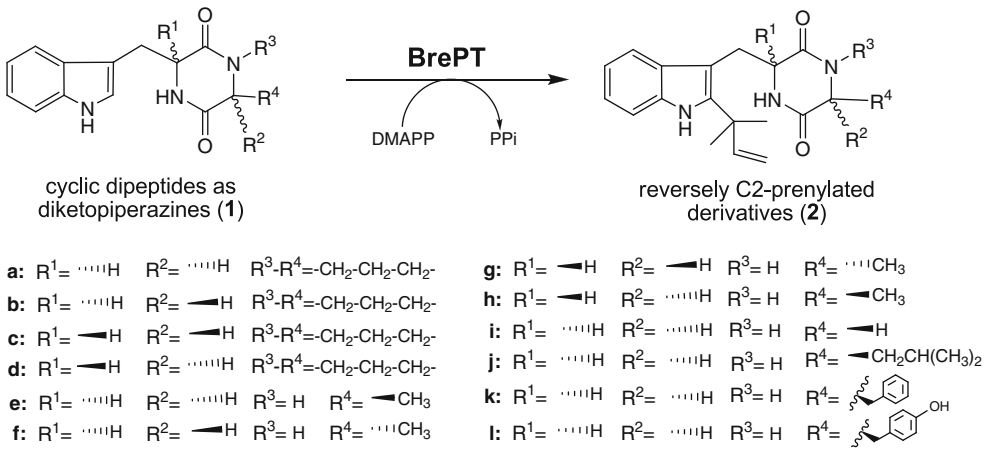

Fig. 5 Conversion of cyclic dipeptides to reversely C2-prenylated derivatives by BrePT

0.276 s^{-1} and 8,639 s^{-1} M^{-1}, respectively. The K_M values of other tested substrates were found to be in the range of 82–2,906 μM. Some of these values are much higher than that of **1a** but still in the concentration range expected for non-natural substrates. Comparing the kinetic data showed that BrePT has much higher catalytic efficiencies towards cyclo-Trp-Pro isomers with L-tryptophanyl moiety, i.e., **1a** and **1b**, than with their D-configured counter partners, i.e., **1c** and **1d**. As aforementioned, cyclo-L-Trp-D-Pro (**1b**) was also very well accepted by BrePT with a K_M value at 82 μM and turnover number at 0.15 s^{-1}. The catalytic efficiency of **1b** was 21 % of that of **1a**. Significant higher K_M values at 0.7 and 2.9 mM were calculated for **1c** and **1d**, respectively. The catalytic efficiency ratios of **1a** to **1c** and **1a** to **1d** were calculated to be approximately 64 and 960, respectively. Similar to the data obtained for cyclo-Trp-Pro isomers, higher catalytic efficiency was also calculated for cyclo-Trp-Ala isomers with L-configured tryptophanyl moiety than for their respective D-configured counter partners, i.e., with ratios of about 1.8 for cyclo-L-Trp-L-Ala (**1e**) to cyclo-D-Trp-L-Ala (**1h**) and cyclo-L-Trp-D-Ala (**1f**) to cyclo-D-Trp-D-Ala (**1g**). Cyclo-L-Trp-L-Leu (**1j**) was also found to be a good substrate for BrePT with a K_M value of 0.106 mM and turnover number of 0.014 s^{-1}, corresponding to a catalytic efficiency of 134 s^{-1} M^{-1}.

Table 3 Kinetic parameters of BrePT for selected substrates

Name	K_M (mM)	k_{cat} (s^{-1})	k_{cat}/K_M (s^{-1} M^{-1})
Cyclo-L-Trp-L-Pro (**1a**)	0.032	0.276	8639
Cyclo-L-Trp-D-Pro (**1b**)	0.082	0.150	1830
Cyclo-D-Trp-D-Pro (**1c**)	0.709	0.095	134
Cyclo-D-Trp-L-Pro (**1d**)	2.906	0.027	9
Cyclo-L-Trp-L-Ala (**1e**)	0.942	0.035	37
Cyclo-L-Trp-D-Ala (**1f**)	0.793	0.013	17
Cyclo-D-Trp-D-Ala (**1g**)	1.318	0.011	9
Cyclo-D-Trp-L-Ala (**1h**)	0.139	0.003	21
Cyclo-L-Trp-Gly (**1i**)	1.300	0.032	25
Cyclo-L-Trp-L-Leu (**1j**)	0.106	0.014	134
Cyclo-L-Trp-L-Phe (**1k**)	0.094	0.004	40
Cyclo-L-Trp-L-Tyr (**1l**)	0.214	0.006	27
DMAPP	0.098	0.489	4,992

Discussion

In a previous study, Ding et al. (2010) showed the high specificity of the brevianamide F reverse prenyltransferase NotF. In that study, the natural substrate cyclo-L-Trp-L-Pro (**1a**) was very well, but cyclo-L-Trp-L-Tyr (**1l**) and cyclo-L-Trp-L-Trp (**1n**) were not accepted by NotF. In this study, we cloned, overexpressed and characterized a NotF homologue BrePT from *A. versicolor*, which accepted all of the 14 tested tryptophan-containing cyclic dipeptides with cyclo-L-Trp-L-Pro (**1a**) as the best substrate. This could indicate the different substrate specificities of BrePT and NotF. BrePT from *A. versicolor* shares a sequence identity of 83 % on the amino acid level with NotF from *Aspergillus* sp. MF297-2 and is of 17 amino acids shorter than NotF. These 17 amino acids were found as three gaps in NotF (Fig. 2). Given the difference of their substrate specificity, it could be speculated that these three gaps would be responsible for the different flexibility of these enzymes towards aromatic substrates.

On the other hand, cyclic dipeptides consisting of two aromatic amino acids were also poor substrates for BrePT (Fig. 4). Cyclo-L-Trp-L-Tyr (**1l**) and cyclo-L-Trp-L-Trp (**1n**) were accepted by BrePT with conversion yields of 13.6 and 12.7 % after incubation with 18 μg of BrePT for 4 h, i.e., a relative activity of 14.8 and 13.9 % of that of cyclo-L-Trp-L-Pro (**1a**), respectively. The catalytic efficiency was calculated for cyclo-L-Trp-L-Tyr (**1l**) at 27 s^{-1} M^{-1}, i.e., only 0.3 % of that of **1a** (Table 3). Unfortunately, the conversion yield of cyclo-L-Trp-L-Pro was not given for NotF in the previous

study (Ding et al. 2010). Given a similar behavior of BrePT and NotF regarding their substrate specificities, it would not be surprising that no product formation was observed for NotF with cyclo-L-Trp-L-Trp (**1n**) and cyclo-L-Trp-L-Tyr (**1l**) as substrates. It would be interesting now to test the acceptance of other substances investigated in this study by NotF, e.g., **1b** or/and **1j**.

From the catalytic efficiencies obtained for the four stereoisomers of cyclo-Trp-Pro (**1a**–**1d**) as well as for those of cyclo-Trp-Ala (**1e**–**1h**), it seems that an acceptance by BrePT is strongly dependent on the configuration of tryptophan. Isomers with L-tryptophanyl moiety were much better substrates for BrePT than those with a D-configuration (Fig. 4). The natural substrate of BrePT is unknown. Base on its high sequence similarity of 83 % on the amino acid level to NotF, the low K_M value and high turnover number with cyclo-L-Trp-L-Pro (**1a**), it can be however speculated that the natural substrate of BrePT should be brevianamide F. As mentioned in the "Introduction," the product of BrePT, i.e., deoxybrevianamide E, is a precursor of brevianamides and notoamides, which were isolated from several strains of *A. versicolor* (Finefield et al. 2011). BrePT is therefore very likely involved in the biosynthesis of these compounds in *A. versicolor* (Finefield et al. 2011; Li et al. 2009).

We demonstrated in this study that BrePT catalyzed the reverse prenyltransfer reaction onto C2 of the indole nucleus of the tryptophan-containing diketopiperazines, at least for the 12 isolated and identified enzyme products (Fig. 5). This feature provides experimental evidence for a possible application of BrePT as a catalyst in the chemoenzymatic synthesis of C2 reversely prenylated cyclic dipeptides.

Acknowledgments This work was financially supported in part by grants from the Deutsche Forschungsgemeinschaft (Li844/1-3 to S.-M. Li) and China Natural Science Foundation (31070067 to X.-Q. Liu). Xia Yu is a recipient of a fellowship from China Scholarship Council.

References

Bivin DB, Kubota S, Pearlstein R, Morales MF (1993) On how a myosin tryptophan may be perturbed. Proc Natl Acad Sci U S A 90:6791–6795

Caballero E, Avendañno C, Menéndez JC (2003) Brief total synthesis of the cell cycle inhibitor tryprostatin B and related preparation of its alanine analogue. J Org Chem 68:6944–6951

Cacciatore I, Cocco A, Costa M, Fontana M, Lucente G, Pecci L, Pinnen F (2005) Biochemical properties of new synthetic carnosine analogues containing the residue of 2,3-diaminopropionic acid: the effect of *N*-acetylation. Amino Acids 28:77–83

Ding Y, Williams RM, Sherman DH (2008) Molecular analysis of a 4-dimethylallyltryptophan synthase from *Malbranchea aurantiaca*. J Biol Chem 283:16068–16076

Ding Y, Wet JR, Cavalcoli J, Li S, Greshock TJ, Miller KA, Finefield JM, Sunderhaus JD, McAfoos TJ, Tsukamoto S, Williams RM, Sherman DH (2010) Genome-based characterization of two prenylation steps in the assembly of the stephacidin and notoamide anticancer agents in a marine-derived *Aspergillus* sp. J Am Chem Soc 132:12733–12740

Finefield JM, Greshock TJ, Sherman DH, Tsukamoto S, Williams RM (2011) Notoamide E: biosynthetic incorporation into notoamides C and D in cultures of *Aspergillus versicolor* NRRL 35600. Tetrahedron Lett 52:1987–1989

Grundmann A, Li S-M (2005) Overproduction, purification and characterization of FtmPT1, a brevianamide F prenyltransferase from *Aspergillus fumigatus*. Microbiology 151:2199–2207

Guo JP, Tan JL, Wang YL, Wu HY, Zhang CP, Niu XM, Pan WZ, Huang XW, Zhang KQ (2011) Isolation of talathermophilins from the thermophilic fungus *Talaromyces thermophilus* YM3-4. J Nat Prod 74:2278–2281

Heide L (2009) Prenyl transfer to aromatic substrates: genetics and enzymology. Curr Opin Chem Biol 13:171–179

Kremer A, Li S-M (2008) Potential of a 7-dimethylallyltryptophan synthase as a tool for production of prenylated indole derivatives. Appl Microbiol Biotechnol 79:951–961

Kremer A, Westrich L, Li S-M (2007) A 7-dimethylallyltryptophan synthase from *Aspergillus fumigatus*: overproduction, purification and biochemical characterization. Microbiology 153:3409–3416

Kuramochi K, Ohnishi K, Fujieda S, Nakajima M, Saitoh Y, Watanabe N, Takeuchi T, Nakazaki A, Sugawara F, Arai T, Kobayashi S (2008) Synthesis and biological activities of neoechinulin A derivatives: new aspects of structure-activity relationships for neoechinulin a. Chem Pharm Bull (Tokyo) 56:1738–1743

Laemmli UK (1970) Cleavage of structural proteins during the assembly of the head of bacteriophage T4. Nature 227:680–685

Li S-M (2009a) Applications of dimethylallyltryptophan synthases and other indole prenyltransferases for structural modification of natural products. Appl Microbiol Biotechnol 84:631–639

Li S-M (2009b) Evolution of aromatic prenyltransferases in the biosynthesis of indole derivatives. Phytochemistry 70:1746–1757

Li S-M (2010) Prenylated indole derivatives from fungi: structure diversity, biological activities, biosynthesis and chemoenzymatic synthesis. Nat Prod Rep 27:57–78

Li G-Y, Yang T, Luo Y-G, Chen X-Z, Fang DM, Zhang G-L (2009) Brevianamide J, a new indole alkaloid dimer from fungus *Aspergillus versicolor*. Org Lett 11:3714–3717

Liang PH (2009) Reaction kinetics, catalytic mechanisms, conformational changes, and inhibitor design for prenyltransferases. Biochemistry 48:6562–6570

Ritchie R, Saxton JE (1981) Studies on indolic mould metabolites. Total synthesis of L-prolyl-2-methyltryptophan anhydride and deoxybrevianamide E. Tetrahedron 37:4295–4303

Sambrook J, Russell DW (2001) Molecular cloning: a laboratory manual. Cold Spring Harbor Laboratory Press, New York

Steffan N, Li S-M (2009) Increasing structure diversity of prenylated diketopiperazine derivatives by using a 4-dimethylallyltryptophan synthase. Arch Microbiol 191:461–466

Steffan N, Unsöld IA, Li S-M (2007) Chemoenzymatic synthesis of prenylated indole derivatives by using a 4-dimethylallyltryptophan synthase from *Aspergillus fumigatus*. Chem Bio Chem 8:1298–1307

Steffan N, Grundmann A, Yin W-B, Kremer A, Li S-M (2009) Indole prenyltransferases from fungi: a new enzyme group with high potential for the production of prenylated indole derivatives. Curr Med Chem 16:218–231

Tudzynski P, Holter K, Correia T, Arntz C, Grammel N, Keller U (1999) Evidence for an ergot alkaloid gene cluster in *Claviceps purpurea*. Mol Gen Genet 261:133–141

Wallwey C, Li S-M (2011) Ergot alkaloids: structure diversity, biosynthetic gene clusters and functional proof of biosynthetic genes. Nat Prod Rep 28:496–510

Williams RM, Stocking EM, Sanz-Cervera JF (2000) Biosynthesis of prenylated alkaloids derived from tryptophan. Topics Curr Chem 209:97–173

Woodside AB, Huang Z, Poulter CD (1988) Triammonium germanyl diphosphate. Org Synth 66:211–215

Yazaki K, Sasaki K, Tsurumaru Y (2009) Prenylation of aromatic compounds, a key diversification of plant secondary metabolites. Phytochemistry 70:1739–1745

Yin W-B, Grundmann A, Cheng J, Li S-M (2009) Acetylaszonalenin biosynthesis in *Neosartorya fischeri*: identification of the biosynthetic gene cluster by genomic mining and functional proof of the genes by biochemical investigation. J Biol Chem 284:100–109

Yin W-B, Yu X, Xie X-L, Li S-M (2010) Preparation of pyrrolo[2,3-b] indoles carrying a ß-configured reverse C3-dimethylallyl moiety by using a recombinant prenyltransferase CdpC3PT. Org Biomol Chem 8:2430–2438

Yu X, Liu Y, Xie X, Zheng X-D, Li S-M (2012) Biochemical characterization of indole prenyltransferases: filling the last gap of prenylation positions by a 5-dimethylallyl tryptophansynthase from *Aspergillus clavatus*. J Biol Chem 287:1371–1380

Zou H-X, Xie X-L, Linne U, Zheng X-D, Li S-M (2010) Simultaneous C7- and N1-prenylation of cyclo-L-Trp-L-Trp catalyzed by a prenyltransferase from *Aspergillus oryzae*. Org Biomol Chem 8:3037–3044

Electronic supplementary material for:

Identification of a brevianamide F reverse prenyltransferase BrePT from *Aspergillus versicolor* with a broad substrate specificity towards tryptophan-containing cyclic dipeptides

Suqin Yin[1,2,3], Xia Yu[2,3], Qing Wang[1,2], Xiao-Qing Liu[1*] and Shu-Ming Li[2*]

[1] College of Life Sciences, Capital Normal University, No.105 Xisanhuan Beilu, Beijing, 100048, China

[2] Philipps-Universität Marburg, Institut für Pharmazeutische Biologie und Biotechnologie, Deutschhausstrasse 17A, D-35037 Marburg, Germany.

[3] These authors contributed equally to this work

* correspondence to: Xiao-Qing Liu (liuxq@mail.cnu.edu.cn) and Shu-Ming Li (shuming.li@Staff.uni-Marburg.de)

Figure S1. ^{1}H-NMR spectrum of **2a** in CD_3OD (500 MHz)

Figure S2. ^{1}H-NMR spectrum of **2b** in CD_3OD (500 MHz)

Figure S3. ^{1}H-NMR spectrum of **2c** in CD_3OD (500 MHz)

Figure S4. ^{1}H-NMR spectrum of **2d** in CD_3OD (400 MHz)

Figure S5. ^{1}H-NMR spectrum of **2e** in CD_3OD (400 MHz)

Figure S6. ^{1}H-NMR spectrum of **2f** in CD_3OD (500 MHz)

Figure S7. ^{1}H-NMR spectrum of **2g** in CD_3OD (400 MHz)

Figure S8. ^{1}H-NMR spectrum of **2h** in CD_3OD (400 MHz)

Figure S9. ^{1}H-NMR spectrum of **2i** in CD_3OD (500 MHz)

Figure S10. ^{1}H-NMR spectrum of **2j** in CD_3OD (500 MHz)

Figure S11. ^{1}H-NMR spectrum of **2k** in DMSO-d_6 (400 MHz) after addition of D_2O

Figure S12. ^{1}H-NMR spectrum of **2l** in DMSO-d_6 (400 MHz) after addition of D_2O

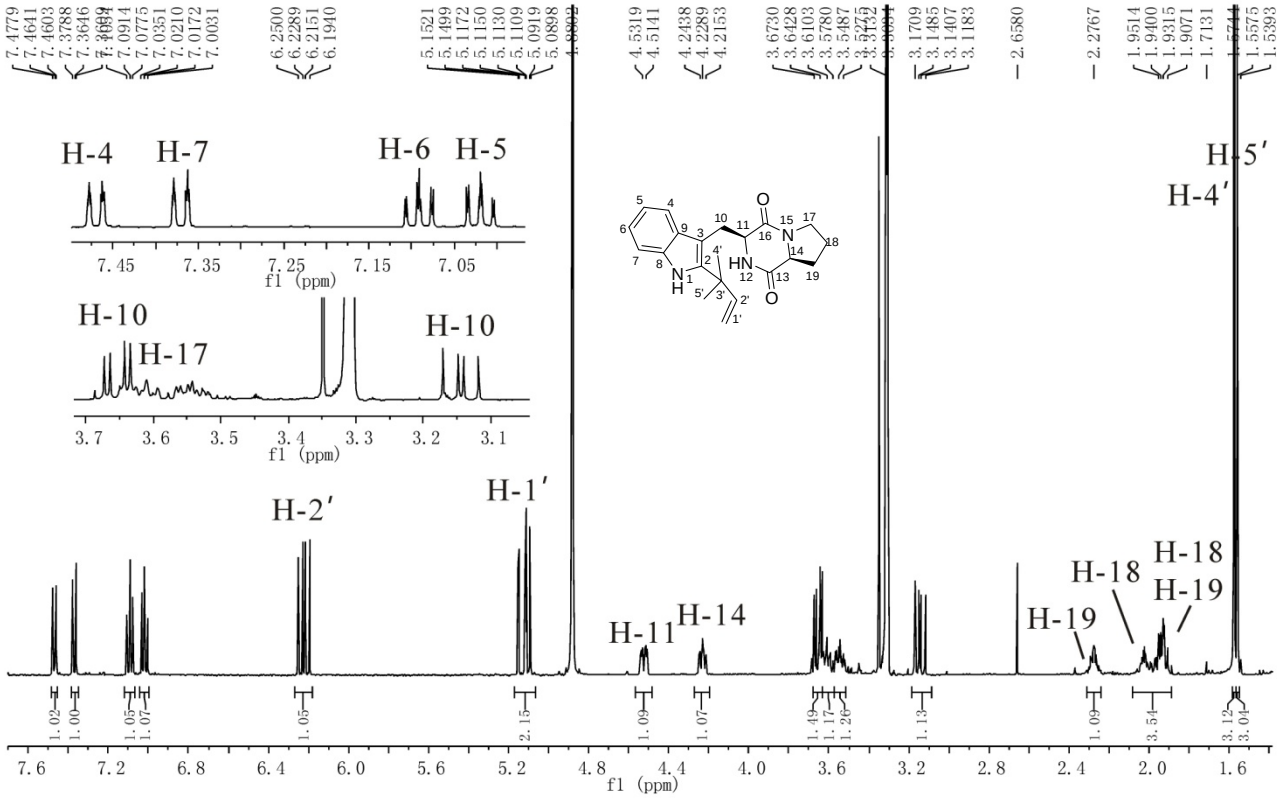

Figure S1. ^{1}H-NMR spectrum of **2a** in CD_3OD (500 MHz)

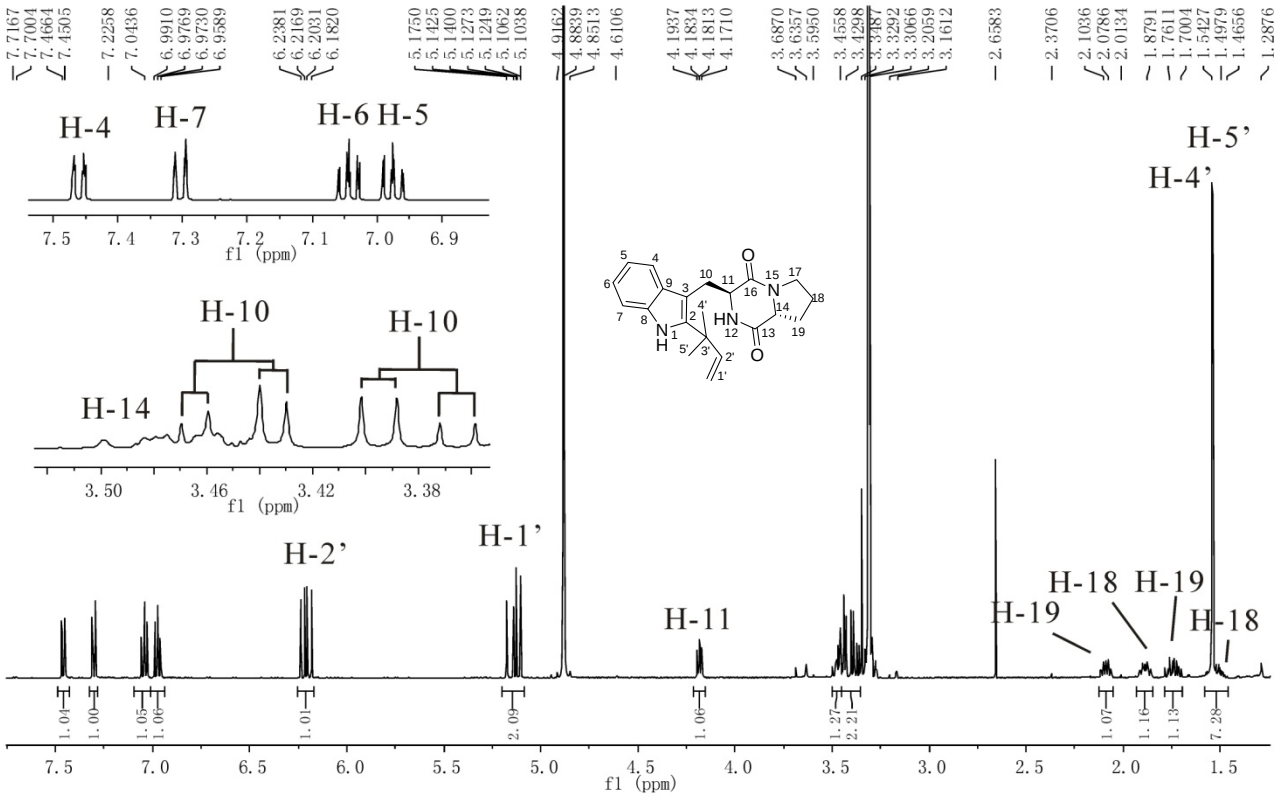

Figure S2. ^{1}H-NMR spectrum of **2b** in CD_3OD (500 MHz)

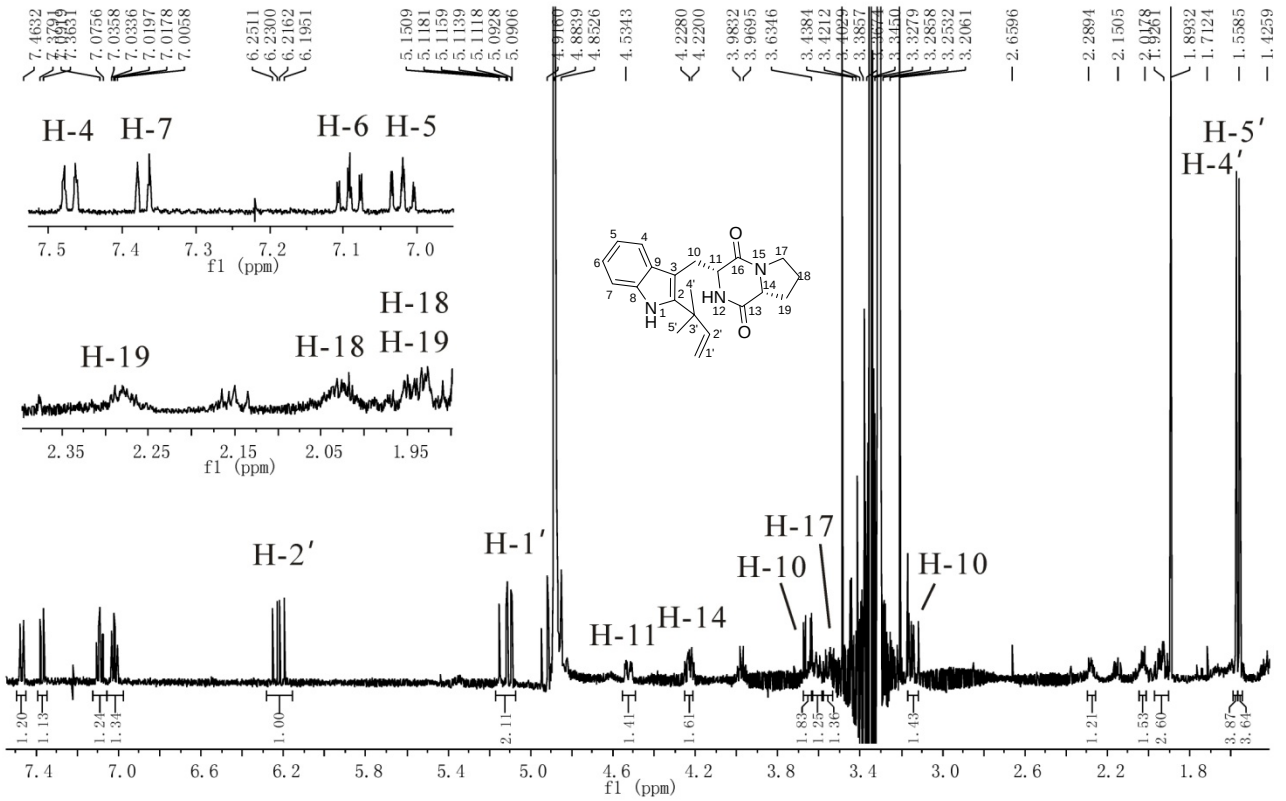

Figure S3. ^{1}H-NMR spectrum of **2c** in CD_3OD (500 MHz)

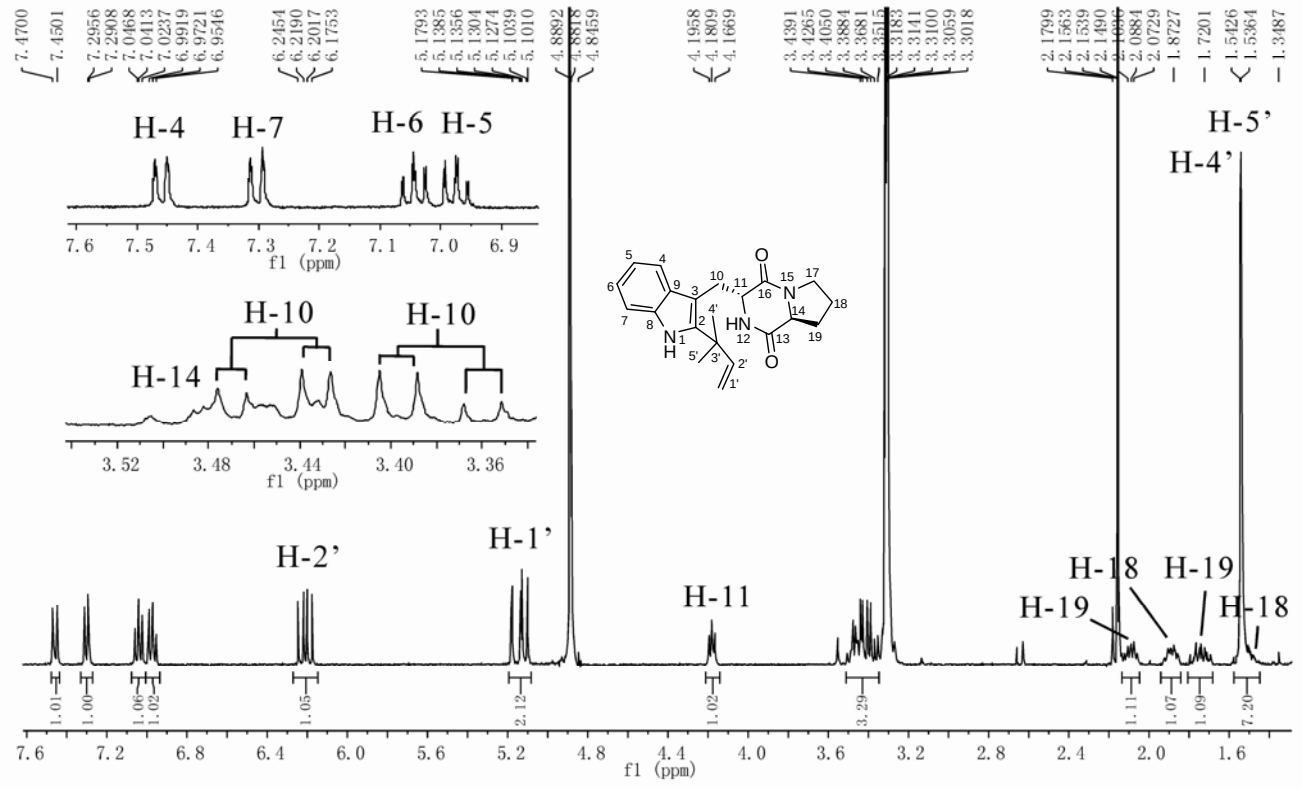

Figure S4. ^{1}H-NMR spectrum of **2d** in CD_3OD (400 MHz)

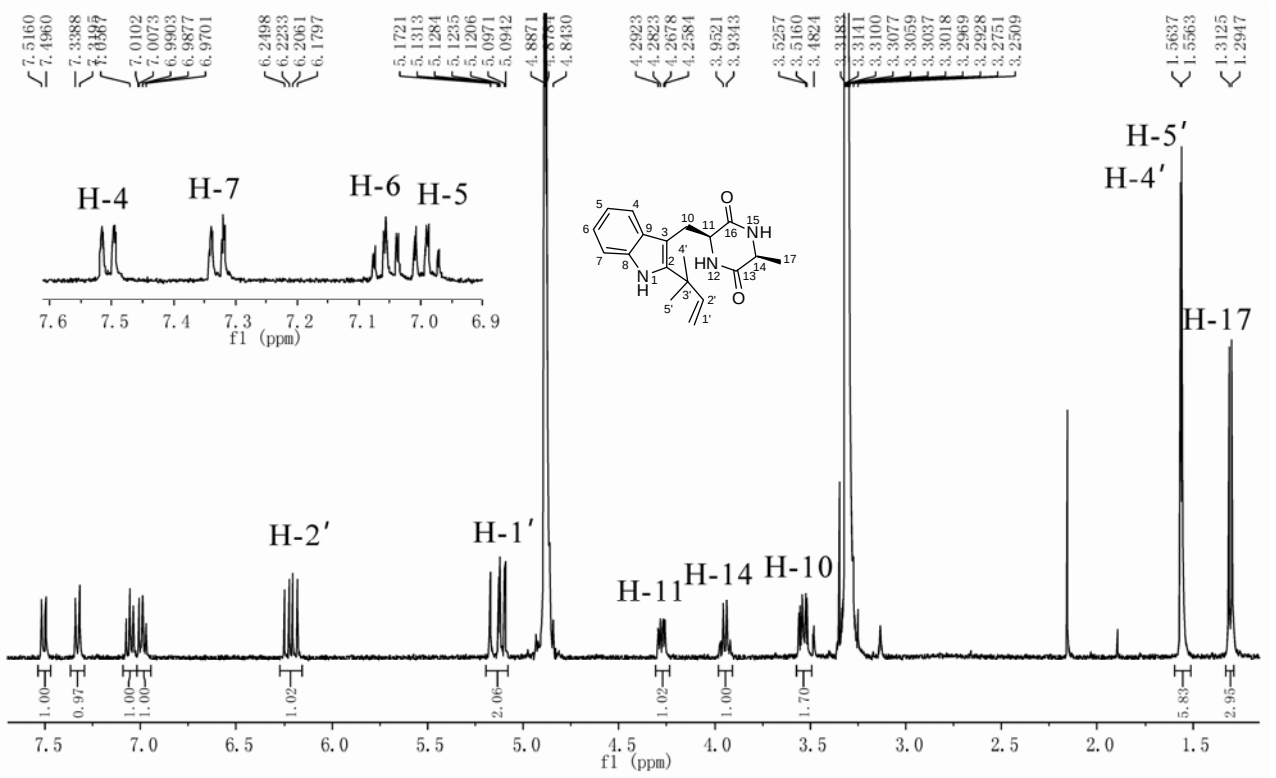

Figure S5. ^{1}H-NMR spectrum of **2e** in CD_3OD (400 MHz)

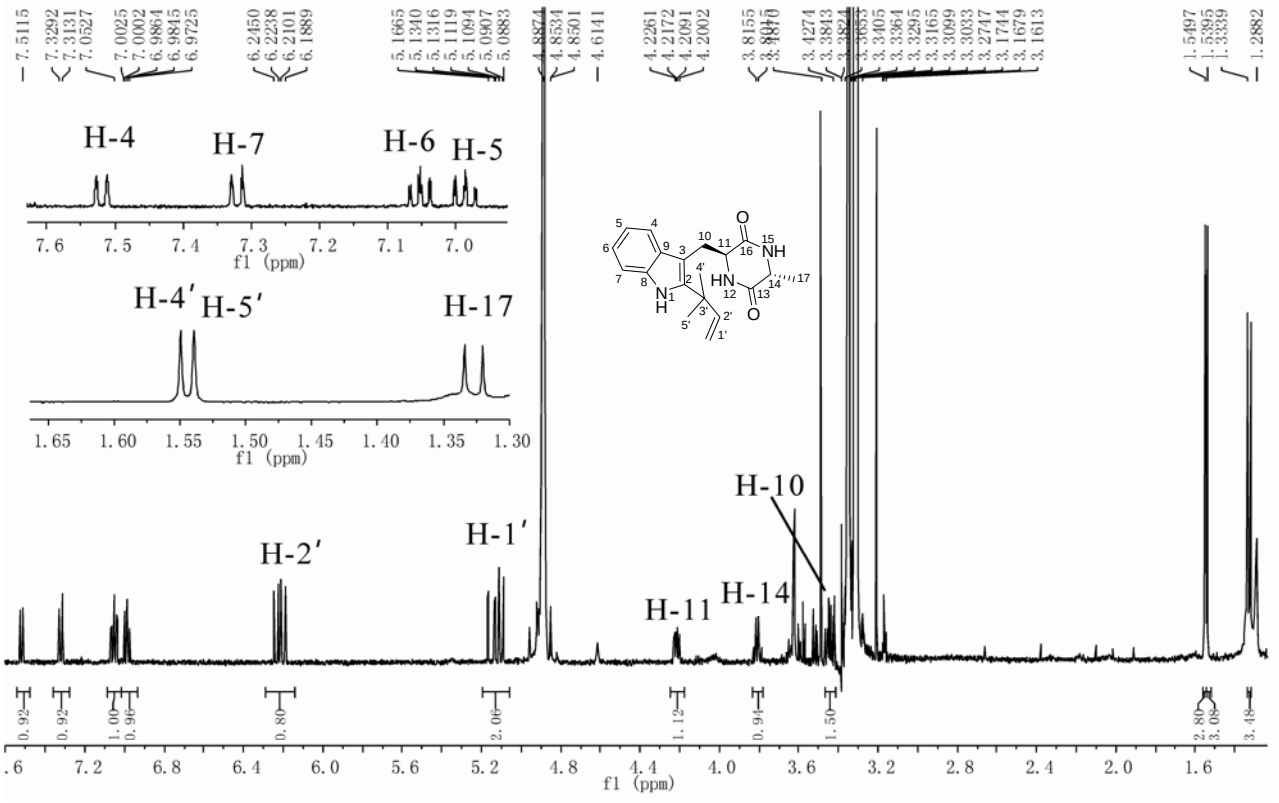

Figure S6. ^{1}H-NMR spectrum of **2f** in CD_3OD (500 MHz)

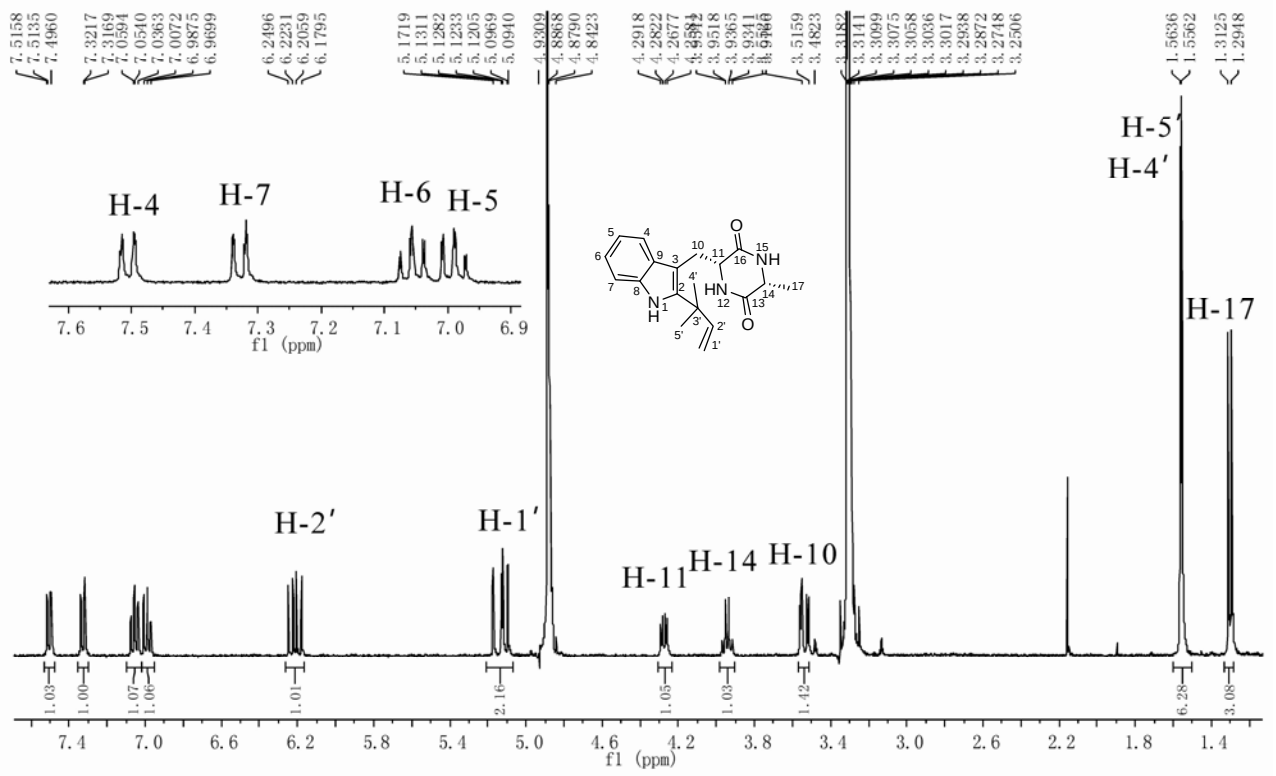

Figure S7. ^{1}H-NMR spectrum of **2g** in CD_3OD (400 MHz)

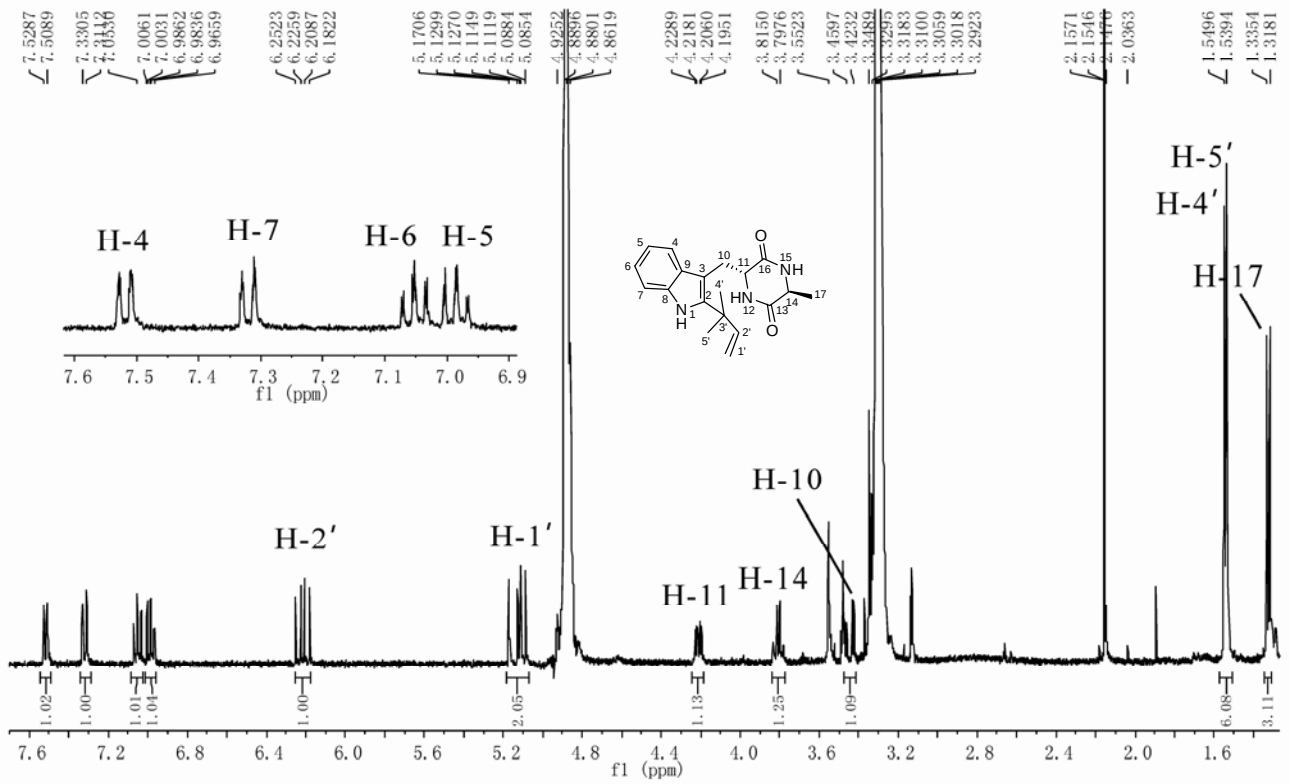

Figure S8. ^{1}H-NMR spectrum of **2h** in CD_3OD (400 MHz)

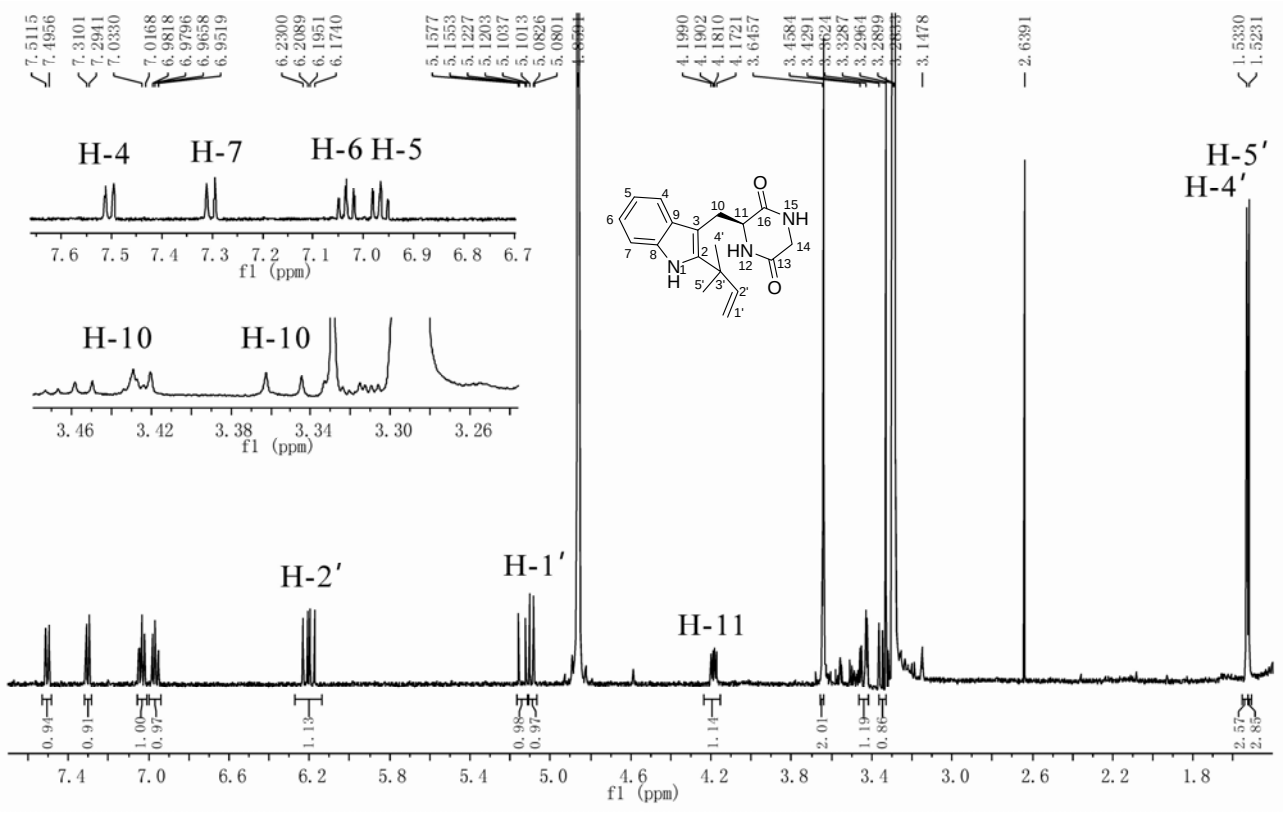

Figure S9. ^{1}H-NMR spectrum of **2i** in CD_3OD (500 MHz)

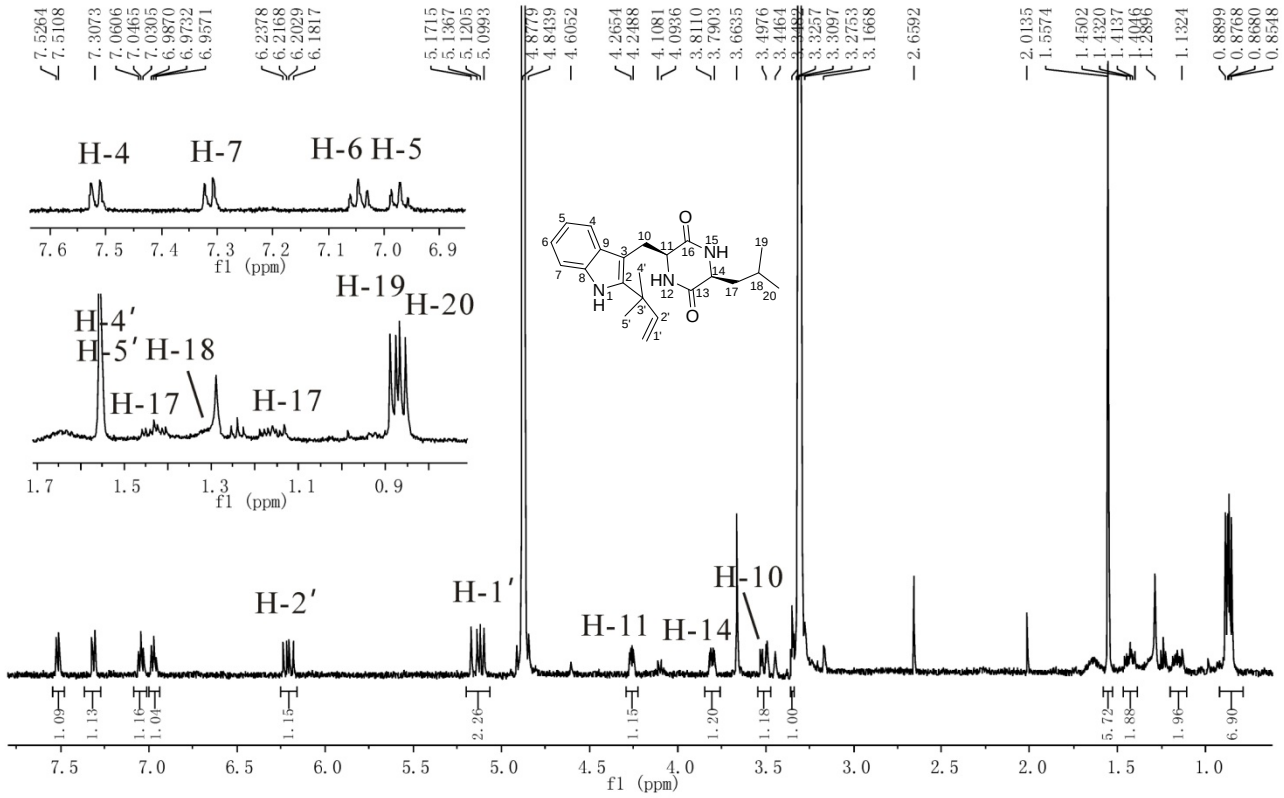

Figure S10. ^{1}H-NMR spectrum of **2j** in CD_3OD (500 MHz)

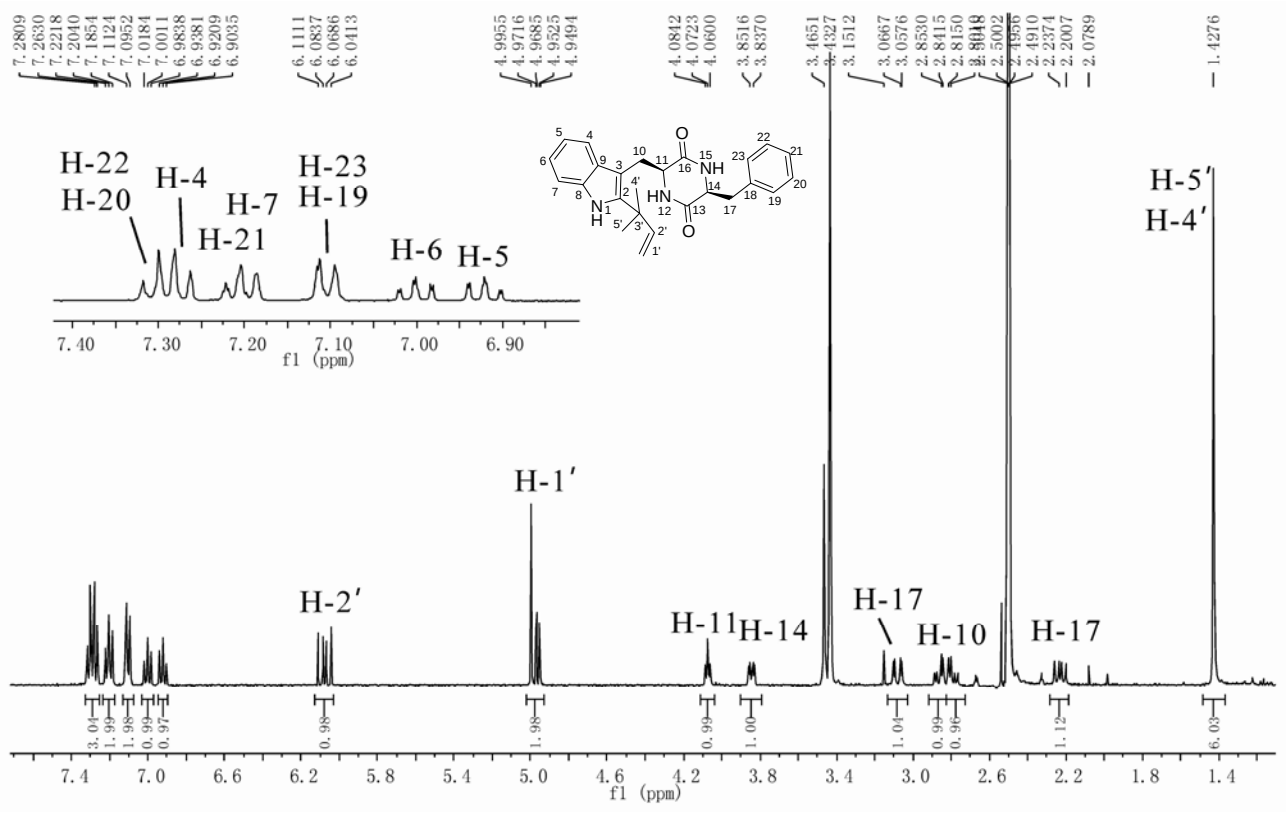

Figure S11. ^{1}H-NMR spectrum of **2k** in DMSO-d_6 (400 MHz) with addition of one drop of D_2O

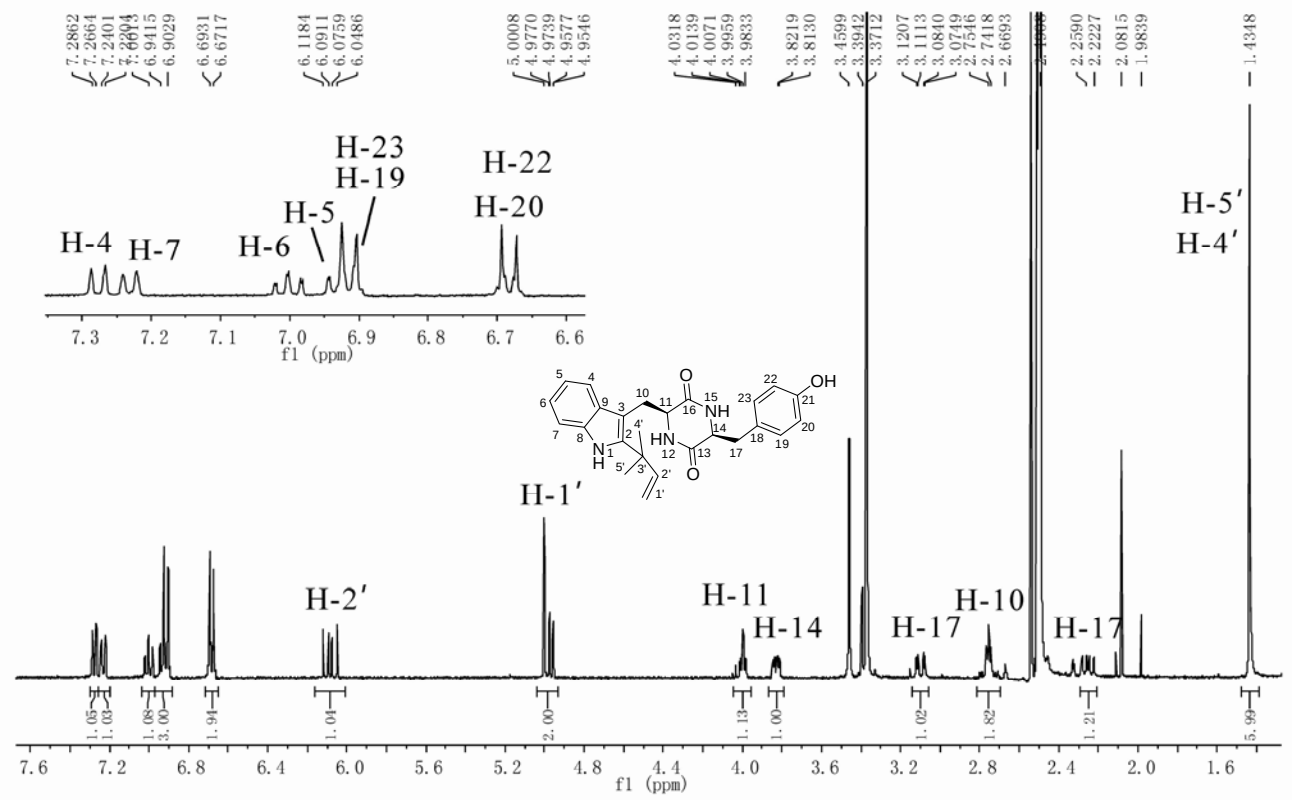

Figure S12. ^{1}H-NMR spectrum of **2l** in DMSO-d_6 (400 MHz) with addition of one drop of D_2O

5.4 Complementary stereospecific synthesis of *cis*-configurated prenylated pyrroloindoline diketopiperazines by indole prenyltransferases of the DMATS superfamily (manuscript)

Organic & Biomolecular Chemistry

Dynamic Article Links ►

131

Cite this: DOI: 10.1039/c0xx00000x

FULL PAPER

www.rsc.org/obc

Complementary stereospecific synthesis of *cis*-configured prenylated pyrroloindoline diketopiperazines by indole prenyltransferases of the DMATS superfamily

Xia Yu,[a] Xiulan Xie,[b] and Shu-Ming Li*[a]

Received (in XXX, XXX) Xth XXXXXXXXX 20XX, ***Accepted Xth XXXXXXXXX 20XX***
DOI: 10.1039/b000000x

Prenylated pyrroloindoline diketopiperazines are a subgroup of prenylated indole alkaloids with a characteristic 6/5/5/6-fused tetracyclic ring system. Three indole prenyltransferases of the dimethylallyltryptophan synthase (DMATS) superfamily, *i.e.*, AnaPT and CdpC3PT from *Neosartorya fischeri* and CdpNPT from *Aspergillus fumigatus*, had been found to catalyze the formation of prenylated pyrroloindoline diketopiperazines from tryptophan-containing cyclic dipeptides in one-step reactions. In this study, we investigated their behavior towards all of the four stereoisomers of cyclo-Trp-Ala and cyclo-Trp-Pro. Our results demonstrated that the enzymes showed different preference for these substrates and different stereospecificity of the product formation. The stereoselectivity of AnaPT and CdpC3PT depends mainly on the configuration of the tryptophanyl moiety in the tested cyclic dipeptides. AnaPT usually catalyze the *anti*-substitution of the prenyl moiety at C-3 to the carbonyl moiety at C-11, while CdpC3PT introduces the prenyl moiety from the opposite side, *i.e. syn*-configuration to the carbonyl moiety at C-11. CdpNPT catalyzes both *syn*- and *anti*-substitution of the prenyl moiety and the structure of the second amino acid moiety of the tested dipeptides is important for the stereospecificity in its enzyme catalysis. These enzymes are therefore efficient tools for enantioselective synthesis of *cis*-configured prenylated pyrroloindoline diketopiperazines. As examples, we prepared in this study eight and six stereoisomers of *cis*-configured prenylated pyrroloindoline diketopiperazines from cyclo-Trp-Ala and cyclo-Trp-Pro isomers, respectively.

Introduction

Prenylated indole alkaloids are mainly found in the family of Clavicipitaceae and Trichocomaceae of Ascomycota, and carry important pharmacological and biological activities.[1-5] Prenylated pyrroloindoline diketopiperazines, a subgroup of these alkaloids, contain a 6/5/5/6-fused tetracyclic core with at least three or four chiral centres (Fig. 1).[6-11] Their structural complexity prohibited a conventional synthesis of these compounds.[12,13] In previous studies, three C3-prenyltransferases belonging to the dimethylallyltryptophan synthase (DMATS) superfamily were identified and characterized biochemically, *i.e.*, AnaPT and CdpC3PT from *Neosartorya fischeri* and CdpNPT from *Aspergillus fumigatus*.[14-16] They introduced a dimethylallyl moiety to position C-3 of a tryptophanyl moiety. In addition, they catalyzed also the formation of a five-membered ring between the original indole and diketopiperazine rings with a *cis*-configuration between H-2 and C3-dimethylallyl moiety, resulting in the formation of prenylated pyrroloindoline diketopiperazines (Fig. 1). Attacking of the dimethylallyl cation by C-3 of the indole ring was proposed to be the first step in the reaction mechanism, resulting in the formation of an intermediate with a positive charge at C-2. This is followed by the formation

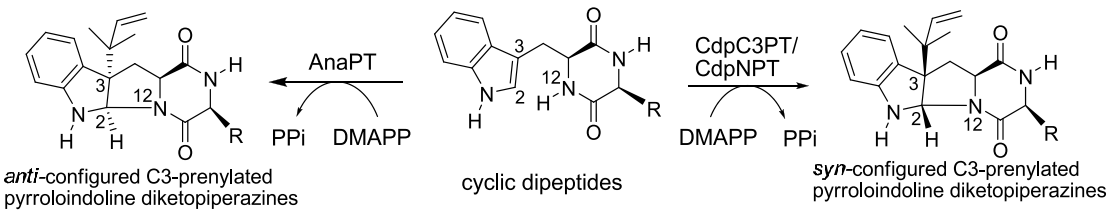

R= H, indole-3-methyl, phenol-4-methyl, phenylmethyl or isobutyl

Fig. 1: Prenyl transfer reactions catalyzed by AnaPT, CdpC3PT and CdpNPT.

Table 1: Conversion of cyclo-Trp-Ala (**1a-4a**) and cyclo-Trp-Pro isomers (**5a-8a**) catalyzed by AnaPT, CdpC3PT and CdpNPT. The assays contained 40 μg of the recombinant enzymes each and were incubated at 37 °C for 3 h.

Subs.	**Conversion (%)**								
	AnaPT			CdpC3PT			CdpNPT		
	S.C.	*Anti-* (**1b-8b**)	*Syn-* (**7c**)	S.C.	*Anti-* (**7b**)	*Syn-* (**1c-8c**)	S.C.	*Anti-* (**1b-5b**, **7b**, **8b**)	*Syn-* (**1c-7c**)
cyclo-L-Trp-L-Ala (**1a**)	39.7	39.7	n.d.	52.4	n.d.	39.5	72.5	38.4	22.0
cyclo-L-Trp-D-Ala (**2a**)	29.1	29.1	n.d.	34.2	n.d.	32.0	86.2	34.3	51.9
cyclo-D-Trp-D-Ala (**3a**)	13.9	10.8	n.d.	15.9	n.d.	11.0	87.0	72.7	2.6 (n.i.)
cyclo-D-Trp-L-Ala (**4a**)	21.7	21.7	n.d.	17.8	n.d.	17.8	62.3	26.1	36.2
cyclo-L-Trp-L-Pro (**5a**)	15.2	15.2	n.d.	88.3	n.d.	58.3	89.6	4.8	75.1
cyclo-L-Trp-D-Pro (**6a**)	30.0	23.9 (n.i.)	n.d.	76.1	n.d.	69.6	68.5	n.d.	62.5
cyclo-D-Trp-D-Pro (**7a**)	7.1	3.2	0.2	26.0	2.7	2.7	98.0	94.1	2.0 (n.i.)
cyclo-D-Trp-L-Pro (**8a**)	8.7	5.6 (n.i.)	n.d.	5.1	n.d.	3.7	86.5	25.6 (n.i.)	n.d.

S.C.: substrate consumption.
Anti-: conversion yields of *anti-cis* configured prenylated pyrroloindoline diketopiperazines.
Syn-: conversion yields of *syn-cis* configured prenylated pyrroloindoline diketopiperazines.
n.d.: not detected.
n.i.: not isolated due to low stability

of a C–N bond between C-2 and N-12 with a positive charge at N-12.[17-19] Release of a proton from N-12 leads to the enzymatic products.[17-19] The substrate promiscuity of AnaPT, CdpC3PT and CdpNPT towards tryptophan-containing cyclic dipeptides provided evidence for their potential application as catalysts for highly regio- and stereoselective conversions.[15-17,19] By using AnaPT and CdpNPT, four aszonalenin stereoisomers were prepared from benzodiazepinedione enantiomers.[20] However, the most of the reported cyclic dipeptides usually contained only L-configured amino acid moieties, and little was known about their behavior on substrates with D-configured amino acid moieties. In order to understand more about the stereospecificity of AnaPT, CdpC3PT and CdpNPT, we carried out enzyme incubation with four cyclo-Trp-Ala isomers (**1a-4a**) and four cyclo-Trp-Pro isomers (**5a-8a**) and analyzed the chemical structures of the enzyme products.

Results and Discussion

The four cyclo-Trp-Ala (**1a-4a**) and cyclo-Trp-Pro isomers (**5a-8a**) (Table 1) were synthesized according to the methods published previously.[21,22] Incubation of these substrates was carried out with 40 μg of AnaPT, CdpC3PT or CdpNPT in the presence of DMAPP for 3 h. Assays with heat-inactivated proteins by boiling for 20 min were used as negative controls. HPLC analysis of the incubation mixtures showed that isomers of cyclo-Trp-Ala (**1a-4a**) were well accepted by all of the three enzymes (Fig. 2). Substrate consumptions were found to be in the range of 13.9-52.4% in the assays with AnaPT and CdpC3PT (Table 1). In comparison to those of 13.9% for cyclo-D-Trp-D-Ala (**3a**) and 21.7% for cyclo-D-Trp-L-Ala (**4a**), AnaPT accepted cyclo-L-Trp-L-Ala (**1a**) and cyclo-L-Trp-D-Ala (**2a**) significantly better (Table 1) with substrate consumption at 39.7% and 29.1%, respectively. These results indicated the preference of AnaPT for L-configured tryptophanyl moiety. CdpC3PT represented a similar behavior as AnaPT. The substrate consumption of cyclo-L-Trp-L-Ala (**1a**) at 52.4% and cyclo-L-Trp-D-Ala (**2a**) at 34.2% were twice or even higher than those for cyclo-D-Trp-D-Ala (**3a**) and cyclo-D-Trp-L-Ala (**4a**). As given in Table 1, CdpNPT showed much higher activity towards four cyclo-Trp-Ala isomers (**1a-4a**) than AnaPT and CdpC3PT. Substrate consumptions in the range of 62.3–87.0% were detected in the enzyme assays with CdpNPT. The comparable activity of CdpNPT towards cyclo-Trp-Ala isomers (**1a-4a**) indicated that CdpNPT exhibited no obvious preference for L- or D-configured cyclic dipeptides.

In the incubation mixtures with the four cyclo-Trp-Pro isomers (**5a-8a**), preference of AnaPT and CdpC3PT towards substrates with L-tryptophanyl moiety was also observed (Fig. 3). By using AnaPT, higher substrate consumption of 15.2% for cyclo-L-Trp-L-Pro (**5a**) and 30.0% for cyclo-L-Trp-D-Pro (**6a**) were detected, in comparison to 7.1% for cyclo-D-Trp-D-Pro (**7a**) and 8.7% for cyclo-D-Trp-L-Pro (**8a**) (Table 1). CdpC3PT represented significant higher activity towards cyclo-L-Trp-L-Pro (**5a**) and cyclo-L-Trp-D-Pro (**6a**) with substrate consumption of 88.3 and 76.1%, respectively, approximately three times or even higher than those for cyclo-D-Trp-D-Pro (**7a**) and cyclo-D-Trp-L-Pro (**8a**). As observed for cyclo-Trp-Ala isomers (**1a-4a**), relative higher activity than those of AnaPT and CdpC3PT was also detected for CdpNPT in the assays with cyclo-Trp-Pro isomers (**5a-8a**). Yields of the product formation were found in the range of 68.5-98.0%.

Detailed inspection of the HPLC chromatograms of the incubation mixtures of **1a-4a** with AnaPT and CdpC3PT (Fig. 2) revealed the formation of one product peak in each assay. The presence of one dominant peak for **3a** or two comparable peaks for **1a**, **2a** and **4a** were observed in the assays of CdpNPT. Incubation of AnaPT with cyclo-L-Trp-L-Pro (**5a**), cyclo-L-Trp-D-Pro (**6a**) and cyclo-D-Trp-L-Pro (**8a**) resulted in the formation of one dominant enzyme product in each assay (Fig. 3). AnaPT catalyzed the conversion of two dominant products from cyclo-D-Trp-D-Pro (**7a**). In cases of the assays with CdpC3PT, one dominant product each was detected for cyclo-L-Trp-D-Pro (**6a**), cyclo-D-Trp-D-Pro (**7a**) and cyclo-D-Trp-L-Pro (**8a**), and three products for cyclo-L-Trp-L-Pro (**5a**). In the incubation mixtures with CdpNPT, one dominant product peak each was observed for cyclo-L-Trp-D-Pro (**6a**) and cyclo-D-Trp-D-Pro (**7a**), while two and three products were for cyclo-L-Trp-L-Pro (**5a**) and cyclo-D-Trp-L-Pro (**8a**), respectively.

UV-detection revealed that **1b-8b** and **1c-8c** were likely prenylated pyrroloindoline diketopiperazines with maximal

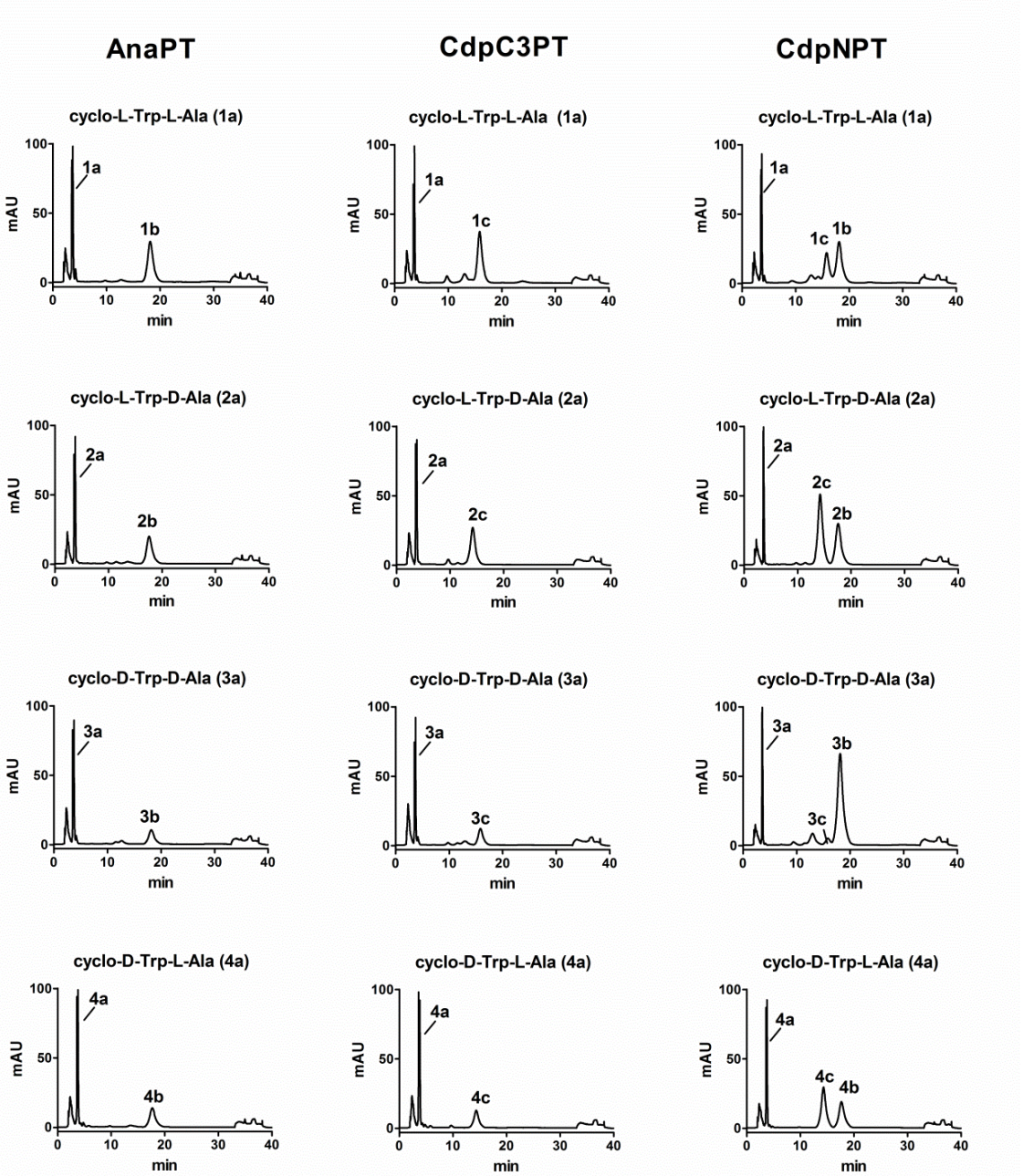

Fig. 2: HPLC chromatograms of incubation mixtures of **1a**-**4a** with AnaPT, CdpC3PT and CdpNPT. The assays contained 40 µg of the recombinant enzymes each and were incubated at 37 °C for 3 h. Detection was carried with a diode array detector and illustrated for absorption at 254 nm.

abosorptions at 205, 240 and 295 nm. The dominant products (**1b**-**4b**, **1c**-**4c**) of the four cyclo-Trp-Ala isomers (**1a**-**4a**) catalyzed by AnaPT and CdpC3PT were isolated on HPLC, respectively, and subjected to ^{1}H-NMR and MS analyses. Products (**1b**-**4b**, **1c**, **2c** and **4c**) were also purified from the incubation mixtures with CdpNPT. ^{1}H-NMR and MS analyses proved that the products from CdpNPT were identical to those from AnaPT and CdpC3PT assays. Similar experiments were also carried out for the four cyclo-Trp-Pro isomers (**5a**-**8a**). Products **5b**-**8b** and **7c** from the reaction mixtures of AnaPT, **5c**-**8c**, **7b**, **5d** and **6d** of CdpC3PT and **5b**, **7b**, **8b**, **5c**-**7c**, **6d** and **8d** of CdpNPT were isolated on HPLC and subjected to MS and NMR analyses.

Positive EI-MS or ESI-MS (see Electronic Supplementary Information, Table S1) confirmed the presence of one dimethylallyl moiety each in **1b**-**5b**, **7b** and **1c**-**8c** by detection of masses, which are 68 daltons larger than those of the respective substrates. In the ^{1}H-NMR spectra of all of the enzyme products (taken in $CDCl_3$), signals at δ_H 5.15-5.07 (d, 2H-1'), 5.94-5.99 (dd, H-2'), 1.11-1.14 (s, 3H-4'), 0.99-1.11 (s, 3H-5') were observed (Tables S2-3 and Figs. S1-S17), proving unequivocally the presence of a reverse dimethylallyl moiety in their structures.[15,19]

Cross peaks in HSQC spectra of **5b**, **5c** and **6c** revealed that the singlets of H-2 (δ_H 5.39-5.71, 1H, s) correlated with C-2 (δ_C 77.2-79.4), proving the disappearance of the double bond between C-2 and C-3 of the original indole ring. Connectivities from H-2 to C-

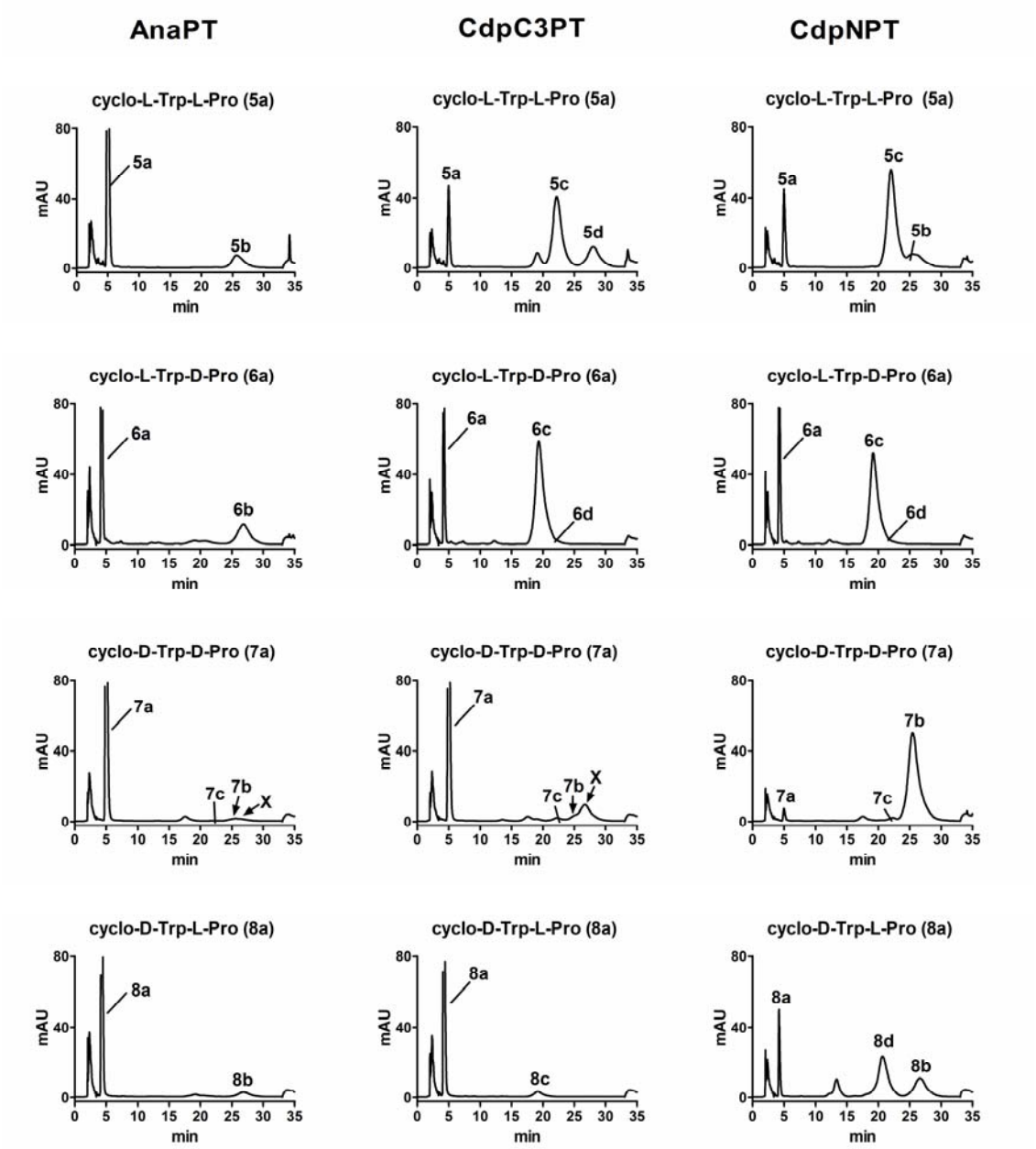

Fig. 3: HPLC chromatograms of incubation mixtures of **5a-8a** with AnaPT, CdpC3PT and CdpNPT. The assays contained 40 µg of the recombinant enzymes each and were incubated at 37 °C for 3 h. Detection was carried with a diode array detector and illustrated for absorption at 254 nm. X: enzyme products with unknown structures.

11 (δ_C 59.1-60.5) in the HMBC spectra of **5b**, **5c** and **6c** showed clearly that a chemical bond between C-2 and N-12 was formed and therefore the three C3-prenylated products contained a fused five-membered ring between the indoline and diketopiperazine ring. In the HMBC spectra of **5b**, **5c** and **6c** (Figs. S9-S11), connectivities from H-2 of the indoline ring to C-3' (δ_C 40.8-41.6) of the prenyl moiety, and from both H-4' (δ_H 1.11-1.14, 3H, s) and H-5' (δ_H 0.99-1.01, 3H, s) of the prenyl moiety to C-3 (δ_C 61.9-62.8) of the indoline ring, proved unequivocally the attachment of the dimethylallyl moiety to C-3 of the indoline ring. NOESY experiments provided unambiguous evidences for a *cis*-configuration between H-2 and C3-prenyl moiety (Figs. S9-S11). For example, strong or medium NOE correlations were observed for H-2 with H-2', H-4' and H-5' of the dimethylallyl moieties. For compound **5b**, strong NOE correlation was observed between H-4' of the prenyl moiety and H-10b, which has the *anti*-configuration to the carbonyl moiety at C-11. NOE correlation was not observed for the protons of the prenyl moiety with H-10a, which has the *syn*-configuration to the carbonyl moiety at C-11. Therefore, H-2 and C3-prenyl moiety must be substituted on the same side to H-10b, consequently the opposite side of the carbonyl moiety at C-11 and proving that **5b** is an *anti-cis* configured prenylated pyrroloindoline diketopiperazine. In contrast to **5b**, weak or none NOE correlations were observed

Table 2: Signals of H-10b and H-11 in the ^{1}H-NMR spectra of *cis*-configured prenylated pyrroloindoline diketopiperazines from the incubation mixtures of C3-prenyltransferases with cyclic dipeptides.

Substrates	Enzymes	Products					
		Configu-rations	H-11, multi.	$J_{H11\text{-}H10a}$ (Hz)	$J_{H11\text{-}H10b}$ (Hz)	H-10b, δ_H, ppm	Ref.
cyclo-L-Trp-L-Pro	AnaPT CdpNPT	*anti-cis*	t	8.9	8.9	2.79	this study
cyclo-D-Trp-D-Pro	AnaPT CdpNPT CdpC3PT	*anti-cis*	t	8.9	8.9	2.79	this study
cyclo-L-Trp-L-Leu	AnaPT	*anti-cis*	t	8.5	8.5	2.81	19
cyclo-L-Trp-L-Trp	AnaPT	*anti-cis*	t	9.2	9.2	2.79	19
cyclo-L-Trp-L-Phe	AnaPT	*anti-cis*	t	9.2	9.2	2.81	19
cyclo-L-Trp-L-Tyr	AnaPT	*anti-cis*	t	8.8	8.8	2.81	19
cyclo-L-Trp-Gly	AnaPT	*anti-cis*	t	9.0	9.0	2.84	19
cyclo-L-Trp-L-Ala	AnaPT CdpNPT	*anti-cis*	t	8.7	8.7	2.81	this study
cyclo-L-Trp-D-Ala	AnaPT CdpNPT	*anti-cis*	t	9.1	9.1	2.87	this study
cyclo-D-Trp-D-Ala	AnaPT CdpNPT	*anti-cis*	t	8.8	8.8	2.81	this study
cyclo-D-Trp-L-Ala	AnaPT CdpNPT	*anti-cis*	t	9.2	9.2	2.87	this study
cyclo-L-Trp-L-Pro	CdpC3PT CdpNPT	*syn-cis*	dd	6.7	10.8	2.54	this study
cyclo-L-Trp-D-Pro	CdpC3PT CdpNPT	*syn-cis*	dd	5.3	12.0	2.51	this study
cyclo-D-Trp-L-Pro	CdpC3PT	*syn-cis*	dd	5.3	12.0	2.51	this study
cyclo-L-Trp-L-Leu	CdpC3PT CdpNPT	*syn-cis*	dd	5.1	10.5	2.55	15
cyclo-L-Trp-L-Trp	CdpC3PT CdpNPT	*syn-cis*	dd	6.2	11.1	2.52	15
cyclo-L-Trp-L-Phe	CdpC3PT CdpNPT	*syn-cis*	dd	6.2	11.2	2.52	15
cyclo-L-Trp-L-Tyr	CdpC3PT CdpNPT	*syn-cis*	dd	6.1	10.7	2.52	15
cyclo-L-Trp-Gly	CdpC3PT CdpNPT	*syn-cis*	dd	5.9	11.0	2.56	15
cyclo-L-Trp-L-Ala	CdpC3PT CdpNPT	*syn-cis*	dd	6.2	11.1	2.55	this study
cyclo-L-Trp-D-Ala	CdpC3PT CdpNPT	*syn-cis*	dd	6.2	11.2	2.57	this study
cyclo-D-Trp-D-Ala	CdpC3PT CdpNPT	*syn-cis*	dd	6.5	10.9	2.55	this study
cyclo-D-Trp-L-Ala	CdpC3PT CdpNPT	*syn-cis*	dd	6.2	11.3	2.57	this study

H-10a and H-10b has the *syn*- and *anti*-configuration to to the carbonyl moiety at C-11, respectively.

for protons of the prenyl moiety with H-10b and H-11 in the spectra of compounds **5c** and **6c**. Moreover, H-4' of the dimethylallyl moieties showed strong or medium NOE correlation with H-10a. Therefore, H-2 and C3-prenyl moiety of **5c** and **6c** must be situated on the opposite side to H-10b, consequently the same side of the carbonyl moiety at C-11. Products **5c** and **6c** were therefore assigned to be *syn-cis* configured prenylated pyrroloindoline diketopiperazines. Compound **5c** was also reported as enzyme product of the G115T mutant of FtmPT1.[18] The NMR data of **5c** corresponded well to those published previously.[18]

The ^{1}H-NMR spectrum of the enzyme product **7b** obtained from substrate **7a** was identical to that of **5b** obtained from **5a** (Figs. S9 and S12). Considering that **7a** is the enantiomer of **5a**, **7b** and **5b** should also be enantiomers. The structure of **7b** was therefore assigned to be an *anti-cis* configured prenylated pyrroloindoline diketopiperazine. Similar phenomena were also observed for enzyme product **7c** and **5c** as well as **8c** and **6c**. It can be therefore concluded that the prenyl moiety has a *syn*-configuration to the carbonyl moiety at C-11 in **7c** and **8c**.

Detailed inspection of the ^{1}H-NMR spectra revealed significant difference between *anti*-configured (**5b** and **7b**) and *syn*-configured derivatives (**5c**, **6c** and **8c**) for the coupling patterns of H-11 and chemical shift of H-10b. A triplet was detected for H-11 in **5b** and **7b**, while a double doublet was observed for H-11 in **5c**, **6c**, and **8c**. Concerning the chemical shifts for H-10b, it seems that H-10b in products with an *anti*-configured prenyl moiety was low-field shifted approximate 0.25 ppm in comparison to H-10b in those with a *syn*-configured prenyl moiety (Table 2). To understand the observed difference for H-11 and H-10b, ^{1}H-NMR data of known *anti-cis* and *syn-cis* configured prenylated pyrroloindoline diketopiperazines from literature and from this study are summarized in Table 2.[15,19] The observed difference for H-11 and H-10b in this study can be indeed also found for other product pairs of known compounds. In addition, similar coupling constants were observed for H-11 in products bearing a prenyl moiety in the same orientation. The coupling constants of H-11 were approximately 9 Hz for the triplets in *anti-cis* configured prenylated pyrroloindoline diketopiperazines and about 11 Hz and 6 Hz for the double doublets in *syn-cis* configured prenylated pyrroloindoline diketopiperazines. Therefore, the ^{1}H-^{1}H vicinal coupling patterns of H-11 and chemical shifts for H-10b in ^{1}H-NMR spectra could be used for prediction of the stereochemistry of *cis*-configured prenylated pyrroloindoline diketopiperazines.

In the ^{1}H-NMR spectra of the product pairs obtained from cyclo-Trp-Ala isomers, triplets with coupling constants of 8.7-9.1 Hz were observed for H-11 in products **1b**-**4b**, while double doublets with coupling constants of 11.1-11.2 Hz and 6.2 Hz were detected for H-11 in **1c**-**4c**. Furthermore, comparison of the signals in the ^{1}H-NMR spectra of **1b** to **1c**, **2b** to **2c**, **3b** to **3c** and **4b** to **4c** revealed that H-10b of the former was low-field shifted 0.26-0.30 ppm to the latter in respective product pairs. Thus, **1b**-**4b** and **1c**-**4c** were assigned to be *anti*- and *syn-cis* configured prenylated pyrroloindoline diketopiperazines, respectively. A literature search revealed that the ^{1}H-NMR data of **2c** corresponded well to those published previously.[23] Unfortunately, **6b** and **8b** were very unstable and their structures cannot be elucidated in this study. In addition to *cis*-configured prenylated pyrroloindoline diketopiperazines, N-regularly prenylated derivatives of cylco-Trp-Pro (**5d**, **6d** and **8d**) were also detected in the enzyme assays of CdpNPT and CdpC3PT, and their structures were confirmed by ^{1}H-NMR and MS analyses (Figs. S15-S17).

From the obtained data, it is obvious that the configuration of tryptophanyl moiety in the tested cyclic dipeptides has a significant influence on the attack direction of the indole ring to the dimethylllalyl cation. AnaPT converted all cyclo-Trp-Ala stereoisomers (**1a**-**4a**) to *anti-cis* configured prenylated pyrroloindoline diketopiperazines (**1b**-**4b**). This means that the

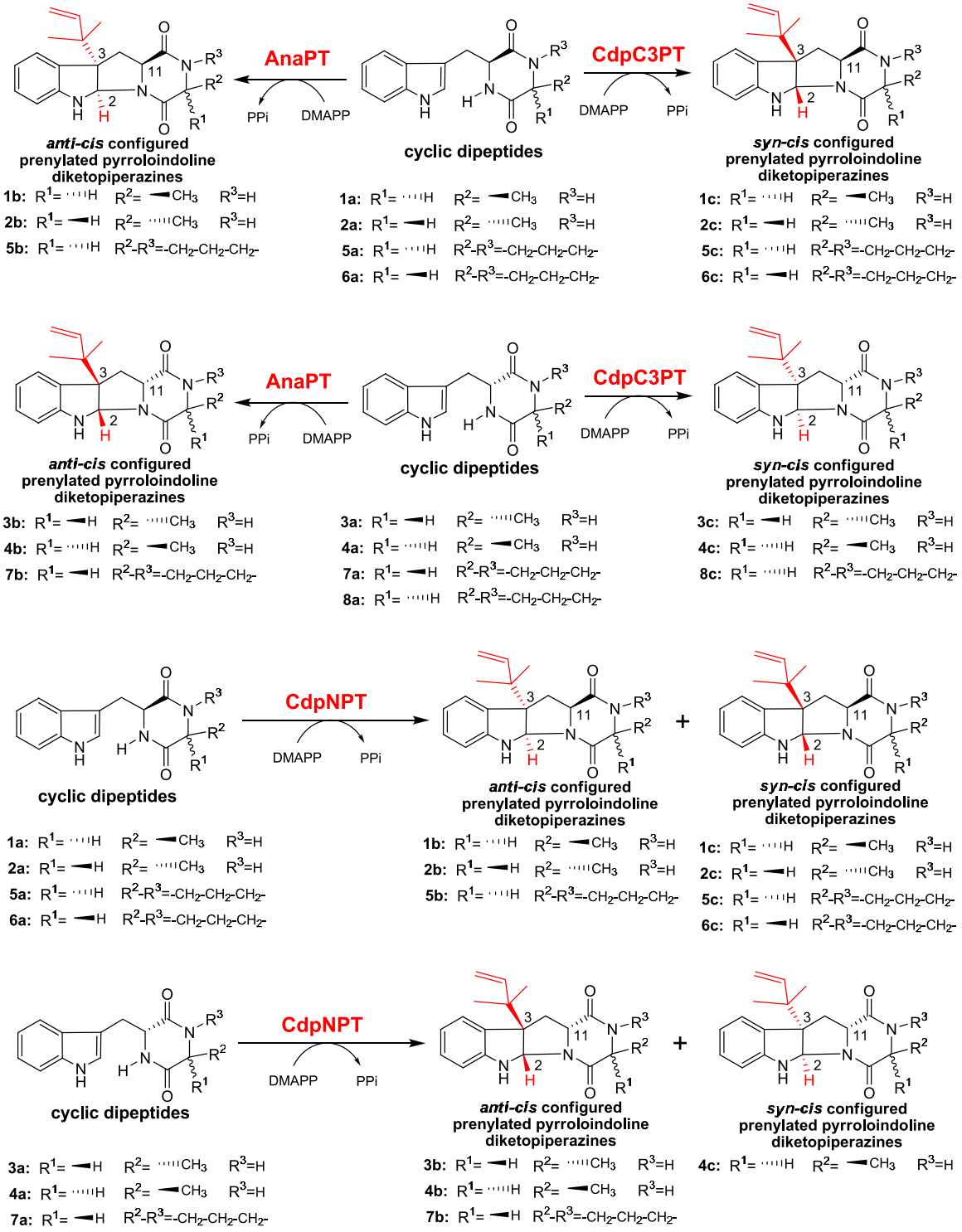

Fig. 4: Prenyl transfer reactions catalyzed by AnaPT, CdpC3PT and CdpNPT towards **1a**-**4a** and **5a**-**8a**. Only C3-prenylated products with yields more than 3% are illustrated.

prenyl moiety was always attached at the opposite side of the carbonyl moiety at C-11. Similar phenomena were also observed for assays of AnaPT with cyclo-L-Trp-L-Pro (**5a**) and cyclo-D-Trp-D-Pro (**7a**). In the incubation mixture with cyclo-L-Trp-L-Pro (**5a**), only the product with *anti*-configured prenylation was detected. Although both *anti*- and *syn-cis* configured prenylated pyrroloindoline diketopiperazines were isolated from assays of AnaPT with cyclo-D-Trp-D-Pro (**7a**), the *anti-cis* configured product with 94% of the C3-prenylated deivatives (Table 1) was the clearly dominant product.

^{1}H-NMR spectra confirmed the formation of *syn-cis* configured prenylated pyrroloindoline diketopiperazines (**1c**-**8c**) from all substrates with CdpC3PT. In the incubation mixture of cyclo-D-Trp-D-Pro (**7a**) with CdpC3PT, conversion yield of C3-

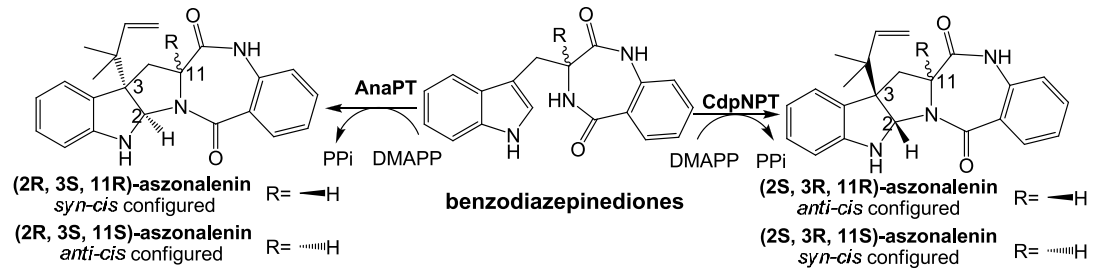

Fig. 5. Prenylations of (R)- and (S)-benzodiazepinedione catalyzed by AnaPT and CdpNPT.

prenylated products was very low. In this case, one additional *anti-cis* configured prenylated pyrroloindoline diketopiperazine **7b** was also isolated. These data confirmed that the stereospecificity of CdpC3PT was also mainly influenced by the configuration of tryptophanyl moiety other than alaninyl or prolinyl moiety in the tested cyclic dipeptides. The prenylation almost took place at the same side of the carbonyl moiety at C-11.

It was reported in a previous study that CdpNPT catalyzed only *syn*-prenylation of cyclo-L-Trp-L-Pro (**5a**).[17] Detailed inspection of the HPLC chromatogram of incubation mixture of CdpNPT with **5a** revealed that one minor peak with a ratio of 6 : 94 to the *syn-cis* configured prenylated pyrroloindoline diketopiperazine **5c** with the characteristic UV absorption of prenylated pyrroloindoline diketopiperazines was also detected. The minor peak had the same retention time with the *anti-cis* configured prenylated pyrroloindoline diketopiperazine (**5b**) produced by AnaPT and was subsequently confirmed to be an identical structure by the ^{1}H-NMR analysis. Similar to **5a**, one minor peak each (**3c** and **7c**) with a characteristic UV absorption of prenylated pyrroloindoline diketopiperazines, in addition to the *anti-cis* configured prenylated pyrroloindoline diketopiperazines (**3b** and **7b**), were also detected in the assays of CdpNPT with cyclo-D-Trp-D-Ala (**3a**) and cyclo-D-Trp-D-Pro (**7a**). The ratio of the products was found to be about 3 : 97 for **3c** and **3b** and 2 : 98 for **7c** and **7b** in these assays. Products **3c** and **7c** formed by CdpNPT had the same retention time with *syn-cis* configured prenylated pyrroloindoline diketopiperazines **3c** and **7c** formed by CdpC3PT, and thereby could be assigned to *syn-cis* configured prenylated pyrroloindoline diketopiperazines. It seems that CdpNPT showed different stereospecificity towards the four isomers of cyclo-Trp-Ala isomers (**1a-4a**) and cyclo-Trp-Pro isomers (**5a-7a**). CdpNPT preferred to catalyze the formation of *syn-cis* configured prenylated pyrroloindoline diketopiperazines (**5c** and **6c**) from cyclo-L-Trp-L-Pro (**5a**) and cyclo-L-Trp-D-Pro (**6a**), and an *anti-cis* configured prenylated pyrroloindoline diketopiperazine (**7c**) from cyclo-D-Trp-D-Pro (**7a**). These products were found as major products in the enzyme assays with **5a-7a**. Although a main product (**3b**) with *anti*-configured prenyl moiety was observed in the assay with cyclo-D-Trp-D-Ala (**3a**), product yields of derivatives with *syn*- and *anti*-configured prenyl moiety were comparable in the assays with cyclo-L-Trp-L-Ala (**1a**), cyclo-L-Trp-D-Ala (**2a**) and cyclo-D-Trp-L-Ala (**4a**). In contrast to AnaPT and CdpC3PT, it is likely that not the configuration of amino acids moiety in the tested cyclic dipeptides, but the size of the second amino acid moiety plays an important role for the stereospecificity of CdpNPT. The size reduction from cyclo-Trp-Pro (**5a-8a**) to cyclo-Trp-Ala (**1a-4a**) leaded to lower stereoselectivity of CdpNPT.

Furthermore, free rotation of the residue at C-14 of the diketopiperazine ring plays also an important role for the stereoselectivity observed in this study. In a previous study,[20] we have observed that the stereoselectivity of a given enzyme for benzodiazepinedinones differed clearly from that of tested diketopiperazines. AnaPT introduced in that case a prenyl moiety from different sides of (R)- and (S)-benzodiazepinedinone, so that an α-prenylation took place in both cases, resulting in the formation of *anti-cis* and *syn-cis* configured aszonalenin, respectively (Fig. 5). In contrast, CdpNPT catalyzed a ß-prenylation of both substrates, *i.e.* introduced the prenyl moiety from the opposite side of the AnaPT reactions, resulting in the formation of other two *anti-cis* and *syn-cis* configured isomers (Fig. 5). In all of the four reactions, only one of the four stereoisomers was detected as enzyme product.

Conclusions

In this study, we presented the substrate promiscuity of AnaPT, CdpC3PT and CdpNPT towards all of the four stereoisomers of cyclo-Trp-Ala and cyclo-Trp-Pro, and demonstrated clearly the distinct stereospecific preference of the three C3-prenyltransferases. The configuration of tryptophanyl moiety in the tested cyclic dipeptides strongly influences the prenylation orientation of the AnaPT and CdpC3PT reactions, but not that of CdpNPT. The stereoselectivity of the AnaPT and CdpC3PT reactions were approximately 100% in incubation mixtures with different stereoisomers and complemented to each other. In comparison to AnaPT and CdpC3PT, CdpNPT showed lower stereospecificity, but higher conversion yields towards most of the tested substrates. Therefore, CdpNPT could be useful for prenylation of poor substrates of AnaPT and CdpC3PT.

Experimental Section

Chemicals

Dimethylallyl diphosphate (DMAPP) was prepared according to the methods described for GPP.[24] Synthesis of the four cyclo-Trp-Ala (**1a-4a**) isomers and cyclo-Trp-Pro isomers (**5a-8a**) was according to the method published previously.[21,22]

Overproduction and purification of the recombinant proteins as well as enzyme assays with recombinant purified protein

AnaPT, CdpNPT and CdpC3PT were overproduced in *E. coli* and purified as described.[14-16] The enzymatic reaction mixtures (100

µl) for determination of the relative activities with different tryptophan-containing cyclic dipeptides contained 50 mM Tris-HCl (pH 7.5), 10 mM $CaCl_2$, 1 mM substrate, 2 mM DMAPP, 0.15-2% (v/v) glycerol, 5% (v/v) DMSO and 40 µg of purified recombinant protein. The reaction mixtures were incubated at 37 °C for 3 h. The enzyme reactions were terminated by addition of 100 µl methanol per 100 µl reaction mixtures. Enzymatic assays for isolation of the enzyme products contained 2 mM DMAPP, 1 mM cyclic dipeptide, 10 mM $CaCl_2$, 50 mM Tris-HCl (pH 7.5), and 2 mg of purified recombinant protein per 10 ml assay. The reaction mixtures were incubated at 37 °C for 16 h and extracted subsequently with ethyl acetate. After evaporation of the solvent, the residues were dissolved in methanol and purified on HPLC.

HPLC conditions for analysis and isolation of synthetic products

The enzyme products of the incubation mixtures were analyzed on HPLC with an Agilent series 1200 by using a Multospher 120 RP-18 column (250 x 4 mm, 5 µm, C+S Chromatographie Service, Langerwehe, Germany) at a flow rate of 1 ml•min^{-1}. Water (solvent A) and acetonitrile (solvent B) each with 0.5% (v/v) trifluoroacetic acid were used as solvents. For analysis of enzyme products, 37% (v/v) solvent B in 30 min was used. The column was then washed with 85% solvent B for 5 min and equilibrated with 37% (v/v) solvent B for 5 min. Detection was carried out by a photodiode array detector at 254 nm.

For isolation, the same HPLC equipment with a Multospher 120 RP-18 column (250 x 10 mm, 5 um, C＋S Chromatographie) at a flow rate of 2.5 ml•min^{-1} was used. Water (solvent C) and acetonitrile (solvent D) without acid were used as solvents. Repeated chromatography was carried out with different gradients for isolation.

NMR spectroscopic analysis and high resolution mass spectra

NMR spectra were recorded on a JEOL ECX-400, Bruker Avance 500 MHz or Bruker Avance 600 MHz spectrometer. Chemical shifts were referenced to the signal of $CDCl_3$ at 7.26 ppm. All spectra were processed with MestReNova 5.2.2. The isolated products were also analyzed by mass spectroscopy on a Q-Trap Quantum (Applied Biosystems) using an electron spray ionization (ESI) or on an Auto SPEC with an electron impact (HR-EI) mode.. Positive MS data are given in Table S1 in Electronic Supplementary Information.

Acknowledgements

This work was financially supported in part by a grant from the Deutsche Forschungsgemeinschaft (Li844/4-1 to S.-M. Li). Xia Yu is a recipient of a fellowship from China Scholarship Council.

Notes and references

[a] *Philipps-Universität Marburg, Institut für Pharmazeutische Biologie und Biotechnologie, Deutschhausstrasse 17A, D-35037 Marburg, Germany. Fax: 0049-6421-2825365; Tel: 0049-6421-2822461; Email: shuming.li@staff.uni-marburg.de*

[b] *Philipps-Universität Marburg, Fachbereich Chemie, Hans-Meerwein-Strasse, 35032 Marburg, Germany.*

† Electronic Supplementary Information (ESI) available: [details of any supplementary information available should be included here]. See DOI: 10.1039/b000000x/

1 R. M. Williams, E. M. Stocking, and J. F. Sanz-Cervera, *Topics Curr. Chem.*, 2000, **209**, 97-173.
2 S.-M. Li, *Nat. Prod. Rep.*, 2010, **27**, 57-78.
3 C. Wallwey and S.-M. Li, *Nat. Prod. Rep.*, 2011, **28**, 496-510.
4 C. L. Schardl, D. G. Panaccione, and P. Tudzynski, *The Alkaloids, Chem. Biol.*, 2006, **63**, 45-86.
5 S. Uhlig, C. J. Botha, T. Vralstad, E. Rolen, and C. O. Miles, *J. Agric. Food Chem.*, 2009, **57**, 11112-11119.
6 L. Du, X. Yang, T. Zhu, F. Wang, X. Xiao, H. Park, and Q. Gu, *Chem. Pharm. Bull.*, 2009, **57**, 873-876.
7 S. Takase, Y. Kawai, I. Uchida, H. Tanaka, and H. Aoki, *Tetrahedron*, 1985, **41**, 3037-3048.
8 D. Wakana, T. Hosoe, T. Itabashi, K. Nozawa, K. Okada, G. M. d. C. Takaki, T. Yaguchi, K. Fukushima, and K. I. Kawai, *Mycotoxins*, 2006, **56**, 3-6.
9 P. M. Scott and B. P. C. Kennedy, *J. Agric. Food Chem.*, 1976, **24**, 865-868.
10 T. A. Reshetilova, N. G. Vinokurova, V. N. Khmelenina, and A. G. Kozlovskii, *Mikrobiology (Moscow)*, 1995, **64**, 27-29.
11 M. O'Brien, K. F. Nielsen, P. O'Kiely, P. D. Forristal, H. T. Fuller, and J. C. Frisvad, *J. Agric. Food Chem.*, 2006, **54**, 9268-9276.
12 P. Ruiz-Sanchis, S. A. Savina, F. Albericio, and M. Alvarez, *Chemistry.*, 2011, **17**, 1388-1408.
13 T. Lindel, N. Marsch, and S. K. Adla, *Top. Curr. Chem.*, 2012, **309**, 67-129.
14 W.-B. Yin, A. Grundmann, J. Cheng, and S.-M. Li, *J. Biol. Chem.*, 2009, **284**, 100-109.
15 W.-B. Yin, X. Yu, X.-L. Xie, and S.-M. Li, *Org. Biomol. Chem.*, 2010, **8**, 2430-2438.
16 W.-B. Yin, H.-L. Ruan, L. Westrich, A. Grundmann, and S.-M. Li, *Chembiochem*, 2007, **8**, 1154-1161.
17 J. M. Schuller, G. Zocher, M. Liebhold, X. Xie, M. Stahl, S.-M. Li, and T. Stehle, *J. Mol. Biol.*, 2012, **422**, 87-99.
18 M. Jost, G. Zocher, S. Tarcz, M. Matuschek, X. Xie, S.-M. Li, and T. Stehle, *J. Am. Chem. Soc.*, 2010, **132**, 17849-17858.
19 W.-B. Yin, X.-L. Xie, M. Matuschek, and S.-M. Li, *Org. Biomol. Chem.*, 2010, **8**, 1133-1141.
20 W.-B. Yin, J. Cheng, and S.-M. Li, *Org. Biomol. Chem.*, 2009, **7**, 2202-2207.
21 B. Wollinsky, L. Ludwig, A. Hamacher, X. Yu, M. U. Kassack, and S.-M. Li, *Bioorg. Med. Chem. Lett.*, 2012, **22**, 3866-3869.
22 S. Yin, X. Yu, Q. Wang, X. Q. Liu, and S.-M. Li, *Appl. Microbiol. Biotechnol.*, 2012, DOI: 10.1007/s00253-012-4130-0.
23 K. M. Depew, S. P. Marsden, D. Zatorska, A. Zatorski, W. G. Bornmann, and S. J. Danishefsky, *J . Am. Chem. Soc.*, 1999, **121**, 11953-11963.
24 A. B. Woodside, Z. Huang, and C. D. Poulter, *Org. Synth.*, 1988, **66**, 211-215.

Supplementary information for:

Complementary stereospecific synthesis of *cis*-configurated prenylated pyrroloindoline diketopiperazines by indole prenyltransferases of the DMATS superfamily

Xia Yu,[a] Xiulan Xie,[b] and Shu-Ming Li*[a]

[a] Philipps-Universität Marburg, Institut für Pharmazeutische Biologie und Biotechnologie, Deutschhausstrasse 17A, D-35037 Marburg, Germany. Email: shuming.li@staff.uni-marburg.de, Tel: 0049-6421-2822461, Fax: 0049-6421-2825365.

[b] Philipps-Universität Marburg, Fachbereich Chemie, Hans-Meerwein-Strasse, 35032 Marburg, Germany.

Correspondence to: Shu-Ming Li, Institut für Pharmazeutische Biologie und Biotechnologie, Philipps-Universität Marburg, Deutschhausstrasse 17A, 35037 Marburg, Germany, Tel: 0049-6421-2822461, Fax: 0049-6421-2825365, email: shuming.li@staff.uni-marburg.de

Contents

Table S1: HR-EI-MS and ESI-MS data of enzyme products.

Comp.	Chemical formula	MS	Calculated	Measured	Deviation (ppm)
1b	$C_{19}H_{23}N_3O_2$	ESI-MS	326.2 $[M+H]^+$	326.1	-
1c	$C_{19}H_{23}N_3O_2$	ESI-MS	326.2 $[M+H]^+$	326.1	-
2b	$C_{19}H_{23}N_3O_2$	ESI-MS	326.2 $[M+H]^+$	326.1	-
2c	$C_{19}H_{23}N_3O_2$	ESI-MS	326.2 $[M+H]^+$	326.1	-
3b	$C_{19}H_{23}N_3O_2$	ESI-MS	326.2 $[M+H]^+$	326.1	-
3c	$C_{19}H_{23}N_3O_2$	ESI-MS	326.2 $[M+H]^+$	326.1	-
4b	$C_{19}H_{23}N_3O_2$	ESI-MS	326.2 $[M+H]^+$	326.1	-
4c	$C_{19}H_{23}N_3O_2$	ESI-MS	326.2 $[M+H]^+$	326.1	-
5b	$C_{21}H_{25}N_3O_2$	HR-EI-MS	351.1947 $[M]^+$	351.1952	-1.5
5c	$C_{21}H_{25}N_3O_2$	HR-EI-MS	351.1947 $[M]^+$	351.1967	-5.8
5d	$C_{21}H_{25}N_3O_2$	ESI-MS	352.2 $[M+H]^+$	352.1	-
6c	$C_{21}H_{25}N_3O_2$	HR-EI-MS	351.1947 $[M]^+$	351.1974	-7.8
6d	$C_{21}H_{25}N_3O_2$	ESI-MS	352.2 $[M+H]^+$	352.1	-
7b	$C_{21}H_{25}N_3O_2$	ESI-MS	352.2 $[M+H]^+$	352.2	-
7c	$C_{21}H_{25}N_3O_2$	HR-EI-MS	351.1947 $[M]^+$	351.1981	-9.6
8c	$C_{21}H_{25}N_3O_2$	ESI-MS	352.2 $[M+H]^+$	352.2	-
8d	$C_{21}H_{25}N_3O_2$	ESI-MS	352.2 $[M+H]^+$	352.2	-

142

Table S2. ^{1}H-NMR data of enzyme products obtained from cyclo-Trp-Ala isomers (**1a**-**4a**) in $CDCl_3$ (400 MHz). Chemical shifts (δ) were given in ppm and coupling constants (J) in Hz.

Compd	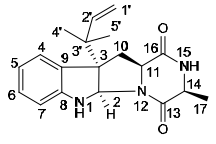 **1b***	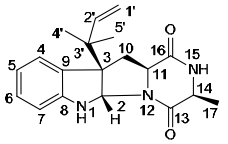 **1c**	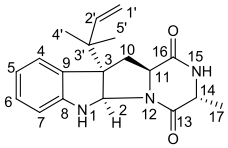 **2b**	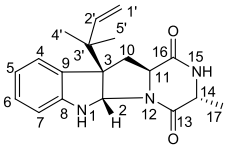 **2c**	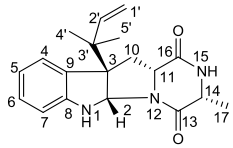 **3b***	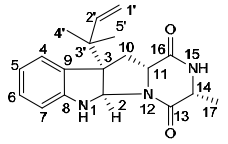 **3c**	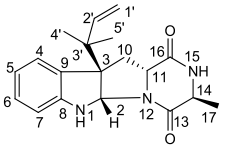 **4b***	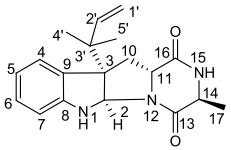 **4c**
Pos.	δ_H, multi., J in Hz	δ_H, multi., J in Hz	δ_H, multi., J in Hz	δ_H, multi., J in Hz	δ_H, multi., J in Hz	δ_H, multi., J in Hz	δ_H, multi., J in Hz	δ_H, multi., J in Hz
2	5.41, s	5.52, s	5.38, s	5.57, s	5.40, s	5.51, s	5.39, s	5.58, s
4	7.18, d, 7.6	7.16, d, 7.6	7.15, d, 7.6	7.16, d, 7.6	7.17, d, 7.6	7.16, d, 7.5	7.16, d, 7.6	7.17, d, 7.4
5	6.76, t, 7.6	6.77, t, 7.6	6.74, t, 7.6	6.77, t, 7.6	6.75, t, 7.6	6.76, t, 7.5	6.76, t, 7.6	6.78, t, 7.4
6	7.09, t, 7.6	7.11, t, 7.6	7.08, t, 7.6	7.11, t, 7.6	7.08, t, 7.6	7.10, t, 7.5	7.09, t, 7.6	7.12, t, 7.4
7	6.61, d, 7.6	6.60, d, 7.6	6.57, d, 7.6	6.60, d, 7.6	6.58, d, 7.6	6.58, d, 7.5	6.61, d, 7.6	6.61, d, 7.4
10a	2.54, dd, 13.9, 8.7	2.48, dd, 12.7, 11.1	2.44, dd, 13.8, 9.1	2.43, dd, 12.6, 11.2	2.54, dd, 13.9, 8.8	2.47, dd, 12.7, 10.9	2.43, dd, 13.8, 9.2	2.43, dd, 12.6, 11.3
10b	2.81, dd, 13.9, 8.7	2.55, dd, 12.7, 6.2	2.87, dd, 13.8, 9.1	2.57, dd, 12.6, 6.2	2.81, dd, 13.9, 8.8	2.55, dd, 12.7, 6.5	2.87, dd, 13.8, 9.2	2.57, dd, 12.6, 6.2
11	4.13, t, 8.7	3.96, dd, 11.1, 6.2	4.09, t, 9.1	3.93, dd, 11.2, 6.2	4.13, t, 8.8	3.96, dd, 10.9, 6.5	4.09, t, 9.2	3.93, dd, 11.3, 6.2
14	4.06, q, 6.9	4.05, q, 6.9	3.96, qd, 7.2, 3.7	4.01, qd, 7.1, 3.8	4.06, q, 6.9	4.04, q, 6.9	3.96, qd, 7.2, 3.8	4.01, qd, 7.1, 3.8
17	1.42, d, 6.9	1.47, d, 6.9	1.48, d, 7.2	1.41, d, 7.1	1.42, d, 6.9	1.46, d, 6.9	1.47, d, 7.2	1.41, d, 7.1
1'	5.16, d, 10.8	5.13, d, 10.8	5.17, d, 10.8	5.13, d, 10.8	5.16, d, 10.8	5.12, d, 10.8	5.17, d, 10.8	5.13, d, 10.8
1'	5.13, d, 17.4	5.08, d, 17.4	5.13, d, 17.4	5.08, d, 17.3	5.12, d, 17.4	5.08, d, 17.4	5.14, d, 17.4	5.08, d, 17.4
2'	5.95, dd, 17.4, 10.8	5.98, dd, 17.4, 10.8	5.95, dd, 17.4, 10.8	5.97, dd, 17.3, 10.8	5.95, dd, 17.4, 10.8	5.98, dd, 17.4, 10.8	5.94, dd, 17.4, 10.8	5.97, dd, 17.4, 10.8
4'	1.15, s	1.12, s	1.15, s	1.12, s	1.14, s	1.12, s	1.15, s	1.12, s
5'	0.99, s	1.02, s	0.99, s	1.01, s	0.99, s	1.02, s	0.99, s	1.01, s

H-10a and H-10b: has the *syn*- and *anti*-configuration to the carbonyl moiety at C-11, respectively.

*: measured on 500 MHz spectrometer.

Table S3. ^{1}H- and ^{13}C- NMR data of enzyme products obtained from cyclo-Trp-Pro isomers (**5a**-**8a**) in $CDCl_3$ (400 MHz). Chemical shifts (δ) were given in ppm and coupling constants (J) in Hz.

Compd	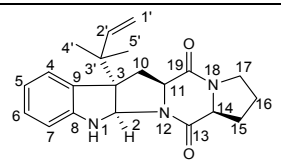 **5b***		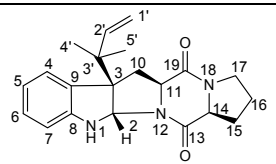 **5c$^{\Delta}$**		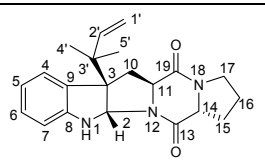 **6c***		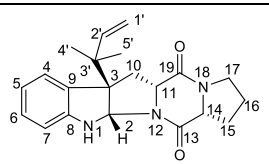 **7b**	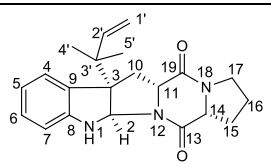 **7c**	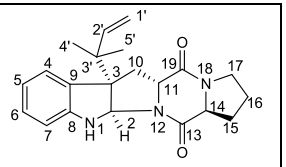 **8c**
Pos.	^{13}C NMR δ ppm	^{1}H NMR δ_H, multi., J in Hz	^{13}C NMR δ ppm	^{1}H NMR δ_H, multi., J in Hz	^{13}C NMR δ ppm	^{1}H NMR δ_H, multi., J in Hz	^{1}H NMR δ_H, multi., J in Hz	^{1}H NMR δ_H, multi., J in Hz	^{1}H NMR δ_H, multi., J in Hz
2	79.4	5.39, s	77.4	5.46, s	77.2	5.71, s	5.39, s	5.46, s	5.71, s
3	62.3	/	61.9	/	62.8	/	/	/	/
4	125.8	7.17, d, 7.6	125.1	7.16, d, 7.6	125.5	7.17, d, 7.6	7.17, d, 7.6	7.16, d, 7.6	7.17, d, 7.6
5	118.7	6.73, t, 7.6	119.0	6.77, t, 7.6	119.0	6.74, t, 7.6	6.73, t, 7.6	6.77, t, 7.6	6.75, t, 7.6
6	128.3	7.06, t, 7.6	128.9	7.11, t, 7.6	129.0	7.08, t, 7.6	7.07, t, 7.6	7.11, t, 7.6	7.08, t, 7.6
7	108.9	6.55, d, 7.6	109.4	6.59, d, 7.6	108.7	6.56, d, 7.6	6.55, d, 7.6	6.59, d, 7.6	6.57, d, 7.6
8	148.4	/	149.9	/	150.3	/	/	/	/
9	131.5	/	129.4	/	128.6	/	/	/	/
10a	35.7	2.56, dd, 14.0, 8.9	35.1	2.49, dd, 12.9, 10.8	38.3	2.31, t, 12.0	2.56, dd, 14.0, 8.9	2.48, §	2.31, t, 12.0
10b	35.7	2.79, dd, 14.0, 8.9	35.1	2.54, dd, 12.9, 6.7	38.3	2.51, dd, 12.0, 5.3	2.79, dd, 14.0, 8.9	2.54, §	2.51, dd, 12.0, 5.3
11	59.1	4.16, t, 8.9	60.5	3.99, dd, 10.8, 6.7	59.9	3.97, dd, 12.0, 5.3	4.16, t, 8.9	3.99, §	3.98, dd, 12.0, 5.3
13	168.7	/	166.2	/	164.2	/	/	/	/
14	60.7	4.09, t, 8.0	60.5	4.05, †	60.7	4.02, dd, 11.7, 5.7	4.09, dd, 8.9, 7.2	4.05, §	4.03, dd, 11.6, 5.6
15	27.8	2.31, m 2.05, m	27.7	2.32, m 2.12, m	29.4	2.40, m 1.75, m	2.32, m 2.06, m	2.31, m 2.12, m	2.41, m 1.75, m
16	23.0	1.97, m 1.86, m	22.9	2.04, m, 1.89, m	21.5	1.98, m 1.89, m	1.97, m 1.87, m	2.03, m 1.89, m	1.98, m 1.89, m
17	44.9	3.42, m	45.1	3.56, m 3.50, m	44.4	3.91, m 3.28, m	3.43, m	3.56, m 3.50, m	3.90, ddd, 12.2, 8.8, 7.3 3.29, ddd, 12.2, 9.9, 4.1
19	165.7	/	167.0	/	164.5	/	/	/	/
1’	114.6	5.15, d, 10.8 5.12, d, 17.4	114.5	5.12, d, 10.8 5.07, d, 17.4	114.6	5.12, d, 10.8 5.08, d, 17.4	5.15, d, 10.8 5.12, d, 17.3	5.11, d, 10.8 5.07, d, 17.3	5.12, d, 10.8 5.08, d, 17.4
2’	143.7	5.95, dd, 17.4, 10.8	143.7	5.98, dd, 17.4, 10.8	143.5	5.94, dd, 17.4, 10.8	5.95, dd, 17.3, 10.8	5.99, dd, 17.3, 10.8	5.94, dd, 17.4, 10.8
3’	41.6	/	40.8	/	41.0	/	/	/	/
4’	22.2	1.14, s	22.4	1.11, s	22.1	1.12, s	1.14, s	1.11, s	1.12, s
5’	22.4	0.99, s	22.7	1.01, s	23.0	1.01, s	0.99, s	1.01, s	1.01, s

H-10a and H-10b: has the *syn*- and *anti*-configuration to the carbonyl moiety at C-11, respectively.
†: the coupling constant can't be determined due to overlapping of this peak with impurity.
§: the coupling constants can't be determined due to low resolution of these peaks.
*: measured on 500 MHz spectrometer.
$^{\Delta}$: measured on 600 MHz spectrometer

144
Table S3 (continued)

Compd	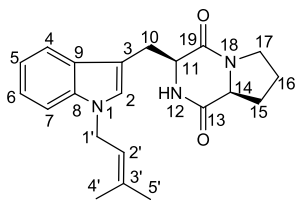 **5d***	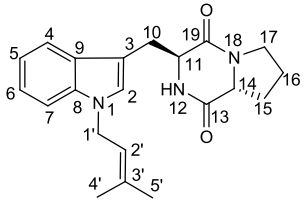 **6d***	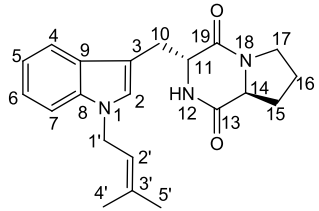 **8d**
Pos.	^{1}H NMR δ_H, multi., J in Hz	^{1}H NMR δ_H, multi., J in Hz	^{1}H NMR δ_H, multi., J in Hz
2	7.01, s	6.96, s	6.95, s
4	7.56, d, 8.1	7.59, d, 8.1	7.59, d, 8.1
5	7.12, dd, 8.1, 7.0	7.12, dd, 8.1, 7.0	7.11, dd, 8.1, 7.0
6	7.24, dd, 8.1, 7.0	7.20, dd, 8.1, 7.0	7.20, dd, 8.1, 7.0
7	7.33, d, 8.1	7.30, d, 8.1	7.30, d, 8.1
10	3.76, dd, 15.1, 3.7 2.92, dd, 15.1, 11.1	3.35, dd, 14.5, 6.7 3.20, dd, 14.5, 3.7	3.35, dd, 14.4, 6.7 3.20, dd, 14.4, 3.7
11	4.36, dd, 11.1, 3.7	4.23, dt, 6.7, 3.7	4.23, dt, 6.7, 3.7
14	4.08, t, 8.2	3.57, dt, 12.0, 8.6	3.57, dt, 12.2, 8.6
15	2.33, m 2.02, m‡	2.11, m 1.74, m‡	2.10, m 1.72, m‡
16	2.02, m‡ 1.91, m‡	1.86, m‡ 1.48, m‡	1.86, m‡ 1.47, m‡
17	3.65, m 3.59, m	3.22, overlaps 2.92, dd, 10.9, 6.4	3.22, overlaps 2.91, dd, 11.0, 6.5
1’	4.67, d, 6.9	4.65, d, 6.9	4.65, d, 6.9
2’	5.38, tm, 6.9	5.31, tm, 6.9	5.31, tm, 6.9
4’	1.83, s	1.82, s	1.82, s
5’	1.78, s	1.76, s	1.76, s

*: measured on 500 MHz spectrometer.
‡: assignments interchangeable.

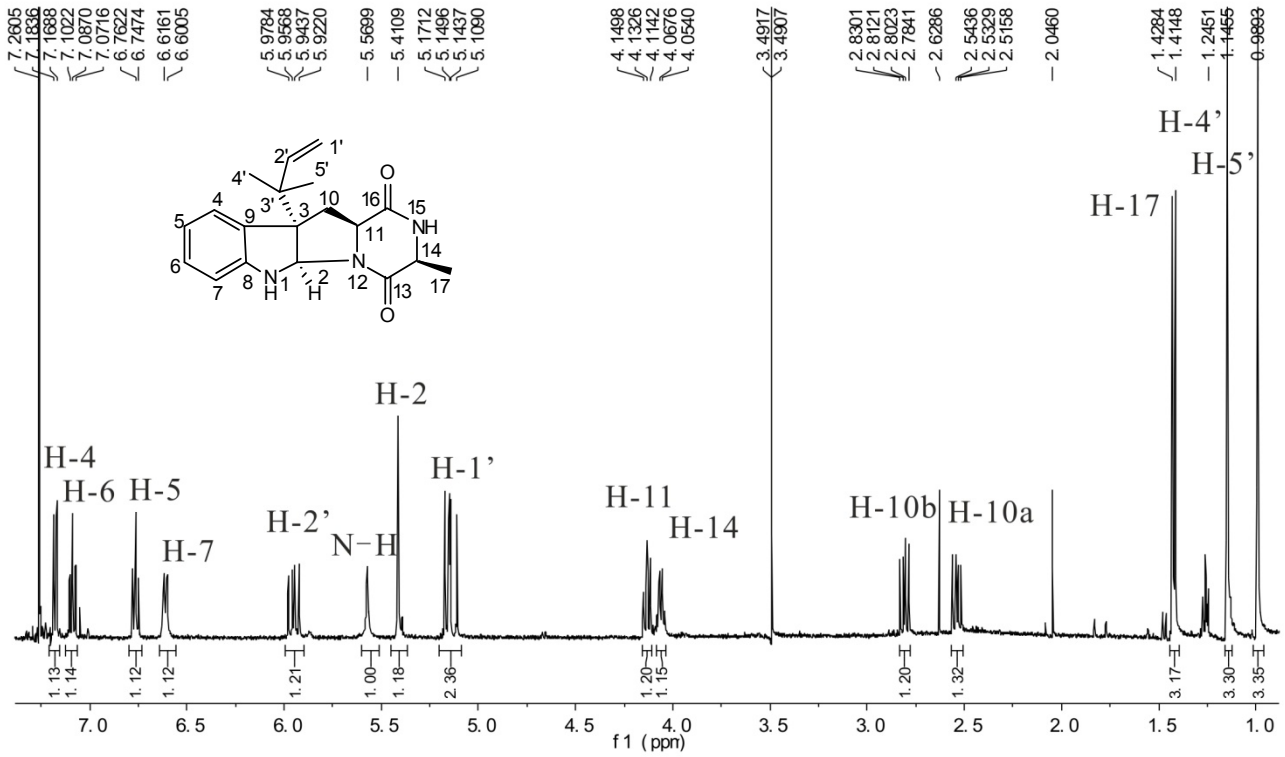

Fig. S1: ^{1}H-NMR spectrum of **1b** in $CDCl_3$ (500 MHz).

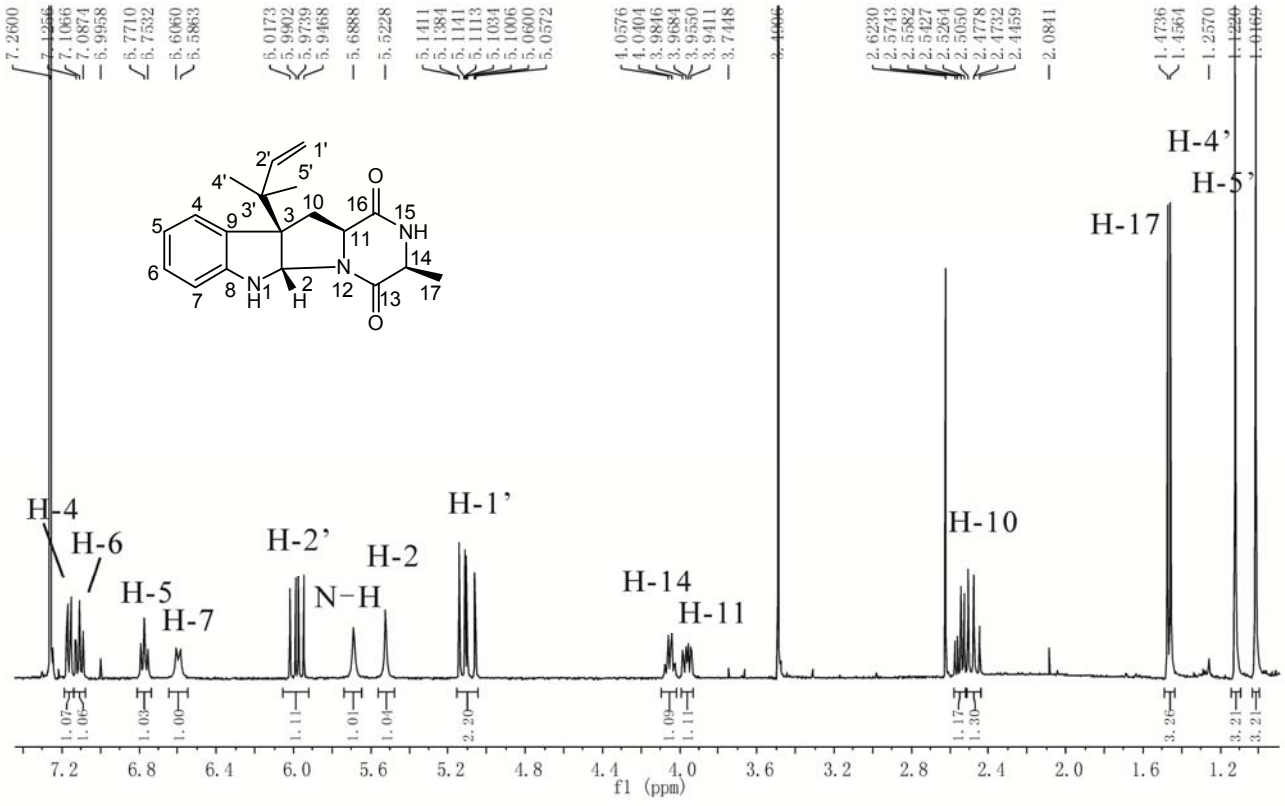

Fig. S2: ^{1}H-NMR spectrum of **1c** in $CDCl_3$ (400 MHz).

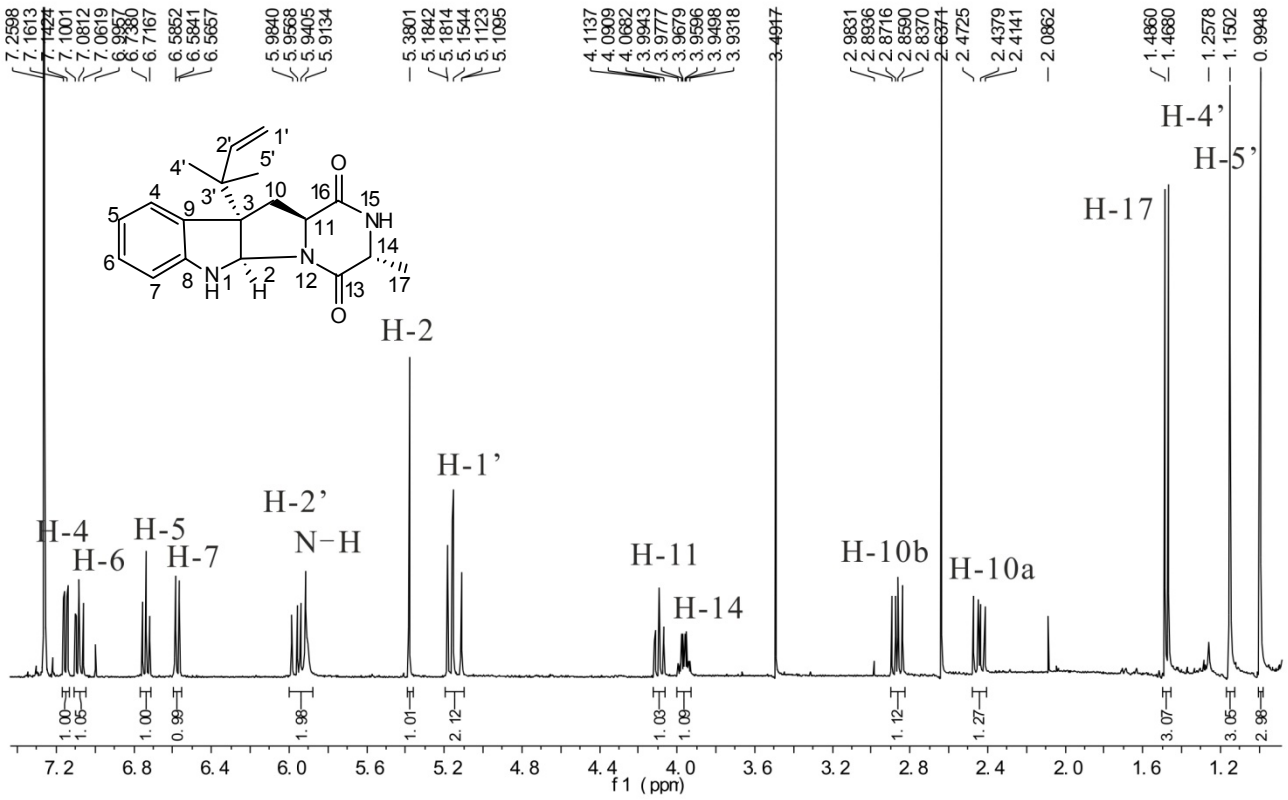

Fig. S3: ^{1}H-NMR spectrum of **2b** in $CDCl_3$ (400 MHz).

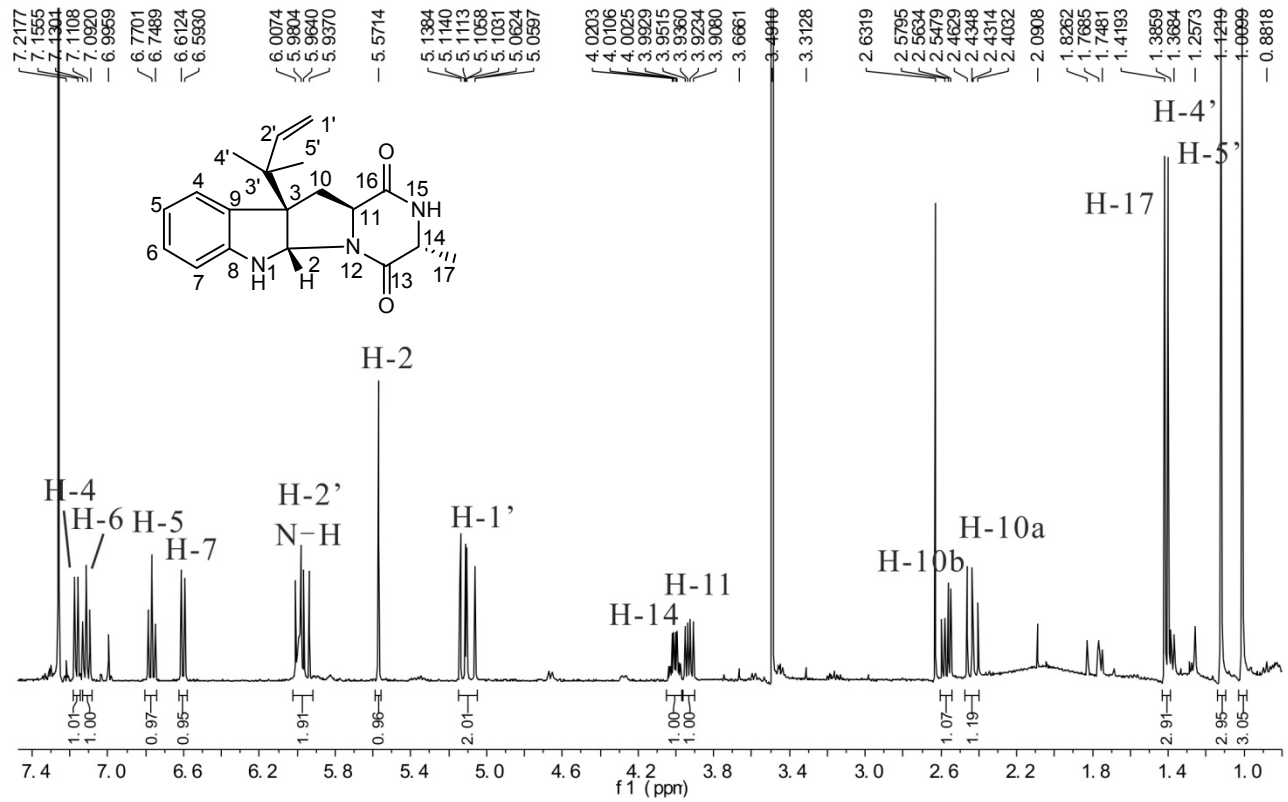

Fig. S4: ^{1}H-NMR spectrum of **2c** in $CDCl_3$ (400 MHz).

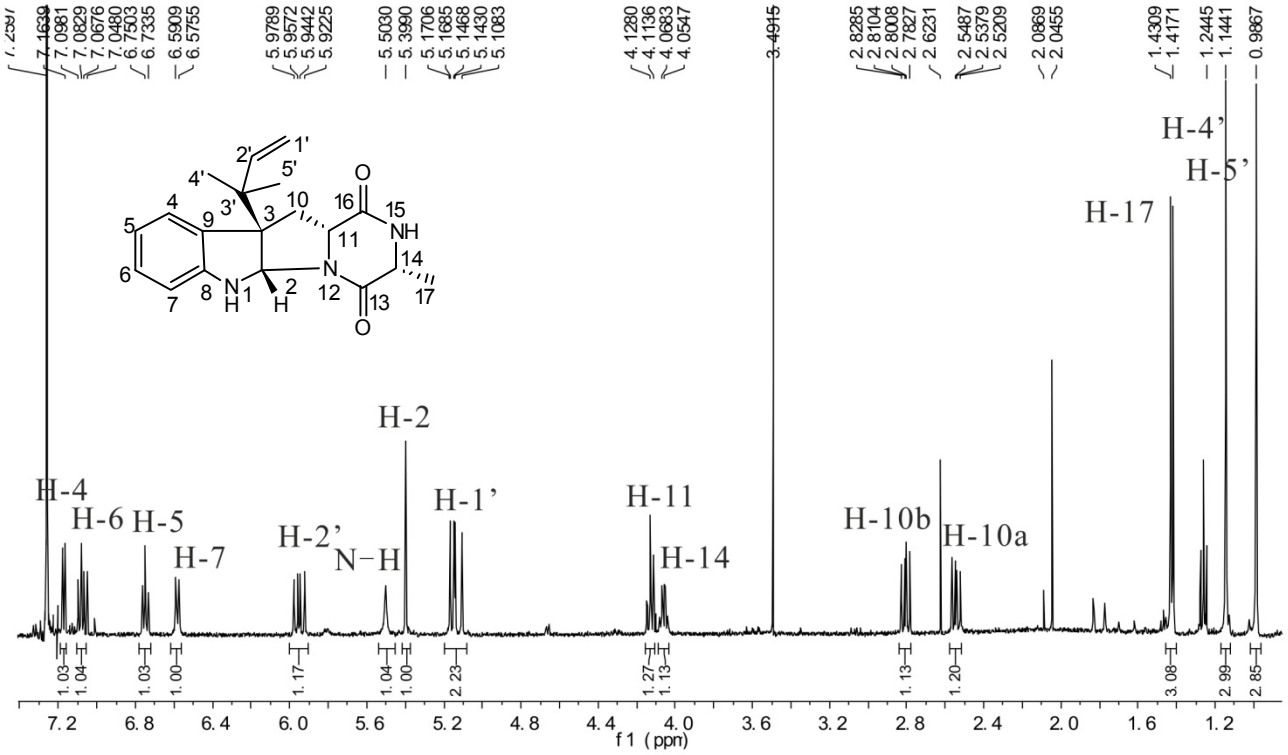

Fig. S5: ^{1}H-NMR spectrum of **3b** in $CDCl_3$ (500 MHz).

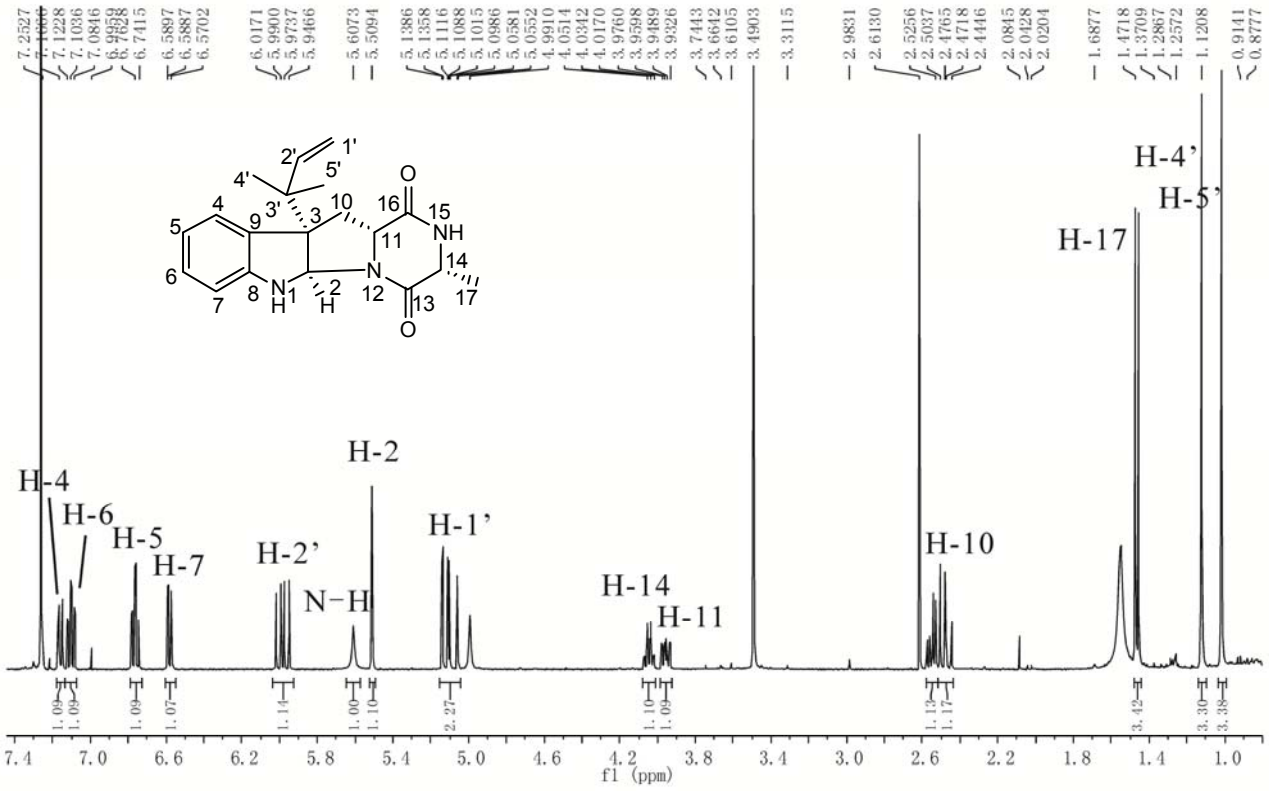

Fig. S6: ^{1}H-NMR spectrum of **3c** in $CDCl_3$ (400 MHz).

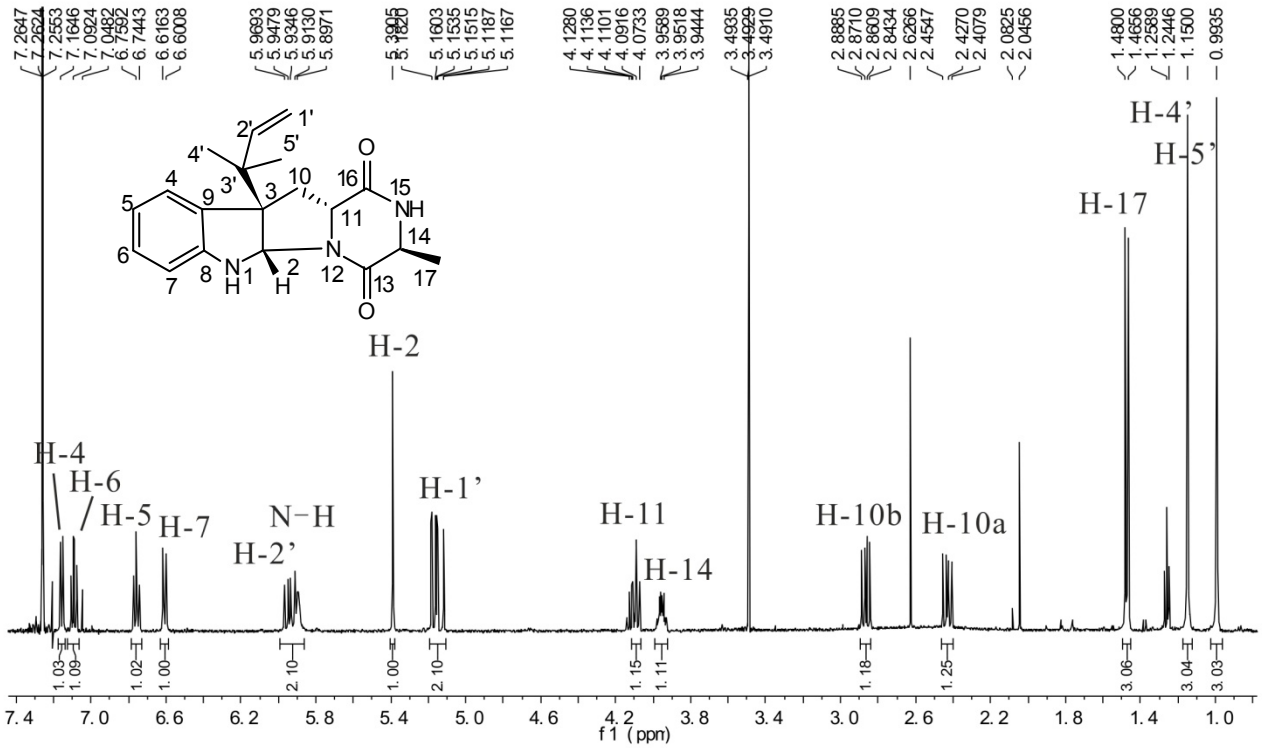

Fig. S7: ^{1}H-NMR spectrum of **4b** in $CDCl_3$ (500 MHz).

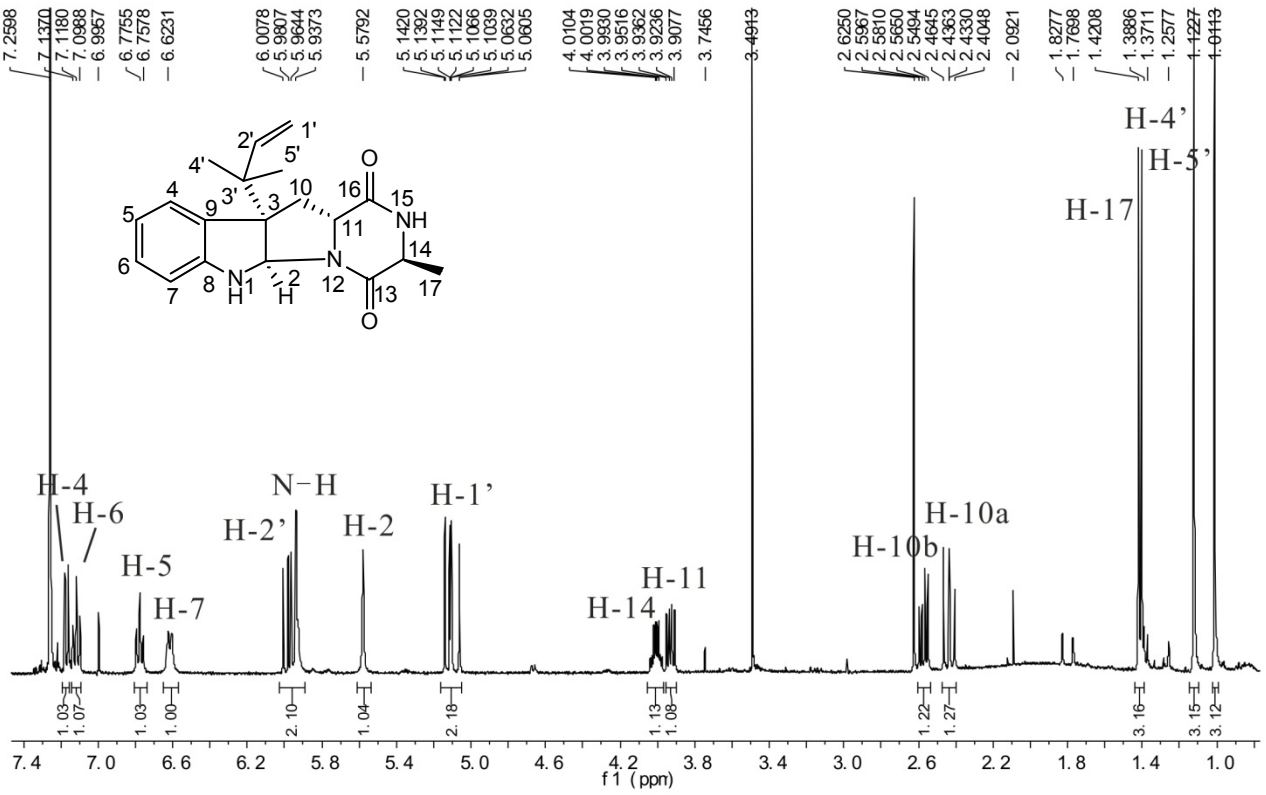

Fig. S8: ^{1}H-NMR spectrum of **4c** in $CDCl_3$ (400 MHz).

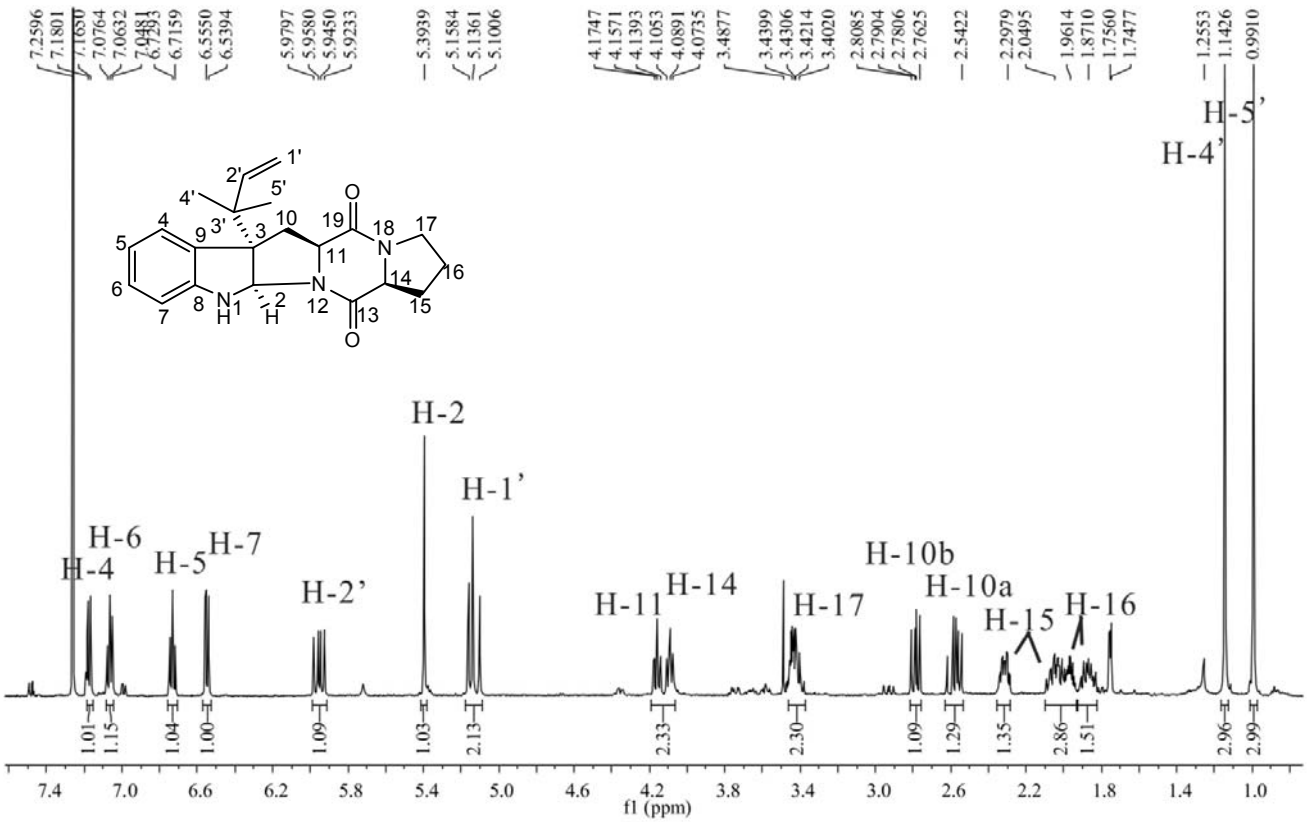

Fig. S9.1: ^{1}H-NMR spectrum of **5b** in $CDCl_3$ (500 MHz).

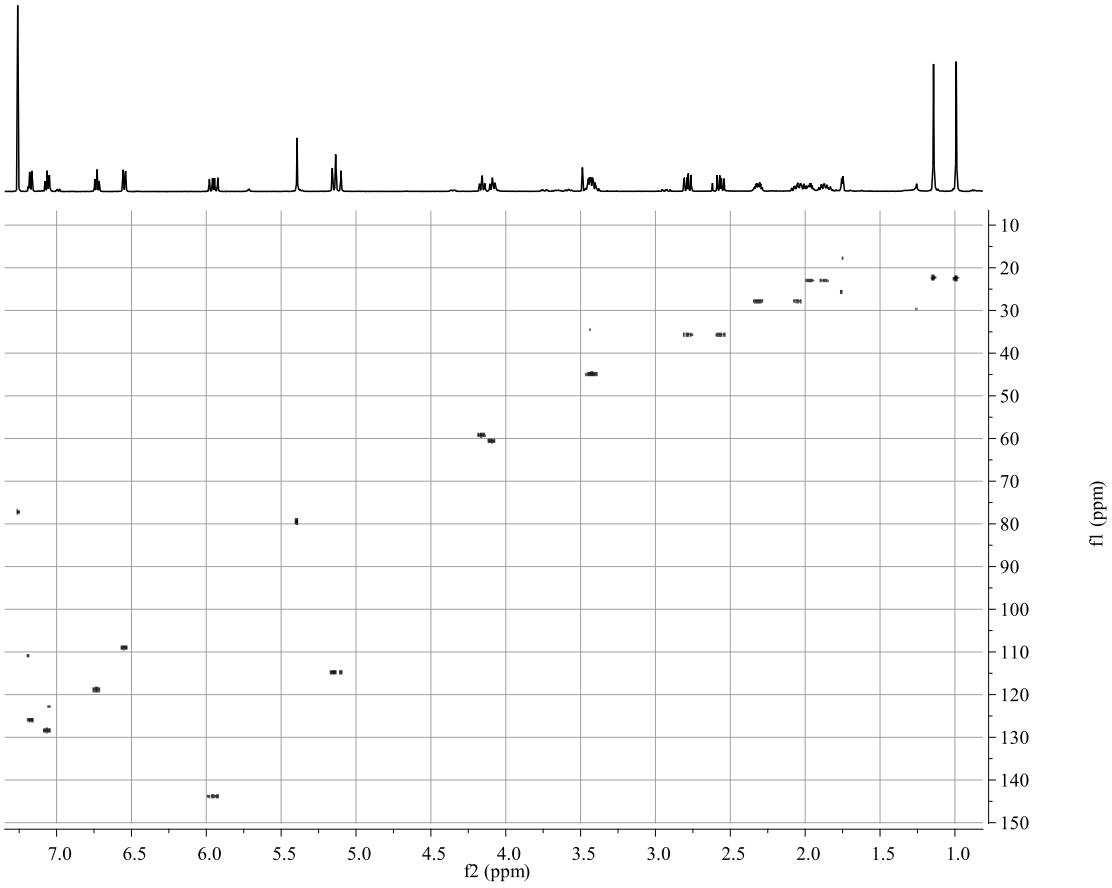

Fig. S9.2: HSQC spectrum of **5b** in $CDCl_3$ (500 MHz).

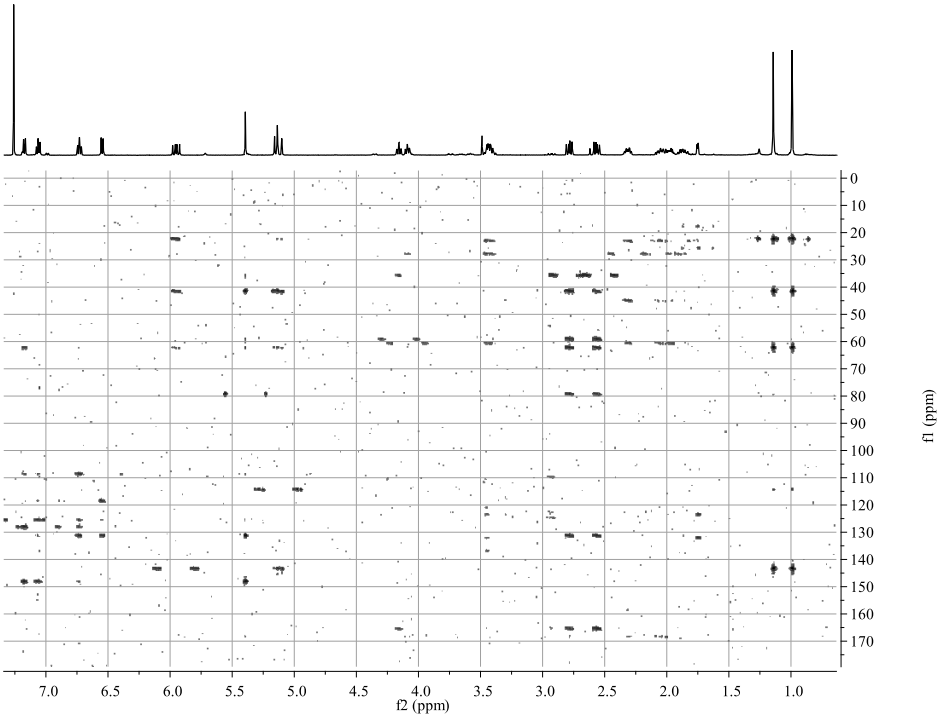

Fig. S9.3: HMBC spectrum of **5b** in $CDCl_3$ (500 MHz).

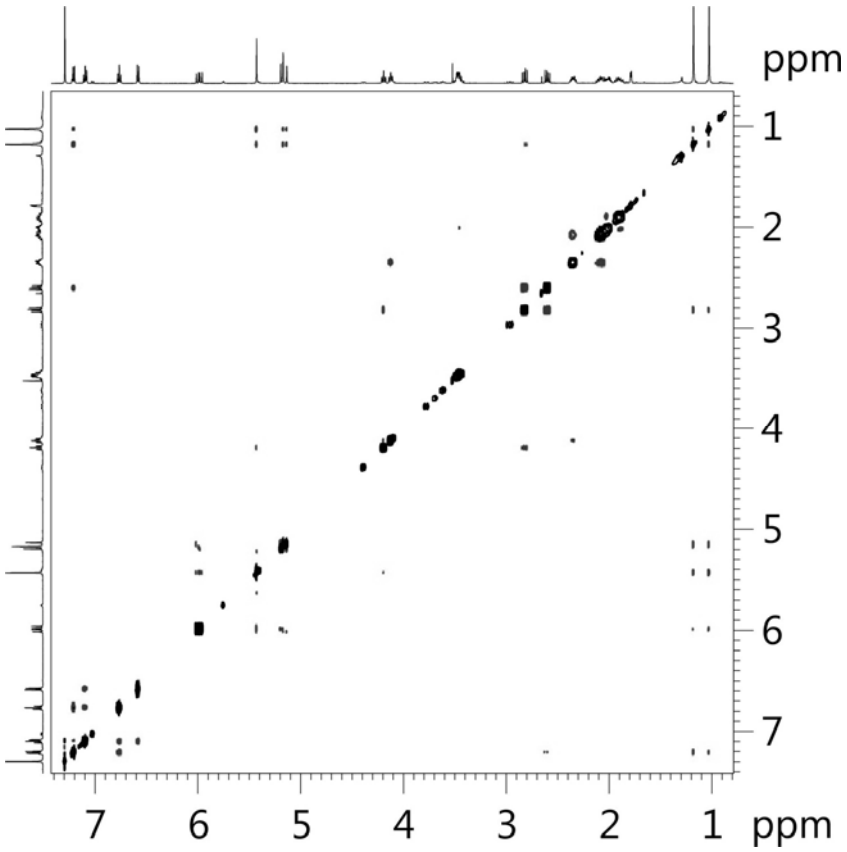

Fig. S9.4: NOESY spectrum of **5b** in $CDCl_3$ (500 MHz).

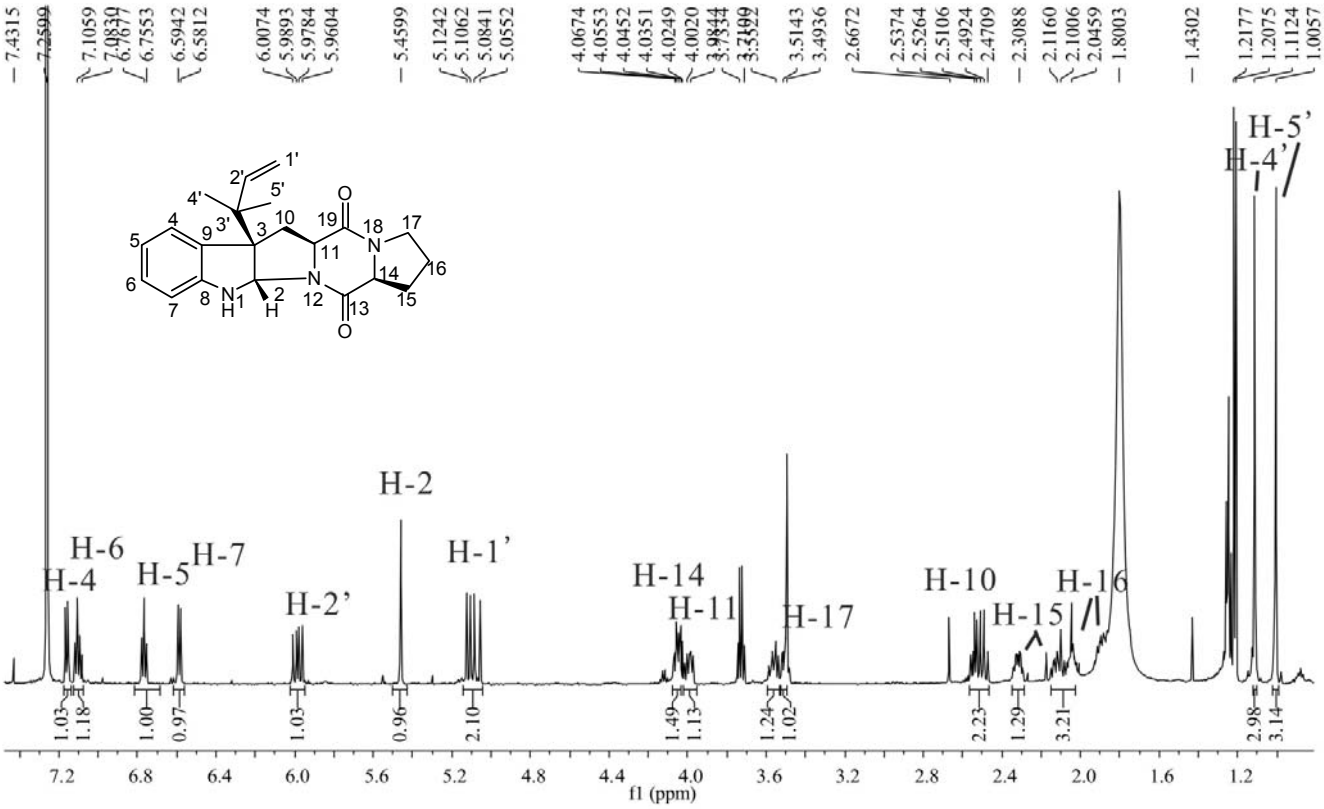

Fig. S10.1: ^{1}H-NMR spectrum of **5c** in $CDCl_3$ (600 MHz).

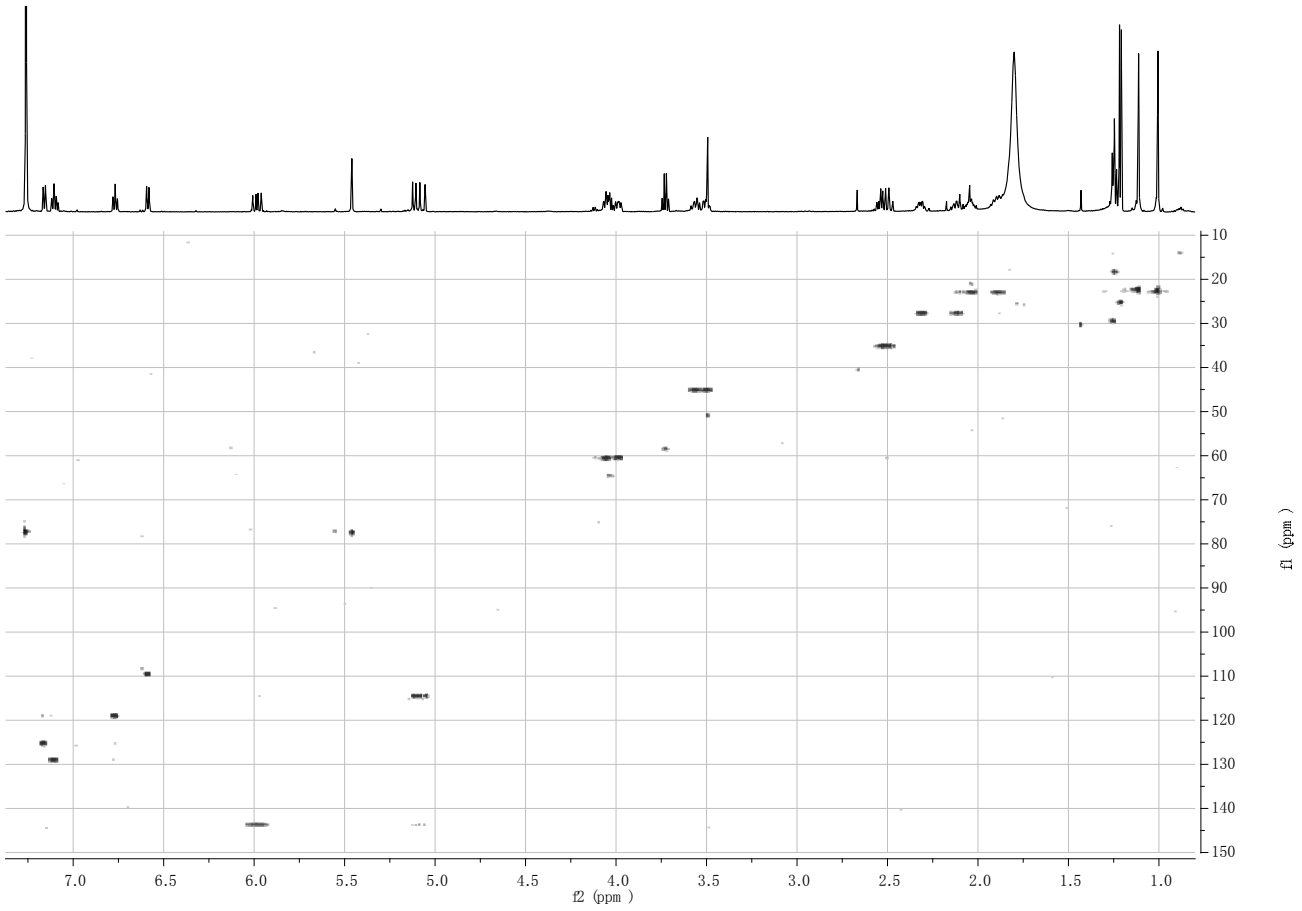

Fig. S10.2: HSQC spectrum of **5c** in $CDCl_3$ (600 MHz).

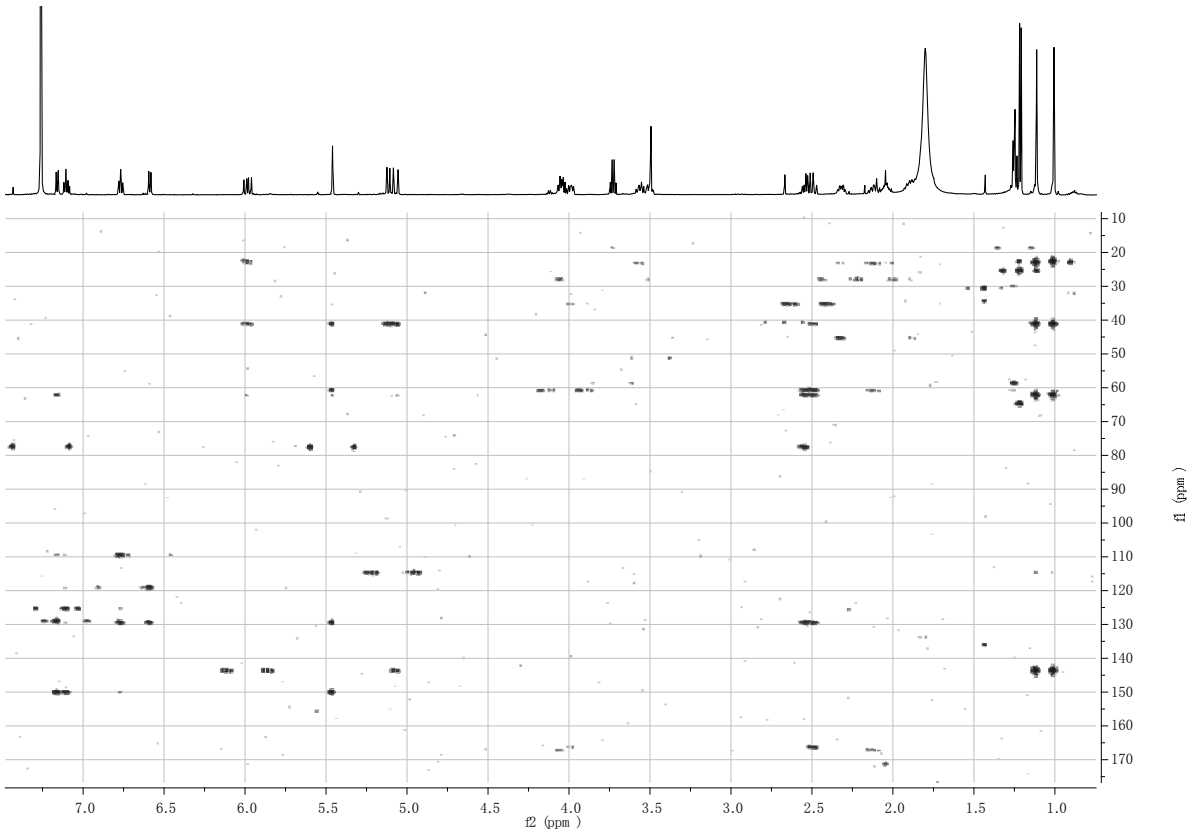

Fig. S10.3: HMBC spectrum of **5c** in $CDCl_3$ (600 MHz).

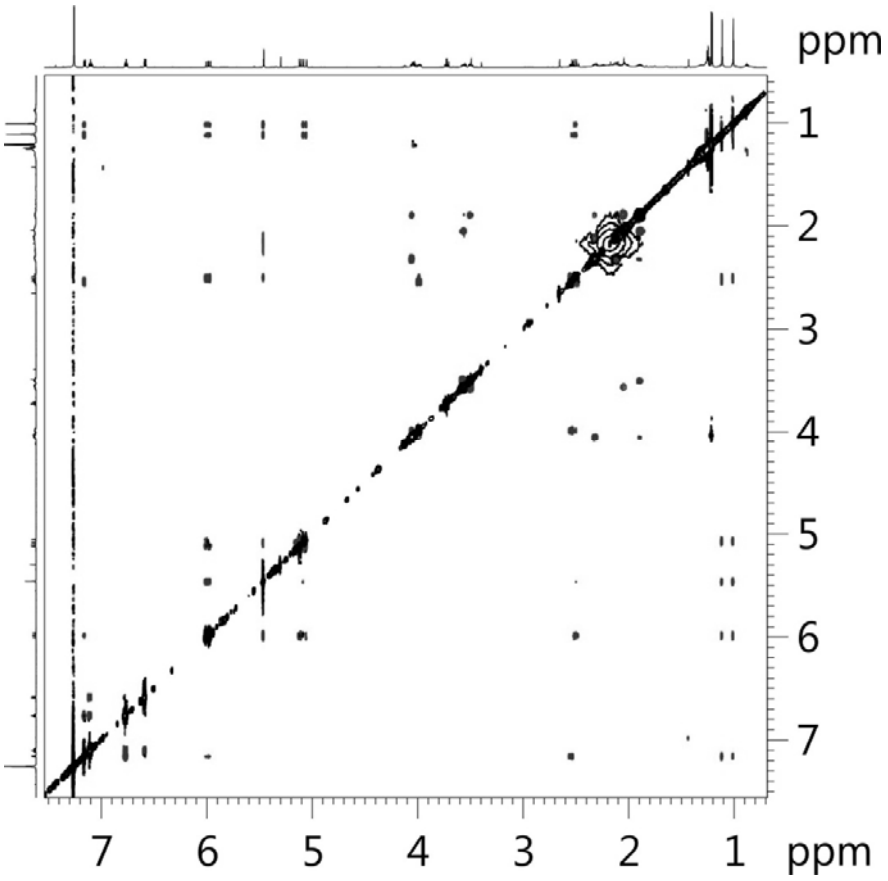

Fig. S10.4: NOESY spectrum of **5c** in $CDCl_3$ (600 MHz).

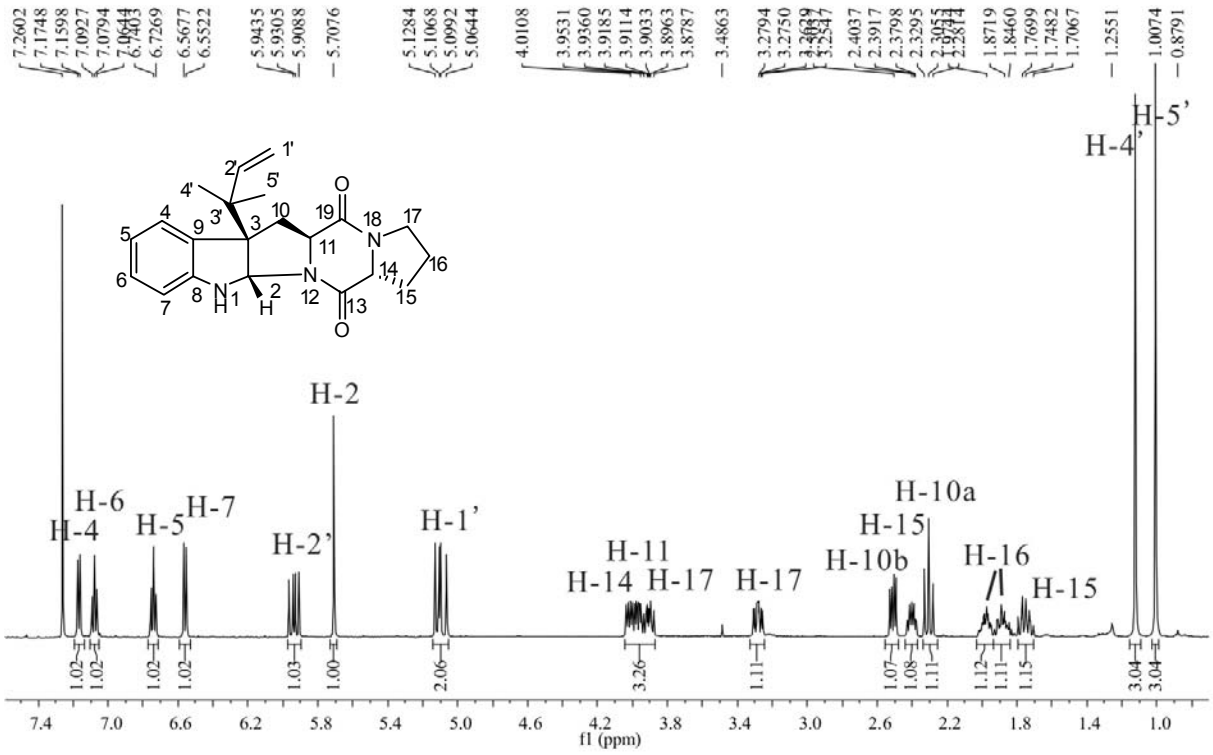

Fig. S11.1: ^{1}H-NMR spectrum of **6c** in $CDCl_3$ (500 MHz).

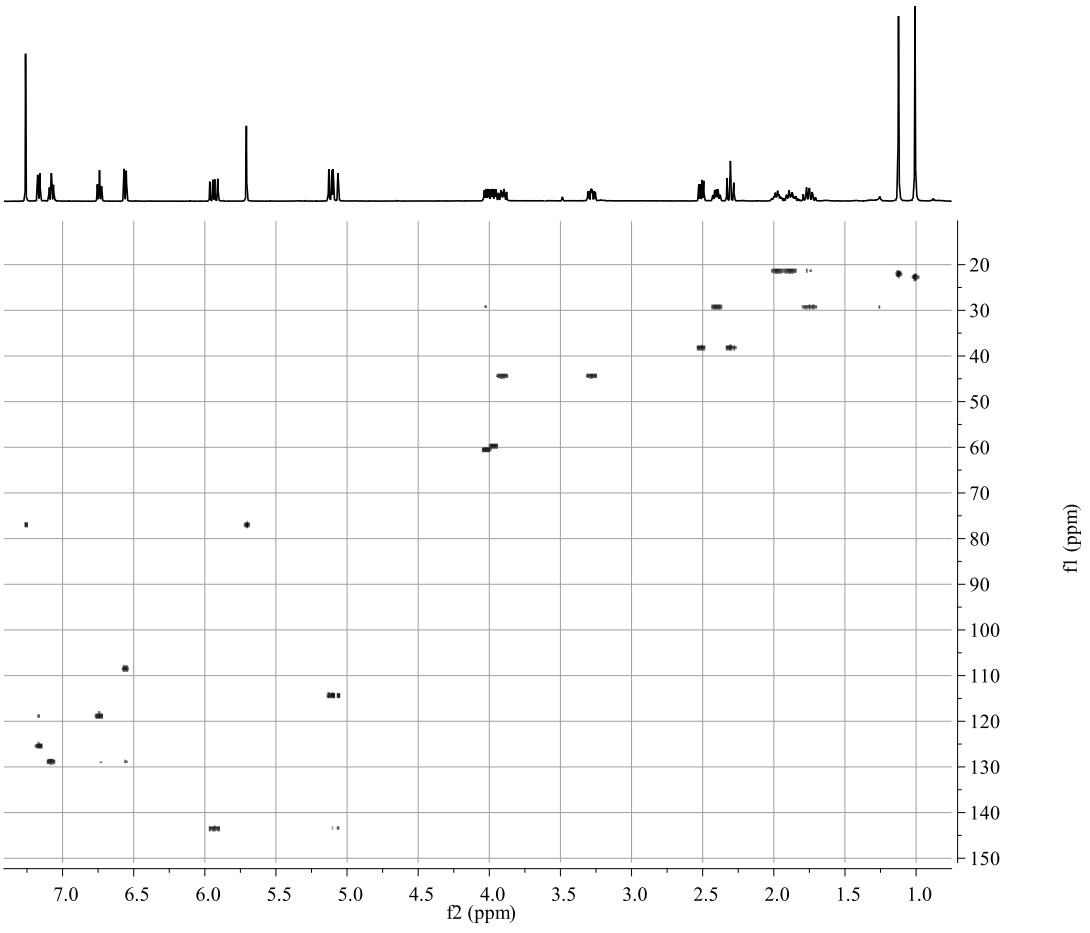

Fig. S11.2: HSQC spectrum of **6c** in $CDCl_3$ (500 MHz).

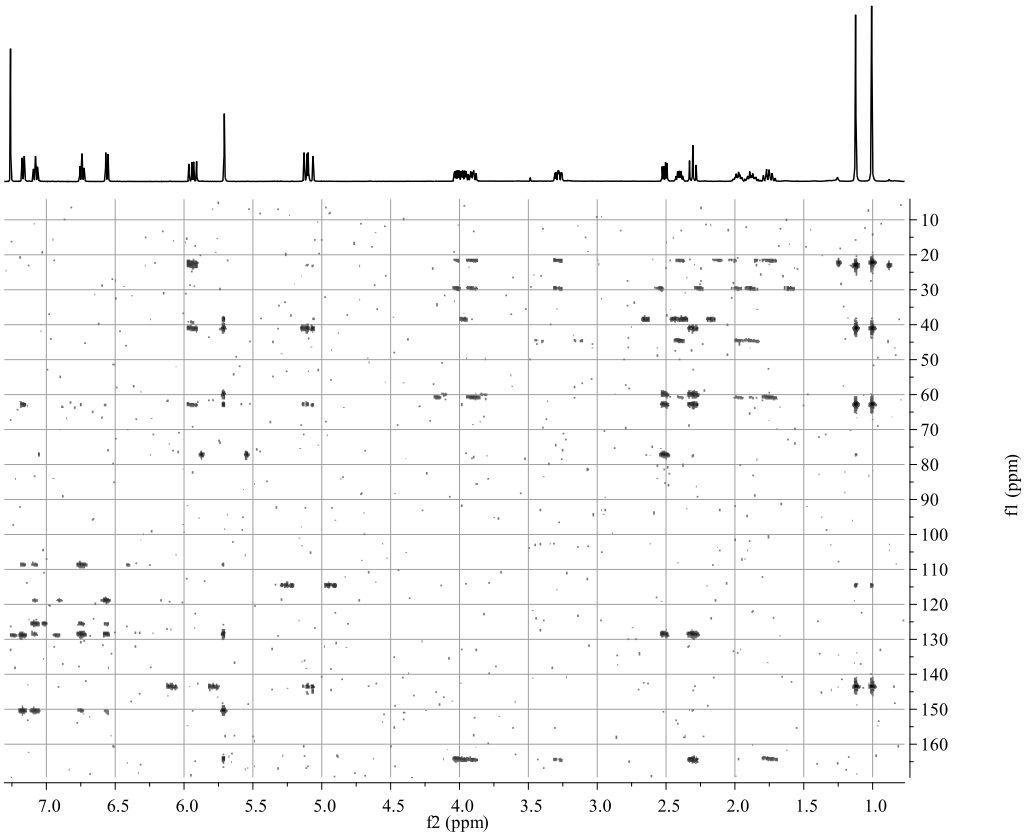

Fig. S11.3: HMBC spectrum of **6c** in $CDCl_3$ (500 MHz).

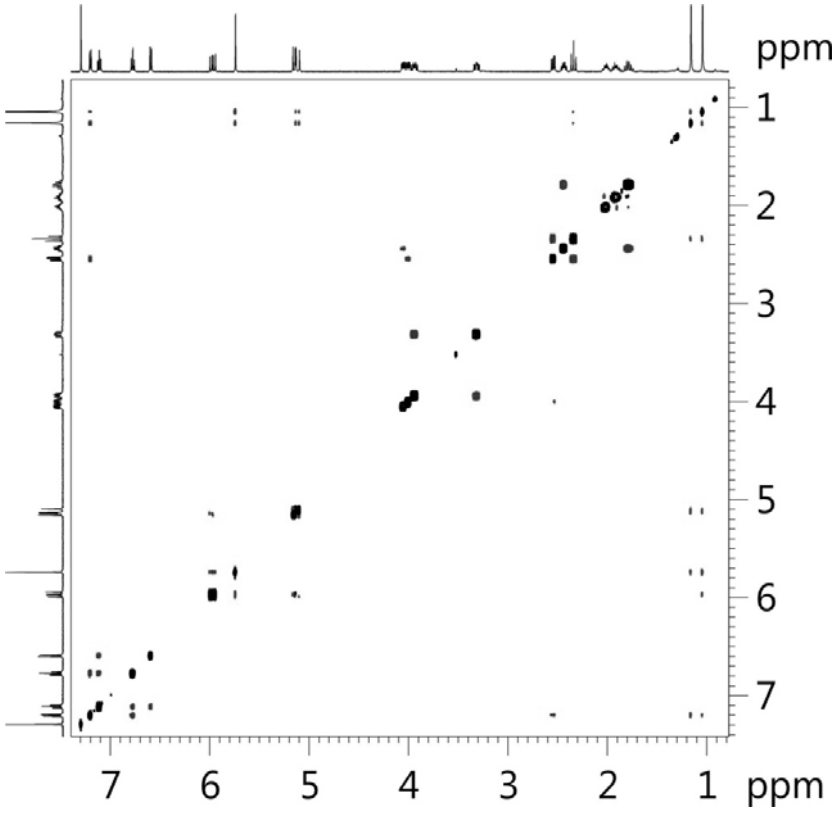

Fig. S11.4: NOESY spectrum of **6c** in $CDCl_3$ (500 MHz).

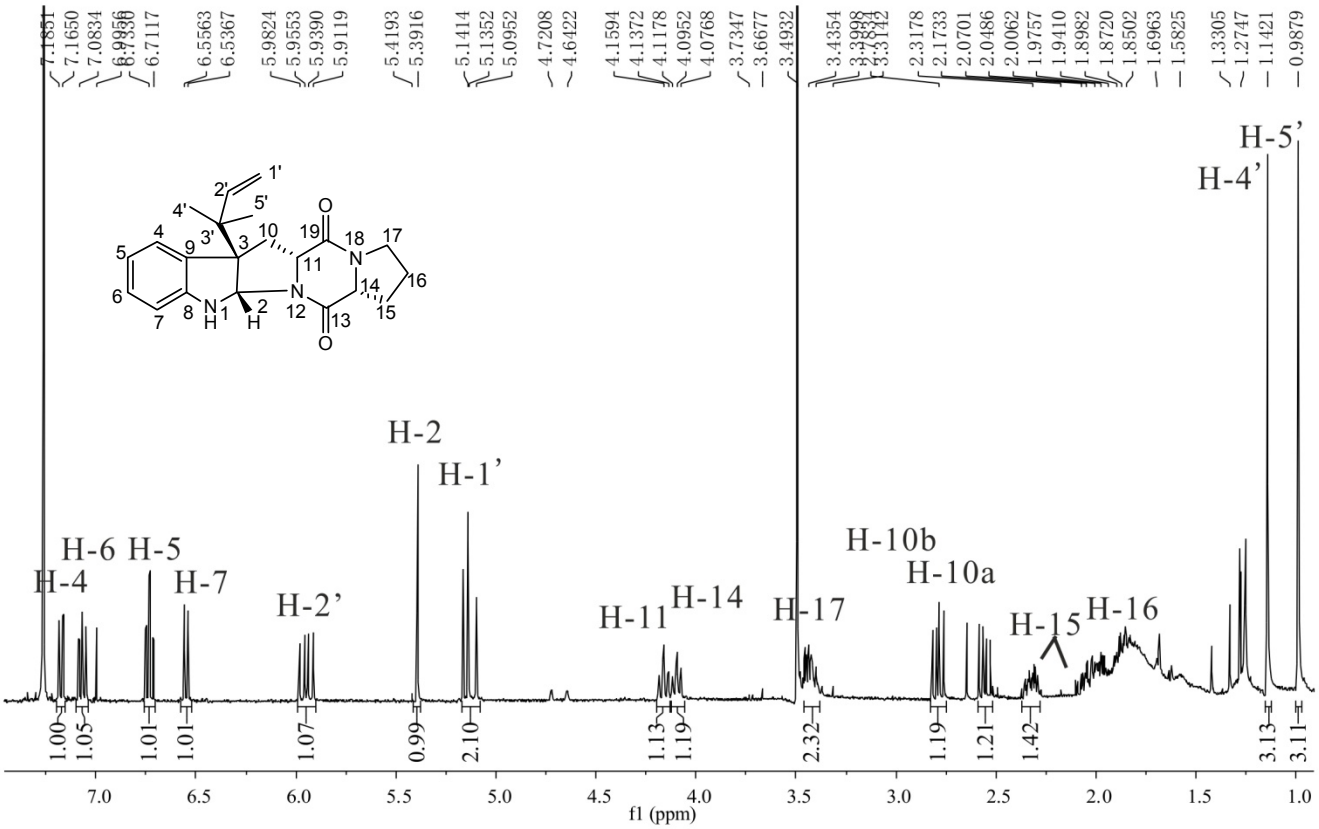

Fig. S12: ^{1}H-NMR spectrum of **7b** in $CDCl_3$ (400 MHz).

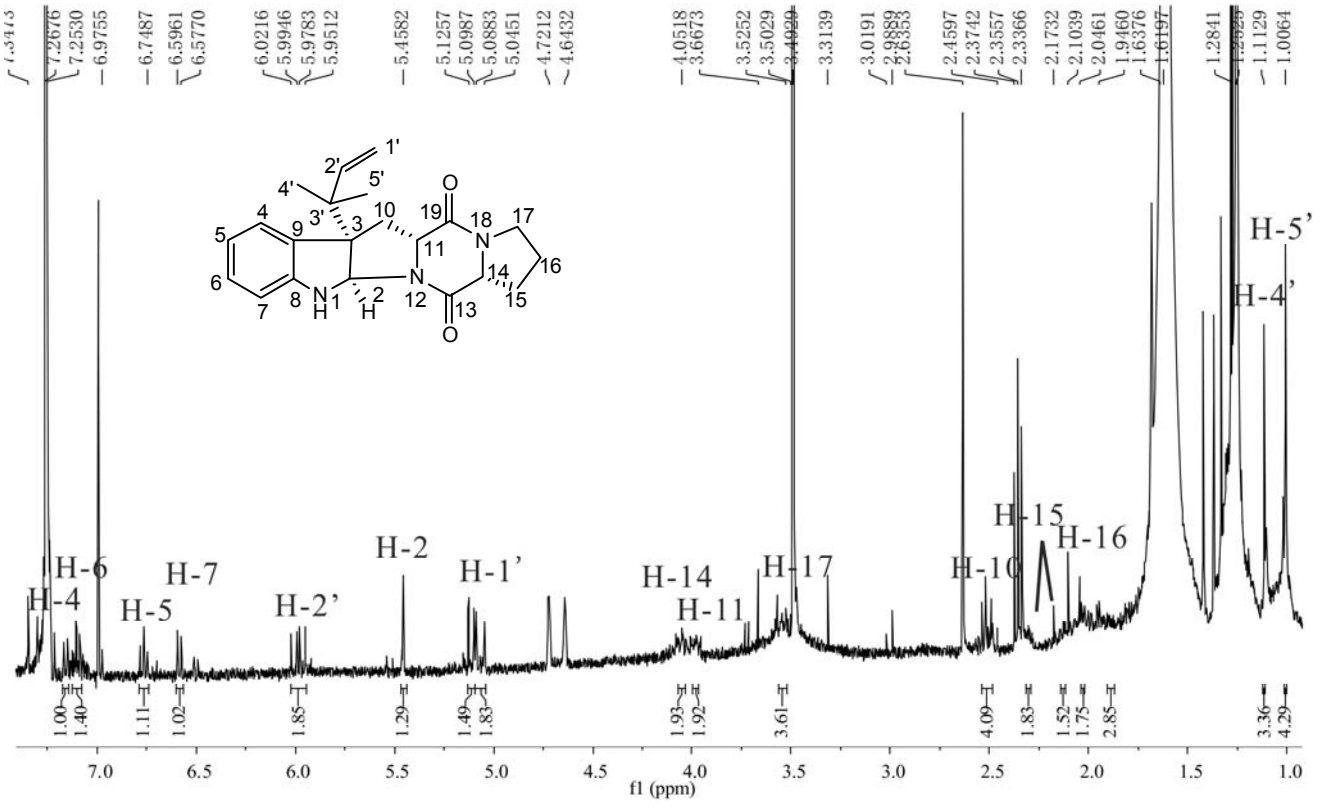

Fig. S13: ^{1}H-NMR spectrum of **7c** in $CDCl_3$ (400 MHz).

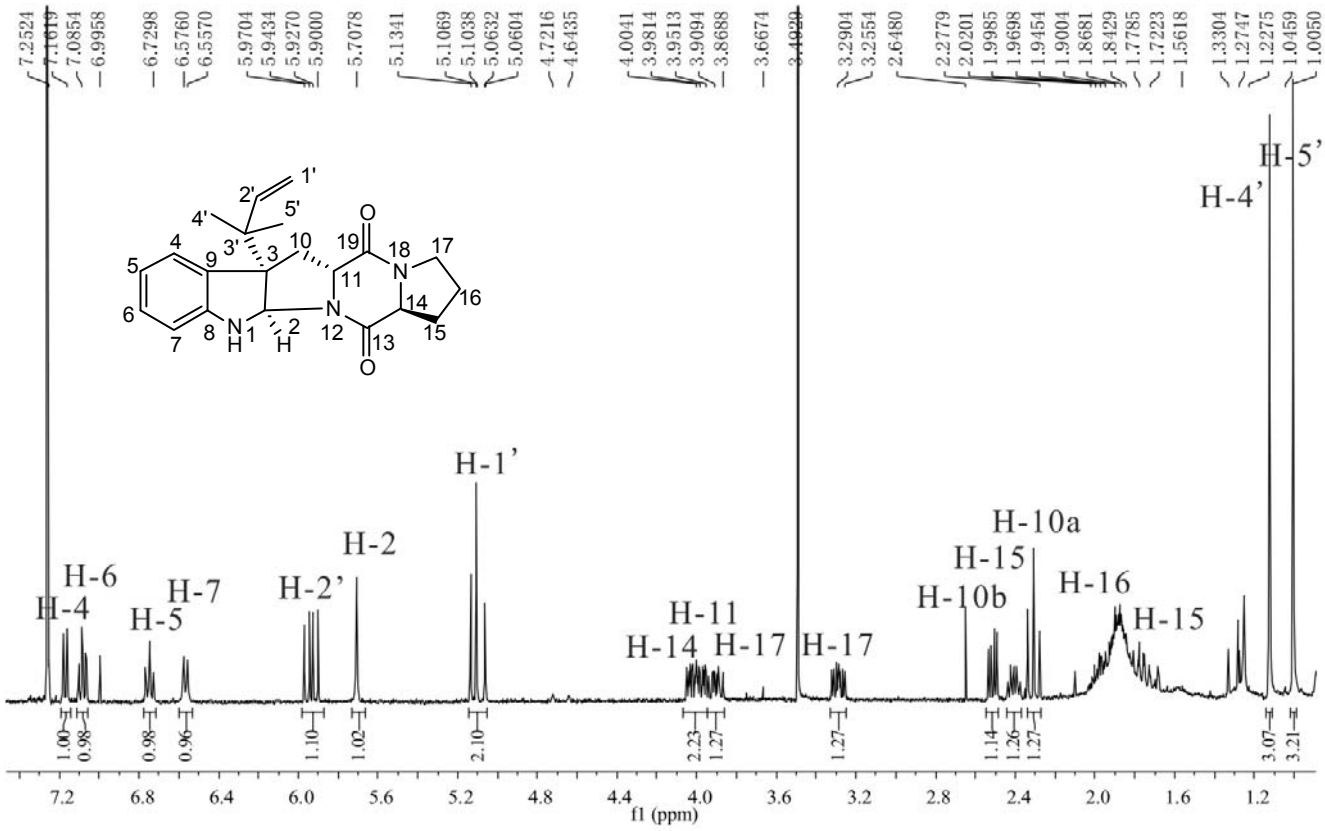

Fig. S14: ^{1}H-NMR spectrum of **8c** in $CDCl_3$ (400 MHz).

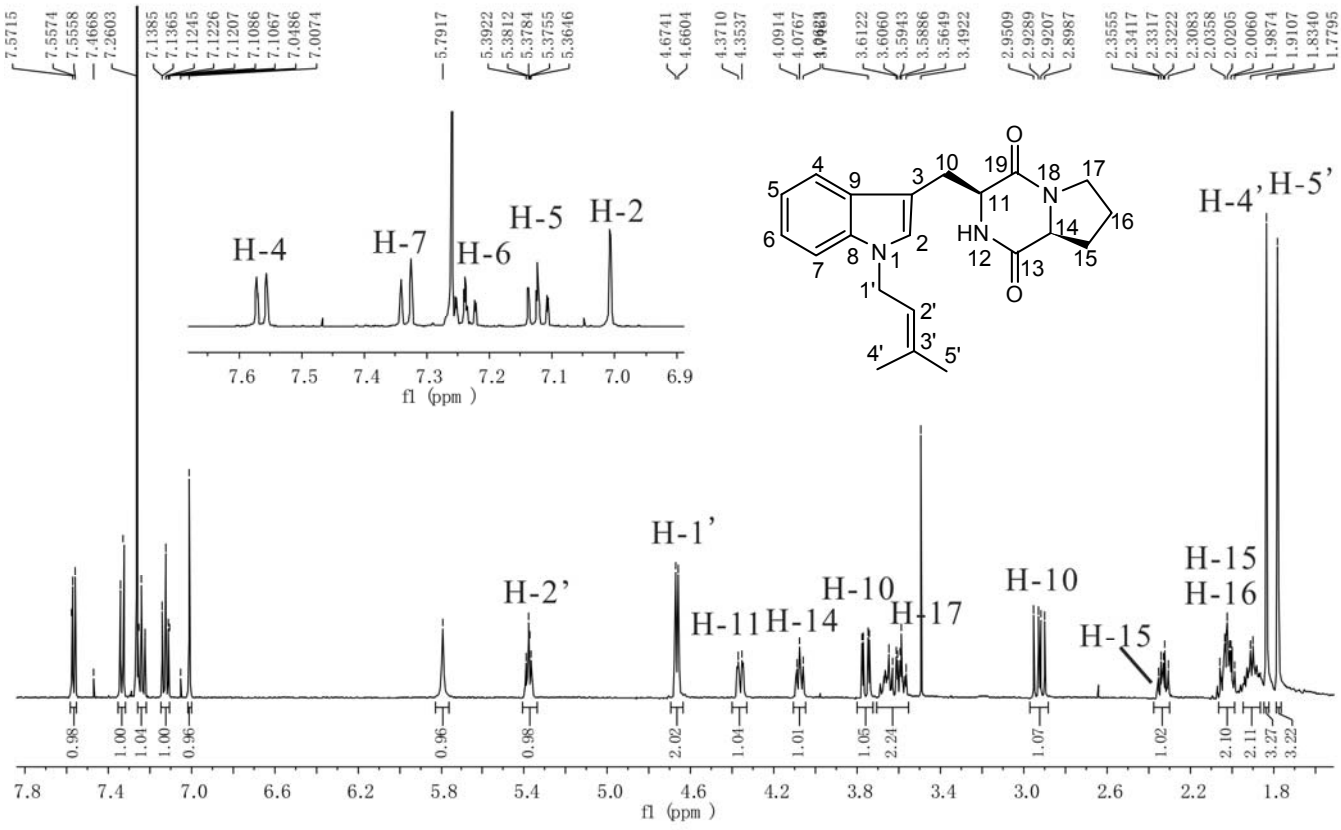

Fig. S15: ^{1}H-NMR spectrum of **5d** in $CDCl_3$ (500 MHz).

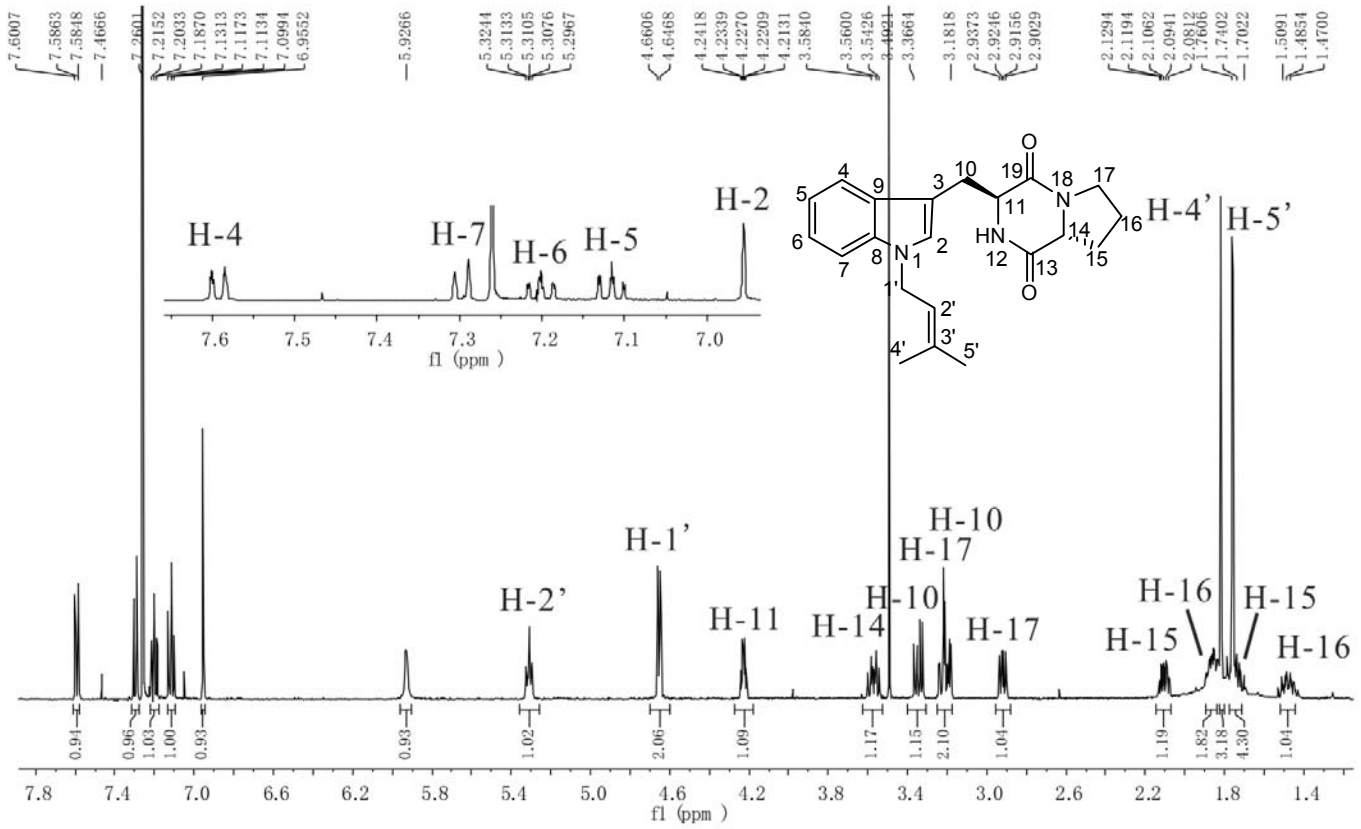

Fig. S16: ^{1}H-NMR spectrum of **6d** in $CDCl_3$ (500 MHz).

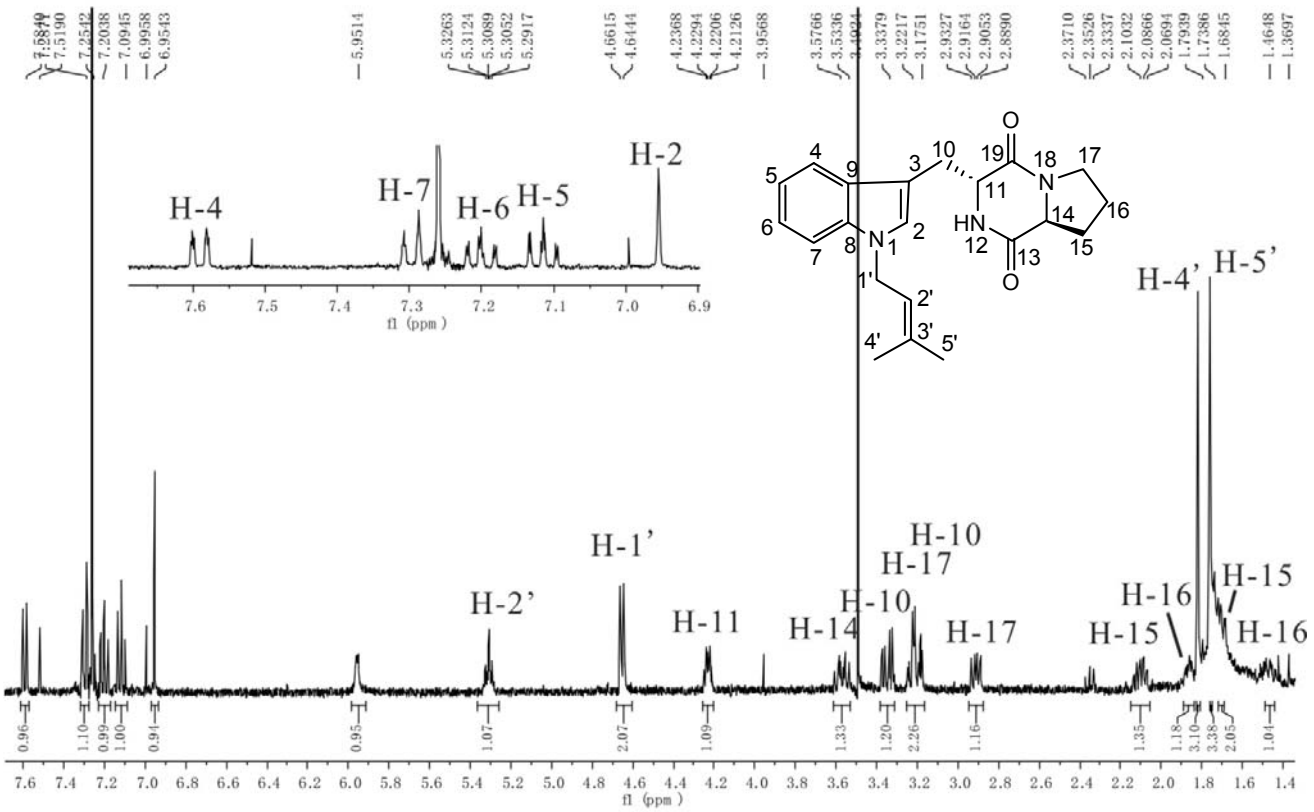

Fig. S17: ^{1}H-NMR spectrum of **8d** in $CDCl_3$ (400 MHz).

5.5 Friedel–Crafts alkylation on indolocarbazoles catalyzed by two dimethylallyltryptophan synthases from *Aspergillus*

Tetrahedron Letters 53 (2012) 6861–6864

Contents lists available at SciVerse ScienceDirect

Tetrahedron Letters

journal homepage: www.elsevier.com/locate/tetlet

Friedel–Crafts alkylation on indolocarbazoles catalyzed by two dimethylallyltryptophan synthases from *Aspergillus*

Xia Yu [a], Aigang Yang [b], Wenhan Lin [b], Shu-Ming Li [a,c,*]

[a] *Institut für Pharmazeutische Biologie und Biotechnologie, Philipps-Universität Marburg, Marburg 35037, Germany*
[b] *State Key Laboratory of Natural and Biomimetic Drugs, Peking University, Beijing 100191, China*
[c] *Zentrum für Synthetische Mikrobiologie, Philipps-Universität Marburg, Marburg 35032, Germany*

ARTICLE INFO

Article history:
Received 24 August 2012
Revised 5 October 2012
Accepted 9 October 2012
Available online 16 October 2012

Keywords:
Aspergillus
Enzyme catalysis
Indolocarbazoles
Prenylation

ABSTRACT

Prenylated indolocarbazoles have been reported neither from natural sources, nor by chemical synthetic approaches. In this Letter, we report a regiospecific prenylation of indolocarbazoles at the *para*-position of the indole N-atom by two recombinant enzymes from the dimethylallyltryptophan synthase (DMATS) superfamily, that is, 5-DMATS from *Aspergillus clavatus* and FgaPT2 from *Aspergillus fumigatus*.

Indolocarbazoles are a class of natural products with well known remarkable biological activities, especially their inhibitory effects against protein kinases in various organisms. Several of these compounds have already entered clinical trials for treatment of cancer and other diseases.[1,2] To overcome the activity promiscuity of naturally occurring indolocarbazoles such as staurosporine and K252d (Fig. 1) toward kinases,[3–5] numerous chemical strategies have been developed for the synthesis of their mimetics to provide specific kinase inhibitors.[6,7] Significant progress has also been achieved in the biosynthetic studies of indolocarbazoles. Identification and proof of biosynthetic genes for indolocarbazoles provided additional possibilities to create novel derivatives by combinatorial biosynthesis.[2,8] However, prenylated indolocarbazoles have been reported, neither from natural sources, nor from chemical synthetic approaches, although diverse prenylated carbazoles have been isolated from different sources.[6]

Prenylated derivatives are formed in the nature by transfer of $n \times$ C5 (n = 1, 2, 3, 4, or larger) units from their active forms, usually as diphosphate esters, to diverse acceptors. The responsible enzymes for the transfer reactions are different prenyltransferases, which are also successfully used as biocatalysts for the synthesis of prenylated compounds.[9–12] A large group of prenyltransferases belong to the dimethylallyltryptophan synthase (DMATS) superfamily. The members of this superfamily are involved in the biosynthesis of fungal secondary metabolites and catalyzed mainly the prenylation of diverse indole derivatives.[13] For example, FgaPT2 from *Aspergillus fumigatus* and 5-DMATS from *Aspergillus clavatus* catalyze the prenylation of L-tryptophan at C-4 and C-5, respectively, and therefore function as dimethylallyltryptophan synthases (Scheme 1).[14,15] It has also been demonstrated that some members of the DMATS superfamily catalyze even the prenylation of hydroxynaphthalenes and flavonoids.[16,17] These results encouraged us to test the acceptance of indolocarbazoles by members of the DMATS superfamily.

For this purpose, we synthesized four indolocarbazoles **1a**–**4a** (Scheme 2). Treatment of indole-3-acetamide with methyl indolyl-3-glyoxylate in the presence of KOBu^t afforded the intermediate arcyriarubin A,[18] which was converted to *N*-methylarcyriarubin A by treatment with methyl iodide.[19] Arcyriaflavin A (**1a**) and its N6-methylated derivative **4a** were obtained after oxidative

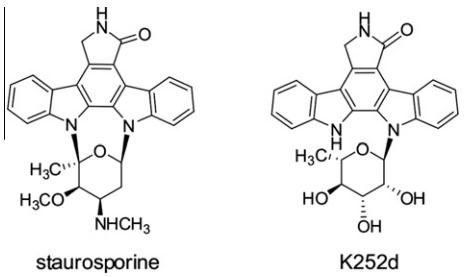

Figure 1. Structures of staurosporine and K252d.

* Corresponding author. Tel.: +49 6421 2822461; fax: +49 6421 2826678.
E-mail address: shuming.li@staff.uni-marburg.de (S.-M. Li).

0040-4039/$ - see front matter © 2012 Elsevier Ltd. All rights reserved.
http://dx.doi.org/10.1016/j.tetlet.2012.10.039

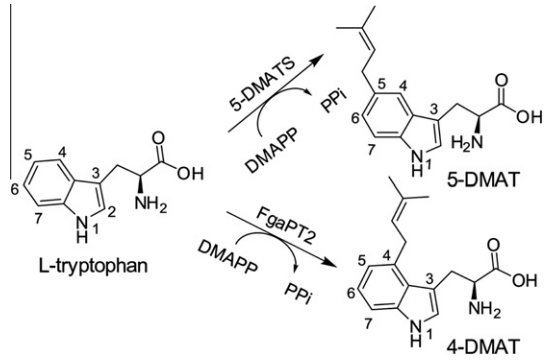

Scheme 1. Prenyltransfer reactions of 5-DMATS and FgaPT2 for their natural substrate L-tryptophan.

cyclization of the two bisindolylmaleimides arcyriarubin A and *N*-methylarcyriarubin A, respectively.[20,21] Reduction of **1a** with tin metal in AcOH/HCl and $LiAlH_4$ in THF resulted in the formation of K252c (**2a**)[21] and 7-hydroxy-K252c (**3a**),[22] respectively. The identities of the obtained compounds were confirmed by NMR and MS analyses. Unexpectedly, two product peaks **3a** and **3a*** were observed in the HPLC chromatogram of **3a** (Fig. 2). Reanalysis of the isolated single peak **3a** on HPLC revealed still the presence of both peaks. Furthermore, the ratios of **3a*** to **3a** were found to be nearly identical in all of the incubation mixtures with **3a**. However,

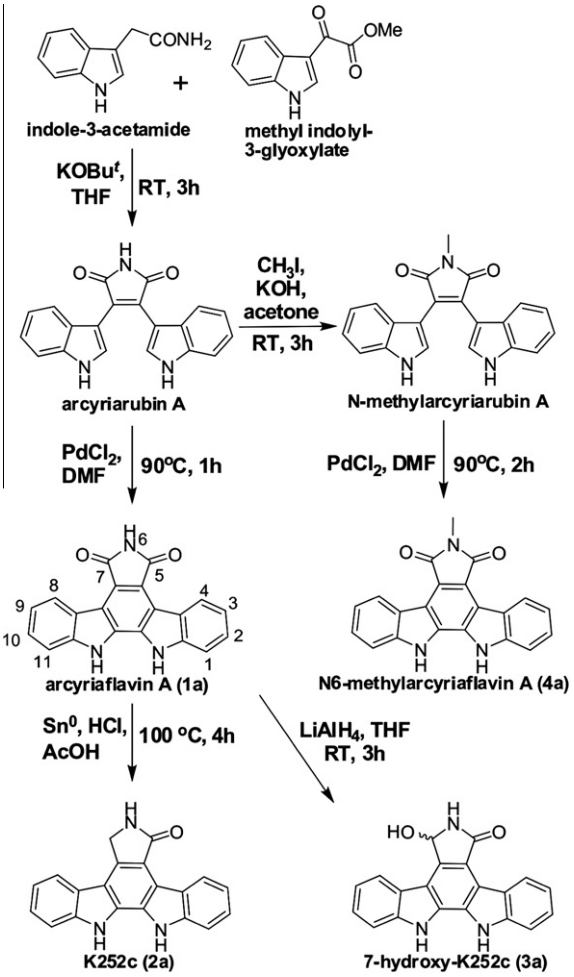

Scheme 2. Synthesis of bisindolylmaleimides and indolocarbazoles as substrates.

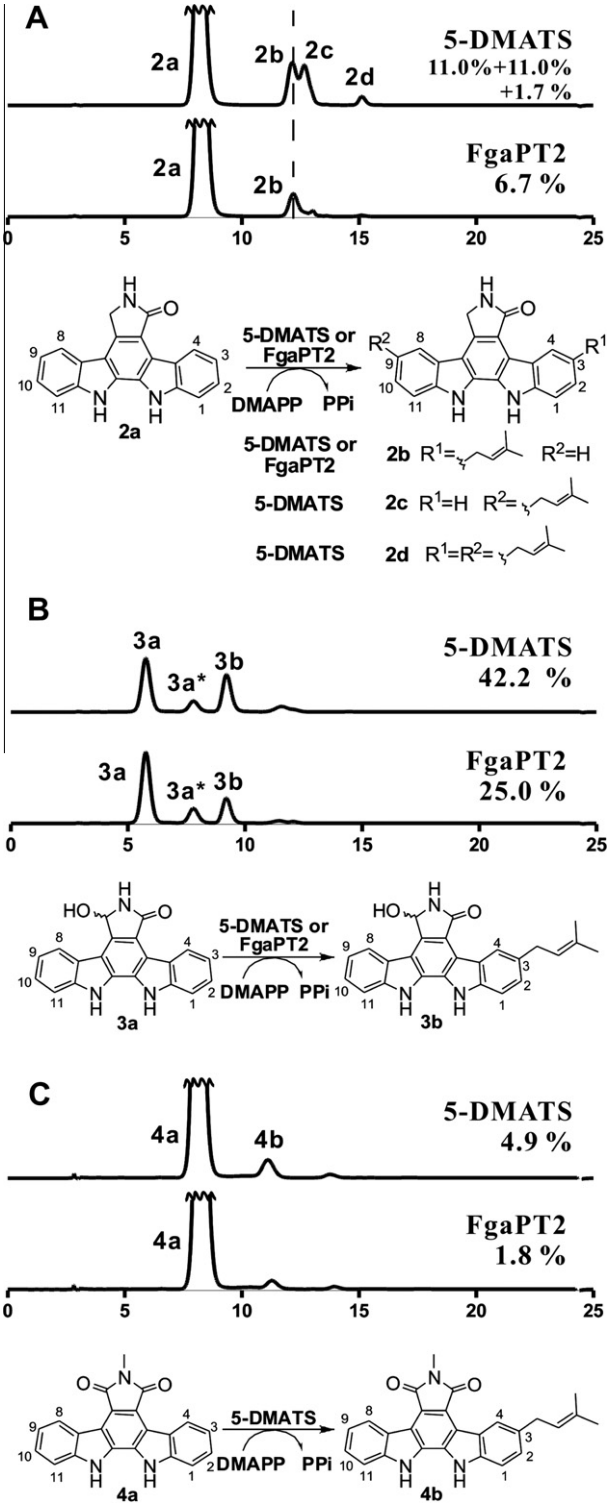

Figure 2. HPLC chromatograms and prenyl transfer reactions onto indolocarbazoles catalyzed by 5-DMATS and FgaPT2. The reaction mixtures (100 μl) containing 0.2 μg μl^{-1} of purified recombinant protein, 0.5 mM of aromatic substrate, and DMAPP in 50 mM Tris–HCl (pH 7.5) were incubated at 37 °C for 3 h. Detection was carried out on a Photodiode array detector and illustrated for absorption at 290 nm.

a ^{1}H NMR spectrum in DMSO-d_6 showed only signals for the structure of **3a**. It seems therefore that **3a*** is an isomer of **3a**, for example, a keto–enol tautomer at C-5 and N-6.

The two bisindolylmaleimides arcyriarubin A and *N*-methylarcyriarubin A, the four indolocarbazoles **1a**–**4a**, and two indolocarbazole glycosides staurosporine and K252d, which had been isolated from

Streptomyces nitrosporeus CQT14-24, were then incubated with nine prenyltransferases from the DMATS superfamily in the presence of dimethylallyl diphosphate (DMAPP). The tested enzymes included five cyclic dipeptide prenyltransferases AnaPT, BrePT, CdpC3PT, CdpNPT, and FtmPT1 with prenylation positions at C-2 or C-3 of the indole ring,[23–27] three dimethylallyltryptophan synthases FgaPT2, 5-DMATS, and 7-DMATS with prenylation positions at C-4, C-5, and C-7,[14,15,28] respectively. One tyrosine *O*-prenyltransferase SirD[29] was also tested. HPLC analysis showed that 5-DMATS from *Aspergillus clavatus* and FgaPT2 from *Aspergillus fumigatus* displayed more substrate flexibilities toward the tested substances than other enzymes (data not shown) and were studied in detail.

HPLC analysis of incubation mixtures with a 20 μg of 5-DMATS or FgaPT2 in 100 μl assay indicated that **1a** was poor substrate for both enzymes. 5-DMATS accepted **1a** only with a total conversion yield of 0.3%, while no product peak was detected in its incubation mixture with FgaPT2. Other three indolocarbazoles (**2a**–**4a**) were clearly accepted by both 5-DMATS and FgaPT2 (Fig. 2). Product formation was only detected in the incubation mixtures with active, but not in those with heat-inactivated proteins (by boiling for 20 min, data not shown). This demonstrated the importance of the oxidation grade at position C-7. Hydroxylation at this position seems better for acceptance by 5-DMATS than with a keto group. Detailed inspection of the HPLC chromatograms with **2a**–**4a** revealed that FgaPT2 showed generally a lower activity than 5-DMATS, proving again that different DMATS enzymes display different preference toward aromatic substrates.[17] Furthermore, more than one product peaks were detected in the reaction mixtures and the main product of both enzymes for a given substrate was proven to be identical (see below). For example, **2a** was converted by 5-DMATS into **2b**, **2c**, and **2d** with yields of 11, 11, and 1.7 %, respectively. **2a** was converted by FgaPT2 mainly into **2b** with a yield of 6.7 % (Fig. 2A). **3a**/**3a*** were converted into **3b** by 5-DMATS and FgaPT2 with conversion yields of 42 and 25%, respectively. The non-bridged intermediates of indolocarbazoles, that is, arcyriarubin A and *N*-methylarcyriarubin A, were not accepted by 5-DMATS and FgaPT2, indicating the importance of the presence of the indolocarbazole skeleton. Glycosides of indolocarbazoles, that is, staurosporine or K252d (Fig. 1), were also not prenylation substrates for the enzymes of the DMATS superfamily (data not shown).

For structure elucidation, three enzyme products **2b**, **2c**, and **2d** were isolated from the incubation mixture of 5-DMATS with **2a** and one each, that is, **3b** and **4b**, from those with **3a** and **4a**, respectively. **2b** and **3b** were also isolated from the reaction mixtures of FgaPT2 with **2a** and **3a**. All isolated enzyme products were subjected to MS and NMR analyses.

In the HPLC chromatograms of the incubation mixtures with **3a**, a minor product peak eluted after **3b** was also observed (Fig. 2B), which could be a prenylation product of **3a*** or formed by tautomerism of **3b**. Due to the low quantity, this minor product could not be isolated and identified. For the same reason, no enzyme product of **4a** with FgaPT2 and **1a** with 5-DMATS was isolated.

HR-EI-MS confirmed the monoprenylation in **2b**, **2c**, **3b**, and **4b** and diprenylation in **2d**, by detection of the molecular masses that are 68 and 136 Da larger than those of the respective substrate (Supplementary Table S1). The main enzyme products of FgaPT2 with **2a** and **3a** had identical ^{1}H NMR spectra as those of **2b** and **3b** from the 5-DMATS assays, respectively, proving the same structure of the enzyme products. The ^{1}H NMR signals at δ_H 3.48–3.52 (d, 2H-1′ or 2H-1″), 5.40–5.44 (t sep, H-2′ or H-2″), 1.77–1.79 (d, 3H-4′ or 3H-4″), and 1.73–1.75 ppm (d, 3H-5′ or 3H-5″) in the spectra of **2b**, **2c**, **2d, 3b**, and **4b** (Supplementary Figs. S1–S5, Table S2) revealed clearly the attachment of one regular dimethylallyl moiety to a C-atom.[17,30]

In the ^{1}H NMR spectra of the substrates **2a**–**4a** (Supplementary Figs. S6–S8), the aromatic signals appeared as two identical (**4a**) or different sets of four vicinal coupling protons (**2a** and **3a**). Each set contains two doublets and two triplets with coupling constants in the range of 7–9 Hz. In comparison, one set of signals in the ^{1}H NMR spectra of their enzyme products **2b**, **2c**, **3b**, and **4b** represent merely three protons. Two of these protons couple with each other with coupling constants of 7–9 Hz and the third one appears as a singlet or doublet with a small coupling constant of less than 2 Hz. These changes indicated that the prenylation had taken place at position C-2, C-3, C-9, or C-10. Similar phenomenon was also observed in both sets of aromatic signals in the ^{1}H NMR spectrum of **2d**, suggesting that one prenylation took place at C-2 or C-3 and the other at C-9 or C-10. Comparing the signals in the spectra of **2b**, **3b**, and **4b** with those of the respective substrate (Supplementary Figs. S6–S8) revealed that the H-4 was changed from a doublet with coupling constants of 7-9 Hz to another doublet with coupling constants small than 2 Hz, which was found in the low field in ^{1}H NMR spectra at approximately δ_H 9 ppm due to a characteristic deshielding effect from the lactam carbonyl,[31] confirming the prenylation at C-3 of **2b**, **3b**, and **4b**. In the ^{1}H NMR spectrum of **2c**, the signal of H-8 rather than that of H-4 was changed from a doublet to a singlet (Figure S6),[31] confirming that the prenylation had taken place at C-9. The structure of **2d** was assigned to a product with two prenyl moieties at C-3 and C-9, since both H-4 and H-8 were altered from doublets to singlets (Supplementary Fig. S6). This proved that both DMATS enzymes catalyzed the regiospecific C-prenyltion on the indolocarbazole system, that is, the *para*-position to the indole N-atom (C3, C9, or both) and function therefore as catalysts for Friedel–Crafts alkylations. A Friedel–Crafts alkylation catalyzed by strong Lewis acids would involve an allyl cation. This is also the case for the enzyme-catalyzed Friedel–Crafts alkylation described in this study. The formation of a dimethylallyl cation in an enzyme-catalyzed prenyl transfer reaction would be facilitated by interactions of several basic amino acid residues of the enzyme with pyrophosphate group of DMAPP.[32,33]

To elucidate the behavior of 5-DMATS and FgaPT2 toward indolocarbazoles, kinetic parameters were determined for the best accepted substrate **3a** with both enzymes by Hanes–Woolf and Eadia–Hofstee plots. Michaelis–Menten constants (K_M) were calculated to be at 87 and 136 μM for 5-DMATS and FgaPT2, respectively, while turnover numbers (k_{cat}) were found at 6.8 and 7.3 min^{-1}. The catalytic efficiency (k_{cat}/K_M) of 5-DMATS toward **3a** was 1302 s^{-1} M^{-1}, that is, 5.0 % of that of its best substrate L-tryptophan.[14] Similarly, A k_{cat}/K_M value of 891 s^{-1} M^{-1} was calculated for FgaPT2 toward **3a**, which is 3.0 % of that of L-tryptophan.[15] These data provided evidence that dimethylallyltryptophan synthases could also be used for the production of C-prenylated indolocarbazoles.

In conclusion, the present work demonstrated the acceptance of indolocarbazoles by fungal dimethylallyltryptophan synthases of the DMATS superfamily, which expands the potential usage of these enzymes in the structural modifications. To the best of our knowledge, this is the first report on the (chemoenzymatic) synthesis of prenylated indolocarbazoles.

Acknowledgments

This work was supported within the LOEWE program of the State of Hessen (SynMikro to S.-M. Li). Xia Yu is a recipient of a fellowship from China Scholarship Council. We thank Dr. Ortmann and Laufenberg for taking NMR and mass spectra.

Supplementary data

Supplementary data associated with this article can be found, in the online version, at http://dx.doi.org/10.1016/j.tetlet.2012.10.039.

References and notes

1. Sánchez, C.; Méndez, C.; Salas, J. A. *Nat. Prod. Rep.* **2006**, *23*, 1007–1045.
2. Nakano, H.; Ômura, S. *J. Antibiot.* **2009**, *62*, 17–26.
3. Karaman, M. W.; Herrgard, S.; Treiber, D. K.; Gallant, P.; Atteridge, C. E.; Campbell, B. T.; Chan, K. W.; Ciceri, P.; Davis, M. I.; Edeen, P. T.; Faraoni, R.; Floyd, M.; Hunt, J. P.; Lockhart, D. J.; Milanov, Z. V.; Morrison, M. J.; Pallares, G.; Patel, H. K.; Pritchard, S.; Wodicka, L. M.; Zarrinkar, P. P. *Nat. Biotechnol.* **2008**, *26*, 127–132.
4. Ruggeri, B. A.; Miknyoczki, S. J.; Singh, J.; Hudkins, R. L. *Curr. Med. Chem.* **1999**, *6*, 845–857.
5. Perez, S.; Sanchez, R.; Fernandez, B.; Mendez, F.; Salas, F.; Moris, V. WO Patent 2009125042A1, 2009.
6. Schmidt, A. W.; Reddy, K. R.; Knölker, H.-J. *Chem. Rev.* **2012**, *112*, 3193–3328.
7. Knölker, H.-J.; Reddy, K. R. *Chem. Rev.* **2002**, *102*, 4303–4427.
8. Salas, J. A.; Mendez, C. *Curr. Opin. Chem. Biol.* **2009**, *13*, 152–160.
9. Li, S.-M. *Appl. Microbiol. Biotechnol.* **2009**, *84*, 631–639.
10. Heide, L. *Curr. Opin. Chem. Biol.* **2009**, *13*, 171–179.
11. Sacchettini, J. C.; Poulter, C. D. *Science* **1997**, *277*, 1788–1789.
12. Yu, X.; Li, S.-M. In *Natural Product Biosynthesis by Microorganisms and Plants, Part B*; Hopwood, D. A., Ed.; Elsevier Science: California, 2012; Vol. 516, pp 259–278.
13. Li, S.-M. *Nat. Prod. Rep.* **2010**, *27*, 57–78.
14. Yu, X.; Liu, Y.; Xie, X.; Zheng, X.-D.; Li, S.-M. *J. Biol. Chem.* **2012**, *287*, 1371–1380.
15. Unsöld, I. A.; Li, S.-M. *Microbiology* **2005**, *151*, 1499–1505.
16. Yu, X.; Li, S.-M. *Chembiochem* **2011**, *12*, 2280–2283.
17. Yu, X.; Xie, X.; Li, S.-M. *Appl. Microbiol. Biotechnol.* **2011**, *92*, 737–748.
18. Faul, M. M.; Winneroski, L. L.; Krumrich, C. A. *J. Org. Chem.* **1998**, *63*, 6053–6058.
19. Nakazono, M.; Nanbu, S.; Uesaki, A.; Kuwano, R.; Kashiwabara, M.; Zaitsu, K. *Org. Lett.* **2007**, *9*, 3583–3586.
20. Burtin, G. E.; Madge, D. J.; Selwood, D. L. *Heterocycles* **2000**, *53*, 2119–2122.
21. Wilson, L. J.; Yang, C.; Murray, W. V. *Tetrahedron Lett.* **2007**, *48*, 7399–7403.
22. Harris, W.; Hill, C. H.; Keech, E.; Malsher, P. *Tetrahedron Lett.* **1993**, *34*, 8361–8364.
23. Yin, W.-B.; Grundmann, A.; Cheng, J.; Li, S.-M. *J. Biol. Chem.* **2009**, *284*, 100–109.
24. Yin, S.; Yu, X.; Wang, Q.; Liu, X. Q.; Li, S.-M. *Appl. Microbiol. Biotechnol.* **2012**. http://dx.doi.org/10.1007/s00253-012-4130-0.
25. Yin, W.-B.; Yu, X.; Xie, X.-L.; Li, S.-M. *Org. Biomol. Chem.* **2010**, *8*, 2430–2438.
26. Yin, W.-B.; Cheng, J.; Li, S.-M. *Org. Biomol. Chem.* **2009**, *7*, 2202–2207.
27. Grundmann, A.; Li, S.-M. *Microbiology* **2005**, *151*, 2199–2207.
28. Kremer, A.; Westrich, L.; Li, S.-M. *Microbiology* **2007**, *153*, 3409–3416.
29. Kremer, A.; Li, S.-M. *Microbiology* **2010**, *156*, 278–286.
30. Zou, H.-X.; Xie, X.; Zheng, X.-D.; Li, S.-M. *Appl. Microbiol. Biotechnol.* **2011**, *89*, 1443–1451.
31. Hudkins, R. L.; Johnson, N. W. *J. Heterocycl. Chem.* **2001**, *38*, 591–595.
32. Metzger, U.; Schall, C.; Zocher, G.; Unsöld, I.; Stec, E.; Li, S.-M.; Heide, L.; Stehle, T. *Proc. Natl. Acad. Sci. U.S.A.* **2009**, *106*, 14309–14314.
33. Jost, M.; Zocher, G.; Tarcz, S.; Matuschek, M.; Xie, X.; Li, S.-M.; Stehle, T. *J. Am. Chem. Soc.* **2010**, *132*, 17849–17858.

Electronic Supplementary Material for:

Friedel-Crafts alkylation on indolocarbazoles catalyzed by two dimethylallyltryptophan synthases from *Aspergillus*

Xia Yu [a], Aigang Yang [b], Wenhan Lin[b] and Shu-Ming Li [a,c,*]

[a] Institut für Pharmazeutische Biologie und Biotechnologie, Philipps-Universität Marburg, Marburg, Germany

[b] State Key Laboratory of Natural and Biomimetic Drugs, Peking University, Beijing, China

[c] Zentrum für Synthetische Mikrobiologie, Philipps-Universität Marburg, Marburg, Germany

* Corresponding author: Shu-Ming Li. Institut für Pharmazeutische Biologie und Biotechnologie, Philipps-Universität Marburg, Deutschhausstrasse 17A, 35037 Marburg, Germany

Tel.: +49 6421 2822461; fax: +49 6421 2826678.

E-mail address: shuming.li@staff.uni-marburg.de

Experimental section

Overproduction and purification of the recombinant proteins as well as enzyme assays with recombinant proteins

HPLC conditions for analysis and isolation of the enzyme products

Spectroscopic analyses

HR-EI-MS and NMR data

Table S1. HR-EI-MS data of the enzyme products of indolocarbazoles.

Table S2. ^{1}H-NMR data (400 MHz) of prenylated products in DMSO-d_6. Chemical shifts (δ) are given in ppm and coupling constants (J) in Hz.

NMR spectra

Figure S1. ^{1}H-NMR spectrum of **2b** in DMSO-d_6 (400 MHz).

Figure S2. ^{1}H-NMR spectrum of **2c** in DMSO-d_6 (400 MHz).

Figure S3. ^{1}H-NMR spectrum of **2d** in DMSO-d_6 (400 MHz).

Figure S4.1. ^{1}H-NMR spectrum of **3b** in DMSO-d_6 (400 MHz).

Figure S4.2. ^{1}H-NMR spectrum of **3b** in DMSO-d_6 (400 MHz) with addition of D_2O.

Figure S5 ^{1}H-NMR spectrum of **4b** in DMSO-d_6 (400 MHz).

Figure S6. Comparison of the aromatic signals in the ^{1}H-NMR spectrum of substrate **2a** with those of its prenylated products **2b**, **2c** and **2d** (in DMSO-d_6, 400 MHz).

Figure S7. Comparison of the aromatic signals in the ^{1}H-NMR spectrum of substrate **3a** with that of its prenylated product **3b** (in DMSO-d_6, 400 MHz).

Figure S8. Comparison of the aromatic signals in the ^{1}H-NMR spectrum of substrate **4a** with that of its prenylated product **4b** (in DMSO-d_6, 400 MHz).

Experimental section

Overproduction and purification of the recombinant proteins as well as enzyme assays with recombinant proteins

Protein overproduction and purification were carried out as described previously.[1, 2] The enzyme mixtures (100 µl) for determination of the relative activities (Figure 2) contained each of 50 mM Tris–HCl (pH 7.5), 0.5 mM aromatic substrate, 0.5 mM DMAPP, 5 mM $CaCl_2$, 5 % (v/v) DMSO, 0.15–1.5% (v/v) glycerol and 20 µg of purified protein. After incubation at 37°C for 3 h, the reaction mixtures were stopped by extraction with ethyl acetate for three times. For structure elucidation, enzyme products were isolated from large-scale incubations of 20-50 ml with the same condition described above.

HPLC conditions for analysis and isolation of the enzyme products

The enzyme products of the incubation mixtures were analyzed by HPLC on an Agilent series 1200 by using a Multospher 120 RP 18–5 µ column (250 x 4 mm, 5 µm, C+S Chromatographie Service, Langerwehe, Germany) at a flow rate of 1 ml•min^{-1}. Water (solvent A) and methanol (solvent B) were used as solvents. For analysis of enzyme assays with **2a** and **3a**, a linear gradient of 70-100 % (v/v) solvent B in 15 min was used. The column was then washed with 100 % solvent B for 5 min and equilibrated with 70 % (v/v) solvent B for 5 min. For analysis of enzyme assays with **4a**, a linear gradient of 85-100 % (v/v) solvent B in 15 min was used. The column was then washed with 100 % solvent B for 5 min and equilibrated with 85 % (v/v) solvent B for 5 min. For isolation of the enzyme products, the same HPLC equipment with a Multospher 120 RP 18–5 µ column (250 x 10 mm, 5 µm, C+S Chromatographie Service) was used. The flow rate was 2.5 ml•min^{-1}.

Spectroscopic analyses

High-resolution electron impact mass spectrometry (HR-EI-MS) was taken on Auto SPEC. Positive HR-EI-MS data of the enzyme products are listed in Table S1. NMR Spectra (Figures S1-S8) were recorded on a JEOL ECX-400 spectrometer. Chemical shifts (Table S2) were referenced to the signal of DMSO-d_6 at 2.50 ppm.

HR-EI-MS and NMR data

Table S1. HR-EI-MS data of the enzyme products of indolocarbazoles.

Compound	Chemical formula	HR-EI-MS data		Deviation (ppm)
		Calculated (M^+)	Measured	
2b	$C_{25}H_{21}N_3O$	379.1685	379.1699	-3.7
2c	$C_{25}H_{21}N_3O$	379.1685	379.1667	4.8
2d	$C_{30}H_{29}N_3O$	447.2311	447.2328	-3.9
3b	$C_{25}H_{21}N_3O_2$	395.1634	395.1681	-12.1
4b	$C_{26}H_{21}N_3O_2$	407.1634	407.1650	-3.9

Table S2. ^{1}H-NMR data of prenylated products in DMSO-d_6 (400 MHz). Chemical shifts (δ) are given in ppm and coupling constants (J) in Hz.

Compd	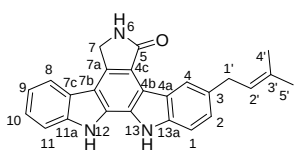 **2b**	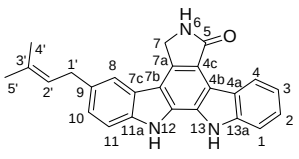 **2c**	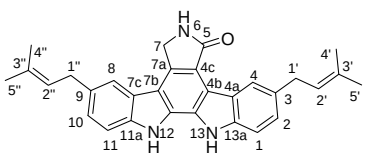 **2d**	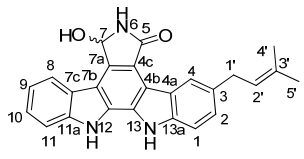 **3b**	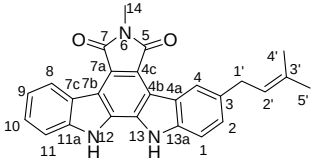 **4b**
Pos.	δ_H, multi., J	δ_H, multi., J	δ_H, multi., J	δ_H, multi., J	δ_H, multi., J
1	7.61, d, 8.3	7.71, br d, 8.3	7.60, d, 8.2	7.62, d, 8.3	7.67, d, 8.4
2	7.23, dd, 8.3, 1.5	7.41, ddd, 8.3, 7.1, 1.3	7.22, dd, 8.2, 1.8	7.24, dd, 8.3, 1.4	7.33, dd, 8.4, 1.7
3	-	7.22, ddd, 7.9, 7.1, 1.0	-	-	-
4	9.03, d, 1.5	9.20, br d, 7.9	9.02, br s	8.97, d, 1.4	8.80, d, 1.7
7	4.95, s	4.94, s	4.93, s	6.38, dd, 10.2, 1.1	-
8	8.03, br d, 7.8	7.81, br s	7.80, br s	8.36, br d, 7.9	8.96, dd, 8.0, 1.2
9	7.30, ddd, 7.8, 7.1, 0.9	-	-	7.27, ddd, 7.9, 7.1, 0.9	7.31, ddd, 8.0, 7.1, 0.9
10	7.46, ddd, 8.2, 7.1, 1.1	7.27, dd, 8.3, 1.6	7.26, dd, 8.3, 1.5	7.45, ddd, 8.2, 7.1, 1.2	7.51, ddd, 8.4, 7.1, 1.2
11	7.77, br d, 8.2	7.69, d, 8.3	7.67, d, 8.3	7.75, br d, 8.2	7.76, dd, 8.4, 0.9
14	-	-	-	-	3.15, s
1'	3.49, d, 7.4	3.52, d, 7.4	3.48, d, 7.3	3.49, d, 7.3	3.49, d, 7.3
2'	5.41, t sep, 7.4, 1.1	5.44, t sep, 7.4, 1.0	5.41, t sep, 7.3, 1.2	5.41, t sep, 7.3, 1.0	5.40, t sep, 7.3, 1.1
4'	1.79, d, 1.1	1.79, d, 1.0	1.79, d, 1.2	1.79, d, 1.0	1.77, d, 1.1
5'	1.74, d, 1.1	1.75, d, 1.0	1.74, d	1.74, d, 1.0	1.73, d, 1.1
1"	-	-	3.52, d, 7.4	-	-
2"	-	-	5.43, t sep, 7.4, 1.1	-	-
4"	-	-	1.78, d, 1.1	-	-
5"	-	-	1.74, d	-	-
NH	11.56, s	11.47, s	11.47, s	11.52, s	11.98, s
NH	11.29, s	11.39, s	11.29, s	11.29, s	11.98, s
NH	8.45, s	8.48, s	8.42, s	8.69, br s	-
OH	-	-	-	6.42, d, 10.2	-

NMR spectra

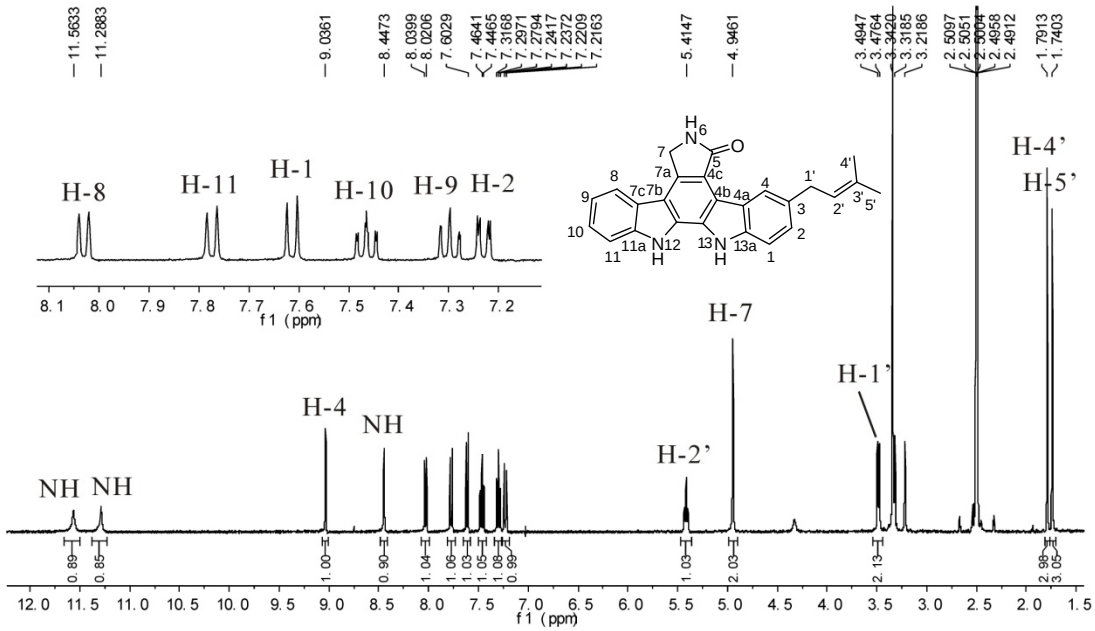

Figure S1. ^{1}H-NMR spectrum of **2b** in DMSO-d_6 (400 MHz).

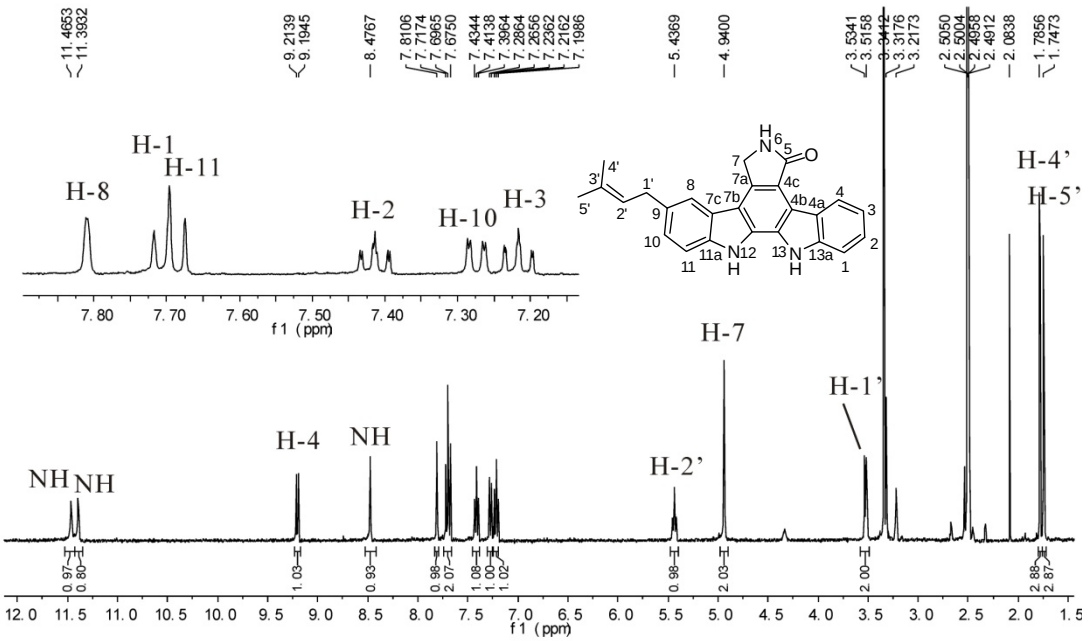

Figure S2. ^{1}H-NMR spectrum of **2c** in DMSO-d_6 (400 MHz).

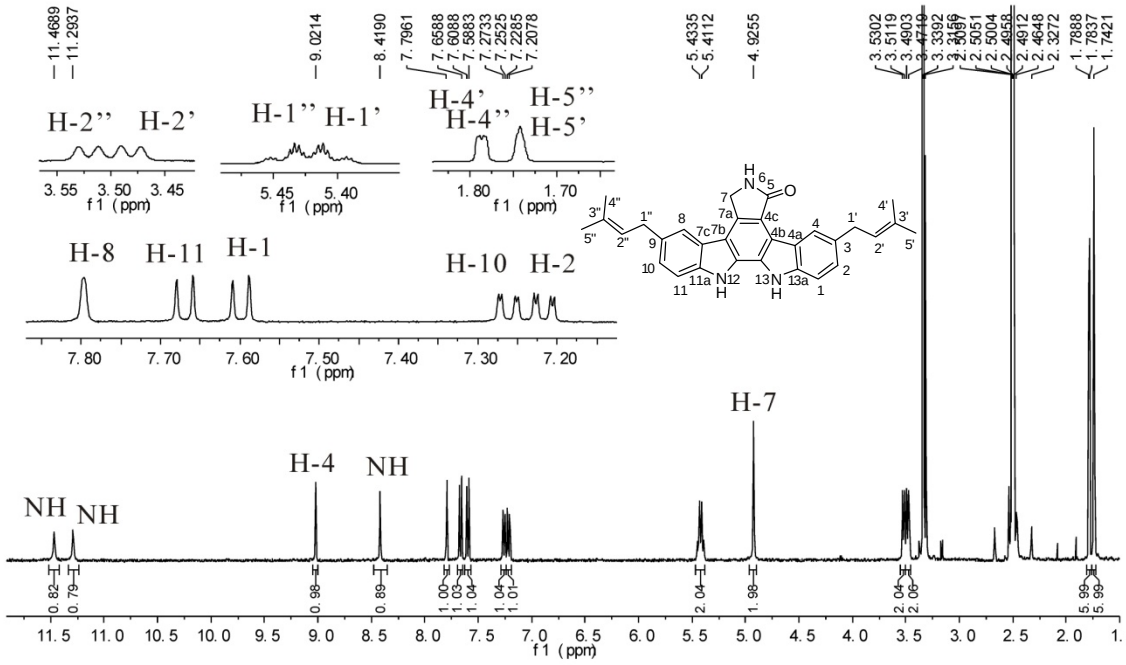

Figure S3. ^{1}H-NMR spectrum of **2d** in DMSO-d_6 (400 MHz).

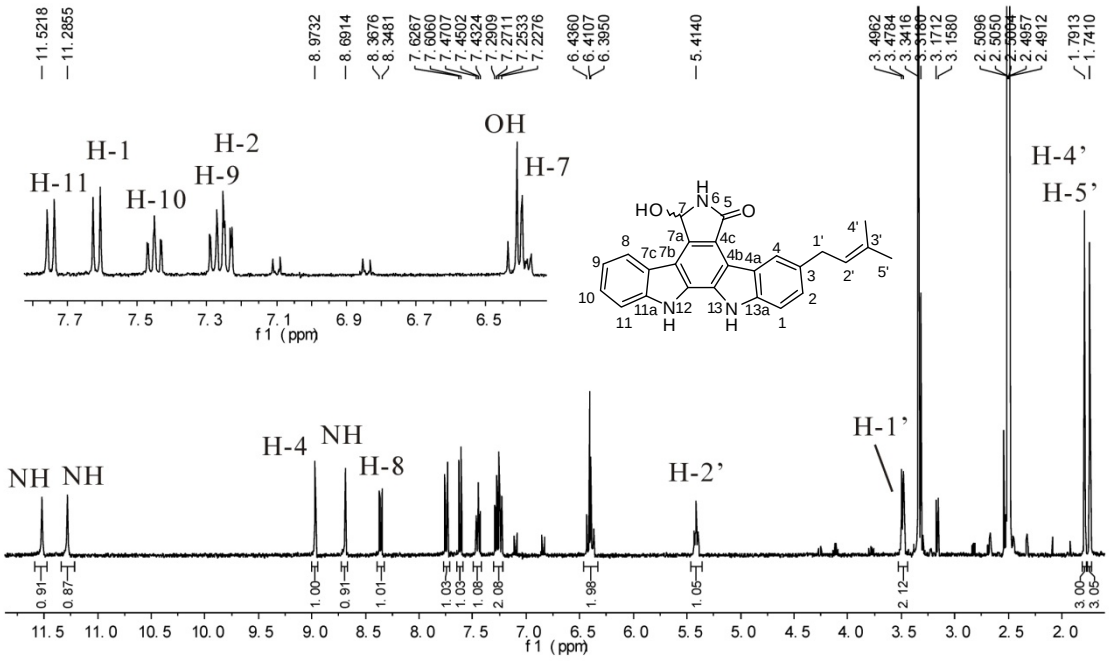

Figure S4.1. ^{1}H-NMR spectrum of **3b** in DMSO-d_6 (400 MHz).

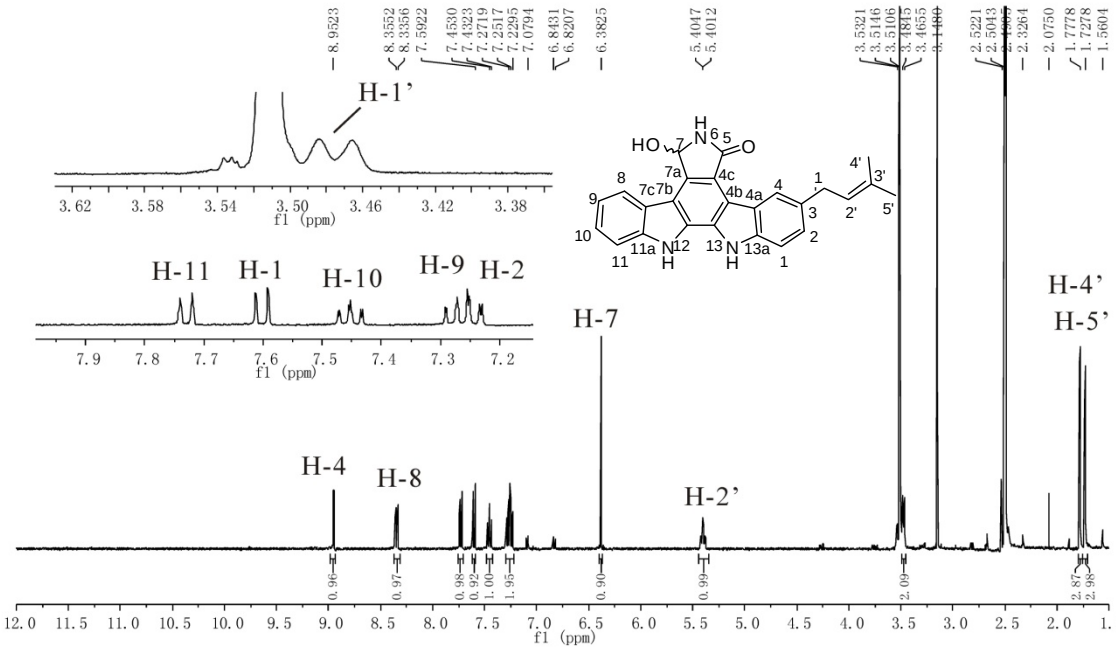

Figure S4.2. ^{1}H-NMR spectrum of **3b** in DMSO-d_6 (400 MHz) with addition of D_2O.

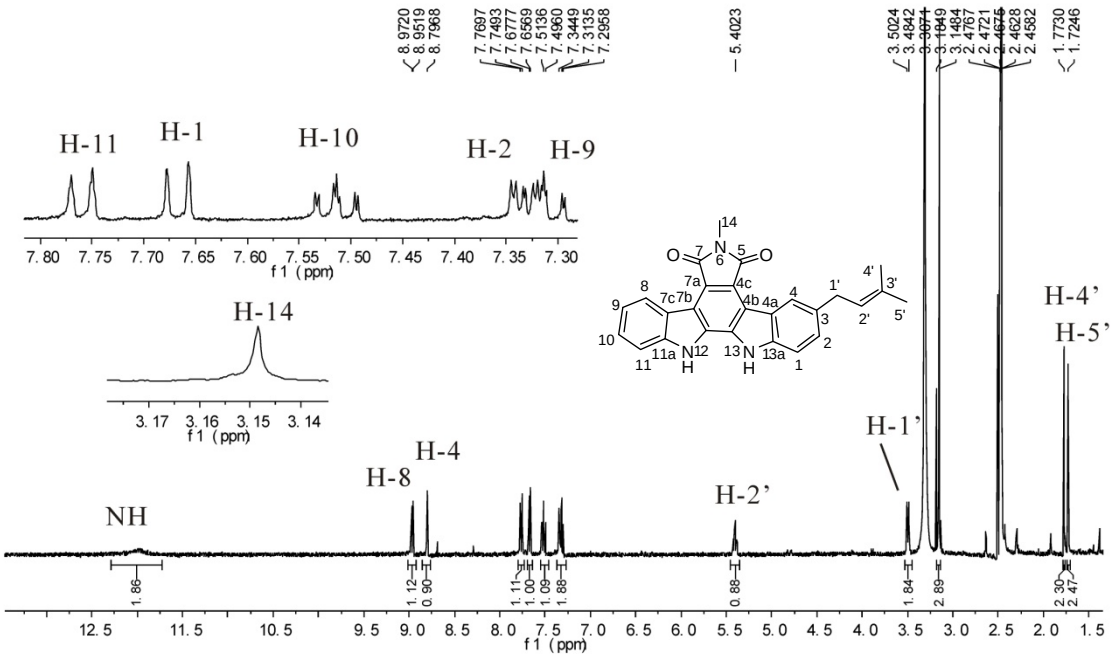

Figure S5 ^{1}H-NMR spectrum of **4b** in DMSO-d_6 (400 MHz).

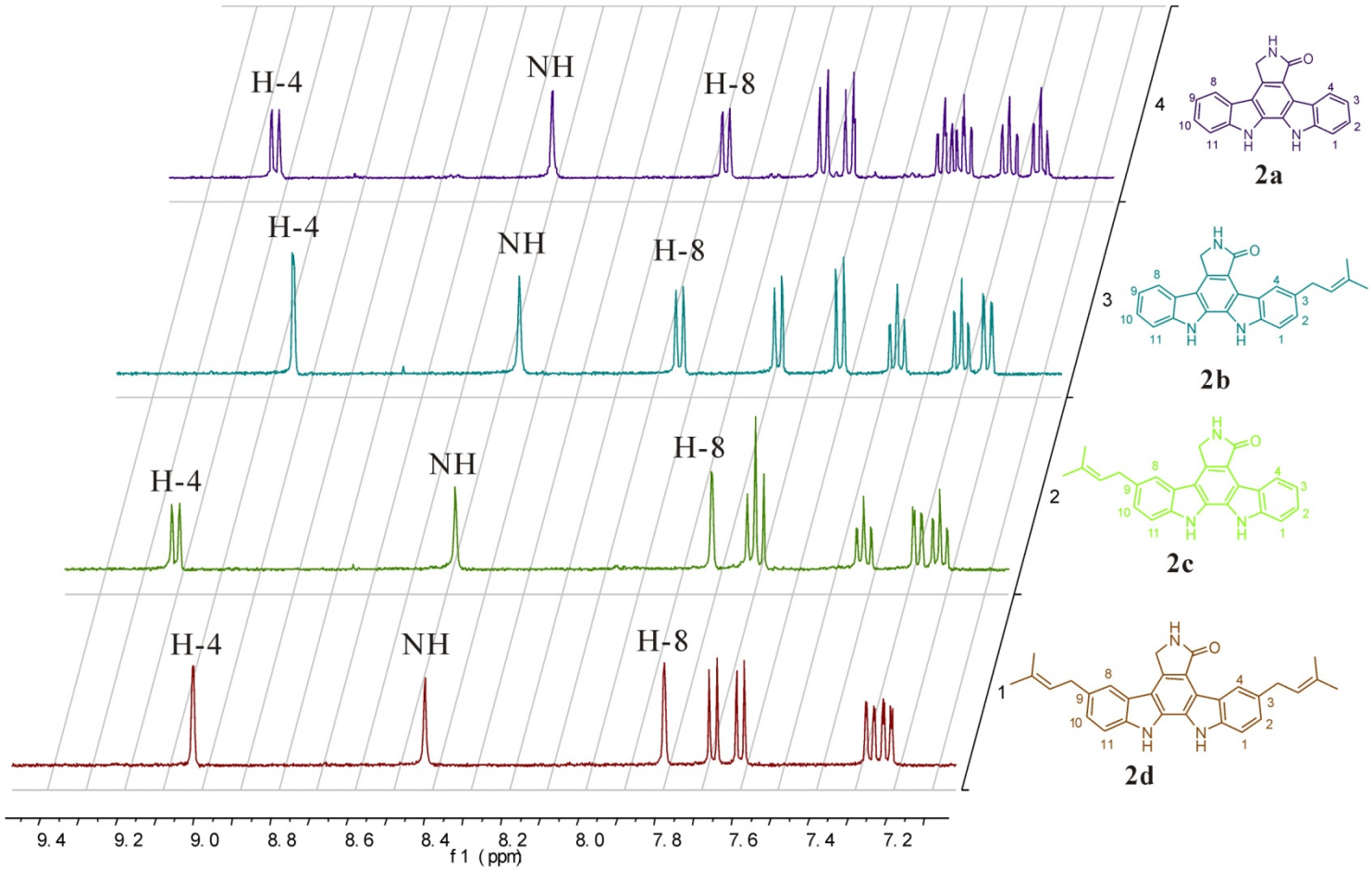

Figure S6. Comparison of the aromatic signals in the ^{1}H-NMR spectrum of substrate **2a** with those of its prenylated products **2b**, **2c** and **2d (**in DMSO-d_6, 400 MHz**)**.

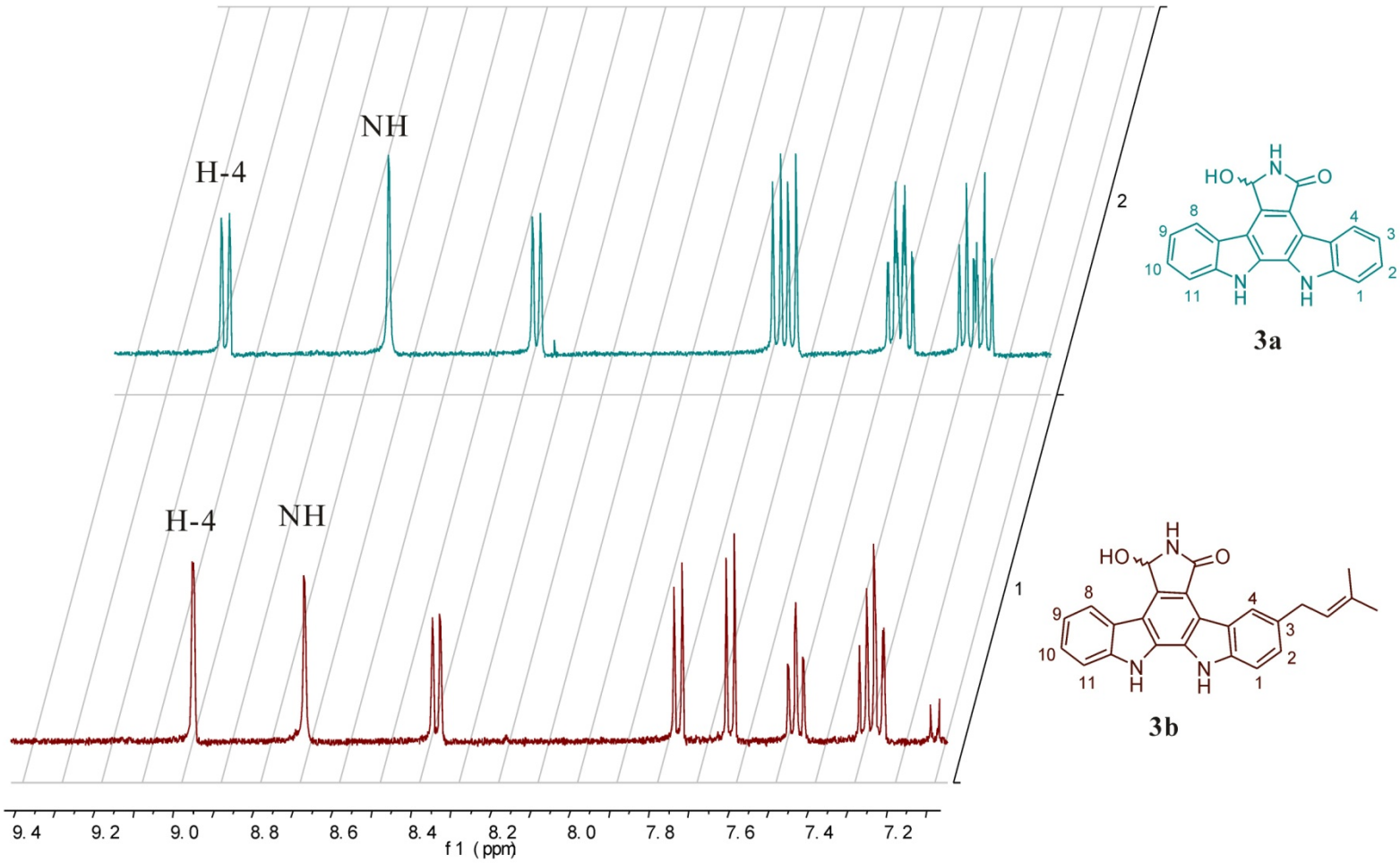

Figure S7. Comparison of the aromatic signals in the ^{1}H-NMR spectrum of substrate **3a** with that of its prenylated product **3b** (in DMSO-d_6, 400 MHz).

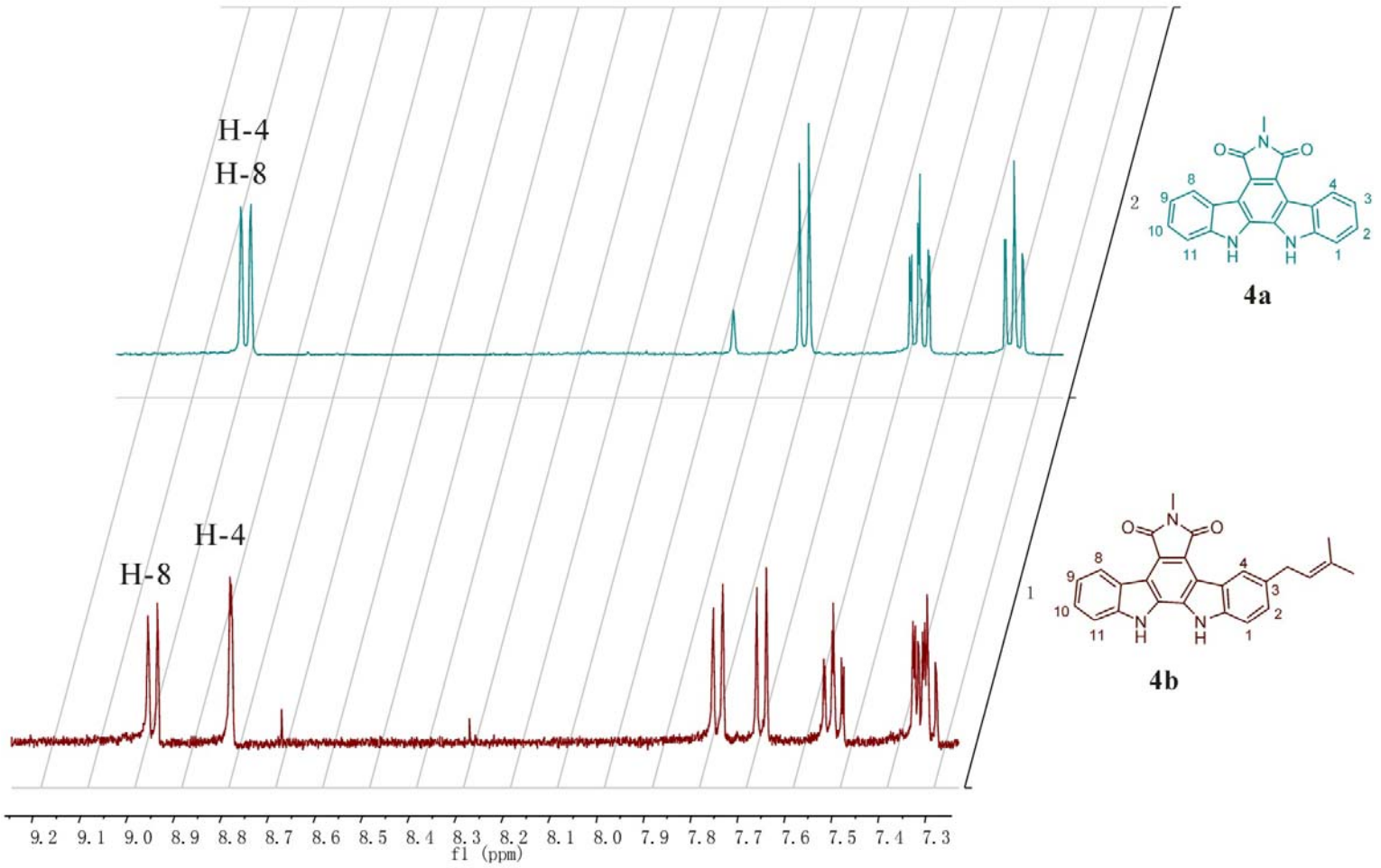

Figure S8. Comparison of the aromatic signals in the ^{1}H-NMR spectrum of substrate **4a** with that of its prenylated product **4b** (in DMSO-d_6, 400 MHz).

Reference List

1. Yu, X.; Liu, Y.; Xie, X.; Zheng, X.-D.; Li, S.-M. *J.Biol.Chem.* **2012**, *287*, 1371-1380.

2. Steffan, N.; Unsöld, I. A.; Li, S.-M. *Chembiochem* **2007**, *8*, 1298-1307.

5.6 Substrate promiscuity of secondary metabolite enzymes: prenylation of hydroxynaphthalenes by fungal indole prenyltransferases

Appl Microbiol Biotechnol (2011) 92:737–748
DOI 10.1007/s00253-011-3351-y

BIOTECHNOLOGICALLY RELEVANT ENZYMES AND PROTEINS

Substrate promiscuity of secondary metabolite enzymes: prenylation of hydroxynaphthalenes by fungal indole prenyltransferases

Xia Yu · Xiulan Xie · Shu-Ming Li

Received: 24 February 2011 / Revised: 9 April 2011 / Accepted: 20 April 2011 / Published online: 4 June 2011

Abstract Fungal prenyltransferases of the dimethylallyltryptophan synthase (DMATS) superfamily share no sequence, but structure similarity with the prenyltransferases of the CloQ/NphB group. The members of the DMATS superfamily have been reported to catalyze different prenylations of diverse indole or tyrosine derivatives, while some members of the CloQ/NphB group used hydroxynaphthalenes as prenylation substrates. In this study, we report for the first time the prenylation of hydroxynaphthalenes by the members of the DMATS superfamily. Three tryptophan-containing cyclic dipeptide prenyltransferases (AnaPT, CdpNPT and CdpC3PT), one tryptophan C7-prenyltransferase and one tyrosine *O*-prenyltransferase (SirD) were incubated with naphthalene and 11 derivatives. The enzyme activity and preference of the tested prenyltransferases towards hydroxynaphthalenes differed clearly from each other. For an accepted substrate, however, different enzymes produced usually the same major prenylation product, i.e. with a regular *C*-prenyl moiety at *para*- or *ortho*-position to a hydroxyl group. Regularly, *O*-prenylated and diprenylated derivatives were also identified as enzyme products of substrates with low conversion rates and regioselectivity. This was unequivocally proven by mass spectrometry and nuclear magnetic resonance analyses. The K_M values and turnover numbers (k_{cat}) of the enzymes towards selected hydroxynaphthalenes were determined to be in the range of 0.064–2.8 mM and 0.038–1.30 s^{-1}, respectively. These data are comparable to those obtained using indole derivatives. The results presented in this study expanded the potential usage of the members of the DMATS superfamily for production of prenylated derivatives including hydroxynaphthalenes.

Keywords Enzyme promiscuity · Fungal indole prenyltransferase · DMATS superfamily · Prenylated hydroxynaphthalenes

Electronic supplementary material The online version of this article (doi:10.1007/s00253-011-3351-y) contains supplementary material, which is available to authorized users.

X. Yu · S.-M. Li
Institut für Pharmazeutische Biologie und Biotechnologie,
Philipps-Universität Marburg,
Deutschhausstrasse 17A,
35037 Marburg, Germany

S.-M. Li (✉)
Zentrum für Synthetische Mikrobiologie,
Philipps-Universität Marburg,
35032 Marburg, Germany
e-mail: shuming.li@staff.uni-marburg.de

X. Xie
Fachbereich Chemie, Philipps-Universität Marburg,
Hans-Meerwein-Strasse,
35032 Marburg, Germany

Introduction

Prenyltransferases catalyze the transfer reactions of a prenyl moiety from a prenyl donor, usually as diphosphate, to a terpenoid, serine residue of a protein or an aromatic nucleus. They are found in all domains of the life and involved in the biosynthesis of primary and secondary metabolites (Heide 2009; Li 2009; Liang 2009; Yazaki et al. 2009). The prenylated compounds often possess pharmacological activity distinct from their non-prenylated precursors (Sings and Singh 2003; Williams et al. 2000), which makes prenyltransferases attractive not only for biologists but also for medicinal chemists and biotechnologists. Significant progress has been achieved in the last years on the molecular biological, biochemical and structural biological investigations of

prenyltransferases for aromatic substrates, such as benzoic acid, naphthalene or indole derivatives (Heide 2009; Li 2010). A number of indole prenyltransferases have been identified in fungi, mainly by genome mining, and characterized biochemically (Li 2010). These enzymes share clear sequence similarity with the dimethylallyltryptophan synthase (DMATS) from *Claviceps purpurea* (Tudzynski et al. 1999) and therefore referred as prenyltransferases of the DMATS superfamily (Haug-Schifferdecker et al. 2010). The members of the DMATS superfamily showed significant flexibility towards their aromatic substrates. Most of them used tryptophan-containing cyclic dipeptides as natural (AnaPT, FtmPT1 and NotF; Ding et al. 2010; Grundmann and Li 2005; Yin et al. 2009) or best substrates (CdpNPT and CdpC3PT; Ruan et al. 2008; Yin et al. 2010c) (Fig. 1a). FgaPT2 and 7-DMATS accepted tryptophan as substrate and function therefore as DMATS (Fig. 1b) (Kremer et al. 2007; Unsöld and Li 2005). At higher enzyme concentration, FgaPT2 accepted also cyclic dipeptides and FtmPT1 and CdpNPT tryptophan derivatives as prenylation substrates (Steffan and Li 2009; Zou et al. 2009). SirD shares significant sequence similarities with other enzymes from the DMATS superfamily and uses L-tyrosine as natural substrate (Fig. 1c) (Kremer and Li 2010; Zou et al. 2011).

The enzymes of the DMATS superfamily share almost no sequence similarity with other known prenyltransferases, e.g. the soluble prenyltransferases of the CloQ/NphB group from bacteria and fungi, which catalyze the prenylation of 4-hydroxyphenylpyruvate, phenazine and naphthalenes in the biosynthesis of secondary metabolites (Haug-Schifferdecker et al. 2010; Heide 2009). For example, the naphthalene prenyltransferases Fnq26, Fur7 and NphB from the CloQ/NphB group are involved in the biosynthesis of furanonaphthoquinone I (Haagen et al. 2007), furaquinocins (Kumano et al. 2010) and naphterpin

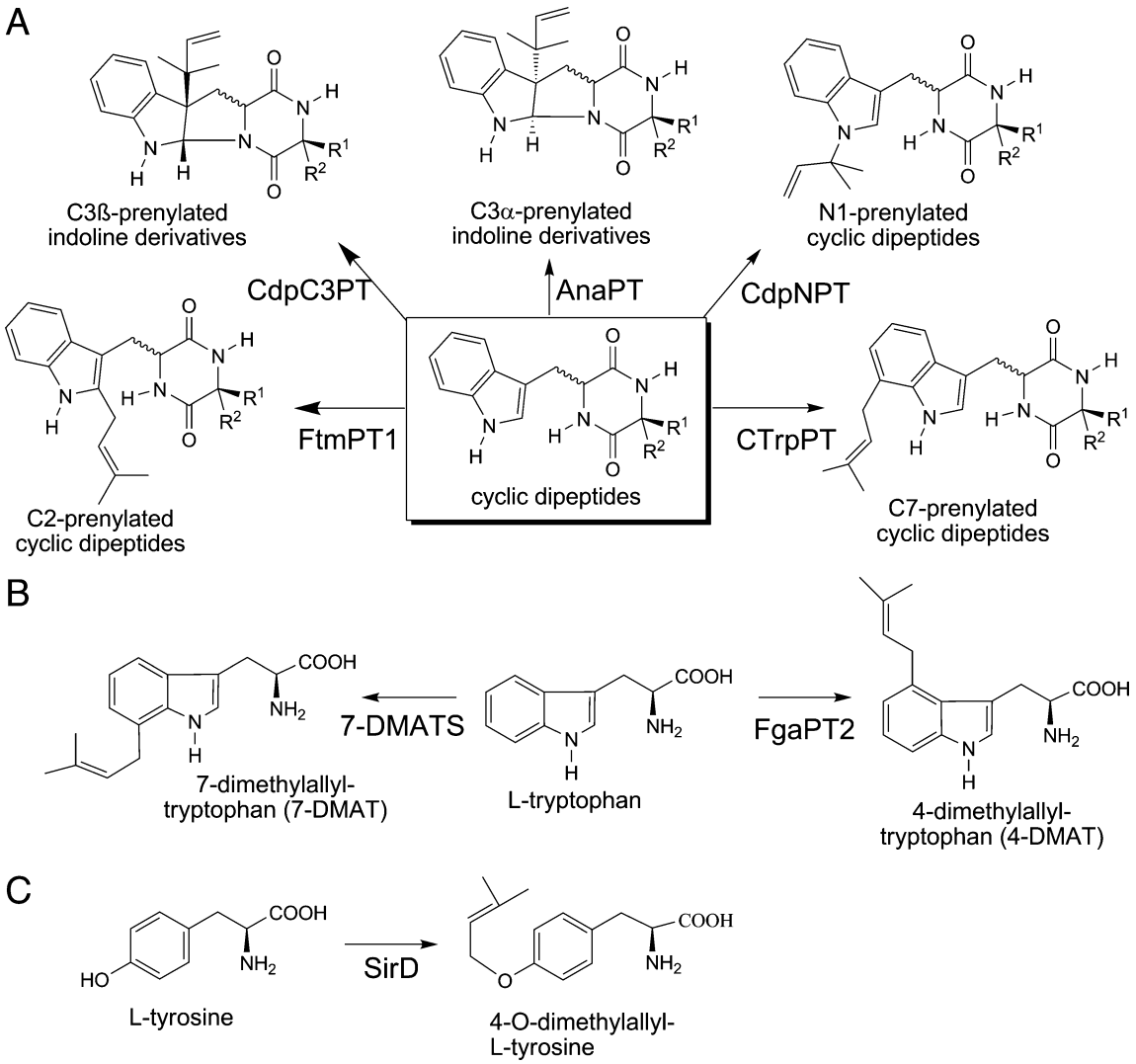

Fig. 1 Prenyl transfer reactions catalyzed by prenyltransferases of the DMATS superfamily towards **a** cyclic dipeptides; **b** L-tryptophan and **c** L-tyrosine

(Kumano et al. 2008), respectively. An acceptance of hydroxynaphthalenes by a member of the DMATS superfamily was not reported previously. Correspondingly, tyrosine or indole derivatives were not prenylated by enzymes of the CloQ/NphB group.

Interestingly, structure analysis revealed that FgaPT2 and FtmPT1 from the DMATS superfamily contain a PT barrel (Jost et al. 2010; Metzger et al. 2009), which has been only found in the bacterial aromatic prenyltransferases of the CloQ/NphB group (Kuzuyama et al. 2005; Metzger et al. 2010). This finding prompted us to investigate the acceptance of naphthalene derivatives by the members of the DMATS superfamily. Acceptance of hydroxynaphthalenes by prenyltransferases of the DMATS superfamily would increase structure diversity of prenylated hydroxynaphthalenes by chemoenzymatic synthesis approaches.

Materials and methods

Chemicals

Dimethylallyl diphosphate (DMAPP) was prepared according to the method described for geranyl diphosphate by Woodside et al. (1988). Naphthalene derivatives of the highest available purity were purchased from Fluka, TCI, Acros Organics, Aldrich and Alfa Aesar.

Overproduction and purification of recombinant proteins

Protein overproduction and purification were carried out as described previously: FgaPT2 (Steffan et al. 2007), FtmPT1 (Grundmann and Li 2005), AnaPT (Yin et al. 2009), CdpNPT (Yin et al. 2007), CdpC3PT (Yin et al. 2010b), 7-DMATS (Kremer et al. 2007), CTrpPT (Zou et al. 2010) and SirD (Kremer and Li 2010).

Enzyme assays with different prenyltransferases

The enzymatic reaction mixtures (100 μl) for determination of the relative activities with different hydroxynaphthalenes contained 50 mM Tris–HCl (pH 7.5), 5 mM (CdpC3PT and SirD) or 10 mM $CaCl_2$ (other enzymes), 1 mM aromatic substrate, 2 mM DMAPP, 0.15–1.5% (*v*/*v*) glycerol, 5% (*v*/*v*) dimethyl sulphoxide (DMSO) and 20 μg of purified recombinant protein. Under this condition, naphthalene (**1a**, Table 1) reached a final concentration of 0.2 mM, while other substrates were dissolved completely. The reaction mixtures were incubated at 37°C for 1 or 7 h. For structure elucidation, enzyme products were isolated from large-scale incubations of 5–70 ml with 0.2–0.3 mg protein per milliliter assay. For the determination of the kinetic parameters, the assays contained DMAPP at final concentrations of 2 or 5 mM (for CdpC3PT) and hydroxynaphthalenes at final concentrations of 0.02, 0.05, 0.1, 0.2, 0.5, 1, 2 and 5 mM. The protein amount and incubation time are given in Table 2.

Table 1 List of naphthalene and derivatives used in this study

Compounds	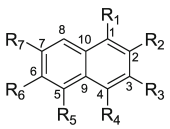						
	R_1	R_2	R_3	R_4	R_5	R_6	R_7
naphthalene (**1a**)	H	H	H	H	H	H	H
1-naphthol (**1b**)	OH	H	H	H	H	H	H
2-naphthol (**1c**)	H	OH	H	H	H	H	H
1,4-dihydroxynaphthalene (**1d**)	OH	H	H	OH	H	H	H
1,5-dihydroxynaphthalene (**1e**)	OH	H	H	H	OH	H	H
1,6-dihydroxynaphthalene (**1f**)	OH	H	H	H	H	OH	H
1,7-dihydroxynaphthalene (**1g**)	OH	H	H	H	H	H	OH
2,3-dihydroxynaphthalene (**1h**)	H	OH	OH	H	H	H	H
2,6-dihydroxynaphthalene (**1i**)	H	OH	H	H	H	OH	H
2,7-dihydroxynaphthalene (**1j**)	H	OH	H	H	H	H	OH
3,5-dihydroxy-2-naphthoic acid (**1k**)	H	COOH	OH	H	OH	H	H
3,7-dihydroxy-2-naphthoic acid (**1l**)	H	COOH	OH	H	H	H	OH

Table 2 Kinetic parameters of the tested prenyltransferases

Enzyme/substrate	Incubation		K_M (mM)	k_{cat} (s^{-1})	k_{cat}/K_M (s^{-1} M^{-1})	Percent[f]
	Protein (μg)	Time (min)				
AnaPT						
1-Naphthol (**1b**)	10	20	1.30	0.74	569	8.72
1,7-Dihydroxynaphthalene (**1g**)	10	20	0.30	0.34	1,133	17.4
2,6-Dihydroxynaphthalene (**1i**) [a]	20	20	1.90	0.043	23	0.35
3,5-Dihydroxy-2-naphthoic acid (**1k**)	20	20	0.68	0.063	93	1.43
3,7-Dihydroxy-2-naphthoic acid (**1l**)	20	20	1.10	0.10	91	1.40
(*R*)-Benzodiazepinedione [b]			0.23	1.5	6,522	100
CdpNPT						
1-Naphthol (**1b**)	5	5	0.25	1.30	5,200	1,040
1,6-Dihydroxynaphthalene (**1f**) [c]	5	5	0.20	0.16	800	160
Cyclo-L-Trp-L-Trp	2.5	10	0.18	0.09	500	100
CdpC3PT						
1-Naphthol (**1b**)	20	10	1.30	0.31	238	15.6
1,7-Dihydroxynaphthalene (**1g**)[d]	20	20	0.37	0.14	378	24.7
Cyclo-L-Trp-L-Leu	1.5	30	0.53	0.81	1,528	100
7-DMATS						
1-Naphthol (**1b**)	20	30	0.83	0.038	46	2.80
1,6-Dihydroxynaphthalene (**1f**)	10	15	0.29	0.12	414	25.2
1,7-Dihydroxynaphthalene (**1g**)	10	15	0.064	0.077	1,203	73.2
3,5-Dihydroxy-2-naphthoic acid (**1k**)	10	20	2.8	0.053	19	1.16
L-Trp[e]			0.14	0.23	1,643	100

The mean values from two independent experiments were calculated from Hanes–Woolf and Eadie–Hofstee plots

[a] Due to solubility, the concentration was only tested up to 5 mM

[b] Data were adopted from Yin et al. (2009)

[c] Substrate inhibition at 0.5 mM or higher concentrations

[d] Substrate inhibition at 1.0 mM or higher concentrations

[e] Data were adopted from Kremer et al. (2007)

[f] k_{cat}/K_M obtained by using indole derivatives as substrate was defined as 100%

The enzyme reactions were terminated by addition of 60 μl methanol per 100 μl reaction mixtures. The proteins were removed by centrifugation at 13,000×*g* for 20 min. For quantification of the enzyme activity, two independent incubations were carried out routinely.

Quantification of the enzyme products

Due to the unknown absorption coefficients of the enzyme products and the low quality of the isolated substances, conversion rates of the enzyme reactions were calculated with the help of ^{1}H-NMR spectra. For this purpose, incubations were taken in a large scale (10 ml) containing each of 1 mM aromatic substrate, 2 mM DMAPP, 5 or 10 mM $CaCl_2$ as mentioned above and 2 mg of purified protein. The reaction mixtures were extracted three times with ethyl acetate after incubation at 37°C for 24 h. After evaporation of the solvent, the residues of the ethyl acetate phase containing both substrate and enzyme products were subjected to ^{1}H-NMR analysis. The conversion rate of a given substrate was determined by comparison of the integrals of the enzyme products and the remained substrate in ^{1}H-NMR spectra. The absorption coefficients of the enzyme products were then calculated by high-performance liquid chromatography (HPLC) analysis of the samples after NMR analysis. For incubations with low conversion rates, e.g. <5%, ratio of peak areas of the product to sum of product and substrate was used.

HPLC conditions for analysis and isolation of the enzyme products

The enzyme products of the incubation mixtures were analyzed by HPLC on an Agilent series 1200 using a LiChrospher RP 18–5 column (125×4 mm, 5 μm, Agilent) at a flow rate of 1 ml min^{-1}. Water with 0.5% trifluoroacetic

acid (TFA; solvent A) and methanol with 0.5% TFA (solvent B) were used as solvents. For analysis of enzyme products, a linear gradient of 50–100% (*v*/*v*) solvent B in 20 min was used. The column was then washed with 100% solvent B for 5 min and equilibrated with 50% (*v*/*v*) solvent B for 5 min. For comparison of the enzyme activities towards 1-naphthol (**1b**, Table 1) versus tyrosine or indole derivatives shown in Fig. 2, a linear gradient of 40–100% (*v*/*v*) solvent B in 20 min was used. The column was then washed with 100% solvent B for 5 min and equilibrated with 40% (*v*/*v*) solvent B for 5 min. Detection was carried out by a photo diode array detector.

For isolation of the enzyme products, the same HPLC equipment with a Multospher 120 RP-18 column (250× 10 mm, 5 μm, C+S Chromatographie Service, Langenfeld, Germany) was used. A linear gradient of 65–100% (*v*/*v*) solvent B in 20 min at a flow rate of 2.5 ml min^{-1} was used. The column was then washed with 100% solvent B

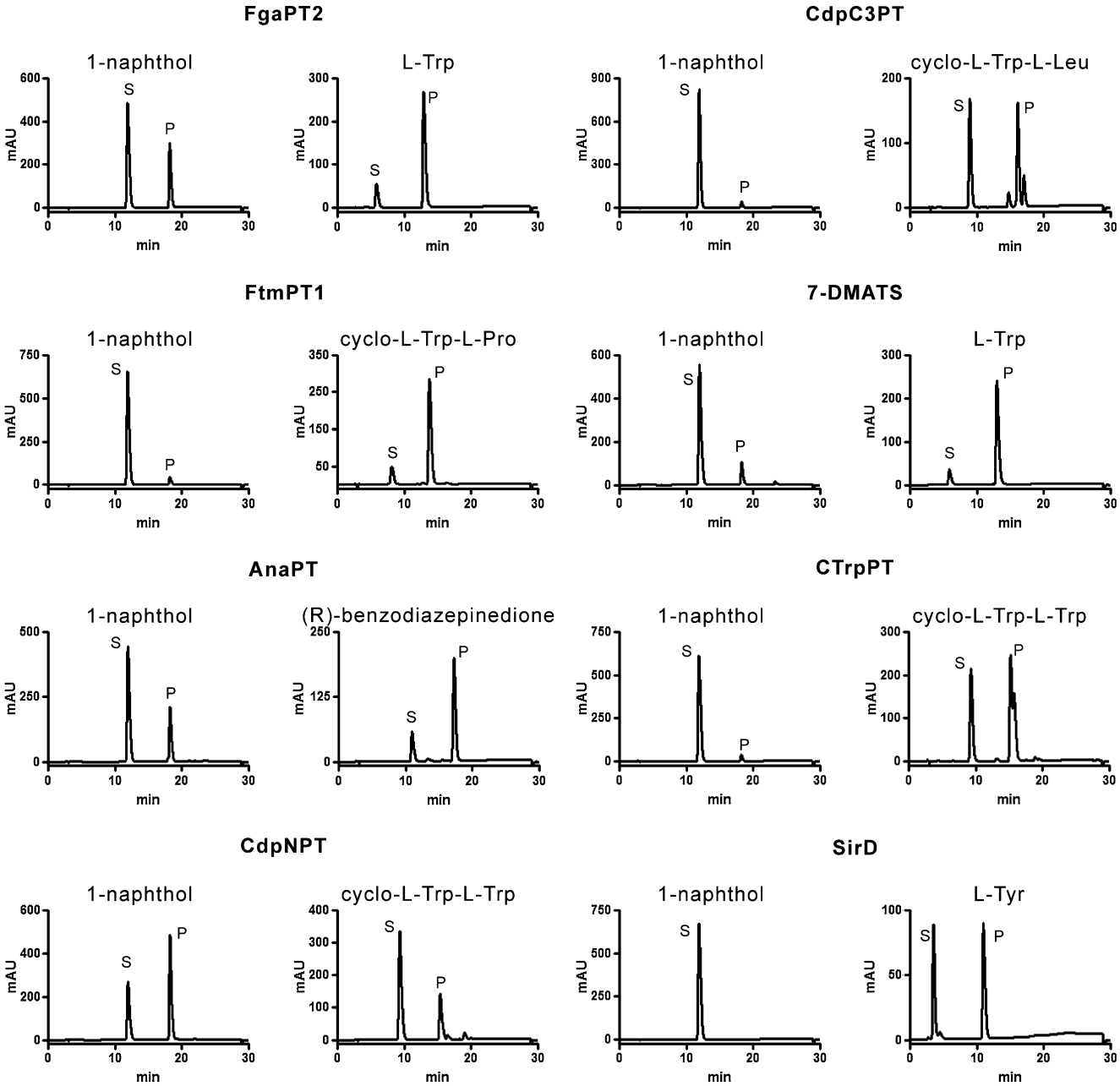

Fig. 2 HPLC chromatograms of incubation mixtures of 1-naphthol (**1b**) and tyrosine or indole derivatives with purified recombinant FgaPT2 (4.2 μg), FtmPT1 (5.0 μg), AnaPT (2.0 μg), CdpNPT (8.0 μg), CdpC3PT (5.0 μg), 7-DMATS (4.5 μg), CTrpPT (20 μg) or SirD (2.0 μg). The reaction mixtures in 100 μl scale contained 2 mM DMAPP and 1 mM aromatic substrate and were incubated at 30°C (FgaPT2 and FtmPT1) or 37°C (other enzymes) for 2 h. Detection was carried with a diode array detector and illustrated for absorption of 1-naphthol and indole derivatives at 296 nm. For L-tyrosine, the absorption at 277 nm was given (*S* substrate; *P* product)

for 8 min and equilibrated with 65% (*v*/*v*) solvent for 8 min. For isolation of the enzyme products from the incubation mixtures of **1i** and **1j**, repeated chromatography was carried out with different gradients. If necessary, acetonitrile instead of methanol was used as elution solvent.

NMR spectroscopic analysis

The isolated enzyme products were dissolved in 0.3 ml of CD_3OD. Samples were filled into 3 mm thin wall NMR sample tubes of Wilmad Labglass from Rototec-Spintec. Spectra were recorded at room temperature on a JEOL ECX 400 MHz, a Bruker Avance 500 MHz or an Avance 600 MHz spectrometer. The heteronuclear single quantum coherence (HSQC) and heteronuclear multiple bond correlation (HMBC) spectra were recorded with standard methods (Berger and Braun 2004). For HSQC spectra, 16 transients were used, while 32–64 transients were used for the HMBC spectra. ^1H spectra were acquired with 65,536 data points, while 2D spectra were collected using 4,096 points in the F_2 dimension and 512 increments in the F_1 dimension. Chemical shifts were referenced to those of CD_3OD. All spectra were processed with MestReNova.5.2.2

High-resolution electron impact mass spectra

The isolated products were also analyzed by high-resolution electron impact mass spectrometry (HR-EI-MS) on Auto SPEC. Positive HR-EI-MS data of the enzyme products are as following: **2b**, *m/z* 212.1230 (M^+) (calculated for $C_{15}H_{16}O$, 212.1201); **2f**: *m/z* 228.1162 (M^+) (calculated for $C_{15}H_{16}O_2$, 228.1150); **2g**, *m/z* 228.1154 (M^+) (calculated for $C_{15}H_{16}O_2$, 228.1150); **2i**, *m/z* 228.1163 (M^+) (calculated for $C_{15}H_{16}O_2$, 228.1150); **3i**, *m/z* 228.1146 (M^+) (calculated for $C_{15}H_{16}O_2$, 228.1150); **4i**, *m/z* 296.1787 (M^+) (calculated for $C_{20}H_{24}O_2$: 296.1776); **5i**: *m/z* 296.1789 (M^+) (calculated for $C_{20}H_{24}O_2$, 296.1776); **6i**, *m/z* 296.1768 (M^+) (calculated for $C_{20}H_{24}O_2$, 296.1776); **7i**, *m/z* 296.1762 (M^+) (calculated for $C_{20}H_{24}O_2$, 296.1776); **2j**, *m/z* 228.1180 (M^+) (calculated for $C_{15}H_{16}O_2$, 228.1150); **3j**, *m/z* 228.1161 (M^+) (calculated for $C_{15}H_{16}O_2$, 228.1150); **4j**, *m/z* 228.1159 (M^+) (calculated for $C_{15}H_{16}O_2$, 228.1150); **5j**: *m/z* 296.1781 (M^+) (calculated for $C_{20}H_{24}O_2$, 296.1776); **6j**, *m/z* 296.1772 (M^+) (calculated for $C_{20}H_{24}O_2$, 296.1776); **7j**, *m/z* 296.1773 (M^+) (calculated for $C_{20}H_{24}O_2$, 296.1776); **8j**, *m/z* 296.1787 (M^+) (calculated for $C_{20}H_{24}O_2$, 296.1776); **9j**, *m/z* 296.1786 (M^+) (calculated for $C_{20}H_{24}O_2$, 296.1776); **2k**, *m/z* 272.1068 (M^+) (calculated for $C_{16}H_{16}O_4$, 272.1049); **3k**, *m/z* 272.1087 (M^+) (calculated for $C_{16}H_{16}O_4$, 272.1049); **2l**, *m/z* 272.1083 (M^+) (calculated for $C_{16}H_{16}O_4$, 272.1049).

Results

1-Naphthol was accepted by seven of eight prenyltransferases of the DMATS superfamily

For initial investigation, eight prenyltransferases of the DMATS superfamily including five cyclic dipeptide prenyltransferases (FtmPT1, AnaPT, CdpC3PT, CdpNPT and CTrpPT), two dimethylallyltryptophan synthases (FgaPT2 and 7-DMATS) and one tyrosine *O*-prenyltransferase (SirD) were incubated with the simple naphthalene derivative 1-naphthol (**1b**, Table 1). Enzyme assays with the respective natural or best substrate described in previous studies (Grundmann and Li 2005; Kremer et al. 2007; Kremer and Li 2010; Unsöld and Li 2005; Yin et al. 2007, 2009, 2010c; Zou et al. 2010), i.e. L-tyrosine for SirD or indole derivatives for other enzymes, were used as positive controls. HPLC analysis was used for monitoring of product formation and carried out under the same condition. As shown in Fig. 2, product formation was observed in the incubation mixtures of all of the enzymes with tyrosine or indole derivatives, as reported previously (Kremer et al. 2007; Kremer and Li 2010; Ruan et al. 2008; Unsöld and Li 2005; Yin et al. 2009, 2010c; Zou et al. 2010). One additional peak each was also clearly detected in the incubation mixtures of FgaPT2, FtmPT1, AnaPT, CdpNPT, CdpC3PT, 7-DMATS and CTrpPT with **1b** and DMAPP. Formation of these peaks was strictly dependent on the presence of DMAPP and active enzymes (data not shown). These results demonstrated that these enzymes accepted not only tryptophan or tryptophan-containing cyclic dipeptides but also the hydroxynaphthalene **1b** as substrate. Product formation was not observed in the incubation mixture of SirD with **1b** and DMAPP.

Comparison of the relative enzyme activities towards indole derivatives and **1b** revealed a clear preference of most of the enzymes for indole derivatives (Fig. 2). However, high conversion rates of 33.9% and 28.8% were observed in the incubation mixtures of **1b** with FgaPT2 and AnaPT, respectively, although these values are lower than those with their natural substrates L-tryptophan at 80.4% and (*R*)-benzodiazepinedinone at 74.2%. The conversion rate of CdpNPT with **1b** was found to be 60.2%, significantly higher than that with one of the best substrates cyclo-L-Trp-L-Trp of 14.8%, (Ruan et al. 2008). Inspection of the HPLC chromatograms revealed additionally that the enzyme products of **1b** with the seven mentioned indole prenyltransferases had the same retention time of 18.2 min, indicating the possibility of the presence of the same product. The intriguing results obtained with **1b** encouraged us to test the acceptance of more hydroxynaphthalenes by the members of the DMATS family.

Different preference of indole prenyltransferases towards hydroxynaphthalenes

Five enzymes including AnaPT, CdpC3PT, CdpNPT, 7-DMATS and SirD were selected for incubation with naphthalene (**1a**) and 11 derivatives listed in Table 1. The reaction mixtures containing 5% (*v*/*v*) DMSO and 20 μg of purified protein each were incubated in the presence of DMAPP for 1 and 7 h. HPLC analysis was used for monitoring the enzyme product formation. Incubations with heat-inactivated proteins by boiling the proteins for 20 min were used as control assays.

As given in Table S1 (Electronic supplementary material), naphthalene (**1a**) in a final concentration of 0.2 mM was accepted by none of the tested enzymes, indicating the importance of activation of the naphthalene ring, e.g. by hydroxylation. All of the 11 hydroxynaphthalenes (**1b**–**1l**) were accepted by AnaPT. A conversion rate of more than 10% was observed for eight substrates after 1 h and for ten after 7 h. 7-DMATS and CdpNPT accepted nine of the 11 substrates after incubation for 1 h. In comparison to AnaPT, CdpNPT and 7-DMATS, hydroxynaphthalenes were poor substrates for CdpC3PT and SirD. Although CdpC3PT accepted most of the tested hydroxynaphthalenes, the conversion rates were very low (Table S1). Comparison of the conversion rates showed that 1-naphthol (**1b**) and 1,7-dihydroxynaphthalene (**1g**) were well accepted by AnaPT, 7-DMATS and CdpNPT. In addition, 1,6-dihydroxynaphthalene (**1f**) was found to be the best substrate for 7-DMATS with conversion rates of 73.3% and 92.6% after incubation for 1 and 7 h, respectively.

The data in Table S1 showed furthermore that the positions of the hydroxyl groups are important for the acceptance of these compounds. Reduction in enzyme activities of more than 75% was observed for AnaPT, CdpNPT, CdpC3PT and 7-DMATS if the hydroxyl group of **1b** was moved from position C1 to C2 as in the structure of **1c**. No product formation with **1c** was detected after incubation with CdpC3PT for 1 h. Addition of one hydroxyl group to position C4 of **1b** as in the structure of **1d** caused even more loss of enzyme activities. Addition of one hydroxyl group to C6 at the second ring (**1f**) increased the activity of 7-DMATS to 333% after 1 h, in comparison to that of **1b**. Placing this hydroxyl group to C7 (**1g**) increased slightly the activity of AnaPT, but strongly that of 7-DMATS, in comparison to those of **1b**. Dihydroxynaphthalenes with one of the hydroxyl groups at C1 were generally better accepted by indole prenyltransferases than those with a hydroxyl group at C2, as detected for 7-DMATS, CdpNPT and CdpC3PT in the incubation mixtures with **1f** and **1i**. Similar phenomenon was also observed in the reaction mixtures of **1g** and **1j** with AnaPT, 7-DMATS, CdpNPT and CdpC3PT. Interestingly, moderate conversion rates of 14–20% after incubation for 1 h were observed for naphthoic acids like **1k** with AnaPT and 7-DMATS as well as **1l** with AnaPT.

Same prenyl transfer reaction onto hydroxynaphthalenes catalyzed by different indole prenyltransferases

For product isolation and structure elucidation, HPLC chromatograms of incubation mixtures of seven hydroxynaphthalenes (**1b**, **1f**, **1g**, **1i**, **1j**, **1k** and **1l**) with AnaPT, 7-DMATS, CdpNPT, CdpC3PT and SirD for 7 h (Fig. 3) are inspected in detail. Conversion rates of 15% or more were observed in 14 of the 35 incubation mixtures. With the exceptions of incubation mixtures of **1i** and **1k** with AnaPT and **1j** with CdpNPT, 7-DMATS and AnaPT (Fig. 3d–f), one or one dominant product was detected in these mixtures. In the case of **1k** (Fig. 3f), two products with comparable yields were observed. Incubations with low conversions showed more frequently two or more product peaks, e.g. AnaPT and 7-DMATS with **1i** and **1j** (Fig. 3d, e) as well as CdpNPT with **1j** (Fig. 3e).

Most interestingly, the major products of one given substrate with different enzymes had usually the same retention time (Fig. 3a–f), as observed for **1b** mentioned above (Fig. 2). To prove that the product peaks with the same retention time deal really with the same compound, the dominant products of **1b** and **1g** in the incubation mixtures of AnaPT, CdpNPT, CdpC3PT and 7-DMATS, i.e. **2b** and **2g** (Fig. 3a, c), were isolated on HPLC separately and subjected to ^{1}H-NMR analysis. Similar experiments were also carried out for **2f** from the incubation mixtures of **1f** with 7-DMATS and CdpNPT (Fig. 3b) as well as **2j** from those of **1j** with AnaPT, 7-DMATS and CdpNPT (Fig. 3e). The four samples (**2b**, Fig. 3a**)** isolated from the incubation mixtures of AnaPT, CdpNPT, CdpC3PT and 7-DMATS with **1b** showed identical ^{1}H-NMR spectra (data not shown) and confirmed the presence of the identical structure. This proved that the four enzymes catalyzed the same prenylation reaction on **1b**. It can be deduced that the enzyme products of FgaPT2, FtmPT1 and CTrpPT with **1b** mentioned above (Fig. 2) have also the same structure as that of **2b**. The same conclusion was also proven to be valid for **2f**, **2g** and **2j** from different reaction mixtures. In addition, the products of **1i**, **1k** and **1l** (Fig. 3d, f and g) were isolated from their incubation mixtures with AnaPT.

para-Position to the hydroxyl group at C1 of naphthalene ring is the favored prenylation position for indole prenyltransferases

The main products **2b**, **2f**, **2g**, **2i**, **2j**, **2k**, **3k** and **2l** were subjected to MS and NMR analyses. HR-EI-MS (see 'Materials and methods') confirmed the monoprenylation in the isolated enzyme products by detection of molecular

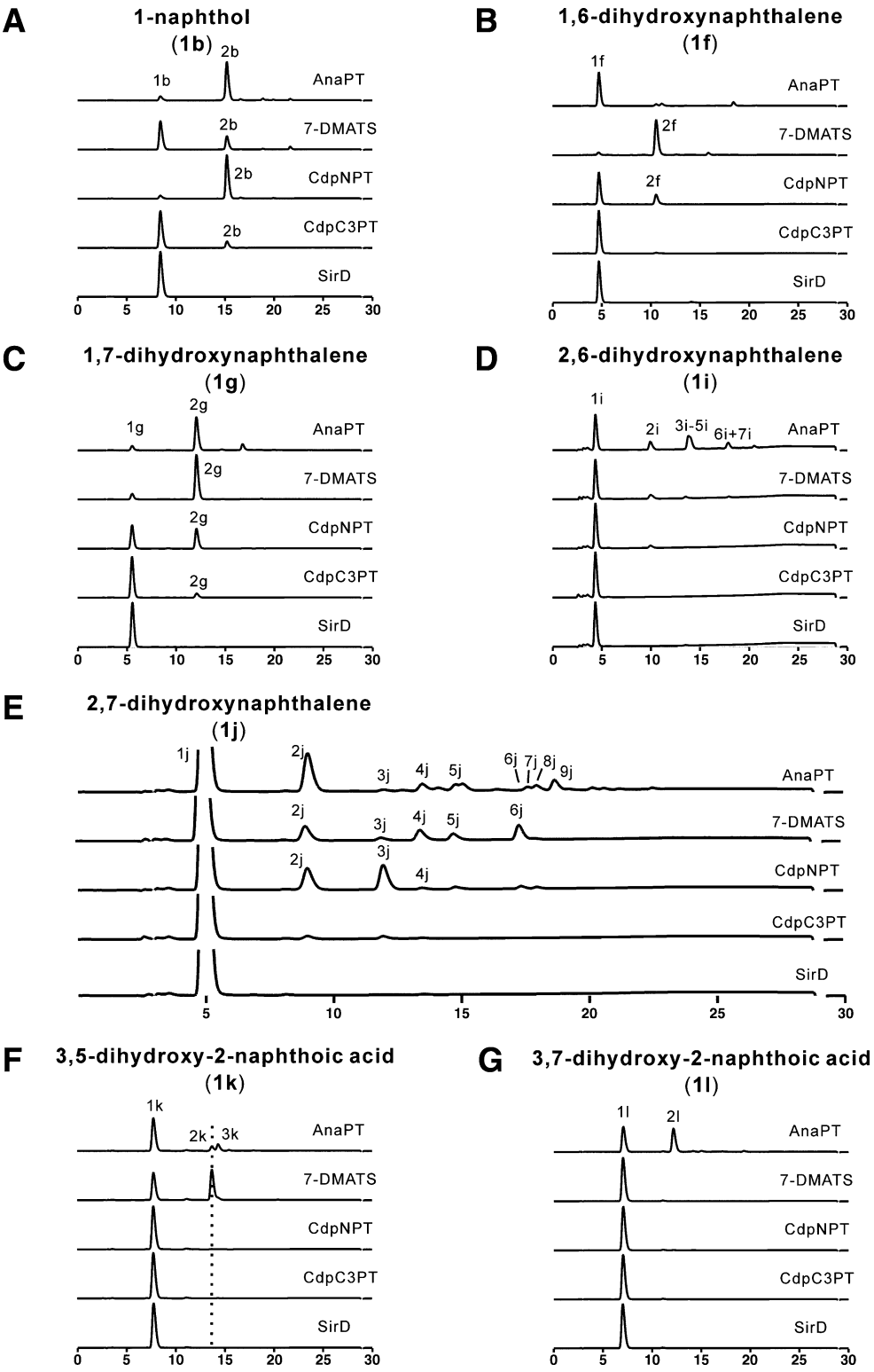

Fig. 3 HPLC chromatograms of incubation mixtures of selected hydroxynaphthalenes with recombinant AnaPT, CdpNPT, CdpC3PT, 7-DMATS and SirD after incubation for 7 h. Detection was carried with a diode array detector and illustrated for absorption at 296 nm

masses, which are 68 Da larger than the respective substrates. Inspection of the ^{1}H-NMR data of the isolated products revealed clearly the presence of signals for a regular dimethylallyl moiety at δ_H 3.49–3.73 (d, 2H-1′), 5.17–5.35 (br t, H-2′), 1.78–1.92 (s, 3H-4′), 1.67–1.75 (s, 3H-5′) (Table S2, Electronic supplementary material). Comparing the signals of the aromatic protons of **2b**, **2f**, **2g**, **2k** and **3k** with those of the respective substrates (data not shown), the disappearance of one triplet was observed. This indicated that the prenyl moiety was very likely attached to position 2 or 4 of **2f** and **2g**, position 6 or 8 of **2k** and **3k** and position 2, 4, 5 or 8 of **2b** (please see

Table S2 for numbering of the naphthalene ring). For determination of the prenylation position, connectivities in HMBC of the isolated compounds are taken in consideration and summarized in Fig. S1 (Electronic supplementary material). In the HMBC spectra of **2f** and **2g**, connectivities from H-1′ of the dimethylallyl moiety at 3.54–3.59 ppm to C9 at δ_C 128.9–135.8 ppm confirmed the attachment of the prenyl residue at position C4. Connectivities from H-1′ to δ_C 127.8 ppm of C10 in **2k** and to δ_C 148.4 ppm of C-5 in **3k**, proved unequivocally the presence of the prenyl moiety at position C8 in **2k** and position C6 in **3k**, i.e. the *para*- and *ortho*-position of the hydroxyl group, respectively. The observation of two doublets of double doublets at 7.45 (ddd, H-6) and 7.40 (ddd, H-7) in ^{1}H-NMR spectrum and connectivity from H-1′ to δ_C 134.0 of C9 in the HMBC spectrum confirmed the prenylation at position C4 in **2b**.

Comparison of the signals for aromatic protons in the spectra of **2i**, **2j** and **2l** with those of the respective substrates revealed the disappearance of one doublet with a coupling constant of about 2–2.5 Hz, indicating the prenylations at position C1 of **2i** and **2j** and position C8 of **2l**. In the HMBC spectra of **2i** and **2j**, connectivities from H-1′ of the dimethylallyl residue to C2 at δ_C 150.3–152.8 ppm and to C10 at δ_C 129.3–136.1 ppm, proved unambiguously the attachment of the prenyl moieties at C1 in **2i** and **2j**. The observation of H-1′ to δ_C 150.9 ppm for C7 and δ_C 128.1 ppm for C10, H-6 to δ_C 121.4 ppm for C8 in the HMBC spectrum confirmed the prenylation at position C8 in **2l**. The structures of the enzyme products are summarized in Table S2. **2i** and **2j** have been also identified as prenylation products of **1i** and **1j** by NovQ, an enzyme from the CloQ/NphB group (Macone et al. 2009; Ozaki et al. 2009).

Inspection of the structures of the enzyme products revealed clearly that prenylation has preferentially taken place at *para*-position of the hydroxyl group at C1, as in the cases of 2**b**, **2f**, **2g** and **2k**. If this was not possible, as for **2i**, **2j**, and **2l**, the *ortho*-position to the hydroxyl group at C2 was prenylated (Fig. 4). Detection of more than two product peaks in the incubation mixtures of **1i** and **1j** (Fig. 3d, e) indicated the presence of further derivatives, in addition to the two possible monoprenylated products at *ortho*-position to one of the two hydroxyl groups.

O-Prenylated and diprenylated derivatives were identified as minor products in the incubation mixtures of **1i** and **1j**

To get structure information of the minor products, **3i**, **4i**, **5i, 6i** and **7i** were also isolated by repeated chromatography

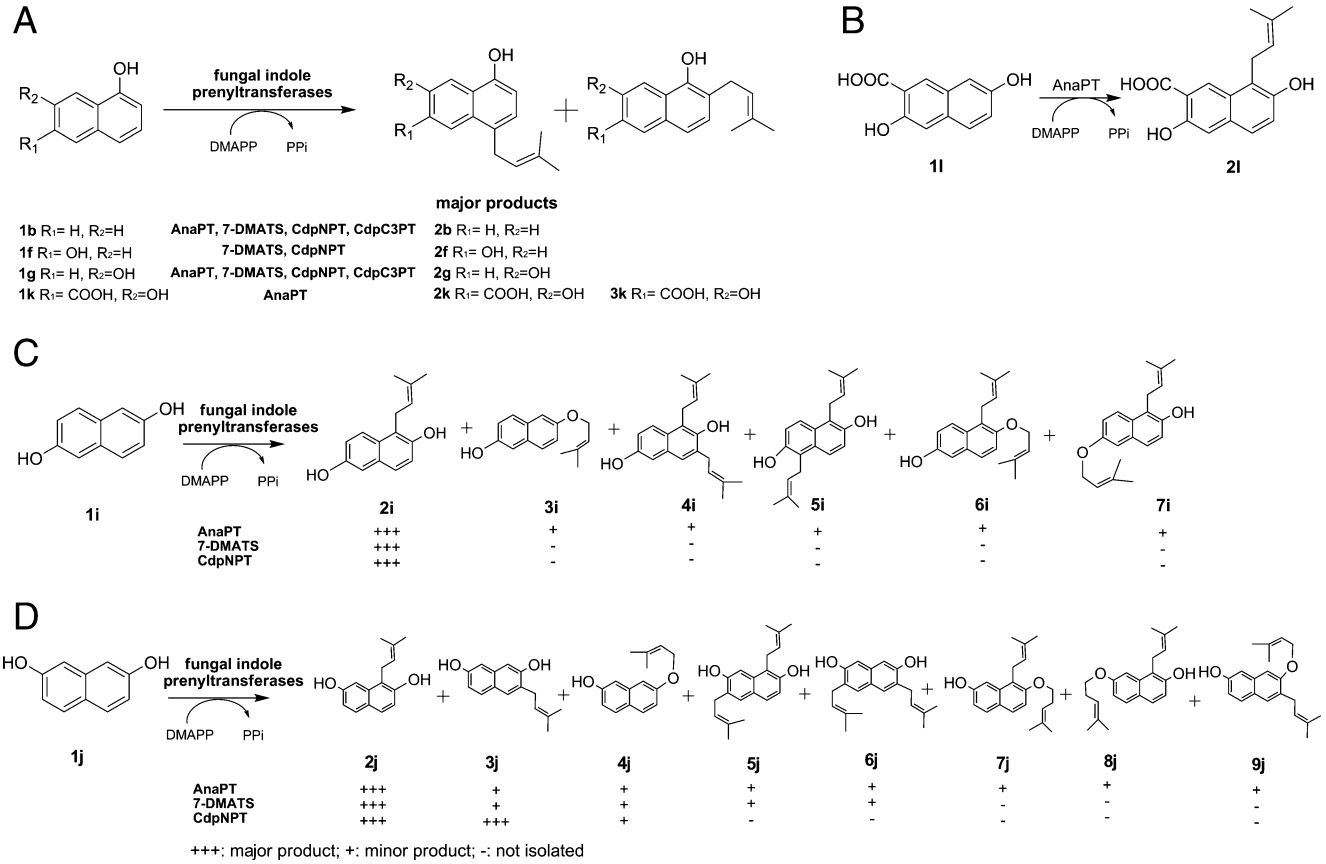

Fig. 4 Prenyl transfer reactions catalyzed by prenyltransferases of the DMATS superfamily towards **a** 1-naphthol and derivatives (**1b**, **1f**, **1g** and **1k**), **b** 3,7-dihydroxy-2-naphtholic acid (**1l**), **c** 2,6-dihydroxynaphthalene (**1i**) and **d** 2,7-dihydroxynaphthalene (**1j**)

on HPLC from the incubation mixtures of **1i** with AnaPT (Fig. 3d). In analogous manner, products of **1j** were obtained from the incubation mixtures of AnaPT (**3j–9j**), 7-DMATS (**3j–6j**) and CdpNPT (**3j** and **4j**) (Fig. 3e). ^{1}H-NMR spectra revealed again that products with same retention times have also same ^{1}H-NMR spectra.

The structures of **3i**, **4i**, **5i, 6i**, **7i**, **3j**, **4j**, **5j** and **6j** (Fig. 4 and Tables S2 and S3) were elucidated by comparison of their ^{1}H-NMR spectra with those of the respective substrate and the aforementioned products **2i** and **2j**. Characteristic signals for *O*-prenyl moieties were found for H-2′ at approximately 5.5 ppm and for H-1′at 4.6 ppm (Zou et al. 2011). The corresponding signals for *C*-prenyl groups appeared in the range of 5.1–5.4 and 3.3–3.7 ppm, respectively (Kremer and Li 2008; Steffan et al. 2007). In the case of the *O*-prenylated derivatives **3i** and **4j**, the number and coupling pattern of the aromatic protons were not changed. For **3j**, **5j** and **6j**, signal for one or two aromatic protons had disappeared and the structures have been elucidated by interpretation of the coupling pattern of the aromatic protons.

The structures of **7j**, **8j** and **9j** were elucidated by interpretation of the connectivities in their HMBC spectra (Fig. S1, Electronic supplementary material), as described for the main products discussed above. All of the structures were also confirmed by high-resolution electron impact mass spectrometry. It is obvious that in the incubation mixtures of substrates with low conversion rates and low regioselectivity like **1i** and **1j**, *O*-prenylation and diprenylation took place more frequently than those with a better acceptance.

Kinetic parameters of the indole prenyltransferases towards hydroxynaphthalenes

To get information on the catalytic efficiency of indole prenyltransferases towards hydroxynaphthalenes, kinetic parameters of AnaPT, CdpNPT, CdpC3PT and 7-DMATS, including Michaelis–Menten constants (K_M) and turnover numbers (k_{cat}) of six selected substrates were determined by Hanes–Woolf and Eadie–Hofstee plots. The obtained data are given in Table 2 and compared with those of indole derivatives with the respective enzyme. With an exception of (*R*)-benzodiazepinedione for AnaPT, the natural substrates of CdpNPT, CdpC3PT and 7-DMATS are unknown. Therefore, the best reported indole derivatives were used in these experiments. Due to the very low conversion, kinetic parameters of SirD towards hydroxynaphthalenes were not determined.

The K_M values of these enzymes for hydroxynaphthalenes are in the similar concentration range as those for indole derivatives, at least for some of hydroxynaphthalenes. For example, AnaPT accepted **1g** with a K_M of 0.30 mM, slightly higher than that for its natural substrate (*R*)-benzodiazepindinone at 0.23 mM. Comparable K_M values were found for CdpNPT towards hydroxynaphthalenes and cyclo-L-Trp-L-Trp. Similar or even lower K_M values were observed for CdpC3PT and 7-DMATS. Notably, low K_M value of 0.064 mM was determined for **1g** with 7-DMATS, while L-tryptophan was accepted by this enzyme with a K_M value of 0.14 mM.

Maximal reaction velocities of AnaPT, CdpC3PT and 7-DMATS determined with hydroxynaphthalenes are slightly slower than those with indole derivatives. Turnover numbers of AnaPT with **1b** and **1g** were found to be 0.74 and 0.34 s^{-1}, i.e. 49% and 23% of that with its natural substrate (*R*)-benzodiazepinedinone, respectively. For CdpC3PT, turnover numbers at 0.31 and 0.14 s^{-1} were determined for **1b** and **1g**, i.e. 38% and 17% of that of cyclo-L-Trp-L-Leu, respectively. Turnover numbers of 7-DMATS with **1f** and **1g** were found to be 52% and 33% of that of its best substrate L-tryptophan. CdpNPT showed a much higher maximal reaction velocity with **1b** and **1f** than with cyclo-L-Trp-L-Trp, approximate 14- and 1.8-fold, respectively.

As a consequence, the catalytic efficiencies (k_{cat}/K_M) of AnaPT determined with hydroxynaphthalenes were found to be about 17% of that with (*R*)-benzodiazepindinone. This low value is, however, due to the high turnover number and catalytic efficiency of AnaPT with its natural substrate. The catalytic efficiencies of AnaPT with **1b** and **1g** at 569 and 1,133 s^{-1} M^{-1} should be categorized as high. In comparison to the data obtained with AnaPT, higher relative catalytic efficiencies for hydroxynaphthalenes were calculated for CdpC3PT and 7-DMATS. The catalytic efficiency of 7-DMATS with **1g** was found to be 73.2% of that with L-tryptophan.

Discussion

Prenyltransferases of the DMATS superfamily showed broad substrate specificity and were successfully used for production of prenylated tyrosine and indole derivatives by chemoenzymatic synthesis (Li 2010; Yin et al. 2010c; Zou et al. 2011). However, prenylation of hydroxynaphthalenes by these enzymes have not been reported previously.

After initial observation of the acceptance of 1-naththol (**1b**) by seven of the eight tested enzymes, we chose AnaPT, CdpC3PT, CdpNPT, 7-DMATS and SirD for detailed investigation with 11 hydroxynaphthalenes as potential prenylation substrates. As shown in Fig. 1, AnaPT, CdpC3PT and CdpNPT accept tryptophan-containing cyclic dipeptides as natural or best substrates (Ruan et al. 2008; Yin et al. 2010a, c). These enzymes are therefore the best candidates to elucidate the behaviour of very similar indole

prenyltransferases towards hydroxynaphthalenes. The dimethylallyltryptophan synthase 7-DMATS catalyzes the regular C7-prenylation of L-tryptophan derivatives (Kremer et al. 2007; Kremer and Li 2008). SirD represents a tyrosine *O*-prenyltransferase (Kremer and Li 2010). The substrates and catalyzed prenylation reactions of 7-DMATS and SirD differ clearly from those of the three cyclic dipeptide prenyltrasnferases AnaPT, CdpC3PT and CdpNPT. The five enzymes are therefore the best candidates to elucidate the behaviour of very different prenyltransferases towards hydroxynaphthalenes. In this study, we have shown that the substrate specificity of the members of DMATS superfamily towards hydroxynaphthalene derivatives did not correlate with those obtained for tyrosine or indole derivatives. For example, SirD showed the most flexible substrate specifity within the DMATS superfamily, accepted both tyrosine and tryptophan derivatives as substrates and catalyzed *O*-, *N*- and *C*-prenylation (Zou et al. 2011). However, hydroxynaphthalenes were poor substrates for this enzyme and only four of them were accepted with very low velocities (Table S1, Electronic supplementary material). Furthermore, in contrast to the different prenylation patterns and positions of a given indole derivative by different enzymes, same prenylation products of a hydroxynaphthalene were identified in the reaction mixtures with different enzymes. As shown in Fig. 3, naphthalenes with a hydroxyl group at C1 such as **1b**, **1f**, **1g** and **1k** produced usually one dominant product, i.e. with a regular prenyl moiety at *para*-position to this hydroxy group. Naphthalenes with a hydroxyl group at C2 such as **1i** and **1j** showed a lowed regioselectivity. In addition to the major product with a regular prenyl moiety at *ortho*-position of the hydroxyl group, i.e. **2i** and **2j**, up to seven minor products including *O*-prenylated, *C*- and *C*- as well as *C*- and *O*-diprenylated derivatives were obtained from the incubation mixtures (Fig. 4).

The relative high turnover numbers and catalytic efficiencies of these enzymes towards hydroxynaphthalenes provided experimental evidence for their potential application as catalysts for chemoenzymatic synthesis of prenylated hydroxynaphthalenes. It can be expected that high efficiency of the prenylation reaction for a given substrate could be achieved by choice of a suitable indole prenyltransferase, as demonstrated in this study.

As mentioned in 'Introduction', prenyltransferases of the DMATS superfamily show no noteworthy sequence similarity with prenyltransferases of the CloQ/NphB group, which use hydroxynaphthalenes or other nitrogen-free aromatic compounds as prenylation substrates (Haug-Schifferdecker et al. 2010; Kumano et al. 2008). However, they share the common PT barrel in their protein structures (Jost et al. 2010; Kuzuyama et al. 2005; Metzger et al. 2009, 2010). Structural analysis of FgaPT2 and FtmPT1 revealed the presence of only one reaction chamber (Jost et al. 2010; Metzger et al. 2010). The acceptance of hydroxynaphthalenes by enzymes of the DMATS superfamily demonstrates probably just the flexibility of such reaction chambers. It would be now interesting to investigate the acceptance of tyrosine or indole derivatives by the members of the CloQ/NphB group.

Acknowledgements This work was supported within the LOEWE program of the State of Hessen (SynMikro to S.-M. Li). Xie acknowledges the Deutsche Forschungsgemeinschaft for funding the Bruker AVANCE 600 spectrometer. Xia Yu is a recipient of a fellowship from China Scholarship Council. We thank Dr. Laufenberg for taking mass spectra and Marco Matuschek for synthesis of DMAPP.

References

Berger S, Braun S (2004) 200 and more NMR experiments. A practical course. Weiley-VCH, Weinheim

Ding Y, Wet JR, Cavalcoli J, Li S, Greshock TJ, Miller KA, Finefield JM, Sunderhaus JD, McAfoos TJ, Tsukamoto S, Williams RM, Sherman DH (2010) Genome-based characterization of two prenylation steps in the assembly of the stephacidin and notoamide anticancer agents in a marine-derived *Aspergillus* sp. J Am Chem Soc 132:12733–12740

Grundmann A, Li S-M (2005) Overproduction, purification and characterization of FtmPT1, a brevianamide F prenyltransferase from *Aspergillus fumigatus*. Microbiology 151:2199–2207

Haagen Y, Unsöld I, Westrich L, Gust B, Richard SB, Noel JP, Heide L (2007) A soluble, magnesium-independent prenyltransferase catalyzes reverse and regular C-prenylations and O-prenylations of aromatic substrates. FEBS Lett 581:2889–2893

Haug-Schifferdecker E, Arican D, Brueckner R, Heide L (2010) A new group of aromatic prenyltransferases in fungi, catalyzing a 2,7-dihydroxynaphthalene dimethylallyltransferase reaction. J Biol Chem 285:16487–16494

Heide L (2009) Prenyl transfer to aromatic substrates: genetics and enzymology. Curr Opin Chem Biol 13:171–179

Jost M, Zocher G, Tarcz S, Matuschek M, Xie X, Li S-M, Stehle T (2010) Structure–function analysis of an enzymatic prenyl transfer reaction identifies a reaction chamber with modifiable specificity. J Am Chem Soc 132:17849–17858

Kremer A, Li S-M (2008) Potential of a 7-dimethylallyltryptophan synthase as a tool for production of prenylated indole derivatives. Appl Microbiol Biotechnol 79:951–961

Kremer A, Li S-M (2010) A tyrosine O-prenyltransferase catalyses the first pathway-specific step in the biosynthesis of sirodesmin PL. Microbiology 156:278–286

Kremer A, Westrich L, Li S-M (2007) A 7-dimethylallyltryptophan synthase from *Aspergillus fumigatus*: overproduction, purification and biochemical characterization. Microbiology 153:3409–3416

Kumano T, Richard SB, Noel JP, Nishiyama M, Kuzuyama T (2008) Chemoenzymatic syntheses of prenylated aromatic small molecules using *Streptomyces* prenyltransferases with relaxed substrate specificities. Bioorg Med Chem 16:8117–8126

Kumano T, Tomita T, Nishiyama M, Kuzuyama T (2010) Functional characterization of the promiscuous prenyltransferase responsible for furaquinocin biosynthesis: identification of a physiological polyketide substrate and its prenylated reaction products. J Biol Chem 285:39663–39671

Kuzuyama T, Noel JP, Richard SB (2005) Structural basis for the promiscuous biosynthetic prenylation of aromatic natural products. Nature 435:983–987

Li S-M (2009) Applications of dimethylallyltryptophan synthases and other indole prenyltransferases for structural modification of natural products. Appl Microbiol Biotechnol 84:631–639

Li S-M (2010) Prenylated indole derivatives from fungi: structure diversity, biological activities, biosynthesis and chemoenzymatic synthesis. Nat Prod Rep 27:57–78

Liang PH (2009) Reaction kinetics, catalytic mechanisms, conformational changes, and inhibitor design for prenyltransferases. Biochemistry 48:6562–6570

Macone A, Lendaro E, Comandini A, Rovardi I, Matarese RM, Carraturo A, Bonamore A (2009) Chromane derivatives of small aromatic molecules: chemoenzymatic synthesis and growth inhibitory activity on human tumor cell line LoVo WT. Bioorg Med Chem 17:6003–6007

Metzger U, Schall C, Zocher G, Unsöld I, Stec E, Li S-M, Heide L, Stehle T (2009) The structure of dimethylallyl tryptophan synthase reveals a common architecture of aromatic prenyltransferases in fungi and bacteria. Proc Natl Acad Sci USA 106:14309–14314

Metzger U, Keller S, Stevenson CE, Heide L, Lawson DM (2010) Structure and mechanism of the magnesium-independent aromatic prenyltransferase CloQ from the clorobiocin biosynthetic pathway. J Mol Biol 404:611–626

Ozaki T, Mishima S, Nishiyama M, Kuzuyama T (2009) NovQ is a prenyltransferase capable of catalyzing the addition of a dimethylallyl group to both phenylpropanoids and flavonoids. J Antibiot (Tokyo) 62:385–392

Ruan H-L, Yin W-B, Wu J-Z, Li S-M (2008) Reinvestigation of a cyclic dipeptide N-prenyltransferase reveals rearrangement of N-1 prenylated indole derivatives. Chembiochem 9:1044–1047

Sings H, Singh S (2003) Tremorgenic and nontremorgenic 2,3-fused indole diterpenoids. Alkaloids Chem Biol 60:51–163

Steffan N, Li S-M (2009) Increasing structure diversity of prenylated diketopiperazine derivatives by using a 4-dimethylallyltryptophan synthase. Arch Microbiol 191:461–466

Steffan N, Unsöld IA, Li S-M (2007) Chemoenzymatic synthesis of prenylated indole derivatives by using a 4-dimethylallyltryptophan synthase from *Aspergillus fumigatus*. Chembiochem 8:1298–1307

Tudzynski P, Holter K, Correia T, Arntz C, Grammel N, Keller U (1999) Evidence for an ergot alkaloid gene cluster in *Claviceps purpurea*. Mol Gen Genet 261:133–141

Unsöld IA, Li S-M (2005) Overproduction, purification and characterization of FgaPT2, a dimethylallyltryptophan synthase from *Aspergillus fumigatus*. Microbiology 151:1499–1505

Williams RM, Stocking EM, Sanz-Cervera JF (2000) Biosynthesis of prenylated alkaloids derived from tryptophan. Topics Curr Chem 209:97–173

Woodside AB, Huang Z, Poulter CD (1988) Triammonium germanyl diphosphate. Org Synth 66:211–215

Yazaki K, Sasaki K, Tsurumaru Y (2009) Prenylation of aromatic compounds, a key diversification of plant secondary metabolites. Phytochemistry 70:1739–1745

Yin W-B, Ruan H-L, Westrich L, Grundmann A, Li S-M (2007) CdpNPT, an N-prenyltransferase from *Aspergillus fumigatus*: overproduction, purification and biochemical characterisation. Chembiochem 8:1154–1161

Yin W-B, Grundmann A, Cheng J, Li S-M (2009) Acetylaszonalenin biosynthesis in *Neosartorya fischeri*: Identification of the biosynthetic gene cluster by genomic mining and functional proof of the genes by biochemical investigation. J Biol Chem 284:100–109

Yin W-B, Xie X-L, Matuschek M, Li S-M (2010a) Reconstruction of pyrrolo[2,3-b]indoles carrying an α-configured reverse C3-dimethylallyl moiety by using recombinant enzymes. Org Biomol Chem 8:1133–1141

Yin W-B, Yu X, Xie X-L, Li S-M (2010b) Preparation of pyrrolo[2,3-b]indoles carrying a ?-configured reverse C3-dimethylallyl moiety by using a recombinant prenyltransferase CdpC3PT. Org Biomol Chem 8:2430–2438

Zou H, Zheng X, Li S-M (2009) Substrate promiscuity of the cyclic dipeptide prenyltransferases from *Aspergillus fumigatus*. J Nat Prod 72:44–52

Zou H-X, Xie X-L, Linne U, Zheng X-D, Li S-M (2010) Simultaneous C7- and N1-prenylation of cyclo-L-Trp-L-Trp catalyzed by a prenyltransferase from *Aspergillus oryzae*. Org Biomol Chem 8:3037–3044

Zou H-X, Xie X, Zheng X-D, Li S-M (2011) The tyrosine O-prenyltransferase SirD catalyzes O-, N-, and C-prenylations. Appl Microbiol Biotechnol 89:1443–1451

Electronic Supplementary Material for:

Substrate promiscuity of secondary metabolite enzymes: Prenylation of hydroxynaphthalenes by fungal indole prenyltransferases

Xia Yu, Xiulan Xie, and Shu-Ming Li *

Xia Yu, Shu-Ming Li*

Institut für Pharmazeutische Biologie und Biotechnologie, Philipps-Universität Marburg, Deutschhausstrasse 17A, 35037 Marburg, Germany

* Correspondence: shuming.li@staff.uni-marburg.de

Shu-Ming Li

Zentrum für Synthetische Mikrobiologie, Philipps-Universität Marburg, 35032 Marburg

Xiulan Xie

Fachbereich Chemie, Philipps-Universität Marburg, Hans-Meerwein-Strasse, 35032 Marburg, Germany

Table S1: Conversion rates of the five enzymes towards different substrates after incubation for 1h or 7h

Substrate	Conversion rate （%）									
	AnaPT		7-DMATS		CdpNPT		CdpC3PT		SirD	
	1h	7h	1h	7h	1h	7h	1h	7h	1h	7h
naphthalene (**1a**)	-	-	-	-	-	-	-	-	-	-
1-naphthol (**1b**)	64.7	91.5	22.0	45.4	84.4	93.3	9.1	14.1	-	-
2-naphthol (**1c**)	13.3	19.7	5.1	9.7	8.1	14.3	-	0.9	-	-
1,4-dihydroxynaphthalene (**1d**)	0.7	1.1	-	0.7	1.0	1.3	0.6	0.7	1.8	4.4
1,5-dihydroxynaphthalene (**1e**)	6.7	13.2	14.6	37.9	10.3	16.4	0.7	1.1	-	-
1,6-dihydroxynaphthalene (**1f**)	11.8	17.8	73.3	92.6	21.3	24.7	0.4	2.1	1.1	2.3
1,7-dihydroxynaphthalene (**1g**)	68.8	88.7	50.6	88.5	37.3	46.7	3.5	9.8	0.8	1.1
2,3-dihydroxynaphthalene (**1h**)	13.8	21.9	9.1	26.4	4.1	6.4	0.5	1.5	-	-
2,6-dihydroxynaphthalene (**1i**)	14.4	47.7	4.9	13.0	2.1	4.9	-	0.5	1.0	1.3
2,7-dihydroxynaphthalene (**1j**)	7.8	18.6	3.1	10.5	7.8	12.1	0.6	1.1	-	-
3,5-dihydroxy-2-naphthoic acid (**1k**)	14.0	25.7	19.9	59.0	-	0.6	-	0.6	-	-
3,7-dihydroxy-2-naphthoic acid (**1l**)	20.5	42.7	-	-	-	0.9	-	-	-	-

-: not detected, conversion rate ≤0.3 %

Table S2: ^{1}H- and ^{13}C-NMR data of monoprenylted products in CD_3OD. Chemical shifts (δ) are given in ppm and coupling constants (*J*) in Hz.

Compd	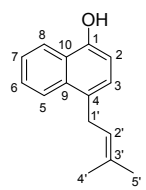 **2b**		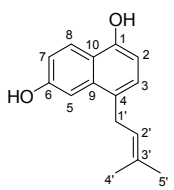 **2f**		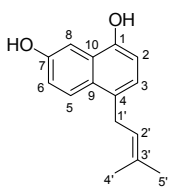 **2g**		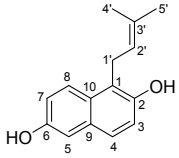 **2i**		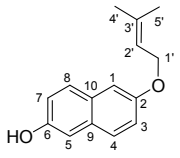 **3i**	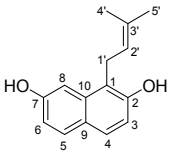 **2j**	
Pos.	δ_C	δ_H, multi., *J*	δ_C	δ_H, multi.,*J*	δ_C	δ_H, multi.,*J*	δ_C	δ_H, multi.,*J*	δ_H, multi., *J*	δ_C	δ_H, multi.,*J*
1	152.7	\	152.8	\	151.4	\	120.5	\	7.04, overlaps [c]	118.6	\
2	108.1	6.72, d, 7.7	105.5	6.52, d, 7.6	108.6	6.64, d, 7.6	150.3	\	\	152.8	\
3	126.4	7.09, d, 7.7	126.9	7.00, d, 7.0	123.5	6.88, d, 7.6	118.9	7.01, overlaps	7.04, dd, 9.2, 2.5[a]	115.5	6.87, d, 8.8
4	129.2	\	127.7	\	129.4	\	126.1	7.36, d, 8.8	7.53, d, 8.9[b]	127.7	7.44, d, 8.8
5	124.5	7.90, d, 8.4	106.6	7.18, d, 2.4	126.4	7.78, d, 9.1	110.4	7.02, overlaps	7.13, d, 2.4 [c]	130.6	7.56, d, 8.8
6	126.5	7.45, ddd, 8.4, 6.8, 1.5	156.1	\	118.4	7.04, dd, 9.1, 2.6	153.2	\	\	115.0	6.83, dd, 8.7, 2.4
7	124.8	7.40, ddd, 8.3, 6.8,1.3	116.7	6.98, dd, 9.1, 2.4	154.8	\	118.6	7.01, overlaps	7.02, dd, 9.0, 2.5 [a]	156.0	\
8	123.4	8.21, d, 8.4	125.2	8.07, d, 9.0	105.5	7.49, d, 2.6	125.4	7.70, d, 8.7	7.60, d, 8.8 [b]	105.9	7.12, d, 2.4
9	134.0	\	135.8	\	128.9	\	131.4	\	\	124.9	\
10	126.5	\	121.1	\	128.0	\	129.3	\	\	136.1	\
11	\	\	\	\	\	\	\	\	\	\	\
1'	31.8	3.65, d, 7.3	32.1	3.54, d, 6.8	32.0	3.59, d, 6.8	24.6	3.69, d, 6.6	4.60, overlaps	24.5	3.64, d, 6.7
2'	124.8	5.33, br.t, 7.0	124.7	5.33, br.t, 6.9	124.9	5.32, br.t, 7.0	124.8	5.17, br.t, 6.7	5.52, m	124.6	5.17, br.t, 6.6
3'	132.3	\	132.4	\	132.1	\	131.2	\	\	131.3	\
4'	17.5	1.80, s	17.6	1.79, s	17.6	1.78, s	17.7	1.87, s	1.81, s	17.7	1.87, s
5'	25.5	1.74, s	25.6	1.74, s	25.5	1.73, s	25.4	1.67, s	1.78, s	25.4	1.68, s

[a], [b], [c]: exchangeable protons

Signals were assigned by comparison of the spectra of the enzyme products with those of the substrate, and with each other, as well as by HSQC and HMBC correlations.

Table S2 (continued)

Compd	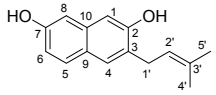 **3j**		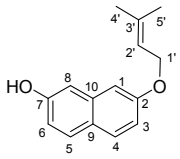 **4j**		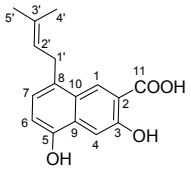 **2k**		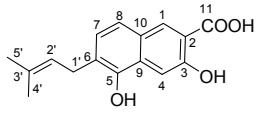 **3k**		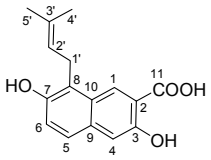 **2l**	
Pos.	δ_H, multi., *J*		δ_H, multi., *J*		δ_C	δ_H, multi.,*J*	δ_C	δ_H, multi.,*J*	δ_C	δ_H, multi.,*J*
1	6.87, s		7.00, overlaps		129.9	8.64, s	133.2	8.42, s	128.9	8.58, s
2	\		\		115.2	\	115.4	\	115.2	\
3	\		6.88, dd, 8.9, 2.5		156.9	\	157.3	\	155.1	\
4	7.35, s		7.59, d, 8.8		107.6	7.57, s	106.3	7.54, s	112.3	7.15, s
5	7.49, d, 9.1		7.59, d, 8.8		151.5	\	148.4	\	126.2	7.44, d, 8.9
6	6.79, dd, 8.7, 2.4		6.88, dd, 8.8, 2.4		110.8	6.74, d, 7.6	126.6	\	122.5	7.15, d, 8.8
7	\		\		124.6	6.96, d, 7.6	126.9	7.08, d, 8.4	150.9	\
8	6.85, d, 2.4		7.00, overlaps		131.0	\	122.2	7.35, d, 8.5	121.4	\
9	\		\		131.4	\	131.6	\	134.7	\
10	\		\		127.8	\	128.2	\	128.1	\
11	\		\		173.2	\	173.3	\	173.2	\
1'	3.38, d, 6.9		4.61, d, 6.6		32.4	3.64, d, 7.0	29.3	3.49, d, 7.3	24.7	3.73, d, 6.8
2'	5.40, m		5.52, m		124.8	5.29, br.t, 7.1	123.4	5.35, br.t, 7.3	124.4	5.17, br.t, 6.9
3'	\		\		132.7	\	133.2	\	131.6	\
4'	1.77, s		1.81, s		17.7	1.84, s	17.7	1.78, s	17.7	1.92, s
5'	1.74, s		1.79, s		25.7	1.74, s	25.7	1.75, s	25.5	1.68, s

Signals were assigned by comparison of the spectra of the enzyme products with those of the substrate, and with each other, as well as by HSQC and HMBC correlations.

Table S3: ^{1}H- and ^{13}C-NMR data of diprenylted products in CD_3OD. Chemical shifts (δ) are given in ppm and coupling constants (*J*) in Hz.

Compd	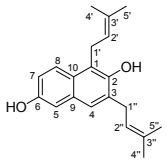 **4i**	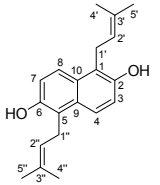 **5i**	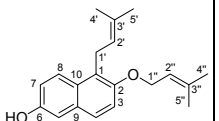 **6i**	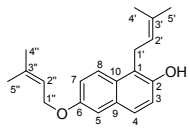 **7i**	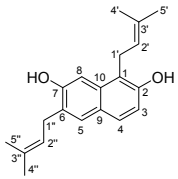 **5j**	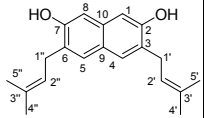 **6j**	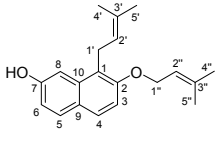 **7j**		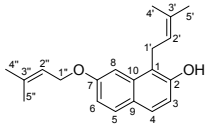 **8j**		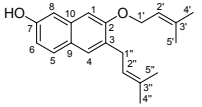 **9j**	
Pos.	δ_H, multi., *J*	δ_H, multi., *J*	δ_H, multi., *J*	δ_H, multi., *J*	δ_H, multi., *J*	δ_H, multi., *J*	δ_C	δ_H, multi., *J*	δ_C	δ_H, multi., *J*	δ_C	δ_H, multi., *J*
1	\	\	\	\	\	6.83, s	123.0	\	119.4	\	105.5	6.96, s
2	\	\	\	\	\	\	154.9	\	153.3	\	157.2	\
3	\	7.03, d, 9.0	7.23, d, 9.0	7.04, d, 8.8	6.83, d, 8.7	\	113.5	7.10, d, 8.9	116.1	6.92, d, 8.7	129.7	\
4	6.92, s	7.58, d, 9.0	7.49, d, 9.0	7.46, d, 8.8	7.36, d, 9.3	7.27, s	128.1	7.58, d, 8.9	127.8	7.47, d, 8.7	128.3	7.39, s
5	7.21, d, 2.4		7.05, overlaps	7.12, d, 2.6	7.35, s	7.27, s	130.8	7.62, d, 8.8	130.6	7.60, d, 8.9	129.4	7.52, d, 8.7
6	\	\	\	\	\	\	116.4	6.90, dd, 8.8, 2.3	115.9	6.88, dd, 8.8, 2.4	116.1	6.85, dd, 8.7, 2.4
7	7.00, dd, 9.1, 2.5	7.03, d, 9.0	7.04, overlaps	7.06, dd, 9.3, 2.6	\	\	156.5	\	158.2	\	156.0	\
8	7.71, d, 9.1	7.58, d, 9.0	7.76, d, 10.0	7.74, d, 9.3	7.11, s	6.83, s	106.2	7.17, d, 2.2	104.1	7.13, d, 2.4	108.9	6.98, d, 2.3
9	\	\	\	\	\	\	125.8	\	125.6	\	125.0	\
10	\	\	\	\	\	\	135.8	\	136.0	\	136.2	\
1'	3.66, d, 6.6	3.69, d, 6.6	3.73, d, 6.6	3.70, d, 6.7	3.62, d, 6.4	3.36, d, 6.8	24.8	3.67, d, 6.6	24.7	3.69, d, 6.6	65.5	4.61, d, 6.5
2'	5.16, m	5.16, m	5.13, m	5.17, m	5.19, m	5.40, m	124.6	5.14, m	124.9	5.17, m	121.3	5.55, m
3'	\	\	\	\	\	\	131.6	\	131.5	\	138.2	\
4'	1.86, s	1.87, s	1.86, s	1.87, s	1.87, s	1.77, s	17.8	1.86, s	17.8	1.90, s	25.7	1.82, s
5'	1.67, s	1.67, s	1.67, s	1.67, s	1.67, s	1.73, s	25.5	1.67, s	25.6	1.69, s	17.9	1.79, s
1''	3.59, d, 7.0	3.69, d, 6.6	4.59, d, 6.8	4.60, d, 6.6	3.38, d, 7.0	3.36, d, 6.8	67.2	4.62, d, 6.7	65.5	4.62, d, 6.5	29.6	3.36, d, 7.4
2''	5.37, m	5.16, m	5.51, m	5.52, m	5.41, m	5.40, m	121.6	5.51, m	121.3	5.52, m	123.9	5.34, m
3''	\	\	\	\	\	\	138.1	\	138.0	\	132.8	\
4''	1.79, s	1.87, s	1.80, s	1.81, s	1.77, s	1.77, s	25.5	1.78, s	25.5	1.81, s	25.6	1.74, s
5''	1.77, s	1.67, s	1.73, s	1.78, s	1.74, s	1.73, s	17.8	1.75, s	17.9	1.79, s	17.5	1.72, s

Signals were assigned by comparison of the spectra of the enzyme products with those of the substrate, and with each other, as well as by HSQC and HMBC correlations.

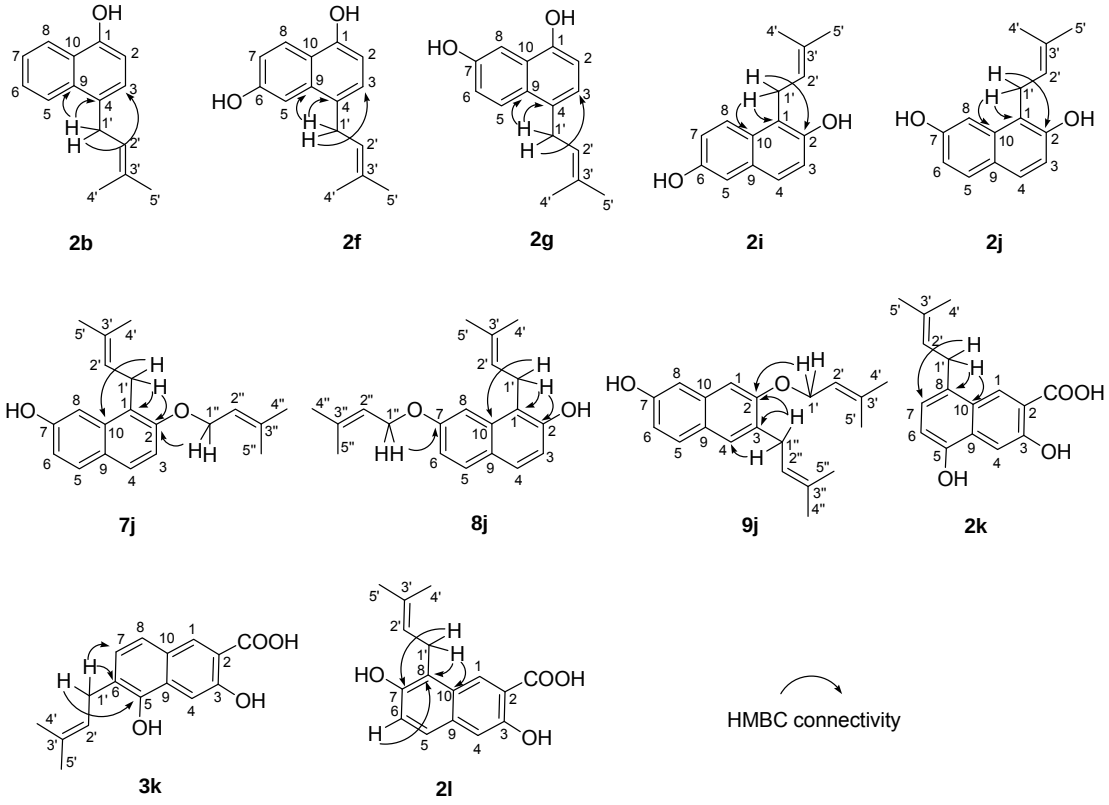

Figure. S1 HMBC connectivities of enzyme products **2b, 2f, 2g, 2i, 7j, 8j, 9j, 2j, 2k, 3k** and **2l**.

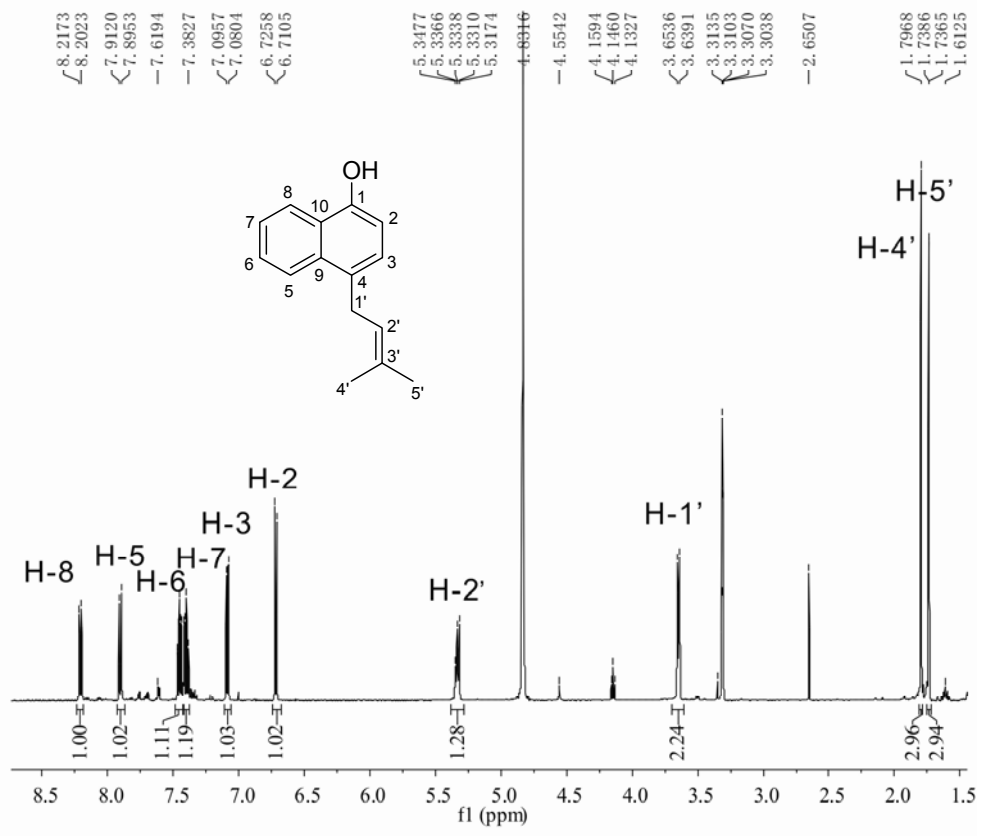

Figure S2.1 ^{1}H-NMR spectrum of **2b** in CD_3OD (500 MHz)

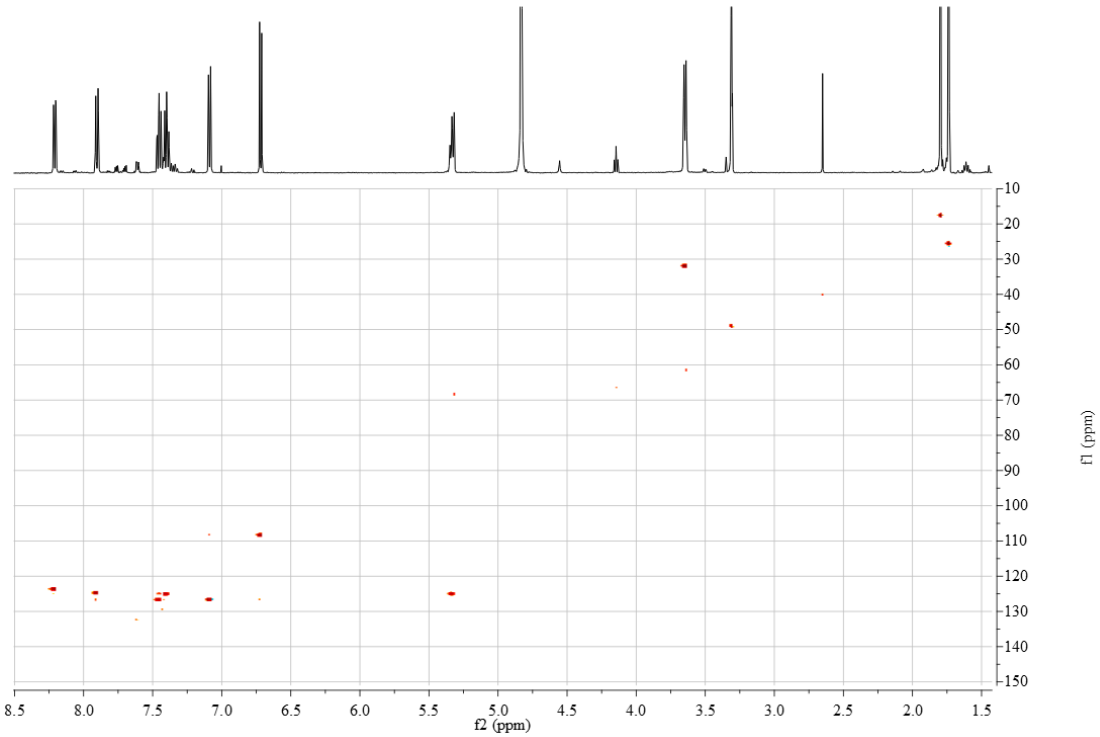

Figure S2.2 HSQC spectrum of **2b** in CD_3OD (500 MHz)

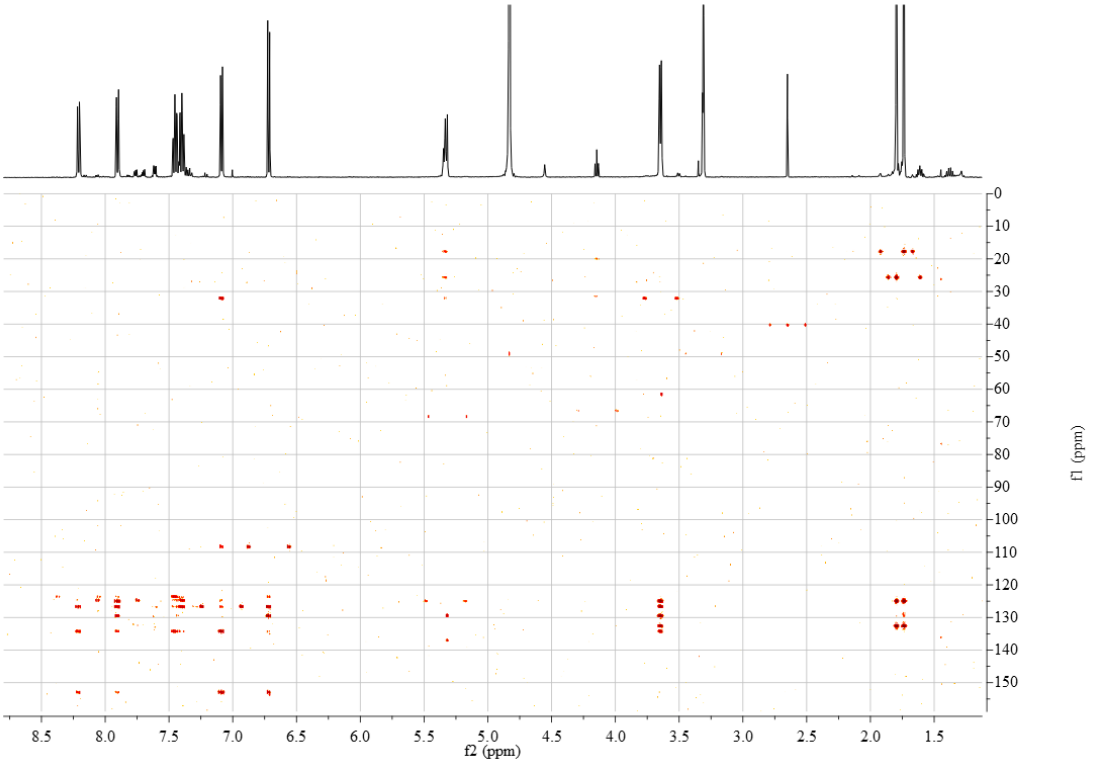

Figure S2.3 HMBC spectrum of **2b** in CD_3OD (500 MHz)

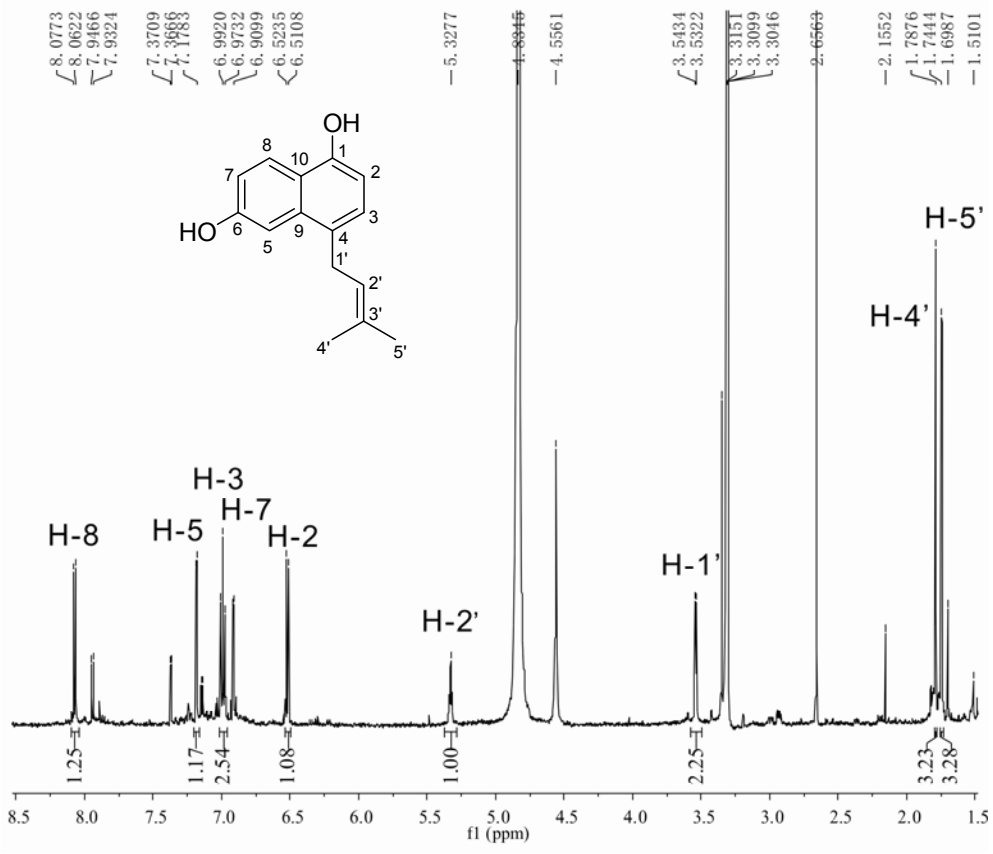

Figure S3.1 ^{1}H-NMR spectrum of **2f** in CD_3OD (600 MHz)

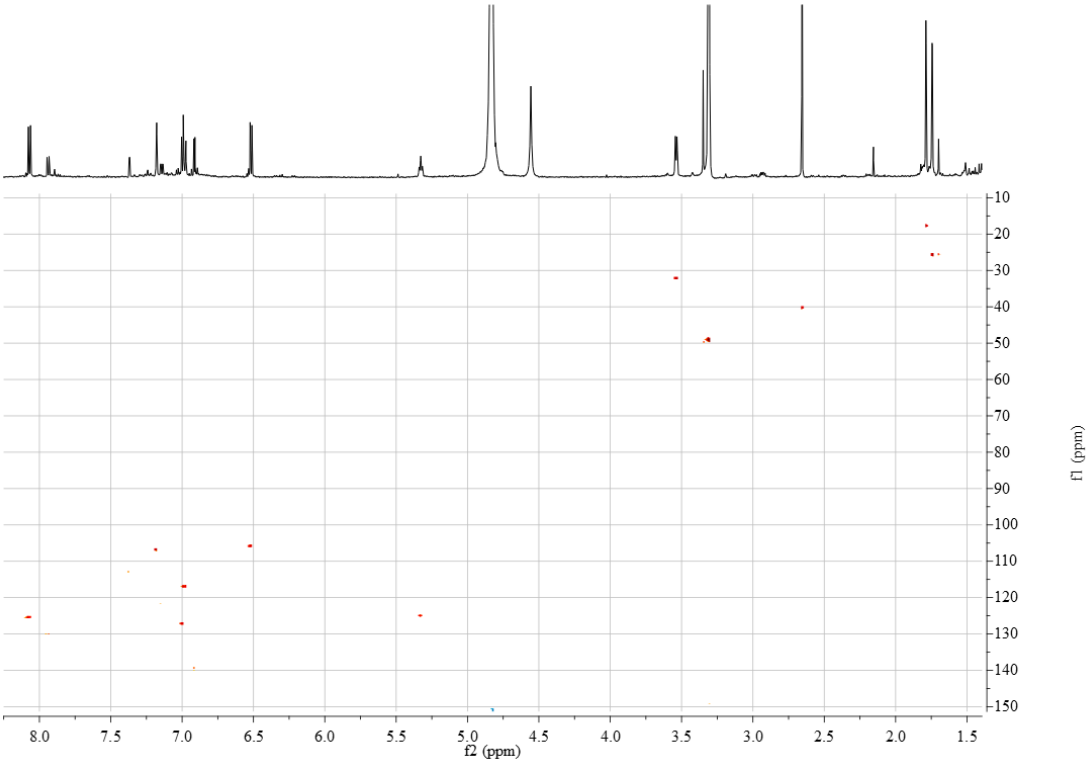

Figure S3.2 HSQC spectrum of **2f** in CD_3OD (600 MHz)

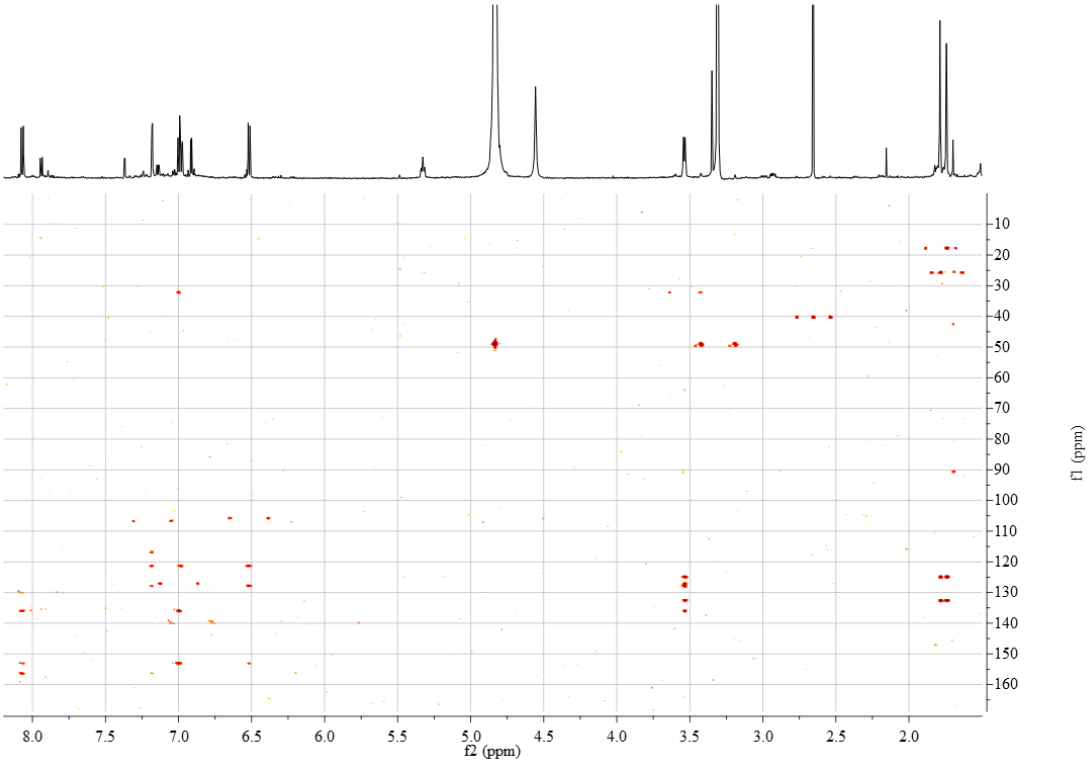

Figure S3.3 HMBC spectrum of **2f** in CD_3OD (600 MHz)

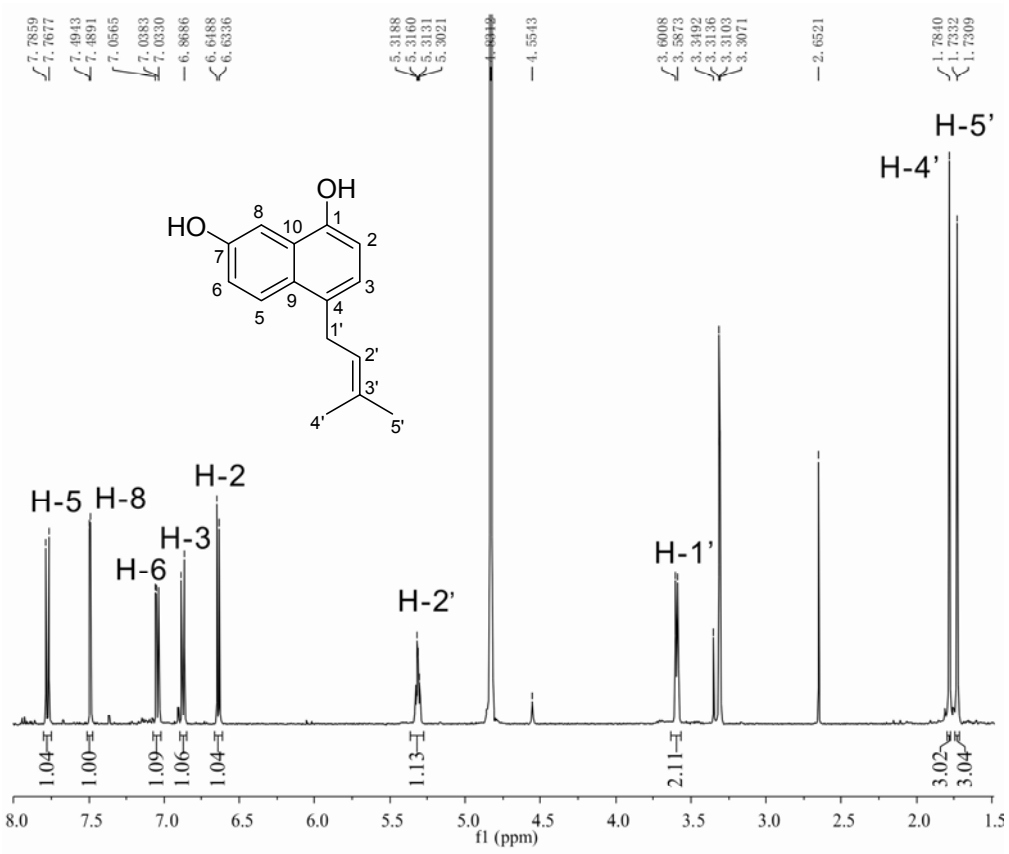

Figure S4.1 ^{1}H-NMR spectrum of **2g** in CD_3OD (500 MHz)

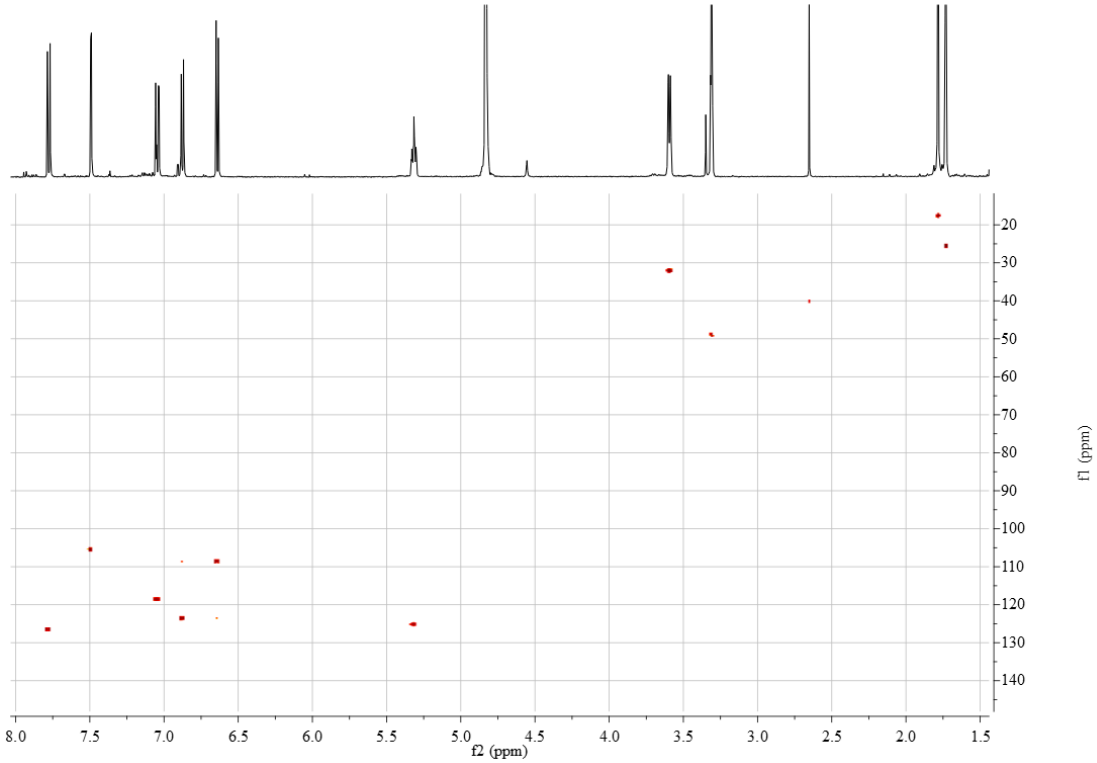

Figure S4.2 HSQC spectrum of **2g** in CD_3OD (500 MHz)

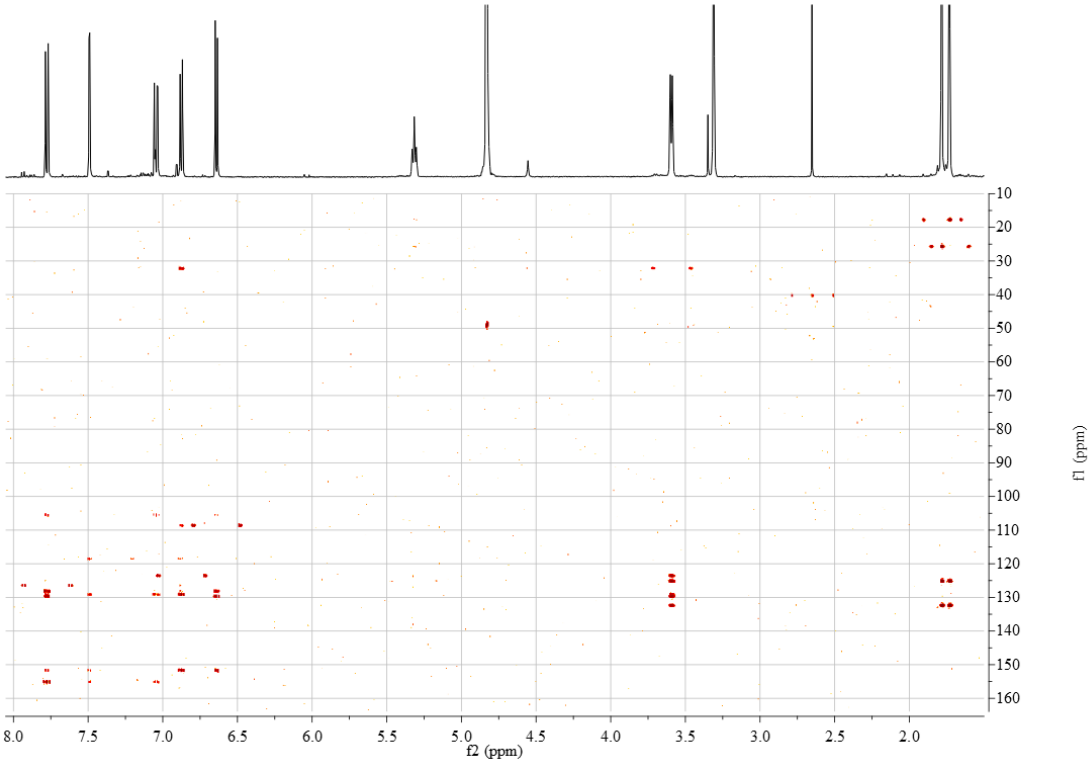

Figure S4.3 HMBC spectrum of **2g** in CD_3OD (500 MHz)

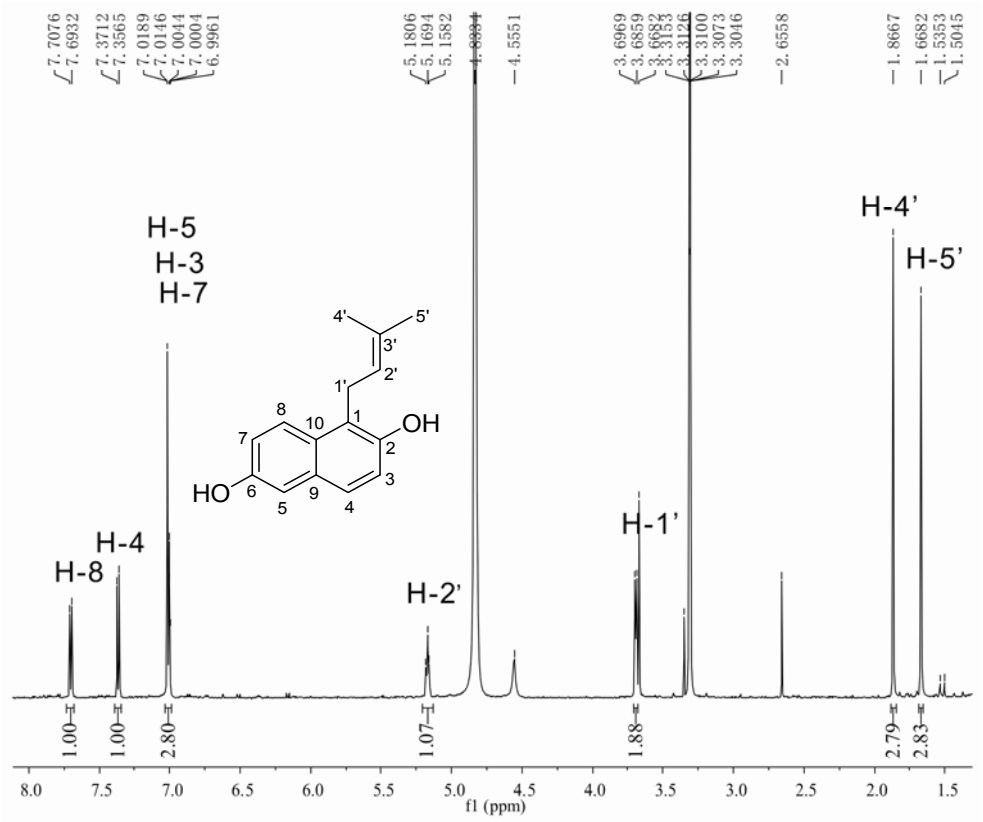

Figure S5.1 ^{1}H-NMR spectrum of **2i** in CD_3OD (600 MHz)

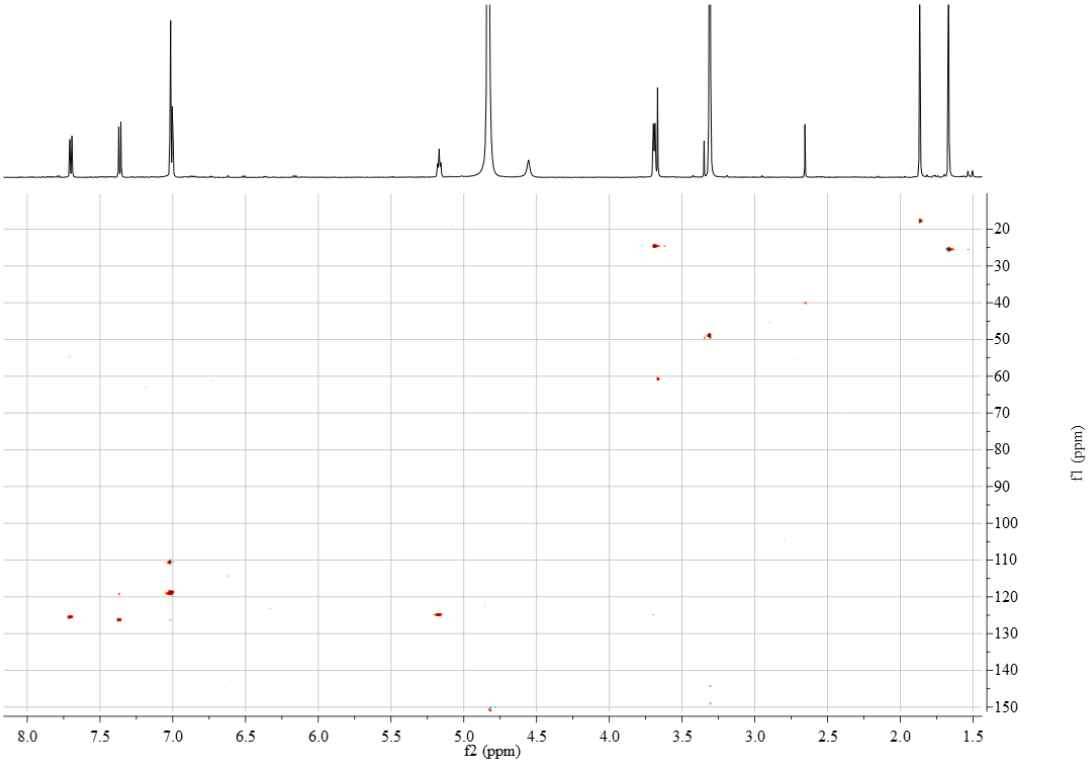

Figure S5.2 HSQC spectrum of **2i** in CD_3OD (600 MHz)

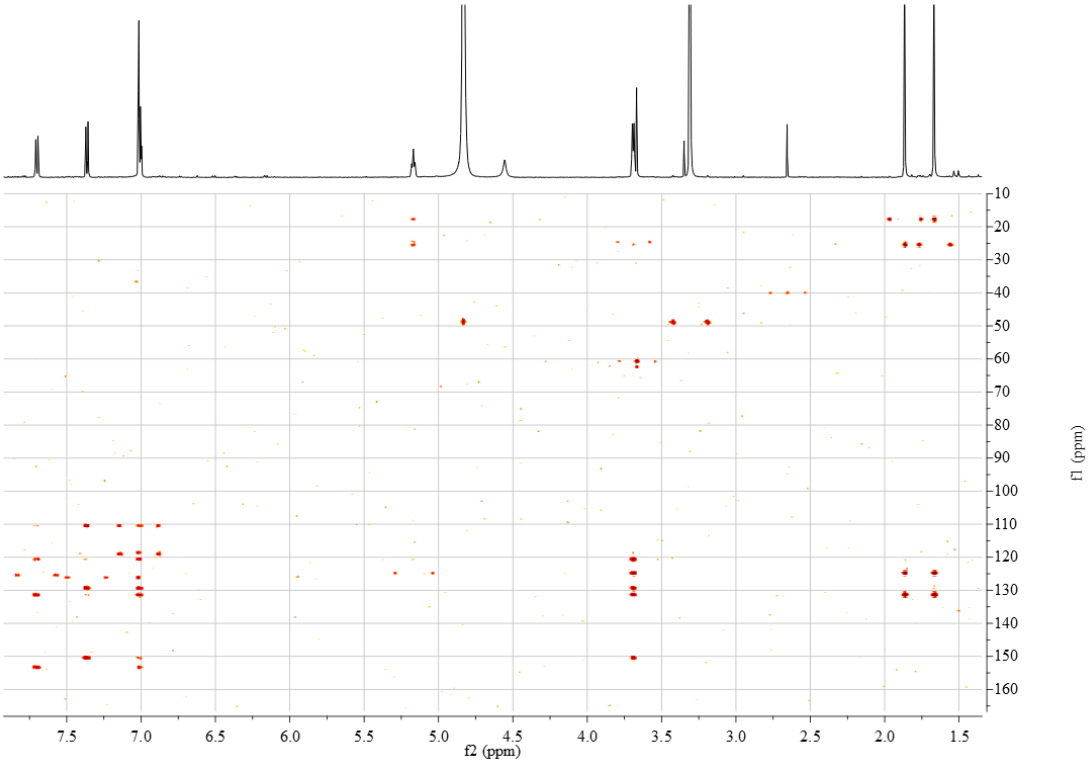

Figure S5.3 HMBC spectrum of **2i** in CD_3OD (600 MHz)

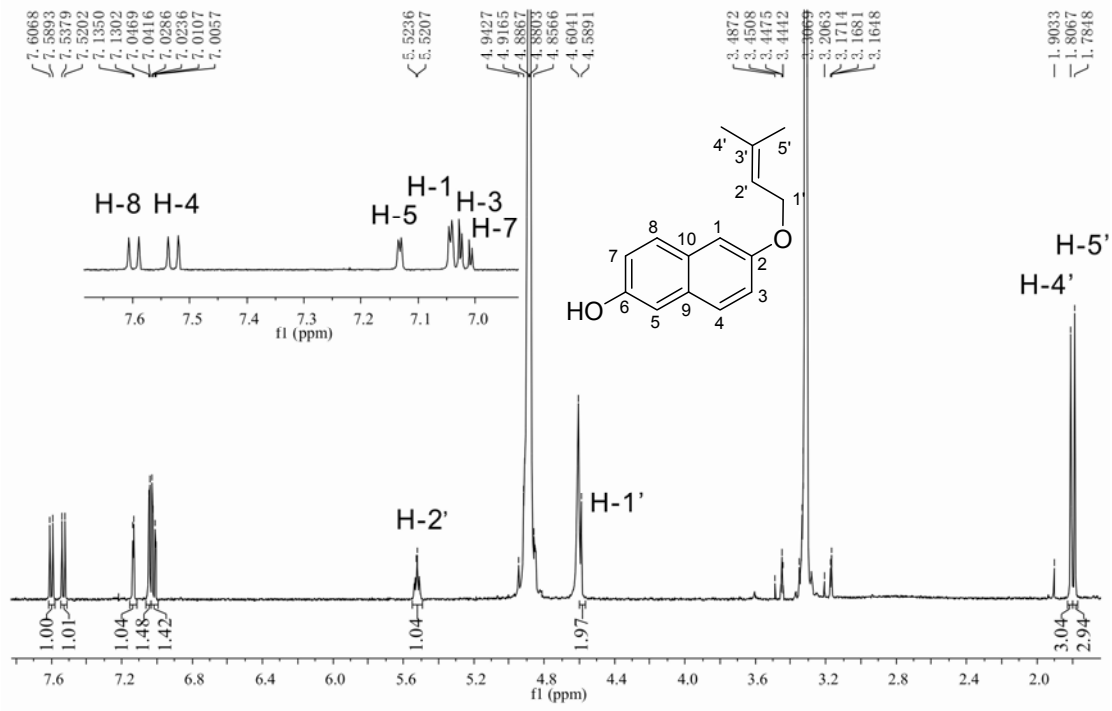

Figure S6 ^{1}H-NMR spectrum of **3i** in CD_3OD (500 MHz)

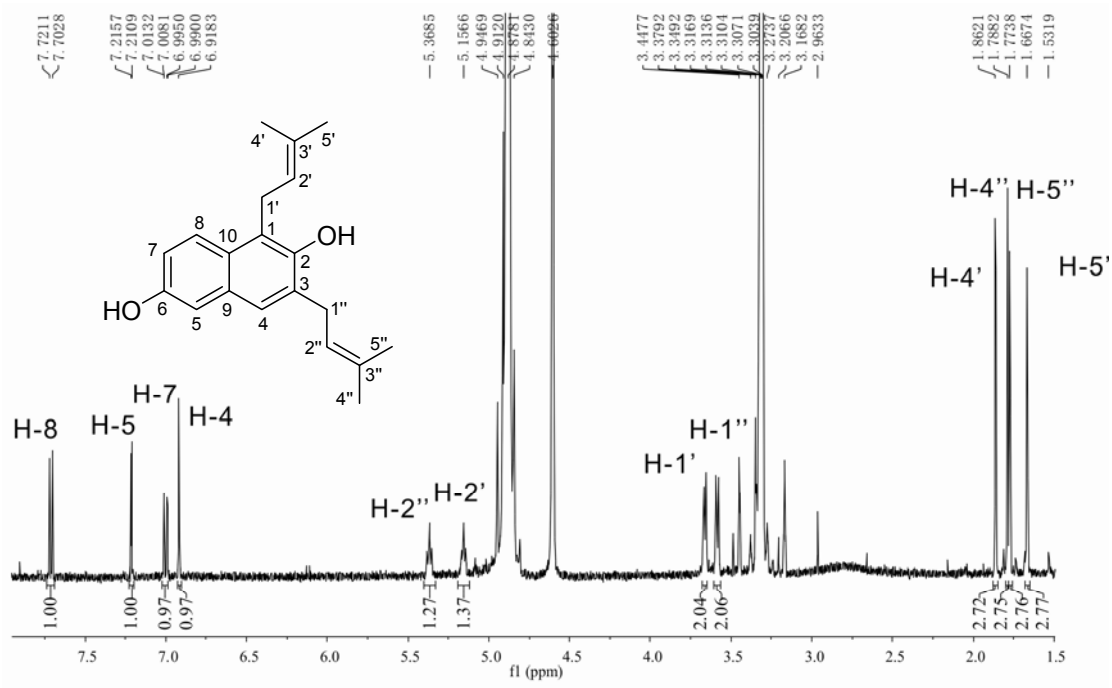

Figure S7 ^{1}H-NMR spectrum of **4i** in CD_3OD (500 MHz)

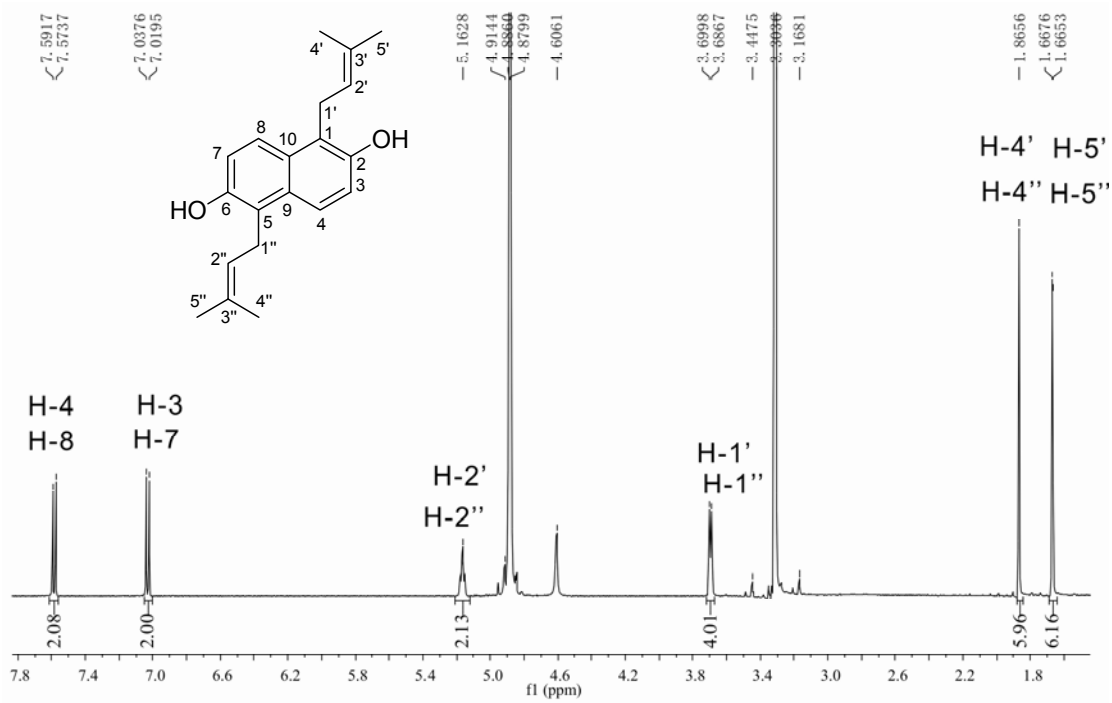

Figure S8 ^{1}H-NMR spectrum of **5i** in CD_3OD (500 MHz)

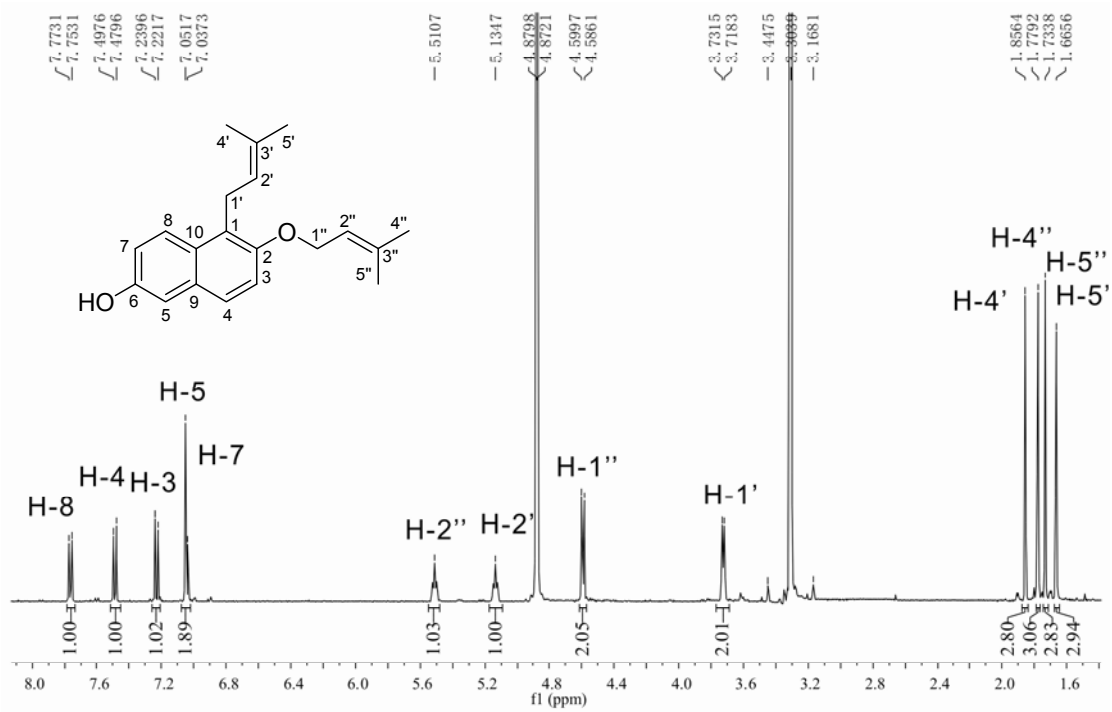

Figure S9 ^{1}H-NMR spectrum of **6i** in CD_3OD (500 MHz)

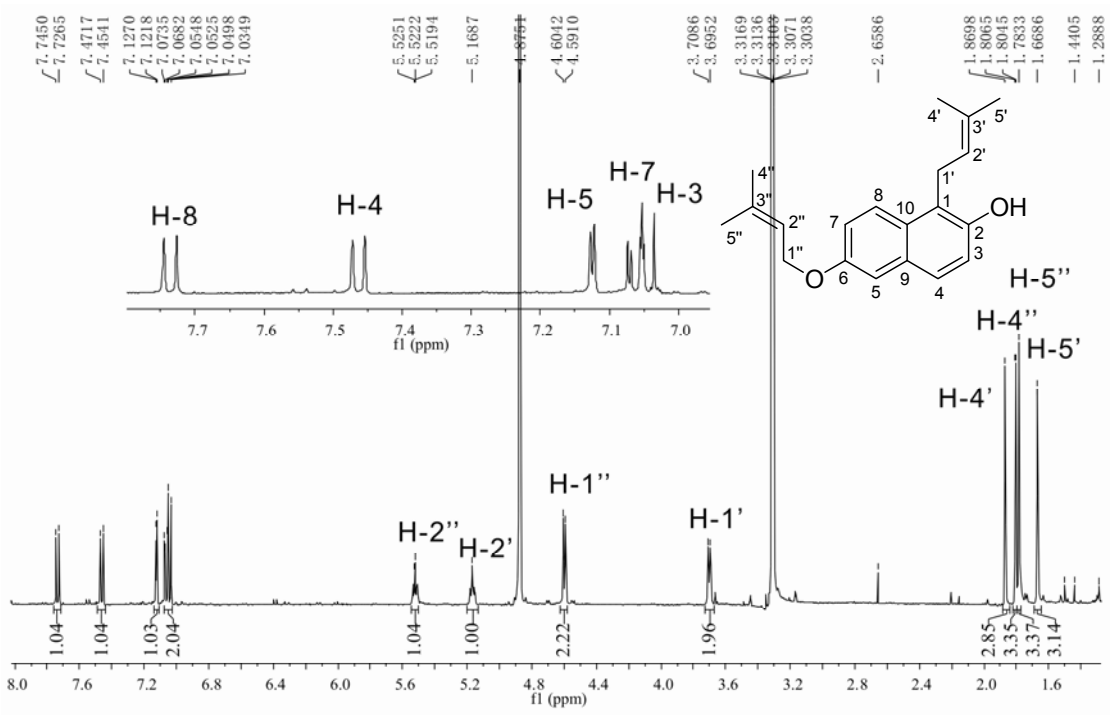

Figure S10 ^{1}H-NMR spectrum of **7i** in CD_3OD (500 MHz)

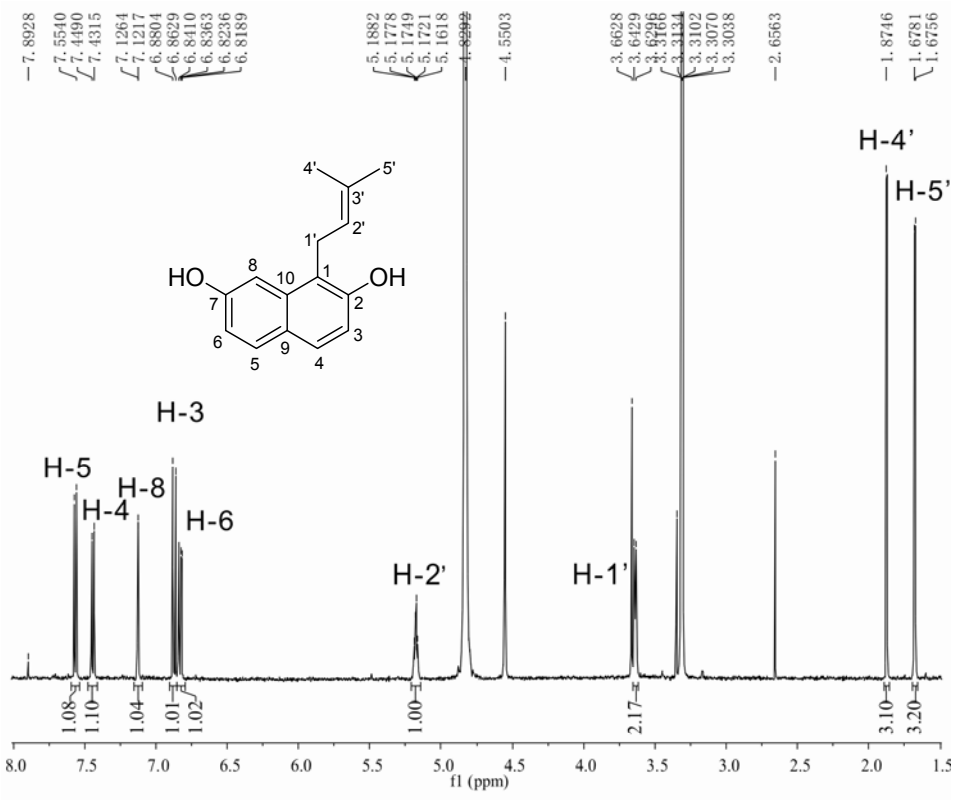

Figure S11.1 ^{1}H-NMR spectrum of **2j** in CD_3OD (500 MHz)

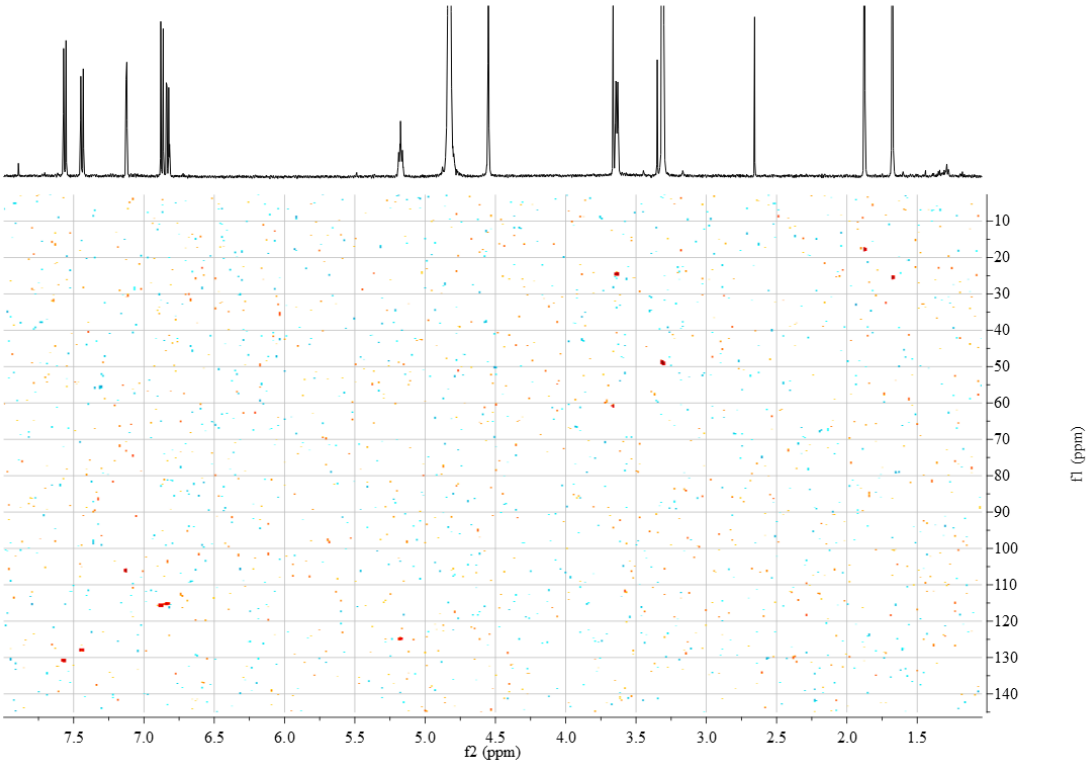

Figure S11.2 HSQC spectrum of **2j** in CD_3OD (500 MHz)

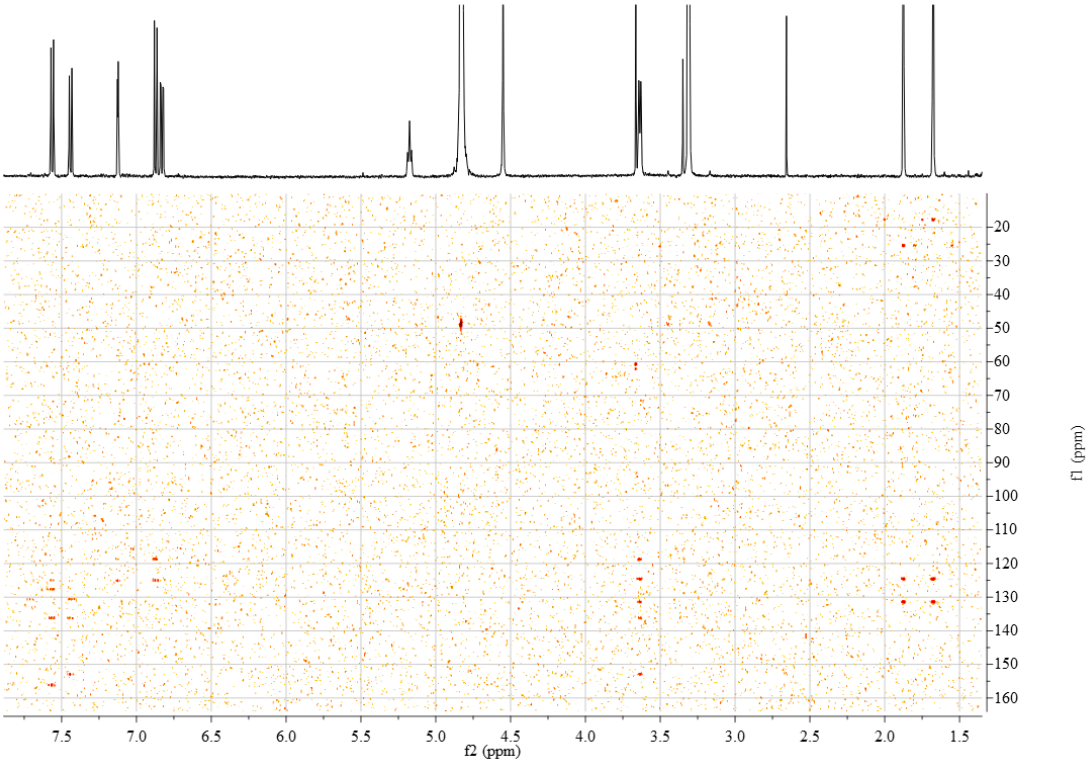

Figure S11.3 HMBC spectrum of **2j** in CD_3OD (500 MHz)

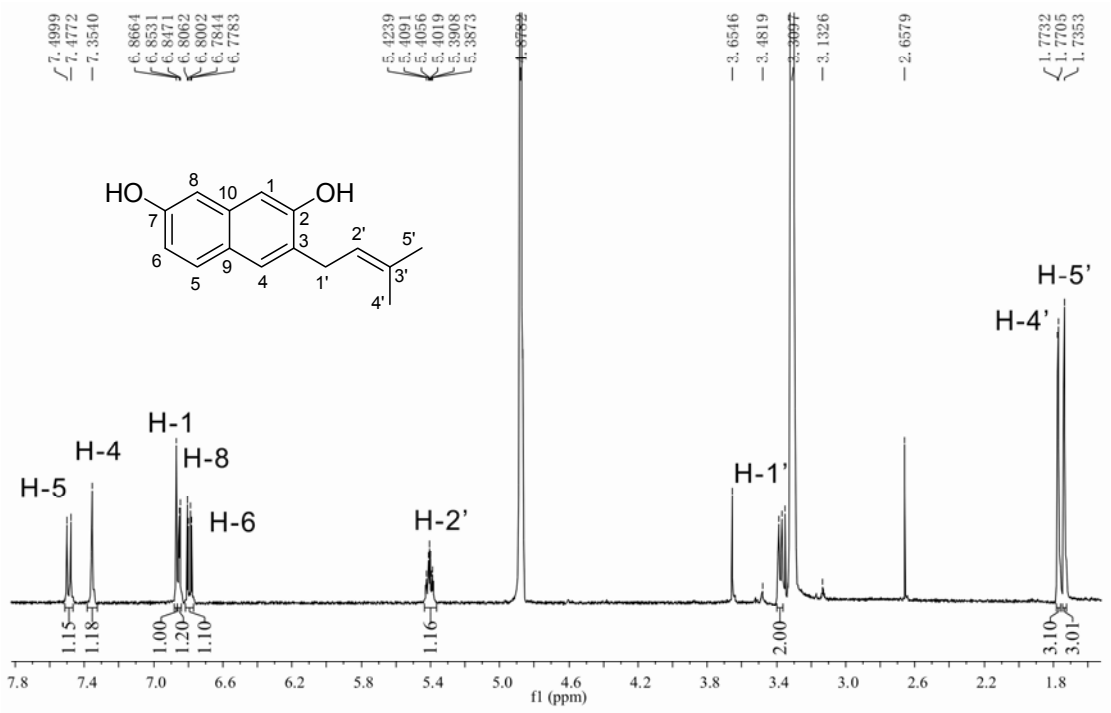

Figure S12 ^{1}H-NMR spectrum of **3j** in CD_3OD (400 MHz)

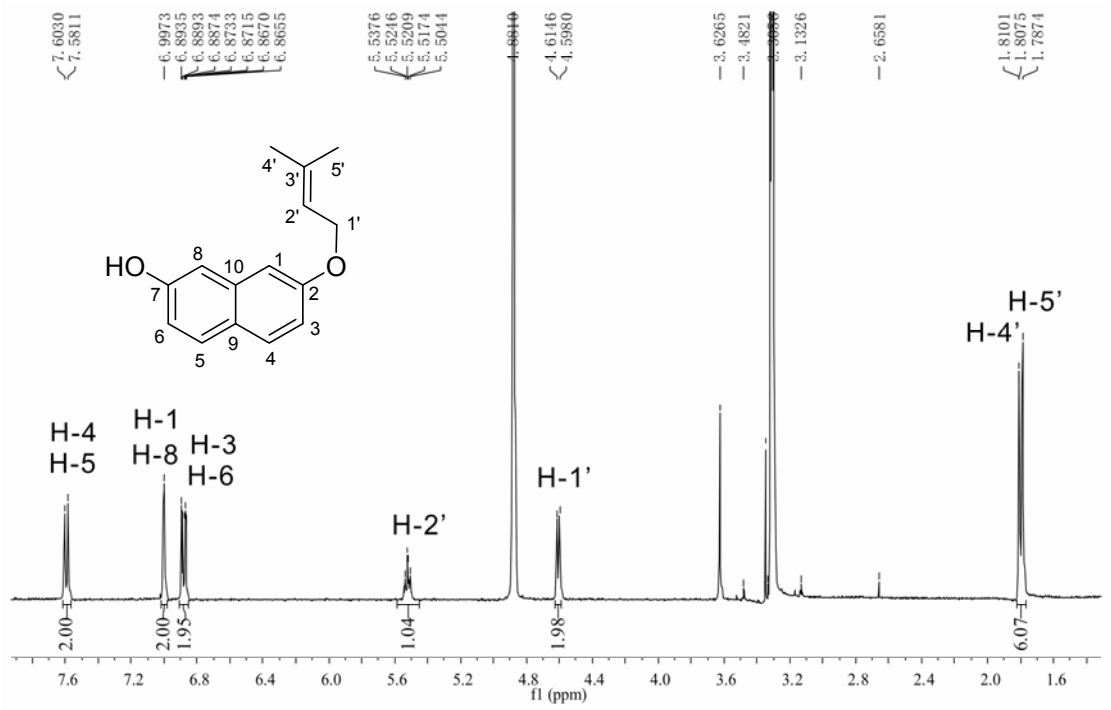

Figure S13 ^{1}H-NMR spectrum of **4j** in CD_3OD (400 MHz)

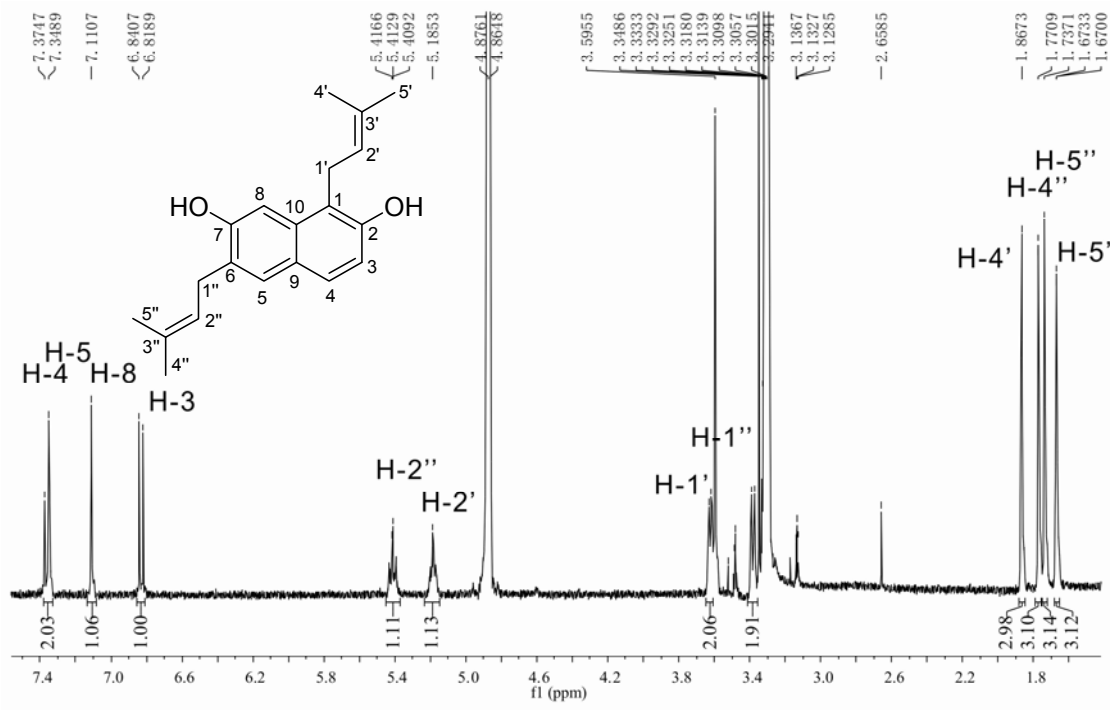

Figure S14 ^{1}H-NMR spectrum of **5j** in CD_3OD (400 MHz)

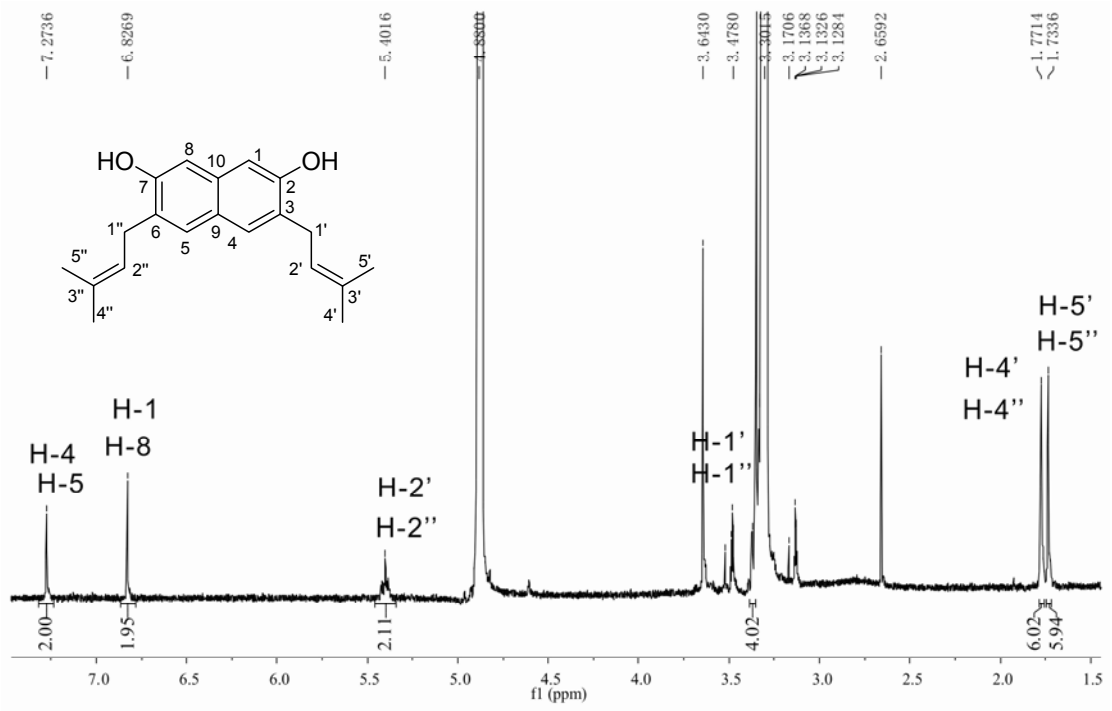

Figure S15 ^{1}H-NMR spectrum of **6j** in CD_3OD (400 MHz)

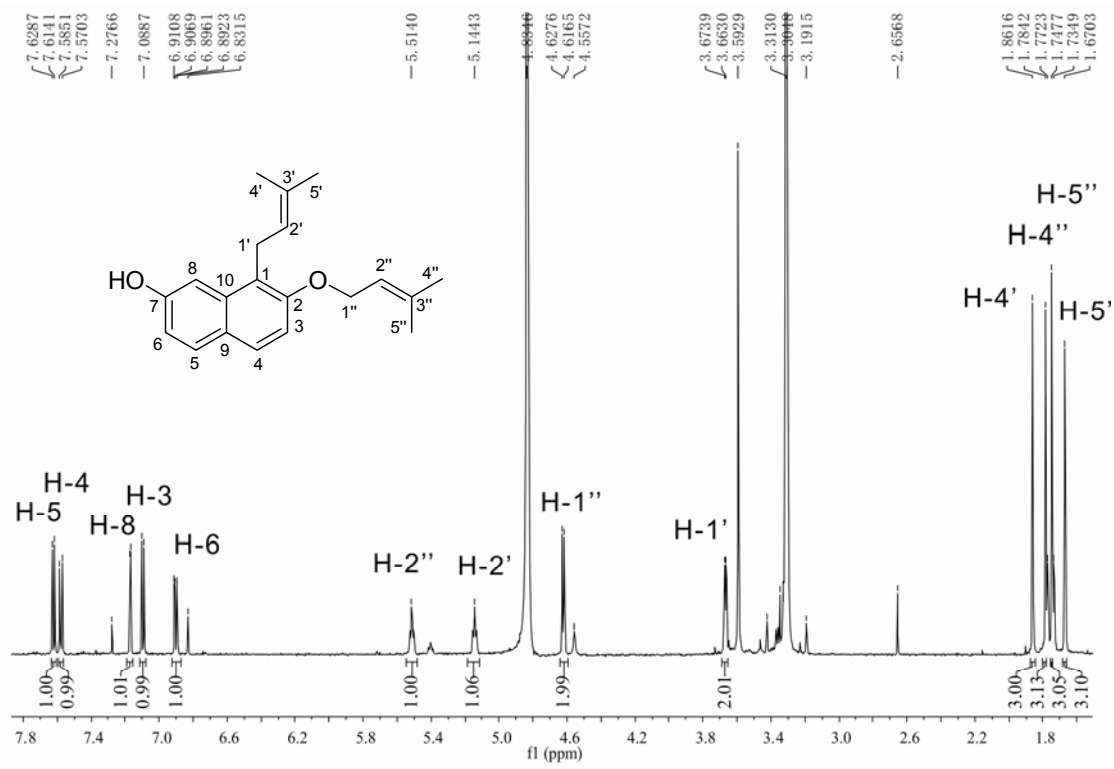

Figure S16.1 ^{1}H-NMR spectrum of **7j** in CD_3OD (600 MHz)

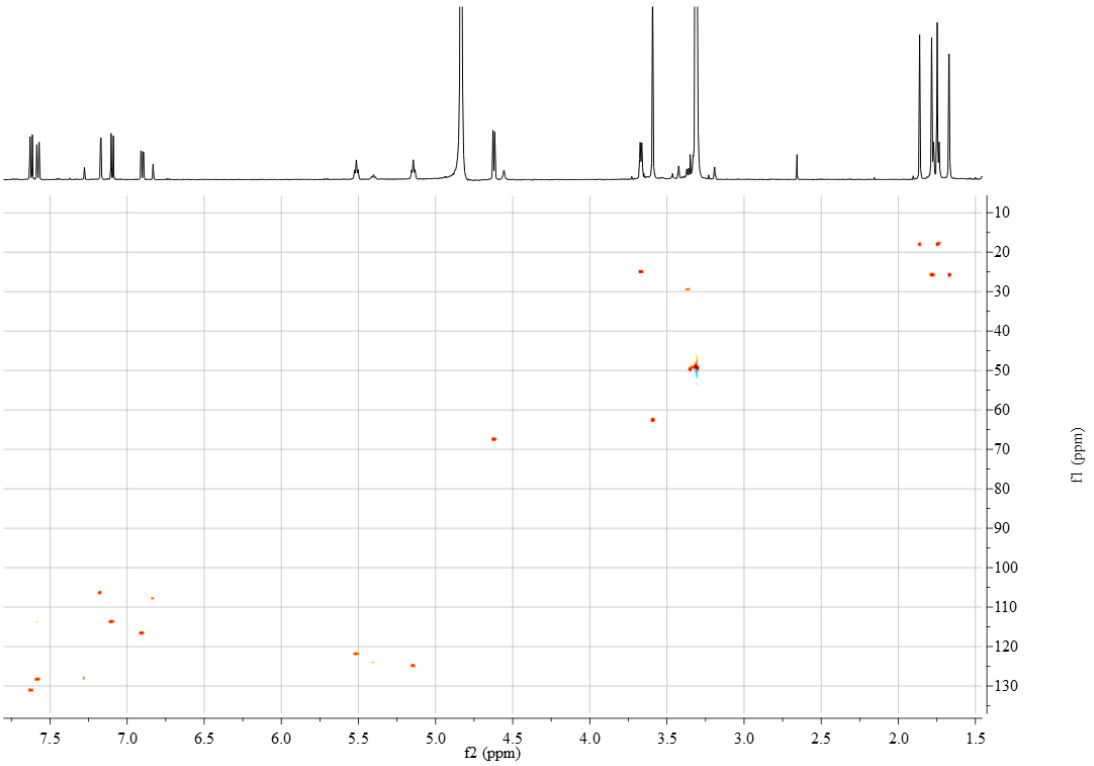

Figure S16.2 HSQC spectrum of **7j** in CD_3OD (600 MHz)

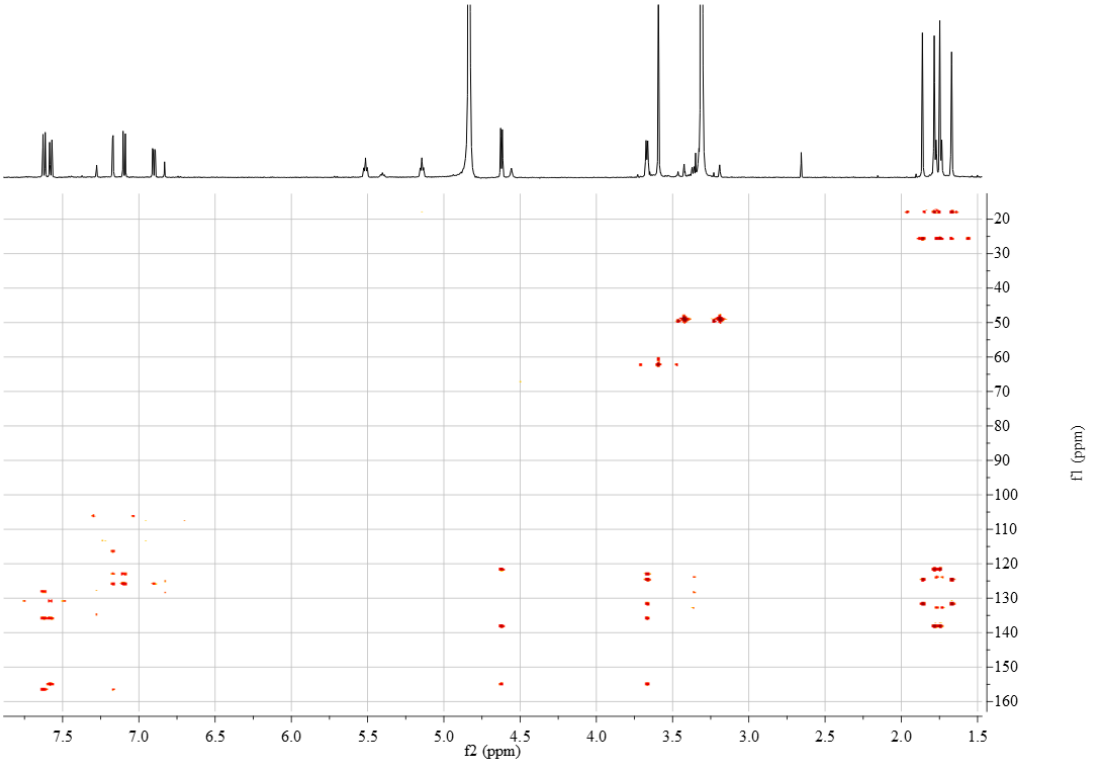

Figure S16.3 HMBC spectrum of **7j** in CD_3OD (600 MHz)

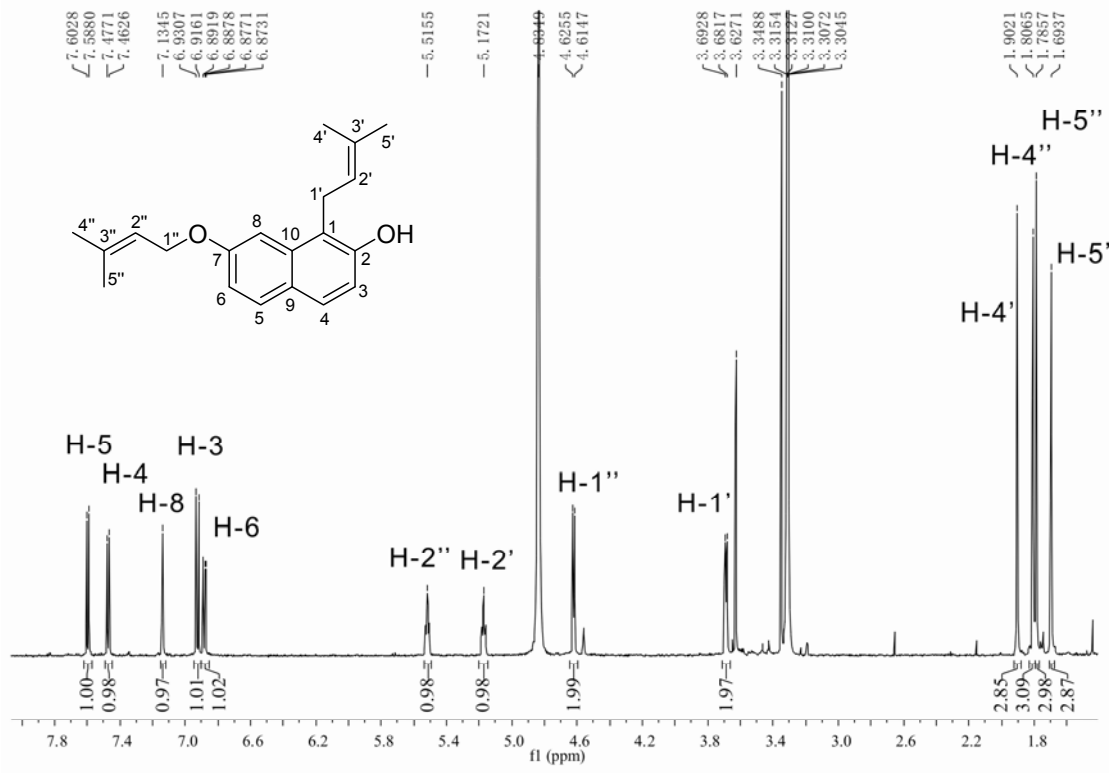

Figure S17.1 ^{1}H-NMR spectrum of **8j** in CD_3OD (600 MHz)

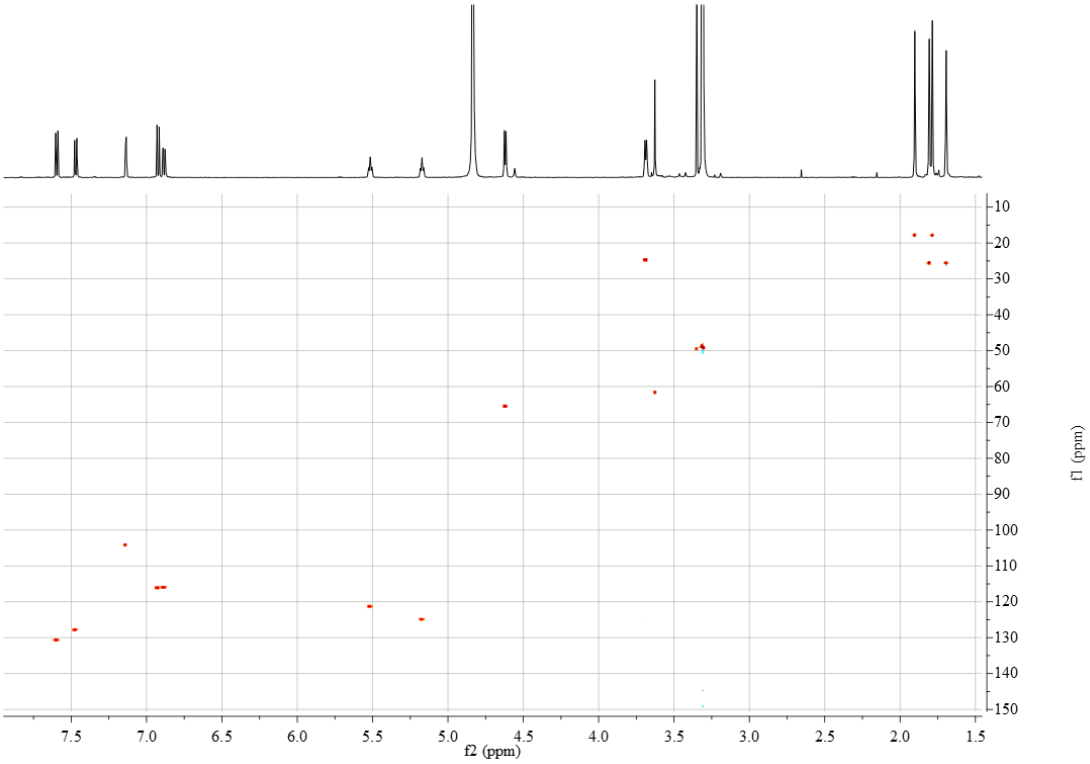

Figure S17.2 HSQC spectrum of **8j** in CD_3OD (600 MHz)

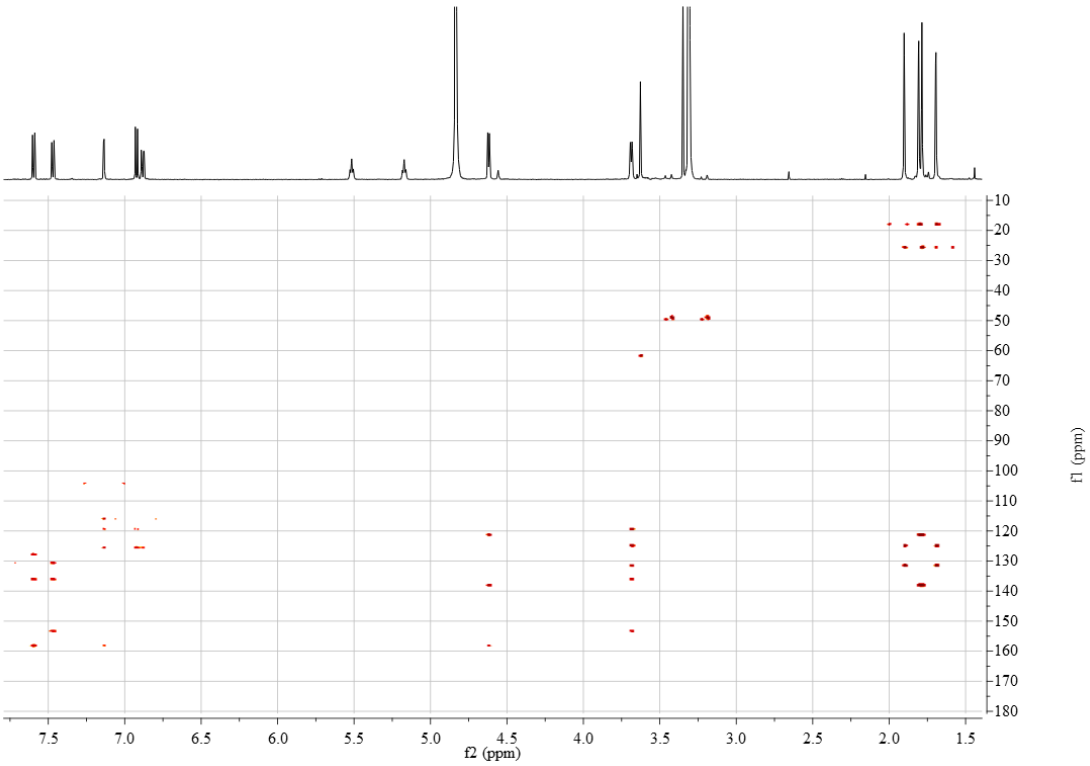

Figure S17.3 HMBC spectrum of **8j** in CD_3OD (600 MHz)

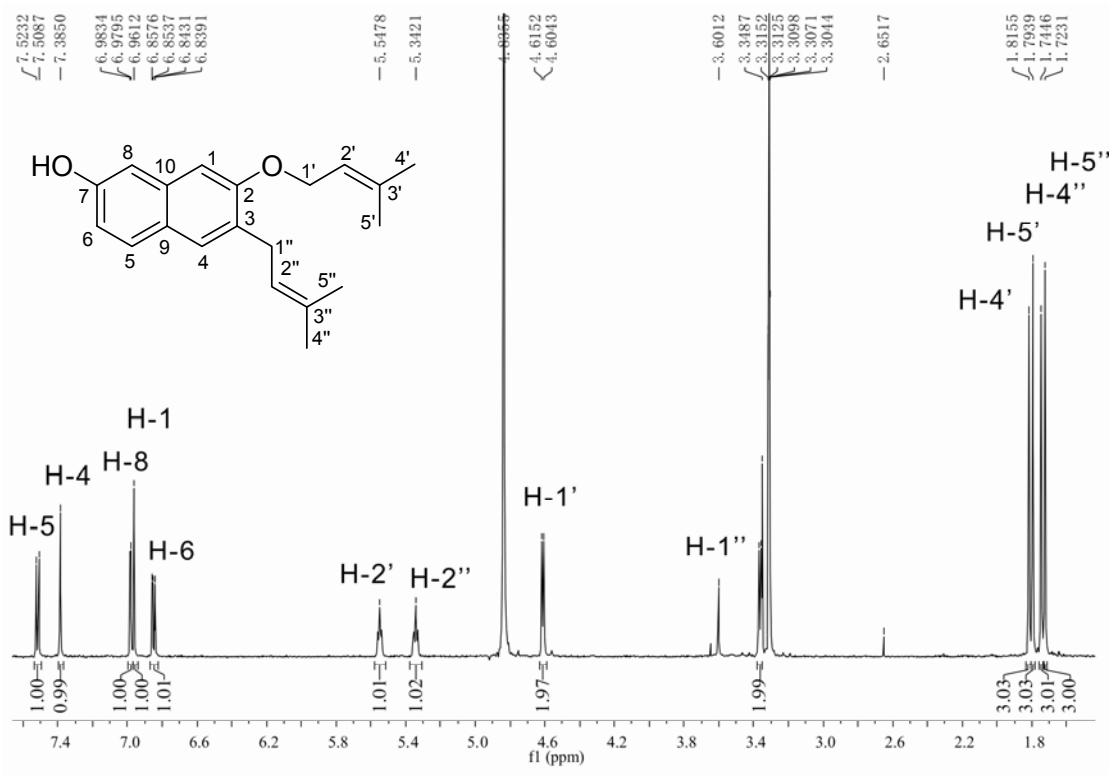

Figure S18.1 ^{1}H-NMR spectrum of **9j** in CD_3OD (600 MHz)

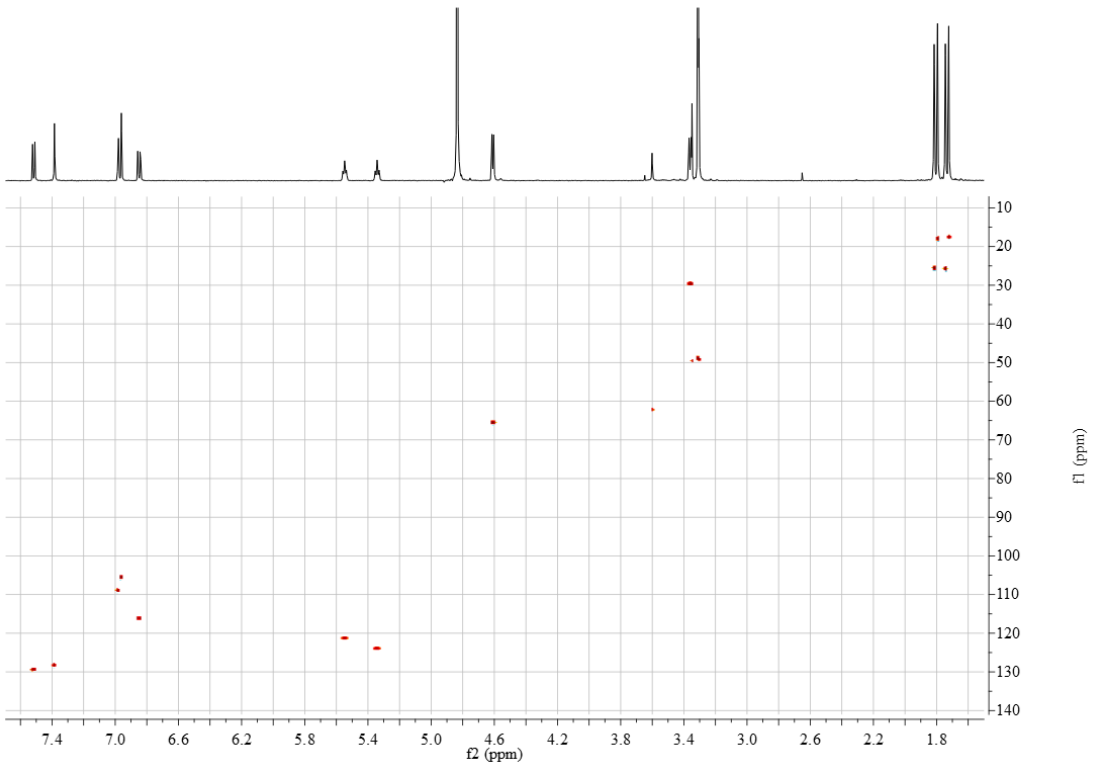

Figure S18.2 HSQC spectrum of **9j** in CD_3OD (600 MHz)

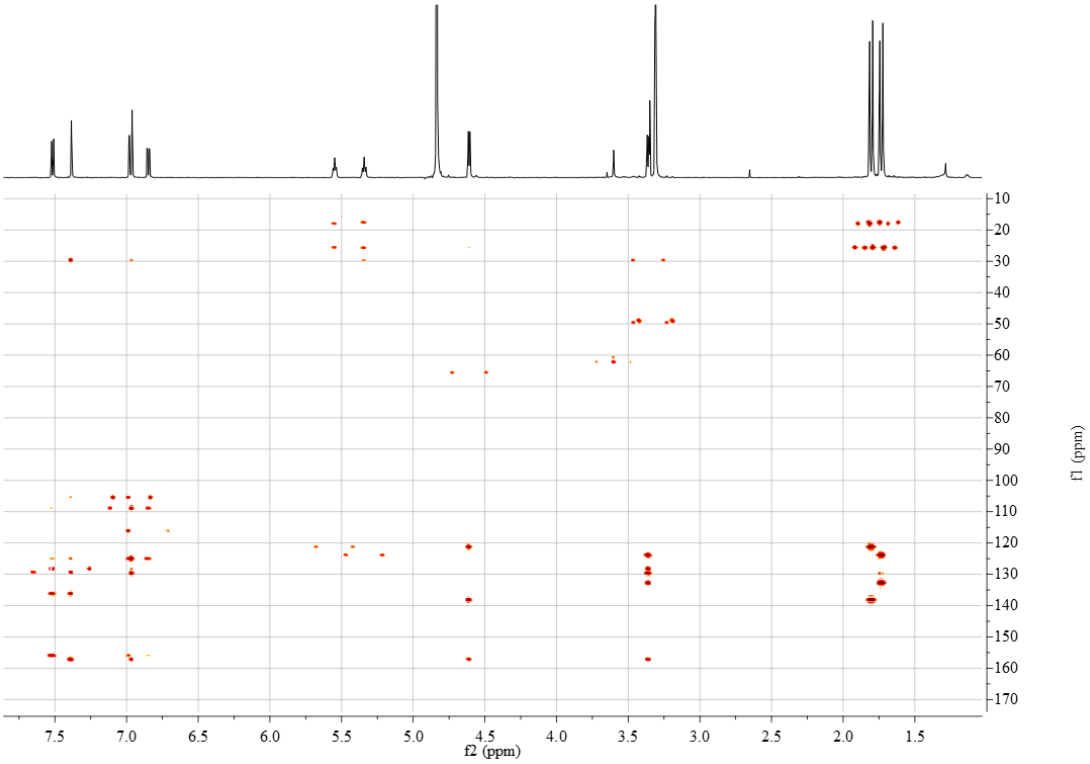

Figure S18.3 HMBC spectrum of **9j** in CD_3OD (600 MHz)

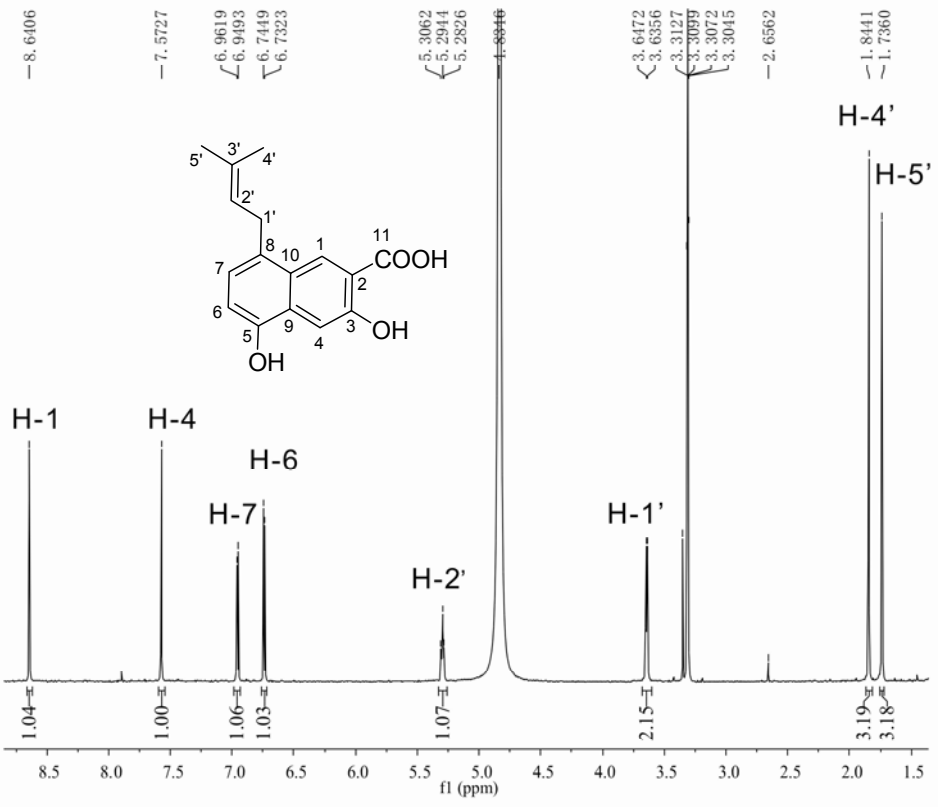

Figure S19.1 ^{1}H-NMR spectrum of **2k** in CD_3OD (600 MHz)

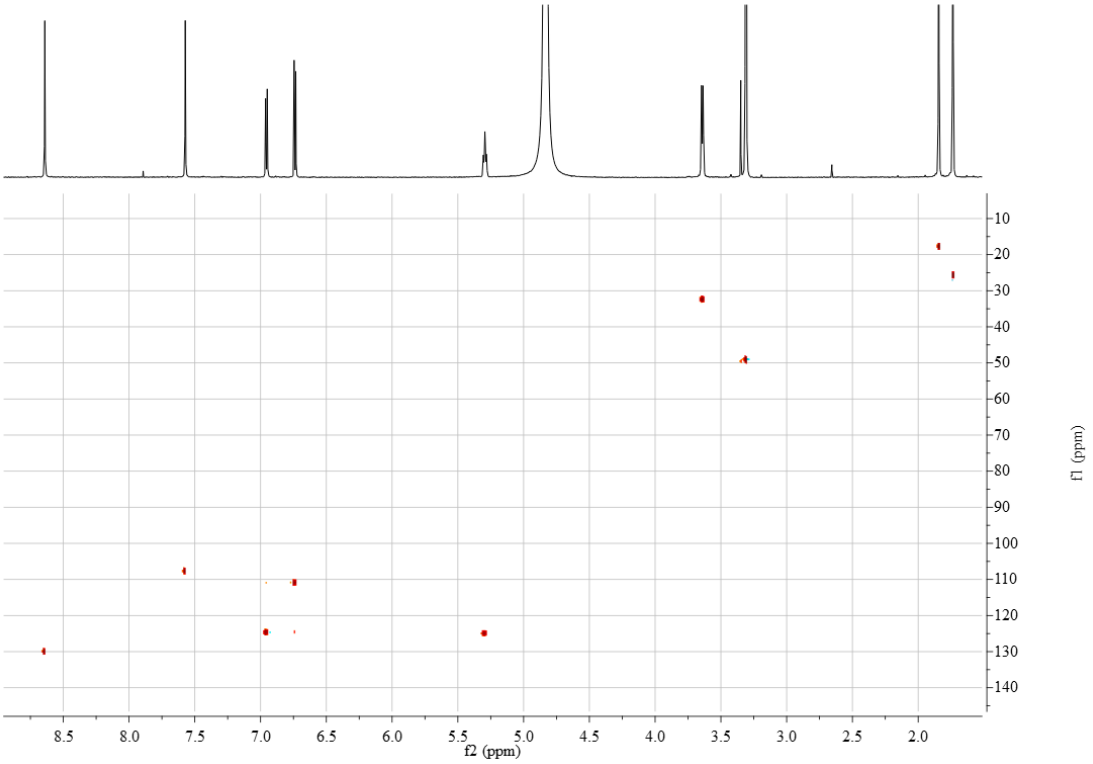

Figure S19.2 HSQC spectrum of **2k** in CD_3OD (600 MHz)

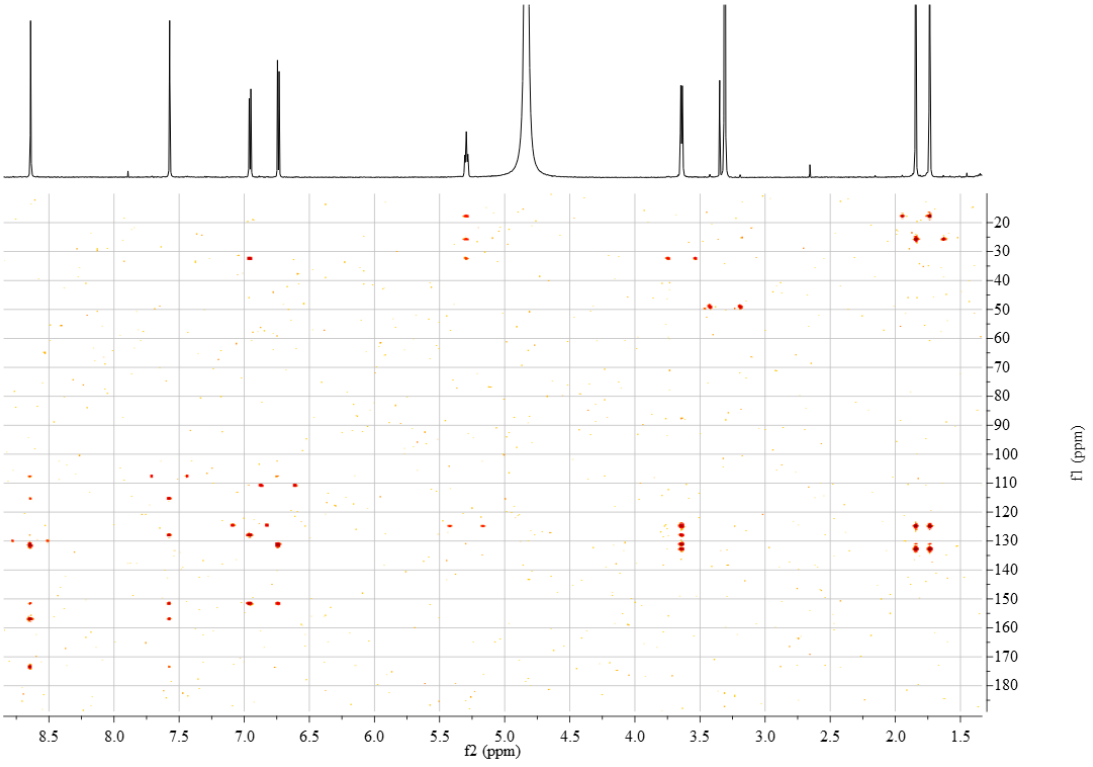

Figure S19.3 HMBC spectrum of **2k** in CD_3OD (600 MHz)

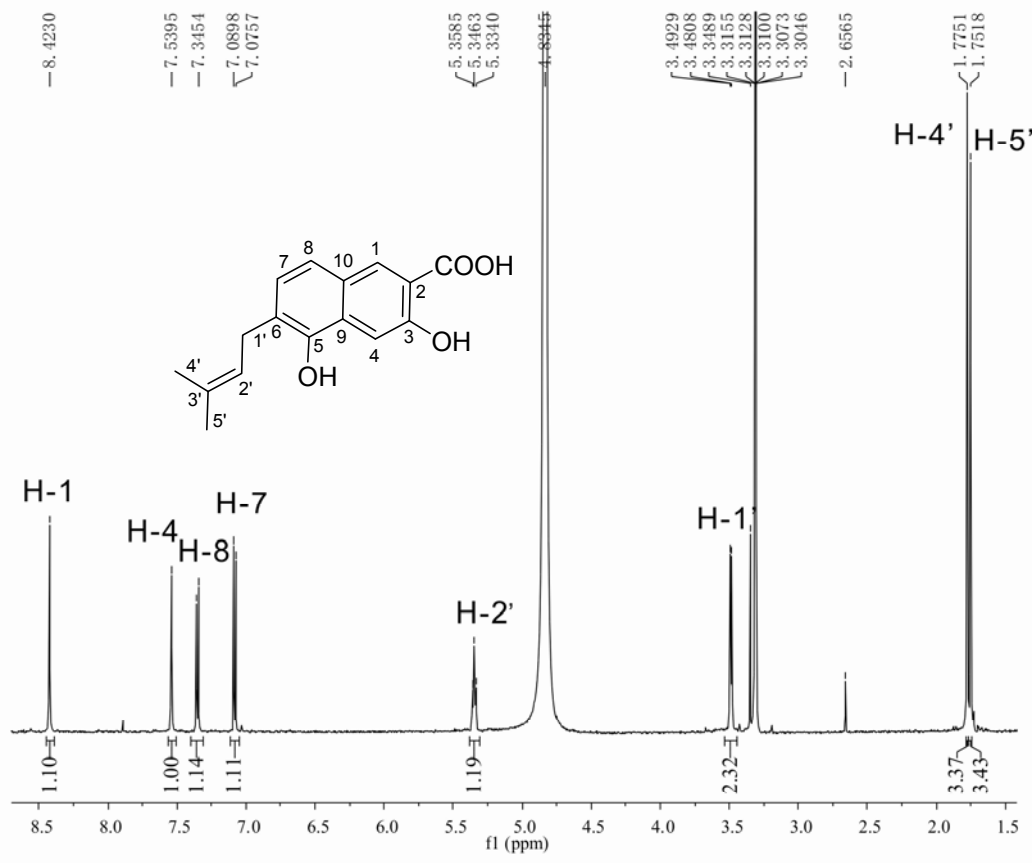

Figure S20.1 ^{1}H-NMR spectrum of **3k** in CD_3OD (600 MHz)

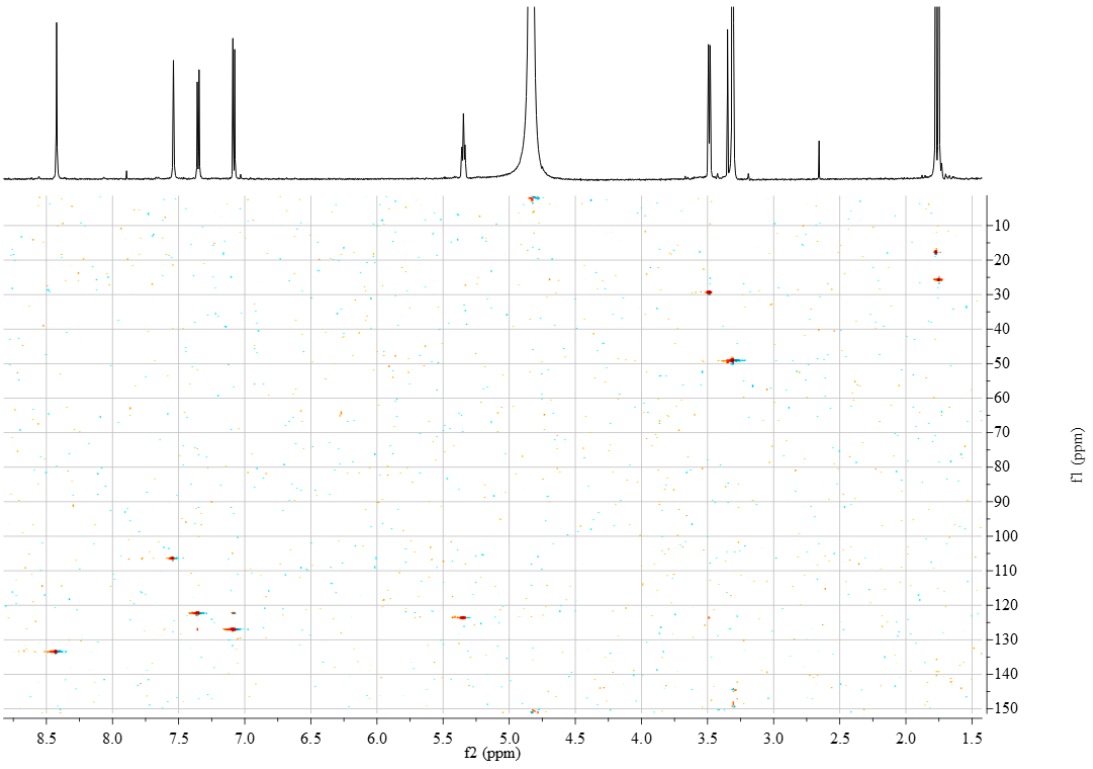

Figure S20.2 HSQC spectrum of **3k** in CD_3OD (600 MHz)

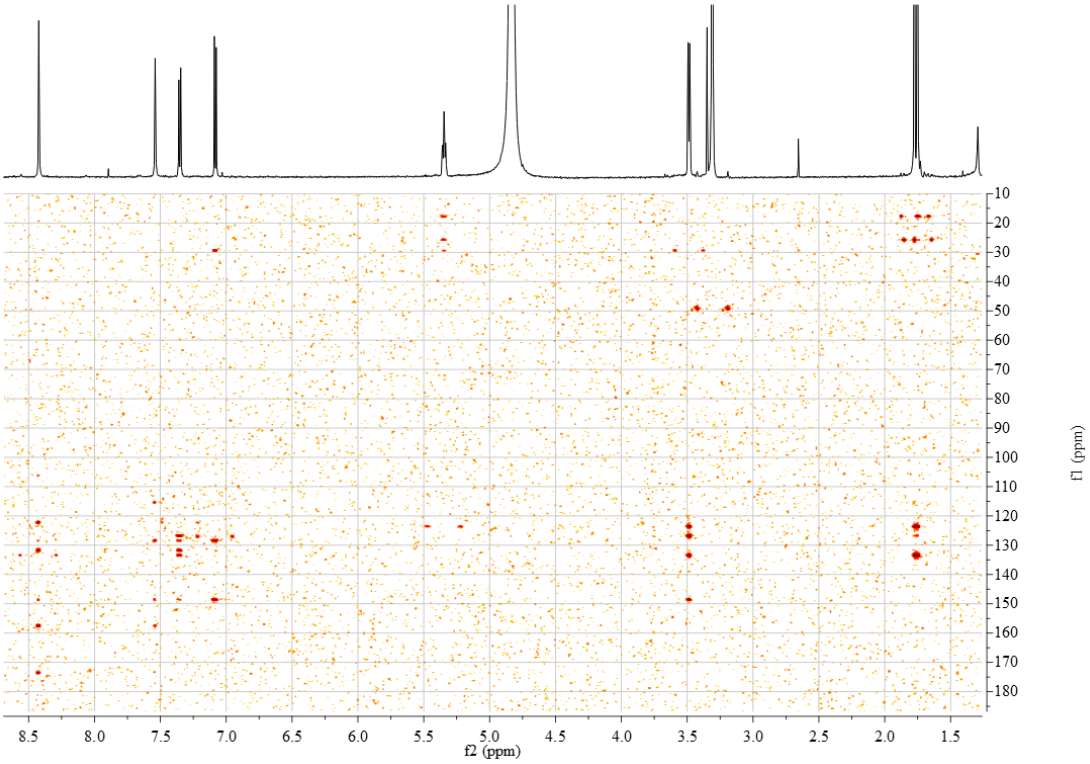

Figure S20.3 HMBC spectrum of **3k** in CD_3OD (600 MHz)

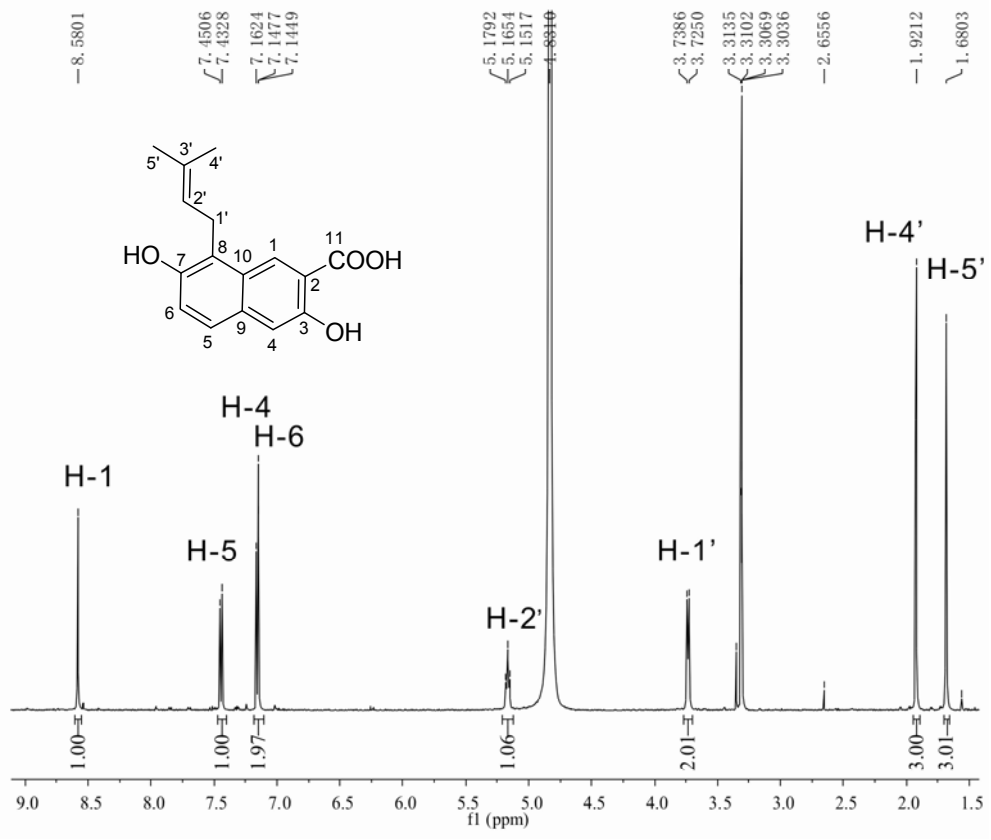

Figure S21.1 ^{1}H-NMR spectrum of **2l** in CD_3OD (500 MHz)

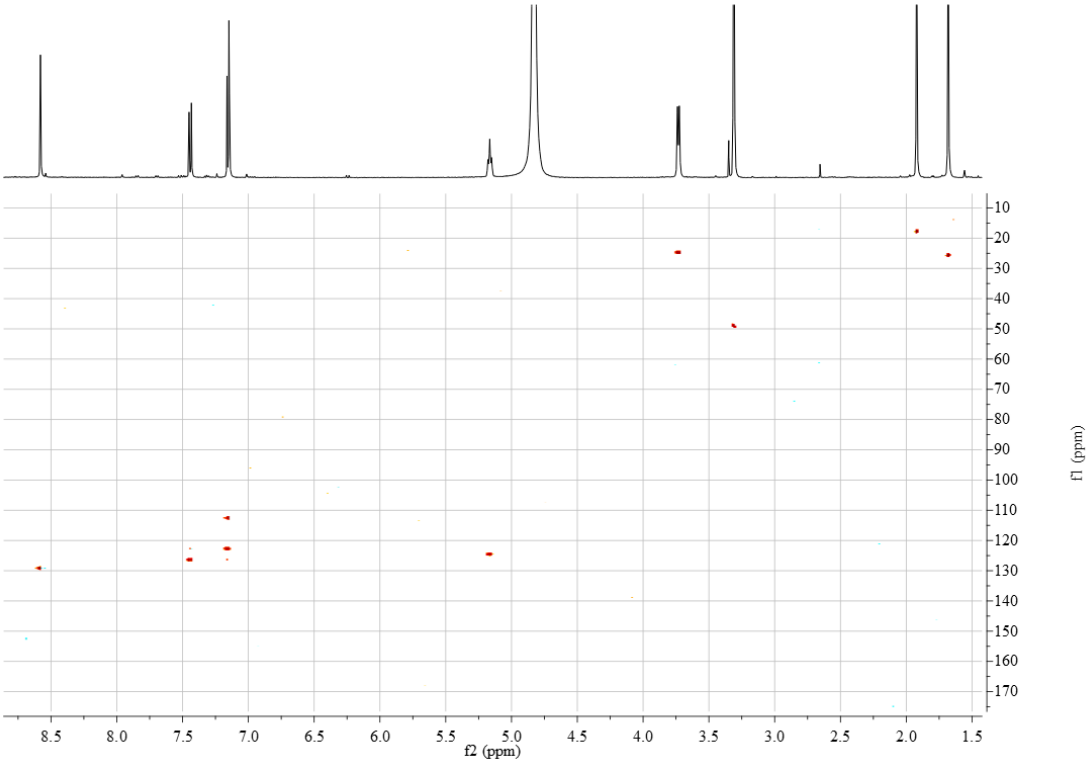

Figure S21.2 HSQC spectrum of **2l** in CD_3OD (500 MHz)

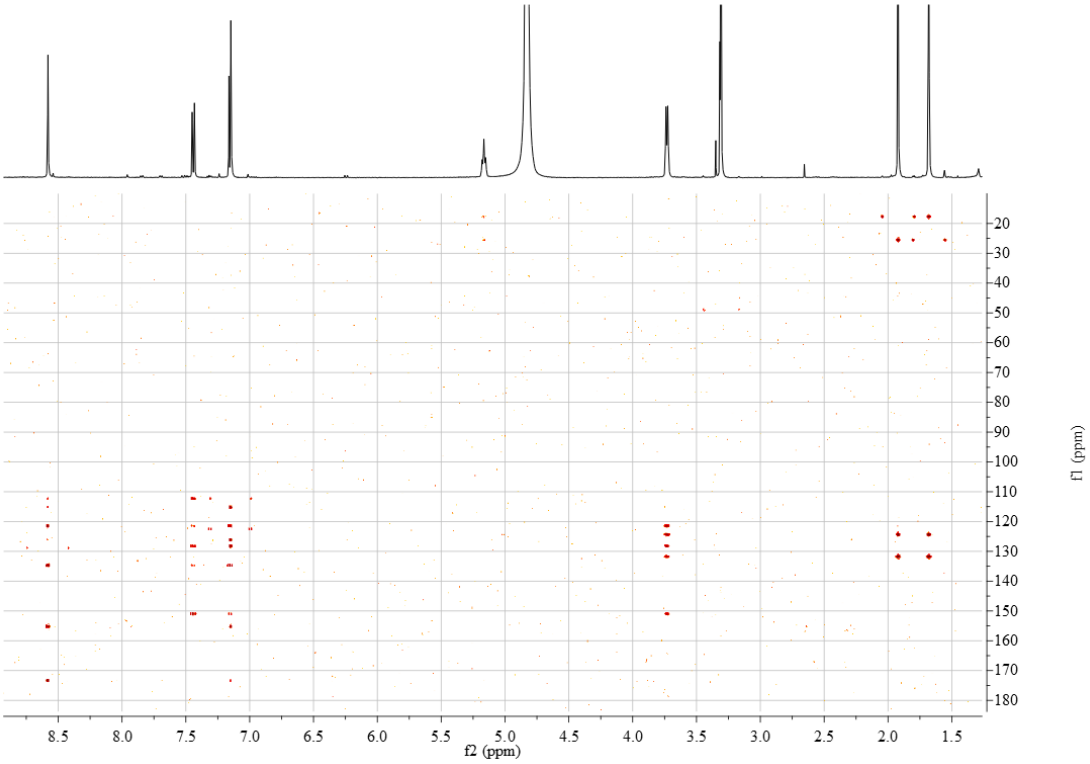

Figure S21.3 HMBC spectrum of **2l** in CD_3OD (500 MHz)

5.7 Prenylation of flavonoids by using a dimethylallyltryptophan synthase 7-DMATS from *Aspergillus fumigatus*

DOI: 10.1002/cbic.201100413

Prenylation of Flavonoids by Using a Dimethylallyltryptophan Synthase, 7-DMATS, from *Aspergillus fumigatus*

Xia Yu[a] and Shu-Ming Li*[a, b]

Prenylated flavonoids including prenylated chalcones and isoflavonoids are widely distributed in the nature, predominantly in plants.[1,2] Prenylation often improves the affinity for biomembranes and the interaction with proteins of a compound,[2] and therefore dramatically increases the biological activity. Diverse biological and pharmacological activities such as antifungal, antibacterial, antiviral, antiparasitic, anti-inflammatory, antitumor, cancer chemoprevention, estrogenic, and antiestrogenic activities have been described for prenylated flavonoids.[1–3]

Due to the broad pharmacological activities of prenylated flavonoids, various strategies have been developed for their regioselective chemical synthesis, especially for C-prenylated derivatives.[4,5] Meanwhile, significant progress has also been made in the identification of enzymes that catalyze the transfer of prenyl moieties onto the flavonoid skeleton.[6] Three membrane-bound prenyltransferases from *Sophora flavescens* have been cloned, expressed, and characterized biochemically.[7,8] The identified enzymes include a naringenin 8-prenyltransferase (SfN8DT-1),[8] an isoflavone-specific C6-prenyltransferase (SfG6DT), and the chalcone-specific isoliquiritigenin dimethylallyltransferase (SfiLDT).[7] Those enzymes showed very high substrate specificities and accepted only their natural substrates or just a few substances with very similar structures. This feature prohibits their potential application as catalysts for the chemoenzymatic synthesis of prenylated flavonoids. Furthermore, these membrane-bound enzymes are generally more difficult to overproduce and purify than soluble enzymes.

Fortunately, it has been demonstrated that some prenyltransferases of the CloQ/NphB group from the soil bacteria *Streptomyces* are also capable of catalyzing the prenylation of flavonoids. For example, the 4-hydroxyphenylpyruvate C3-prenyltransferase NovQ also accepted flavonoids and isoflavonoids as substrates and catalyzed O- and C-prenylations at ring B.[9] NphB is a hydroxynaphthalene geranyltransferase.[10] This enzyme also catalyzed O- and C-geranylation at 7-OH or C-6 in flavonoid and isoflavonoid ring A.[11] The SCO7190 protein, a homologue of NphB from *Streptomyces coelicolor*, catalyzed the prenylation of naringenin at position C-6 in the presence of dimethylallyl diphosphate (DMAPP).[11] In summary, many prenylated flavonoids have been produced by using recombinant enzymes. However, only a few such derivatives have a dimethylallyl moiety at position C-6. No acceptance of flavonoids by a prenyltransferase from the DMATS superfamily had been reported prior to this study. This is not surprising because fungi produce almost no flavonoids. The members of the DMATS superfamily are secondary-metabolite enzymes of ascomycota and mainly involved in the biosynthesis of prenylated indole alkaloids.[12] They catalyze prenylation at the indole moieties of diverse substrates including tryptophan and tryptophan-containing cyclic dipeptides.[12] Recent studies have shown that several members of the DMATS superfamily also accept tyrosine or xanthones as natural substrates.[13,14] Furthermore, we have recently demonstrated that some of the fungal indole prenyltransferases also accept hydroxynaphthalene derivatives, and convert them to prenylated derivatives.[15] (Hydroxynaphthalenes are natural substrates of some prenyltransferases of the CloQ/NphB group.[16]) These results encouraged us to test the acceptance of flavonoids, including chalcones and isoflavonoids, by members of the DMATS superfamily.

Incubation of up to 30 flavonoids with seven fungal prenyltransferases, 7-DMATS, AnaPT, CdpC3PT, CdpNPT, SirD, FtmPT1 and FgaPT2,[12,13] showed that 7-DMATS has a more flexible substrate specificity towards these compounds than the other enzymes (data not shown). A detailed study was therefore carried out with 7-DMATS from *Aspergillus fumigatus*, which catalyzes the prenylation of tryptophan and derivatives at position C7.[17,18] In total, 16 flavonoids and analogues were incubated with purified, recombinant 7-DMATS from *Escherichia coli* in the presence of DMAPP (Supporting Information).[18] HPLC analysis was used to monitor product formation. Incubation with protein that had been heat-inactivated by being boiled for 20 min was used as a negative control. Product formation was detected for 14 substrates after incubation with 14 μg protein per 100 μL assay at 37 °C for 16 h (data not shown), six yields were more than 12% (**1a**–**6a**, Figure 1). Chalcones, isoflavonoids, and flavanones were much better accepted than flavones and flavonols. For example, total conversion yields of 22.8, 18.7, 12.3, 46.2, 24.1, and 14.5%, respectively, were calculated for the isoflavones **1a** and **2a**, flavanones **3a**, **4a** and **5a** as well as for the chalcone **6a**. The corresponding flavones of **3a** and **4a**, that is, apigenin and luteuolin, were also accepted by 7-DMATS, but only with conversion yields of 3.8 and 8.2%, respectively. The corresponding flavonols of these compounds, that is, kaempferol and quercetin, were accepted with conversion yields of 4.7 and 2.7%, respectively.

As shown in Figure 1, one dominant product peak was detected for each of the incubation mixtures of **1a**, **2a**, **3a**, and **6a**. In the cases of **4a** and **5a**, at least two product peaks

[a] X. Yu, Prof. Dr. S.-M. Li
Institut für Pharmazeutische Biologie und Biotechnologie
Philipps-Universität Marburg
Deutschhausstrasse 17A, 35037 Marburg (Germany)
E-mail: shuming.li@staff.uni-marburg.de

[b] Prof. Dr. S.-M. Li
Zentrum für Synthetische Mikrobiologie, Philipps-Universität Marburg
35032 Marburg (Germany)

Supporting information for this article is available on the WWW under http://dx.doi.org/10.1002/cbic.201100413.

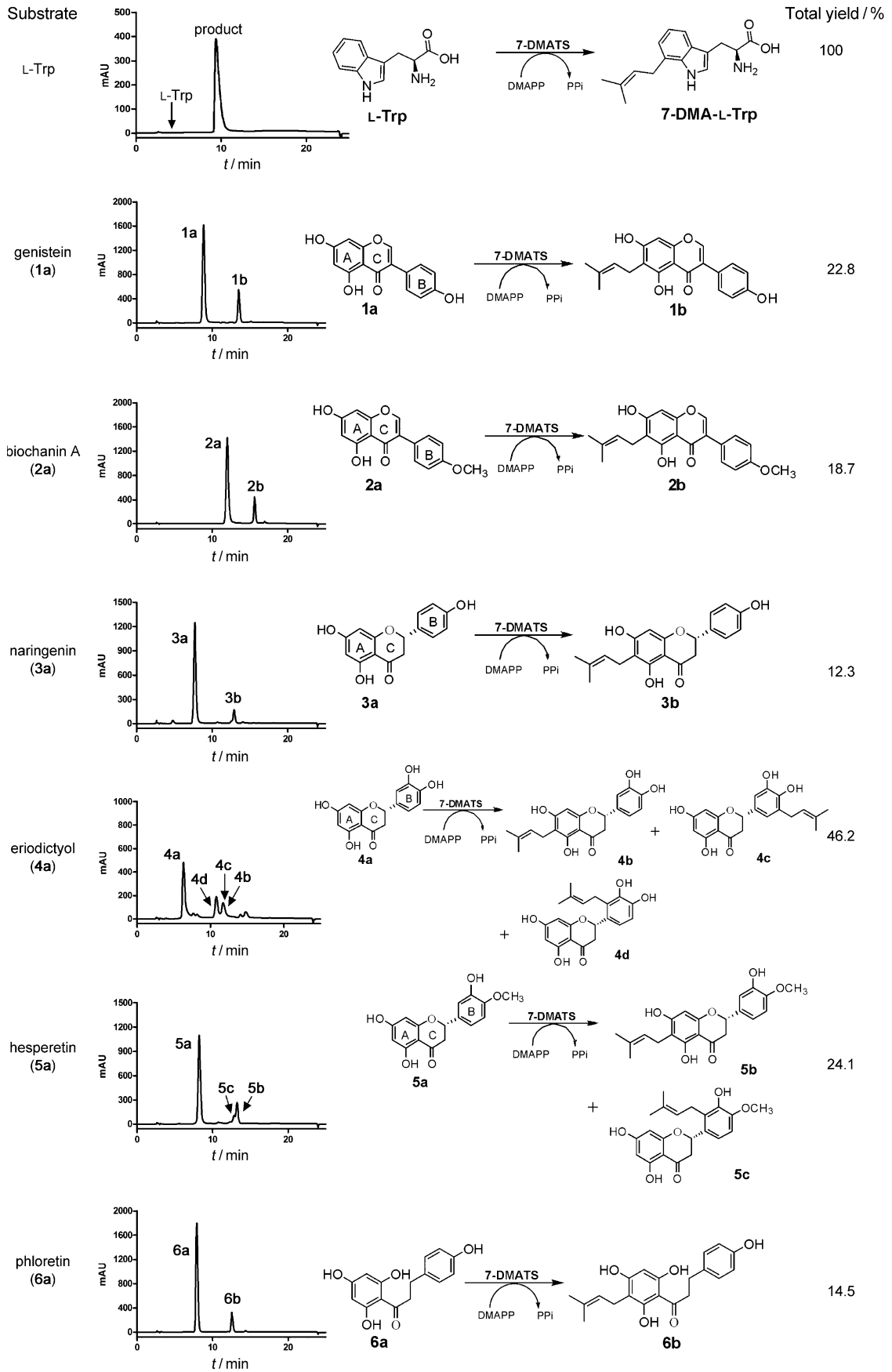

Figure 1. HPLC chromatograms and prenyltransfer reactions catalyzed by 7-DMATS. The absorption at 277 nm is illustrated.

were observed. To elucidate the structures, nine products were isolated from the incubation mixtures of these six substrates and subjected to MS and NMR analyses (Supporting Information). HR-EI-MS (Table S1) indicated the presence of one prenyl moiety each in the enzyme products by showing molecular masses that are 68 Da larger than those of the respective substrates. The ^{1}H NMR signals at $\delta_H = 3.21–3.53$ (d, 2H-1′), 5.15–5.35 (m, H-2′), 1.68–1.78 (s, 3H-4′), and 1.62–1.71 ppm (s, 3H-5′; Figures S1–S9 and Table S2) confirmed the presence of a regular dimethylallyl moiety. The resonance of H-1′ in the range of 3.21–3.53 ppm proved their attachment to aromatic carbon atoms.[15] A literature search revealed that the ^{1}H NMR data of **1b**, **2b**, **3b**, **4b**, **4c**, and **6b** corresponded well to those of the plant metabolites wighteone,[5] gancaonin A,[19,20] 6-prenylnaringenin,[21] 6-prenyleriodictyol,[22] sigmoidin B,[23] and 6-dimethylallyl-5,7,9,1′-tetrahydroxydihydrochalcone,[24] respectively.

Comparing the signals in the spectrum of **5b** with those of the substrate (data not shown) revealed that the signals of the ABX system in ring B were almost unchanged. The singlet at $\delta_H = 6.04$ ppm represented one aromatic proton in ring A and indicated that the prenylation was at position C-6 or C-8. The singlet of 5-OH at $\delta_H = 12.46$ confirmed the attachment of the dimethylallyl moiety at position C-6.[22] Comparing the signals of **4d** and **5c** in the NMR spectra with those of the respective substrate (data not shown) showed that the ABX systems for ring B protons in the spectra of substrates had disappeared. Instead, two doublets with a coupling constant of 8.3 or 8.5 Hz were observed, thus proving the prenylation at position C-2′ (Figure 1 and Table S2). The structure of **4d** was assigned to a prenylated flavanone isolated from *Lycopersicon esculentum* seeds[25] and *Erythrina suberose* roots.[26] Nearly identical chemical shifts were given in these works, which clearly differed from those obtained in this study (all taken in [D$_6$]acetone). However, no coupling constants were presented in the publication by Gangwal et al.[25] In the second case, the observed coupling constant of 2 Hz was too small for the two protons in *ortho*- position (H-5′ and H-6′). It can therefore be concluded that the data obtained in the previous studies[25,26] are inconsistent with the structure of **4d**, and that **4d** reported in this study is a new structure. The structures of **5b** and **5c** have not been described previously.

From the structures of the enzyme products, it is obvious that the favorable prenylation position for 7-DMATS was C-6, between the two hydroxyl groups. C6-prenylated derivatives were isolated from all of the six investigated substrates. In the incubation mixtures of four compounds (**1a**, **2a**, **3a**, and **6a**), only compounds with C6-prenyl moieties were detected (Figure 1). Even in the incubation mixture of **5a**, in which a product with prenylation at ring B was also observed, the C6-prenylated derivative remained the dominant product.

To test the acceptance of prenylated flavonoids, the nine isolated products (0.2–0.4 mM) were incubated with 7-DMATS in the presence of DMAPP for 16 h and then analyzed by HPLC. Product peaks were detected in eight of the incubation mixtures; no conversion was detected for **2b**. Conversion yields of between 0.9 and 7.7% were calculated for **1b**, **3b**, **5b**, **5c**, and **6b**. Much higher conversion yields of 71, 100, and 48% were observed for **4b–d**, respectively. Unfortunately, at least three product peaks were detected in each of the incubation mixtures of **4b–d**, respectively. Due to the low amounts, the structures of these products could not be elucidated in this study.

To get information on the catalytic efficiency of 7-DMATS toward flavonoids, kinetic parameters including Michaelis–Menten constants (K_M) and turnover numbers (k_{cat}) were determined for **1a–6a** by Hanes–Woolf and Eadie–Hofstee plots and compared to those obtained by using L-tryptophan as substrate (Table 1). Compounds **1a**, **2a**, and **6a** were found to have comparable affinities to L-Trp for 7-DMATS (Table 1), with K_M values in the range of 0.07 to 0.16 mM. The K_M values of **3a**, **4a**, and **5a**, at about 1 mM, are significantly higher, but still within the concentration range expected for many secondary-metabolite enzymes. The turnover numbers were found to be from 0.019 to 0.39 s^{-1}. The calculated catalytic efficiencies (k_{cat}/K_M) of 7-DMATS toward flavonoids are in the range of 20 to 320 $s^{-1}\,M^{-1}$, that is, 1.4–19.0% of that of the best substrate, L-Trp. These data provide evidence that the tryptophan prenyltransferase 7-DMATS can also be used for the production of prenylated flavonoids, especially for C6- or ring B-prenylated flavanones and isoflavonoids by chemoenzymatic approach and therefore complement the production gap of other reported prenyltransferases for prenylated flavonoids.[7,9,11,27] It may be expected that other members of the DMATS superfamily from fungi could also be used for the production of prenylated flavonoids.

Table 1. Kinetic parameters of 7-DMATS toward L-tryptophan and flavonoids.

Substrate	K_M [mM]	k_{cat} [s^{-1}]	k_{cat}/K_M [$s^{-1}\,M^{-1}$]	[%][a]
L-Trp[b]	0.14	0.23	1643	100
genistein (**1a**)	0.16	0.027	171	10.4
biochanin A (**2a**)	0.07	0.019	261	15.9
naringenin (**3a**)	0.99	0.023	23	1.4
eriodictyol (**4a**)	1.26	0.39	312	19.0
hesperetin (**5a**)	1.10	0.026	24	1.4
phloretin (**6a**)[c]	0.13	0.036	286	17.4

[a] The k_{cat}/K_M obtained with L-tryptophan as substrate was defined as 100%. [b] Data are taken from ref. [18]. [c] Substrate inhibition at 1 mM or higher concentrations.

Experimental Section

For materials and methods as well as spectra and data see the Supporting Information.

Acknowledgements

This work was supported within the LOEWE program of the State of Hessen (SynMikro to S.-M.L.). X.Y. is a recipient of a fellowship from the China Scholarship Council. We thank Dr. Thomas Kämpchen for NMR and Dr. Gabriele Laufenberg for MS analysis.

Keywords: flavonoids · fungi · indoles · prenylation · synthases · transferases

[1] B. Botta, P. Menendez, G. Zappia, R. A. de Lima, R. Torge, G. D. Monachea, *Curr. Med. Chem.* **2009**, *16*, 3414 – 3468.
[2] B. Botta, A. Vitali, P. Menendez, D. Misiti, M. G. Delle, *Curr. Med. Chem.* **2005**, *12*, 713 – 739.
[3] W. Wätjen, N. Weber, Y. J. Lou, Z. Q. Wang, Y. Chovolou, A. Kampkötter, R. Kahl, P. Proksch, *Food Chem. Toxicol.* **2007**, *45*, 119 – 124.
[4] S. Tischer, P. Metz, *Adv. Synth. Catal.* **2007**, *349*, 147 – 151.
[5] M. M. Hossain, Y. Kawamura, K. Yamashita, M. Tsukayama, *Tetrahedron* **2006**, *62*, 8625 – 8635.
[6] K. Yazaki, K. Sasaki, Y. Tsurumaru, *Phytochemistry* **2009**, *70*, 1739 – 1745.
[7] K. Sasaki, Y. Tsurumaru, H. Yamamoto, K. Yazaki, *J. Biol. Chem.* **2011**, *286*, 24125 – 24134.
[8] K. Sasaki, K. Mito, K. Ohara, H. Yamamoto, K. Yazaki, *Plant Physiol.* **2008**, *146*, 1075 – 1084.
[9] T. Ozaki, S. Mishima, M. Nishiyama, T. Kuzuyama, *J. Antibiot.* **2009**, *62*, 385 – 392.
[10] T. Kuzuyama, J. P. Noel, S. B. Richard, *Nature* **2005**, *435*, 983 – 987.
[11] T. Kumano, S. B. Richard, J. P. Noel, M. Nishiyama, T. Kuzuyama, *Bioorg. Med. Chem.* **2008**, *16*, 8117 – 8126.
[12] S.-M. Li, *Nat. Prod. Rep.* **2010**, *27*, 57 – 78.
[13] A. Kremer, S.-M. Li, *Microbiology* **2010**, *156*, 278 – 286.
[14] J. F. Sanchez, R. Entwistle, J. H. Hung, J. Yaegashi, S. Jain, Y. M. Chiang, C. C. Wang, B. R. Oakley, *J. Am. Chem. Soc.* **2011**, *133*, 4010 – 4017.
[15] X. Yu, X. Xie, S.-M. Li, *Appl. Microbiol. Biotechnol.* **2011**; DOI: 10.1007s00253-011-3351-y.
[16] L. Heide, *Curr. Opin. Chem. Biol.* **2009**, *13*, 171 – 179.
[17] A. Kremer, S.-M. Li, *Appl. Microbiol. Biotechnol.* **2008**, *79*, 951 – 961.
[18] A. Kremer, L. Westrich, S.-M. Li, *Microbiology* **2007**, *153*, 3409 – 3416.
[19] T. Fukai, J. Nishizawa, T. Nomura, *Phytochemistry* **1994**, *36*, 225 – 228.
[20] T. Fukai, Q.-H. Wang, M. Takayama, T. Nomura, *Heterocycles* **1990**, *31*, 373 – 382.
[21] S. Tahara, Y. Katagiri, J. L. Ingham, J. Mizutani, *Phytochemistry* **1994**, *36*, 1261 – 1271.
[22] T. Fukai, T. Nomura, *Heterocycles* **1990**, *31*, 1861 – 1872.
[23] J. C. Ndom, J. T. Mbafor, Z. T. Fomum, *Magn. Reson. Chem.* **1993**, *31*, 210 – 211.
[24] Y. Komazawa, S. Takeda, K. Hosaka, H. Mitsuhashi, T. Watanabe, *Antiulcer Agents Containing Chalcone Derivatives as Effective Ingredients and Novel Chalcone Derivatives* (Tsumura Juntendo, Inc., Japan), WO 8804288, **1988**.
[25] M. L. Gangwal, D. K. Vardhan, A. Sharma, P. Patidar, R. Kushwah, *Res. J. Chem. Environ.* **1998**, *2*, 73 – 74.
[26] P. Chauhan, V. K. Saxena, *Planta Med.* **1987**, *53*, 221 – 222.
[27] B. Botta, G. D. Monache, P. Menendez, A. Boffi, *Trends Pharmacol. Sci.* **2005**, *26*, 606 – 608.

Received: June 27, 2011
Published online on August 25, 2011

CHEMBIOCHEM

Supporting Information

Prenylation of Flavonoids by Using a Dimethylallyltryptophan Synthase, 7-DMATS, from *Aspergillus fumigatus*

Xia Yu[a] and Shu-Ming Li*[a, b]

cbic_201100413_sm_miscellaneous_information.pdf

Experimental section

Chemicals

Dimethylallyl diphosphate (DMAPP) was prepared according to the method described for geranyl diphosphate by Woodside *et al.*. [1] Flavonoids of the highest available purity were purchased from Alfa Aesar, Roth and TCI.

Overproduction and purification of the recombinant protein as well as enzyme assays with recombinant 7-DMATS

7-DMATS was overproduced in *E. coli* and purified as described by Kremer et al.[2] The enzymatic reaction mixtures (100 µl) for determination of the relative activities with different flavonoids contained 50 mM Tris-HCl (pH 7.5), 10 mM $CaCl_2$, 1 mM substrate, 2 mM DMAPP, 0.15 % (v/v) glycerol, 5 % (v/v) DMSO and 14 µg of purified recombinant protein. The reaction mixtures were incubated at 37 °C for 16 h. The enzyme reactions were terminated by addition of 100 µl methanol per 100 µl reaction mixtures. For determination of the kinetic parameters, the assays contained DMAPP at a final concentration of 2 mM and flavonoids at final concentrations of 0.02, 0.05, 0.1, 0.2, 0.5, 1 and 2 mM. For **1a** and **2a**, the final concentrations were up to 1 and 0.5 mM, respectively. The protein amount was 2 µg (**4a**) or 7 µg (other substrates), and the incubation time was 30 min.

HPLC conditions for analysis and isolation of the enzyme products

The enzyme products of the incubation mixtures were analyzed by HPLC on an Agilent series 1200 by using a Multospher 120 RP-18 column (125 x 4 mm, 5 µm) at a flow rate of 1 ml•min^{-1}. Water (solvent A) and methanol (solvent B) were used as solvents. For analysis of enzyme products, a linear gradient of 50 - 80 % (v/v) solvent B in 10 min and then 80- 100 % (v/v) solvent B in 5 min were used. The column was then washed with 100 % solvent B for 5 min and equilibrated with 50 % (v/v) solvent B for 5 min. Conversion yields of the enzyme reactions were calculated by ratios of peak areas of the product to sum of product and substrate detected at 277 nm. For isolation of the enzyme products, the same HPLC equipment with a Multospher 120 RP-18 column (250 x 10 mm, 5 µm) was used. The flow rate was 2.5 mL•min^{-1}.

Spectroscopic analysis

High-resolution electron impact mass spectrometry (HR-EI-MS) was taken on Auto SPEC. Positive HR-EI-MS data of the enzyme products are listed in Table S1. NMR Spectra (Figures S1-S9) were recorded on a JEOL ECA-500 spectrometer. Chemical shifts (Table S2) were referenced to the signal of acetone-d_6 or DMSO- d_6.

HR-EI-MS and ^{1}H- NMR data

Table S1: HR-EI-MS data of the enzyme products of flavonoids.

Compound	Chemical formula	HR-EI-MS data		Deviation (ppm)
		Calculated (M^+)	Measured	
1b	$C_{20}H_{18}O_5$	338.1154	338.1165	-3.0
2b	$C_{21}H_{20}O_5$	352.1311	352.1321	-3.0
3b	$C_{20}H_{20}O_5$	340.1311	340.1333	-6.4
4b	$C_{20}H_{20}O_6$	356.1260	356.1238	6.0
4c	$C_{20}H_{20}O_6$	356.1260	356.1262	-0.7
4d	$C_{20}H_{20}O_6$	356.1260	356.1236	6.6
5b	$C_{21}H_{22}O_6$	370.1416	370.1402	3.8
5c	$C_{21}H_{22}O_6$	370.1416	370.1379	10.1
6b	$C_{20}H_{22}O_5$	342.1467	342.1419	14.0

Table S2: ^{1}H-NMR data (500 MHz) of prenylated products in $(CD_3)_2CO$ or DMSO-d_6 (**4c**). Chemical shifts (δ) are given in ppm and coupling constants (*J*) in Hz.

Compd	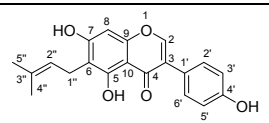 **1b**	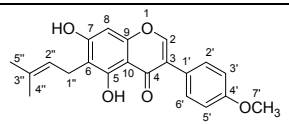 **2b**	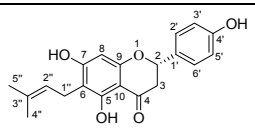 **3b**	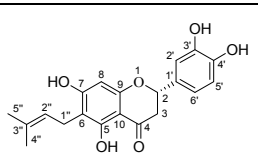 **4b**	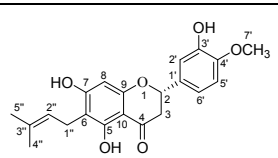 **5b**	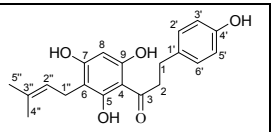 **6b**[1]
Pos.	$\delta_{H,}$ multi., *J*	$\delta_{H,}$ multi., *J*	$\delta_{H,}$ multi., *J*	$\delta_{H,}$ multi., *J*	$\delta_{H,}$ multi., *J*	$\delta_{H,}$ multi., *J*
1	/	/	/	/	/	2.88, t, 7.8
2	8.15, s	8.18, s	5.43, dd, 12.9, 3.0	5.37, dd, 12.8, 3.0	5.41, dd, 12.6, 3.1	3.33, t, 7.7
3	/	/	3.17, dd, 17.1, 12.9	3.12, overlaps	3.14, dd, 17.1, 12.6	/
3	/	/	2.72, dd, 17.1, 3.0	2.71, dd, 17.1, 2.9	2.74, dd, 17.1, 3.1	/
6	/	/	/	/	/	/
8	6.50, s	6.50, s	6.03, s	6.03, s	6.04, s	6.07, s
2'	7.45, d, 8.8	7.54, d, 8.9	7.39, d, 8.3	7.02, br.s	7.04, d, 2.0	7.09, d, 8.5
3'	6.90, d, 8.8	7.00, d, 8.9	6.89, d, 8.6	/	/	6.74, d, 8.5
5'	6.90, d, 8.8	7.00, d, 8.9	6.89, d, 8.6	6.86, br.s	6.99, d, 8.2	6.74, d, 8.5
6'	7.45, d, 8.8	7.54, d, 8.9	7.39, d, 8.3	6.86, br.s	6.96, dd, 8.3, 2.0	7.09, d, 8.5
7'	/	3.84, s	/	/	3.86, s	/
1"	3.37, d, 7.2	3.37, d, 7.2	3.25, d, 7.2	3.24, d, 7.1	3.24, d, 7.2	3.24, d, 2.3
2"	5.28, m	5.28, m	5.23, m	5.23, m	5.23, m	5.22, m
4"	1.78, s	1.78, s	1.75, s	1.75, s	1.75, s	1.74, s
5"	1.65, s	1.65, s	1.64, s	1.63, s	1.64, s	1.62, s
OH	13.33, s	13.30, s	12.47, s	12.47, s	12.46, s	9.49, s
OH	9.65, s	9.67, s	8.52, s	8.02, s	7.74, s	9.05, s
OH	8.49, s	/	/	/	/	8.05, s

[1]: Addition of D_2O was used to prove active protons.

Table S2 (continued)

Compd	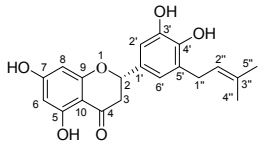 **4c**	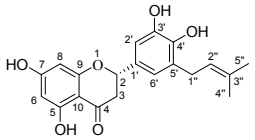 **4c**[2]	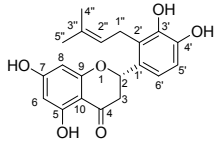 **4d**	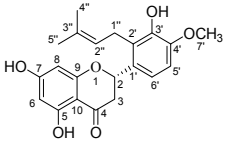 **5c**
Pos.	δ_H, multi., *J*	δ_H, multi., *J*	δ_H, multi., *J*	δ_H, multi., *J*
2	5.36, dd, 12.6, 3.1	5.35, dd, 12.2, 3.0	5.61, dd, 13.3, 2.7	5.65, dd, 13.3, 2.8
3	3.12, dd, 17.1, 12.6	3.13, dd, 17.2, 12.2	3.17, dd, 17.1, 13.3	3.19, dd, 17.1, 13.2
3	2.71, dd, 17.1, 3.1	2.67, dd, 17.1, 3.2	2.65, dd, 17.2, 2.8	2.67, dd, 17.1, 2.8
6	5.94, d, 2.2	5.85, s	5.95, s	5.96, s
8	5.94, d, 2.2	5.85, s	5.95, s	5.96, s
2'	6.90, d, 2.1	6.75, d, 2.0	/	/
3'	/	/	/	/
5'	/	/	6.81, d, 8.3	6.93, d, 8.5
6'	6.81, d, 2.1	6.63, d, 2.0	6.96, d, 8.3	7.08, d, 8.5
7'	/	/	/	3.88, s
1''	3.35, d, 7.4	3.21, d, 7.3	3.53, d, 6.8	3.53, d, 6.9
2''	5.35, m	5.26, m	5.16, m	5.15, m
4''	1.72, s	1.68, s	1.68, s	1.68, s
5''	1.71, s	1.66, s	1.64, s	1.64, s
OH	12.18, s	/	12.19, s	12.19, s
OH	8.02, s	/	/	7.57, s

[2]: Taken in DMSO- d_6.

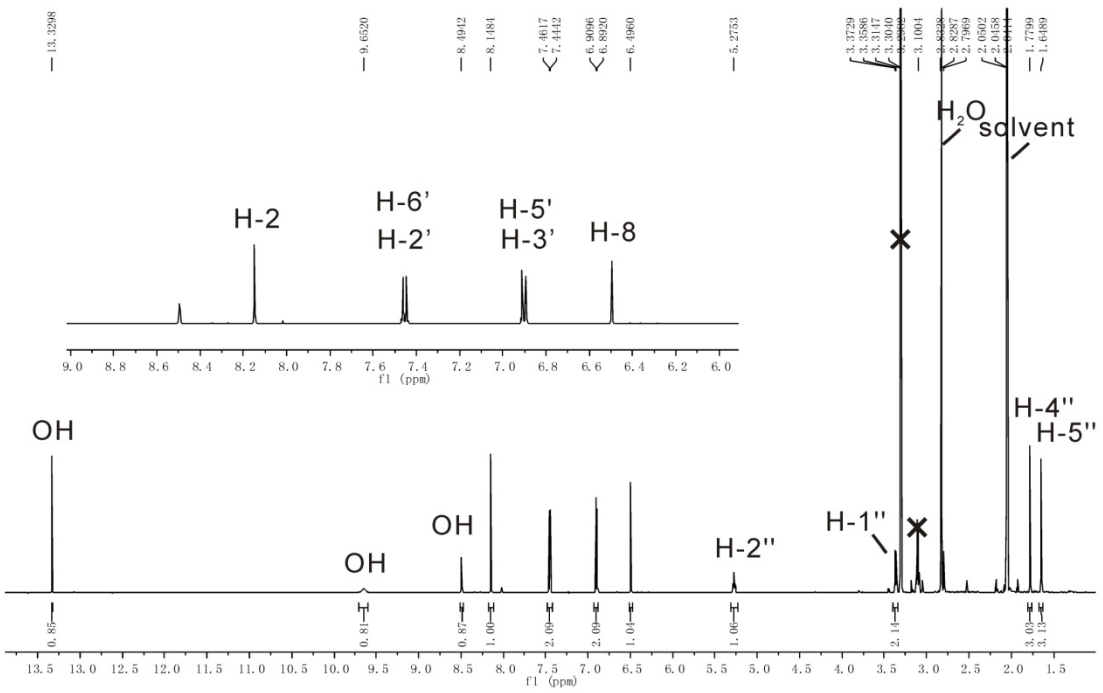

Figure S1 ^{1}H-NMR spectrum of **1b** in $(CD_3)_2CO$ (500 MHz)

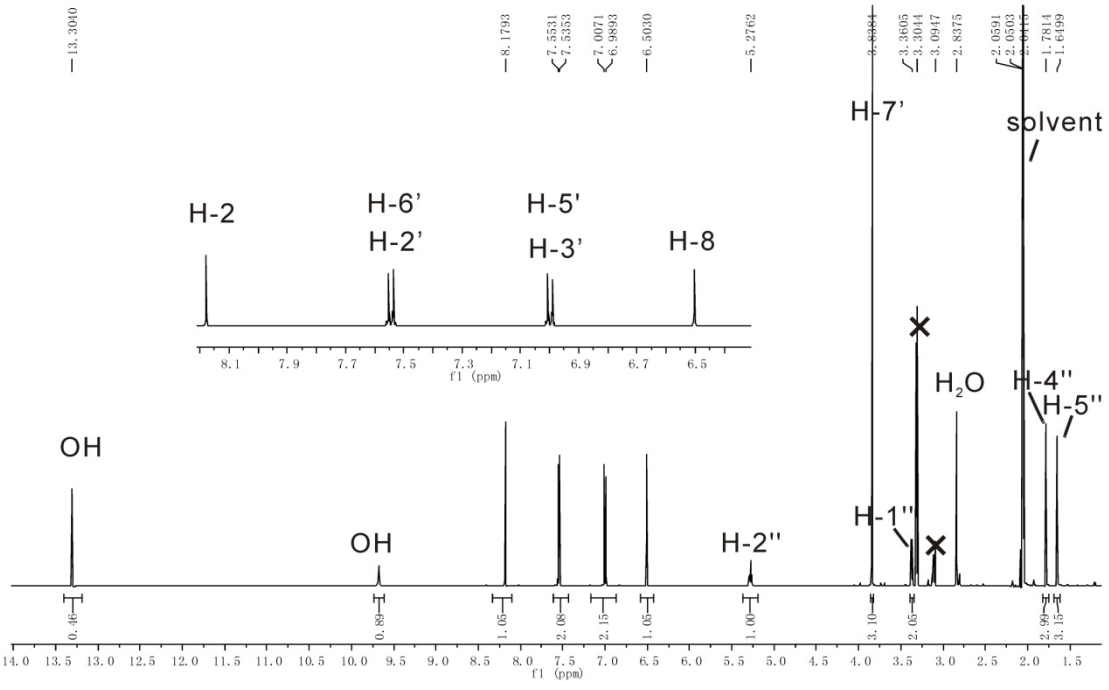

Figure S2 ^{1}H-NMR spectrum of **2b** in $(CD_3)_2CO$ (500 MHz)

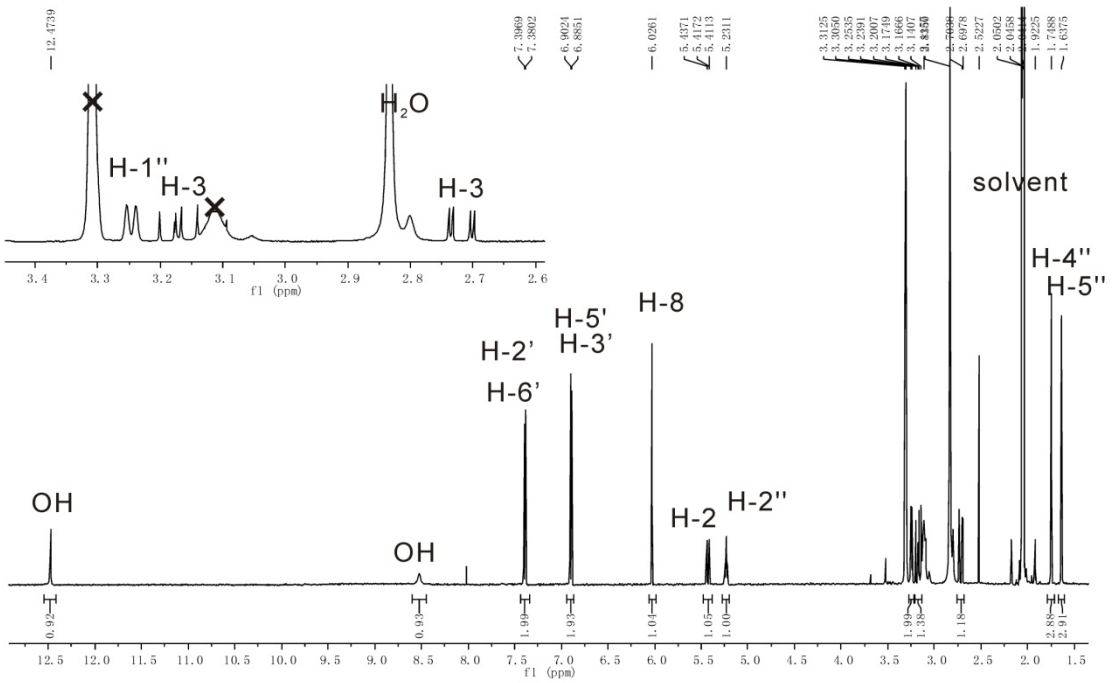

Figure S3 ^{1}H-NMR spectrum of **3b** in $(CD_3)_2CO$ (500 MHz)

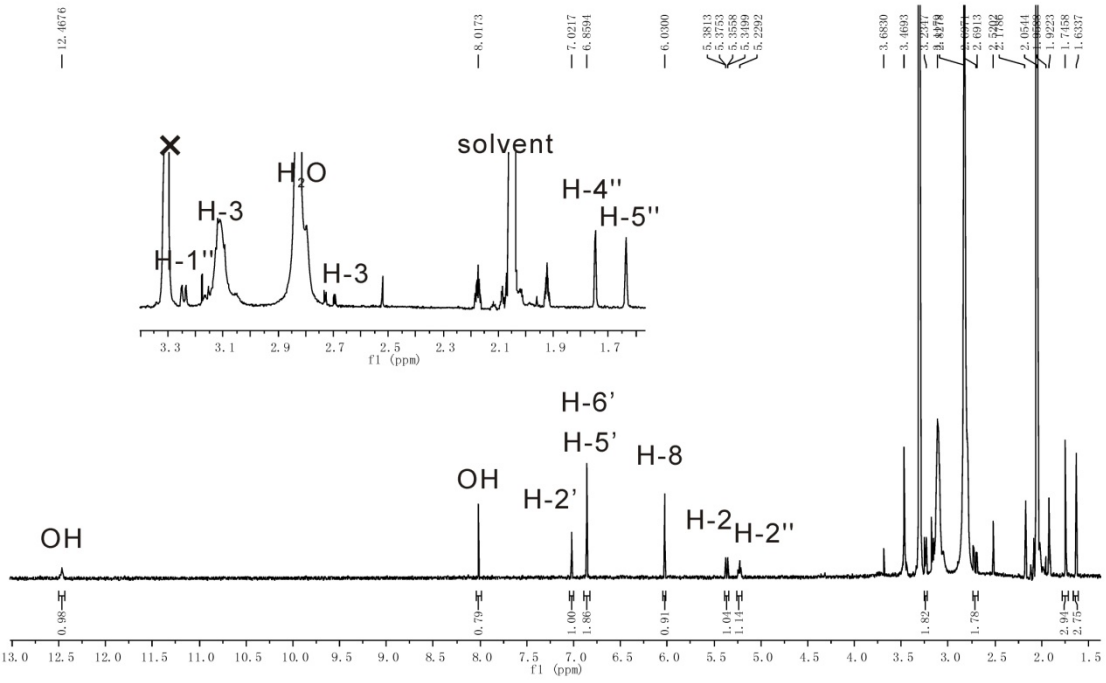

Figure S4 ^{1}H-NMR spectrum of **4b** in $(CD_3)_2CO$ (500 MHz)

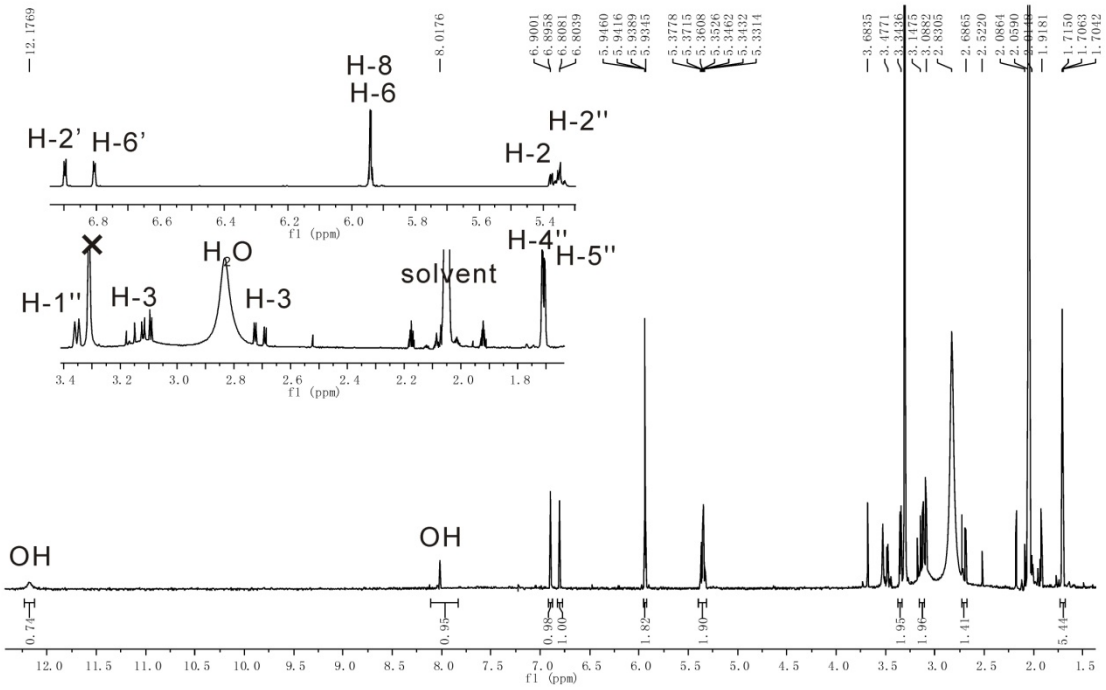

Figure S5.1 ^{1}H-NMR spectrum of **4c** in $(CD_3)_2CO$ (500 MHz)

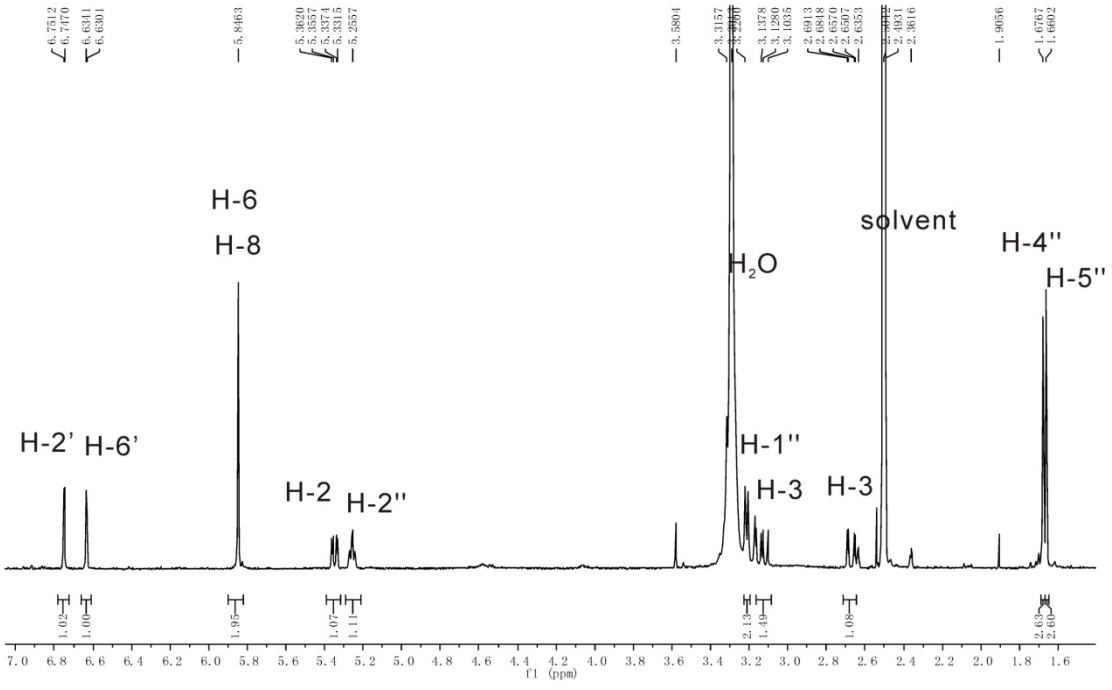

Figure S5.2 ^{1}H-NMR spectrum of **4c** in DMSO-d_6 (500 MHz)

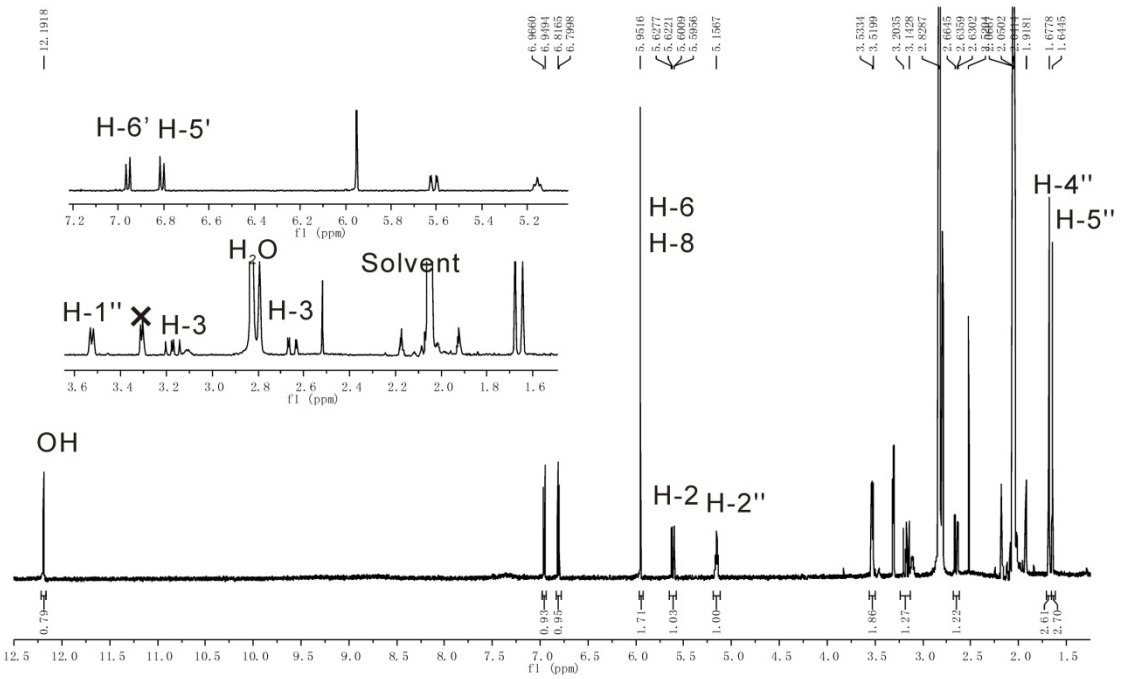

Figure S6 ^{1}H-NMR spectrum of **4d** in $(CD_3)_2CO$ (500 MHz)

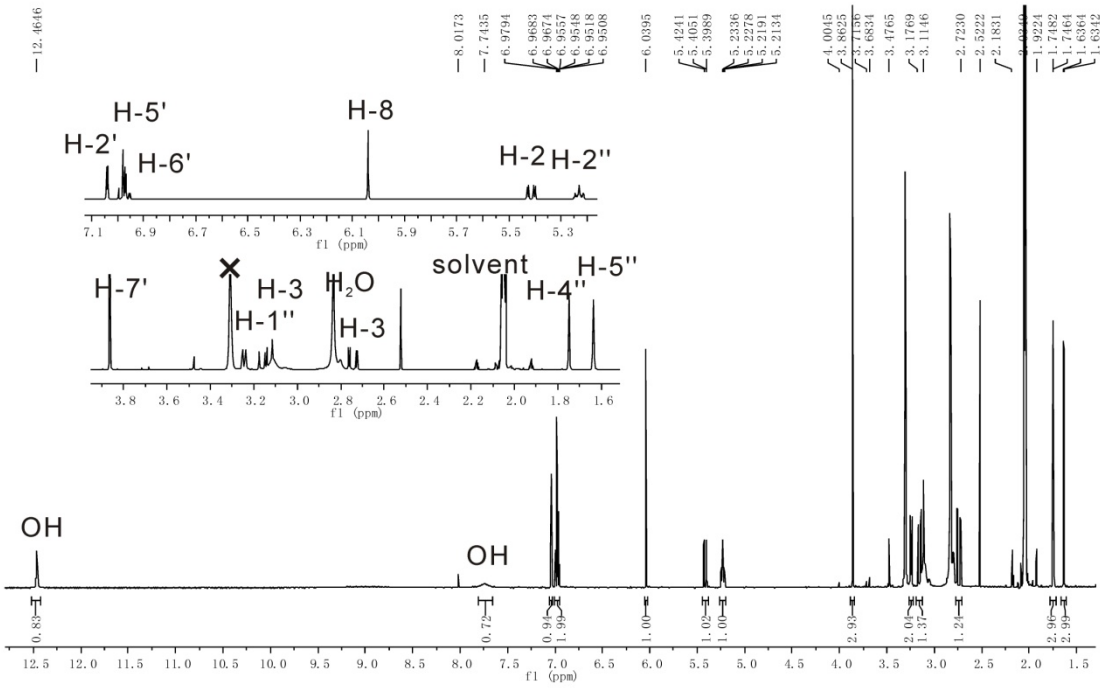

Figure S7 ^{1}H-NMR spectrum of **5b** in $(CD_3)_2CO$ (500 MHz)

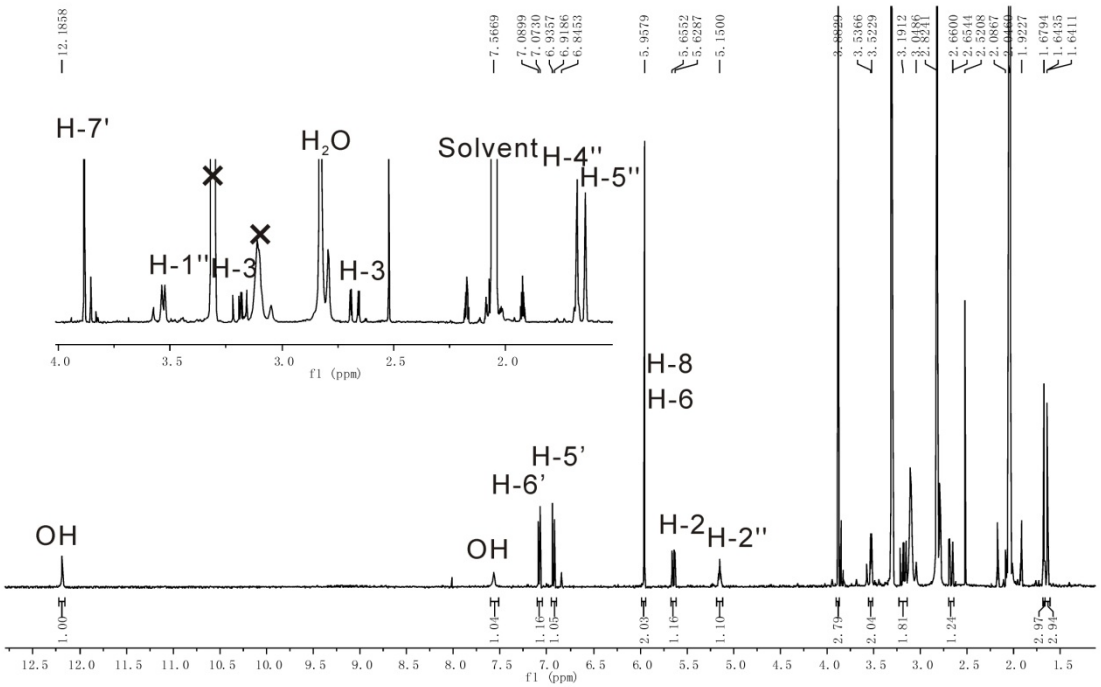

Figure S8 ^{1}H-NMR spectrum of **5c** in $(CD_3)_2CO$ (500 MHz)

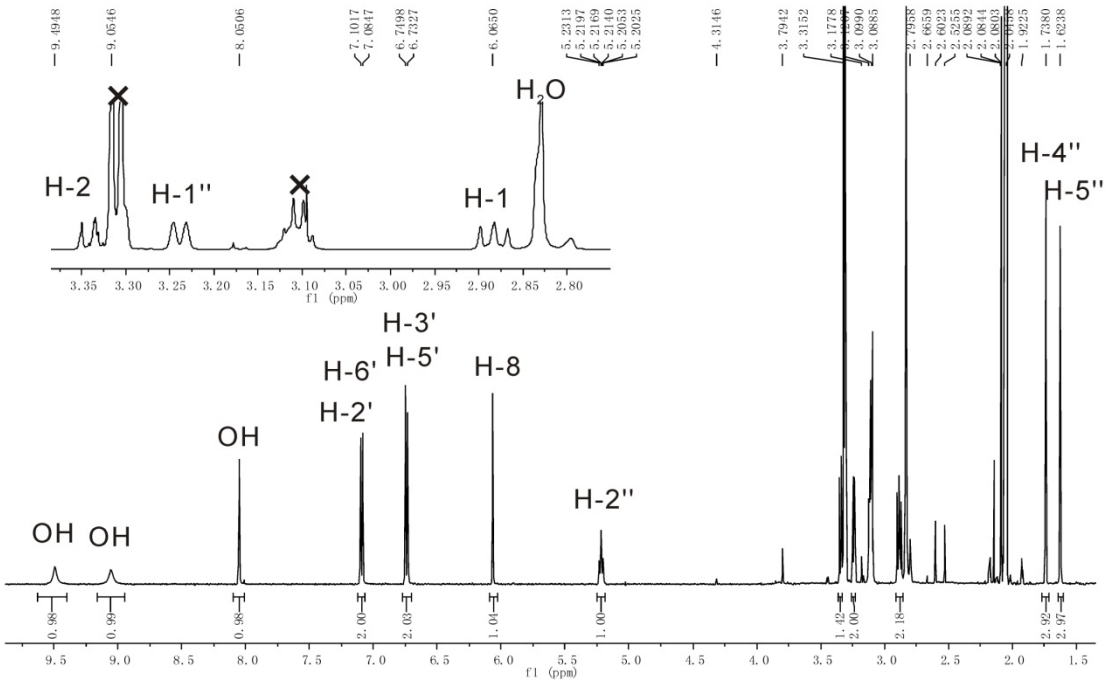

Figure S9.1 ^{1}H-NMR spectrum of **6b** in $(CD_3)_2CO$ (500 MHz)

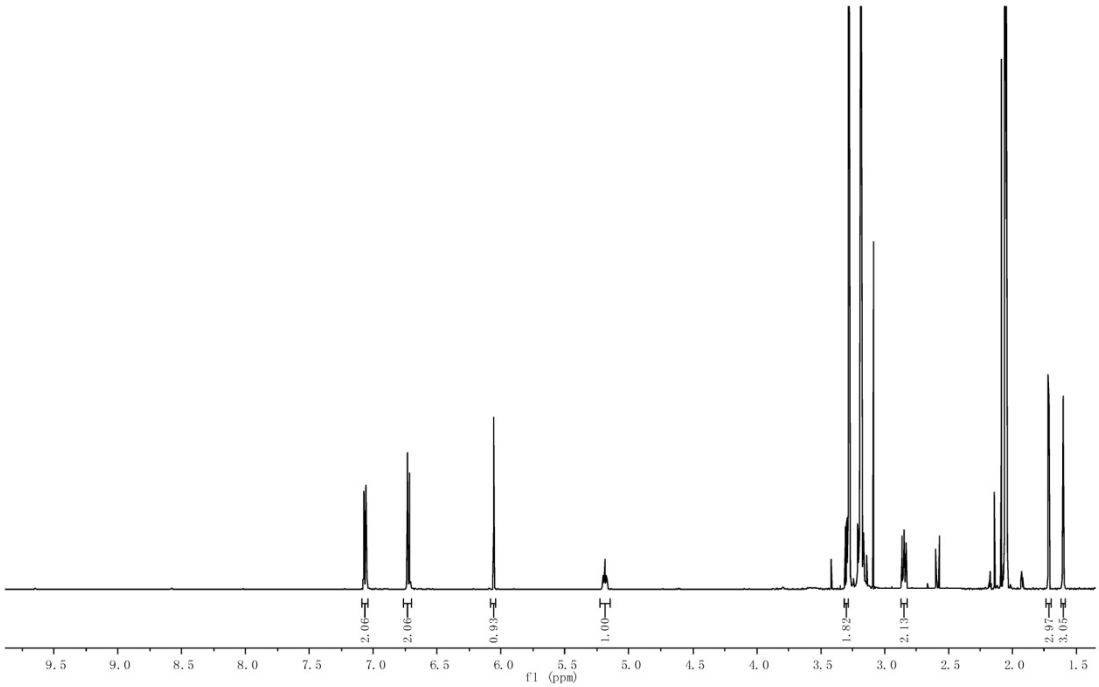

Figure S9.2 ^{1}H-NMR spectrum of **6b** in $(CD_3)_2CO$ after addition of D_2O (500 MHz)

Reference List

[1.] A. B. Woodside, Z. Huang, C. D. Poulter, *Org.Synth.* **1988,** *66*, 211-215.

[2.] A. Kremer, L. Westrich, S.-M. Li, *Microbiology* **2007,** *153*, 3409-3416.

5.8 Prenyltransferases of the dimethylallyltryptophan synthase superfamily

CHAPTER THIRTEEN

Prenyltransferases of the Dimethylallyltryptophan Synthase Superfamily

Xia Yu, Shu-Ming Li[1]
Institut für Pharmazeutische Biologie und Biotechnologie, Philipps-Universität Marburg, Deutschhausstrasse 17A, Marburg, Germany
[1]Corresponding author: e-mail address: shuming.li@staff.uni-marburg.de

Contents

Abstract

Prenylated natural products often have interesting biological and pharmacological activities clearly distinct from their nonprenylated precursors. Prenyltransferases are

Methods in Enzymology, Volume 516
ISSN 0076-6879
http://dx.doi.org/10.1016/B978-0-12-394291-3.00005-8

responsible for the attachment of prenyl moieties to a number of acceptors and contribute significantly to structural and biological diversity of these compounds in nature. In the past 8 years, significant progress has been achieved in the molecular biological, biochemical, and structural biological investigation of the prenyltransferases of the dimethylallyltryptophan synthase (DMATS) superfamily. These soluble enzymes are involved in the biosynthesis of fungal secondary metabolites and mainly catalyze prenylation of diverse indole derivatives, including tryptophan and tryptophan-containing cyclic dipeptides. The members of the DMATS superfamily show promising flexibility toward their aromatic substrates and catalyze highly regio- and stereoselective prenyltransfer reactions. These features were successfully used for chemoenzymatic synthesis, not only for production of prenylated simple indoles and cyclic dipeptides but also for prenylated hydroxynaphthalenes and flavonoids, which are usually found in bacteria and plants, respectively.

1. INTRODUCTION

*Dim*ethyl*a*llyl*t*ryptophan *s*ynthase (DMATS) was identified as the first pathway-specific enzyme in the biosynthesis of ergot alkaloids (Tsai, Wang, Gebler, Poulter, & Schardl, 1995; Unsöld & Li, 2005). It catalyzes the prenylation of L-tryptophan at C-4 of the indole ring and therefore functions as an indole prenyltransferase (Steffan, Grundmann, Yin, Kremer, & Li, 2009; Unsöld & Li, 2005). Analysis of a vast volume of released sequences from fungal genome projects revealed nearly 200 putative genes with sequence homology to DMATS by bioinformatic approaches (at the beginning of 2012, GenBank). These genes are classified as prenyltransferase genes of the DMATS superfamily. Biochemical characterization of the encoded enzymes began in summer 2004 after availability of the genome sequence for *Aspergillus fumigatus* (Unsöld & Li, 2005). To the end of January 2012, results for 17 such enzymes have been reported, for example, six from *A. fumigatus* (Li, 2009b) and two each from *Neosartorya fischeri* (Li, 2009b; Yin, Yu, Xie, & Li, 2010), *Aspergillus oryzae* (Liu & Walsh, 2009; Zou, Xie, Linne, Zheng, & Li, 2010), and *Aspergillus* sp. (Ding et al., 2010). The characterized enzymes accepted almost only dimethylallyl diphosphate (DMAPP) as prenyl donor and catalyzed via enzyme-bound cations the prenyltransfer reactions to aromatic substrates in "regular" or "reverse" connection (Figs. 13.1 and 13.2) (Luk & Tanner, 2009; Metzger et al., 2009; Yin et al., 2010; Zou et al., 2010). In the enzyme products of the "regular" prenyltransferases, for example, 5-DMATS,

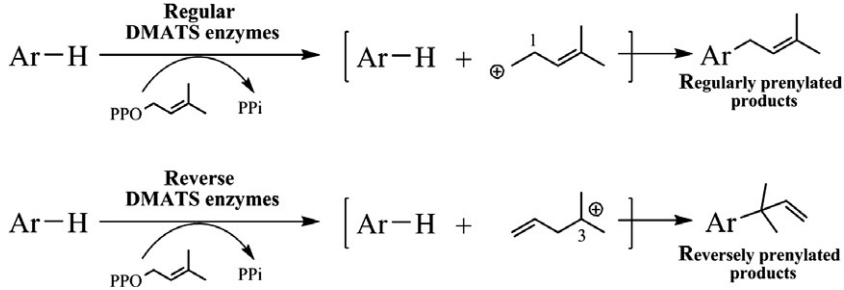

Figure 13.1 Regular and reverse prenylations catalyzed by prenyltransferases of the DMATS superfamily.

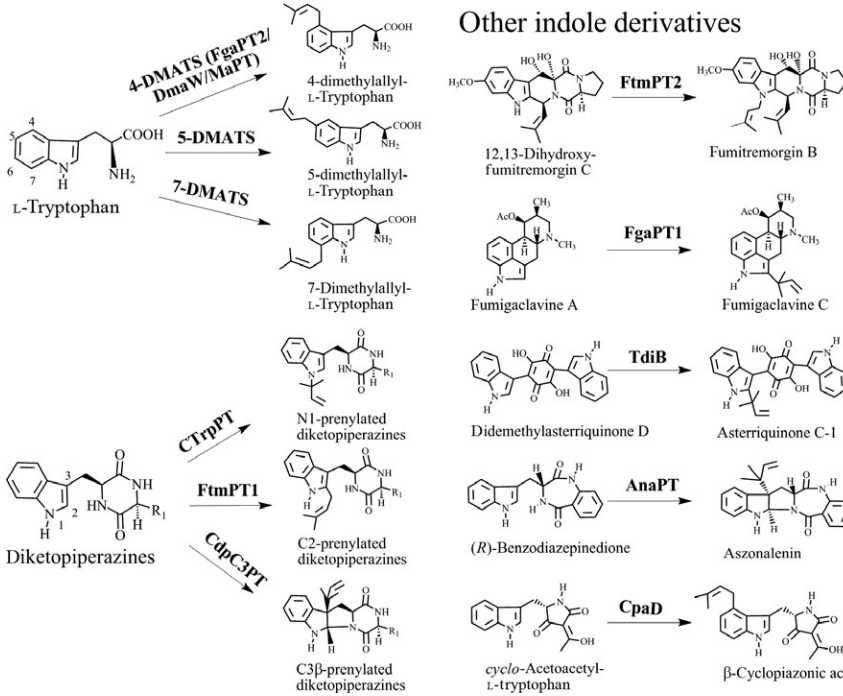

Figure 13.2 Examples of enzyme reactions catalyzed by prenyltransferases of the DMATS superfamily.

7-DMATS, CpaD, DmaW, FgaPT2, FtmPT1, FtmPT2, and MaPT, (Ding, Williams, & Sherman, 2008; Grundmann, Kuznetsova, Afiyatullov, & Li, 2008; Grundmann & Li, 2005; Kremer, Westrich, & Li, 2007; Liu & Walsh, 2009; Markert et al., 2008; Unsöld & Li, 2005; Yu, Liu, Xie, Zheng, & Li, 2012), the prenyl moiety is attached via its C-1 to the

aromatic nucleus. In contrast, the "reverse" prenyltransferases, for example, AnaPT, CdpC3PT, CTrpPT, and FgaPT1 (Unsöld & Li, 2006; Yin, Grundmann, Cheng, & Li, 2009; Yin et al., 2010; Zou et al., 2010), catalyze connection of the prenyl moieties via C-3 to the aromatic substrate.

The prenyltransferases of the DMATS superfamily are involved in the biosynthesis of diverse fungal secondary metabolites, especially prenylated indole alkaloids (Li, 2010). Prenylated indole alkaloids, including a number of important mycotoxins and drugs, are hybrid natural products containing both indole and isoprenoid moieties. They are widely distributed in terrestrial and marine organisms and mainly found in ascomycetes, for example, members of the genera *Claviceps*, *Penicillium*, and *Aspergillus* (Li, 2010). These compounds often possess biological activities clearly distinct from their non-prenylated precursors (Jain et al., 2008). Most prenyltransferases of the DMATS superfamily catalyze prenylation reactions at the indole ring and play an important role in the biosynthesis of structurally diverse prenylated indole alkaloids in fungi. Many of these enzymes accept tryptophan and tryptophan-containing cyclic dipeptides as aromatic substrates and catalyze regio- and stereospecific prenylation reactions. As mentioned above, DmaW, FgaPT2, and MaPT catalyze prenylation of L-tryptophan at C-4 of the indole ring and function as 4-DMATS. 5-DMATS and 7-DMATS accept also L-tryptophan as substrate but prenylate it at C-5 and C-7, respectively (Fig. 13.2). CTrpPT, FtmPT1, and CdpC3PT accept tryptophan-containing cyclic dipeptides and catalyze regiospecific prenylations at N-1, C-2, and C-3, respectively. As shown in Fig. 13.2, members of the DMATS superfamily also accept more complicated indole derivatives as substrates. For example, FtmPT2, FgaPT1, TdiB, AnaPT, and CpaD use 12,13-dihydroxy fumitremorgin C, fumigaclavine A, didemethylasterriquinone D, (*R*)-benzodiazepinedione, and *cyclo*-acetoacetyl-L-tryptophan as substrates and catalyze regiospecific prenylations at the indole ring (Fig. 13.2).

In contrast to the indole prenyltransferases mentioned above, some members of the DMATS superfamily accept other aromatic substances as substrates. For example, SirD is an *O*-prenyltransferase for tyrosine (Kremer & Li, 2010). Based on results obtained from knockout mutants, it was suggested that XptA and XptB are involved in the prenylation of xanthones (Sanchez et al., 2011).

Sequence analysis revealed that the members of the DMATS superfamily contain no DDxxD motifs, which are essential for binding of prenyl diphosphate via metal ions, for example, Mg^{2+} or Mn^{2+}, in *trans*-prenyltransferases (Lu, Liu, & Liang, 2009) in the biosynthesis of terpenoids or membrane-bound aromatic prenyltransferases in the biosynthesis of

prenylated flavonoids or benzoic acids (Yazaki, Sasaki, & Tsurumaru, 2009). Biochemical investigations showed that reactions catalyzed by members of the DMATS superfamily were independent of metal ions, although Ca^{2+} enhanced the reaction velocity (Li, 2010; Steffan et al., 2009). Structural biological analysis and site-directed mutagenesis experiments have proven that the formation of prenyl cations is facilitated by binding of the phosphate residues of DMAPP with several basic amino acids (Jost et al., 2010; Metzger et al., 2009; Stec et al., 2008).

Detailed investigations on the substrate specificities of the DMATS enzymes in recent years have provided experimental evidence for their effective use in the production of prenylated compounds. They accepted a number of structural analogues of their natural substrates such as tryptophan, tyrosine, or cyclic dipeptides and catalyzed regio- and stereospecific prenylations. Promisingly, prenylated hydroxynaphthalenes or flavonoids can also be regiospecifically produced by using prenyltransferases of the DMATS superfamily (Yu & Li, 2011; Yu, Xie, & Li, 2011). These compounds have not been found in fungi, but in bacteria or plants, respectively.

In this chapter, we provide general protocols for biochemical investigation of prenyltransferases of the DMATS superfamily, including DNA and RNA propagation, gene cloning and expression, enzyme assays, and chemoenzymatic synthesis of prenylated compounds.

2. SPORE PREPARATION

1. Prepare sterile 0.1% (v/v) Tween-20 and sterile 20% (v/v) glycerol.
2. Prepare Czapek-Dox with yeast extract solid medium consisting of 3.5% (w/v) Czapek-Dox, 0.5% (w/v) yeast extract, and 2% (w/v) agar; autoclave at 121 °C for 20 min; and use for preparation of agar plates.
3. Spread 1000–10,000 spores on each plate and cultivate the plates for approximately 2 weeks at 26 °C in darkness.
4. Wash each plate thoroughly (spores and mycelia) three times with 4 ml of 0.1% Tween-20 and collect and transfer the suspension to sterile 50-ml Falcon tubes with some autoclaved glass beads with a diameter of 2.85–3.3 mm. Vortex the suspension exhaustively.
5. Filter the suspension over sterile cotton wool. Centrifuge for 5 min at 3000 rpm and resuspend the pellets in 20% (v/v) glycerol (use 100 μl for spores from one plate). Use fresh spores for inoculation or store them at −80 °C.

3. CULTIVATION OF FUNGI

Fungal mycelia are used for RNA and DNA isolation.

1. Prepare liquid yeast extract medium with sucrose, consisting of 0.6% (w/v) yeast extract and 0.2% (w/v) sucrose, pH 5.8, for cultivation of *N. fischeri* (Yin et al., 2009, 2010) and *A. oryzae* (Zou et al., 2010). Solid media for agar plates contain 2% (w/v) agar.
2. Prepare yeast malt extract medium consisting of 0.4% (w/v) yeast extract, 1% (w/v) malt extract, and 0.4% (w/v) glucose, pH 7.3, for cultivation of *Aspergillus clavatus* (Yu et al., 2012). Solid media for agar plates contain 2% (w/v) agar.
3. Spread a small portion of spore suspensions on agar plates and incubate at 30 °C or 26 °C for 5–7 days.
4. Take mycelia with agar (1 × 1 cm) from the agar plates and inoculate into 300-ml Erlenmeyer flasks containing 100 ml liquid medium from step 1 or 2.
5. Cultivate at 26 °C or 30 °C and 160 rpm in a dark room for 3–7 days.

4. RNA AND DNA ISOLATION AND cDNA Synthesis

4.1. RNA isolation and cDNA synthesis

1. Prepare sterile, RNase-free glass and plastic wares and double distilled water by twice autoclaving.
2. Prepare buffer RB/2-mercaptoethanol by adding 20 μl 2-mercaptoethanol to 1 ml of buffer RB from E.Z.N.A.™ Fungal RNA Kit (Omega Bio-Tek) before use.
3. Collect fungal cultures in 50-ml Falcon tubes by centrifugation at 5000 rpm for 5 min. Wash the pellets with ice-cold double distilled water twice by suspension and centrifugation.
4. Add liquid nitrogen to the pellets and grind the frozen mycelia to a fine powder in a twice-autoclaved mortar.
5. Take 50 mg of the powder and transfer it to a 1.5-ml microtube. Immediately add 500 μl of buffer RB/2-mercaptoethanol to the tube.
6. Isolate the RNA by using a Homogenization Spin Column (Green) followed by a HiBind® RNA spin column from the kit according to the manufacturer's protocol.
7. Use the isolated RNA directly to synthesize cDNA or store it at − 80 °C.

8. For synthesis of cDNA, carry out the reaction with RNA in a volume of 20 µl by using Transcriptor High Fidelity cDNA Synthesis Kit (Roche Diagnostics GmbH).
9. Heat to 85 °C for 5 min to inactivate reverse transcriptase. Then store it at −20 °C.

4.2. DNA isolation

1. Prepare sterile phosphate-buffered saline buffer (PBS buffer, 137 m*M* NaCl, 2.7 m*M* KCl, 1.0 m*M* Na_2HPO_4, and 0.18 m*M* KH_2PO_4).
2. Prepare sterile digestion buffer consisting of 100 m*M* NaCl, 10 m*M* Tris–HCl, 25 m*M* EDTA, and 0.5% (w/v) SDS, pH 8.0. Add proteinase K to a final concentration of 0.1 mg ml^{-1} before use.
3. Collect fungal cultures in sterile 50-ml Falcon tubes by centrifugation at 5000 rpm at 4 °C for 5 min, and then wash the pellets with ice-cold PBS buffer twice by suspension and centrifugation.
4. Add liquid nitrogen to the pellets and grind the frozen mycelia to a fine powder in an autoclaved mortar.
5. Transfer 100 mg of mycelial powder into a sterile 1.5-ml microtube and add 1.2 ml digestion buffer. Incubate the mixture at 50 °C and 160 rpm for 2 h.
6. Extract twice with 1 volume of phenol/chloroform/isoamyl alcohol mixture (25:24:1) by inversion for 10 min and centrifuge at 4 °C and 4000 rpm for 5–10 min.
7. Add 1/10 volume of ice-cold 3 *M* sodium acetate and 1 volume of ice-cold isopropanol to the aqueous phase and keep for 20 min at −80 °C.
8. Centrifuge at 4 °C and 6000 rpm for 30 min and wash the DNA pellets twice with 3 ml ice-cold 70% (v/v) ethanol.
9. Dry DNA pellets at 60 °C for approximately 30 min. Dissolve DNA in sterile double distilled water and store at −20 °C.

5. GENE CLONING

Analysis of genomic DNA and cDNA sequences of the known prenyltransferase genes of the DMATS superfamily revealed the presence of one to three short intron sequences at the 3′-end of the genes (Steffan et al., 2009). For heterologous gene expression in *Escherichia coli* or *Saccharomyces cerevisiae*, these intron sequences must be removed. This can be achieved by PCR amplification of the coding region from cDNA or by fusion PCR from genomic DNA.

5.1. PCR amplification from cDNA

1. Synthesize cDNA with the Transcriptor High Fidelity cDNA Synthesis Kit (Roche Diagnostics GmbH) from mRNA as described above (Section 4.1).
2. Synthesize primers with mutations at the start and stop codon to generate the respective restriction sites for cloning into expression vector and His-tagged fusion protein for purification.
3. Use synthesized cDNA as template in a gradient PCR with Taq polymerase in a volume of 50 µl to optimize PCR conditions.
4. Carry out PCR amplification in a volume of 50 µl by using Expand High Fidelity Kit (Roche Diagnostics GmbH) and the conditions in step 3.

5.2. Fusion PCR amplification from genomic DNA

Fusion PCR amplification consists of at least two rounds and is therefore somewhat more complicated than normal PCR. We demonstrate this approach by using genes containing only one intron as an example (Fig. 13.3):

1. Synthesize two PCR primer pairs: exon1a and exon1b for the first exon at the 5′-end and exon2a and exon2b for the second exon at the 3′-end of the gene. The primers exon1b and exon2a contain approximately 36 bp overlapping sequence of the two exons. Primers exon1a and exon2b contain suitable restriction sites at the start and stop codon, respectively, which are considered for cloning into the expression vector and for His-tagged fusion protein.

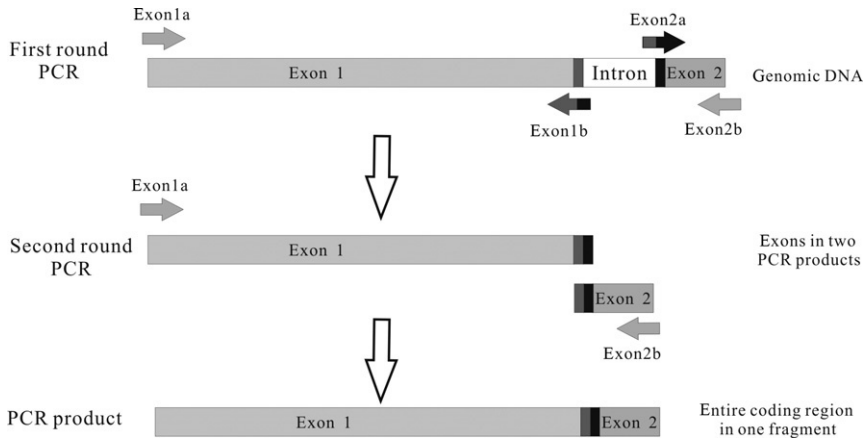

Figure 13.3 Amplification of the coding sequence of a gene of interest from gDNA by two rounds fusion PCR.

2. In the first round, amplify the two exons from genomic DNA by using primers exon1a and exon1b, and exon2a and exon2b, respectively. Optimize PCR conditions by gradient PCR with Taq polymerase and carry out PCR amplification by using Expand High Fidelity Kit (Roche Diagnostics GmbH).
3. Use PCR products of the two exons from the first round PCR as primers and templates (in a molar ratio of 1:1) for the second round PCR to obtain the entire coding region. Addition of the primers exon1a and exon2b to the reaction mixture often enhances the yield of the PCR amplification.

6. PROTEIN OVERPRODUCTION

The PCR product is subsequently cloned into an expression vector directly (Schneider, Weber, & Hoffmeister, 2008; Yin, Ruan, Westrich, Grundmann, & Li, 2007) or via a cloning vector, for example, pGEM-T easy or pBlueskript KS (−) (Grundmann et al., 2008; Grundmann & Li, 2005; Kremer et al., 2007; Markert et al., 2008; Steffan, Unsöld, & Li, 2007; Unsöld & Li, 2005, 2006). Protein overproduction can be carried out in *E. coli* or *S. cerevisiae* (Steffan et al., 2009).

6.1. Protein overproduction in *E. coli*

6.1.1 Gene induction

Most prenyltransferases of the DMATS superfamily were successfully overproduced in *E. coli* strains. The commonly used vectors are pQE60 and pQE70 with *E. coli* XL1 Blue or M15 as expression hosts (Kremer et al., 2007; Yin et al., 2009, 2007, 2010; Yu et al., 2012; Zou et al., 2010). pRSET B and pET28 or its derivative pHis8 was expressed in *E. coli* BL21 (Schneider et al., 2008; Steffan et al., 2007; Unsöld & Li, 2006). For overproduction of soluble proteins in *E. coli*, the following steps are involved:

1. Prepare sterile Luria-Bertani (LB) medium consisting of 1.0% (w/v) tryptone, 1.0% (w/v) NaCl, and 0.5% (w/v) yeast extract.
2. Prepare sterile potassium phosphate buffer (0.17 *M* KH_2PO_4 and 0.72 *M* K_2HPO_4).
3. Prepare sterile Terrific-Broth medium (TB medium, per 900 ml medium: 12 g tryptone, 24 g yeast extract, and 4 ml glycerol; add 100 ml potassium phosphate buffer before use).

4. Transfer the expression plasmid by transformation into calcium-competent *E. coli* cells.
5. Inoculate a colony from the LB agar plate or take several microliter glycerol stocks into glass tubes containing 5 ml LB or TB medium supplemented with the respective antibiotics. Cultivate at 37 °C and 220 rpm overnight.
6. Inoculate 2 ml overnight culture into a 250-ml Erlenmeyer flask containing 100 ml liquid LB or TB medium supplemented with the respective antibiotics. Grow the cells at 37 °C and 220 rpm to an adsorption of approximately 0.6 at 600 nm.
7. Add isopropyl thiogalactoside (IPTG) to a final concentration of 0.1–2 m*M* and cultivate the cells for further 6–16 h at 18–37 °C before harvest. Change temperature and IPTG concentration to obtain the desired recombinant soluble protein.
8. Carry out cultivation in 2000-ml Erlenmeyer flasks containing 1000 ml medium, if necessary.
9. Collect *E. coli* cells by centrifugation at 3000 rpm for 20 min and store the cells at −20 °C.

6.1.2 Protein purification

His-tagged fusion proteins can be purified by using Ni-NTA agarose and judged by SDS-PAGE. The amount of Ni-NTA resin, pH value, and imidazole concentration in buffers are important factors influencing the yield and purity of the purified proteins. For condition optimization, please take these factors into consideration.

1. Prepare lysis buffer (10 m*M* imidazole, 50 m*M* NaH_2PO_4, and 300 m*M* NaCl, pH 8.0), wash buffer (20–50 m*M* imidazole, 50 m*M* NaH_2PO_4, and 300 m*M* NaCl, pH 8.0), and elution buffer (250 m*M* imidazole, 50 m*M* NaH_2PO_4, and 300 m*M* NaCl, pH 8.0).
2. All the following steps are carried out at 4 °C.
3. Resuspend the frozen *E. coli* cells in lysis buffer at 2–5 ml g^{-1} wet weight. Add lysozyme to a final concentration of 1 mg ml^{-1} and incubate for 30 min. Sonicate the cells six times for 10 s, each time at 200 W, with 10 s for cooling after each burst.
4. Centrifuge the lysate at 13,000 rpm for 30 min to separate soluble proteins from cellular debris. If the lysate is very viscous, for example, the lysate of *E. coli* BL21 cells, add RNAase and DNAase to a final concentration of 10 and 5 μg ml^{-1} 15 min before sonication, respectively.

5. Mix soluble proteins with Ni-NTA agarose resin (Qiagen) according to the manufacturer's instructions and stir the mixture for 1 h. The volume of resin depends on the yield of protein; try 50 μl for the lysate from 100 ml culture first.
6. Load the mixture to a column with bottom sieve. Wash the residue on the sieve with 4 ml wash buffer twice to remove nonbound proteins.
7. Elute the target protein with 2.5 ml elution buffer and check protein purity on SDS-PAGE.
8. Change the protein buffer by passing a column with Sephadex G-25, for example, PD-10 (GE Healthcare), which has been equilibrated with 50 m*M* Tris–HCl containing 15% (v/v) glycerol, pH 7.5, previously.
9. Collect the purified protein and store aliquots at −80 °C for enzyme assays.

6.2. Protein overproduction in *S. cerevisiae*

6.2.1 Gene expression

A few prenyltransferases were overproduced in *S. cerevisiae* INVSc1 with pYES2/NT as expression vector (Grundmann et al., 2008; Markert et al., 2008; Unsöld & Li, 2005). For overproduction of soluble proteins in *S. cerevisiae*, the following steps are involved:

1. Prepare sterile minimal medium consisting of 0.67% (w/v) yeast nitrogen base (without amino acids but with ammonium sulfate), 0.01% (w/v) each of adenine, arginine, cysteine, leucine, lysine, threonine, and tryptophan, 0.005% (w/v) each of aspartic acid, histidine, isoleucine, methionine, phenylalanine, proline, serine, tyrosine, and valine. Add 2% (w/v) agar for a solid medium.
2. Transfer the expression plasmid into *S. cerevisiae* cells by electroporation and select the resulting transformants on minimal medium plate.
3. Grow cells in 500-ml Erlenmeyer flasks containing 250 ml liquid minimal medium with 2% (w/v) glucose at 30 °C for 36 h.
4. Centrifuge cells at 3000 rpm for 5 min and wash the pellets with liquid minimal medium without glucose.
5. Transfer the washed cells into 1000-ml Erlenmeyer flasks containing 500 ml induction medium consisting of minimal medium with 1% (w/v) raffinose and 2% (w/v) galactose. Incubate at 30 °C for 16 h before harvest.
6. Collect the cells by centrifugation at 3000 rpm for 5 min and store them at −20 °C.

6.2.2 Protein purification

The purification procedure of proteins from *S. cerevisiae* is similar to that from *E. coli*, that is, breaking cells followed by affinity chromatography with Ni-NTA agarose.

1. Prepare extraction buffer consisting of 50 m*M* Tris–HCl, 15% (v/v) glycerol, 1 m*M* DTT, and 1 m*M* phenylmethylsulfonyl fluoride, pH 7.5. Prepare buffers for purification as described in step 1 in Section 6.1.2.
2. All the following steps are carried out at 4 °C.
3. Resuspend the resulting yeast pellets (Section 6.2.1) in an adequate amount of ice-cold water and press the suspension by using an injection syringe into a mortar with liquid nitrogen. Grind the cells to a fine powder.
4. Resuspend 1 g powder in 2 ml extraction buffer and stir the mixture for 15 min.
5. Centrifuge the mixture at 13,000 rpm for 15 min to separate soluble proteins from cellular debris and use the supernatant for protein purification.
6. Do the same as steps 5–9 in Section 6.1.2.

7. PREPARATION OF STOCK SOLUTIONS FOR ENZYME ASSAYS

Stock solutions for DMAPP, tryptophan-containing cyclic dipeptides, hydroxynaphthalenes, flavonoid aglycones, simple indoles, tyrosine derivatives, and Ca^{2+} are prepared as follows:

1. Weigh accurately desired amount of a given substance in a 1.5-ml microtube.
2. Dissolve DMAPP in a calculated volume of 50 m*M* Tris–HCl buffer (pH 7.5) to give a final concentration of 20 m*M*.
3. Considering the difference in their solubility in aqueous system, stock solutions of 20 m*M*, 10 m*M*, or 4 m*M* in DMSO, 50 m*M* Tris–HCl buffer (pH 7.5), or both are prepared for simple indoles and tyrosine derivatives. Owing to the inhibiting potential of DMSO for enzyme reactions, keep the DMSO concentration as low as possible.
4. Dissolve tryptophan-containing cyclic dipeptides, hydroxynaphthalenes, and flavonoid aglycones in DMSO to give a final concentration of 20 m*M*.
5. Dissolve $CaCl_2$ in 50 m*M* Tris–HCl buffer (pH 7.5) to give a final concentration of 100 m*M*.

8. BIOCHEMICAL CHARACTERIZATION OF PRENYLTRANSFERASES

8.1. Enzyme assays

Purified prenyltransferases are incubated with different aromatic substrates in the presence of DMAPP. The reaction mixtures are analyzed on HPLC.

1. In general, each assay (100 μl) contains 50 m*M* Tris–HCl (pH 7.5), 5 or 10 m*M* Ca^{2+}, 1 m*M* aromatic substrate, 2 m*M* DMAPP, 0.3–5% (v/v) glycerol, 0–5% (v/v) DMSO, and 1–20 μg of purified recombinant protein.
2. Add a calculated volume of 50 m*M* Tris–HCl (pH 7.5) in a 1.5-ml microtube to ensure the final volume to be 100 μl, followed by adding stock solutions of Ca^{2+} and aromatic substrate.
3. Add DMAPP and protein solution as last assay components and mix thoroughly by pipetting.
4. Incubate the reaction mixture at 37 °C or 30 °C for 0.5–7 h and terminate the enzyme reaction by adding 100 μl methanol to the mixture.
5. Centrifuge the mixture at 13,000 rpm for 20 min to remove proteins before injection on HPLC.
6. Carry out negative controls with heat-inactivated protein by boiling it for 20 min.

Keep in mind that the reactions catalyzed by the prenyltransferases of the DMATS superfamily are usually independent of the presence of metal ions. However, Ca^{2+} often enhanced the reaction velocity. The optimal Ca^{2+} concentration was estimated in the range of 5–10 m*M* for known enzymes (Steffan et al., 2009).

8.2. Kinetic parameters

Kinetic parameters of the prenyltransferases for aromatic substrates and DMAPP are determined in 100 μl assays. Linear dependences of the enzyme reactions on reaction time and protein amount should be carried out previously. The values for known prenyltransferases were estimated to be up to 150 min and 20 μg, respectively. The K_M values of the best known prenyltransferases of the DMATS superfamily were found to be 1–500 μ*M* for DMAPP and 2–300 μ*M* for natural or best aromatic substrates.

8.2.1 Kinetic parameter for DMAPP

1. Use natural or the best accepted aromatic substrate for kinetic assays for DMAPP.

2. Dilute the 20 m*M* DMAPP stock solution to different concentrations for assays. Always use newly prepared stock solution.
3. Each assay contains 50 m*M* Tris–HCl (pH 7.5), 5 or 10 m*M* Ca^{2+}, 1 m*M* aromatic substrate, 0.3–5% (v/v) glycerol, 0–5% (v/v) DMSO, a given amount of purified recombinant protein and DMAPP at final concentrations of 0.01, 0.02, 0.05, 0.1, 0.2, 0.5, 1, and 2 m*M*.
4. Carry out assay incubation and termination and sample preparation for HPLC in the same manner as described in steps 2–5 of Section 8.1. Use protein amount and incubation time in the linear region of the reactions.
5. Use assays without DMAPP as negative controls.
6. Adjust DMAPP concentrations and repeat the experiments, if necessary.

8.2.2 Kinetic parameters for aromatic substrates

1. Use the same solvents as described in Section 7 to prepare 100 m*M* stock solutions and dilute them to concentrations of 40, 20, 10, 4, 2, 1, 0.4, and 0.2 m*M*. Owing to limited solubility, stock solutions with a maximal concentration of 40 or 20 m*M* are prepared for some substrates.
2. Each assay contains 50 m*M* Tris–HCl (pH 7.5), 5 or 10 m*M* of Ca^{2+}, 2 m*M* DMAPP, 0.3–5% (v/v) glycerol, 0–5% (v/v) DMSO, a given amount of purified recombinant protein and aromatic substrate at final concentrations of 0.01, 0.02, 0.05, 0.1, 0.2, 0.5, 1, 2, and 5 m*M*. Owing to different solubility, the maximal concentration can be changed.
3. Carry out assay incubation and termination and sample preparation for HPLC in the same manner as described in steps 2–5 of Section 8.1. Use protein amount and incubation time in the linear region of reactions.
4. Use assays without aromatic substrate as negative controls.
5. Adjust the concentrations of aromatic substrate and repeat the experiments, if necessary.

9. CHEMOENZYMATIC SYNTHESIS OF PRENYLATED COMPOUNDS

Prenyltransferases of the DMATS superfamily have been successfully used for production of prenylated compounds including analogues of their natural substrates such as simple indoles, tryptophan-containing cyclic dipeptides, and tyrosine derivatives (Li, 2009a, 2010; Zou, Xie, Zheng & Li, 2011; Fig. 13.4). Interestingly, some enzymes from this family are also able to prenylate hydroxynaphthalenes and flavonoid aglycones, resulting in formation of prenylated derivatives (Yu & Li, 2011; Yu, Xie & Li, 2011).

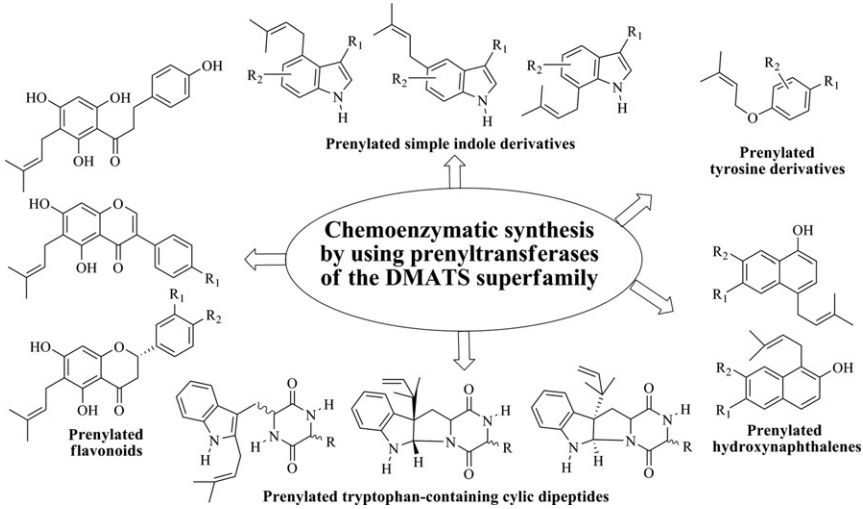

Figure 13.4 Chemoenzymatic synthesis achieved by prenyltransferases of the DMATS superfamily.

9.1. Incubations

Reactions for chemoenzymatic synthesis and structure elucidation are taken in large scales (10–50 ml), which are carried out as following:

1. Each assay contains 50 m*M* Tris–HCl (pH 7.5), 5 or 10 m*M* Ca^{2+}, 1 m*M* aromatic substrate, 2 m*M* DMAPP, 0.3–5% (v/v) glycerol, 0–5% (v/v) DMSO, and 0.5–4 mg purified recombinant protein for 10 ml assays.
2. First add the calculated volume of 50 m*M* Tris–HCl (pH 7.5) to a 50- or 100-ml glass flask, followed by adding Ca^{2+} and aromatic substrate solutions.
3. Add DMAPP and protein solution as last components and mix thoroughly.
4. Incubate the mixture at 30 °C or 37 °C for 16–24 h. Mix occasionally during the incubation.

9.2. Sample preparation for HPLC

Owing to solubility difference of the enzyme products, reaction mixtures are treated in different ways before purification on an HPLC system.

9.2.1 Reaction mixtures with simple indoles and tyrosine derivatives

1. After incubation for 16–24 h, terminate the assays by mixing with an equal volume of methanol. Centrifuge at 13,000 rpm for 20 min to remove precipitated proteins.

2. Concentrate the resulting supernatant on a rotating vacuum evaporator at 30 °C to a final volume of 1–3 ml before injection onto HPLC.
3. Transfer the sample for HPLC into an autosampler tube or a new reaction tube for manual injection. Keep in mind that insoluble particles in the samples could block and damage the column and HPLC system. If the reaction mixture is poorly dissolved, try to improve the solubility by adding DMSO. However, DMSO in the sample could influence the chromatographic behavior of the compounds. It is preferable to centrifuge the samples for 10 min at 13,000 rpm or filter them through a 13-mm syringe filter (0.2 μm PTFE) before injection, to remove insoluble components.

9.2.2 Reaction mixtures with tryptophan-containing cyclic dipeptides, hydroxynaphthalenes, and flavonoid aglycones

1. After 16–24 h incubation, transfer the reaction mixture to a separatory funnel and extract it with an equal volume of ethyl acetate three times. Collect the upper layers (ethyl acetate phase) in a flask.
2. Evaporate solvents with a rotating vacuum evaporator at 30 °C to obtain the residues containing both substrate and enzyme products.
3. Dissolve the residues in methanol (500 μl or more if necessary). As described in Section 9.2.1, DMSO can also be used to improve the solubility. It is recommended to centrifuge or filter the sample before injection.
4. Transfer the sample into an autosampler tube or a new reaction tube for the application on HPLC.

10. HPLC

HPLC is used for analysis and purification of the enzyme products.

10.1. HPLC components

1. Use an HPLC system equipped with a photo diode array detector and an autosampler, if possible.
2. Use an RP-18 column (250 × 4 mm, 5 μm) for analyzing enzyme assays and RP-18 column (250 × 10 mm, 5 μm) for purifying enzyme products.
3. Use solvents A and B as mobile phases for analyzing enzyme assays. Solvent A: water with 0.5% (v/v) trifluoroacetic acid (TFA); solvent B: methanol with 0.5% (v/v) TFA.

4. Use solvents C and D for purification. Solvent C: water without acid; solvent D: methanol without acid. TFA in the mobile phase for reverse phase HPLC sharpens the peaks and improves resolution. However, it can influence the stability of some compounds and is better not used in the mobile phases for substance isolation.
5. Use flow rate of 1 ml min^{-1} for analysis and 2.5 ml min^{-1} for purification of the enzyme products.
6. Set detection wavelength between 250 and 300 nm.

10.2. HPLC conditions

10.2.1 Analysis of enzyme assays with simple indoles or tyrosine derivatives as substrates

1. Equilibrate the HPLC column with 20% (v/v) solvent B in A for 5 min.
2. Inject the sample and use a linear gradient from 20% (v/v) solvent B in A to 100% (v/v) solvent B in 15 min for separation.
3. Rinse the column with 100% (v/v) solvent B for 5 min and equilibrate subsequently with 20% (v/v) solvent B in A for 5 min.

10.2.2 Purification of prenylated products of simple indoles or tyrosine derivatives

1. Equilibrate the HPLC column with 20% (v/v) solvent D in C for 8 min.
2. Inject the sample and use a linear gradient from 20% (v/v) solvent D in C to 100% (v/v) solvent D for 30 min for separation.
3. Rinse the column with 100% (v/v) solvent D for 8 min and equilibrate subsequently with 20% (v/v) solvent D in C for 8 min.
4. For assays with more than one product, optimize the method for better separation, if necessary.
5. Collect product peaks and evaporate at 30 °C to dryness.
6. Use the purified products for NMR and MS analyses.

10.2.3 Analysis of enzyme assays with tryptophan-containing cyclic dipeptides, hydroxynaphthalenes, or flavonoid aglycones as substrates

1. Equilibrate the HPLC column with 40% (v/v) solvent B in A for 5 min.
2. Inject the sample and use a linear gradient from 40% (v/v) solvent B in A to 100% (v/v) solvent B for 15 min for separation.
3. Rinse the column with 100% (v/v) solvent B for 5 min and equilibrate subsequently with 40% (v/v) solvent B in A for 5 min for elution.

10.2.4 Purification of prenylated tryptophan-containing cyclic dipeptides, hydroxynaphthalenes, or flavonoid aglycones

1. Equilibrate the HPLC column with 40% (v/v) solvent D in C for 8 min.
2. Inject the sample and use a linear gradient from 40% (v/v) solvent D in C to 100% (v/v) solvent D for 30 min for separation.
3. Rinse the column with 100% (v/v) solvent D for 8 min and equilibrate subsequently with 40% (v/v) solvent D in C for 8 min for elution.
4. For assays with more than one product, optimize the method for better separation, if necessary.
5. Do the same as described in steps 5 and 6 in Section 10.2.2.

11. SUMMARY

Prenyltransferases of the DMATS superfamily mainly catalyze the prenylation of diverse indole derivatives and are involved in the biosynthesis of indole alkaloids in ascomycetes. Recent studies have revealed that these enzymes showed high tolerance toward diverse tryptophan and tyrosine derivatives and accepted even hydroxynaphthalenes and flavonoid aglycones as substrates. They usually catalyze regio- and stereospecific prenylations and can be used as efficient catalysts for chemoenzymatic synthesis of novel prenylated compounds, which can be then tested for their biological activities in drug discovery and development programs. Therefore, these enzymes are attractive not only for biologists but also for biotechnologists and medicinal chemists. We hope that the described procedures for biochemical characterization of prenyltransferases in this chapter can meet the challenges for finding additional enzymes to be used as novel catalysts.

ACKNOWLEDGMENTS

Work in the authors' laboratory was supported by a grant from the Deutsche Forschungsgemeinschaft (LI844/4-1 to S.-M. Li). X. Y. is a recipient of a fellowship from the China Scholarship Council.

REFERENCES

Ding, Y., Wet, J. R., Cavalcoli, J., Li, S., Greshock, T. J., Miller, K. A., et al. (2010). Genome-based characterization of two prenylation steps in the assembly of the stephacidin and notoamide anticancer agents in a marine-derived *Aspergillus* sp. *Journal of the American Chemical Society*, *132*, 12733–12740.

Ding, Y., Williams, R. M., & Sherman, D. H. (2008). Molecular analysis of a 4-dimethylallyltryptophan synthase from *Malbranchea aurantiaca*. *The Journal of Biological Chemistry*, *283*, 16068–16076.

Grundmann, A., Kuznetsova, T., Afiyatullov, S. S., & Li, S.-M. (2008). FtmPT2, an N-prenyltransferase from *Aspergillus fumigatus*, catalyses the last step in the biosynthesis of fumitremorgin B. *Chembiochem*, *9*, 2059–2063.

Grundmann, A., & Li, S.-M. (2005). Overproduction, purification and characterization of FtmPT1, a brevianamide F prenyltransferase from *Aspergillus fumigatus*. *Microbiology*, *151*, 2199–2207.

Jain, H. D., Zhang, C., Zhou, S., Zhou, H., Ma, J., Liu, X., et al. (2008). Synthesis and structure-activity relationship studies on tryprostatin A, a potent inhibitor of breast cancer resistance protein. *Bioorganic & Medicinal Chemistry*, *16*, 4626–4651.

Jost, M., Zocher, G., Tarcz, S., Matuschek, M., Xie, X., Li, S.-M., et al. (2010). Structure-function analysis of an enzymatic prenyl transfer reaction identifies a reaction chamber with modifiable specificity. *Journal of the American Chemical Society*, *132*, 17849–17858.

Kremer, A., & Li, S.-M. (2010). A tyrosine O-prenyltransferase catalyses the first pathway-specific step in the biosynthesis of sirodesmin PL. *Microbiology*, *156*, 278–286.

Kremer, A., Westrich, L., & Li, S.-M. (2007). A 7-dimethylallyltryptophan synthase from *Aspergillus fumigatus*: Overproduction, purification and biochemical characterization. *Microbiology*, *153*, 3409–3416.

Li, S.-M. (2009a). Applications of dimethylallyltryptophan synthases and other indole prenyltransferases for structural modification of natural products. *Applied Microbiology and Biotechnology*, *84*, 631–639.

Li, S.-M. (2009b). Evolution of aromatic prenyltransferases in the biosynthesis of indole derivatives. *Phytochemistry*, *70*, 1746–1757.

Li, S.-M. (2010). Prenylated indole derivatives from fungi: Structure diversity, biological activities, biosynthesis and chemoenzymatic synthesis. *Natural Product Reports*, *27*, 57–78.

Liu, X., & Walsh, C. T. (2009). Characterization of cyclo-acetoacetyl-L-tryptophan dimethylallyltransferase in cyclopiazonic acid biosynthesis: Substrate promiscuity and site directed mutagenesis studies. *Biochemistry*, *48*, 11032–11044.

Lu, Y. P., Liu, H. G., & Liang, P. H. (2009). Different reaction mechanisms for *cis*- and *trans*-prenyltransferases. *Biochemical and Biophysical Research Communications*, *379*, 351–355.

Luk, L. Y. P., & Tanner, M. E. (2009). Mechanism of dimethylallyltryptophan synthase: Evidence for a dimethylallyl cation intermediate in an aromatic prenyltransferase reaction. *Journal of the American Chemical Society*, *131*, 13932–13933.

Markert, A., Steffan, N., Ploss, K., Hellwig, S., Steiner, U., Drewke, C., et al. (2008). Biosynthesis and accumulation of ergoline alkaloids in a mutualistic association between *Ipomoea asarifolia* (Convolvulaceae) and a Clavicipitalean fungus. *Plant Physiology*, *147*, 296–305.

Metzger, U., Schall, C., Zocher, G., Unsöld, I., Stec, E., Li, S.-M., et al. (2009). The structure of dimethylallyl tryptophan synthase reveals a common architecture of aromatic prenyltransferases in fungi and bacteria. *Proceedings of the National Academy of Sciences of the United States of America*, *106*, 14309–14314.

Sanchez, J. F., Entwistle, R., Hung, J. H., Yaegashi, J., Jain, S., Chiang, Y. M., et al. (2011). Genome-based deletion analysis reveals the prenyl xanthone biosynthesis pathway in *Aspergillus nidulans*. *Journal of the American Chemical Society*, *133*, 4010–4017.

Schneider, P., Weber, M., & Hoffmeister, D. (2008). The *Aspergillus nidulans* enzyme TdiB catalyzes prenyltransfer to the precursor of bioactive asterriquinones. *Fungal Genetics and Biology*, *45*, 302–309.

Stec, E., Steffan, N., Kremer, A., Zou, H., Zheng, X., & Li, S.-M. (2008). Two lysine residues are responsible for the enzymatic activities of indole prenyltransferases from fungi. *Chembiochem*, *9*, 2055–2058.

Steffan, N., Grundmann, A., Yin, W.-B., Kremer, A., & Li, S.-M. (2009). Indole prenyltransferases from fungi: A new enzyme group with high potential for the production of prenylated indole derivatives. *Current Medicinal Chemistry*, *16*, 218–231.

Steffan, N., Unsöld, I. A., & Li, S.-M. (2007). Chemoenzymatic synthesis of prenylated indole derivatives by using a 4-dimethylallyltryptophan synthase from *Aspergillus fumigatus*. *Chembiochem*, *8*, 1298–1307.

Tsai, H. F., Wang, H., Gebler, J. C., Poulter, C. D., & Schardl, C. L. (1995). The *Claviceps purpurea* gene encoding dimethylallyltryptophan synthase, the committed step for ergot alkaloid biosynthesis. *Biochemical and Biophysical Research Communications*, *216*, 119–125.

Unsöld, I. A., & Li, S.-M. (2005). Overproduction, purification and characterization of FgaPT2, a dimethylallyltryptophan synthase from *Aspergillus fumigatus*. *Microbiology*, *151*, 1499–1505.

Unsöld, I. A., & Li, S.-M. (2006). Reverse prenyltransferase in the biosynthesis of fumigaclavine C in *Aspergillus fumigatus*: Gene expression, purification and characterization of fumigaclavine C synthase FgaPT1. *Chembiochem*, 7, 158–164.

Yazaki, K., Sasaki, K., & Tsurumaru, Y. (2009). Prenylation of aromatic compounds, a key diversification of plant secondary metabolites. *Phytochemistry*, *70*, 1739–1745.

Yin, W.-B., Grundmann, A., Cheng, J., & Li, S.-M. (2009). Acetylaszonalenin biosynthesis in *Neosartorya fischeri*: Identification of the biosynthetic gene cluster by genomic mining and functional proof of the genes by biochemical investigation. *The Journal of Biological Chemistry*, *284*, 100–109.

Yin, W.-B., Ruan, H.-L., Westrich, L., Grundmann, A., & Li, S.-M. (2007). CdpNPT, an N-prenyltransferase from *Aspergillus fumigatus*: Overproduction, purification and biochemical characterisation. *Chembiochem*, *8*, 1154–1161.

Yin, W.-B., Yu, X., Xie, X.-L., & Li, S.-M. (2010). Preparation of pyrrolo[2,3-b]indoles carrying a ß-configured reverse C3-dimethylallyl moiety by using a recombinant prenyltransferase CdpC3PT. *Organic and Biomolecular Chemistry*, *8*, 2430–2438.

Yu, X., & Li, S.-M. (2011). Prenylation of flavonoids by using a dimethylallyltryptophan synthase 7-DMATS from *Aspergillus fumigatus*. *Chembiochem*, *12*, 2280–2283.

Yu, X., Liu, Y., Xie, X., Zheng, X.-D., & Li, S.-M. (2012). Biochemical characterization of indole prenyltransferases: Filling the last gap of prenylation positions by a 5-dimethylallyl tryptophansynthase from *Aspergillus clavatus*. *The Journal of Biological Chemistry*, *287*, 1371–1380.

Yu, X., Xie, X., & Li, S.-M. (2011). Substrate promiscuity of secondary metabolite enzymes: Prenylation of hydroxynaphthalenes by fungal indole prenyltransferases. *Applied Microbiology and Biotechnology*, *92*, 737–748.

Zou, H.-X., Xie, X.-L., Linne, U., Zheng, X.-D., & Li, S.-M. (2010). Simultaneous C7- and N1-prenylation of cyclo-L-Trp-L-Trp catalyzed by a prenyltransferase from *Aspergillus oryzae*. *Organic and Biomolecular Chemistry*, *8*, 3037–3044.

Zou, H.-X., Xie, X., Zheng, X.-D., & Li, S.-M. (2011). The tyrosine O-prenyltransferase SirD catalyzes O-, N-, and C-prenylations. *Applied Microbiology and Biotechnology*, *89*, 1443–1451.

6 Conclusions and future prospects

In this thesis, novel strategies for chemoenzymatic synthesis of prenylated compounds were developed by function elucidation of indole prenyltransferases as well as by substrate promiscuity study.

Firstly, three indole prenyltransferases of the DMATS superfamily were characterized. The C3-prenyltransferase CdpC3PT from *N. fischeri* catalyzed reverse prenylation of tryptophan-containing cyclic dipeptides of the indole ring and the formation of a 6/5/5/6 tetracyclic ring system. Five monoprenylated and one diprenylated derivatives were obtained from five cyclic dipeptides containing L-form tryptophanyl moiety. 5-DMATS was identified from *A. clavatus* and proven to catalyze the regiospecific C5-prenylation of indole derivatives. It is the first enzyme reported to catalyze prenylation at position C-5 of indole derivatives and fills herewith the last gap in the search for indole prenyltransferases regarding their prenylation positions. Twelve C5-prenylated derivatives of simple indole derivatives were produced. In contrast to the low flexibility of NotF from *Aspergillus* sp. MF297-2, we demonstrated that the NotF homologue BrePT from *A. versicolor* showed substrate promiscuity for at least twelve substrates from which reversely C2-prenylated products were produced and subsequently identified by MS and NMR analyses. The broad substrate promiscuity and high regiospecificity of CdpC3PT, 5-DMATS and BrePT provides experimental evidence for their application as effective biocatalysts for chemoenzymatic synthesis. The natural substrates of CdpC3PT and 5-DMATS can't be detected in this thesis. Concerning BrePT, it can be speculated that the natural substrate of BrePT should be brevianamide F based on the high sequence similarity of BrePT with NotF.

Subsequently, CdpC3PT, 5-DMATS and BrePT obtained in this thesis as well as other known indole prenyltransferases of the DMATS superfamily were successfully applied for chemoenzymatic synthesis of prenylated derivatives. AnaPT, CdpC3PT and CdpNPT constructed eight prenylated pyrroloindoline diketopiperazine stereoisomers with one 6/5/5/6 tetracyclic framework and six prenylated pyrroloindoline diketopiperazine stereoisomers containing one 6/5/5/6/5 pentacyclic framework from cyclo-Trp-Ala and cyclo-Trp-Pro isomers, respectively. Experimental data in this thesis provided information on the structure dependence of the stereoselectivity of these enzymes towards the tested cyclic dipeptides. The stereoselectivity of AnaPT and CdpC3PT was largely dependent on the configuration of tryptophanyl moiety in substrates and always complemented to each other, while CdpNPT showed lower stereoselectivity but higher conversion ability. Indolocarbazoles were also accepted by indole prenyltransferases. 5-DMATS and FgaPT2 were capable to catalyze regiospecific prenylation of indolocarbazoles at the *para*-position of the indole N-atom. Five prenylated indolocarbazoles were generated in this study. Since prenylated indolocarbazoles

have been reported neither from natural sources, nor by chemical synthetic approaches, this is the first report on prenylated indolocarbazoles.

Indole prenyltransferases of the DMATS superfamily also showed substrate specificity towards hydroxynaphthalene derivatives, which were substrates for enzymes of the CloQ/NphB group. In contrast to the different prenylation patterns and positions of a given indole derivative by different enzymes, the same major prenylated products were identified in the reaction mixtures with hydroxynaphthalenes, *i.e.* with a regular C-prenyl moiety at *para*- or *ortho*-position to a hydroxyl group. O-prenylated and diprenylated derivatives were also identified as enzyme products in incubation mixtures with low conversion. Twenty prenylated hydroxynaphthalenes have been isolated in this study. Furthermore, 7-DMATS showed the capability to catalyze C-prenylation of flavonoids, which were substrates for the members of the UbiA superfamily. Regularly C6-prenylated flavonoids were identified in all of six investigated flavonoids as enzyme products, revealing that the catalytic preference of prenylation at position C-6 between two hydroxyl groups in flavonoids by 7-DMATS.

These results expand the potential usage of prenyltransferases of the DMATS superfamily as biocatalysts for chemoenzymatic synthesis, and meanwhile, increase the structural diversity of prenylated compounds and provide new opportunities for drug discovery and development.

In addition to the works on indole prenyltransferases, another two genes involved in the biosynthetic pathway of the prenylated indole alkaloid HAS were successfully cloned, *i.e.* the putative O-methyltransferase gene *hasC* and the putative cytochrome P450 gene *hasH*. The gene *hasC* was cloned into pQE60 and overexpressed in *E. coli*. Recombinant His_6-HasC was successfully overproduced and detected by SDS-PAGE. Three expression vectors have been constructed for the overexpression of *hasH*, including the normal expression vectors with myc epitope tag or His_6-tag and the co-expression vector containing the reductase gene *NFIA_083630*. Unfortunately, due to time limit of scholarship, these projects can't be finished.

For the future prospects, the following works should be performed:

(1) Further investigation on the putative O-methyltransferase gene *hasC* and the putative cytochrome P450 gene *hasH* from *A. fumigatus*.

(2) Investigation on the prenylation of indole alkaloids by prenyltransferases of the CloQ/NphB group and the UbiA superfamily.

7 References

Akashi, T., Sasaki, K., Aoki, T., Ayabe, S. & Yazaki, K. (**2009**). Molecular cloning and characterization of a cDNA for pterocarpan 4-dimethylallyltransferase catalyzing the key prenylation step in the biosynthesis of glyceollin, a soybean phytoalexin. *Plant Physiol.* **149**, 683-693.

Akazawa, H., Kohno, H., Tokuda, H., Suzuki, N., Yasukawa, K., Kimura, Y., Manosroi, A., Manosroi, J. & Akihisa, T. (**2012**). Anti-inflammatory and anti-tumor-promoting effects of 5-deprenyllupulonol C and other compounds from Hop (*Humulus lupulus* L.). *Chem. Biodivers.* **9**, 1045-1054.

Albini, A., Dell'Eva, R., Vene, R., Ferrari, N., Buhler, D. R., Noonan, D. M. & Fassina, G. (**2006**). Mechanisms of the antiangiogenic activity by the hop flavonoid xanthohumol: NF-kappaB and Akt as targets. *FASEB J.* **20**, 527-529.

Arai, K., Kimura, K., Mushiroda, T. & Yamamoto, Y. (**1989**). Structures of fructigenines A and B, new alkaloids isolated from *Penicillium fructigenum* Takeuchi. *Chem. Pharm. Bull.* **37**, 2937-2939.

Arung, E. T., Shimizu, K. & Kondo, R. (**2006**). Inhibitory effect of isoprenoid-substituted flavonoids isolated from *Artocarpus heterophyllus* on melanin biosynthesis. *Planta Med.* **72**, 847-850.

Bankeu, J. J., Khayala, R., Lenta, B. N., Noungoue, D. T., Ngouela, S. A., Mustafa, S. A., Asaad, K., Choudhary, M. I., Prigge, S. T., Hasanov, R., Nkengfack, A. E., Tsamo, E. & Ali, M. S. (**2011**). Isoflavone dimers and other bioactive constituents from the figs of *Ficus mucuso*. *J. Nat. Prod.* **74**, 1370-1378.

Barron, D., Ibrahim, R. K. (**1996**). Isoprenylated flavonoids–a survey. *Phytochemistry* **43**, 921-982.

Barrow, K. D., Quigley, F. R. (**1975**). Ergot alkaloids III: The isolation of N-methyl-4-dimethylallyltryptophan from *claviceps fusiformis*. *Tetrahedron Lett.* **16**, 4269-4270.

Belofsky, G., Carreno, R., Goswick, S. M. & John, D. T. (**2006**). Activity of isoflavans of *Dalea aurea* (Fabaceae) against the opportunistic ameba *naegleria fowleri*. *Planta Med.* **72**, 383-386.

Belofsky, G. N., Gloer, J. B., Wicklow, D. T. & Dowd, P. F. (**1995**). Antiinsectan alkaloids: Shearinines A-C and a new paxilline derivative from the ascostromata of *Eupenicillium shearii*. *Tetrahedron* **51**, 3959-3968.

Bivin, D. B., Kubota, S., Pearlstein, R. & Morales, M. F. (**1993**). On how a myosin tryptophan may be perturbed. *Proc. Natl. Acad. Sci. U. S. A.* **90**, 6791-6795.

Bonitz, T., Alva, V., Saleh, O., Lupas, A. N. & Heide, L. (**2011**). Evolutionary relationships of microbial aromatic prenyltransferases. *PLoS One* **6**, e27336.

Boonnak, N., Karalai, C., Chantrapromma, S., Ponglimanont, C., Fun, H. K., Kanjana-Opas, A. & Laphookhieo, S. (**2006**). Bioactive prenylated xanthones and anthraquinones from *Cratoxylum formosum* ssp. *pruniflorum*. *Tetrahedron* **62**, 8850-8859.

Boonnak, N., Karalai, C., Chantrapromma, S., Ponglimanont, C., Kanjana-Opas, A., Chantrapromma, K. & Fun, H. K. (**2007**). Quinonoids from the barks of *Cratoxylum formosum* subsp.*pruniflorum*. *Can. J. Chem.* **85**, 341-345.

Botta, B., Delle Monache, F., Delle Monache, G., MariniBettolo, G. B. & Oguakwa, J. U. (**1983**). 3-Geranyloxy-6-methyl-1,8-dihydroxyanthraquinone and vismiones C, D and E from *Psorospermum febrifugum*. *Phytochemistry* **22**, 539-542.

Botta, B., Menendez, P., Zappia, G., de Lima, R. A., Torge, R. & Monachea, G. D. (**2009**). Prenylated isoflavonoids: Botanical distribution, structures, biological activities and biotechnological studies. An update (1995-2006). *Curr. Med. Chem.* **16**, 3414-3468.

Botta, B., Monache, G. D., Menendez, P. & Boffi, A. (**2005a**). Novel prenyltransferase enzymes as a tool for flavonoid prenylation. *Trends Pharmacol. Sci.* **26**, 606-608.

Botta, B., Vitali, A., Menendez, P., Misiti, D. & Delle, M. G. (**2005b**). Prenylated flavonoids: pharmacology and biotechnology. *Curr. Med. Chem.* **12**, 717-739.

Burtin, G. E., Madge, D. J. & Selwood, D. L. (**2000**). New synthesis of KT5823 indolocarbazole aglycone. *Heterocycles* **53**, 2119-2122.

Caballero, E., Avendaño, C. & Menéndez, J. C. (**1998**). Stereochemical issues related to the synthesis and reactivity of pyrazino[2',1'-5,1]pyrrolo[2,3-b]indole-1,4-diones. *Tetrahedron: Asymmetry* **9**, 967-981.

Cacciatore, I., Cocco, A., Costa, M., Fontana, M., Lucente, G., Pecci, L. & Pinnen, F. (**2005**). Biochemical properties of new synthetic carnosine analogues containing the residue of 2,3-diaminopropionic acid: the effect of N-acetylation. *Amino Acids* **28**, 77-83.

Chen, L. G., Yang, L. L. & Wang, C. C. (**2008**). Anti-inflammatory activity of mangostins from *Garcinia mangostana*. *Food Chem. Toxicol.* **46**, 688-693.

Chexal, K. K., Holker, J. S., Simpson, T. J. & Young, K. (**1975**). The biosynthesis of fungal metabolites. Part V. Structure of variecoxanthones A, B, and C, metabolites of *Aspergillus variecolor*; conversion of variecoxanthone A into (±)-de-c-prenylepishamixanthone. *J. Chem. Soc. ,Perkin 1*543-548.

Chi, Y. S., Jong, H. G., Son, K. H., Chang, H. W., Kang, S. S. & Kim, H. P. (**2001**). Effects of naturally occurring prenylated flavonoids on enzymes metabolizing arachidonic acid: Cyclooxygenases and lipoxygenases. *Biochem. Pharmacol.* **62**, 1185-1191.

Cho, J. K., Ryu, Y. B., Curtis-Long, M. J., Kim, J. Y., Kim, D., Lee, S., Lee, W. S. & Park, K. H. (**2011**). Inhibition and structural reliability of prenylated flavones from the stem bark of *Morus lhou* on beta-secretase (BACE-1). *Bioorg. Med. Chem. Lett.* **21**, 2945-2948.

Chooi, Y. H., Fang, J., Liu, H., Filler, S. G., Wang, P. & Tang, Y. (**2013**). Genome mining of a prenylated and immunosuppressive polyketide from pathogenic Fungi. *Org. Lett.* **15**, 780-783.

Chooi, Y. H., Wang, P., Fang, J., Li, Y., Wu, K., Wang, P. & Tang, Y. (**2012**). Discovery and characterization of a group of fungal polycyclic polyketide prenyltransferases. *J. Am. Chem. Soc.* **134**, 9428-9437.

Cole, R. J., Dorner, J. W., Springer, J. P. & Cox, R. H. (**1981**). Indole metabolites from a strain of *Aspergillus flavus*. *J. Agr. Food Chem.* **29**, 293-295.

Coyle, C. M., Cheng, J. Z., O'Connor, S. E. & Panaccione, D. G. (**2010**). An old yellow enzyme gene that controls the branch point between *Aspergillus fumigatus* and *Claviceps purpurea* ergot alkaloid pathways. *Appl. Environ. Microbiol.* **76**, 3898-3903.

Cui, C. B., Kakeya, H., Okada, G., Onose, R. & Osada, H. (**1996**). Novel mammalian cell cycle inhibitors, tryprostatins A, B and other diketopiperazines produced by *Aspergillus fumigatus*. I. Taxonomy, fermentation, isolation and biological properties. *J. Antibiot.* **49**, 527-533.

Cui, C. B., Kakeya, H., Okada, G., Onose, R., Ubukata, M., Takahashi, I., Isono, K. & Osada, H. (**1995**). Tryprostatins A and B, novel mammalian cell cycle inhibitors produced by *Aspergillus fumigatus*. *J. Antibiot.* **48**, 1382-1384.

Deachathai, S., Mahabusarakam, W., Phongpaichit, S. & Taylor, W. C. (**2005**). Phenolic compounds from the fruit of *Garcinia dulcis*. *Phytochemistry* **66**, 2368-2375.

Ding, Y., Wet, J. R., Cavalcoli, J., Li, S., Greshock, T. J., Miller, K. A., Finefield, J. M., Sunderhaus, J. D., McAfoos, T. J., Tsukamoto, S., Williams, R. M. & Sherman, D. H. (**2010**). Genome-based characterization of two prenylation steps in the assembly of the stephacidin and notoamide anticancer agents in a marine-derived *Aspergillus* sp. *J. Am. Chem. Soc.* **132**, 12733-12740.

Ding, Y., Williams, R. M. & Sherman, D. H. (**2008**). Molecular analysis of a 4-dimethylallyltryptophan synthase from *Malbranchea aurantiaca*. *J. Biol. Chem.* **283**, 16068-16076.

Djiogue, S., Halabalaki, M., Alexi, X., Njamen, D., Fomum, Z. T., Alexis, M. N. & Skaltsounis, A. L. (**2009**). Isoflavonoids from *Erythrina poeppigiana*: evaluation of their binding affinity for the estrogen receptor. *J. Nat. Prod.* **72**, 1603-1607.

Edwards, D. J., Gerwick, W. H. (**2004**). Lyngbyatoxin biosynthesis: sequence of biosynthetic gene cluster and identification of a novel aromatic prenyltransferase. *J. Am. Chem. Soc.* **126**, 11432-11433.

El-Masry, S., Amer, M. E., Abdel-Kader, M. S. & Zaatout, H. H. (**2002**). Prenylated flavonoids of *Erythrina lysistemon* grown in Egypt. *Phytochemistry* **60**, 783-787.

El-Seedi, H. R., El-Barbary, M. A., El-Ghorab, D. M. H., Bohlin, L., Borg-Karlson, A. K., Göransson, U. & Verpoorte, R. (**2010**). Recent insights into the biosynthesis and biological activities of natural xanthones. *Curr. Med. Chem.* **17**, 854-901.

El-Seedi, H. R., El-Ghorab, D. M. H., El-Barbary, M. A., Zayed, M. F., Göransson, U., Larsson, S. & Verpoorte, R. (**2009**). Naturally occurring xanthones; latest investigations: isolation, structure elucidation and chemosystematic significance. *Curr. Med. Chem.* **16**, 2581-2626.

Ellestad, G. A., Mirando, P. & Kunstmann, M. P. (**1973**). Structure of the metabolite LL-S490ß from an unidentified *Aspergillus* species. *J. Org. Chem.* **38**, 4204-4205.

Epifano, F., Genovese, S., Fiorito, S., Mathieu, V. & Kiss, R. (**2013**). Lapachol and its congeners as anticancer agents: a review. *Phytochem. Rev.*DOI: 10.1007/s11101-013-9289-1.

Erasto, P., Bojase-Moleta, G. & Majinda, R. R. (**2004**). Antimicrobial and antioxidant flavonoids from the root wood of *Bolusanthus speciosus*. *Phytochemistry* **65**, 875-880.

Faul, M. M., Winneroski, L. L. & Krumrich, C. A. (**1998**). A new, efficient method for the synthesis of bisindolylmaleimides. *J. Org. Chem.* **63**, 6053-6058.

Finefield, J. M., Greshock, T. J., Sherman, D. H., Tsukamoto, S. & Williams, R. M. (**2011a**). Notoamide E: Biosynthetic incorporation into notoamides C and D in cultures of *Aspergillus versicolor* NRRL 35600. *Tetrahedron Lett.* **52**, 1987-1989.

Finefield, J. M., Kato, H., Greshock, T. J., Sherman, D. H., Tsukamoto, S. & Williams, R. M. (**2011b**). Biosynthetic studies of the notoamides: isotopic synthesis of stephacidin a and incorporation into notoamide B and sclerotiamide. *Org. Lett.* **13**, 3802-3805.

Finefield, J. M., Sherman, D. H., Tsukamoto, S. & Williams, R. M. (**2011c**). Studies on the biosynthesis of the notoamides: synthesis of an isotopomer of 6-hydroxydeoxybrevianamide e and biosynthetic incorporation into notoamide J. *J. Org. Chem.* **76**, 5954-5958.

Fredenhagen, A., Petersen, F., Tintelnot-Blomley, M., Rosel, J., Mett, H. & Hug, P. (**1997**). Semicochliodinol A and B: inhibitors of HIV-1 protease and EGF-R protein tyrosine kinase related to asterriquinones produced by the fungus *Chrysosporium merdarium*. *J. Antibiot.* **50**, 395-401.

Fujimoto, H., Fujimaki, T., Okuyama, E. & Yamazaki, M. (**1999**). Immunomodulatory constituents from an ascomycete, *Microascus tardifaciens*. *Chem. Pharm. Bull.* **47**, 1426-1432.

Gallagher, R. T., Latch, G. C. M. (**1977**). Production of the tremorgenic mycotoxins verruculogen and fumitremorgin B by *Penicillium piscarium* Westling. *Appl. Envir. Microbiol.* **33**, 730-731.

Gallagher, R. T., Wilson, B. J. (**1978**). Aflatrem, the tremorgenic mycotoxin from *Aspergillus flavus*. *Mycopathologia* **66**, 183-185.

Ge, H. M., Peng, H., Guo, Z. K., Cui, J. T., Song, Y. C. & Tan, R. X. (**2010**). Bioactive alkaloids from the plant endophytic fungus *Aspergillus terreus*. *Planta Med.* **76**, 822-824.

Ge, H. M., Yu, Z. G., Zhang, J., Wu, J. H. & Tan, R. X. (**2009**). Bioactive alkaloids from endophytic *Aspergillus fumigatus*. *J. Nat. Prod.* **72**, 753-755.

Gerhauser, C. (**2005**). Broad spectrum anti-infective potential of xanthohumol from hop (*Humulus lupulus* L.) in comparison with activities of other hop constituents and xanthohumol metabolites. *Mol. Nutr. Food Res.* **49**, 827-831.

Gerhauser, C., Alt, A., Heiss, E., Gamal-Eldeen, A., Klimo, K., Knauft, J., Neumann, I., Scherf, H. R., Frank, N., Bartsch, H. & Becker, H. (**2002**). Cancer chemopreventive activity of xanthohumol, a natural product derived from hop. *Mol. Cancer Ther.* **1**, 959-969.

Grundmann, A., Kuznetsova, T., Afiyatullov, S. S. & Li, S.-M. (**2008**). FtmPT2, an N-prenyltransferase from *Aspergillus fumigatus*, catalyses the last step in the biosynthesis of fumitremorgin B. *Chembiochem* **9**, 2059-2063.

Grundmann, A., Li, S.-M. (**2005**). Overproduction, purification and characterization of FtmPT1, a brevianamide F prenyltransferase from *Aspergillus fumigatus*. *Microbiology* **151**, 2199-2207.

Gunasekera, S. P., Jayatilake, G. S., Selliah, S. S. & Sultanbawa, M. U. (**1977**). Chemical investigation of ceylonese plants. Part 27. Extractives of *Calophyllum cuneifolium* Thw. and *Calophyllum soulattri* Burm. f. (Guttiferae). *J. Chem. Soc. ,Perkin Trans. 1*1505-1511.

Haagen, Y., Unsöld, I., Westrich, L., Gust, B., Richard, S. B., Noel, J. P. & Heide, L. (**2007**). A soluble, magnesium-independent prenyltransferase catalyzes reverse and regular C-prenylations and O-prenylations of aromatic substrates. *FEBS Lett.* **581**, 2889-2893.

Han, Q. B., Yang, N. Y., Tian, H. L., Qiao, C. F., Song, J. Z., Chang, D. C., Chen, S. L., Luo, K. Q. & Xu, H. X. (**2008**). Xanthones with growth inhibition against HeLa cells from *Garcinia xipshuanbannaensis*. *Phytochemistry* **69**, 2187-2192.

Harris, W., Hill, C. H., Keech, E. & Malsher, P. (**1993**). Oxidative cyclisations with palladium acetate. A short synthesis of staurosporine aglycone. *Tetrahedron Lett.* **34**, 8361-8364.

Heide, L. (**2009**). Prenyl transfer to aromatic substrates: genetics and enzymology. *Curr. Opin. Chem. Biol.* **13**, 171-179.

Ho, C. K., Huang, Y. L. & Chen, C. C. (**2002**). Garcinone E, a xanthone derivative, has potent cytotoxic effect against hepatocellular carcinoma cell lines. *Planta Med.* **68**, 975-979.

Hochlowski, J. E., Mullally, M. M., Spanton, S. G., Whittern, D. N., Hill, P. & McAlpine, J. B. (**1993**). 5-N-acetylardeemin, a novel heterocyclic compound which reverses multiple drug resistance in tumor cells. II. Isolation and elucidation of the structure of 5-N-acetylardeemin and two congeners. *J. Antibiot.* **46**, 380-386.

Hossain, M. M., Kawamura, Y., Yamashita, K. & Tsukayama, M. (**2006**). Microwave-assisted regioselective synthesis of natural 6-prenylpolyhydroxyisoflavones and their hydrates with hypervalent iodine reagents. *Tetrahedron* **62**, 8625-8635.

Huang, Y. L., Chen, C. C., Chen, Y. J., Huang, R. L. & Shieh, B. J. (**2001**). Three xanthones and a benzophenone from *Garcinia mangostana*. *J. Nat. Prod.* **64**, 903-906.

Hussain, H., Krohn, K., Ahmad, V. U., Miana, G. A. & Green, I. R. (**2007**). Lapachol: An overview. *ARKIVOC (Gainesville,FL,U. S.)*145-171.

Hussein, A. A., Barberena, I., Capson, T. L., Kursar, T. A., Coley, P. D., Solis, P. N. & Gupta, M. P. (**2004**). New cytotoxic naphthopyrane derivatives from *Adenaria floribunda*. *J. Nat. Prod.* **67**, 451-453.

Hussein, A. A., Bozzi, B., Correa, M., Capson, T. L., Kursar, T. A., Coley, P. D., Solis, P. N. & Gupta, M. P. (**2003**). Bioactive constituents from three *Vismia* species. *J. Nat. Prod.* **66**, 858-860.

Iinuma, M., Tosa, H., Toriyama, N., Tanaka, T., Ito, T. & Chelladurai, V. (**1996**). Six xanthones from *Calophyllum austroindicum*. *Phytochemistry* **43**, 681-685.

Jain, H. D., Zhang, C., Zhou, S., Zhou, H., Ma, J., Liu, X., Liao, X., Deveau, A. M., Dieckhaus, C. M., Johnson, M. A., Smith, K. S., Macdonald, T. L., Kakeya, H., Osada, H. & Cook, J. M. (**2008**). Synthesis and structure-activity relationship studies on tryprostatin A, a potent inhibitor of breast cancer resistance protein. *Bioorg. Med. Chem.* **16**, 4626-4651.

Jang, D. S., Cuendet, M., Hawthorne, M. E., Kardono, L. B., Kawanishi, K., Fong, H. H., Mehta, R. G., Pezzuto, J. M. & Kinghorn, A. D. (**2002**). Prenylated flavonoids of the leaves of *Macaranga conifera* with inhibitory activity against cyclooxygenase-2. *Phytochemistry* **61**, 867-872.

Jost, M., Zocher, G., Tarcz, S., Matuschek, M., Xie, X., Li, S.-M. & Stehle, T. (**2010**). Structure-function analysis of an enzymatic prenyl transfer reaction identifies a reaction chamber with modifiable specificity. *J. Am. Chem. Soc.* **132**, 17849-17858.

Jung, H. A., Su, B. N., Keller, W. J., Mehta, R. G. & Kinghorn, A. D. (**2006**). Antioxidant xanthones from the pericarp of *Garcinia mangostana* (Mangosteen). *J. Agric. Food Chem.* **54**, 2077-2082.

Kagan, R. M., Clarke, S. (**1994**). Widespread occurrence of three sequence motifs in diverse S-adenosylmethionine-dependent methyltransferases suggests a common structure for these enzymes. *Arch. Biochem. Biophys.* **310**, 417-427.

Kaji, A., Iwata, T., Kiriyama, N., Wakusawa, S. & Miyamoto, K. (**1994**). Four new metabolites of *Aspergillus terreus*. *Chem. Pharm. Bull.* **42**, 1682-1684.

Kanokmedhakul, S., Kanokmedhakul, K., Phonkerd, N., Soytong, K., Kongsaeree, P. & Suksamrarn, A. (**2002**). Antimycobacterial anthraquinone-chromanone compound and diketopiperazine alkaloid from the fungus *Chaetomium globosum* KMITL-N0802. *Planta Med.* **68**, 834-836.

Kato, N., Suzuki, H., Takagi, H., Asami, Y., Kakeya, H., Uramoto, M., Usui, T., Takahashi, S., Sugimoto, Y. & Osada, H. (**2009**). Identification of cytochrome P450s required for fumitremorgin biosynthesis in *Aspergillus fumigatus*. *Chembiochem* **10**, 920-928.

Kikuchi, H., Ohtsuki, T., Koyano, T., Kowithayakorn, T., Sakai, T. & Ishibashi, M. (**2010**). Activity of mangosteen xanthones and teleocidin a-2 in death receptor expression enhancement and tumor necrosis factor related apoptosis-inducing ligand assays. *J. Nat. Prod.* **73**, 452-455.

Ko, H. H., Yu, S. M., Ko, F. N., Teng, C. M. & Lin, C. N. (**1997**). Bioactive constituents of *Morus australis* and *Broussonetia papyrifera*. *J. Nat. Prod.* **60**, 1008-1011.

Kozlovsky, A. G., Vinokurova, N. G., Adanin, V. M., Burkhardt, G., Dahse, H. M. & Gräfe, U. (**2000**). New diketopiperazine alkaloids from *Penicillium fellutanum*. *J. Nat. Prod.* **63**, 698-700.

Kozlovsky, A. G., Vinokurova, N. G., Adanin, V. M., Burkhardt, G., Dahse, H.-M. & Gräfe, U. (**2001**). New diketopiperazine alkaloids from *Penicillium fellutanum*. *J. Nat. Prod.* **64**, 553-554.

Kremer, A., Li, S.-M. (**2008**). Potential of a 7-dimethylallyltryptophan synthase as a tool for production of prenylated indole derivatives. *Appl. Microbiol. Biotechnol.* **79**, 951-961.

Kremer, A., Li, S.-M. (**2010**). A tyrosine O-prenyltransferase catalyses the first pathway-specific step in the biosynthesis of sirodesmin PL. *Microbiology* **156**, 278-286.

Kremer, A., Westrich, L. & Li, S.-M. (**2007**). A 7-dimethylallyltryptophan synthase from *Aspergillus fumigatus*: overproduction, purification and biochemical characterization. *Microbiology* **153**, 3409-3416.

Kumano, T., Richard, S. B., Noel, J. P., Nishiyama, M. & Kuzuyama, T. (**2008**). Chemoenzymatic syntheses of prenylated aromatic small molecules using *Streptomyces* prenyltransferases with relaxed substrate specificities. *Bioorg. Med. Chem.* **16**, 8117-8126.

Kumano, T., Tomita, T., Nishiyama, M. & Kuzuyama, T. (**2010**). Functional characterization of the promiscuous prenyltransferase responsible for furaquinocin biosynthesis: identification of a physiological polyketide substrate and its prenylated reaction products. *J. Biol. Chem.* **285**, 39663-39671.

Kuzuyama, T., Noel, J. P. & Richard, S. B. (**2005**). Structural basis for the promiscuous biosynthetic prenylation of aromatic natural products. *Nature* **435**, 983-987.

Laphookhieo, S., Maneerat, W. & Koysomboon, S. (**2009**). Antimalarial and cytotoxic phenolic compounds from *Cratoxylum maingayi* and *Cratoxylum cochinchinense*. *Molecules* **14**, 1389-1395.

Lee, B. W., Lee, J. H., Lee, S. T., Lee, H. S., Lee, W. S., Jeong, T. S. & Park, K. H. (**2005**). Antioxidant and cytotoxic activities of xanthones from *Cudrania tricuspidata*. *Bioorg. Med. Chem. Lett.* **15**, 5548-5552.

Lenta, B. N., Kamdem, L. M., Ngouela, S., Tantangmo, F., Devkota, K. P., Boyom, F. F., Rosenthal, P. J. & Tsamo, E. (**2011a**). Antiplasmodial constituents from the fruit pericarp of *Pentadesma butyracea*. *Planta Med.* **77**, 377-379.

Lenta, B. N., Kamdem, L. M., Ngouela, S., Tantangmo, F., Devkota, K. P., Boyom, F. F., Rosenthal, P. J. & Tsamo, E. (**2011b**). Antiplasmodial constituents from the fruit pericarp of *Pentadesma butyracea*. *Planta Med.* **77**, 377-379.

Li, S., Finefield, J. M., Sunderhaus, J. D., McAfoos, T. J., Williams, R. M. & Sherman, D. H. (**2012**). Biochemical characterization of NotB as an FAD-dependent oxidase in the biosynthesis of notoamide indole alkaloids. *J. Am. Chem. Soc.* **134**, 788-791.

Li, S.-M. (**2009**). Evolution of aromatic prenyltransferases in the biosynthesis of indole derivatives. *Phytochemistry* **70**, 1746-1757.

Li, S.-M. (**2010**). Prenylated indole derivatives from fungi: structure diversity, biological activities, biosynthesis and chemoenzymatic synthesis. *Nat. Prod. Rep.* **27**, 57-78.

Lindel, T., Marsch, N. & Adla, S. K. (**2012**). Indole prenylation in alkaloid synthesis. *Top. Curr. Chem.* **309**, 67-129.

Liu, X., Walsh, C. T. (**2009**). Characterization of cyclo-acetoacetyl-L-tryptophan dimethylallyltransferase in cyclopiazonic acid biosynthesis: substrate promiscuity and site directed mutagenesis studies. *Biochemistry* **48**, 11032-11044.

Liu, X., Wang, L., Steffan, N., Yin, W.-B. & Li, S.-M. (**2009**). Ergot alkaloid biosynthesis in *Aspergillus fumigatus*: FgaAT catalyses the acetylation of fumigaclavine B. *Chembiochem* **10**, 2325-2328.

Lukaseder, B., Vajrodaya, S., Hehenberger, T., Seger, C., Nagl, M., Lutz-Kutschera, G., Robien, W., Greger, H. & Hofer, O. (**2009**). Prenylated flavanones and flavanonols as chemical markers in *Glycosmis species* (Rutaceae). *Phytochemistry* **70**, 1030-1037.

Ma, J., Zuo, D., Song, Y., Wang, B., Huang, H., Yao, Y., Li, W., Zhang, S., Zhang, C. & Ju, J. (**2012**). Characterization of a single gene cluster responsible for methylpendolmycin and pendolmycin biosynthesis in the deep sea bacterium *Marinactinospora thermotolerans*. *Chembiochem* **13**, 547-552.

Macone, A., Lendaro, E., Comandini, A., Rovardi, I., Matarese, R. M., Carraturo, A. & Bonamore, A. (**2009**). Chromane derivatives of small aromatic molecules: Chemoenzymatic synthesis and growth inhibitory activity on human tumor cell line LoVo WT. *Bioorg. Med. Chem.* **17**, 6003-6007.

Magalhaes, P. J., Carvalho, D. O., Cruz, J. M., Guido, L. F. & Barros, A. A. (**2009**). Fundamentals and health benefits of xanthohumol, a natural product derived from hops and beer. *Nat. Prod. Commun.* **4**, 591-610.

Maiya, S., Grundmann, A., Li, S.-M. & Turner, G. (**2006**). The fumitremorgin gene cluster of *Aspergillus fumigatus*: identification of a gene encoding brevianamide F synthetase. *Chembiochem.* **7**, 1062-1069.

Matsumoto, K., Akao, Y., Kobayashi, E., Ohguchi, K., Ito, T., Tanaka, T., Iinuma, M. & Nozawa, Y. (**2003**). Induction of apoptosis by xanthones from mangosteen in human leukemia cell lines. *J. Nat. Prod.* **66**, 1124-1127.

Melzer, M., Heide, L. (**1994**). Characterization of polyprenyldiphosphate: 4-hydroxybenzoate polyprenyltransferase from *Escherichia coli*. *Biochim. Biophys. Acta* **1212**, 93-102.

Metzger, U., Keller, S., Stevenson, C. E., Heide, L. & Lawson, D. M. (**2010**). Structure and mechanism of the magnesium-independent aromatic prenyltransferase CloQ from the clorobiocin biosynthetic pathway. *J. Mol. Biol.* **404**, 611-626.

Metzger, U., Schall, C., Zocher, G., Unsöld, I., Stec, E., Li, S.-M., Heide, L. & Stehle, T. (**2009**). The structure of dimethylallyl tryptophan synthase reveals a common architecture of aromatic prenyltransferases in fungi and bacteria. *Proc. Natl. Acad. Sci. U. S. A* **106**, 14309-14314.

Mishra, B. B., Kishore, N., Tiwari, V. K., Singh, D. D. & Tripathi, V. (**2010a**). A novel antifungal anthraquinone from seeds of *Aegle marmelos* Correa (family Rutaceae). *Fitoterapia* **81**, 104-107.

Mishra, B. B., Singh, D. D., Kishore, N., Tiwari, V. K. & Tripathi, V. (**2010b**). Antifungal constituents isolated from the seeds of *Aegle marmelos*. *Phytochemistry* **71**, 230-234.

Mocek, U., Schultz, L., Buchan, T., Baek, C., Fretto, L., Nzerem, J., Sehl, L. & Sinha, U. (**1996**). Isolation and structure elucidation of five new asterriquinones from *Aspergillus*, *Humicola* and *Botryotrichum* species. *J. Antibiot.* **49**, 854-859.

Monache, F. D., Botta, B., Monache, G. D. & Bettolo, G. B. M. (**1985**). Prenylated anthranoids from *Psorospermum* species. *Phytochemistry* **24**, 1855-1856.

Morikawa, T., Xu, F., Matsuda, H. & Yoshikawa, M. (**2006**). Structures of new flavonoids, erycibenins D, E, and F, and NO production inhibitors from *Erycibe expansa* originating in Thailand. *Chem. Pharm. Bull.* **54**, 1530-1534.

Na, Z., Xu, Y. K. (**2010**). A new prenylated xanthone from *Garcinia xipshuanbannaensis* Y.H. Li. *Nat. Prod. Res.* **24**, 1648-1653.

Nakahara, K., Roy, M. K., Ono, H., Maeda, I., Ohnishi-Kameyama, M., Yoshida, M. & Trakoontivakorn, G. (**2003**). Prenylated flavanones isolated from flowers of *Azadirachta indica* (the neem tree) as antimutagenic constituents against heterocyclic amines. *J. Agric. Food Chem.* **51**, 6456-6460.

Nakano, H., Ômura, S. (**2009**). Chemical biology of natural indolocarbazole products: 30 years since the discovery of staurosporine products. *J. Antibiot.* **62**, 17-26.

Nakazono, M., Nanbu, S., Uesaki, A., Kuwano, R., Kashiwabara, M. & Zaitsu, K. (**2007**). Bisindolylmaleimides with large stokes shift and long-lasting chemiluminescence properties. *Org. Lett.* **9**, 3583-3586.

Noike, M., Liu, C., Ono, Y., Hamano, Y., Toyomasu, T., Sassa, T., Kato, N. & Dairi, T. (**2012**). An enzyme catalyzing O-prenylation of the glucose moiety of fusicoccin A, a diterpene glucoside produced by the fungus *Phomopsis amygdali*. *Chembiochem* **13**, 566-573.

O'Brien, M., Nielsen, K. F., O'Kiely, P., Forristal, P. D., Fuller, H. T. & Frisvad, J. C. (**2006**). Mycotoxins and other secondary metabolites produced in vitro by *Penicillium paneum* Frisvad and *Penicillium roqueforti* Thom isolated from baled grass silage in Ireland. *J. Agric. Food Chem.* **54**, 9268-9276.

Ohara, K., Muroya, A., Fukushima, N. & Yazaki, K. (**2009**). Functional characterization of LePGT1, a membrane-bound prenyltransferase involved in the geranylation of p-hydroxybenzoic acid. *Biochem. J.* **421**, 231-241.

Ohmomo, S., Utagawa, T. & Abe, M. (**1977**). Identification of roquefortine C produced by *Penicillium roqueforti*. *Agric. Biol. Chem.* **41**, 2097-2098.

Oku, H., Ueda, Y., Iinuma, M. & Ishiguro, K. (**2005**). Inhibitory effects of xanthones from guttiferae plants on PAF-induced hypotension in mice. *Planta Med.* **71**, 90-92.

Ooike, M., Nozawa, K., Udagawa, S. I. & Kawai, K. I. (**1997**). Bisindolylbenzenoids from ascostromata of *Petromyces muricatus*. *Can. J. Chem.* **75**, 625-628.

Ovenden, S. P., Nielson, J. L., Liptrot, C. H., Willis, R. H., Wright, A. D., Motti, C. A. & Tapiolas, D. M. (**2011**). Comosusols A-D and comosone A: cytotoxic compounds from the brown alga *Sporochnus comosus*. *J. Nat. Prod.* **74**, 739-743.

Overk, C. R., Yao, P., Chadwick, L. R., Nikolic, D., Sun, Y., Cuendet, M. A., Deng, Y., Hedayat, A. S., Pauli, G. F., Farnsworth, N. R., van Breemen, R. B. & Bolton, J. L. (**2005**). Comparison of the in vitro estrogenic activities of compounds from hops (*Humulus lupulus*) and red clover (*Trifolium pratense*). *J. Agric. Food Chem.* **53**, 6246-6253.

Ozaki, T., Mishima, S., Nishiyama, M. & Kuzuyama, T. (**2009**). NovQ is a prenyltransferase capable of catalyzing the addition of a dimethylallyl group to both phenylpropanoids and flavonoids. *J. Antibiot. (Tokyo)* **62**, 385-392.

Ozaki, T., Nishiyama, M. & Kuzuyama, T. (**2013**). Novel tryptophan metabolism by a potential gene cluster that is widely distributed among Actinomycetes. *J. Biol. Chem.* **288**, 9946-9956.

Park, K. H., Park, Y. D., Han, J. M., Im, K. R., Lee, B. W., Jeong, I. Y., Jeong, T. S. & Lee, W. S. (**2006**). Anti-atherosclerotic and anti-inflammatory activities of catecholic xanthones and flavonoids isolated from *Cudrania tricuspidata*. *Bioorg. Med. Chem. Lett.* **16**, 5580-5583.

Peters, L., Konig, G. M., Terlau, H. & Wright, A. D. (**2002**). Four new bromotryptamine derivatives from the marine bryozoan *Flustra foliacea*. *J. Nat. Prod.* **65**, 1633-1637.

Peters, L., König, G. M., Wright, A. D., Pukall, R., Stackebrandt, E., Eberl, L. & Riedel, K. (**2003**). Secondary metabolites of *Flustra foliacea* and their influence on bacteria. *Appl. Environ. Microbiol.* **69**, 3469-3475.

Pierrel, F., Hamelin, O., Douki, T., Kieffer-Jaquinod, S., Muhlenhoff, U., Ozeir, M., Lill, R. & Fontecave, M. (**2010**). Involvement of mitochondrial ferredoxin and para-aminobenzoic acid in yeast coenzyme Q biosynthesis. *Chem. Biol.* **17**, 449-459.

Pinto, M. M., Sousa, M. E. & Nascimento, M. S. (**2005**). Xanthone derivatives: new insights in biological activities. *Curr. Med. Chem.* **12**, 2517-2538.

Pockrandt, D., Ludwig, L., Fan, A., Konig, G. M. & Li, S. M. (**2012**). New insights into the biosynthesis of prenylated xanthones: Xptb from *Aspergillus nidulans* catalyses an O-prenylation of xanthones. *Chembiochem* **13**, 2764-2771.

Raju, R., Piggott, A. M., Huang, X. C. & Capon, R. J. (**2011**). Nocardioazines: a novel bridged diketopiperazine scaffold from a marine-derived bacterium inhibits p-glycoprotein. *Org. Lett.* **13**, 2770-2773.

Rank, C., Phipps, R. K., Harris, P., Frisvad, J. C., Gotfredsen, C. H. & Larsen, T. O. (**2006**). *epi*-Aszonalenins A, B, and C from *Aspergillus novofumigatus*. *Tetrahedron Lett.* **47**, 6099-6102.

Ren, Y., Matthew, S., Lantvit, D. D., Ninh, T. N., Chai, H., Fuchs, J. R., Soejarto, D. D., de Blanco, E. J., Swanson, S. M. & Kinghorn, A. D. (**2011**). Cytotoxic and NF-kappaB inhibitory constituents of the stems of *Cratoxylum cochinchinense* and their semisynthetic analogues. *J. Nat. Prod.* **74**, 1117-1125.

Rigbers, O., Li, S.-M. (**2008**). Ergot alkaloid biosynthesis in *Aspergillus fumigatus*: overproduction and biochemical characterisation of a 4-dimethylallyltryptophan N-methyltransferase. *J. Biol. Chem.* **283**, 26859-26868.

Rochfort, S. J., Moore, S., Craft, C., Martin, N. H., Van Wagoner, R. M. & Wright, J. L. (**2009**). Further studies on the chemistry of the flustra alkaloids from the bryozoan *Flustra foliacea*. *J. Nat. Prod.* **72**, 1773-1781.

Ruiz-Sanchis, P., Savina, S. A., Albericio, F. & Alvarez, M. (**2011**). Structure, bioactivity and synthesis of natural products with hexahydropyrrolo[2,3-b]indole. *Chemistry.* **17**, 1388-1408.

Rukachaisirikul, V., Kamkaew, M., Sukavisit, D., Phongpaichit, S., Sawangchote, P. & Taylor, W. C. (**2003**). Antibacterial xanthones from the leaves of *Garcinia nigrolineata*. *J. Nat. Prod.* **66**, 1531-1535.

Ryu, H. W., Cho, J. K., Curtis-Long, M. J., Yuk, H. J., Kim, Y. S., Jung, S., Kim, Y. S., Lee, B. W. & Park, K. H. (**2011**). Alpha-glucosidase inhibition and antihyperglycemic activity of prenylated xanthones from *Garcinia mangostana*. *Phytochemistry* **72**, 2148-2154.

Ryu, H. W., Lee, B. W., Curtis-Long, M. J., Jung, S., Ryu, Y. B., Lee, W. S. & Park, K. H. (**2010**). Polyphenols from *Broussonetia papyrifera* displaying potent alpha-glucosidase inhibition. *J. Agric. Food Chem.* **58**, 202-208.

Sabater-Vilar, M., Nijmeijer, S. & Fink-Gremmels, J. (**2003**). Genotoxicity assessment of five tremorgenic mycotoxins (fumitremorgen B, paxilline, penitrem A, verruculogen, and verrucosidin) produced by molds isolated from fermented meats. *J. Food Prot.* **66**, 2123-2129.

Saleh, O., Gust, B., Boll, B., Fiedler, H.-P. & Heide, L. (**2009**). Aromatic prenylation in phenazine biosynthesis: dihydrophenazine-1-carboxylate dimethylallyltransferase from *Streptomyces anulatus*. *J. Biol. Chem.* **284**, 14439-14447.

Sánchez, C., Méndez, C. & Salas, J. A. (**2006**). Indolocarbazole natural products: occurrence, biosynthesis, and biological activity. *Nat. Prod. Rep.* **23**, 1007-1045.

Sansom, C. E., Larsen, L., Perry, N. B., Berridge, M. V., Chia, E. W., Harper, J. L. & Webb, V. L. (**2007**). An antiproliferative bis-prenylated quinone from the New Zealand brown alga *Perithalia capillaris*. *J. Nat. Prod.* **70**, 2042-2044.

Sasaki, H., Kashiwada, Y., Shibata, H. & Takaishi, Y. (**2012**). Prenylated flavonoids from *Desmodium caudatum* and evaluation of their anti-MRSA activity. *Phytochemistry* **82**, 136-142.

Sasaki, K., Mito, K., Ohara, K., Yamamoto, H. & Yazaki, K. (**2008**). Cloning and characterization of naringenin 8-prenyltransferase, a flavonoid-specific prenyltransferase of *Sophora flavescens*. *Plant Physiol.* **146**, 1075-1084.

Sasaki, K., Tsurumaru, Y., Yamamoto, H. & Yazaki, K. (**2011**). Molecular characterization of a membrane-bound prenyltransferase specific for isoflavone from *Sophora flavescens*. *J. Biol. Chem.* **286**, 24125-24134.

Schardl, C. L., Panaccione, D. G. & Tudzynski, P. (**2006**). Ergot alkaloids--biology and molecular biology. *The Alkaloids, Chem. Biol.* **63**, 45-86.

Scherlach, K., Hertweck, C. (**2006**). Discovery of aspoquinolones A-D, prenylated quinoline-2-one alkaloids from *Aspergillus nidulans*, motivated by genome mining. *Org. Biomol. Chem.* **4**, 3517-3520.

Schmidt, A. W., Reddy, K. R. & Knölker, H.-J. (**2012**). Occurrence, biogenesis, and synthesis of biologically active carbazole alkaloids. *Chem. Rev.* **112**, 3193-3328.

Schuller, J. M., Zocher, G., Liebhold, M., Xie, X., Stahl, M., Li, S.-M. & Stehle, T. (**2012**). Structure and catalytic mechanism of a cyclic dipeptide prenyltransferase with broad substrate promiscuity. *J. Mol. Biol.* **422**, 87-99.

Schultz, A. W., Lewis, C. A., Luzung, M. R., Baran, P. S. & Moore, B. S. (**2010**). Functional characterization of the cyclomarin/cyclomarazine prenyltransferase CymD directs the biosynthesis of unnatural cyclic peptides. *J. Nat. Prod.* **73**, 373-377.

Seeger, K., Flinspach, K., Haug-Schifferdecker, E., Kulik, A., Gust, B., Fiedler, H. P. & Heide, L. (**2011**). The biosynthetic genes for prenylated phenazines are located at two different chromosomal loci of *Streptomyces cinnamonensis* DSM 1042. *Microb. Biotechnol.* **4**, 252-262.

Sekita, S. (**1983**). Isocochliodinol and neocochliodinol, bis(3-indolyl)-benzoquinones from *Chaetomium* spp. *Chem. Pharm. Bull.* **31**, 2998-3001.

Seto, H., Watanabe, H. & Furihata, K. (**1996**). Simultaneous operation of the mevalonate and non-mevalonate pathways in the biosynthesis of isopentenyl diphosphate in *Streptomyces aeriouvifer*. *Tetrahedron Lett.* **37**, 7979-7982.

Shen, G., Huhman, D., Lei, Z., Snyder, J., Sumner, L. W. & Dixon, R. A. (**2012**). Characterization of an isoflavonoid-specific prenyltransferase from *Lupinus albus*. *Plant Physiol.* **159**, 70-80.

Shin-Ya, K., Furihata, K., Hayakawa, Y. & Seto, H. (**1990a**). Biosynthetic studies of naphterpin, a terpenoid metabolite of *Streptomyces*. *Tetrahedron Lett.* **31**, 6025-6026.

Shin-Ya, K., Imai, S., Furihata, K., Hayakawa, Y., Kato, Y., Vanduyne, G. D., Clardy, J. & Seto, H. (**1990b**). Isolation and structural elucidation of an antioxidative agent, naphterpin. *J. Antibiot.* **43**, 444-447.

Shindo, K., Tachibana, A., Tanaka, A., Toba, S., Yuki, E., Ozaki, T., Kumano, T., Nishiyama, M., Misawa, N. & Kuzuyama, T. (**2011**). Production of novel antioxidative prenyl naphthalen-ols by combinational bioconversion with dioxygenase PhnA1A2A3A4 and prenyltransferase NphB or SCO7190. *Biosci. Biotechnol. Biochem.* **75**, 505-510.

Singh, S. B., Ondeyka, J. G., Jayasuriya, H., Zink, D. L., Ha, S. N., Dahl-Roshak, A., Greene, J., Kim, J. A., Smith, M. M., Shoop, W. & Tkacz, J. S. (**2004**). Nodulisporic acids D-F: structure, biological activities, and biogenetic relationships. *J. Nat. Prod.* **67**, 1496-1506.

Sofia, H. J., Chen, G., Hetzler, B. G., Reyes-Spindola, J. F. & Miller, N. E. (**2001**). Radical SAM, a novel protein superfamily linking unresolved steps in familiar biosynthetic pathways with radical mechanisms: functional characterization using new analysis and information visualization methods. *Nucleic Acids Res.* **29**, 1097-1106.

Stec, E., Pistorius, D., Müller, R. & Li, S.-M. (**2011**). AuaA, a membrane-bound farnesyltransferase from *Stigmatella aurantiaca*, catalyzes the prenylation of 2-methyl-4-hydroxyquinoline in the biosynthesis of aurachins. *Chembiochem* **12**, 1724-1730.

Steffan, N., Grundmann, A., Yin, W.-B., Kremer, A. & Li, S.-M. (**2009a**). Indole prenyltransferases from fungi: a new enzyme group with high potential for the production of prenylated indole derivatives. *Curr. Med. Chem.* **16**, 218-231.

Steffan, N., Grundmann, A., Afiyatullov, A., Ruan, H. & Li, S.-M. (**2009b**). FtmOx1, a non heme Fe(II) and alpha-ketoglutarate-dependent dioxygenase, catalyses the endoperoxide formation of verruculogen in *Aspergillus fumigatus*. *Org. Biomol. Chem.* **7**, 4082-4087.

Steffan, N., Li, S.-M. (**2009**). Increasing structure diversity of prenylated diketopiperazine derivatives by using a 4-dimethylallyltryptophan synthase. *Arch. Microbiol.* **191**, 461-466.

Steffan, N., Unsöld, I. A. & Li, S.-M. (**2007**). Chemoenzymatic synthesis of prenylated indole derivatives by using a 4-dimethylallyltryptophan synthase from *Aspergillus fumigatus*. *Chembiochem* **8**, 1298-1307.

Stevens, J. F., Page, J. E. (**2004**). Xanthohumol and related prenylflavonoids from hops and beer: to your good health! *Phytochemistry* **65**, 1317-1330.

Stipanovic, R. D., Schroeder, H. W. (**1976**). Preechinulin, a metabolite of *Aspergillus chevalieri*. *Trans. Br. Mycol. Soc.* **66, Pt. 1**, 178-179.

Subramanian, S., Shen, X., Yuan, Q. & Yan, Y. (**2012**). Identification and biochemical characterization of a 5-dimethylallyltryptophan synthase in *Streptomyces coelicolor* A3(2). *Process Biochem.* **47**, 1419-1422.

Sunassee, S. N., Davies-Coleman, M. T. (**2012**). Cytotoxic and antioxidant marine prenylated quinones and hydroquinones. *Nat. Prod. Rep.*

Tahara, S. (**2007**). A journey of twenty-five years through the ecological biochemistry of flavonoids. *Biosci. Biotechnol. Biochem.* **71**, 1387-1404.

Takahashi, S., Takagi, H., Toyoda, A., Uramoto, M., Nogawa, T., Ueki, M., Sakaki, Y. & Osada, H. (**2010**). Biochemical characterization of a novel indole prenyltransferase from *Streptomyces* sp. SN-593. *J. Bacteriol.* **192**, 2839-2851.

Tanaka, H., Etoh, H., Watanabe, N., Shimizu, H., Ahmad, M. & Rizwani, G. H. (**2001**). Erysubins C–F, four isoflavonoids from *Erythrina suberosa* var. glabrescences. *Phytochemistry* **56**, 769-773.

Tischer, S., Metz, P. (**2007**). Selective C-6 prenylation of flavonoids *via* europium(III)-catalyzed claisen rearrangement and cross-metathesis. *Adv. Synth. Catal.* **349**, 147-151.

Tsai, H. F., Wang, H., Gebler, J. C., Poulter, C. D. & Schardl, C. L. (**1995**). The *Claviceps purpurea* gene encoding dimethylallyltryptophan synthase, the committed step for ergot alkaloid biosynthesis. *Biochem. Biophys. Res. Commun.* **216**, 119-125.

Tsurumaru, Y., Sasaki, K., Miyawaki, T., Uto, Y., Momma, T., Umemoto, N., Momose, M. & Yazaki, K. (**2012**). HlPT-1, a membrane-bound prenyltransferase responsible for the biosynthesis of bitter acids in hops. *Biochem. Biophys. Res. Commun.* **417**, 393-398.

Tuntiwachwuttikul, P., Taechowisan, T., Wanbanjob, A., Thadaniti, S. & Taylor, W. C. (**2008**). Lansai A-D, secondary metabolites from *Streptomyces* sp. SUC1. *Tetrahedron* **64**, 7583-7586.

Uhlig, S., Botha, C. J., Vralstad, T., Rolen, E. & Miles, C. O. (**2009**). Indole-diterpenes and ergot alkaloids in *Cynodon dactylon* (Bermuda Grass) infected with *Claviceps cynodontis* from an outbreak of tremors in cattle. *J. Agric. Food Chem.* **57**, 11112-11119.

Unsöld, I. A., Li, S.-M. (**2005**). Overproduction, purification and characterization of FgaPT2, a dimethylallyltryptophan synthase from *Aspergillus fumigatus*. *Microbiology* **151**, 1499-1505.

Unsöld, I. A., Li, S.-M. (**2006**). Reverse prenyltransferase in the biosynthesis of fumigaclavine C in *Aspergillus fumigatus*: gene expression, purification and characterization of fumigaclavine C synthase FgaPT1. *Chembiochem* **7**, 158-164.

Versiani, M. A., Diyabalanage, T., Ratnayake, R., Henrich, C. J., Bates, S. E., McMahon, J. B. & Gustafson, K. R. (**2011**). Flavonoids from eight tropical plant species that inhibit the multidrug resistance transporter ABCG2. *J. Nat. Prod.* **74**, 262-266.

Vieira, L. M., Kijjoa, A. (**2005**). Naturally-occurring xanthones: recent developments. *Curr. Med. Chem.* **12**, 2413-2446.

Wakana, D., Hosoe, T., Itabashi, T., Nozawa, K., Okada, K., Takaki, G. M. d. C., Yaguchi, T., Fukushima, K. & Kawai, K. I. (**2006**). Isolation of isoterrein from *Neosartorya fischeri*. *Mycotoxins* **56**, 3-6.

Wallwey, C., Li, S.-M. (**2011**). Ergot alkaloids: structure diversity, biosynthetic gene clusters and functional proof of biosynthetic genes. *Nat. Prod. Rep.* **28**, 496-510.

Wallwey, C., Matuschek, M. & Li, S.-M. (**2010a**). Ergot alkaloid biosynthesis in *Aspergillus fumigatus*: conversion of chanoclavine-I to chanoclavine-I aldehyde catalyzed by a short-chain alcohol dehydrogenase FgaDH. *Arch. Microbiol.* **192**, 127-134.

Wallwey, C., Matuschek, M., Xie, X.-L. & Li, S.-M. (**2010b**). Ergot alkaloid biosynthesis in *Aspergillus fumigatus*: Conversion of chanoclavine-I aldehyde to festuclavine by the festuclavine synthase FgaFS in the presence of the old yellow enzyme FgaOx3. *Org. Biomol. Chem.* **8**, 3500-3508.

Wang, F., Fang, Y., Zhu, T., Zhang, M., Lin, A., Gu, Q. & Zhu, W. (**2008**). Seven new prenylated indole diketopiperazine alkaloids from holothurian-derived fungus *Aspergillus fumigatus*. *Tetrahedron* **64**, 7986-7991.

Wang, W. L., Lu, Z. Y., Tao, H. W., Zhu, T. J., Fang, Y. C., Gu, Q. Q. & Zhu, W. M. (**2007a**). Isoechinulin-type alkaloids, variecolorins A-L, from halotolerant *Aspergillus variecolor*. *J. Nat. Prod.* **70**, 1558-1564.

Wang, W. L., Zhu, T. J., Tao, H. W., Lu, Z. Y., Fang, Y. C., Gu, Q. Q. & Zhu, W. M. (**2007b**). Three novel, structurally unique spirocyclic alkaloids from the halotolerant B-17 fungal strain of *Aspergillus variecolor*. *Chem. Biodivers.* **4**, 2913-2919.

Wang, Y., Gloer, J. B., Scott, J. A. & Malloch, D. (**1995**). Terezines A-D: New amino acid-derived bioactive metabolites from the coprophilous fungus *Sporormiella teretispora*. *J. Nat. Prod.* **58**, 93-99.

Wang, Y., Xia, Z., Xu, J. R., Wang, Y. X., Hou, L. N., Qiu, Y. & Chen, H. Z. (**2012**). Alpha-mangostin, a polyphenolic xanthone derivative from mangosteen, attenuates beta-amyloid oligomers-induced neurotoxicity by inhibiting amyloid aggregation. *Neuropharmacology* **62**, 871-881.

Wang, Y. H., Hou, A. J., Zhu, G. F., Chen, D. F. & Sun, H. D. (**2005**). Cytotoxic and antifungal isoprenylated xanthones and flavonoids from *Cudrania fruticosa*. *Planta Med.* **71**, 273-274.

Wätjen, W., Weber, N., Lou, Y. J., Wang, Z. Q., Chovolou, Y., Kampkötter, A., Kahl, R. & Proksch, P. (**2007**). Prenylation enhances cytotoxicity of apigenin and liquiritigenin in rat H4IIE hepatoma and C6 glioma cells. *Food Chem. Toxicol.* **45**, 119-124.

Williams, R. M., Stocking, E. M. & Sanz-Cervera, J. F. (**2000**). Biosynthesis of prenylated alkaloids derived from tryptophan. *Topics Curr. Chem.* **209**, 97-173.

Wilson, L. J., Yang, C. & Murray, W. V. (**2007**). Novel cycloalkene indole carbazole alkaloids via the ring closing metathesis reaction. *Tetrahedron Lett.* **48**, 7399-7403.

Wollinsky, B., Ludwig, L., Hamacher, A., Yu, X., Kassack, M. U. & Li, S.-M. (**2012a**). Prenylation at the indole ring leads to a significant increase of cytotoxicity of tryptophan-containing cyclic dipeptides. *Bioorg. Med. Chem. Lett.* **22**, 3866-3869.

Wollinsky, B., Ludwig, L., Xie, X. & Li, S.-M. (**2012b**). Breaking the regioselectivity of indole prenyltransferases: identification of regular C3-prenylated hexahydropyrrolo[2,3-b]indoles as side products of the regular C2-prenyltransferase FtmPT1. *Org. Biomol. Chem.* **10**, 9262-9270.

Woodside, A. B., Huang, Z. & Poulter, C. D. (**1988**). Trisammonium geranyl diphosphate. *Org. Synth.* **66**, 211-215.

Xu, M., Gessner, G., Groth, I., Lange, C., Christner, A., Bruhn, T., Deng, Z., Li, X., Heinemann, S. H., Grabley, S., Bringmann, G., Sattler, I. & Lin, W. (**2007**). Shearinines D-K, new indole triterpenoids from an endophytic *Penicillium* sp. (strain HKI0459) with blocking activity on large-conductance calcium-activated potassium channels. *Tetrahedron* **63**, 435-444.

Yamamoto, Y., Kiriyama, N., Shimizu, S. & Koshimura, S. (**1976a**). Antitumor activity of asterriquinone, a metabolic product from *Aspergillus terreus*. *Gann* **67**, 623-624.

Yamamoto, Y., Nishimura, K. & Kiriyama, N. (**1976b**). Studies on the metabolic products of *Aspergillus terreus*. I. Metabolites of the strain IFO 6123. *Chem. Pharm. Bull.* **24**, 1853-1859.

Yamazaki, M., Sasago, K. & Miyaki, K. (**1974**). Structure of fumitremorgin B (FTB), a tremorgenic toxin from *Aspergillus fumigatus*. *J. Chem. Soc. , Chem. Commun.*408-409.

Yamazaki, M., Suzuki, S. (**1986**). Toxicology of tremorgenic mycotoxins, fumitremorgin A and B. *Dev. Toxicol. Environ. Sci.* **12**, 273-282.

Yang, Z. G., Matsuzaki, K., Takamatsu, S. & Kitanaka, S. (**2011**). Inhibitory effects of constituents from *Morus alba* var. multicaulis on differentiation of 3T3-L1 cells and nitric oxide production in RAW264.7 cells. *Molecules* **16**, 6010-6022.

Yazaki, K., Sasaki, K. & Tsurumaru, Y. (**2009**). Prenylation of aromatic compounds, a key diversification of plant secondary metabolites. *Phytochemistry* **70**, 1739-1745.

Yin, S., Yu, X., Wang, Q., Liu, X. Q. & Li, S.-M. (**2013a**). Identification of a brevianamide F reverse prenyltransferase BrePT from *Aspergillus versicolor* with a broad substrate specificity towards tryptophan-containing cyclic dipeptides. *Appl. Microbiol. Biotechnol.* **97**, 1649-1660.

Yin, W.-B., Baccile, J. A., Bok, J. W., Chen, Y., Keller, N. P. & Schroeder, F. C. (**2013b**). A nonribosomal peptide synthetase-derived iron(III) complex from the pathogenic fungus *Aspergillus fumigatus*. *J. Am. Chem. Soc.* **135**, 2064-2067.

Yin, W.-B., Grundmann, A., Cheng, J. & Li, S.-M. (**2009**). Acetylaszonalenin biosynthesis in *Neosartorya fischeri*: Identification of the biosynthetic gene cluster by genomic mining and functional proof of the genes by biochemical investigation. *J. Biol. Chem.* **284**, 100-109.

Yin, W.-B., Ruan, H.-L., Westrich, L., Grundmann, A. & Li, S.-M. (**2007**). CdpNPT, an N-prenyltransferase from *Aspergillus fumigatus*: overproduction, purification and biochemical characterisation. *Chembiochem* **8**, 1154-1161.

Yin, W.-B., Xie, X.-L., Matuschek, M. & Li, S.-M. (**2010a**). Reconstruction of pyrrolo[2,3-b]indoles carrying an α-configured reverse C3-dimethylallyl moiety by using recombinant enzymes. *Org. Biomol. Chem.* **8**, 1133-1141.

Yin, W.-B., Yu, X., Xie, X.-L. & Li, S.-M. (**2010b**). Preparation of pyrrolo[2,3-b]indoles carrying a ß-configured reverse C3-dimethylallyl moiety by using a recombinant prenyltransferase CdpC3PT. *Org. Biomol. Chem.* **8**, 2430-2438.

Yu, X., Liu, Y., Xie, X., Zheng, X.-D. & Li, S.-M. (**2012**). Biochemical characterization of indole prenyltransferases: Filling the last gap of prenylation positions by a 5-dimethylallyltryptophansynthase from *Aspergillus clavatus*. *J. Biol. Chem.* **287**, 1371-1380.

Zhang, M., Wang, W.-L., Fang, Y.-C., Zhu, T.-J., Gu, Q.-Q. & Zhu, W.-M. (**2008**). Cytotoxic alkaloids and antibiotic nordammarane triterpenoids from the marine-derived fungus *Aspergillus sydowi*. *J. Nat. Prod.* **71**, 985-989.

Zhang, P. C., Wang, S., Wu, Y., Chen, R. Y. & Yu, D. Q. (**2001**). Five new diprenylated flavonols from the leaves of *Broussonetia kazinoki*. *J. Nat. Prod.* **64**, 1206-1209.

Zhao, S., Smith, K. S., Deveau, A. M., Dieckhaus, C. M., Johnson, M. A., Macdonald, T. L. & Cook, J. M. (**2002**). Biological activity of the tryprostatins and their diastereomers on human carcinoma cell lines. *J. Med. Chem.* **45**, 1559-1562.

Zou, H.-X., Xie, X., Zheng, X.-D. & Li, S.-M. (**2011**). The tyrosine O-prenyltransferase SirD catalyzes O-, N-, and C-prenylations. *Appl. Microbiol. Biotechnol.* **89**, 1443-1451.

Zou, H.-X., Xie, X.-L., Linne, U., Zheng, X.-D. & Li, S.-M. (**2010**). Simultaneous C7- and N1-prenylation of cyclo-L-Trp-L-Trp catalyzed by a prenyltransferase from *Aspergillus oryzae*. *Org. Biomol. Chem.* **8**, 3037-3044.

8 Acknowledgments

Firstly, I would like to express my deepest gratitude to Prof. Dr. Shu-Ming Li for his excellent supervision, support and care for my work. I learned a lot of knowledge on biochemistry and molecular biology from him, and my personal development has greatly benefited from his scientific thinking as well as high efficiency in work.

I am grateful to Prof. Dr. Michael Keusgen for acting as second referee and examinator.

I am especially grateful to the financial support of China Scholarship Council during the PhD period.

Great thanks to Dr. Xiulan Xie for 2D-NMR measurement for enzyme products of cyclic dipeptides, simple indole derivatives and hydroxynaphthalenes catalyzed by indole prenyltransferases.

I would like to thank Dr. Thomas Kämpchen, Dr. Regina Ortmann and Stefan Newel for taking ^{1}H-NMR spectra and Dr. Gabriela Laufenberg for taking mass spectra.

I am grateful to Dr. Wen-Bing Yin and Yan Liu for their works on CdpC3PT and 5-DMATS, respectively, as well as Qing Wang and Suqin Yin for their study on BrePT.

I would like to thank Lena and Dr. Marco Matuschek for synthesis of DMAPP and Dr. Edyta Stec for synthesis of GPP and FPP, as well as their help during the works.

Many thanks to Dr. Edyta Stec, Dr. Ole Rigbers, Dr. Christiane Wallwey and Kathrin Mundt for their kindly help for my living in Marburg as well as help and discussion during the work.

I would like to thank Mr. Rudl for preparing media for *E. coli* cultivation.

I express my thanks to AOR Dr. Dieter Kreusch and Sabine Bouaraba for ordering chemicals as well as lab supplies and maintenance of laboratory equipment.

Especial thanks to Kathrin Mundt and Carsten Wunsch for translating the abstract into German as well as Beate Wollinsky for reading this thesis.

Thanks also go to all current and former colleagues at the institute for the wonderful time that we shared as well as the help and discussion during the work, including Aili Fan, Alexander Frehse, Anne Döring, Daniel Pockrandt, Jennifer Robinson, Julia Winkelblech, Kirsten Brockmeyer, Lennart Poppe, Mike Liebhold, Nina Gerhards, Peter Mai, Soheil Pezeshki, Stefan Wolters, Sylwia Tarcz, Viola Wohlgemuth.

I am deeply indebted to my parents who always give me love and support me over the past years. I would like to give my personal thanks to my friends outside of the laboratory for the nice friendship.

9 Curriculum vitae

Personal data

Name: Xia Yu

Date of Birth: 05.08.1986

Place of Birth: Hunan Province, P. R. China

Education

1991-1994	Primary school student at Affiliated School to Xiangzhong Machinery Factory, Hunan Province, P. R. China.
1994-1997	Primary school student at Affiliated School to Huada Machinery Factory, Hunan Province, P. R. China.
1997-1999	Junior middle school student at Affiliated School to Huada Machinery Factory, Hunan Province, P. R. China.
1999-2000	Junior middle school student at the No. 1 Middle School of Loudi, Hunan Province, P. R. China.
2000-2003	Senior middle school student at the No. 1 Middle School of Loudi, Hunan Province, P. R. China.
09/2003-06/2007	Undergraduate student at Peking University, School of Pharmaceutical Sciences, Beijing, P. R. China.
06/2007	Bachelor of Science
09/2007-06/2009	Master candidate at Peking University, School of Pharmaceutical Sciences, Beijing, P. R. China. Master thesis supervised by Prof. Dr. Wenhan Lin; Title: “Investigation on chemical constituents and their bioactivities from Chinese Mangrove plant *Cerbera manghas* L.”.
06/2009	Master of Science
10/2009–07/2013	PhD candidate at the University of Marburg, Institute of Pharmaceutical biology and biotechnology, Marburg, Germany. Doctoral thesis supervised by Prof. Dr. Shu-Ming Li; Title: “Molecular biological and biochemical investigations on the biosynthetic enzymes of prenylated indole alkaloids from fungi”.